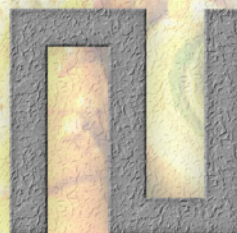


TENTH INTERNATIONAL WORKSHOP  
ON MEASUREMENT AND COMPUTATION OF  
TURBULENT (NON)PREMIXED FLAME

TNFF

Workshop

TSINGHUA UNIVERSITY, BEIJING, CHINA  
JULY 29-31, 2010

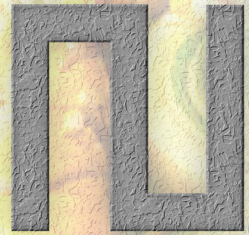


TENTH INTERNATIONAL WORKSHOP  
ON MEASUREMENT AND COMPUTATION OF  
TURBULENT (NON)PREMIXED FLAME

TNFI

Workshop

TSINGHUA UNIVERSITY, BEIJING, CHINA  
JULY 29-31, 2010



SFB 568 | Technical University of Darmstadt



imagination at work

edgewave

The Leverhulme Trust  
Stratified Combustion Network



Sirah  
Tunable Lasers  
[www.sirah.com](http://www.sirah.com)

Continuum®  
The High Energy Laser Company™

Sponsorship funds are used to reduce registration fees for academic participants and students

## SUMMARY

### **Tenth International Workshop on Measurement and Computation of Turbulent Nonpremixed Flames (TNF10)**

**29-31 July 2010  
Beijing, China**

R.S. Barlow, J.-Y. Chen, A. Dreizler, M.J. Dunn, J.H. Frank, R. Gordon,  
S. Hochgreb, J. Janicka, A. Kempf, E.W. Knudsen, A. Kronenburg, R.P. Lindstedt,  
A.R. Masri, H. Pitsch, S.B. Pope, E.S. Richardson, D. Roekaerts

### **INTRODUCTION**

The series of workshops on Measurement and Computation of Turbulent Nonpremixed Flames (TNF) facilitates collaboration and information exchange among experimental and computational researchers in the field of turbulent combustion. The emphasis is on fundamental issues of turbulence-chemistry interaction in flames that are relatively simple in terms of both geometry and chemistry. The TNF Workshop series was initiated to address validation of RANS based models for turbulent nonpremixed flames, as well as partially premixed flames where combustion occurs mainly in a diffusion flame mode. Although the title has not changed, our scope is expanding, and the TNF10 agenda emphasized recent progress toward addressing three challenges that were elaborated at TNF9 in Montreal (2008). These challenges are:

- Development and validation of modeling approaches which are accurate over a broad range of combustion modes and regimes (nonpremixed, partially premixed, stratified, and premixed).
- Extension of quantitative validation work to include more complex fuels (beyond CH<sub>4</sub>) and fuel mixtures that are of practical interest.
- Establishment of a more complete framework for verification and validation of combustion LES, including quality assessment of calculations, as well as development and utilization of approaches which extract knowledge and understanding from comparisons of detailed experimental measurements with detailed simulations.

One of the most useful functions of this workshop series has been to provide a framework for collaborative comparisons of measured and modeled results. Such comparisons are most informative when multiple modeling approaches are represented and when there has been early communication and cooperation regarding how the calculations should be carried out and what results should be compared. Experience had shown that comparisons on new target flames can generate significant new insights, but also many new questions. These questions motivate further research, both computational and experimental, and subsequent rounds of model comparisons. Our overall goal is to accelerate the development of advanced combustion models that are soundly based in fundamental science, rigorously tested against experiments, and capable of predicting flame behavior over a wide range of turbulent combustion modes and regimes.

During the two years between workshops, we have made greatest progress on the first of the three challenges, as demonstrated by the inclusion of model comparisons on two new target burners for premixed and stratified combustion.

TNF10 was attended by 93 researchers from 13 countries. The main sessions topics included:

- Overview and recent progress on lifted flames in hot coflow
- Model comparisons on the Sydney Piloted Premixed Jet Burner (PPJB)
- Overview of stratified combustion experiments
- Overview of modeling approaches for partially premixed and stratified combustion
- Model comparisons on the Darmstadt stratified flames
- Progress on kinetics and diagnostics for “new” fuels
- Best practice in LES

This summary briefly outlines the presentations and discussions. Comments and conclusions given here are based on the perspectives of the authors and do not necessarily represent consensus opinions of the workshop participants. This summary does not attempt to address all topics discussed at the workshop or to define all the terms, acronyms, or references. Readers are encouraged to consult the complete TNF10 Proceedings and also the Proceedings of previous TNF Workshops, because each workshop builds upon what has been done before.

The complete Proceedings are available for download in pdf format from [www.sandia.gov/TNF](http://www.sandia.gov/TNF). The pdf file includes the list of participants, workshop agenda, summary abstracts of the presentations, presentation slides, and two-page abstracts of 39 contributed posters.

## **ACKNOWLEDGMENTS**

Local arrangements for the TNF10 Workshop were coordinated by Profs. WU Yuxin and ZHANG Hai. Sponsorship by the German SFB-568 research program, General Electric, Edgewave, The Leverhulme Trust, La Vision, Numeca, Continuum Lasers, Princeton Instruments, and Sirah Lasers is gratefully acknowledged. These contributions allowed for reduction of the registration fees for university faculty and students. Support for Rob Barlow in coordinating TNF10 and past Workshop activities has been provided by the U. S. Department of Energy, Office of Basic Energy Sciences, Division of Chemical Sciences, Geosciences, and Biosciences. Sandia National Laboratories is a multiprogram laboratory operated by Sandia Corporation, a Lockheed Martin Company, for the United States Department of Energy under contract DE-AC04-94-AL85000.

### **IMPORTANT NOTE ON USE OF THIS MATERIAL**

Results in this and other TNF Workshop proceedings are contributed in the spirit of open scientific collaboration. Some results represent completed work, while others are from work in progress. Readers should keep this in mind when reviewing these materials.

**It would be inappropriate to quote or reference specific results from these proceedings without first checking with the individual author(s) for permission and for the latest information on results and references.**

## **HIGHLIGHTS OF PRESENTATIONS AND DISCUSSIONS**

### **Lifted Flames in Hot Coflow**

The coordinators of this session, Rob Gordon and Dirk Roekaerts, provided a detailed review of the state of knowledge on lifted flames in hot coflow, including recent progress and recommendations for future work. Development of their contribution into a published review article is very much encouraged. The session provided a review of the existing experimental and numerical work that has been conducted on burner configurations of a non- or partially premixed jet in a hot coflow. In most cases, the hot coflow is provided from post-combustion gases of lean flames and hence is reduced in oxygen level compared to air (vitiated). This design permits the investigation of conditions in the combustion zone similar to those arising by entrainment of recirculated flue gas occurring in industrial combustion devices but with the advantage that the flow pattern is much simpler, and the chemistry of the coflow is decoupled from the combustion products. This allows the focus of the investigations to be on turbulence-chemistry interaction and flame stabilization mechanisms. In the presentation by the coordinators, characteristics of the available experimental databases and past and recent modeling efforts were reviewed, as well as near future research plans. Planned new experiments considerably extending the scope of the past experiments (high Reynolds number, high pressure, other fuels) were also discussed.

The coordinators would like to highlight the following key results:

- The CO-LIF data collected for the Cabra CH<sub>4</sub>/Air case is known to be high compared to the Raman CO data. This has been identified as a systematic error in the original data processing, and division by a factor of 2.11 corrects the data well.
- New experimental databases are available from experiments in the Delft (Oldenhof et al.) and Lund (Duwig et al.) burners.
- A comparison of LES of the Cabra burner CH<sub>4</sub>/air case, closed with either tabulation of auto-ignition (AI) and premixed flamelets (AI-PF-FPI) or unsteady diffusion flamelet based progress variable (FPV) was made, highlighting some differences in predictions of standard deviation of temperature and CO.
- 1-D Linear Eddy Model computation of autoignition has been undertaken to investigate the role of differential diffusion (Sauer et al.).
- DNS data were used to validate some LES modeling assumptions, with a key result that LES prediction with only diffusion flamelets over predicts liftoff height (LH) and only AI under predicts LH (Knudsen and Pitsch, poster).
- Liftoff height sensitivity to time step choices in the transported PDF modeling due to fractional step methods was pointed out (Naud, poster).
- Unsteady tabulated non-premixed flamelets methods are developed for simulating these flames (Ihme, contribution to presentation; Vicquelin et al., poster)

The need for parametric variation in experiments and for evaluating model development based on ability to match parametric response was re-emphasized. The presently available databases do represent such parameter variation, and this should be followed in modeling efforts.

## Piloted Premixed Jet Burner (PPJB) Comparisons

The aim of the PPJB session, coordinated by Matt Dunn, was to compare some recent numerical computations of the PPJB with the experimental measurements. There were contributions from four modeling groups, two using RANS based PDF methods and two using LES methods. The PPJB features a small diameter jet from which a lean methane-air mixture issues at high velocity. Surrounding the central jet is a stoichiometric pilot, which ensures initial ignition of the central jet. Both the central jet and pilot are surrounded by a large hot coflow of hydrogen-air combustion products, ensuring that the central jet combustion process is not diluted or quenched by ambient air. By varying the central jet velocity and keeping all other parameters constant, a parametric flame series of four flames (PM1-50, PM1-100, PM1-150, and PM1-200) with increasing degrees of finite-rate chemistry effects has been investigated. The flame structure in the series varies from being thin and flamelet like in the lowest velocity flame (PM1-50) to broad and partially extinguished in the higher velocity cases. Flames PM1-150 and PM1-200 exhibit an initial ignition region close to the jet exit, followed by an extinction region, then a re-ignition region further downstream as the turbulence intensity decays. The PPJB experimental measurement database includes single point velocity measurements, planar imaging of temperature, OH and CH<sub>2</sub>O, as well as 1D line imaging using the Raman/Rayleigh/CO LIF technique combined with crossed PLIF of OH.

The modeling results from the Sydney group (*Dunn and Masri*) utilized a transported thermochemistry PDF model coupled with a RANS turbulence model. Generally it was found that the predictive capability of the RANS turbulence model was not optimal, even in the non-reactive case of a variable density jet. By increasing the value of time scale ratio  $C_\phi$ , the degree of the predicted finite-rate effects increased, although correspondingly the error in scalar variance and flame length increased, making the generality of such an increase in  $C_\phi$  difficult to justify. Generally the mean flame length was predicted to be too short and this correlated with the predicted reaction rates being too high compared to the experiments. No significant differences in the predicted results were found between the modified Curl, EMST and IEM micro-mixing models.

The Cornell group (*Rowinski and Pope*) utilized a joint velocity-turbulence frequency-composition PDF model. Generally the mean and rms mixing fields were simulated well for all flames. The reaction progress in the calculations of the flame with the lowest jet velocity, PM1-50, is in reasonable agreement with the measurements. However, as the jet velocity increases, the reaction progress is increasingly overpredicted. An exhaustive parameter sensitivity study was conducted and the primary source of error was concluded to be the modeling of the conditional diffusion term (the micro-mixing model). The importance of the jet to pilot velocity ratio on the variation of jet-pilot and jet-coflow interaction, hence finite-rate chemistry effects through the flame series was raised as an important parameter, experiments keeping this ratio constant were proposed to examine this effect.

Although one of the strengths of the PDF method is the ability to implement complex chemical mechanisms, a question was raised as to whether kinetic mechanisms (such as GRI 3.0) are suitably accurate for the mode of combustion in the PPJB where fresh methane-air mixes with hydrogen-air combustion products. The accurate prediction of the turbulent burning velocity in a premixed flame is a challenge for PDF models, and in particular there is a high sensitivity to the micro-mixing model. The fact that the use of different mixing models was shown to have such little impact on the predicted flame structure indicates that the sensitivity of the flame structure to the predicted turbulent burning velocity is low in the PPJB flame series. This is quite different to the high sensitivity to the turbulent burning velocity experienced in more traditional turbulent

premixed flames. One of the conclusions from the PDF calculations was the need for further calculations (DNS or highly resolved LES) and potentially experimental measurements of conditional diffusion to gain a better understanding of the performance of mixing models in highly turbulent premixed combustion for the regimes experienced in the PPJB. This is in the hope that such studies may provide further insight that leads to the formulation of improved or new mixing models. In PDF methods, although models for variable values of  $C_\phi$  seem well justified, it was shown that for the flames examined varying the value of  $C_\phi$  does not have a significant influence on improving the numerical predictions for the PPJB.

The Stanford group (*Mittal, Pitsch and Knudsen*) utilized an LES flamelet model combined with a level set G-Equation approach. A systematic investigation and validation of the mesh quality was presented using the velocity measurements from four non-reacting cases, which correspond to the bulk flow velocities of the four reacting cases. In addition, it was shown that a correct inflow generation method for the jet and correct modeling of the chamfer on the pilot shroud were important to obtain good velocity field predictions. Using the non-reacting case to validate the code, the mesh and boundary condition treatment was shown to be an important test to gain confidence in these parameters for the reacting cases. Preliminary results for all four reacting case results were presented. Results for the mixing fields were encouraging. However, in general the mean flame length was predicted to be too short, indicating an over prediction of the reaction rate. Future developments of this modeling methodology will include an enhanced ability to incorporate finite-rate chemistry effects.

The Lund/Haldor Topsøe/ Hong Kong Polytechnic group (*Duwig, Nogenmyr and Chan*) presented an LES model termed integrated LES (ILES), where transport equations for all reactive species are solved and the reaction rates are determined directly from the filtered species mass fractions and temperature. The results of a grid and chemical mechanism sensitivity study were presented for the PM1-100 flame. The results for the mixing fields, minor species (CO and OH) and temperature profiles for the PM1-50 and PM1-100 flames indicated that ILES is capable of good results for all of these measures in regions where the mesh is sufficiently fine ( $x/D < 20$ ). Preliminary results for the PM1-150 flame indicated that the ILES method is capable of closely capturing the initial ignition and subsequent extinction region of this flame. Further simulations will be required to see if the ILES method can capture the downstream re-ignition region of the PM1-150 flame and the PM1-200 flame in general. It was proposed that part of the success of this methodology to problems with strong finite-rate chemistry effects is that the characteristic chemistry progress variables are not neglected. It was shown that an important parameter for successful ILES simulations is that sufficient grid resolution must be used to resolve both the flame-front and the flow-fields. Because the ratio of the jet diameter to the flame-front thickness is relatively small for the PPJB, an ILES PPJB simulation requires only a relatively moderate (in terms of LES) computational cost for successful ILES results (e.g.,  $D/40$  mesh resolution). Quantitative measures that determine when the ILES approach will be valid were presented as a work in progress and are under further development.

A general finding for the simulations of the PPJB flame series was that for the PDF calculations (Cornell and Sydney) and the Stanford LES calculations similar findings were found; for the low velocity cases an acceptable predictive capability for the reaction progress field was found, whilst for the higher velocity cases the predictive capability of the reaction progress field decreased (especially for the 200m/s case). The RANS PDF modeling results presented were close to their final form and further improvements in the RANS PDF models predictive capabilities will most probably require the development of a revised or new micro-mixing model. Both of the LES results presented were preliminary results in that issues with boundary conditions, model

development, and simulating the entire flames series (and flame length) are currently being resolved and may deliver further improvement in the results compared to those presented at TNF10.

If significant new progress is made on the PPJB predictions before TNF11, it would be appropriate to have another PPJB session at TNF11. Any new individuals or groups interested in contributing simulations of the PPJB for TNF11 should contact Matthew Dunn ([mjdunn@sandia.gov](mailto:mjdunn@sandia.gov)) to obtain the experimental database.

## **Overview of Stratified Combustion Experiments**

Given that stratified combustion is a new area for the TNF series, the objective of this session was to provide an overview of experimental information on the effects of mixture stratification on flame structure, including published work as well as work in progress. The session was split into two parts, with Simone Hochgreb covering the broad overview and Andreas Dreizler providing details of experiments on the TU Darmstadt Stratified Burner, which was a target for model comparisons at this workshop.

Most of the published experimental research on the structure of stratified flames deals with fuel-lean combustion in laminar or mildly turbulent flows ( $u'/S_L$  not much higher than 1). The mildly turbulent cases include rod stabilized V-flame and expanding, spark-ignited flames in grid-generated turbulence. From this work there is reasonably consistent evidence on the following. Local flame structure and propagation speed are affected by the gradient in equivalence ratio  $\phi$ , and the effects depend on the magnitude and sign of the gradient in  $\phi$ . When a flame propagates through a fuel-lean mixture with decreasing equivalence ratio, it is described as a back supported flame, meaning that the products immediately behind the flame have higher temperature and higher radical concentrations than the corresponding homogeneous flame at the same equivalence ratio. This back-supported structure enhances the local burning rate and extends the lean flammability limit. In mildly turbulent cases, experiments have shown that stratified flames have broader and more symmetric curvature pdfs and increased flame surface density compared to homogeneous premixed flames. There is also evidence that flame thickness is less sensitive to  $\phi$  in stratified cases.

Detailed velocity and scalar data sets from burners with higher turbulence levels and well defined boundary conditions are needed for model validation. Two burners have been developed for this purpose. The TU Darmstadt Stratified Burner has a co-annular design with a central premixed pilot flame. The inner and outer annular flows can have the same or different equivalence ratios, and they have long development lengths to yield fully developed turbulent flow at the burner exit. This burner was designed to isolate the effects of mixture stratification in statistically stationary flames without the modeling complications of swirling or recirculating flows. Turbulence levels ( $u'/S_L$ ) can exceed 20 in this configuration. Velocity measurements have been published and scalar experiments are in progress. A second burner for stratified flames was developed jointly by Cambridge and Sandia, and it was designed to be a next potential modeling target after the Darmstadt burner. It adopts the co-annular concept of the Darmstadt burner, but uses a central bluff body for flame stabilization and allows for variable swirl in the outer annular flow, yielding greater complexity of the overall flow field. Examples of scalar and velocity measurements are included in the Hochgreb presentation.

## Modeling Approaches for Stratified and Partially Premixed Combustion

The goal of this session, which was coordinated by Ed Richardson and Ed Knudsen, was to review the current of state of stratified, partially premixed, and mixed regime turbulent combustion models, and to suggest directions for future work that will help to advance the fidelity of model performance in these challenging conditions.

The first half of the presentation reviewed the combustion physics that characterize mixed-regime burning, and that must be accounted for by any relevant modeling approach. So-called 'front-supported' and 'back-supported' premixed flames were used as example cases that motivate this discussion. In these flames, the equivalence ratio of a co-flow is set as either farther from stoichiometric (front-supported) or closer to stoichiometric (back-supported) than a central jet stream. Newly available DNS data was referenced to demonstrate how these different configurations change the premixed flame's structure and burning speed. Once the possible effects of stratification are understood, it becomes important to understand the conditions under which these effects are expected to appear. Therefore, in an effort to more rigorously distinguish between stratified combustion and purely premixed combustion, the controlling variables that might appear in a regime diagram for stratification were discussed. These include the ratio of the maximum possible change in burning speed to the mean burning speed, the ratio of the Kolmogorov length scale and the mean flame thickness, and the mixing timescale associated with the local fuel concentration.

In the second half of this presentation, several of the most widely used LES combustion models were discussed with respect to how they handle multi-regime burning. The approaches considered were the flamelet model, the thickened flame model, filtered density function approaches, and the linear eddy model. Each of these approaches was noted to have some particular advantages and particular disadvantages in the context of partially premixed combustion. For example, the flamelet model is expected to predict flame structure very accurately in both the non-premixed and premixed limits, but the extent to which descriptions of these asymptotic regimes can be combined to describe a mixed mode flame structure remains unclear.

Finally, several approaches to locally distinguishing between premixed and non-premixed regimes in an LES were discussed. The simplest of these approaches is the flame index, but more detailed approaches that rely on coordinate transformations that explicitly distinguish regimes were also discussed. These approaches are now being actively applied in LES, and are the subject of ongoing model development efforts.

One point that was raised throughout the workshop was the particular challenge that premixed combustion presented, and how this challenge was distinct from the non-premixed modeling challenge. Because stratified and partially premixed combustion inherently have premixed-like behavior, models for premixed flame propagation and flame structure are essential for any predictive multi-regime approach.

Comments on Future Work:

- A continuing need exists for the improvement of regime distinguishing indicators. These indicators will be needed in most combustion models that involve tabulated chemistry, but have only begun to be developed.
- Beyond the need for regime indicators to be used within models, a broad framework (e.g. regime diagrams) for classifying and comparing different partially premixed flows – and

the resultant combustion physics – will be helpful. Further study of the stratified and partially-premixed data sets presented at this workshop may help determine the relevant effects of various equivalence ratio and equivalence ratio length-scale distributions.

### **Darmstadt Stratified Flames: Model Comparisons**

The Darmstadt Stratified Flames were presented as a new test case for the TNF 10 workshop. These flames were developed at the Technical University of Darmstadt and have been investigated by Seffrin, Fuest, Geyer and Dreizler. Model comparisons were coordinated and presented by Andreas Kempf.

Preliminary experimental data for temperature (Rayleigh, Raman-Rayleigh), mixture fraction and CO<sub>2</sub> mass fraction (Raman) were also made available and presented at the workshop in comparison to the numerical simulations. (These preliminary experimental scalar data were only made available for presentation at TNF10. They will not be distributed further, as improved data will become available soon.)

A set of flames was chosen as preferred target for the comparisons, and contributors were encouraged to simulate at least the non-reactive case TSFAi2 and the basic stratified case TSFAr. Only the Stanford group submitted further data for case TSFG.

Cases in descending order of priority:

1. TSFAi2 (isothermic)
2. TSFAr (stratified, no shear)
3. TSFG (not stratified, no shear)
4. TSFCr (stratified, shear)
5. TSFEr (not stratified, shear)

All groups performed Large-Eddy Simulations, using (i) a sub-grid pdf/stochastic fields method in combination with the static Smagorinsky model (Imperial, Jones' Boffin-LES code), (ii) a flamelet model combined with the G-Equation and the Germano model (Stanford, NGA-3DA), (iii) premixed flamelet generated manifolds with local flame thickening and the Germano model (Darmstadt, FASTEST) and (iv) Fureby's flame surface density model with the static Smagorinsky model (Imperial, Kempf's PsiPhi code).

Two approaches were taken to represent the computational domain: Darmstadt and Stanford simulated the flow upstream, using one large domain with local refinement (Darmstadt) and a cascade of precursor simulations (Stanford). Both groups obtained results that were in good agreement with the experimental velocity data. Both groups from Imperial used a more compact computational domain, starting simulations at the outlet of the inner nozzle, prescribing the experimental velocity data.

Overall, all groups achieved good predictions of the data, particularly considering that a new TNF case was simulated. As the scalar data (temperature, mixture fraction and CO<sub>2</sub> mass fraction) only became available very late, the predictions of these quantities can be considered as 'blind'; modellers had no opportunity to tune their simulations to match the data. The features of the flames that were found to be most challenging were the intricate geometry of the flame holder, the chamfer on the nozzle exits, and the relatively low co-flow velocity of only 0.1 m/s, which makes a long simulation time necessary.

For TNF11, it is recommended that the Darmstadt stratified flame series be considered as a test case. The lessons learned for TNF10 should enable all groups to accurately predict the flow and mixing, so that the focus can be shifted towards the effect of stratification on flame-turbulence interaction. It is hoped that groups will be able to start the TNF11 simulations earlier in the cycle than was the case for TNF10, thus allowing sufficient time for detailed simulations to be completed and potentially interesting comparisons to be made.

Any groups interested to contribute simulations of these flames for TNF11 should contact Andreas Kempf (a.kempf@imperial.ac.uk) to be included in the mailing list.

### **Progress on Kinetics and Diagnostics for “New” Fuels**

Extending validation work to fuels more complex than methane was one of the challenges outlined at TNF9. DME and ethanol were identified as relatively simple fuels which have very different properties and are of practical interest. For example, ethanol has a RON of 129, while DME has a cetane number in the range 55-60. Furthermore, molecular transport properties of the two fuels are very similar and, accordingly, differences in fuel behaviour can be directly related to chemistry effects. Peter Lindstedt and J-Y Chen coordinated a session to review progress on kinetics and diagnostics for these “new” fuels. The topics included an assessment of the need to (i) provide a systematic determination of high quality thermodynamic data, (ii) the derivation and testing of alternative detailed reaction mechanisms using data related to flame structures and ignition related properties. (iii) The need to identify critical reaction pathways and assess the impact of uncertainties in key kinetic rate parameters on model predictions, (iv) the reduction of the resulting mechanisms to an acceptable size and, finally, progress in the efforts to procure high quality experimental data in a “friendly” burner configuration (c.f. Sandia A-F series).

Reaction mechanisms have been published for ethanol by UCSD, LLNL and Dryer’s group, and for DME by the LLNL and Dryer groups. Presentation slides from Berkeley and Imperial College included comparisons of predicted ignition delay characteristics across a range of conditions for both fuels, as well as comparisons of predictions from these mechanisms against published experimental data on low pressure flame profiles, laminar flame speed, and ignition delay times. Substantial differences in ignition delay times between the different mechanisms were shown using a Cabra type burner configuration. The differences were such that one ethanol mechanism was found to ignite more readily than the DME variant from another group. Sensitivity analyses were presented that show a strong impact of the thermal dissociation of DME and the need for accurate rate determinations was identified for a number of reactions. It was further shown that in a HCCI type environment temperature changes of up to 30 K were required in order to bring similarity in behaviour between alternative mechanisms. Such differences in temperature should be contrasted with the strong sensitivity to boundary conditions experienced in, for example, the Cabra configuration and as reported by the groups at Berkeley, Cornell and Imperial College among others. On the positive side, a systematically reduced 28-species mechanism from Berkeley, based on the Dryer mechanism, was shown to be in very close agreement with the parent mechanism across a broad range of conditions. Furthermore, work to identify critical reaction pathways in order to select, or determine, appropriate reaction rate parameters was also summarized with examples shown using laminar flame configurations.

Progress at TU Darmstadt and Sandia to extend quantitative Raman/Rayleigh scattering methods to DME flames was also reviewed. Here the main point was that hydrocarbon intermediates in DME flames are much more important for Raman/Rayleigh data interpretation than in methane flames. Raman/Rayleigh signals from DME flames cannot be interpreted usefully unless these

intermediates are accounted for, and a method for doing this, based on information from laminar flame calculations was introduced. Preliminary results for a series of piloted, partially premixed DME/air jet flames were also presented.

### **Other Highlights**

Jonathan Frank and Andreas Kronenburg organized a session to highlight other recent work of direct or potential relevance to the TNF Workshop process. This included:

- Pros and cons of turbulent counterflow flames as potential TNF targets. Bruno Coriton presented work performed at Yale, Sandia, and Imperial College on two different counterflow burners. The Yale burner was shown to produce turbulence Reynolds numbers up to roughly 1000 and methods for separating out low frequency contributions using techniques formulated at Yale and Imperial College were discussed.
- Development of a piloted jet flame burner for sooty fuels (by Shaddix and coworkers at Sandia), along with an overview of experiments using simultaneous OH/PAH PLIF and PLII, laser extinction, 3-color extinction/emission, local radiant emissions, and PIV.
- Results from Raman/Rayleigh/CO-LIF measurements on the Cambridge Swirl Burner showing that preferential transport can significantly alter the mean atom balance across a turbulent premixed flames.
- Slides from Luc Vervisch and coworkers (presented by Kronenburg) describing a multi-scale convergence methodology for DNS, where the meshes of Large-Eddy-Simulations are repeatedly refined until the smallest scales are sufficiently resolved. The target experiment is a premixed swirl flame reported by Meier et al.

### **Best Practice in LES**

The session on best practices for LES was organized by Heinz Pitsch and Johannes Janicka, who solicited and compiled input from many colleagues to lead off the discussion. Some studies on the topic were presented, and some of the open questions were raised first. This was followed by an open discussion.

The presented material includes examples of criteria for mesh refinement, discussions of the effect of numerical schemes on modeled quantities, and sensitivity studies. As an example, an extensive sensitivity study by Janicka was shown, where the Sydney bluff-body flame was computed and results were compared with experimental data. Then variations of grid, boundary conditions, SGS model, combustion model, and several parameters and modeling assumptions included in the combustion model were performed to study the sensitivity of the solution of these parameters. For this validation study, several other configurations were further considered.

Several recommendations for best practices were made:

1. One of the most important issues is the numerical mesh, which typically also defines the LES filter. Mesh refinement studies should be performed. However,
  - a. It is not sufficient to simply do a global refinement. Mesh refinement should be performed using refinement criteria, since also mesh distribution is important. The local resolution should be reported. This can be done in terms of spectra, fractional sub-filter energies, or relevant length scales. It is important that a distribution is shown, not just a few points.

- b. If the mesh resolution is too fine, the model is not tested. Further, a very high mesh resolution that might be achievable in simple canonical cases cannot be used in the application of models to realistic systems for which the models are ultimately developed.
  - c. While the mesh is a numerical parameter, the filter size is a model parameter. The question was discussed whether it is important in changing the mesh, to separate the effect of model from numerics, which is not easily possible.
2. Sensitivity studies for uncertain parameters should be performed. These parameters could include, for example, grid, boundary conditions, models, model parameters, and modeling assumptions. However, there is a large space of uncertain parameters and there is no general guideline for which parametric uncertainty should be investigated.
  3. The simulations should be documented in all details. This should include a description of the mesh, boundary conditions, numerical algorithms, and all models and model parameters.
  4. Report about length scales and length scale ratios (integral scales, filter size, Kolmogorov scales)

Recommendations to experimentalists (most of these are obvious and already considered in most experiments):

1. Boundary conditions need to be specified in as much detail as possible.
2. Experimental uncertainties need to be well characterized and reported.
3. Error bars should be provided.
4. Series of experimental data sets should include ‘easy’ cases and cold flow.

### **Priorities and Planning for TNF11**

TNF11 Workshop will be held in Darmstadt, Germany just prior to the 34<sup>th</sup> Combustion Symposium (Warsaw, August, 2012) and will be hosted by the Technical University of Darmstadt. Andreas Dreizler and Andreas Kempf will be the Program Co-Chairs. Darmstadt is convenient to Frankfurt airport, which is a major international hub.

It is anticipated that more expensive model comparisons will be carried out for the Sydney Piloted Premixed Jet Burner and the Darmstadt Stratified Burner. Interested modeler should contact Matt Dunn or Andreas Kempf, as indicated in their respective summary sections. It is possible that other target flames will be added, and such announcements will be made as early as possible. Those interested in modeling other flames that are relevant to the TNF process are encouraged to contact the authors of work on those specific flames.

We also expect to continue work toward developing a more complete framework for combustion LES validation. Progress and challenges in areas of LES quality assessment, parameter variation, and uncertainty quantification are likely to be on the agenda. Development of better methods for quantitative comparison of experiments and LES will also be a priority for the next workshop.

Blank Page

# TNF10 Workshop Proceedings – Table of Contents

Preface and Acknowledgments .....	16
List of Participants .....	18
Agenda .....	20
<b>Technical Sessions and Coordinators</b>	
Best Practice in LES – <i>H. Pitsch, J. Janicka</i>	
Abstract .....	22
Presentation .....	23
Lifted Flames in Hot Coflow – <i>R. Gordon, D. Roekaerts</i>	
Abstract .....	44
Presentation .....	49
Comment on a Correction to the Cabra CO-LIF Data .....	92
Piloted Premixed Jet Burner Comparisons – <i>M. Dunn</i>	
Abstract .....	98
Presentation .....	100
Overview of Stratified Flame Experiments – <i>S. Hochgreb</i> .....	156
Overview of Modeling Approaches for Stratified and Partially Premixed Combustion – <i>E. Richardson, E. Knudsen</i>	
Abstract .....	172
Presentation .....	173
Stratified Flames from TU Darmstadt – <i>A. Dreizler</i> .....	190
Darmstadt Stratified Burner Model Comparisons – <i>A. Kempf</i>	
Abstract .....	198
Presentation .....	199
Progress on Kinetics and Diagnostics for “New” Fuels – <i>R.P. Lindstedt, J.-Y. Chen</i> .....	214
Highlights from Posters and Other Recent Work – <i>J. Frank, A. Kronenburg</i> .....	237
Slides to Prompt Open Discussion – <i>S. Pope, A. Masri</i> .....	258
<b>Poster Section</b>	
Poster Titles and Authors .....	264
Poster Abstracts (39 submissions, 2-pages).....	268

# T<sub>N</sub>F10 Workshop – Preface and Acknowledgments

Beijing, 29–31 July 2010

## PREFACE:

The TNF Workshop series facilitates collaboration and information exchange among experimental and computational researchers in the field of turbulent combustion. For most of our history, the emphasis has been on nonpremixed and partially premixed jet flames, including a variety of stabilization mechanisms. Our primary focus has been on issues of turbulence-chemistry interaction in flames of relatively simple fuels. Other modeling issues, including radiation, mixing, chemical kinetic mechanisms, turbulence modeling, and boundary conditions, have been addressed to the extent necessary to reduce ambiguity in comparisons of measured and modeled results. This collaborative process benefits from contributions by participants having different areas of expertise and complementary research capabilities.

The 1st TNF Workshop was held in Naples, Italy in July 1996. Its objectives were to select experimental data sets for testing combustion models and to establish guidelines for collaborative comparisons of measured and modeled results on those target flames. Subsequent workshops were held in Heppenheim, Germany (1997), Boulder, Colorado (1998), Darmstadt, Germany (1999), Delft, The Netherlands (2000), Sapporo, Japan (2002), Chicago, Illinois (2004), Heidelberg, Germany (2006), and Montreal, Canada (2008). Proceedings and summaries are available at <http://www.sandia.gov/TNF>.

Over time, a collection of benchmark experiments and calculations has been established in the literature, covering a progression in geometric and chemical kinetic complexity. Collaborative research efforts have expanded the experimental knowledge base for the benchmark flames and lead to a better understanding of the capabilities and limitations of combustion models and experimental methods.

Perhaps the most important function of the workshops themselves has been to provide a framework for comparing multiple combustion models applied to the same target cases. We emphasize that this is not a competition, but rather a means of identifying areas for potential improvements in a variety of modeling approaches and specific submodels. The process also serves to identify gaps or inconsistencies in the experiments.

The TNF10 Workshop program reflects the broadened scope that was outlined at the Montreal workshop (2008) in the context of three challenges:

- Development and validation of modeling approaches which are accurate over a broad range of combustion modes and regimes (nonpremixed, partially premixed, stratified, and premixed).
- Extension of quantitative validation work to include more complex fuels (beyond CH<sub>4</sub>) and fuel mixtures that are of practical interest.
- Establishment of a more complete framework for verification and validation of combustion LES, including quality assessment of calculations, as well as development and utilization of approaches which extract knowledge and understanding from comparisons of detailed experimental measurements with detailed simulations.

# **TNF10 Workshop – Preface and Acknowledgments**

Beijing, 29–31 July 2010

The inclusion of two new target flames for stratified and premixed combustion, as well as sessions to address experimental and computational issues associated with premixed, stratified, and partially premixed combustion contributed to a full program and vibrant discussion.

## **ACKNOWLEDGEMENTS:**

Partial support for organization of the TNF10 Workshop was provided by Sandia National Laboratories, with funding from the United States Department of Energy, Office of Basic Energy Sciences, and by the Technical University of Darmstadt, Germany, with funding from SFB-568.

Sponsorship contributions from the SFB-568 Program, GE, Edgewave, The Leverhulme Trust, La Vision, Numeca, Continuum Lasers, Princeton Instruments, and Sirah Lasers have been used to reduce the registration fees for university participants and students and to pay a portion of the fixed costs of the conference facility.

Our local hosts at Tsinghua University were incredibly helpful in facilitating all the arrangements with the Unisplendor International hotel. The Workshop could not have happened without their generous contributions of time and effort.

Marissa Targowski of Sandia and Jasmin Krenzer of TU Darmstadt EKT provided administrative support for various aspects of this Workshop.

Cover art is by Daniel Strong of Sandia and uses a flame images provided TU Darmstadt, Sandia, and Cambridge.

Special thanks to the people who coordinated the technical sessions and generated detailed and informative presentations. Thanks also to all those who contributed material for those presentations.

## **TNF10 ORGANIZING COMMITTEE:**

R.S. Barlow, J.-Y. Chen, A. Dreizler, J. Janicka, A. Kempf, R.P. Lindstedt, A.R. Masri, J.C. Oefelein, H. Pitsch, S.B. Pope, D. Roekaerts, L. Vervisch.

## **LOCAL ARRANGEMENTS COMMITTEE (TSINGHUA UNIVERSITY)**

Y. Wu, Q. Yao, H. Zhang, S.Q. Li

# TNF10 Workshop – Participants

Beijing, 29–31 July 2010

<u>Name</u>	<u>Affiliation</u>	<u>Email</u>
Jan E. ANKER	NUMECA	jan.anker@numeca.be
Antonio ATTILI	King Abdullah University - KAUST	antonio.attili@kaust.edu.sa
Junkyung BAI	Hanyang University	ymkim@hanyang.ac.kr
Xue-Song BAI	Lund University	xue-song.bai@energy.lth.se
Rob BARLOW	Sandia National Laboratories	barlow@sandia.gov
Matthieu BOILEAU	CNRS, Ecole Central Paris	matthieu.boileau@em2c.ecp.fr
Fabrizio BISETTI	King Abdullah University - KAUST	fabrizio.bisetti@kaust.edu.sa
Qing Nian (Shaun) CHAN	University of Adelaide	qing.chan@adelaide.edu.au
J.-Y. CHEN	University of California, Berkeley	jychen@me.berkeley.edu
Jacqueline CHEN	Sandia National Laboratories	jhchen@sandia.gov
Ying CHEN	Tsinghua University	
Bruno CORITON	Yale University	bruno.coriton@yale.edu
Bassam DALLY	University of Adelaide	bassam.dally@adelaide.edu.au
Reni De MEESTER	Ghent University	reni.demeester@ugent.be
Dibble	University of California, Berkeley	rdibble@me.berkeley.edu
Andreas DREIZLER	TU Darmstadt	dreizler@ekt.tu-darmstadt.de
James DRISCOLL	University of Michigan	jamesfd@umich.edu
Matthew DUNN	Sandia National Laboratories	mjdunn@sandia.gov
Benoit FIORINA	Ecole Centrale Paris	benoit.fiorina@ecp.fr
Jonathan FRANK	Sandia National Laboratories	jhfrank@sandia.gov
Yipeng GE	University of Queensland	y.ge@uq.edu.au
Dirk GEYER	University of Applied Sciences Darmstadt	dirk.geyer@h-da.de
Kok GOH	Imperial College London	henrygohkh@googlemail.com
Sandro GOMEZ	Yale University	alessandro.gomez@yale.edu
Robert GORDON	University of Cambridge	r.gordon@eng.cam.ac.uk
Andrea GRUBER	SINTEF Energy	andrea.gruber@sintef.no
Christian HASSE	University of Technology Freiberg	Christian.Hasse@iec.tu-freiberg.de
Evatt HAWKES	University of New South Wales	evatt.hawkes@unsw.edu.au
Simone HOCHGREB	University of Cambridge	sh372@cam.ac.uk
Andrea HSU	Sandia National Laboratories	aghsu@sandia.gov
K. Y. HUH	POSTECH	huh@postech.ac.kr
Matthias IHME	University of Michigan	mihme@umich.edu
Jean-Francois IZARD	King Abdullah University - KAUST	jeanfrancois.izard@kaust.edu.sa
Johannes JANICKA	TU Darmstadt - EKT	janicka@ekt.tu-darmstadt.de
Bill JONES	Imperial College London	w.jones@imperial.ac.uk
Mrinal JUDDOO	University of Sydney	mrinal.juddoo@sydney.edu.au
Nader KARIMI	TU Darmstadt - CSI	karimi@csi.tu-darmstadt.de
Andreas KEMPF	Imperial College London	a.kempf@imperial.ac.uk
Taehoon KIM	Hanyang University	susyboy@hanmail.net
Yongmo KIM	Hanyang University	ymkim@hanyang.ac.kr
Alex KLIMENKO	The University of Queensland	klimenko@mech.uq.edu.au
Edward KNUDSEN	Stanford University	ewk@stanford.edu
Heeseok KOO	University of Texas, Austin	hkoo@mail.utexas.edu
Andreas KRONENBURG	Imperial College London	a.kronenburg@imperial.ac.uk
Jens KUEHNE	TU Darmstadt - EKT	kuehne@ekt.tu-darmstadt.de
Jeongwon LEE	Hanyang University	

# TNF10 Workshop – Participants

Beijing, 29–31 July 2010

<u>Name</u>	<u>Affiliation</u>	<u>Email</u>
Peter LINDSTEDT	Imperial College London	p.lindstedt@imperial.ac.uk
Zhaohui LIU	Huazhong University	zliu@hust.edu.cn
Kun LUO	Zhejiang University	zjulk@zju.edu.cn
Terence MA	Imperial College London	terence.ma03@imperial.ac.uk
Ulrich MAAS	Karlsruhe Institute of Technology	umaas@itt.uni-karlsruhe.de
Assaad MASRI	The University of Sydney	assaad.masri@sydney.edu.au
Paul MEDWELL	University of Adelaide	paul.medwell@adelaide.edu.au
Wolfgang MEIER	German Aerospace Center	wolfgang.meier@dlr.de
Gus NATHAN	University of Adelaide	graham.nathan@adelaide.edu.au
Bertrand NAUD	Ciemat	bertrand.naud@ciemat.es
Salvador NAVARRO- MARTINEZ	Imperial College London	s.navarro@imperial.ac.uk
Michael PETTIT	Imperial College London	mwp03@ic.ac.uk
Lyle PICKETT	Sandia National Laboratories	LMPicke@sandia.gov
Heinz PITTSCH	Stanford University	h.pitsch@stanford.edu
Steve POPE	Cornell University	s.b.pope@cornell.edu
Xaiolong QIU	Tsinghua University	
Venkat RAMAN	University of Texas, Austin	v.raman@mail.utexas.edu
Michael RENFRO	University of Connecticut	renfro@engr.uconn.edu
Ed RICHARDSON	Sandia National Laboratories	esrich@sandia.gov
Stelios RIGOPOULOS	University of Manchester	stelios.rigopoulos@manchester.ac.uk
Dirk ROEKAERTS	Delft University of Technology	d.j.e.m.roekaerts@tudelft.nl
Damian ROUSON	Sandia National Laboratories	rouson@sandia.gov
David ROWINSKI	Cornell University	dhr46@cornell.edu
Robert SCHEIßL	Karlsruhe Institute of Technology	robert.schiessl@kit.edu
Thomas SCHMITT	Ecole Central Paris	thomas.schmitt@em2c.ecp.fr
Alexis SEVAULT	NTNU Trondheim	alexis.sevault@ntnu.no
Ivana STANKOVIC	Ghent University	Ivana.Stankovic@Ugent.be
Oliver STEIN	University of Stuttgart	o.stein@itv.uni-stuttgart.de
Pete STRAKEY	DOE/NETL	peter.strakey@netl.doe.gov
Jeff SUTTON	The Ohio State University	sutton.235@osu.edu
Mark SWEENEY	University of Cambridge	marksweeney@cantab.net
Chenning TONG	Clemson University	ctong@ces.clemson.edu
Oliver VERMOREL	CERFACS	vermorel@cerfacs.fr
Vicquelin RONAN	Ecole Centrale Paris	ronan.vicquelin@gmail.com
Konstantina VOGIATZAKI	Imperial College London	k.vogiatzaki@imperial.ac.uk
Stefan VOSS	TU Bergakademie Freiberg	stefan.voss@iwtt.tu-freiberg.de
Andrew WANDEL	University of Southern Queensland	andrew.wandel@usq.edu.au
Haifeng WANG	Cornell University	hw98@cornell.edu
Lin WANG	Huazhong University	willwanglin@163.com
Forman WILLIAMS	University of California, San Diego	faw@ucsd.edu
Shaohua WU	Tsinghua University	
Yuxin (Martin) WU	Tsinghua University	wuyx@tsinghua.edu.cn
Zhaopu YAO	Tsinghua University	yzp02@mails.tsinghua.edu.cn
Hai ZHANG	Tsinghua University	haizhang@tsinghua.edu.cn
Jian ZHANG	Tsinghua University	jianzhang@tsinghua.edu.cn
Yunzhe ZHENG	Tsinghua University	zwz03@mails.tsinghua.edu.cn
Min ZHU	Tsinghua University	zhumin@tsinghua.edu.cn

## TNF10 Workshop – Agenda

Beijing, 29–31 July 2010

### Thursday, July 29:

16:00 – 17:00 Registration and Poster Setup

17:00 – 21:00 Poster Session and Reception

### Friday, July 30:

8:00 – 8:15 Introduction and Announcements  
(Rob Barlow)

8:15 – 9:00 Good Practice in LES – Part 1  
(Coordinator: Heinz Pitsch)

9:00 – 10:15 Lifted Flames in Hot Coflow  
(Coordinators: Rob Gordon, Dirk Roekaerts)

10:15 – 10:45 Tea Break (Poster Session)

10:45 – 12:00 Piloted Premixed Jet Burner Comparisons  
(Coordinator: Matt Dunn)

12:00 Lunch

13:30 – 14:00 Overview of Stratified Flame Experiments  
(Coordinator: Simone Hochgreb)

14:00 – 14:45 Overview of Modeling Approaches for Stratified and Partially  
Premixed Combustion  
(Coordinators: Ed Richardson, Ed Knudsen)

14:45 – 15:15 Darmstadt Stratified Burner Experiments  
(Coordinator: Andreas Dreizler)

15:15 – 15:45 Tea Break (Poster Session)

15:45 – 16:30 Darmstadt Stratified Burner Model Comparisons  
(Coordinator: Andreas Kempf)

16:30 – 17:30 Progress on Kinetics and Diagnostics for “New” Fuels (DME, etc.)  
(Coordinators: Peter Lindstedt, J-Y Chen)

18:00 – Dinner

19:30 – 21:30 Poster Session

## **T<sub>N</sub>F10 Workshop – Agenda**

Beijing, 29–31 July 2010

### **Saturday, July 31:**

- |               |   |
|---------------|---|
| 8:30 – 9:30   | Good Practice in LES – Part 2, Discussion<br>(Coordinators: Heinz Pitsch, Johannes Janicka)         |
| 9:30 – 10:15  | Highlights from Posters and Other Recent Work<br>(Coordinators: Jonathan Frank, Andreas Kronenburg) |
| 10:15 – 10:45 | Tea Break (Poster Session)  |
| 10:45 – 11:30 | Open Discussion<br>(Coordinators: Steve Pope, Assaad Masri)   |
| 11:30 – 12:00 | Action Items and Planning for T <sub>N</sub> F11<br>(Coordinators: Rob Barlow, Andreas Dreizler)    |
| 12:00 –       | Adjourn to Lunch  |
| 13:00 –       | Remove Posters  |

# Best Practices in LES

*Heinz Pitsch, Stanford University and Johannes Janicka, TU Darmstadt*

The session on best practices for LES was organized by Heinz Pitsch and Johannes Janicka who solicited and compiled input from many colleagues to lead off the discussion. Some studies on the topic were presented, and some of the open questions were raised first. This was followed by an open discussion.

The presented material is provided in the subsequent slides, and includes examples of criteria for mesh refinement, discussions of the effect of numerical schemes on modeled quantities, and sensitivity studies. As an example, an extensive sensitivity study by Janicka was shown, where the Sidney bluff-body flame was computed and results were compared with experimental data. Then variations of grid, boundary conditions, SGS model, combustion model, and several parameters and modeling assumptions included in the combustion model were performed to study the sensitivity of the solution of these parameters. For this validation study, several other configurations were further considered.

Several recommendations for best practices were made:

1. One of the most important issues is the numerical mesh, which typically also defines the LES filter. Mesh refinement studies should be performed. However,
  - a. It is not sufficient to simply do a global refinement. Mesh refinement should be performed using refinement criteria, since also mesh distribution is important. The local resolution should be reported. This can be done in terms of spectra, fractional sub-filter energies, or relevant length scales. It is important that a distribution is shown, not just a few points.
  - b. If the mesh resolution is too fine, the model is not tested. Further, a very high mesh resolution that might be achievable in simple canonical cases cannot be used in the application of models to realistic systems for which the models are ultimately developed.
  - c. While the mesh is a numerical parameter, the filter size is a model parameter. The question was discussed whether it is important in changing the mesh, to separate the effect of model from numerics, which is not easily possible.
2. Sensitivity studies for uncertain parameters should be performed. These parameters could include, for example, grid, boundary conditions, models, model parameters, and modeling assumptions. However, there is a large space of uncertain parameters and there is no general guideline for which parametric uncertainty should be investigated.
3. The simulations should be documented in all details. This should include a description of the mesh, boundary conditions, numerical algorithms, and all models and model parameters.
4. Report about length scales and length scale ratios (integral scales, filter size, Komogorov scales)

Recommendations to experimentalists (most of these are obvious and already considered in most experiments):

1. Boundary conditions need to be specified in as much detail as possible.
2. Experimental uncertainties need to be well characterized and reported.
3. Error bars should be provided
4. Series of experimental data sets including 'easy' cases including cold flow

# Best Practices in LES

Heinz Pitsch  
and many others

## Outline

---

- Define scope: What means 'Best Practices'
- Purpose of this session
- LES specific issues
- Examples
- Summarize questions
- Discussion

# Best Practices Means What?

---

- Simulation
  - Mesh
  - Models
  - Numerical Methods
  - Parametric uncertainty (e.g. boundary conditions)
- Comparison with experiments
  - How should LES data be compared with experiments
    - LES provides lots of data, what should be compared
  - When is a model validated?
  - Documentation
- What do experiments need to provide to be 'good LES validation' experiments
  - What quantities to provide good set of boundary conditions
  - What validation data?
  - What cases?

➔ Much of this is not specific to LES

# Specific to LES

---

- Simulation
  - Mesh
  - (Models)
  - Numerical Methods
  - Parametric uncertainty (e.g. boundary conditions)
- Validation/Comparison with experiments
  - How should LES data be compared with experiments
    - LES provides lots of data, what should be compared
  - When is a model validated?
  - Documentation
- What do experiments need to provide to be 'good LES validation' experiments
  - What quantities to provide good set of boundary conditions
  - What validation data?
  - What cases?

➔ Much of this is not specific to LES

# Best Practices: Purpose

---

- Purpose is to provide concrete guidelines for
  - Simulation practices
  - Comparison with experiments
  - Experimentalists

# Specific to LES: Mesh&Model

---

- Filter size
  - Free parameter in LES, solution should (within limits) be independent of filter size
    - ➔ Dynamic models
  - Typically tied to mesh resolution (implicit filtering)
  - Function of space
- Mesh refinement
  - Good practice for any discretized simulation
  - Mesh refinement changes model for implicit filtering
  - Mesh refinement study in classical sense not possible
  - How can good mesh/filter size distribution be demonstrated?

## Specific to LES: Numerical Methods

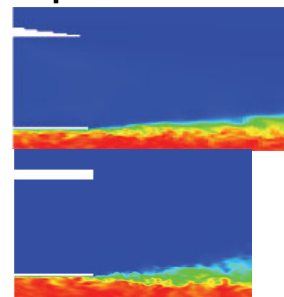
---

- Implicit filtering LES never resolved
  - Always turbulent fluctuations on the scale of the mesh size
  - Simulations always contaminated by large numerical errors on the smallest resolved scales
  - Inherent under-resolution can lead to large dispersion errors
  - Upwind biased schemes or numerical dissipation can kill large-scale turbulence
  - Problem especially for scalars

## Specific to LES: Parametric Uncertainty

---

- Adequate boundary conditions need to be produced
  - Experiments usually provide only moments of velocities, not two-point correlation or unsteady signal
  - Nozzle geometry often slightly complex
    - Perforated plates
    - Contoured nozzles
    - Nozzle wall shape



# Specific to LES: Validation

---

- Modern experiments produce tons of data
  - E.g. instantaneous images
- LES produces multi-point/multi-time (MPMT) statistics
  - What should be compared?
  - How do we use the fact that MPMT data are available
  - How should one compare instantaneous images?
    - MPMT statistics
  - How accurate does two-point correlation or OH temporal spectrum need to be?
- Comparison of filtered ensemble-averaged LES and experimental data
- Documentation
  - Full disclosure: What needs to be reported?

# Specific to LES: Experiment

---

- What is essential for LES in terms of boundary conditions
- What data sets?
  - Cold flow
  - Parameter variations
- What LES specific data are desirable

# Examples

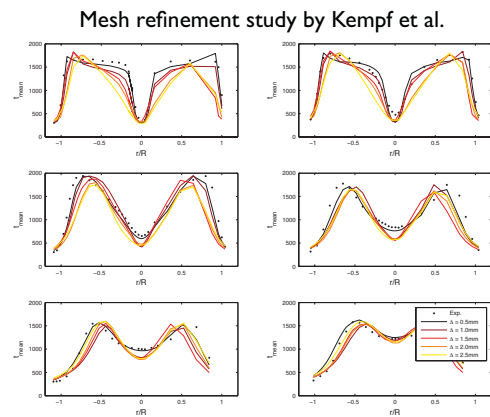
- Simulation
  - Mesh
  - (Models)
  - Numerical Methods
  - Parametric uncertainty (e.g. boundary conditions)
- Validation/Comparison with experiments
  - How should LES data be compared with experiments
    - LES provides lots of data, what should be compared
    - When is a model validated?
  - What do experiments need to provide to be 'good LES validation' experiments
    - What quantities to provide good set of boundary conditions
    - What validation data?
    - What cases?

➔ Much of this is not specific to LES

# Examples: Mesh

## 1. Mesh refinement studies

- What are criteria for good mesh?
  - Compare spectra
  - Comparison with data
  - Changes between grid levels



## 2. Criteria for good filter size distribution

- Ratio of sub-filter to resolved Reynolds stresses
- Ratio of sub-filter to maximum possible scalar variance

# Recursive Filter Refinement

Provided by V. Raman

- **Scalar variance should tend to zero as filter width tends to zero**

→ Normalized scalar variance is used as refinement measure

$$= \frac{Z^2 \leftarrow \text{Instantaneous variance}}{\bar{Z}(1 - \bar{Z}) \leftarrow \text{Maximum variance}}$$

→ Grid should be designed to reduce normalized variance

- **Based on 20% limit for normalized variance**

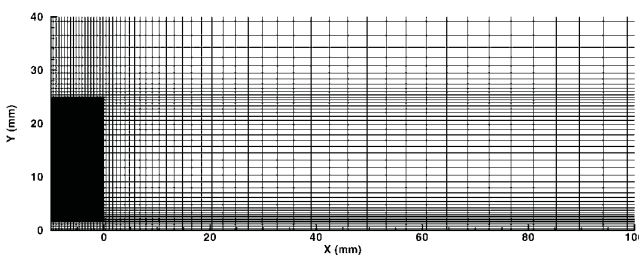
**Filter widths/grid size at current (n) and future level (n+1)**

$$\frac{n+1}{n} = 0.2 \frac{\bar{Z}(1 - \bar{Z})}{Z^2}^{2/3}$$

→ Provides a quantitative estimate of necessary local refinement

# Sydney Bluff-Body Stabilized Flame

Provided by V. Raman



**Grid refined in radial direction to reduce fractional energy**

## Instantaneous Fractional Energy

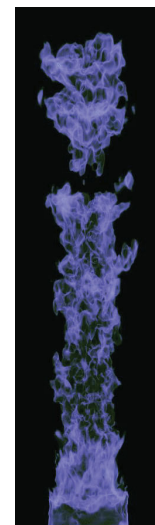
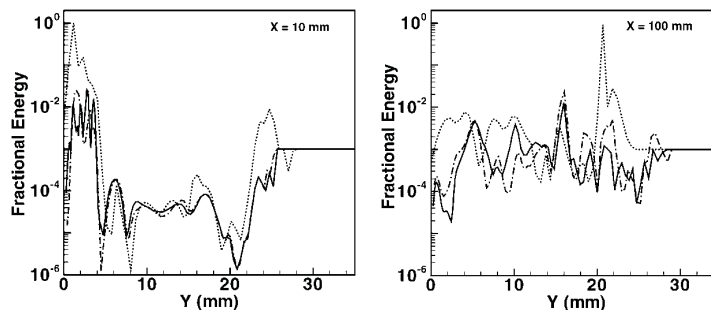
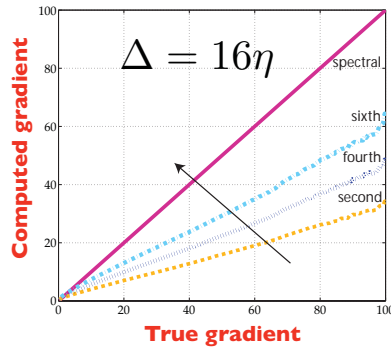


Fig. 1. Radial profiles of the fractional energy resolved at two different axial locations. The dotted line corresponds to the initial grid, the solid line corresponds to the final grid, and the dashed-dotted line represents an intermediate refinement level. The same number of control volumes is used in each case.

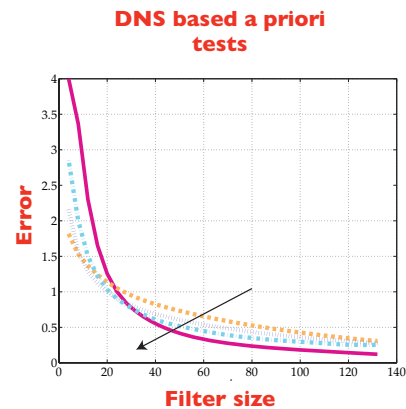
# Examples: Numerical Schemes

- Gradients underpredicted

Provided by V. Raman



- At small filter widths
  - Second order method produces lower error than spectral method



# Example I: Parametric Uncertainty

## LES-Sensitivities

F. Hahn, C. Olbricht, A. Sadiki, J. Janicka



Institute for Energy and  
Powerplant Technology

Technische Universität Darmstadt

## Issues: LES for Applied Systems

- Large number of interacting effects on results

- Resolution
- Boundary conditions
- Models
- ....

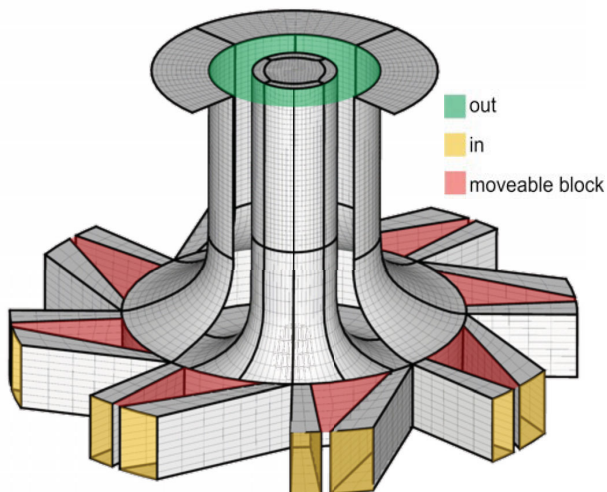
→ Curves through dots means nothing (without demonstrating sensitivities)

- Strategy, show dependence of results on

1. No. of CV's
2. BC's
3. Model assumption
4. Validation by comparisons with flame series

## Grid Dependence Study in Complex Geometries (Configuration)

### Moveable block swirl generator



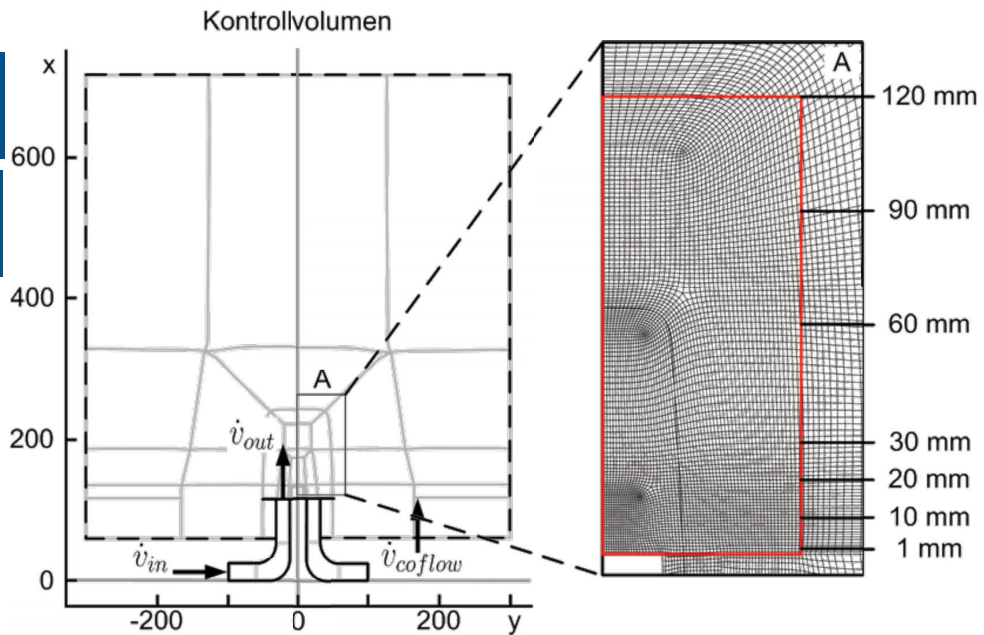
### Operation condition

$P$ [kW]	0
$S_0, th$ [-]	0.75
$\lambda$ [-]	1.2
$\bar{u}_{Austritt}$ [ $m s^{-1}$ ]	4.66
$Re$ [-]	9680
$\dot{Q}_{Gas}$ [ $m^3 h^{-1}$ ]	-
$\dot{Q}_{Luft}$ [ $m^3 h^{-1}$ ]	35.6
$\dot{Q}_{N_2}$ [ $m^3 h^{-1}$ ]	-

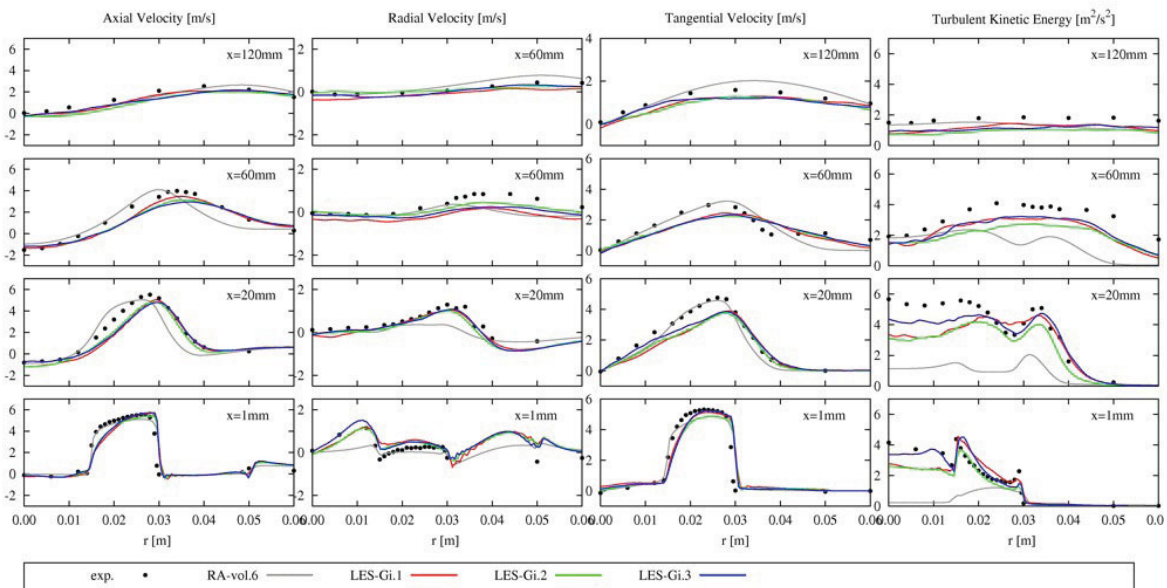
# Grid Dependence Study in Complex Geometries (Grid-Structure)

Basic configuration  
1.76 CV's

Variations  
3.72 CV's  
6.52 CV's

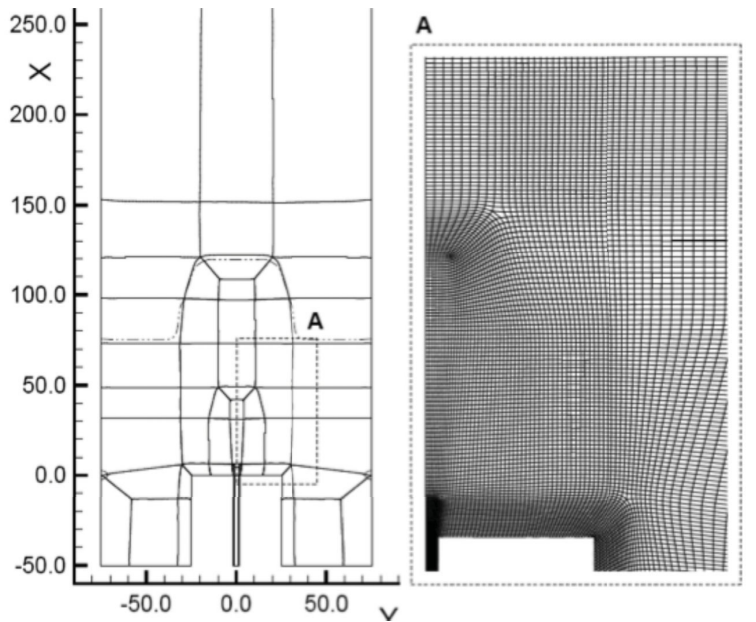


# Grid Dependence Study in Complex Geometries (Results)



Hahn et al., ISTP-19 (2008)

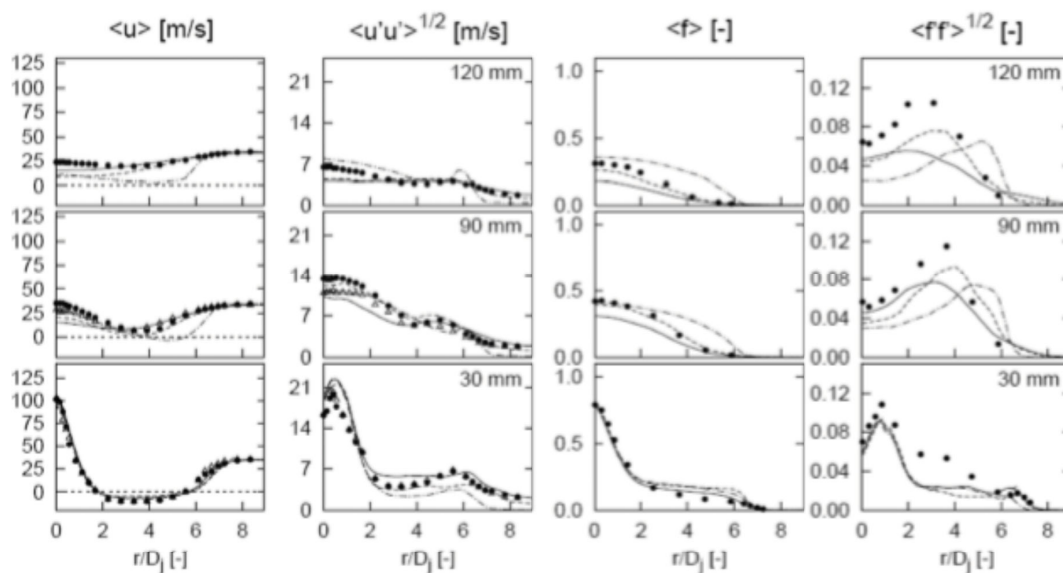
# Sydney Bluff Body Flames Numerical Setup



# Axial and Radial Profiles for Flame HM1E: Sensitivity on Boundary Conditions



$T_{uc} = 5.62\%$  (—),  $T_{uc} = 2.81\%$  (---),  $T_{uc} = 0\%$  (- · -)



## Variation of Models: Flame HM1E

Simulationen:	HM1E	OF1	OF2	MF	PGM1	PGM2	PGM3	NPGM	TPDF
Gitter	MA1	X	-	X	X	X	X	X	-
	MA2	-	X	-	-	-	-	X	-
Turb. Modellierung	Smag.	-	-	-	-	-	-	-	X
	Germ.	X	X	X	X	X	X	X	-
n.-vorg. <i>flamelets</i>	a konst.	X	X	-	-	-	-	-	-
	a var.	-	-	X	-	-	-	X	-
vorg. <i>flamelets</i>	lin. extr.	-	-	-	X	-	-	-	X
	opt. extr.	-	-	-	-	X	X	-	-
Fortschrittsvariable	$Y_{CO_2}$	-	-	-	-	X	X	-	-
	$Y_{H_2+CO_2+H_2O}$	-	-	-	X	-	-	X	X
PDF Modellierung	$\delta$ – PDF	-	-	-	X	-	-	X	-
(Mischungsgrad)	$\beta$ – PDF	X	X	X	-	X	X	-	-
	transp. PDF	-	-	-	-	-	-	-	X
Stat. Unabhängigk.	Gleichung (3.33)	-	-	-	-	-	X	-	-
	Gleichung (3.36)	-	-	-	-	X	-	-	-

## Variation of Models: Flame HM1E

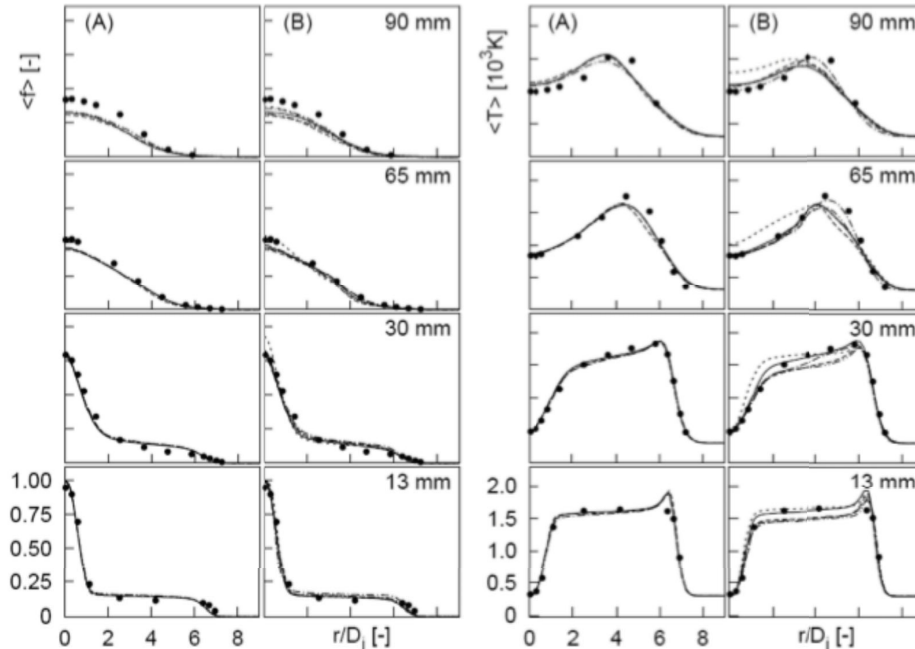
Simulationen:	HM1E
Gitter	MA1
	MA2
Turb. Modellierung	Smag.
	Germ.
n.-vorg. <i>flamelets</i>	a konst.
	a var.
vorg. <i>flamelets</i>	lin. extr.
	opt. extr.
Fortschrittsvariable	$Y_{CO_2}$
	$Y_{H_2+CO_2+H_2O}$
PDF Modellierung	$\delta$ – PDF
(Mischungsgrad)	$\beta$ – PDF
	transp. PDF
Stat. Unabhängigk.	Gleichung (3.33)
	Gleichung (3.36)

### Variation of

- Grids
- SGS models
- Non premixed generated manifolds (NPGM)
- Premixed generated manifolds (PGM)
- Definition of progress variable
- PDF modelling
- Sharp assumption of pdf

# Mean Scaler Profiles of Flame HM1E Model Sensitivity

Spalte A: MF (—), OF-MA2 (---), OF-MA1 (-·-·)  
Spalte B: NPGM (—), PGM2 (---), TPDF (-·-·) Experimente (•, M)



## Investigated Configurations

Flamme	Brennstoff	$f_{st}$ (-)	$u_e$ ( $ms^{-1}$ )	$u_s$ ( $ms^{-1}$ )	$u_j$ ( $ms^{-1}$ )	$Re_s$ (-)	$Re_{jet}$ (-)	$S_g$ (-)	$L_f$ (m)
NRFC	-	-	20.0	-	61.0	-	11900	-	-
HM1E	CNG/H <sub>2</sub> (1:1)	0.050	35.0	-	108.0	-	15800	-	1.00
HM3E	CNG/H <sub>2</sub> (1:1)	0.050	35.0	-	195.0	-	28500	-	1.00
N29S054	-	-	20.0	29.7	66.0	59000	15700	0.54	-
N16S159	-	-	20.0	16.3	66.0	32400	15700	1.59	-
SM1	CNG	0.055	20.0	38.2	32.7	75900	7200	0.50	0.12
SMA2	CNG/Luft (1:2)	0.250	20.0	16.3	66.3	32400	15400	1.59	0.23

## Summary



- Presentation of sensitivities is a crucial for LES quality analysis
- Proof always sensitivities on
  - Numerical resolution
  - BC's
  - Choice of turbulence and combustion modell
- Look at flame series

→ All these aspects may be of importance and bias your conclusion



## Example 2: Parametric Uncertainty

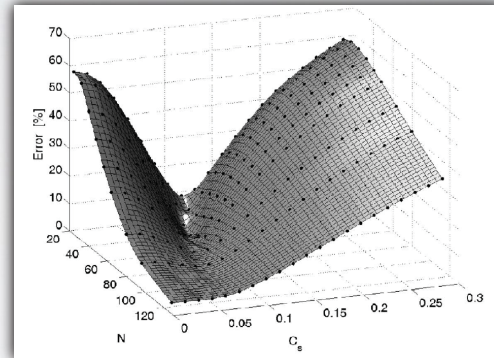
# THE ERROR LANDSCAPE CONCEPT FOR COMBUSTION LES

AM Kempf, J Oefelein, BJ Geurts  
Imperial College London, Sandia Labs, University of Twente

- Rather than performing simple two-point sensitivity analysis, full space of all uncertain parameters, models, mesh sizes, etc could be computed
- Comparison with experiments results in error for each parameter combination, which is the error landscape

# THE ERROR LANDSCAPE

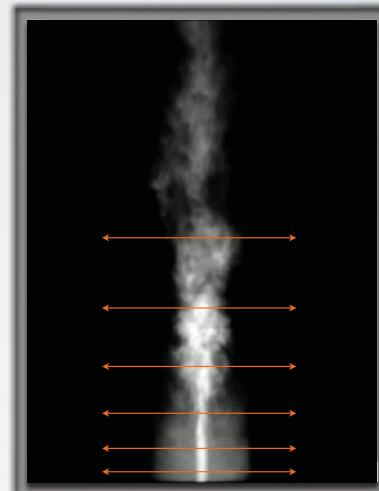
- LES Error as a function of grid resolution and Smagorinsky parameter  $C_s$ .
- Numerical and modelling error may compensate each other.
- An optimum  $C_s$  exists for all filter widths: striking valley structure



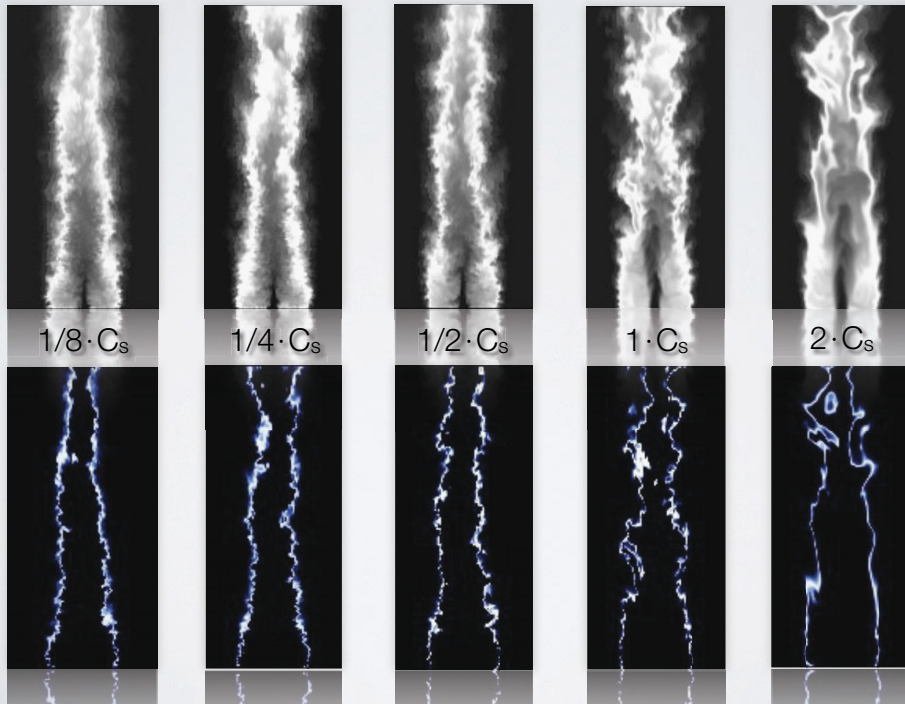
Error Landscape according to Geurts and Meyers. Comparison to the DNS of decaying homogeneous isotropic turbulence 'in a box'.

# EXTENSION TO FLAMES

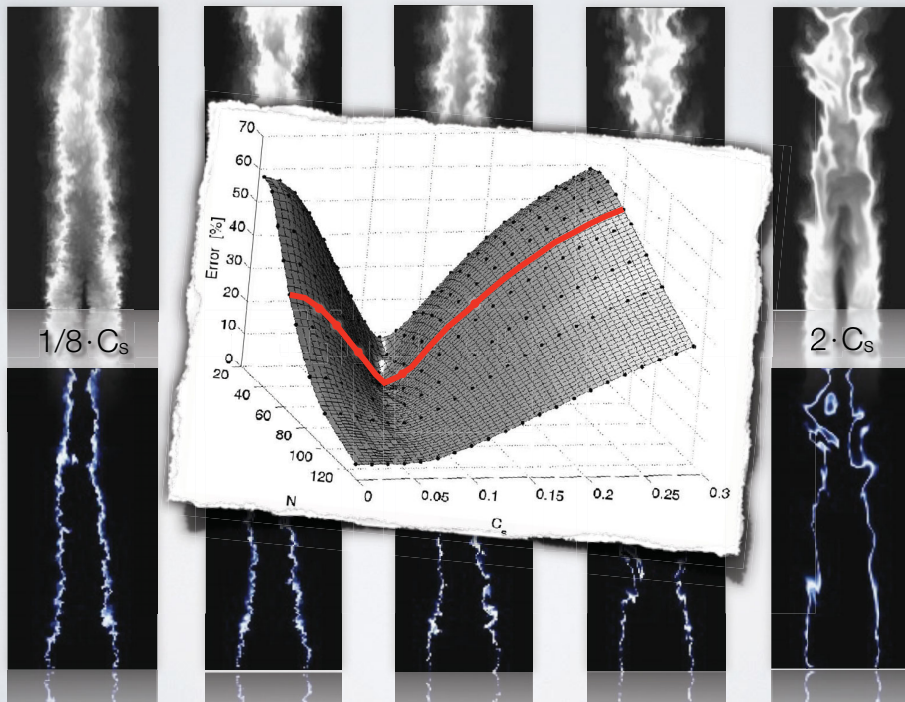
- Can the error landscape be applied to reactive flows with variable density?
- Application to the Sydney Bluff Body Flame.
- Global errors defined in comparison to experimental data (Dally, Masri, Barlow, Kalt) at different radii.



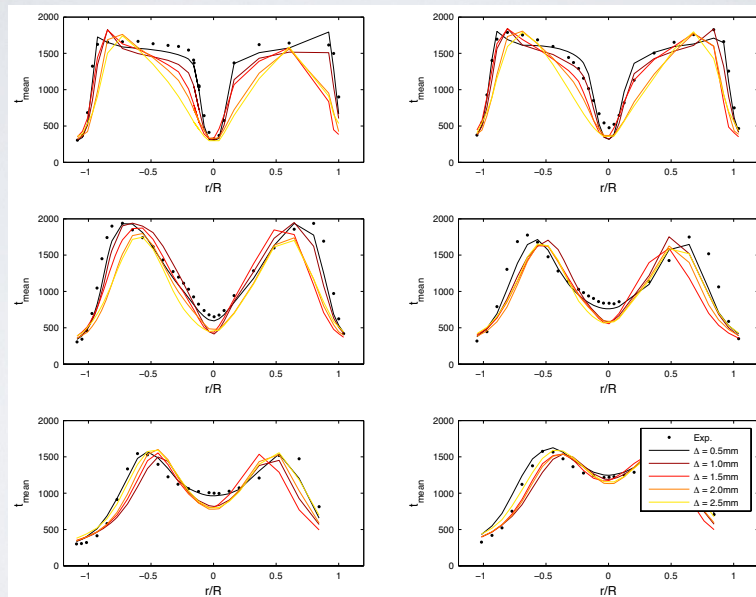
# EFFECT OF $C_S$



# EFFECT OF $C_S$

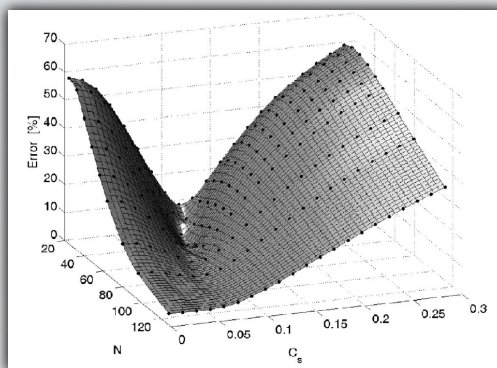


# ERRORS IN PREDICTION

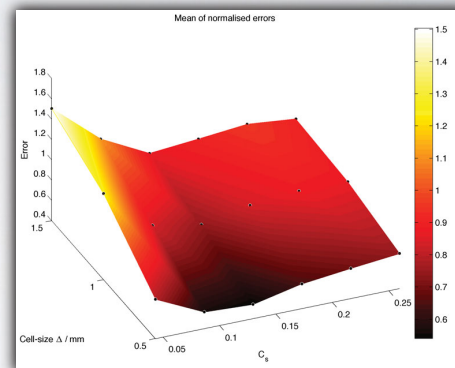


Example: Temperatures for different grids.  
*Simulations and experiments were sampled at identical points.*

# GLOBAL ERROR LANDSCAPE



Error Landscape for decaying isotropic homogeneous turbulences (Geurts, Meyers) against DNS data.



Global Error Landscape for Sydney Bluff Body Flame (Kempf, Geurts, Oefelein) against experimental data (Dally, Masri, Barlow, Kalt).

# SUMMARY

- The error landscape helps understand LES error
- An error minimum exists for optimum value of  $C_s$
- The error minimum is less pronounced for the bluff-body flame than for homogeneous decaying isotropic turbulence
- Calculating an error landscape is cheaper than refining the grid further
- The error landscape cannot be used to estimate LES accuracy in the absence of (experimental) reference data

## Recommendations and Questions

---

- How can good mesh/filter size distribution be demonstrated?
  1. Demonstrate small sub-filter contribution
    - Ratio of sub-filter to resolved Reynolds stresses
    - Ratio of sub-filter to maximum possible scalar variance
  2. Mesh refinement study
    - What are criteria for good mesh/filter size distribution quality?

## Recommendations and Questions

---

- Numerical methods
  - Included in mesh refinement?

## Recommendations and Questions

---

- Parametric uncertainty
  - Full disclosure of all details
  - Sensitivity studies?
    - What is good enough in large space of uncertain parameters?

## Recommendations and Questions

---

- Validation
  - What should be compared (what should we ask for)?
  - How good is good enough?
  - How accurately do higher order statistics need to be?
  - Comparison of filtered ensemble-averaged LES and experimental data?
- Documentation
  - Full disclosure: What needs to be reported?

## Recommendations and Questions

---

- Experiments
  - What is needed to provide an adequate set of boundary conditions?
    - Data in the nozzle
  - What data sets?
    - Cold flow data
    - Parameter variations across regimes going from simple to complex (known to unknown)
  - Error bars

# Issues

---

- Do we need cold flow experiments?
- Mesh refinement and filter size distribution criteria are less meaningful in premixed combustion
- Error bars on experiments
- Boundary conditions: Measure in the nozzle

## Session on Lifted Flames in Hot Coflow

(Rob Gordon and Dirk Roekaerts)

### Summary and highlights

The session on Lifted Flames in Hot Coflow was coordinated by Rob Gordon and Dirk Roekaerts. Other contributors to the session are listed on the first slide of the presentation. The session provided a review of the existing experimental and numerical work that has been conducted on burner configurations of a non- or partially premixed jet in a hot coflow. In most cases, the hot coflow is provided from post-combustion gases of lean flames, and hence are reduced in oxygen level compared to air (vitiating). This design permits the investigation of conditions in the combustion zone similar to those arising by entrainment of recirculated flue gas occurring in industrial combustion devices but with the advantage that the flow pattern is much simpler, and the chemistry of the coflow is decoupled from the combustion products. This allows the focus of the investigations to be on turbulence-chemistry interaction and flame stabilization mechanisms. In the presentation by the coordinators, characteristics of the available experimental databases and past and recent modeling efforts were reviewed, as well as near future research plans. Planned new experiments considerably extending the scope of the past experiments (high Reynolds number, high pressure, other fuels) were also discussed.

The coordinators would like to highlight the following key results:

- The CO-LIF data collected for the Cabra CH<sub>4</sub>/Air case is known to be high compared to the Raman CO data. This has been identified as a systematic error, and division by a factor of 2.11 corrects the data well.
- New experimental databases are available from experiments in the Delft (Oldenhof et al.) and Lund (Duwig et al.) burners.
- A comparison of LES of the Cabra burner CH<sub>4</sub>/air case, closed with either tabulation of auto-ignition (AI) and premixed flamelets (AI-PF-FPI) or unsteady diffusion flamelet based progress variable (FPV) was made, highlighting some differences in predictions of standard deviation of temperature and CO.
- 1-D Linear Eddy Model computation of autoignition has been undertaken to investigate the role of differential diffusion (Sauer et al.).
- DNS data were used to validate some LES modeling assumptions, with a key result that LES prediction with only diffusion flamelets over predicts liftoff height (LH) and only AI under predicts LH (Knudsen and Pitsch, poster).
- Liftoff height sensitivity to time step choices in the transported PDF modeling due to fractional step methods was pointed out (Naud, poster).
- Unsteady tabulated non-premixed flamelets methods are developed for simulating these flames (Ihme, contribution to presentation; Vicquelin et al., poster)

The need for parametric variation in experiments, and for evaluating model development based on ability to match parametric response was re-emphasized. The presently available databases do represent such parameter variation, and this should be followed in modeling efforts.

### Introduction to the burners

Categorisation of flames: The principle parameters that have been used to categorize the jet in hot coflow flames are coflow temperature, Reynolds number of both the fuel and the coflow, and oxygen content. The coflow temperature is recognized as one of the most sensitive parameters for control of flame liftoff. Oxygen content of the coflow at fixed coflow temperature, relative to auto-ignition temperature, should also be considered a key parameter. Figure 1 gives flame type as a function of two controlling variables for methane-air flames. Different experiments from the literature and a recent DNS simulation were compared in the frame of this diagram. In future comparisons, in particular using different fuels, proper normalization with auto-ignition temperature and stoichiometric conditions in each case is recommended.

In the context of the framework proposed at TNF9 (Pope et al.) these are fundamentally adiabatic or non-adiabatic two stream (A2 or N2) flames. However downstream, for some of the burners the quiescent air may be entrained into the coflow and affect flame chemistry, making them N3, and it is possible for the coflow stream to be inhomogeneous in composition, which would introduce a stratification aspect to the flow. Accordingly, models of all categories introduced at TNF9, have been applied, including models applicable to all modes of combustion based on full composition: DNS, PDF and LES/FDF, Eddy dissipation concept (EDC), Linear Eddy Model (LEM), and also models applicable to adiabatic or non-adiabatic two-stream problems.

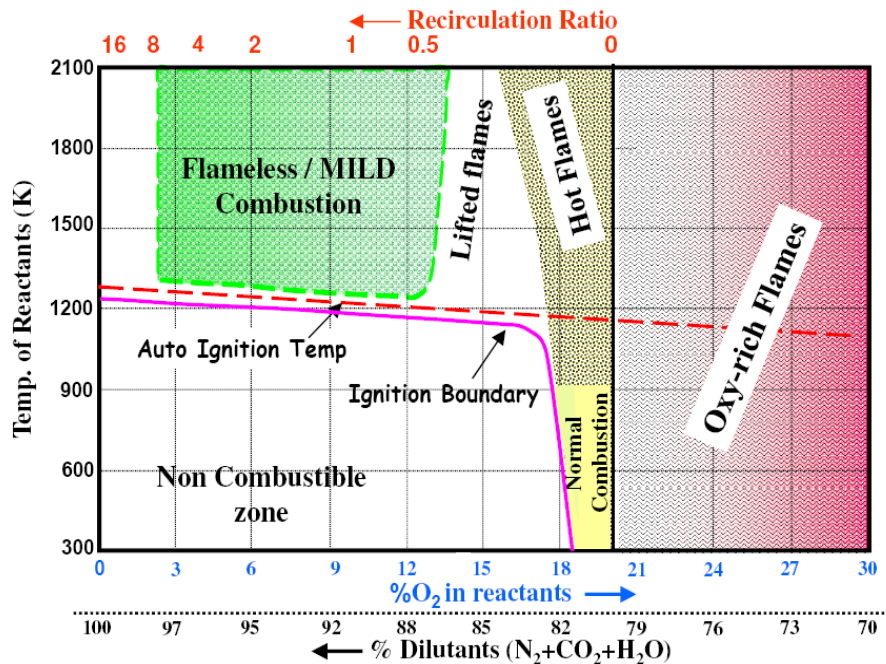


Figure 1: Schematic regime diagram for methane-air JHC flames (Courtesy A. Rao, TU Delft).

**Flame Stabilisation:** The high temperature coflow introduces autoignition as a stabilization mechanism for these lifted flames. Since in general other flame structures are also present, applied models contain a number of ingredients from auto-ignition, premixed flame propagation and diffusion flamelets. These ingredients will appear in the context of a model to describe turbulent mixing (LES, LEM, micromixing model).

### Databases from experiments or DNS

An overview was presented of experiments in five burners, here respectively denoted as Cabra, Adelaide, Delft, Lund, and Cambridge burner. Table 1 gives some key experimental parameters of the geometry and the flows of the five burners, showing the variety in values, with extreme values highlighted. Oxygen concentration in the coflow is very important parameter, and it can be seen that at the low end one has experiments in Adelaide and Lund. Cambridge experiments are with hot air and the experiments on the Cabra burner and the Delft burner are intermediate.

In addition, data from a DNS simulation are included. DNS simulations of lifted flames in slot burner configuration are achieving higher and higher Reynolds numbers. The most recent works include detailed chemistry of Ethylene and Hydrogen at  $Re = 10,000$  and  $Re_t = 300$  at a coflow temperature of 1100 K. This data is available for model development and assessment (J.H. Chen et al).

Table 1 Overview of key parameters for each of the JHC burner types reported on: Reynolds number, coflow mean temperature, jet velocity, coflow velocity, coflow annulus inner diameter, oxygen percentage in coflow.

	Re	Tco (K)	Vjet (m/s)	Vco (m/s)	Dj,co (mm)	%O2
Cabra	11000 – 55000	800 – 1600	50 – 250	1 – 7	4.5 / 200	14 – 16
Adel.	5000 – 20000	1100 – 1300	17 - 31	2.3 – 3.2	4.6 / 82	3 – 12
Delft	3000 – 9500	1400 – 1550	40	2 – 4	4.5 / 80	7.5 – 11
Lund	3000 – 10000	2000	30 – 100	1.4	1.5 / 60	4
Camb.	1500 - 3600	800 - 1200	10 – 120	10 - 35	1.5 – 4.5 / 34	21

### Modelling and Comparison of Models

Lists and tables were compiled of modeling results for the Cabra and the Adelaide burner. For the Adelaide burner the focus was on the experiments with H<sub>2</sub>/CH<sub>4</sub> fuel by Dally et al (PCI, 2002). For the Cabra burner experiments with hydrogen (Cabra et al., 2002) and with methane (Cabra, et al., 2005) were discussed separately.

For the Adelaide burner all published modeling results are RANS-based, with turbulence chemistry interaction treated with EDC, PDF or CMC. (Note: at the Combustion Symposium following the workshop, M. Ihme has reported LES results, using a three-stream steady non-premixed flamelet progress variable model).

After the presentation of the list of published modeling efforts for the Cabra flames, an attempt was made to compare the accuracy of the results. This was done by collecting from the literature the predictions of the specific quantities. The modeling results were grouped in RANS-based and LES-based. Among the RANS based models, PDF methods seem best capable to predict trends in liftoff height with coflow temperature. The LES models found to give best overall agreement involve chemical models based on mixture fraction and a progress variable as independent scalar variables (Z-c-models), in the context of different a priori flame structures. A model based on a combination of auto-ignition events and premixed flamelets (AI-PF-FPI) was compared with a model based on steady or unsteady non-premixed flamelets (FPV). Both models succeed in predicting the axial profile of the standard deviation of temperature, but the former model has a poorer prediction of mean mixture fraction axial profile. The limitations of comparing graphs from published articles were clear. Different authors include plots of different quantities and a systematic comparison is difficult. To come to final conclusions on the performance of the models it would be necessary to systematically compare predictions for a sufficiently large set of variables, from flow field to higher moments and PDF's. It is recommended to include this more systematic comparison in the program of TNF11, for a set of cases to be decided.

The type of flame structures present in the flame stabilization zone can be assessed using the flame index, applied to the resolved field in LES. These LES results with the FPV are in qualitative agreement with the DNS results (which are for a different fuel and burner). Diffusion flame structures are found to be more probable than premixed flame structures.

A first modeling result of the Delft burner, using EDC, shows that this model, for default settings of the parameters, predicts too early ignition (De et al., poster).

## **New Developments and plans**

### LES-DNS comparison

A new development is the comparison of LES predictions with a corresponding DNS. It was found that LES prediction with only diffusion flamelets over predicts lift-off height, while using only auto-ignition under predicts it (Knudsen and Pitsch, poster).

### Higher Carbon Number Fuels

Ethane and propane have been compared to CNG/methane at the University of Sydney under conditions of varying dilution (with N<sub>2</sub>) and varying premixing (with air), with an initial finding that the trends on liftoff height are opposite between propane and methane. (Masri, verbal report)

### Achieving higher Reynolds numbers

TU Darmstadt have plans to develop a high Reynolds number autoignition burner, potentially able to access in the order of  $Re = 100,000$

### Higher Pressure and New Target Fuels

A high pressure vitiated coflow burner is being developed at Lund, and Berkeley are developing the capability to achieve 2-3 bar for DME and ethanol tests

## **Conclusions, Issues and Way Forward**

The following topics have to be investigated in more detail:

- The relation between oxygen content of the coflow and its preheat temperature and the resulting flame structure (transitional vs. lifted flame).
- The transition between auto-ignition stabilized flame and lifted diffusion flame.
- The role of the local flow structure in the auto-ignition process.

The following issues should be addressed in order to reach clear conclusions:

- The low Reynolds number ( $Re < 10000$ ) flows are susceptible to influences of molecular transport through differential diffusion.
- The characterization of the coflow composition in many experiments is still not sufficiently complete. Also radical concentrations may be important. Trace OH and H<sub>2</sub> concentrations can influence the auto-ignition process.

The following recommendations for future work are made:

- Model assumptions can be tested not only by comparison with experiments but also by comparing with DNS databases.
- Trends in liftoff height with parameter variation should be studied both experimentally and in modeling.
- A more systematic model comparison is to be made for the existing experimental cases (flow field, mixing field, species fields, statistics, etc). This could be a part of the program for the next TNF workshop.
- Physical characteristics which so far have received little attention, such as the liftoff height PDF can be important for model validation.
- Studies should be continued or initiated on other fuels (low calorific, DME), high pressure auto-ignition burner design, high Reynolds number burner design, and on DNS of more complex flows and flames.

## **Questions and remarks by the audience**

In the specification of coflow boundary conditions, it is not just traces of OH that are extremely important, but also traces of molecular hydrogen.

Effects on coflow radial temperature profile (e.g. in Delft burner) of a cooling channel between fuel

and coflow channels has also observed in laminar burners (See presentation by Peter Lindstedt)

PDF methods have been shown to predict trends in liftoff height well. So what is the next challenge? It was discussed whether the inclusion of the 'third stream' (entrained air) was a problem. In principle there is no problem, but the calculation has not been made yet. The prediction of the full temperature PDF as measured by Raman-Rayleigh or CARS is an interesting challenge.

## TNF10: session on Lifted flames in hot coflow

Coordinators: Rob Gordon and Dirk Roekaerts

Including contributions by  
B. Dally, P. Medwell, A. Rao,  
J.Y. Chen et al, J.H. Chen et al,  
M. Ihme, B.Naud, E. Oldenhof et al.,  
C. Duwig

### Lifted Jet in Hot Coflow: Outline

#### 0. Introduction to the Burners

##### **Categorisation of flames** ←

Flame Stabilisation

Models

#### 1. Experiments and Databases

*Cabra, Adelaide, Delft, Lund, Cambridge*

DNS

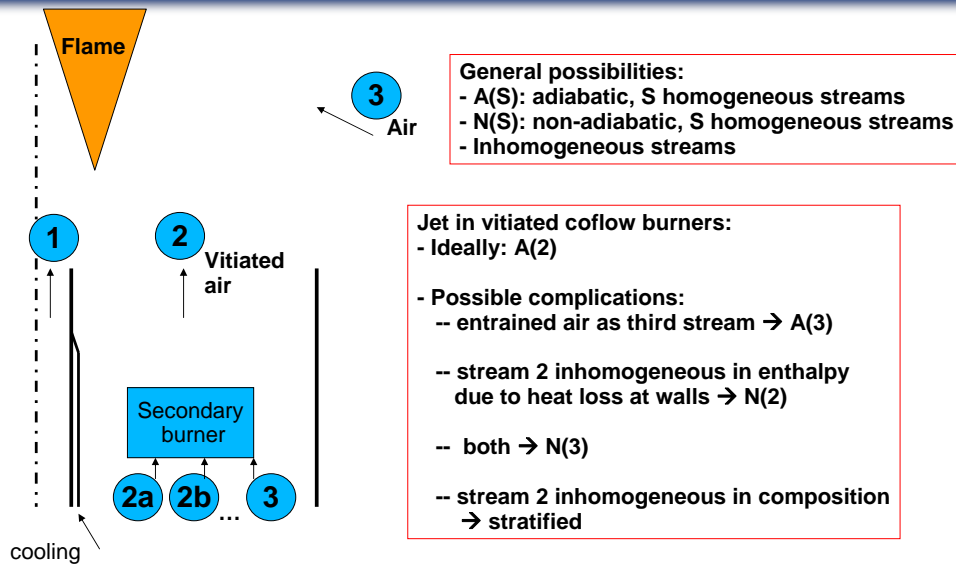
#### 2. Modelling and Comparison of Models

#### 3. New Developments

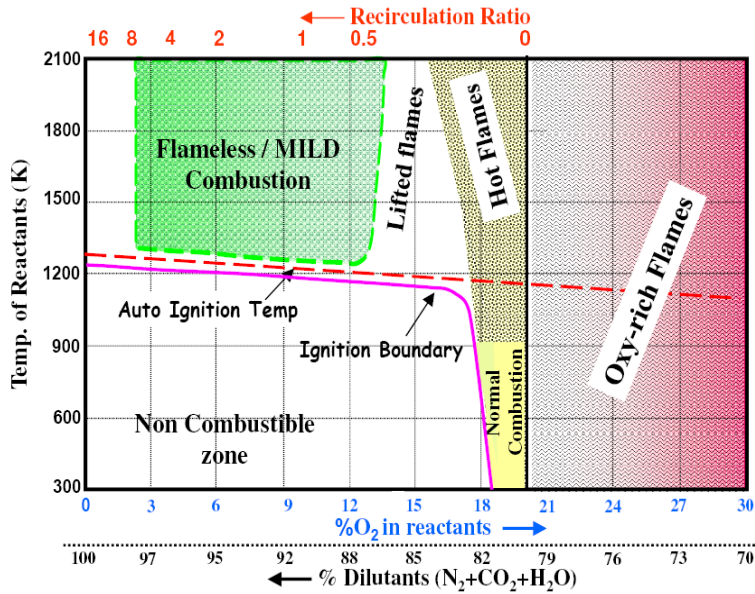
#### 4. Conclusions, Issues and Way Forward

## Categorization of (lifted) flames in hot (vitiated) coflow

### Categorization (following Pope et al. TNF9)



# Role of preheat and dilution

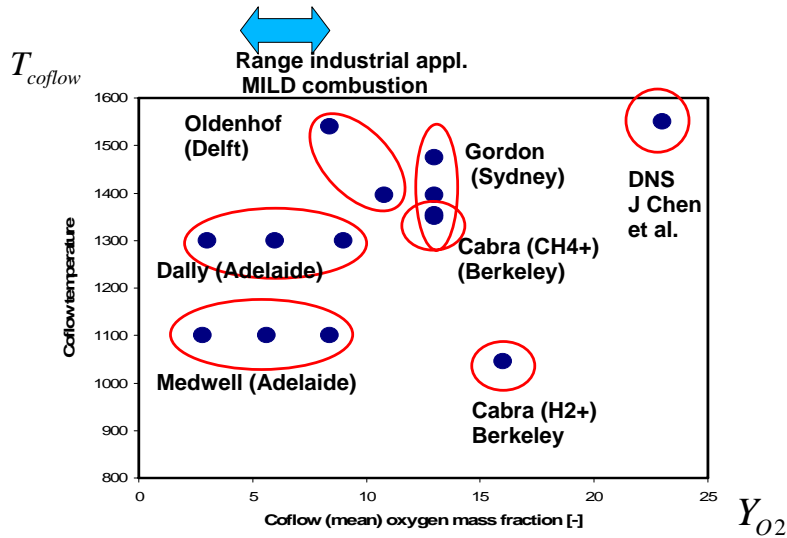


Regime diagram

Case: Methane/air

A. Rao, TU Delft

# Preheat and dilution in experiments and DNS



## Lifted Jet in Hot Coflow: Outline



### 0. Introduction to the Burners

Categorisation of flames

**Flame Stabilisation** ←

Models

### 1. Experiments and Databases

*Cabra, Adelaide, Delft, Lund, Cambridge*

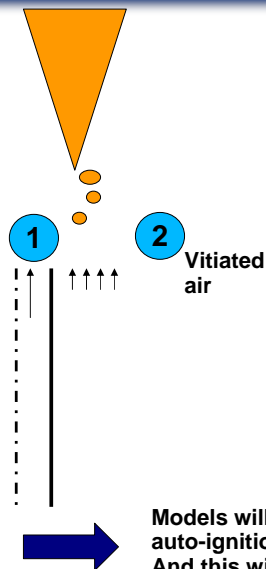
DNS

### 2. Modelling and Comparison of Models

### 3. New Developments

### 4. Conclusions, Issues and Way Forward

## Flame stabilization mechanisms



**Z:** mixture fraction based on jet and coflow

Autoignition delay time of a mixture depends on value of  $Z$ , with minimum at very lean side (most reactive mixture fraction)

Premixed flame propagation with flame speed depending on local mixture fraction (maximal near stoichiometric)

Premixed or edge flame propagation from ignition kernels (growth of kernels)

Unsteady development of diffusion flamelets from ignition kernels, influenced by dynamics of scalar dissipation rate

Models will contain a number of ingredients from:  
auto-ignition, premixed flame propagation and diffusion flamelets.  
And this will appear in the context of a model to describe turbulent mixing



### 0. Introduction to the Burners

Categorisation of flames

Flame Stabilisation

**Models** ←

### 1. Experiments and Databases

*Cabra, Adelaide, Delft, Lund, Cambridge*

DNS

### 2. Modelling and Comparison of Models

### 3. New Developments

### 4. Conclusions, Issues and Way Forward

## Models



### Applicability of models: (from Pope et al. TNF9)

Models applicable to all modes of combustion  
based on full composition

- DNS
- PDF and LES/FDF
- RANS with neglect of fluctuations
- Thickened flame front
- Eddy break-up models
- Eddy dissipation concept (EDC)
- LEM, ODT, other

Models applicable to  
adiabatic two-supply flames (A2)

- $Z, c$  (or  $Z, Y_F$ , or ...)
- $Z, G$

Models applicable to  
non-adiabatic two-supply flames (N2)

- $Z, c, h$
- $Z, G, h$

**Applications to lifted flames  
of almost all these models  
are reviewed or reported today.**

**Did they reveal the relevant  
phenomena ?**

**Did they show to be accurate ?**

## Lifted Jet in Hot Coflow: Outline



### 0. Introduction to the Burners

- Categorisation of flames
- Flame Stabilisation
- Models

### 1. Experiments and Databases

**Cabra, Adelaide, Delft, Lund, Cambridge** ←

DNS

### 2. Modelling and Comparison of Models

### 3. New Developments

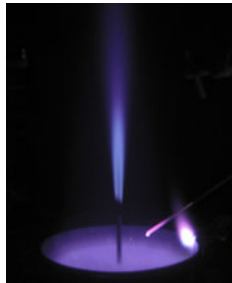
### 4. Conclusions, Issues and Way Forward

## Quick Overview of Burners

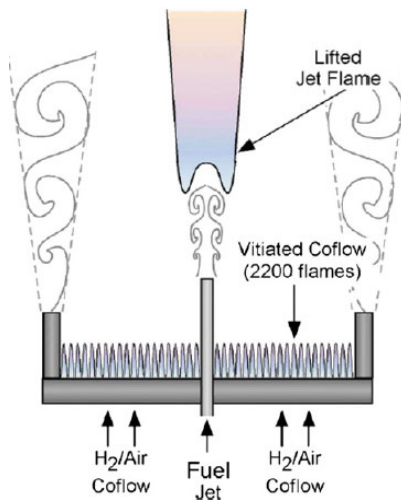


	Re	Tco (K)	Vjet (m/s)	Vco (m/s)	Dj,co (mm)	%O2
Cabra	11000 – <b>55000</b>	800 – 1600	50 – 250	1 – 7	4.5 / 200	14 – 16
Adel.	5000 – 20000	1100 – 1300	17 - 31	2.3 – 3.2	4.6 / 82	<b>3 – 12</b>
Delft	3000 – 9500	<b>1400 – 1550</b>	40	2 – 4	4.5 / 80	7.5 – 11
Lund	3000 – 10000	<b>2000</b>	30 – 100	1.4	1.5 / 60	4
Camb.	1500 - 3600	800 - 1200	10 – 120	<b>10 - 35</b>	1.5 – 4.5 / 34	<b>21</b>

## Berkeley/Sydney JHC burner Experimental results



## Berkeley/Sydney JHC

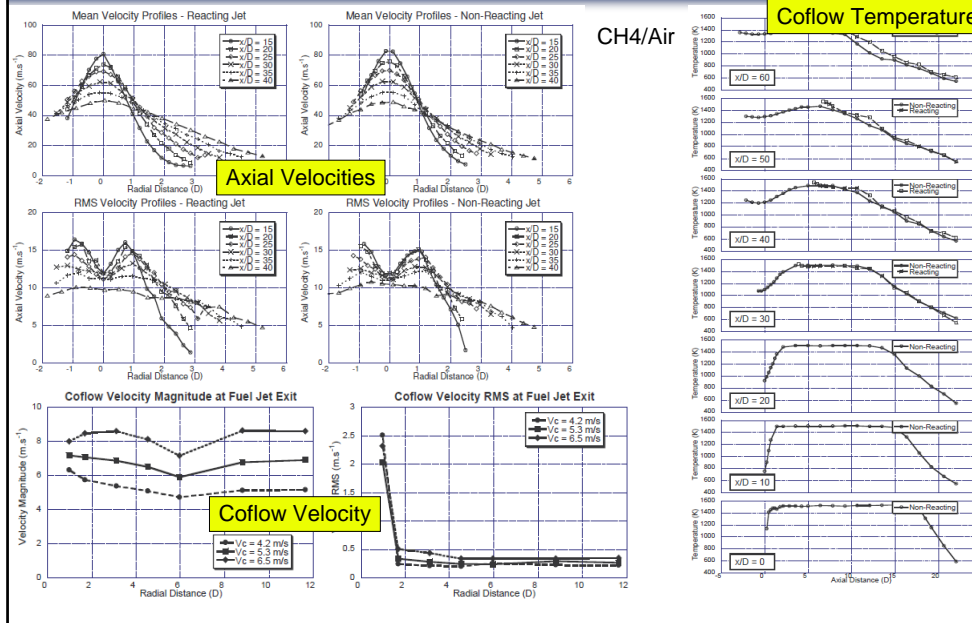


	Central jet		Co-flow
$T_{jet}$ (K)	305	$T_{coflow}$ (K)	1045
$V_{jet}$ (m/s)	107	$V_{coflow}$ (m/s)	3.5
$Re_{jet}$	23,600	$Re_{coflow}$	2,500
$f_{stoich}$	0.47	$\Phi$	0.25
$X_{H2}$	0.25	$X_{O2}$	0.1474
$X_{N2}$	0.75	$X_{H2O}$	0.0989
		$X_{N2}$	0.7534

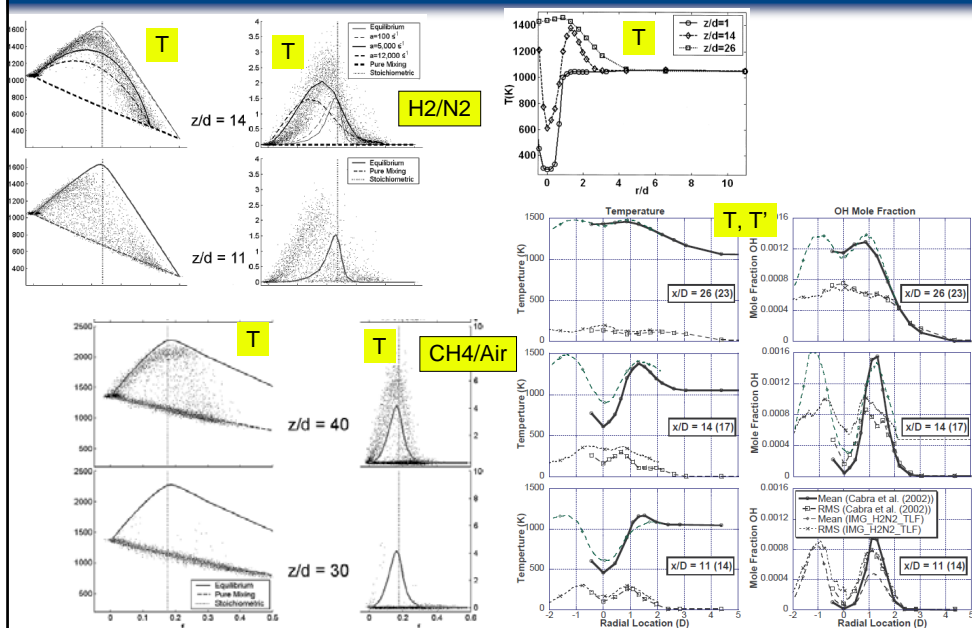


University of Sydney Vitiated  
Coflow Burner

# Flow Characterisation



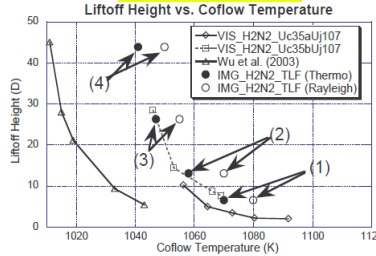
# Radial Profiles, Scatter



# Parametric Variations – H2/N2

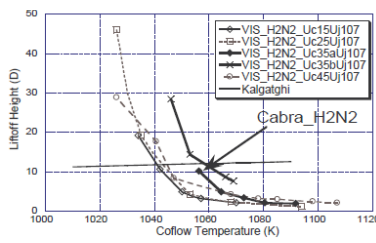
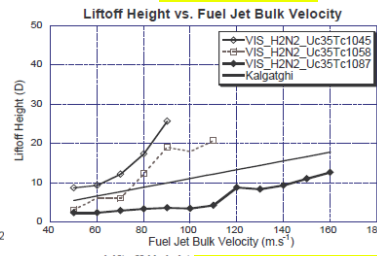


## Liftoff vs Tcoflow

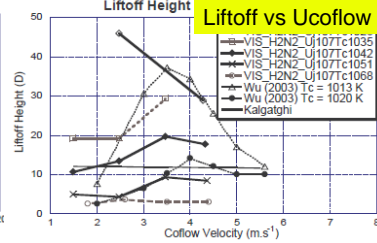


## H2/N2

## Liftoff vs Ufuel



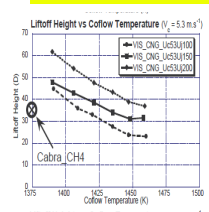
## Liftoff vs Ucoflow



# Parametric Variations – CH4/Air

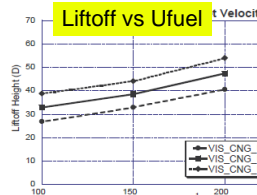


## Liftoff vs Tcoflow

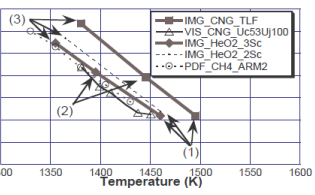
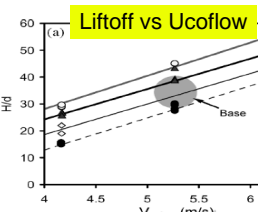


## CH4/Air

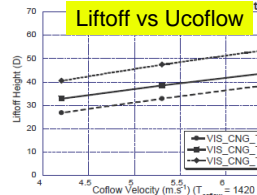
## Liftoff vs Ufuel



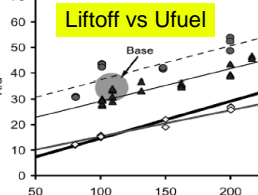
## Liftoff vs Ucoflow



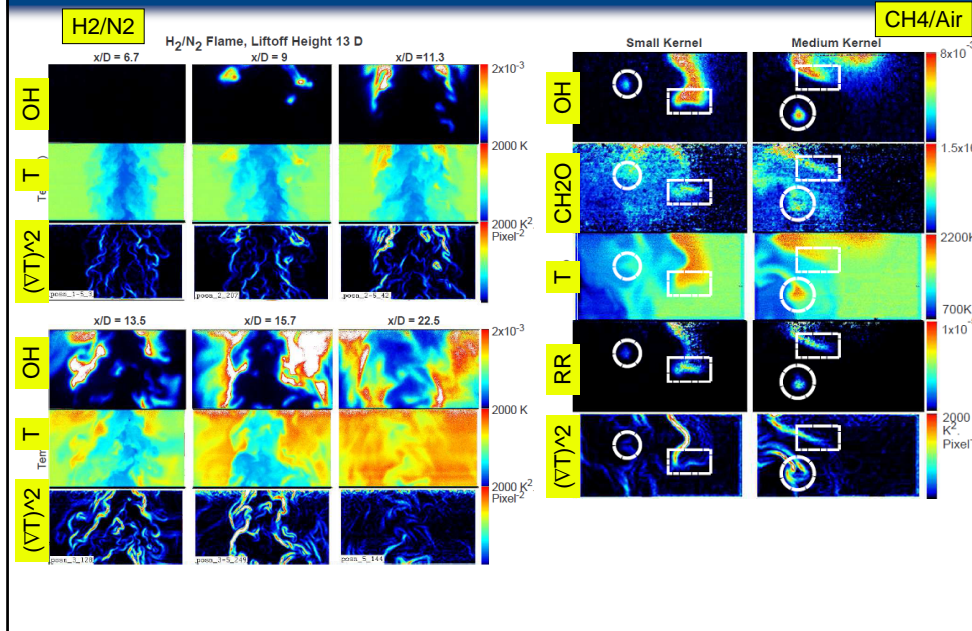
## Liftoff vs Ucoflow



## Liftoff vs Ufuel



# Planar T, $\nabla T$ , OH, semi-quant CH<sub>2</sub>O, RR indicator

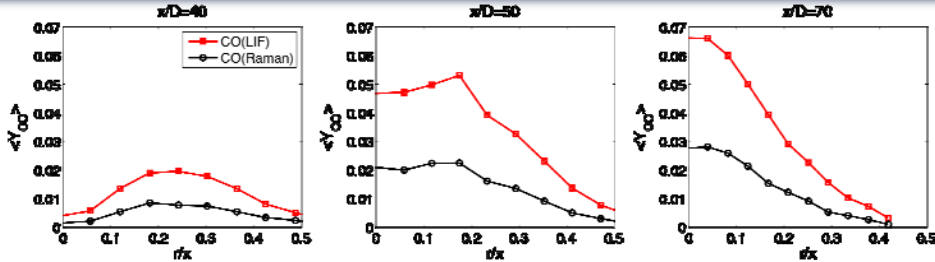


## Summary



- High Reynolds number jets (20,000+)
- Simple Geometry
- Database of species and temperature for CH<sub>4</sub> and H<sub>2</sub>
- Distinct Parametric Trends
- Joint T-OH-CH<sub>2</sub>O imaging (with  $\nabla T$ , and RR proxy)
- Under-investigated Coflow: properties, effects, composition

## CO-Measurements in Lifted Methane/Air flame



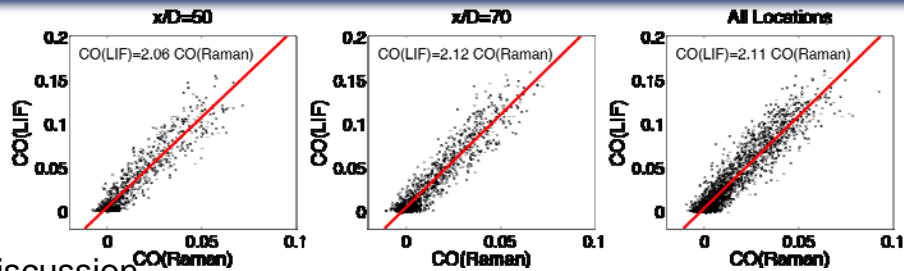
Cabra performed CO-measurements using Raman scattering and LIF

LIF-measurements typically 10% lower than Raman data

TNF recommendation is to use CO(LIF)-data for model comparison

However, analysis of measurements shows that reported CO(LIF) measurements are larger by a factor of two compared to CO(Raman)

## CO-Measurements in Lifted Methane/Air flame



### Discussion

Similar shape for both measurements

Mixture fraction is defined using CO(Raman)-data

→ Suggests no error in LIF-experiments; most-likely only systematic error in data-analysis

### Regression analysis

$$C_{\text{reg}} = \frac{Y_{\text{CO(LIF)}}}{Y_{\text{CO(Raman)}}} = 2.11$$

Linear regression with coefficient:

## CO-Measurements in Lifted Methane/Air flame



Correction of CO(LIF)-measurements (suggested by Barlow)

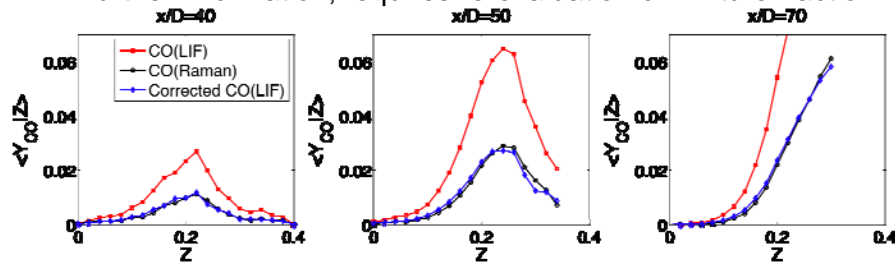
Rescale CO(LIF) by regression coefficient:  $Y_{\overline{\text{CO}}(\text{LIF})} = \frac{C_{\text{exp}}}{C_{\text{reg}}} Y_{\text{CO}(\text{LIF})}$

Re-evaluate mixture fraction and overall mass-fraction balance

### Recommendations

Use CO(Raman)-measurement for model comparisons; reported mixture fraction is consistent with CO(Raman)-data

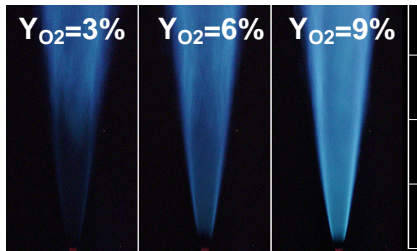
Corrected CO(LIF)-results are of similar quality; can be used as further information; requires re-evaluation of mixture fraction



## Adelaide JHC burner Experimental results

P.R. Medwell, P.A.M. Kalt and B.B. Dally

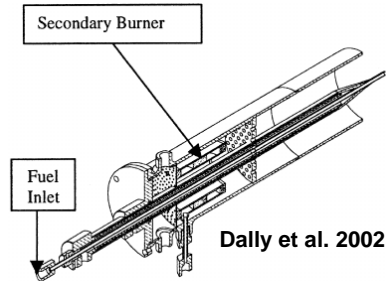
$\text{CH}_4/\text{H}_2$



# Jet in Hot Coflow research at University of Adelaide (experiments)



## JHC burner design



Dally et al. 2002

University of Adelaide

Jet in Hot Coflow (JHC) burner conditions:

Coflow O<sub>2</sub> level: 3%, 6%, 9%, 12%

Coflow temperature: 1100K and 1300K

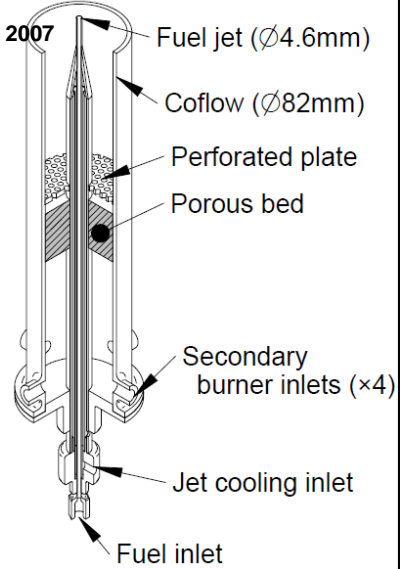
Coflow velocity: 2.3 m/s and 3.2 m/s

Jet Reynolds number; 5000 to 20,000

Jet fuels: natural gas/methane, ethylene, LPG

Fuel diluents: H<sub>2</sub>, N<sub>2</sub>, air

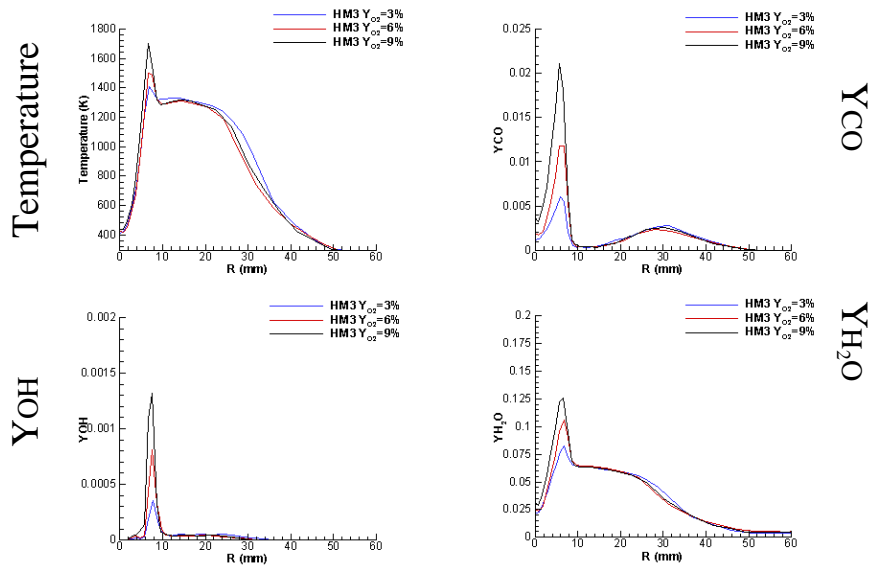
Medwell et al. 2007



## Dally et al: c.2002 – Single-point data



### Turbulent Flame Z = 30 mm



## Dally *et al*: c.2002 – Single-point data

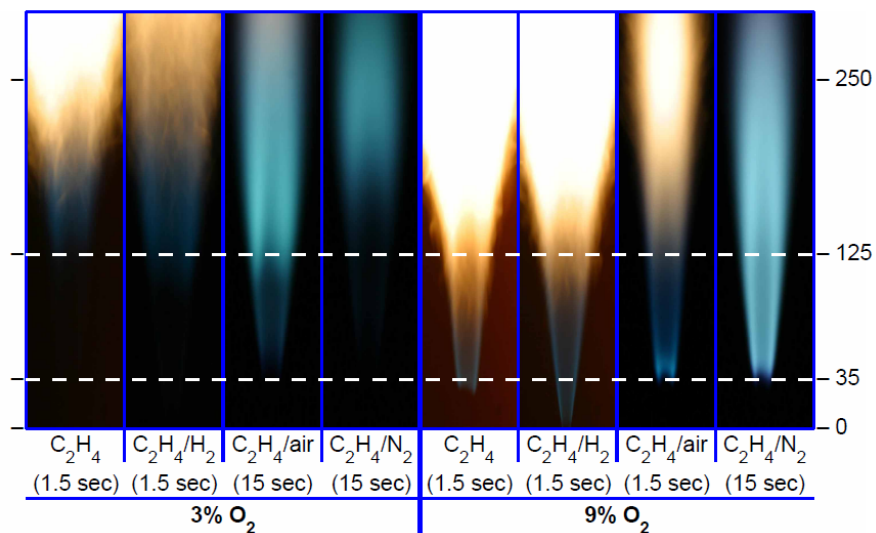


Major changes in the flame structure occur at reduced  $O_2$  coflow;  
at higher jet Reynolds number, oxygen leakage from the surroundings is related to local extinction of the flame

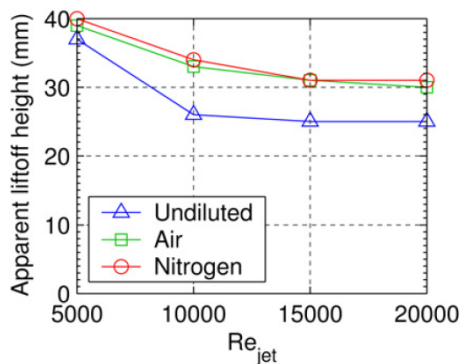
B.B Dally, A.N. Karpets and R.S. Barlow,  
*Proceedings of the Combustion Institute* **29** (2002) 1147-1154.

B.B. Dally, A.N. Karpets and R.S. Barlow, 2002. *Australian Symposium on Combustion and The Seventh Australian Flame Days*, January 2002, Adelaide, Australia

## Medwell *et al*: c.2008 – Fuels and Blends



## Medwell *et al*: c.2008 – Liftoff Height Sensitivity



Increasing the jet velocity (Reynolds number) *appears* to decrease the liftoff height

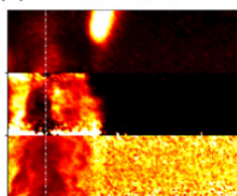
Observation recently also made in JHC exp. Delft

Oldenhof *et al* (2010) Comb. Flame 157 (6), pp. 1167-1178.

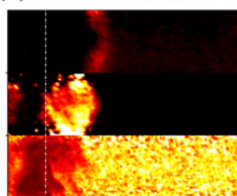
## Medwell *et al*: c.2008 – Transitional flames



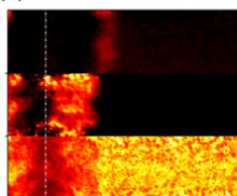
(a) 9% O<sub>2</sub> – C<sub>2</sub>H<sub>4</sub>



(b) 9% O<sub>2</sub> – C<sub>2</sub>H<sub>4</sub>/Air

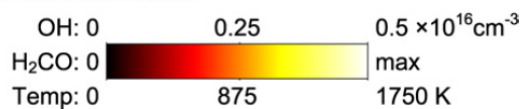


(c) 9% O<sub>2</sub> – C<sub>2</sub>H<sub>4</sub>/N<sub>2</sub>



Beneath the “liftoff height” a clear layer of OH is present  
At the “liftoff height” there is a *transition* from low to high OH

These flames are *transitional* rather than lifted



## Summary



Single-point data has been used for CFD models

- Models show reasonably good agreement

- Third stream poses a challenge

- Capturing low temperature kinetics is important

- Further modelling is continuing

Imaging results collected in “lifted flames”

- A fundamental change in reaction structure occurs under the hot and diluted O<sub>2</sub> (MILD) conditions

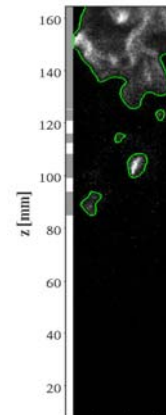
- Precursory reactions occur upstream of the “liftoff” height

  - Flames in the hot and diluted coflow are not genuinely lifted

  - Rather than ‘lifted flames’, these should be termed ‘transitional flames’

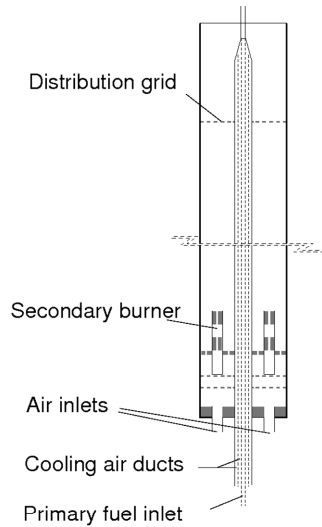


Delft JHC burner  
Experimental results



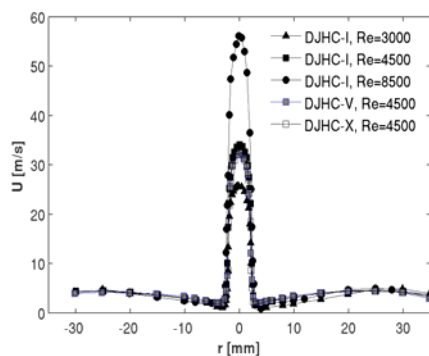
E.Oldenhof, M.J. Tummers, E.H. van Veen and D. Roekaerts  
Department of Multi-Scale Physics  
Delft University of Technology

## DJHC burner – design features



- Based on the Adelaide JHC burner (Dally et al, 2002)
- Secondary burner : ring burner (rich mixture, air)
- Heat loss of coflow by radiation from burner tube
- Seeding added for LDA/PIV measurements

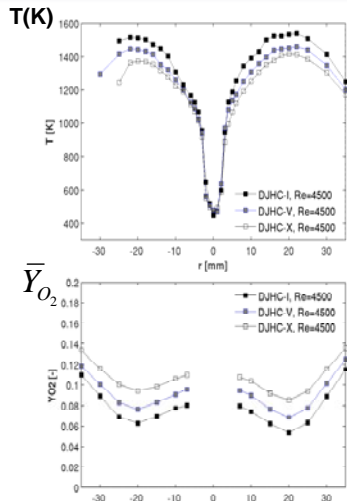
## Jet characteristics



LDA mean axial velocity at  $z=3$  mm  
( $z=0$  at nozzle exit)

- Developed pipe flow (Fuel pipe with  $L/D \sim 150$ )
- Fuel pipe is air-cooled ( $T_{\text{fuel}} \sim 450$  K)
- Studied Re-numbers of jet: 3,000 to 9,500
- So far, operated with *Dutch natural gas* (or similar synthetic mixtures)

# Coflow characteristics

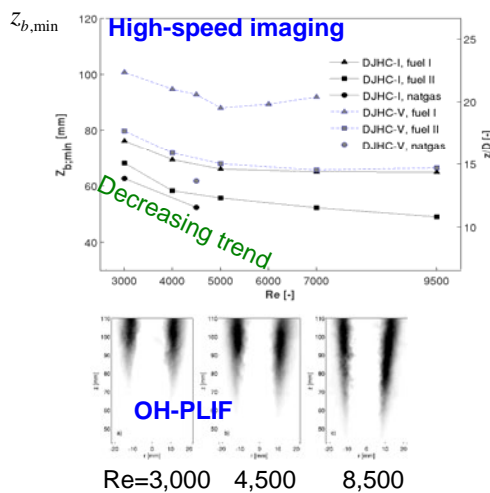


- So far, secondary burner has been operated with *Dutch natural gas*
- Coflow temperature and oxygen at  $z=3$  mm radially inhomogeneous

	$T_{co,max}$ [K]	$Y_{O_2}$ [%]
DJHC-I	1540	7.6
DJHC-V	1460	8.8
DJHC-X	1395	10.9

Temperatures (top) and oxygen mass fractions (bottom),  $z=3$  mm

# Trends with jet Re

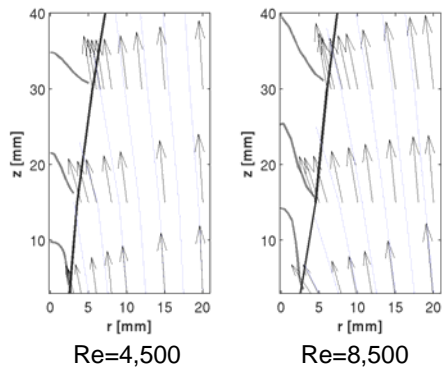


- Ignition kernels appear at lower locations when increasing jet Reynolds number (jet velocity)
- As a result, the lift-off height *decreases* with *increasing* jet velocity
- This is due to the positive radial temperature gradient of the coflow

## Role of entrainment



### Lift-off trends



Streamlines from LDA measurements

- Decrease of lift-off height with jet Reynolds number is due to the positive radial temperature gradient of the coflow:

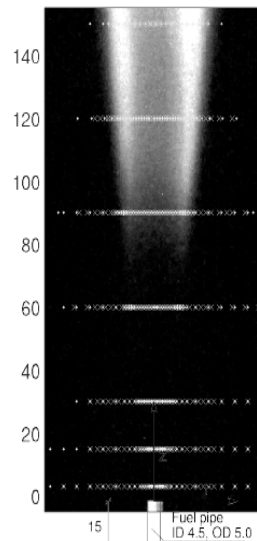
*Hottest part of coflow is entrained faster at faster jet velocities*

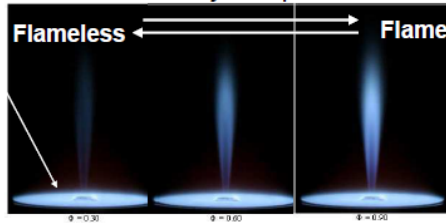
## Experimental Database



- Two-component **velocity** statistics (means and turbulent stresses)
- **Temperature** statistics (means, rms values, pdf's) from **CARS**
- Qualitative **OH-PLIF** fields
- **PIV** fields (in progress)

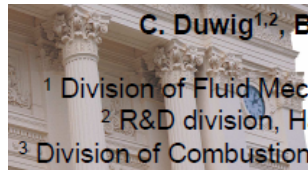
Traverses at:  
z=3, 15, 30, 60, 90, 120, 150 mm  
and r=0 (centerline)





## Lund JHC burner Experimental results

(see poster)



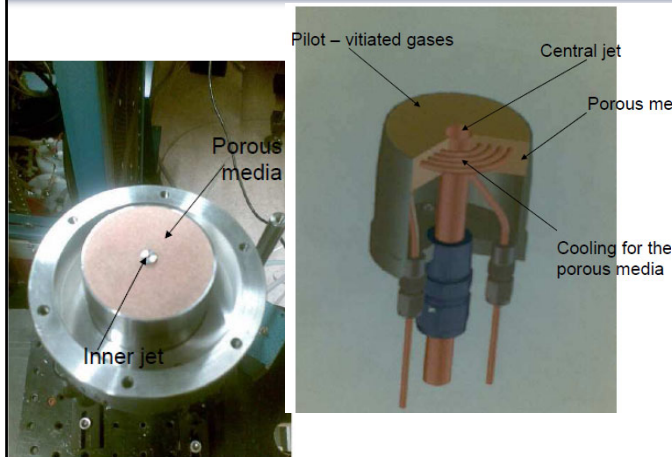
C. Duwig<sup>1,2</sup>, B. Li<sup>3</sup>, Z.S. Li<sup>3</sup>, M. Aldén<sup>3</sup>

<sup>1</sup> Division of Fluid Mechanics, Lund University, Sweden

<sup>2</sup> R&D division, Haldor Topsøe A/S, Denmark

<sup>3</sup> Division of Combustion Physics, Lund University, Sweden

## Lund Burner Design



### •Operating conditions

#### •Jet:

- $U_{JET} = 30 - 100 \text{ m/s}$
- $\Phi = 0.3 - 8.0$
- Methane/air mixture
- Mixing time scale down-to  $\tau \sim 15 \text{ ms}$
- $Re \sim 3000 - 10000$
- $Re - Ka \sim 10^4$

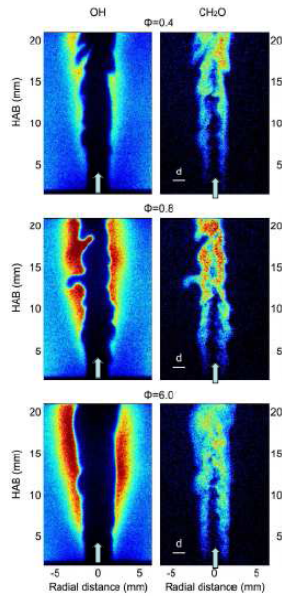
#### •Coflow:

- Flue gas from pilot laminar disk-flame
- Methane/air mixture  $\Phi \sim 0.8$
- $T \sim 2000 \text{ K} - X_{O_2} \sim 4\%$

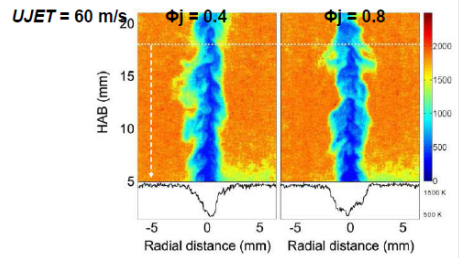
### Dimensions:

- Porous media diameter 60 mm
- Inner Jet 1.5mm

# Experimental Results

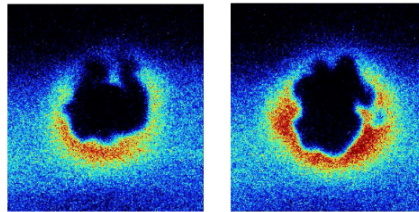


2-D Rayleigh thermometry using the second harmonic radiation (532 nm, 400 mJ)



Spatial resolution  $50 \mu\text{m} \times 50 \mu\text{m} \times 100 \mu\text{m}$

OH-PLIF in cross-section



Cambridge JHC burner  
Experimental results



# Experimental Setup

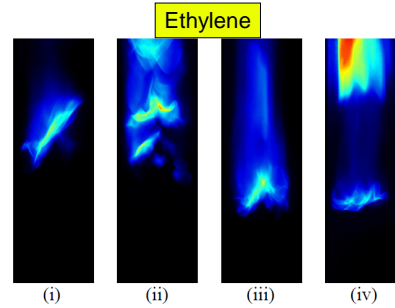
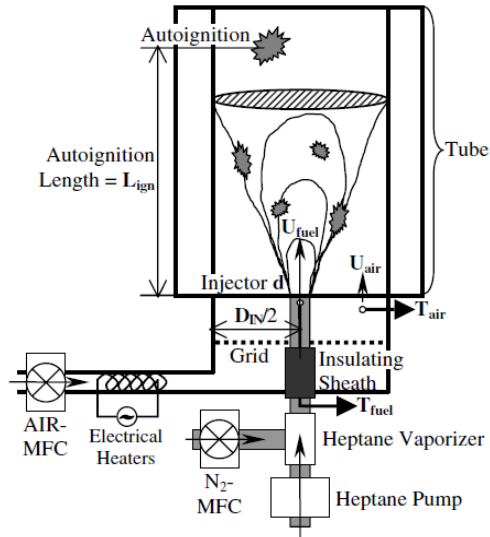
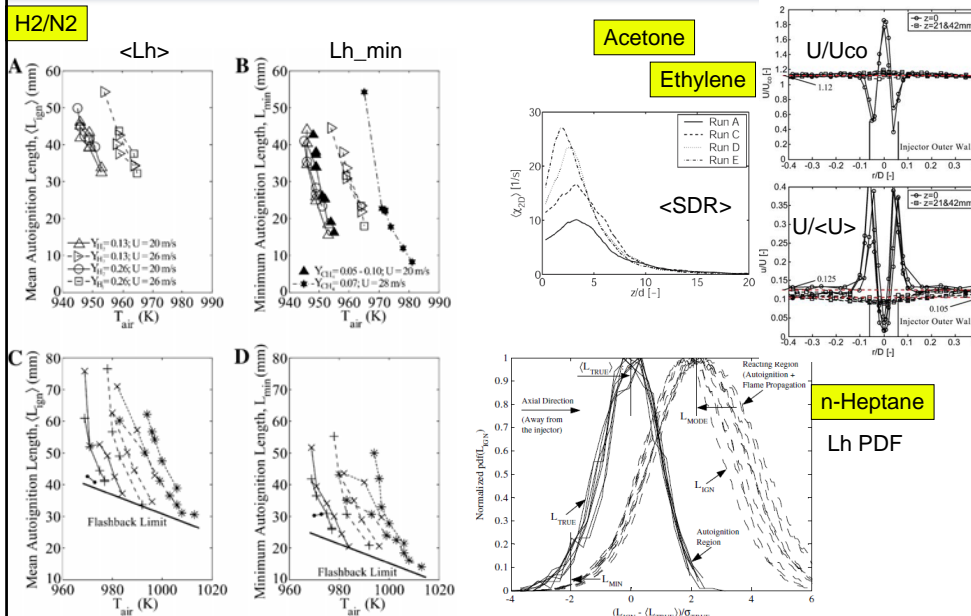


Figure 5: Instantaneous snapshots of autoignition for: (i) and (ii)  $T_{air} = 1059K$ ,  $T_{inj} = 822K$ ,  $U_{air} = 17.8m/s$ ,  $U_{inj}/U_{air} = 2.5$ , and, (iii) and (iv)  $T_{air} = 1051K$ ,  $T_{inj} = 848K$ ,  $U_{air} = 13.2m/s$ ,  $U_{inj}/U_{air} = 3.1$ .

# Experimental Database



# Lifted Jet in Hot Coflow: Outline



## 0. Introduction to the Burners

- Categorisation of flames
- Flame Stabilisation
- Models

## 1. Experiments and Databases

*Cabra, Adelaide, Delft, Lund, Cambridge*

**DNS** ←

## 2. Modelling and Comparison of Models

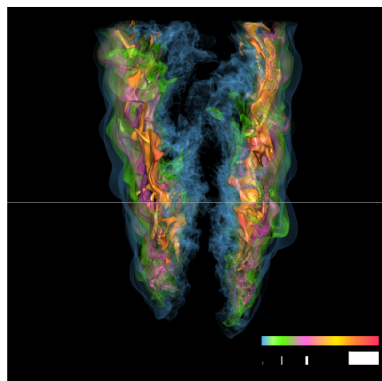
## 3. New Developments

## 4. Conclusions, Issues and Way Forward

# DNS of a Lifted Hydrogen-Air Jet Flame in a Hot Coflow (Yoo et al. JFM 2009)



Re = 11,000 OH Mass Fraction



Turb. Re = 340

$u'/U_j = 0.091$

$T_j = 400\text{ K}$     $T_c = 1100\text{ K}$

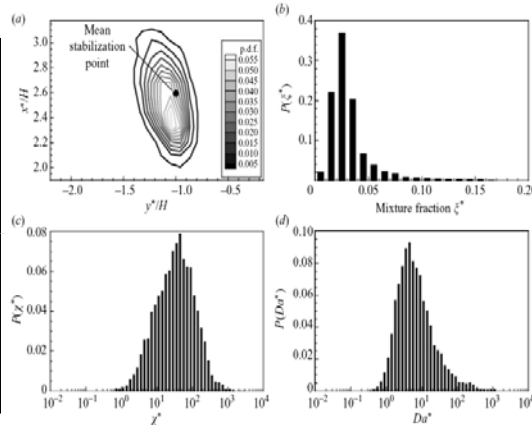


FIGURE 15. The p.d.f. of (a) the flame stabilization point, (b) the mixture fraction, (c) the scalar dissipation rate and (d) the Damköhler number at the local stabilization point.

## DNS of lifted ethylene-air jet flame in a heated coflow



3D slot burner configuration:

$$L_x \times L_y \times L_z = 30 \times 40 \times 6 \text{ mm}^3 \text{ with}$$

1.28 billion grid points

High fuel jet velocity (204m/s); coflow velocity (20m/s)

Nozzle size for fuel jet,  $H = 2.0\text{mm}$

$Re_{\text{jet}} = 10,000$ ;  $\tau_f = 0.15\text{ms}$ ; 3 flow through times

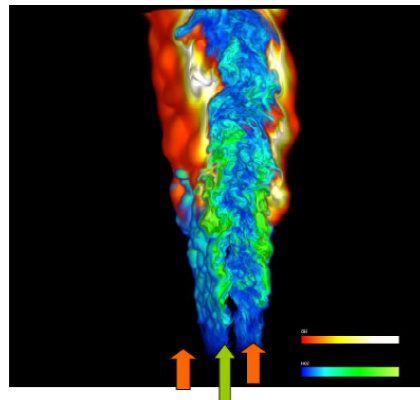
Cold fuel jet (18%  $\text{C}_2\text{H}_4$  + 82%  $\text{N}_2$ ) at 550K,  $\eta_{\text{st}} \approx 0.27$

Detailed  $\text{C}_2\text{H}_4$ /air chemistry, 22 species 18 global reactions, 201 steps

Hot coflow air at 1,550K

Performed on CrayXT4 at ORNL on 30,000 cores and 7.5 million cpu-hrs  
240 TB field data, 50TB particle data

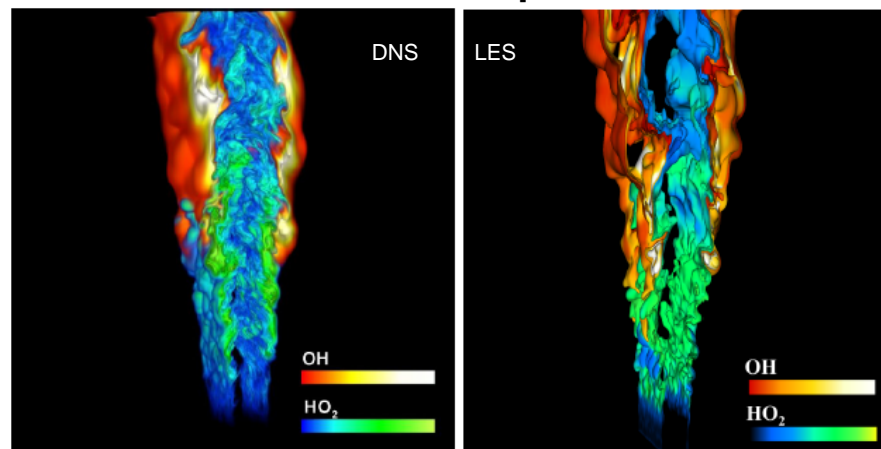
Ethylene-air lifted jet flame at  $Re=10000$



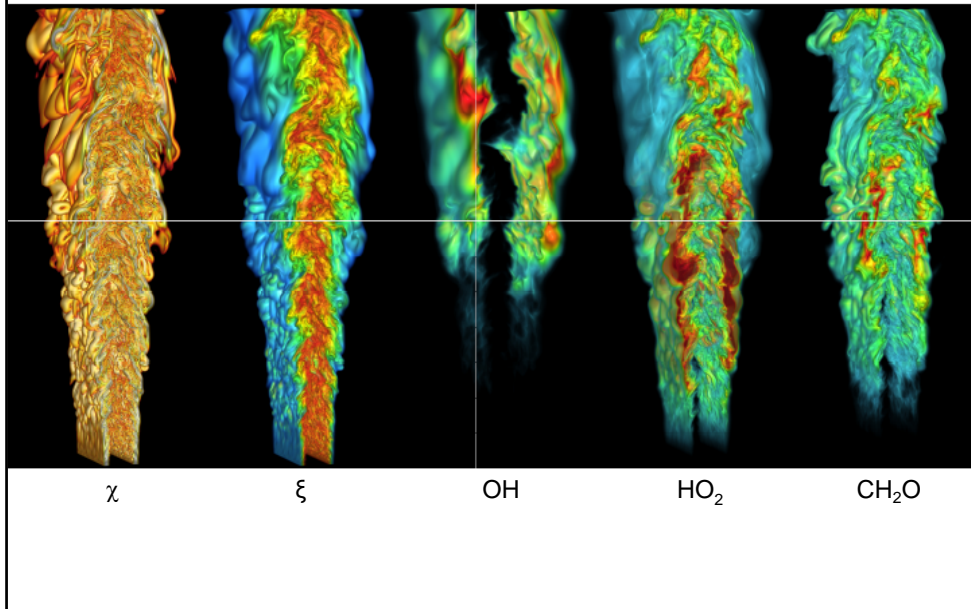
## Comparison of LES model to DNS



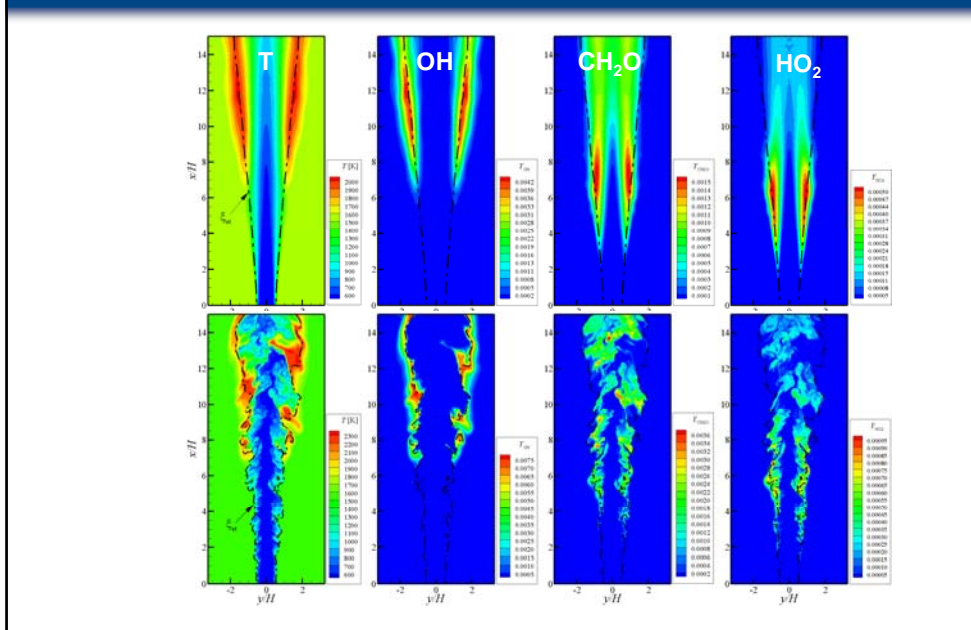
See Ed Knudsen, Heinz Pitsch poster



# Scalar Dissipation Rate $\chi$ , Species and Mixture Fraction $\xi$



# Favre mean and instantaneous temperature and species mass fractions (OH, CH<sub>2</sub>O, HO<sub>2</sub>)



## Summary



Lifted ethylene/air jet flame in heated coflow is stabilized by autoignition upstream of the high temperature flame

Chemical observables include high levels of HO<sub>2</sub>, and low levels of CH<sub>3</sub> and CH<sub>2</sub>O.

Autoignition occurs at a preferred mixture fraction (fuel-lean) and at low scalar dissipation rate.

Stabilization region is affected by large-scale jet mixing structure, with a competition between auto-ignition and extinction of the kernel by scalar dissipation rate.

Low fuel concentration and large stoichiometric mixture fraction together with high jet and coflow velocity prevents upstream flame propagation against adverse convective velocity.

## Lifted Jet in Hot Coflow: Outline



### 0. Introduction to the Burners

Categorisation of flames

Flame Stabilisation

Models

### 1. Experiments and Databases

*Cabra, Adelaide, Delft, Lund, Cambridge*

DNS

### 2. **Modelling** and Comparison of Models

### 3. New Developments

### 4. Conclusions, Issues and Way Forward

## Part 2: Review and comparisons



- Modeling of Adelaide MILD burner
- Modeling of Delft JHC (poster)
- Modeling of Cabra flames
- Comparisons of RANS results for Cabra flames
- Comparisons of LES results for Cabra flames

Many tables and comparisons are included in extra slides

## Modeling of experiments reported in Dally et al., PCI, 29 (2002) 1147-1154 (Adelaide JHC burner )



### Published

- F. Christo and B. Dally, C&F, 142 (2005)117-129 **EDC** **Z/PPDF** **(C05)**
- S.H. Kim, K.Y. Huh, B. Dally, PCI 30, 2005, 751-757 **CMC** **(K05)**
- A. Frassoldati, P. Sharma, A.Cuoci, T. Faravelli, E. Ranzi, App. Therm. Eng., 30 (2010) 376-383 **(F10)** **EDC**
- F.C. Christo, B.B.Dally, 15th Australasian Fluid Mech. Conf., Sydney, 2004
- F. Christo, G. Szego, B.Dally, 5th Asia-Pacific Conf.Combust., Adelaide, 2005, 329-332
- F. Christo, G. Szego, B. Dally, 6th Asia-Pacific Conf.Combust., Nagoya, 2007, 448-451 **(C07)** **EDC** **PDF**

### In press

- Mardani Amir, Tabejamaat Sadegh, Ghamari Mohsen, Numerical study of influence of molecular diffusion in the MILD combustion regime, Comb. Theory & Mod., 2010 **(M10)** **EDC**

Modeling of experiments reported in  
Dally et al., PCI, 29 (2002) 1147-1154  
(Adelaide JHC burner )



Paper	Turbulence	Chemistry	Interaction	Results	Remark
C05	Mod. k-ε	Smooke Mod. GRI 3.0	EDC Z/PDF	-Diff-diff important -EDC performs better than Z/PDF	3,6,9 % cases
K05	Mod. k-ε	GRI 2.11	First order CMC	-Conditional and unconditional profiles - Z-PDF for 3-stream mixing	3,6,9% cases
C07	Mod. k-ε / RSM	ARM, GRI 3.0 Smooke	EDC PDF	- Often EDC better than PDF	
F10	Mod. k-ε / RSM	detailed	EDC	- NOx postprocessor	k-profile at inlet tuned
M10	Mod. k-ε	Several	EDC	- Laminar diffusive effects	

Fluent is used, except in K05

RANS Modeling of experiments reported in  
Cabra et al. 2002 (H2)



**Published – RANS**

- 2002 Proc. Comb. Inst Cabra, Myhrvold, JY Chen, Dibble, Karpets and Barlow *Simultaneous Laser Raman-Rayleigh-LIF measurements and numerical modelling results of a lifted turbulent H2/N2 jet flame in a vitiated coflow* **2002Cab** PDF, EDC
- 2004 CTM Masri, Cao, Pope and Goldin *PDF calculations of turbulent lifted flames of H2/N2 fuel issuing into a vitiated co-flow* **2004Mas** PDF
- 2005 CF Cao, Pope and Masri *Turbulent lifted flames in a vitiated coflow investigated using joint PDF calculations* **2005Cao** PDF
- 2006 CST Myhrvold, Ertesvåg, Gran, Cabra, and JY Chen *A numerical investigation of a lifted H2/N2 turbulent jet flame in a vitiated coflow* **2006Myh** EDC
- 2007 CST Gordon, Masri, Pope, Goldin *A numerical study of auto-ignition in turbulent lifted flames issuing into a vitiated co-flow* **2007Gor-a** PDF
- 2008 JINMF Kang, Kim, Kim and Ahn *Level-set based flamelet approach for simulating turbulent lifted jet flame* **2008Kan** LF+G-eq
- 2009 Proc. Comb. Inst Patwardhan, De, Lakshmisha, Raghunandan *CMC simulations of lifted turbulent jet flame in a vitiated coflow* **2009Pat** CMC
- 2009 J.Eng GT and Pwr. Zhang and Rawat *Simulation of Turbulent Lifted Flames Using a Partially Premixed Coherent Flame Model* **2009Zha** CFM

## RANS Modeling of experiments reported in Cabra et al. 2002 (CH4)



### Published – RANS

2005 CF	<u>Cabra, JY Chen, Dibble, Karpetis and Barlow</u> Lifted methane-air jet flames in a vitiated coflow	<b>2005Cab</b>	<b>PDF</b>
2007 CF	<u>Gordon, Masri, Pope, Goldin</u> Transport Budgets in Turbulent Lifted Flames of Methane Auto-Igniting in a Vitiated Co-flow	<b>2007Gor-b</b>	<b>PDF</b>
2007 PCI	<u>Gkagkas and Lindstedt</u> Transported PDF modelling with detailed chemistry of pre- and auto-ignition in CH4/air mixtures	<b>2007Gka</b>	<b>PDF</b>
2009 CF	<u>Michel, Colin and Angelberger</u> Using the tabulated diffusion flamelet model ADF-PCM to simulate a lifted methane-air jet flame	<b>2009Mic</b>	<b>ADF-PCM</b>
2010 CF	<u>Michel, Colin and Angelberger</u> On the formulation of species reaction rates in the context of multi-species CFD codes using complex chemistry tabulation techniques	<b>2010Mic</b>	<b>Z,c-PCM</b>

## RANS Modeling of experiments reported in Cabra et al. 2002 (H2)



	Turbulence	Chemistry	Interaction	Mixing	Results	Remark
<b>2002Cab</b>	k-ε, LRR-RSM, JM-RSM	GRI2.11	EDC, PDF	MC	-with k-eps, EDC and PDF matched Lh	
<b>2004Mas</b>	k-ε, low Re wall	Mueller, GRI2.11	PDF	MC	the two mechanisms straddled Lh, Ign first at lean Z	
<b>2005Cao</b>	k-ε	Mueller, Li	JPDF	MC, IEM, EMST	best model for T-sensitivity; Lh not sensitive to: mixing model, or its constants, inlet velocity profiles or turbulence intensity;	best agreement at 1033K
<b>2006Myh</b>	k-ε, mod k-ε, LRR-RSM, JM-RSM	GRI2.11	EDC		EDC shows low sensitivity to Tc, over-predicted OH	best agreement at 1053K (JM)
<b>2007Gor-a</b>	k-ε	Li	PDF	MC	TPDF does not capture Lh vs T trend as well as JPDF	best agreement at 1060K
<b>2008Kan</b>	k-ε	Mueller	Level-set + flamelet		OH reproduced well, Lh good	
<b>2009Pat</b>	k-ε	Mueller	1st O CMC		Lh vs T response very shallow	best agreement at 1025K
<b>2009Zha</b>	k-ε	Warnatz 1979	Flame surface density		Good agreement mean T and mean species	Low comp.cost

## RANS Modeling of experiments reported in Cabra et al. 2005 (CH4)



ID	Turbulence	Chemistry	Interaction	Mixing	Results	Remark
2005Cab	k-ε	GRI1.2	PDF	MC, IEM, EMST	parametric variation tested, MC and EMST preferred, Kalghatgi shown not applicable	
2007Gor-b	k-ε	Var. incl. detailed	PDF	EMST	Ignition delay of chemistry important, CH <sub>2</sub> OxOH and COxOH useful ignition markers	best agreement at 1380K
2007Gka	k-ε	Detailed CH <sub>4</sub>	PDF	MC	C <sub>phi</sub> varied with little influence, shallower sensitivity.	RADCAL included,
2009Mic	k-ε	GRI3.0	Flamelet ADF-PCM		including SDR in model improved accuracy	No T <sub>c</sub> sensitivity reported
2010Mic		GRI3.0	PCM-FPI, ADF-PCM		compares mass fraction and reaction rate closure for the mean RR term.	MF applied with ADF-PCM good results

## LES Modeling of experiments reported in Cabra et al. 2002 (H<sub>2</sub>)



### Published

#### H<sub>2</sub>

- 2005 AIAA [Goldin](#) Evaluation of LES Subgrid Reaction Models in a Lifted Flame **SLF, LC** **2005Gol**
- 2007 Comp. & Fluids [Jones and Navarro-Martinez](#) Study of hydrogen **FDF/stoch.field** **2007Jon**  
auto-ignition in a turbulent air co-flow using a Large Eddy Simulation approach
- 2008 CST [Duwig and Fuchs](#) Large Eddy Simulation of a H<sub>2</sub>/N<sub>2</sub> Lifted Flame in a Vitiated Coflow **(Z,T) PresFDF** **2008Duw**
- 2008ASME [Szasz, Duwig and Fuchs](#) Noise Generated by a lifted flame in a vitiated coflow **PresFDF** **2008Sza**

## LES Modeling of experiments reported in Cabra et al. 2005 (CH4)



### Published

- 2008 CF Domingo, Vervisch, Veynante Large-eddy simulation of a lifted methane jet flame in a vitiated coflow (Z,c) FPI 2008Dom
- 2009 PCI Navarro-Martinez and Kronenburg LES-CMC simulations of a lifted methane flame LES-CMC 2009Nav
- 2009 In "LES and DNS of ignition process and complex structure flames with local extinction" Jones and Navarro-Martinez Large Eddy Simulation and the Filtered Probability Density Function Method FDF/stoch.field 2009Jon
- 2009 PCI Godel, Domingo, Vervisch Tabulation of NOx chemistry for Large-Eddy Simulation of non-premixed turbulent flames (Z,c) FPI-NOx 2009God

### Under review

- Ihme & See, Comb. & Flame, accepted (2010) Z-c-UF/PV  
(Z,c) tabulated chemistry  
(Un)steady diffusion flamelet/progress variable

## LES Modeling of Cabra experiments



ID	Turbulence	Chemistry	Interaction	Mixing	Results	Remark
2005Gol	Dyn. Smag.	ARM9	SLF, LC		SLF can't predict ignition, LC surprisingly good.	best agreement at 1040K
2007Jon	Smag.	Yetter/Dryer	FPDF, Eulerian Stochastic Field	LMSE	partial premixed flames and AI successfully modelled. No premixed found	best agreement at 1035K
2008Duw	FSFM	Li	(Z,T) tabulated, MILES		stabilising transport of burnt pocket structures, superposition of 2 spiral modes, $f = 420\text{Hz}$	uses (x-x_ig)/D, POD used in turbulence description, 1040K best match
2008Sza	FSFM	Li	Presumed FDF		shape of acoustic modes identified byPOD, centered at stabilisation and flame tip	
2008Dom		GRI3.0	(Z,c) FPI		Auto-ignition at very lean side + premixed flame propagation; CO, CO2 and OH somewhat underpredicted, but good results	
2009Nav	Smag.	Lindstedt	LES-CMC		OH match is good, shallow response	2D CMC necessary
2009Jon	Smag.	Sung et al.	FPDF, Eulerian Stochastic Field	IEM	concludes partially premixed combustion	no tuning required, also did Markides and Mastorakos burner
2009God			PCM-FPI		New PGV to account for Nox	

# Lifted Jet in Hot Coflow: Outline



## 0. Introduction to the Burners

- Categorisation of flames
- Flame Stabilisation
- Models

## 1. Experiments and Databases

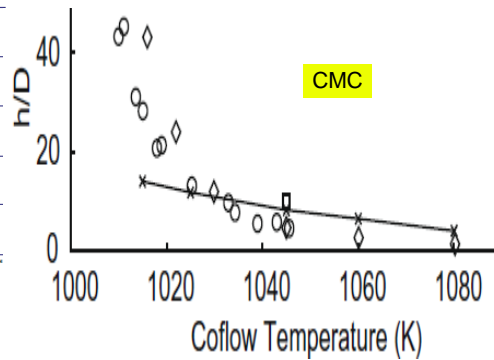
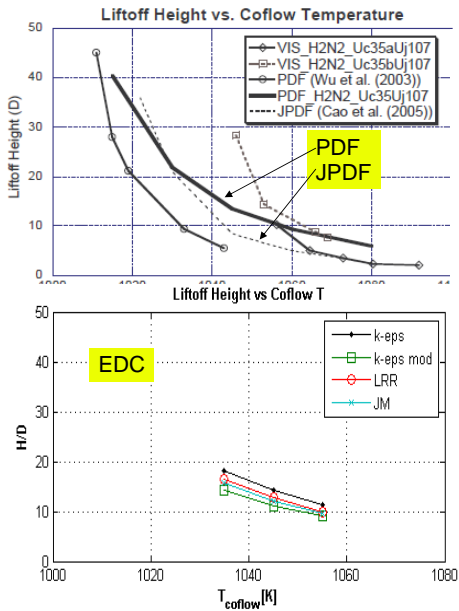
Cabra, Adelaide, Delft, Lund, Cambridge  
DNS

## 2. Modelling and **Comparison of Models** ←

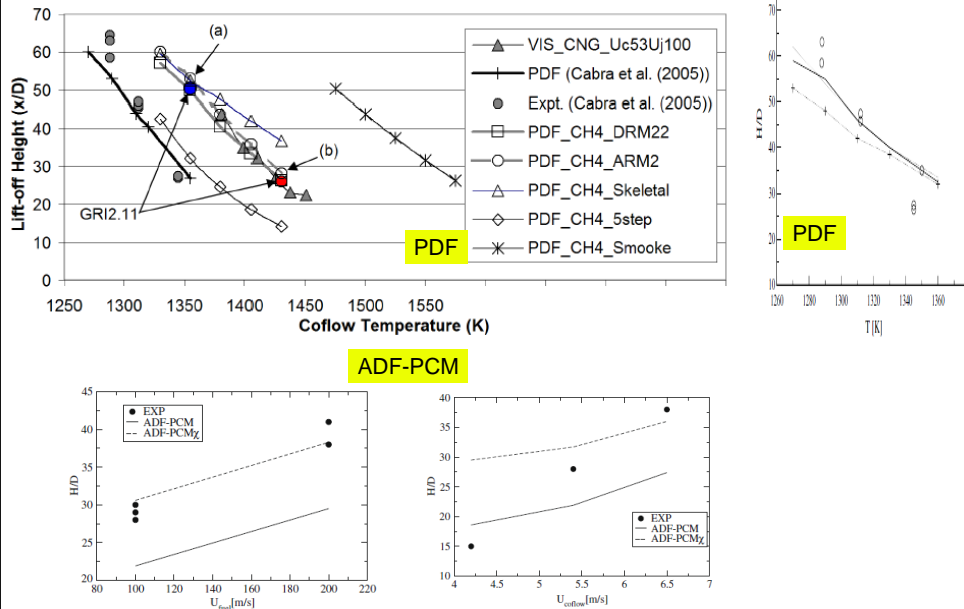
## 3. New Developments

## 4. Conclusions, Issues and Way Forward

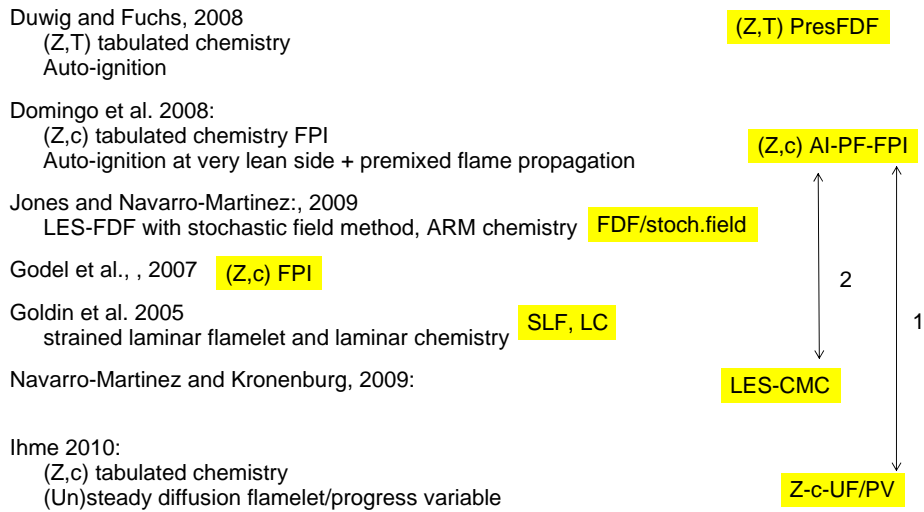
# Cabra (H2) flame liftoff height Model Trends (RANS)



# Cabra (CH4) flame liftoff height Model Trends (RANS)



# Comparison between LES approaches

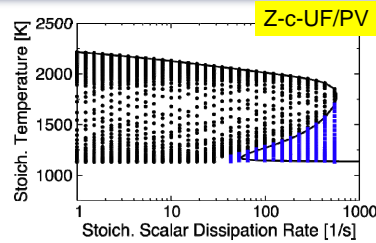


# Unsteady flamelet / progress variable combustion model (1,2)



Unsteady flamelet/progress variable (UFPV) model

Thermochemical quantities (density, viscous-diffusive properties, temperature, species, chemical src-terms, ...) are obtained from solution of **unsteady flamelet equations**



Parameterization of all combustion quantities in terms of (eliminating explicit dependence on Lagr. flamelet time):

- Mixture fraction
- Reaction progress variable
- Scalar dissipation rate

Presumed PDF-closure, consisting of beta-PDF for mixture fraction and statistically most-likely PDF for progress variable

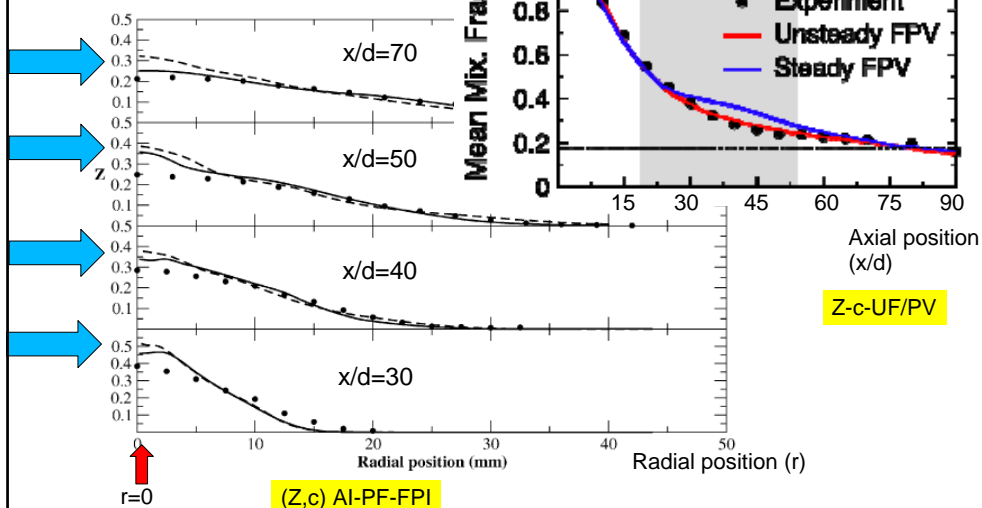
Model was applied in a priori study to assess critical modeling assumption

1 Ihme & See, Comb. & Flame, accepted (2010)  
 2 Pitsch & Ihme, AIAA-Paper 2005-557, (2005)

# Comparison of results Z-c tabulation methods



Mean mixture fraction profiles



Mean mixture fraction axial profile overpredicted by Z-c-AI-PF-FPI

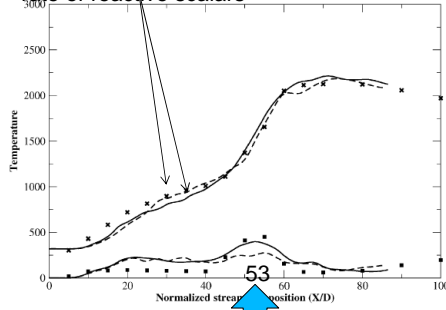
Cabra CH4

# Comparison of results Z-c tabulation methods

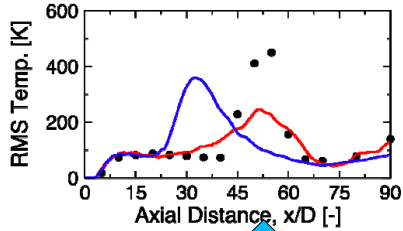
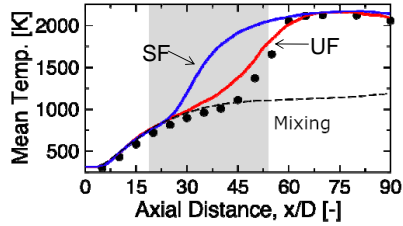


## Temperature centerline profile

Two models for scalar dissipation rate of reactive scalars



(Z,c) AI-PF-FPI

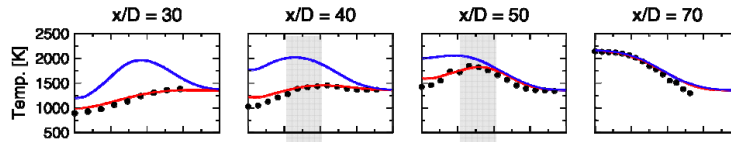


Z-c-UF/PV

Cabra CH4

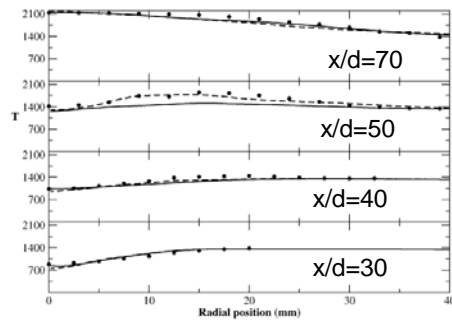
Is the difference in submodel for auto-ignition responsible for better Trms prediction ?

# Comparison of results Z-c tabulation methods



Z-c-UF/PV

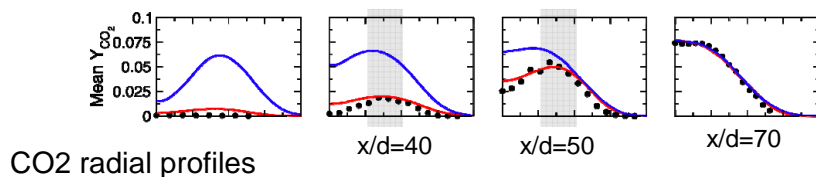
## Temperature radial profile



(Z,c) AI-PF-FPI

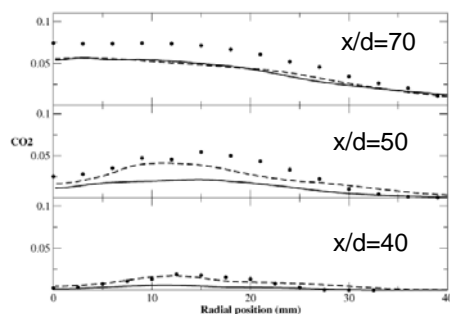
Cabra CH4

## Comparison of results Z-c tabulation methods



CO<sub>2</sub> radial profiles

Z-c-UF/PV



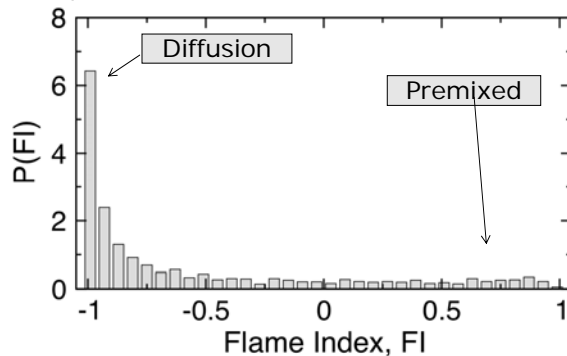
(Z,c) AI-PF-FPI

Cabra CH4

## LES Results on Flame Stabilization Mechanism



Characterize combustion regime of the flame base using **flame index, FI**, (corrected to account for O<sub>2</sub>-content in fuel stream)



Ihme and See, 2010

Note: similar behaviour of Flame Index is also calculated in DNS

Z-c-UF/PV

- 1 Yoo, Sankaran, Chen, JFM, 640, 453 (2009)
- 2 Echehki & Chen, Comb. & Flame, 134, 169, (2003)



### 0. Introduction to the Burners

Categorisation of flames

Flame Stabilisation

Models

### 1. Experiments and Databases

*Cabra, Adelaide, Delft, Lund, Cambridge*

DNS

### 2. Modelling and Comparison of Models

### 3. **New Developments** ←

### 4. Conclusions, Issues and Way Forward

## Part 3: Recent results on Cabra flames



1. Bertrand Naud: study on numerical accuracy questions in PDF modeling (see poster)
2. R. Vicquelin, B. Fiorina, O. Gicquel: using tabulated unsteady non-premixed flamelets (poster)
3. Benjamin Sauer, Ricky Chien, J-Y Chen: modeling of auto-ignition using Senkin, diffusion flamelet and Linear Eddy Modeling
4. Matthias Ihme : LES with unsteady flamelet/ progress variable model

## Autoignition and Linear Eddy Modeling



Modeling of Autoignition of a turbulent  
non-premixed  $H_2/N_2$  jet flame in vitiated  
coflow using Linear Eddy Modeling

Benjamin Sauer\*, Ricky Chien, J-Y Chen  
Department of Mechanical Engineering  
University of California Berkeley  
TNF 10 Workshop 2010

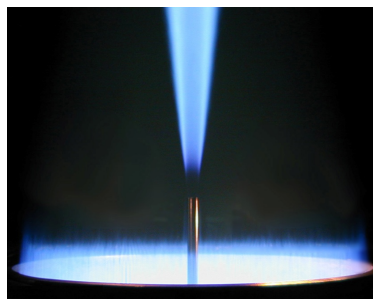
\* Visiting student from Leibniz Universität Hannover

## Motivation



Determine the mixtures at the onset of first auto-ignition  
event (the most reactive mixture)

Study the effect of differential diffusion on autoignition  
delay (laminar & turbulent flames)



$X_{O_2} < 0.21$   
 $T_{\text{coflow}} = [900-2,000] \text{ K}$



**Senkin:** autoignition delay  $\tau_{\text{delay}}$  vs. mixture fraction  $\xi$  of homogeneous hydrogen-air mixtures (no diffusion of heat & mass)

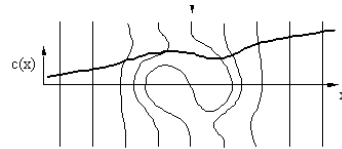
**Transient flamelet:** autoignition delay  $\tau_{\text{delay}}$  as function of scalar dissipation rate

**1-D Laminar Flame Model**

**Linear Eddy Modeling (LEM)**

differential diffusion effects

under simulated turbulent stirring



## Conclusions – effect of differential diffusion in laminar flames



With differential diffusion:

$\tau_{\text{delay}}$  of laminar case (0.25 ms) is smaller than the homogenous case (0.34 ms from Senkin)

With  $Le=1$ :

$\tau_{\text{delay}}$  of laminar case (0.6 ms) is larger than the homogenous case (0.34 ms from Senkin)

Auto-ignition occurs at the same mixture fraction ( $\xi_{\text{mr}} \sim 0.05$ ) with 1-D model independent of diffusion model

Differential diffusion causes  $\chi_{\text{mr}}$  to decrease faster than in the case of equal diffusivity

## Conclusions – effect of turbulent stirring



For  $Re=100 - 300$ :  $\tau_{delays} \sim \tau_{delays}$  of laminar case

For  $Re=500 - 1000$ :  $\tau_{delays} > \tau_{delays}$  of laminar case

Turbulent mixing disperses the radicals: autoignition can occur at mixtures far away from  $\xi_{mr}$  calculated by Senkin

Auto-ignition can occur at multiple locations due to stirring

In LEM for multiple location autoignition,  $\chi_{mr}$  can exceed  $\chi_{critical}$ . The high  $\chi_{mr}$  occurs in the 'leaner' location.

In LEM, turbulence seems always to postpone auto-ignition in contrast to some previous DNS study showing turbulence decreases delays.



Prediction of autoignition in a lifted methane/air flame using an unsteady flamelet/ progress variable model

Matthias Ihme

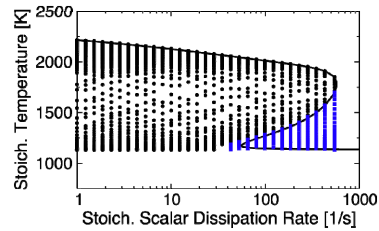
*Department of Aerospace Engineering  
University of Michigan  
Ann Arbor, MI 48109*



### Combustion model<sup>1,2</sup>

Unsteady flamelet/progress variable (UFVP) model

Thermochemical quantities (density, viscous-diffusive properties, temperature, species, chemical src-terms, ...) are obtained from solution of unsteady flamelet equations



Parameterization of all combustion quantities in terms of (eliminating explicit dependence on Lagr. flamelet time):

- Mixture fraction
- Reaction progress variable
- Scalar dissipation rate

Presumed PDF-closure, consisting of beta-PDF for mixture fraction and statistically most-likely PDF for progress variable

Model was applied in a priori study to assess critical modeling assumption

<sup>1</sup> Ihme & See, Comb. & Flame, accepted (2010)  
<sup>2</sup> Pitsch & Ihme, AIAA-Paper 2005-557, (2005)

## Lifted Jet in Hot Coflow: Outline



### 0. Introduction to the Burners

- Categorisation of flames
- Flame Stabilisation
- Models

### 1. Experiments and Databases

*Cabra, Adelaide, Delft, Lund, Cambridge*  
DNS

### 2. Modelling and Comparison of Models

### 3. New Developments

### 4. **Conclusions, Issues and Way Forward** ←

## Lifted jets in hot coflow: Conclusions



- Experiments: a large amount of experimental data is available for model validation
- Interesting models are being developed and applied: but need to
  - apply one model to many flames
  - apply to one flame many models
- Role of oxygen content coflow and preheat temperature to be understood in more detail (transitional vs lifted flame ?)
- To be further investigated:
  - Transition auto-ignition stabilisation to lifted diffusion flame
  - Role of local flow structure in auto-ignition

## Lifted jets in hot coflow: Issues



- Low Re ( $<10000$ ) flows susceptible to influence of molecular transport through differential diffusion
- Characterisation of coflow compositions still not complete, and trace OH compositions can influence autoignition processes
- Parametric variation very important

## Lifted jets in hot coflow: Way Forward



- Testing model assumptions with existing DNS-databases
- Identifying trends in lift off height, both experimentally and in modeling
- More systematic model comparisons for existing experimental cases is needed: task for the next TNF ? (flow field, mixing field, species fields, statistics, etc)
- Explore new physical phenomena for model validation, such as lift off height PDF
- Tests with other fuels (low calorific, DME) - Sydney C<sub>2</sub>H<sub>6</sub>, C<sub>3</sub>H<sub>8</sub>
- High pressure auto-ignition burner design
- High Reynolds number burner design
- DNS of more complex flows and flames

# Comments Regarding CO-Measurements for the Lifted Methane/Air Flame in a Vitiated Coflow

M. Ihme\*, C. Angelberger†, J.-B. Michel† and R.S. Barlow‡

\**Department of Aerospace Engineering, University of Michigan, Ann Arbor, MI 48109*

†*IFP Energies nouvelles, Rueil-Malmaison, France*

‡*Sandia National Laboratories Livermore, CA 94551-0969*

August 10, 2010

## Abstract

This document discusses discrepancies in the reported CO measurements for the lifted methane/air flame, which was investigated by Cabra et al. [1]. Compared to the CO(Raman)-measurements, the reported CO(LIF)-data are higher by a factor of two. Since the differences between both measurements are typically within 10 %, it suggests that the CO(LIF) data are inconsistent. In order to compensate for this discrepancy, a correction was applied to the CO(LIF)-data. The corrected CO(LIF)-data are in quantitative agreement with the Raman-measurements, and can be used for comparisons with simulations.

## 1 Introduction

Measurements for a lifted methane/air flame in a vitiated coflow have been performed by Cabra et al. [1]. The comprehensive experimental database, available at <http://www.me.berkeley.edu/cal/vcb/data/VCMAData.html>, includes single-point measurements and Favre-averaged data at different axial and radial locations in the jet flame. Measurements for CO were performed by Raman scattering and by LIF. Since the CO(Raman) measurements are stronger affected by hydrocarbon fluorescence interferences, a general recommendation of the TNF-workshop is to use the CO(LIF) measurements for comparisons with modeling results [2]. However, an analysis of the CO data showed significant discrepancies between both measurement series. While the sources for these discrepancies remain under investigation, this document shows that the reported CO(Raman) measurements are most consistent with the remaining measurements and the reported mixture fraction data. A correction to the CO(LIF) data is discussed, so that these measurements can also be used to assess modeling results.

## 2 Comparison of CO(LIF) and CO(Raman) data

Results for Reynolds-averaged radial profiles of CO mass fractions at  $x/D = 40, 50,$  and  $60$  are shown in Fig. 1. This comparison shows that the CO(LIF)-measurements are consistently larger by a factor of two throughout the flame. Since the shape of both profiles is similar, it suggests that these differences can be attributed to a systematic error in the measurement-analysis.

Comparisons with other flames (Sandia flame series, DLR-jet flames, and Sydney bluff-body flame; see Appendix) show that values for CO-mass fractions are typically less than 0.08, which indicates that both CO-measurements are plausible. Nevertheless, it is speculated that the CO(Raman)-measurements are more reliable. Some indication for this is that (i) other comparable measurements

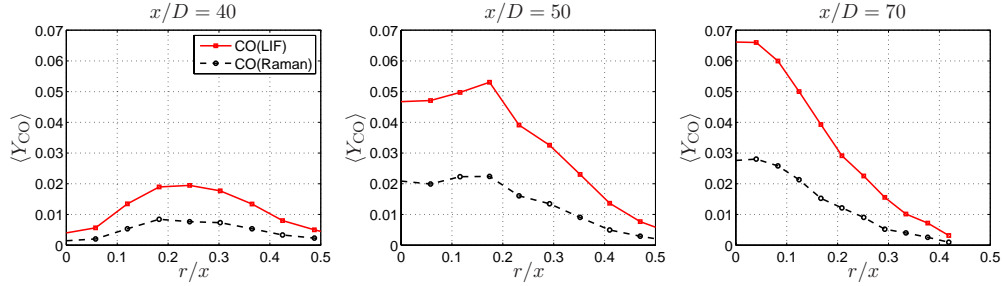


**Figure 1:** Comparison of radial profiles for the Reynolds-averaged mass fractions of CO(LIF) and CO(Raman) in the lifted methane/air flame in vitiated coflow.

indicate that CO(LIF) data are lower than CO(Raman) measurements, and (ii) the CO(Raman)-measurements were used in defining the mixture fraction. The reported mixture fraction is computed from the elemental mass fractions of C, O, and H, following Bilger’s formulation [3]:

$$Z = \frac{\frac{2}{W_C}(Y_C - Y_C^o) + \frac{1}{2W_H}(Y_H - Y_H^o) - \frac{1}{W_O}(Y_O - Y_O^o)}{\frac{2}{W_C}(Y_C^f - Y_C^o) + \frac{1}{2W_H}(Y_H^f - Y_H^o) - \frac{1}{W_O}(Y_O^f - Y_O^o)}, \quad (1)$$

with the subscripts “f” and “o” denoting the fuel and oxidizer streams, respectively. In the following the mixture fraction is computed using either CO(LIF) or CO(Raman) data. Both results are correlated against the mixture fraction which is reported in Ref. [2]. This comparison is presented in Fig. 2, and shows that  $Y_{CO(Raman)}$  was used to determine  $Z$ .

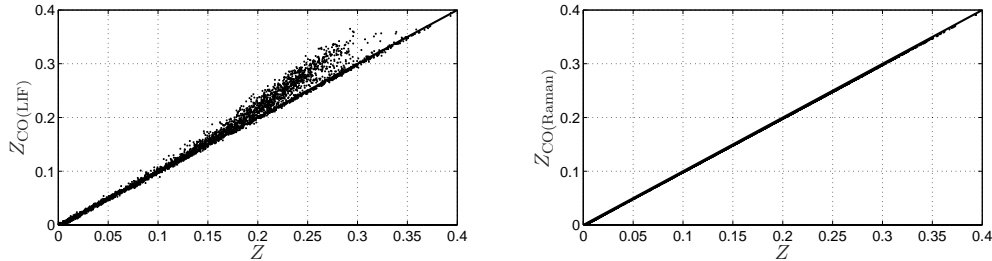


**Figure 2:** Regression plot of the reported mixture fraction,  $Z$ , vs. the mixture fraction, calculated from the CO(LIF) and CO(Raman)-measurements.

In this context it is noted that the mass fraction balance is closed by determining  $Y_{N_2}$  from  $Y_{N_2} = 1 - \sum_{i \neq N_2} Y_i$ . Interestingly, the analysis of the experimental results shows that  $Y_{N_2}$  was determined using the CO(LIF)-measurements. However, it is expected that this inconsistency is most-likely not of practical relevance, since  $N_2$ -comparisons are hardly of interest.

### 3 Correction of CO(LIF) Measurements

A proposed method to correct for the discrepancies between the two CO-measurement series consists in first rescaling the CO(LIF)-data, which is followed by re-evaluating the mixture fraction and correcting  $Y_{N_2}$  to enforce overall species conservation. This procedure provides improved estimates

for CO(LIF) data, and can be used as additional information for comparisons with simulation results. In the following, this correction is applied to the Cabra-flame.

Scatter plots of CO(LIF) and CO(Raman) measurements and the corresponding regression analysis at different axial locations in the flame are illustrated in Fig. 3. The plot at the bottom right combines the single-point measurements at all locations in the flame.

In the following, the corrected CO(LIF) data are denoted by CO\*(LIF), and are obtained by rescaling CO(LIF) as:

$$Y_{\text{CO}^*(\text{LIF})} = \frac{C_{\text{exp}}}{C_{\text{reg}}} Y_{\text{CO}(\text{LIF})} \quad (2)$$

where  $C_{\text{reg}} = 2.11$  is the regression coefficient, which is determined in the bottom right graph of Fig. 3, and the coefficient  $C_{\text{exp}}$  is a correction to account for the correlation between LIF and Raman measurements. This coefficient is set to 0.9 and is evaluated by considering other TNF-flame experiments (see Appendix A). With the corrected CO(LIF)-data, the corresponding mixture

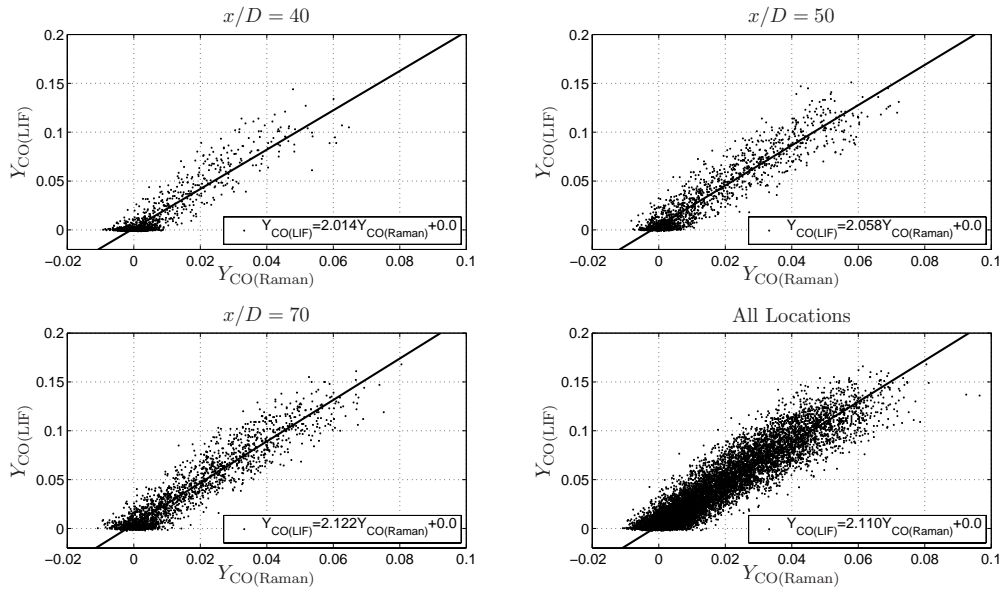


**Figure 3:** Scatter data and regression plots for CO(LIF) and CO(Raman), evaluated at three different axial locations in the flame. The plot at the bottom right combines the single-point measurements at all locations in the Cabra-burner.

fraction can be calculated. A comparison of the mixture-fraction conditioned results for corrected and uncorrected CO(LIF) data is presented in Fig. 4. This comparison shows that the corrected CO(LIF)-data are in very good agreement with the CO(Raman) results; only a slight shift of the profiles toward lean conditions is evident, which is most pronounced at  $x/D = 50$ . This shift is essentially a consequence of the different mixture fraction values. However, these small deviations are considered to be within experimental uncertainties, and therefore not significant.

## 4 Conclusions

Discrepancies between reported CO(LIF) and CO(Raman) measurements in the lifted methane/air flame have been analyzed. The reported CO(LIF) measurements are consistently larger by a factor

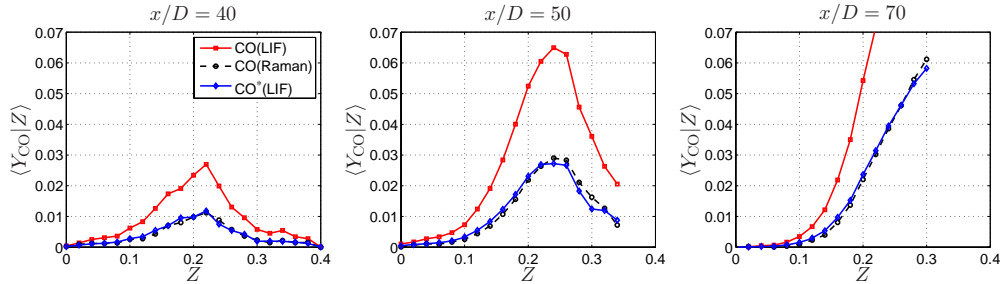


**Figure 4:** Comparison of mixture-fraction conditioned mass fractions of CO(LIF) and CO(Raman) for the lifted methane/air flame in vitiated coflow. Mixture fraction is defined with respect to CO(Raman).

of two throughout the flame. A correction is proposed to compensate for these differences by rescaling the CO(LIF) measurements. The rescaling coefficient is determined from a regression analysis between CO(LIF) and CO(Raman). Applying this method to the measurements provides good agreement between rescaled CO(LIF)-data and CO(Raman)-data. This, in turn, suggests that the differences between both CO measurement series is most-likely not an error in the experiment, and due to a systematic error in the data-analysis. Identifying sources for this discrepancies remains a topic for further investigation.

Because of this discrepancy, it is recommended to use the CO(Raman)-data for model comparisons. The mixture fraction, reported in the experimental database, is evaluated using the CO(Raman) data. The corrected CO(LIF) data are comparable to the CO(Raman) data. In order to use these data for comparisons of conditional results, it is necessary to re-evaluate the corresponding mixture fraction.

## A CO-LIF/Raman Correlations for Other TNF-Experiments

The coefficient  $C_{\text{exp}}$  was introduced in Eq. (2) to consider the correlation between LIF and Raman measurements. To determine this coefficient, CO-measurements for three other TNF-flames have been considered, namely the Sandia flames [2, 4], the DLR-flame [5, 6], and the Sydney bluff-body swirl-stabilized SMH1 flame configuration [7, 8]. For these three flame configurations, regression analyses were performed in order to determine the coefficient  $C_{\text{exp}}$ . The results show that  $C_{\text{exp}}$  can be reasonably well approximated with a value of 0.9.

## References

- [1] R. Cabra, J.-Y. Chen, R. W. Dibble, A. N. Karpetsis, and R. S. Barlow. Lifted methane-air jet flames in a vitiated coflow. *Combust. Flame*, 143:491–506, 2005. data available from <http://www.me.berkeley.edu/cal/vcb/data/VCMADData.html>.
- [2] R. S. Barlow and J. Frank. Piloted CH<sub>4</sub>/air flames C, D, E, and F – Release 2.1. Technical report, Sandia National Laboratories, 2007. available from <http://www.sandia.gov/TNF/DataArch/FlameD/>.
- [3] R. W. Bilger, S. H. Starner, and R. J. Kee. On reduced mechanisms for methane-air combustion in nonpremixed flames. *Combust. Flame*, 80:135–149, 1990.
- [4] R. S. Barlow and J. H. Frank. Effects of turbulence on species mass fractions in methane/air jet flames. *Proc. Combust. Inst.*, 27:1087–1095, 1998.

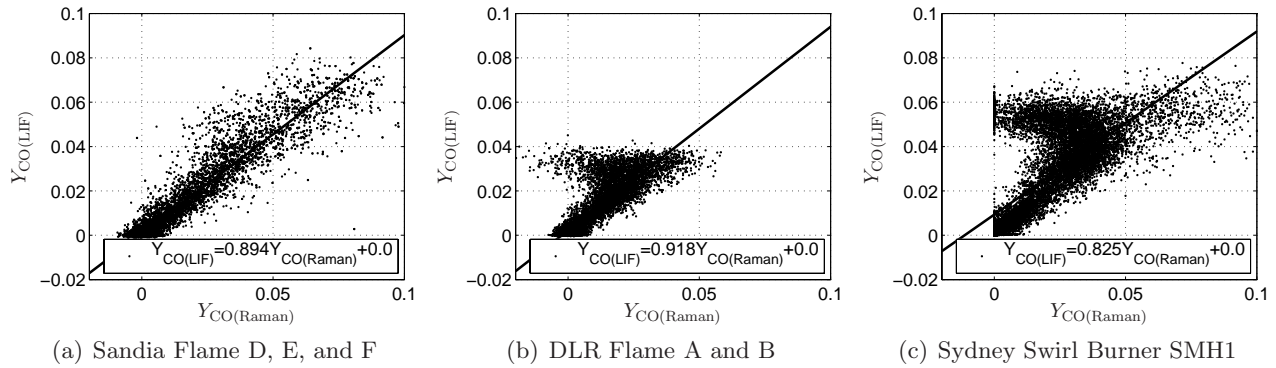


**Figure 5:** Scatter data and regression plots for CO(LIF) and CO(Raman), evaluated at three different axial locations in the flame. The graph at the lower left of radial profiles for the Favre-averaged mass fractions of CO(LIF) and CO(Raman) for the lifted methane/air flame in vitiated coflow.

- [5] V. Bergmann, W. Meier, D. Wolff, and W. Stricker. Application of spontaneous Raman and Rayleigh scattering and 2D LIF for the characterization of a turbulent  $\text{CH}_4/\text{H}_2/\text{N}_2$  jet diffusion flame. *Appl. Phys. B*, 66(4):489–502, 1998.
- [6] W. Meier, R. S. Barlow, Y. L. Chen, and J.-Y. Chen. Raman/Rayleigh/LIF measurements in a turbulent  $\text{CH}_4/\text{H}_2/\text{N}_2$  jet diffusion flame: Experimental techniques and turbulence-chemistry interaction. *Combust. Flame*, 123(3):326–343, 2000.
- [7] P. A. M. Kalt, Y. A. Al-Abdeli, A. R. Masri, and R. S Barlow. Swirling turbulent non-premixed flames of methane: Flow field and compositional structure. *Proc. Combust. Inst.*, 29:1913–1919, 2002.
- [8] Y. A. Al-Abdeli and A. R. Masri. Stability characteristics and flowfields of turbulent non-premixed swirling flames. *Comb. Theory Modelling*, 7:731–766, 2003.

Blank Page

## Comparisons of Experimental Measurements and Numerical Computations of the Piloted Premixed Jet Burner (PPJB)

Contributors:

*M. Dunn, A. Masri, R. Bilger, R. Barlow, G. Wang*, Sandia National Laboratories, The University of Sydney (Experiments)

*M. Dunn, A. Masri*, The University of Sydney (RANS PDF calculations)

*D. Rowinski, S. Pope*, Cornell University (PDF calculations)

*V. Mittal, H. Pitsch, E. Knudsten*, Stanford University (LES calculations)

*C. Duwig, K.-J. Nogenmyr, C.-K. Chan*, Lund University, Haldor Topsøe, Hong Kong Polytechnic University (LES calculations)

The aim of the PPJB session at the TNF10 in Beijing 2010 was to compare some recent numerical computations of the PPJB with the experimental measurements. There were contributions from four different modeling groups, two using RANS based PDF methods and two utilizing LES based methods. The PPJB features a small diameter jet from which a lean methane-air mixture issues at high velocity. Surrounding the central jet is a stoichiometric pilot, which ensures initial ignition of the central jet. Both the central jet and pilot are surrounded by a large hot coflow of hydrogen-air combustion products, ensuring that the central jet combustion process is not diluted or quenched by ambient air. By varying the central jet velocity and keeping all other parameters constant, a parametric flame series of four flames (PM1-50, PM1-100, PM1-150, and PM1-200) with increasing degrees of finite-rate chemistry effects has been investigated. The flame structure in the flame series varies from being thin and flamelet like in the lowest velocity flame (PM1-50) to flames that exhibit an initial ignition region close to the jet exit, flowed by an extinction region (PM1-150 and PM1-200), then a re-ignition region further downstream as the turbulence intensity decays. The PPJB experimental measurement database includes single point velocity measurements, planar imaging of temperature, OH and CH<sub>2</sub>O, as well as 1D line imaging using the Raman/Rayleigh/CO LIF technique combined with crossed PLIF of OH. From the 1D line imaging measurements quantities such as mixture fractions and reaction rates have been calculated, these are valuable quantities for evaluating the numerical model predictions of the mixing and reaction rate fields.

The modeling results from the Sydney group (*Dunn and Masri*) utilized a transported thermo-chemistry PDF model coupled with a RANS turbulence model. Generally it was found that the predictive capability of the RANS turbulence model was not optimal, even in the non-reactive case of a variable density jet. By increasing the value of time scale ratio  $C_\phi$ , the degree of the predicted finite-rate effects increased, although correspondingly the error in scalar variance and flame length increased, making the generality of such an increase in  $C_\phi$  difficult to justify. Generally the mean flame length was predicted to be too short and this correlated with the predicted reaction rates being too high compared to the experiments. No significant differences in the predicted results were found between the modified Curl, EMST and IEM micro-mixing models.

The Cornell group (*Rowinski and Pope*) utilized a joint velocity-turbulence frequency-composition PDF model. Generally the mean and rms mixing fields were simulated well for all flames however the degree of reaction progress was systematically over predicted throughout the flame series. An exhaustive parameter sensitivity study was conducted and the primary source of error was concluded to be the modeling of the conditional diffusion term (the micro-mixing model). The importance of the jet to pilot velocity ratio on the variation of jet-pilot and jet-coflow interaction, hence finite-rate chemistry effects through the flame series was raised as an important parameter, experiments keeping this ratio constant were proposed to examine this effect.

Although one of the strengths of the PDF method is the ability to implement complex chemical mechanisms, a question was raised as to whether kinetic mechanisms (such as GRI 3.0) are suitably accurate for combustion of methane-air mixtures mixing with hydrogen-air combustion products, as occurs in the PPJB. The accurate prediction of the turbulent burning velocity in a premixed flame is a challenge for PDF models, and in particular there is a high sensitivity to the micro-mixing model. The fact that the use of different mixing models was shown to have such little impact on the predicted flame structure indicates that the sensitivity of the flame structure

to the predicted turbulent burning velocity is low in the PPJB flame series. This is quite different to the high sensitivity to the turbulent burning velocity experienced in more traditional turbulent premixed flames. One of the conclusions from the PDF calculations was the need for further calculations (DNS or highly resolved LES) and potentially experimental measurements of conditional diffusion to gain a better understanding of the performance of mixing models in highly turbulent premixed combustion for the regimes experienced in the PPJB. This is in the hope that such studies may provide further insight that leads to the formulation of improved or new mixing models. In PDF methods, although models for variable values of  $C_\phi$  seem well justified, it was shown that for the flames examined varying the value of  $C_\phi$  does not have a significant influence on improving the numerical predictions for the PPJB.

The Stanford group (*Mittal, Pitsch and Knudsten*) utilized an LES flamelet model combined with a level set G-Equation approach. A systematic investigation and validation of the mesh quality was presented using the velocity measurements from four non-reacting cases, which correspond to the bulk flow velocities of the four reacting cases. In addition, it was shown that correct inflow generation method for the jet and correct modeling of the chamfer on the pilot shroud were important to obtain good velocity field predictions. Utilizing the non-reacting case to validate the code, the mesh and boundary condition treatment was shown to be an important test to gain confidence in these parameters for the reacting cases. Preliminary results for all four reacting case results were presented, the results for the mixing fields were encouraging however, in general the mean flame length was predicted to be too short, indicating an over prediction of the reaction rate. Future developments of this modeling methodology will include an enhanced ability to incorporate finite-rate chemistry effects.

The Lund/Haldor Topsøe/ Hong Kong Polytechnic group (*Duwig, Nogenmyr and Chan*) presented an LES model termed integrated LES (ILES), where transport equations for all reactive species are solved and the reaction rates are determined directly from the filtered species transport equations. The results of a grid and chemical mechanism sensitivity study were presented for the PM1-100 flame. The results for the mixing fields, minor species (CO and OH) and temperature profiles for the PM1-50 and PM1-100 flames indicated that ILES is capable of good results for all of these measures in regions where the mesh is sufficiently fine ( $x/D < 20$ ). Preliminary results for the PM1-150 flame indicated that the ILES method is capable of closely capturing the initial ignition and subsequent extinction region of this flame. Further simulations will be required to see if the ILES method can capture the downstream re-ignition region of the PM1-150 flame and the PM1-200 flame in general. It was proposed that part of the success of this methodology to problems with strong finite-rate chemistry effects is that the characteristic chemistry progress variables are not neglected. It was shown that an important parameter for successful ILES simulations is that sufficient grid resolution must be utilized to resolve both the flame-front and the flow-fields. Because the ratio of the jet diameter to the flame-front thickness is relatively small for the PPJB, an ILES PPJB simulation requires only a relatively moderate (in terms of LES) computational cost for successful ILES results (e.g.  $D/40$  mesh resolution). Quantitative measures that determine when the ILES approach will be valid were presented as a work in progress and are under further development.

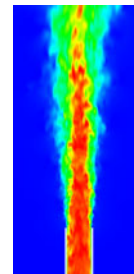
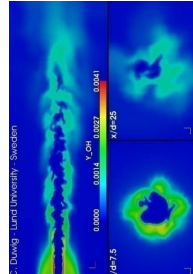
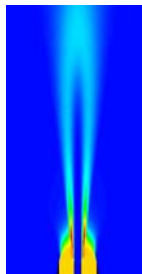
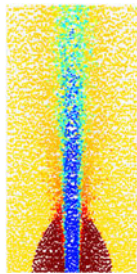
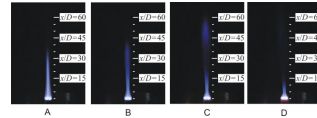
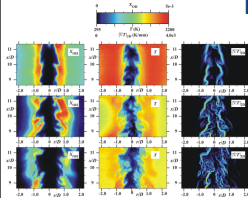
The RANS PDF modeling results presented were close to their final form and further improvements in the RANS PDF models predictive capabilities will most probably require the development of a revised or new micro-mixing model. Both of the LES results presented were preliminary results in that issues with boundary conditions, model development, and simulating the entire flames series (and flame length) are currently being resolved and may possibly deliver further improvement in the results compared to those presented at TNF10.

If significant new progress is made on the PPJB predictions before TNF11, it would be appropriate to have another PPJB session at TNF11. Any new individuals or groups interested in contributing simulations of the PPJB for TNF11 should contact Matthew Dunn ([mjdunn@sandia.gov](mailto:mjdunn@sandia.gov)) to obtain the experimental database.

# Comparisons of Experimental Measurements and Numerical Computations of the Piloted Premixed Jet Burner (PPJB)



Session co-ordinator  
Matthew J. Dunn



TNF 10 Workshop, Beijing 2010

## Contributors



### PPJB Measurements

Matthew J. Dunn<sup>1,2</sup>  
Assaad R. Masri<sup>2</sup>  
Robert W. Bilger<sup>2</sup>  
Robert S. Barlow<sup>1</sup>  
Guanghua Wang<sup>1</sup>

<sup>1</sup>CRF, Sandia National Laboratories  
<sup>2</sup>The University of Sydney



### Sydney PDF Calculations

Matthew J. Dunn<sup>2</sup>  
Assaad R. Masri<sup>2</sup>

<sup>2</sup>The University of Sydney



### Cornell PDF Calculations

David Rowinski<sup>3</sup>  
Steve Pope<sup>3</sup>

<sup>3</sup>Cornell University



LUND  
UNIVERSITY

### Lund LES Calculations

Christophe Duwig<sup>5,6</sup>  
Karl-Johan Nogenmyr<sup>7</sup>  
Cheong-ki Chan<sup>7</sup>

<sup>5</sup>Dept. of Energy Sciences, Lund University, Sweden

<sup>6</sup>Haldor Topsøe A/S, DK-2800 Lyngby

<sup>7</sup>Dept. Applied Mathematics, The Hong Kong Polytechnic University



### Stanford LES Calculations

Varun Mittal<sup>4</sup>  
Heinz Pitsch<sup>4</sup>  
Ed Knudsen<sup>4</sup>

<sup>4</sup>Stanford University

TNF 10 Workshop, Beijing 2010

## Overview

- PPJB development and measurements (Sydney and Sandia)
- RANS PDF computations (Sydney and Cornell) -> PDF discussion
- LES computations (Lund and Stanford) -> LES discussion

TNF 10 Workshop, Beijing 2010

## Burner Development and Measurements



### PPJB Development and Measurements

Matthew J. Dunn<sup>1,2</sup>

Assaad R. Masri<sup>2</sup>

Robert W. Bilger<sup>2</sup>

Robert S. Barlow<sup>1</sup>

Guanghua Wang<sup>1</sup>

<sup>1</sup>CRF, Sandia National Laboratories

<sup>2</sup>The University of Sydney

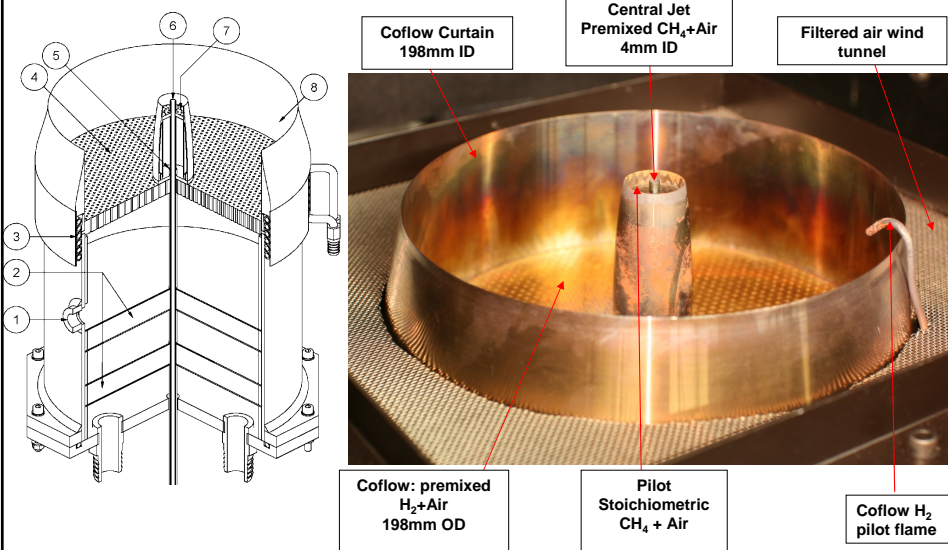
TNF 10 Workshop, Beijing 2010

## Motivation and Aim of Burner Development

- Successes of non-premixed target flames in the TNF workshop
- Platform for success has been to provide well documented parametric flame series measurements that feature varying degrees of turbulence chemistry effects
- Comparatively little development in highly turbulent premixed combustion
- Develop a burner to study finite-rate chemistry effects

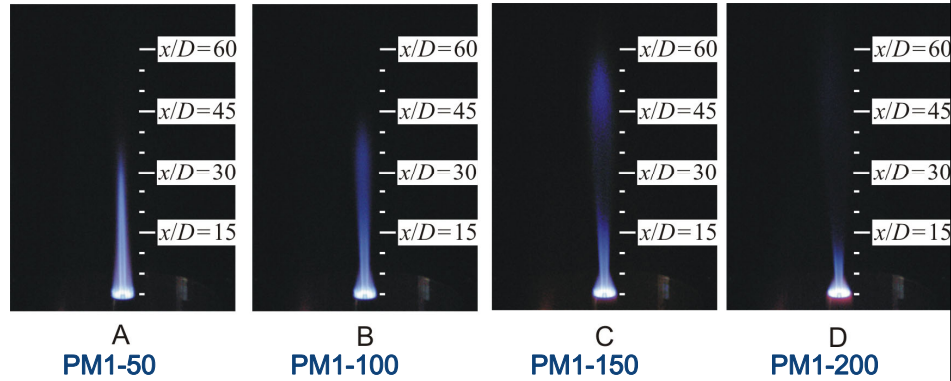
TNF 10 Workshop, Beijing 2010

## PPJB Overview



TNF 10 Workshop, Beijing 2010

## PPJB PM1 Flame Selection



- Transition for central jet velocities 50, 100, 150 and 200m/s:
  - ( $Re \sim 12500, 25000, 37500$  and  $50000$ ),  $T_{\text{Coflow}} = 1500\text{K}$ ,  $\phi_{\text{Jet}} = 0.5$

TNF 10 Workshop, Beijing 2010

## Burner Practical Relevance

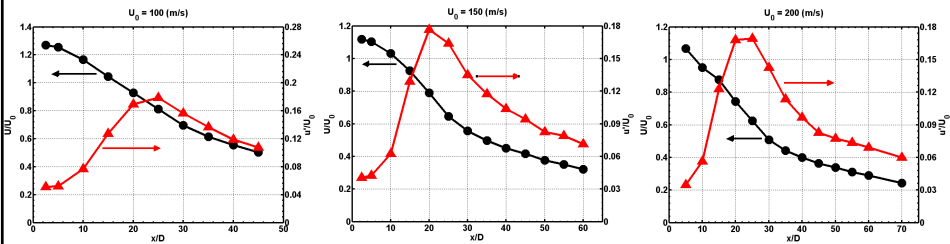
- Relevant to many lean premixed and lean pre-vaporized gas turbine combustors – why?
  - Primary flow of lean pre-mixture stabilized by a near stoichiometric pilot
  - Vary the main flow to vary turn down ratio
- 2nd method to achieve turn down ratio in gas turbines: inject small diameters jets at high velocity of lean pre-mixture into a hot cross flow of lean combustion products
  - Burner does not examine the very complex fluid mechanics of a jet in a cross flow
  - It does allow the study of the turbulence chemistry interaction (similar chemical and turbulence time scales) that is key to stabilizing the jet in hot cross flow problem
- Complications of swirl, recirculation, radiation, heat transfer are removed and the interaction of turbulence chemistry is focused on

TNF 10 Workshop, Beijing 2010

## Velocity and Non-Dimensional Parameters

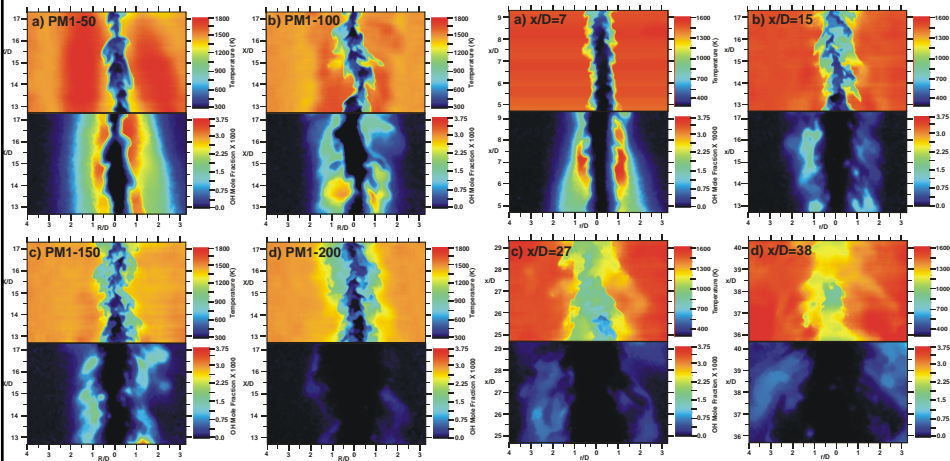
**Table 1** Non-dimensional parameters for the four PM1 series flames

Flame code	$U_0$ (m/s)	$Re$	$q'/S_L$	$\ell_0/\delta_{th}$	$\delta_{th}/\eta$	$Re_t$	$Ka$	$Da$
PM1-50	50	12,500	49.8	2.40	57.1	705	142	0.0482
PM1-100	100	25,000	277	1.78	223	2,923	2,173	0.0064
PM1-150	150	37,500	359	1.64	276	3,486	3,326	0.0046
PM1-200	200	50,000	470	1.79	331	4,979	4,776	0.0038



TNF 10 Workshop, Beijing 2010

## Large Image Region Temperature-OH Imaging

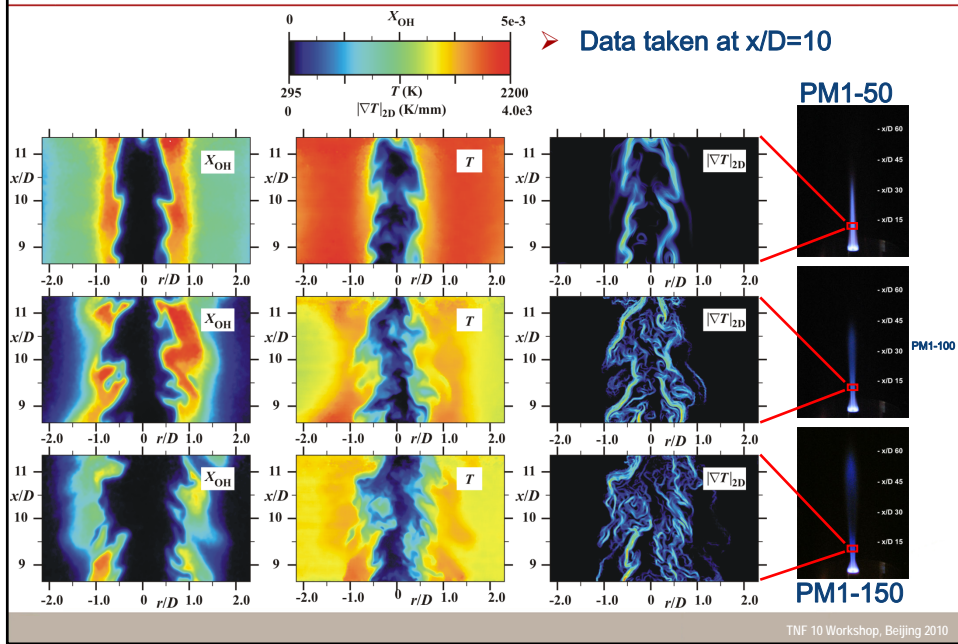


PM1 flame series @  $x/D=15$

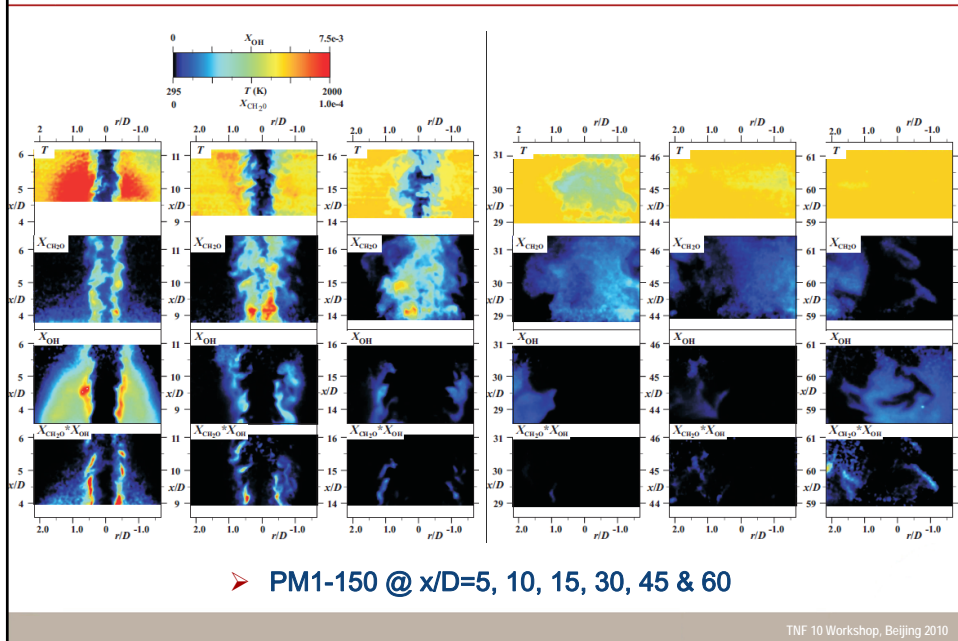
PM1-150 @  $x/D=7, 15, 27$  &  $38$

TNF 10 Workshop, Beijing 2010

## High Resolution Temperature-OH images

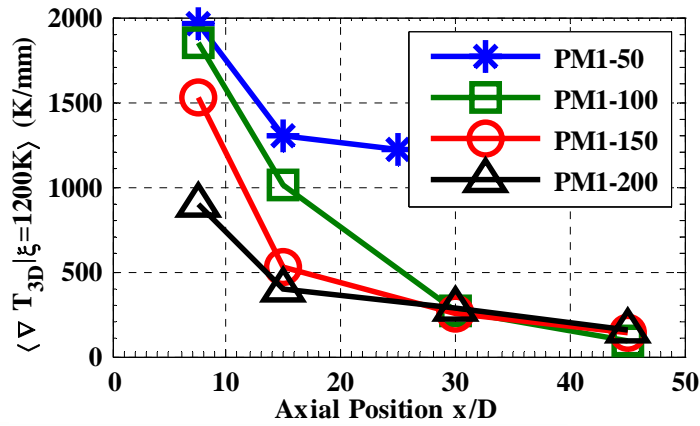


## Temperature-OH-CH<sub>2</sub>O Images



### 3D Temperature Gradients

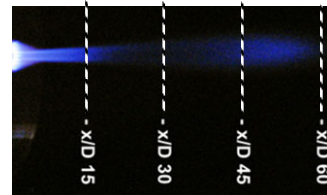
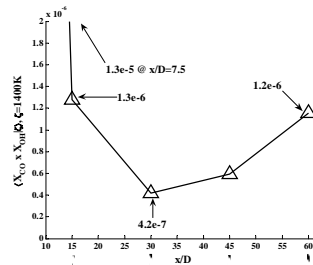
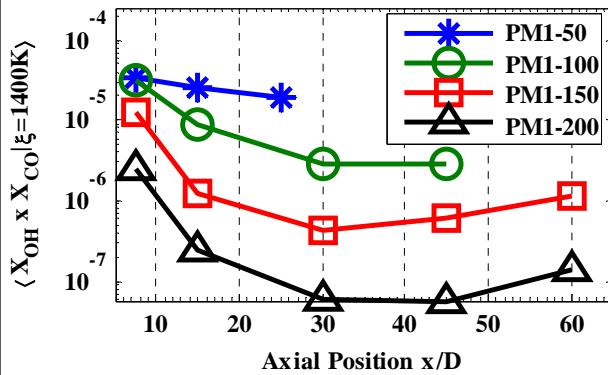
- Compare the corrected conditional 3D gradient across all flames as a function of axial location
- Decrease in gradient with increased turbulence intensity (jet velocity)



TNF 10 Workshop, Beijing 2010

### Application of $\langle [CO][OH] | T \rangle$ to PM1 Flame Series

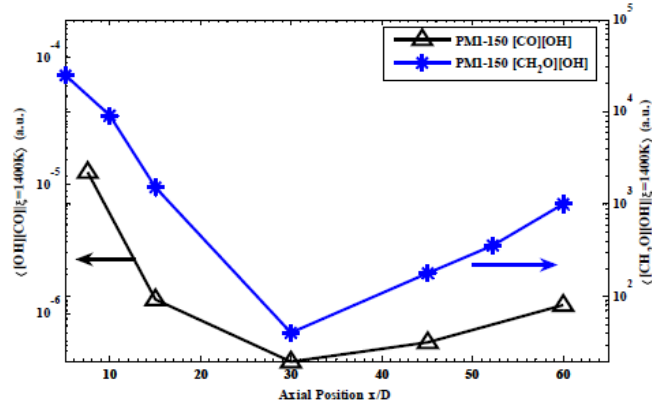
- Results for all flames  $\langle [CO][OH] | \xi = 1400K \rangle$



PM1-150

TNF 10 Workshop, Beijing 2010

## Ignition, Extinction & Re-ignition Hypothesis



- Ignition, extinction then re-ignition hypothesis for the PM1-150 confirmed using two methods

TNF 10 Workshop, Beijing 2010

## Mixture Fractions

- Distinct advantage of using a H<sub>2</sub>-air hot coflow vs. a hydrocarbon-air based hot coflow:
- Can formulate a mixture fraction for each stream (jet, pilot and coflow)

	C	H	O	N
<b>1 (Jet)</b>	0.02127	0.00709	0.2263	0.74534
<b>2 (Pilot)</b>	0.041272	0.013767	0.220172	0.72478
<b>3 (Coflow)</b>	0	0.012373	0.230087	0.75754

$$\xi_{Jet} = \frac{Z_C (Z_{H,Coflow} - Z_{H,Pilot}) + Z_{C,Pilot} (Z_H - Z_{H,Coflow})}{Z_{C,Jet} (Z_{H,Coflow} - Z_{H,Pilot}) + Z_{C,Pilot} (Z_{H,Jet} - Z_{H,Coflow})}$$

$$\xi_{Pilot} = \frac{Z_C (Z_{H,Jet} - Z_{H,Coflow}) + Z_{C,Jet} (Z_{H,Coflow} - Z_H)}{Z_{C,Jet} (Z_{H,Coflow} - Z_{H,Pilot}) + Z_{C,Pilot} (Z_{H,Jet} - Z_{H,Coflow})}$$

$$\xi_{Coflow} = \frac{Z_C (Z_{H,Pilot} - Z_{H,Jet}) + Z_{C,Jet} (Z_H - Z_{H,Pilot}) + Z_{C,2} (Z_{H,Jet} - Z_H)}{Z_{C,Jet} (Z_{H,Coflow} - Z_{H,Pilot}) + Z_{C,Pilot} (Z_{H,Jet} - Z_{H,Coflow})}$$

TNF 10 Workshop, Beijing 2010

## Reaction Progress Variable

- All major species measured plus CO, H<sub>2</sub> and OH:
  - Calculate an adiabatic flame temperature for each measured pixel based on measured species and temperature
  - Use mixture fraction to determine local unburnt value
    - T<sub>u</sub>=300K jet and coflow, T<sub>u</sub>=400K pilot
  - Iterative algorithm using NASA temperature dependant enthalpy polynomials for resolved species, better than 1% accurate

$$C = \frac{T - T_u(\xi_j)}{T_{ad}(T, X_i) - T_u(\xi_j)} = \frac{T - 100(3 + \xi_{pilot})}{T_{ad}(T, X_i) - 100(3 + \xi_{pilot})}$$

TNF 10 Workshop, Beijing 2010

## General Presentation Conclusions (Experiments)

- An experimental platform for the detailed study of finite rate chemistry effects in premixed combustion (the PPJB) has been developed and characterized
- Under certain conditions the burner exhibits a region of initial ignition followed by extinction then re-ignition
- Imaging results indicate a trend of increased thickening with increasing turbulence intensity
- Detailed measurements of the flow-field, the scalar field and minor species support a detailed database of measurements to make this burner a suitably well documented benchmark case for modelers

TNF 10 Workshop, Beijing 2010

## PDF Calculations

- Results from the Sydney group and the Cornell group
- Different approaches similar conclusions
- Important fundamental questions for PDF methods applied to turbulent premixed combustion are raised

TNF 10 Workshop, Beijing 2010

## Sydney PDF Calculations



### Sydney PDF Calculations

Matthew J. Dunn<sup>2</sup>  
Assaad R. Masri<sup>2</sup>

<sup>2</sup> *The University of Sydney*

TNF 10 Workshop, Beijing 2010

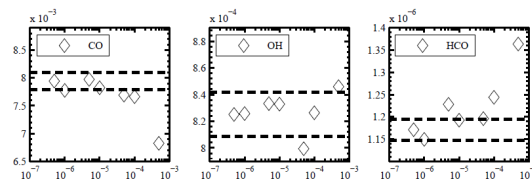
## Model Formulation

- RANS turbulence model and transported PDF for thermo-chemistry
  
- RANS turbulence models
  - $k-\varepsilon$  (std., RNG)
  - $k-\omega$  (Std., SST)
  - Reynolds Stress
  
- Chemistry
  - **DRM22/DRM19**
  - ARM1/ARM2
  
- Mixing models
  - Modified Curl (MC)
  - EMST
  - IEM

TNF 10 Workshop, Beijing 2010

## Domain, Model & Boundary Conditions

- 2D axisymmetric domain, flame region  $20D \times 120D$
  
- 35k cells
  
- 80ppc, (~20ppc ok but 80ppc converges statistics faster)
  
- ISAT  $\varepsilon_{\text{tol}}=5\text{e-}6$ , ~<2% error, ( $\varepsilon_{\text{tol}}=1\text{e-}5$  ~<5% error ~ still ok),

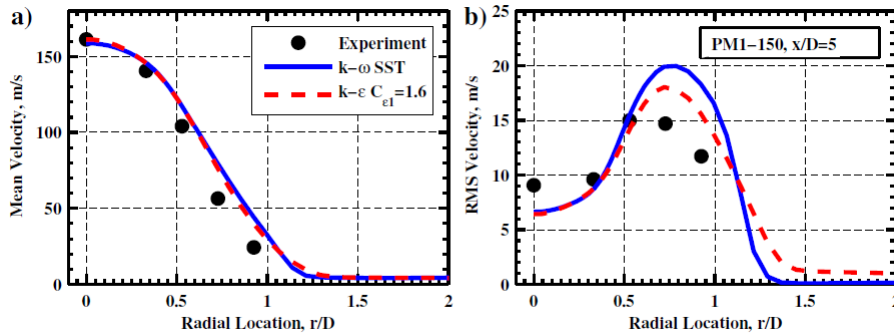


- $C_{\varepsilon 1}=1.44$  & 1.6 for  $k-\varepsilon$  model

TNF 10 Workshop, Beijing 2010

## Focus on PM1-150 Initial Conditions

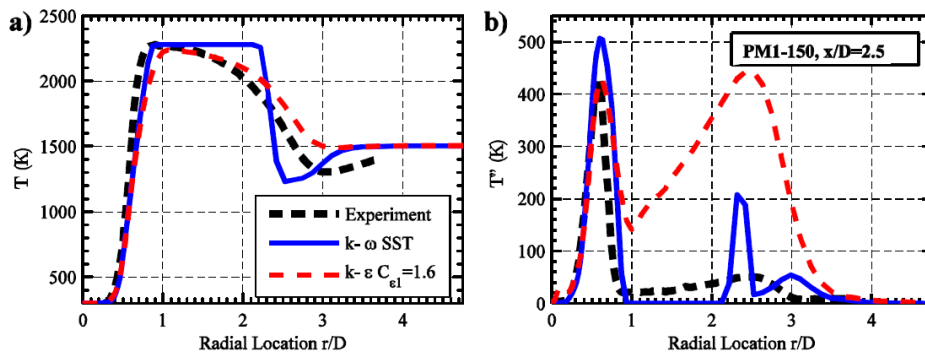
- Base case(s) EMST,  $C_\varphi=1.5$ ,  $k-\varepsilon$  ( $C_{\varepsilon 1}=1.6$ ) and  $k-\omega$ -SST
- Are the initial velocity field conditions (@  $x/D=2.5$ ) correctly predicted?



TNF 10 Workshop, Beijing 2010

## Focus on PM1-150 Initial Conditions

- Are the initial scalar field conditions (@  $x/D=2.5$ ) correctly predicted?

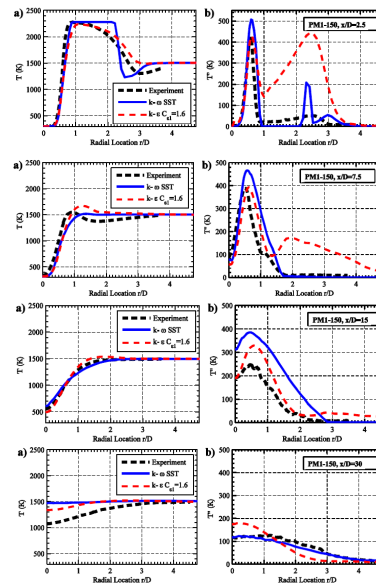


TNF 10 Workshop, Beijing 2010

## Focus on PM1-150 Scalar Results

➤ Is the scalar field simulated correctly?

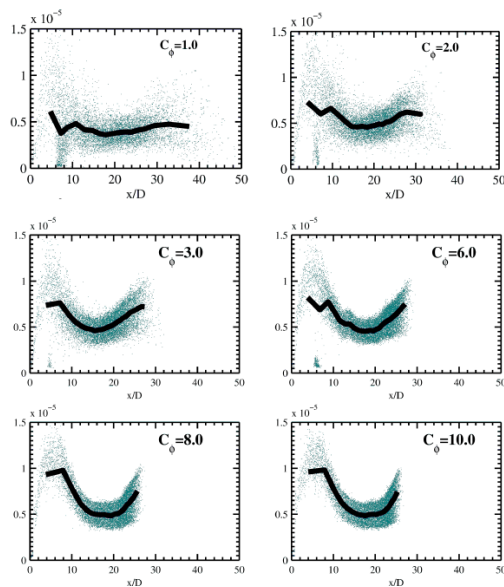
- Flame predicted to be too short
- Peak scalar variance ok, typically to within 20%



TNF 10 Workshop, Beijing 2010

## Finite-Rate Chemistry for PM1-150

- Necessary to change  $C_\phi$  from 1.5 to 6-8 to get significant finite-rate chemistry effects
- Increasing  $C_\phi$  reduces the mean flame length even further!



TNF 10 Workshop, Beijing 2010

## Focus on PM1-150

- Reasonable argument that the time scale ratio is not constant in a premixed flame
- Time scale models
  - Lindstedt *et al.* fractal based closure
  - Recent scalar dissipation models published by Swaminathan *et al.*
- Both seem to give similar results to the constant  $C_\phi=4-6$  cases? What is going on here???

TNF 10 Workshop, Beijing 2010

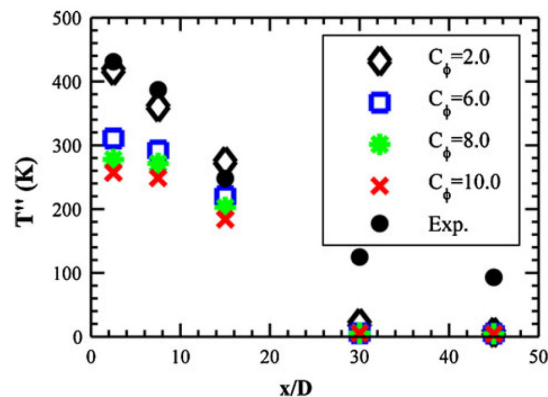
## Focus on PM1-150

- From our knowledge of the optimal value or model for  $C_\phi$  from non-premixed combustion, the correct  $C_\phi$  value or model must also get scalar variance correct

- $C_\phi = 1.5-2.0$  optimal!

- Virtually Identical graphs for:

- EMST (as shown)
- IEM
- MC



TNF 10 Workshop, Beijing 2010

## Sydney PDF Calculation Conclusions (1/2)

- Conventional RANS turbulence models struggle to accurately predict variable density jets (even in the non-reacting case), of the many RANS turbulence models evaluated, the  $k-\varepsilon$  ( $C_{\varepsilon 1}=1.6$ ) and  $k-\omega$ -SST turbulence models seem to perform better than other models tested
- Generally values of  $C_{\varphi}$  in the range 6-8 are required to produce modest degrees of finite-rate chemistry effects for the PM1-150 and PM1-200 flames, reaction-rate reductions that are of an order of magnitude which are observed in the experiments are not possible by simply further increasing  $C_{\varphi}$
- All of the PM1 mean flame lengths are predicted to be too short, implying that the mean reaction rates are over-predicted, increasing  $C_{\varphi}$  only exacerbates this problem

TNF 10 Workshop, Beijing 2010

## Sydney PDF Calculation Conclusions (2/2)

- Though variable time-scale ratio models are well justified, they do not improve the results significantly over constant values of  $C_{\varphi}$
- The optimal value of  $C_{\varphi}$  based on optimizing the scalar variance predictions is in the range 1.5-2.0, which is in agreement with previous results for non-premixed combustion
- No significant improvement in the results between any of the three mixing models evaluated (EMST, MC, IEM) is found
- No significant differences (only computational cost) in the results for ARM1&2 and DRM19&22 mechanisms, though all are based on GRI

TNF 10 Workshop, Beijing 2010

## Cornell PDF Calculations

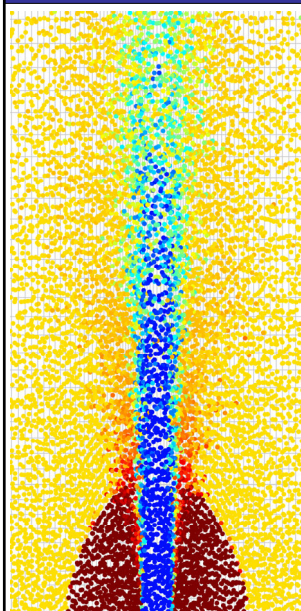


### Cornell PDF Calculations

David Rowinski<sup>3</sup>  
Steve Pope<sup>3</sup>

<sup>3</sup>*Cornell University*

TNF 10 Workshop, Beijing 2010



## RANS-PDF calculations of the Sydney PPJB

David Rowinski and Steve Pope  
*Cornell University*

**10<sup>th</sup> TNF Workshop**  
**Beijing, China**  
**July 30, 2010**

July 30, 2010

10th TNF Workshop

1/28

## Outline

### Comprehensive study of the Sydney PPJB

Rowinski and Pope (2010) "PDF calculations of piloted premixed jet flames",  
*Combustion Theory and Modelling* (submitted)

[www.eccentric.mae.cornell.edu/~tcg](http://www.eccentric.mae.cornell.edu/~tcg)

- Formulation – Joint PDF
- Base case
  - PM1-50:  $U_j = 50$  m/s,  $U_p = 5.3$  m/s,  $U_p/U_j = 0.11$   
*Accurate calculations of mixture fractions and species*
  - PM1-200:  $U_j = 200$  m/s,  $U_p = 5.3$  m/s,  $U_p/U_j = 0.027$   
*Accurate mixture fractions, but reaction overpredicted*
- Sensitivity studies and diagnostic tests of PM1-200
- Conclusions and future work

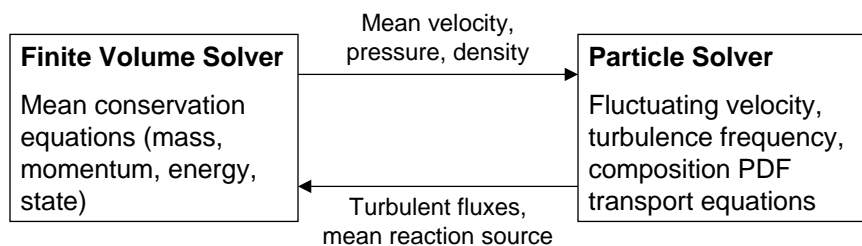
July 30, 2010

10th TNF Workshop

2/28

## Formulation – Joint PDF

- Joint velocity-turbulence frequency-composition PDF method
  - Simplified Langevin model for particle velocity
  - Stochastic frequency model for turbulent frequency
  - EMST mixing model
  - Detailed chemical mechanism, ARM-1 [GRI3.0, et al.]
  - Same method used in many previous studies (e.g., Cao et al. 2005, Wang and Pope 2008)
- Hybrid finite-volume / particle solver

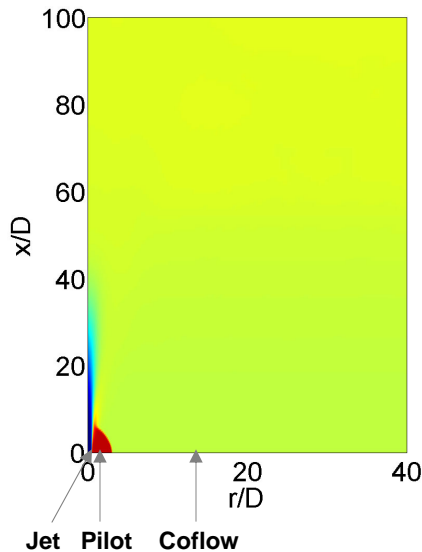


July 30, 2010

10th TNF Workshop

3/28

## Domain and boundary conditions



- Polar cylindrical domain  $(x,r)$  of size  $100D \times 40D$
- Three inlet streams
  - **Jet:** lean ( $\phi=0.5$ ), premixed  $\text{CH}_4/\text{air}$ , 300 K
  - **Pilot:** stoichiometric  $\text{CH}_4/\text{air}$  products, 2280 K
  - **Coflow:** lean ( $\phi=0.43$ )  $\text{H}_2/\text{air}$  products, 1500 K
- Velocity at inlet prescribed from separate calculations on extended domain, going  $100D$  upstream of burner exit plane

July 30, 2010

10th TNF Workshop

4/28

## Base case

- Numerical parameters
  - $144 \times 144$  cells
  - 50 particles per cell
  - 4,000 iterations of time-averaging
  - Maximum numerical errors
    - ~5% for mean of major species, mixture fraction, temperature
    - ~8% for mean of minor species
- Model parameters
  - EMST mixing model,  $C_\phi=1.5$
  - ARM-1 reduced methane mechanism, 16 species
  - Turbulence model constant,  $C_{\omega 1} = 0.7$  (controls jet spreading rate)

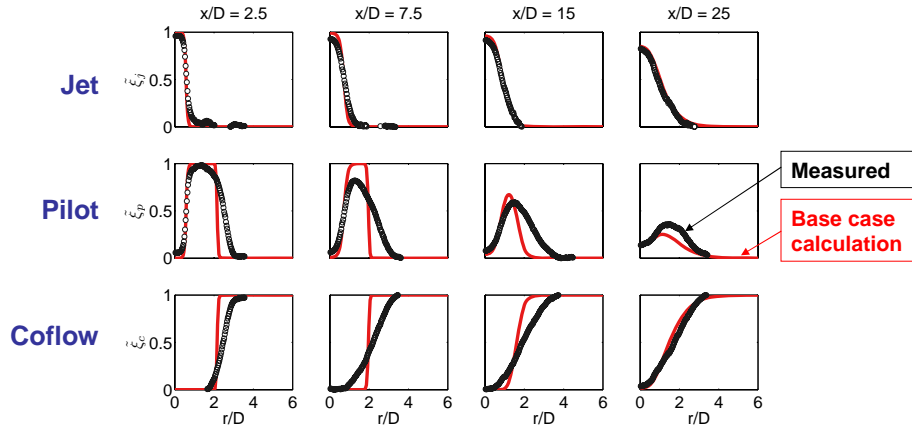
July 30, 2010

10th TNF Workshop

5/28

## Base case PM1-50

### PM1-50, mean mixture fraction fields



- Calculated initial pilot/coflow mixing slower than measured
  - Limited to region of minor importance for reaction of jet fuel
- Mixing in jet/pilot region is well calculated

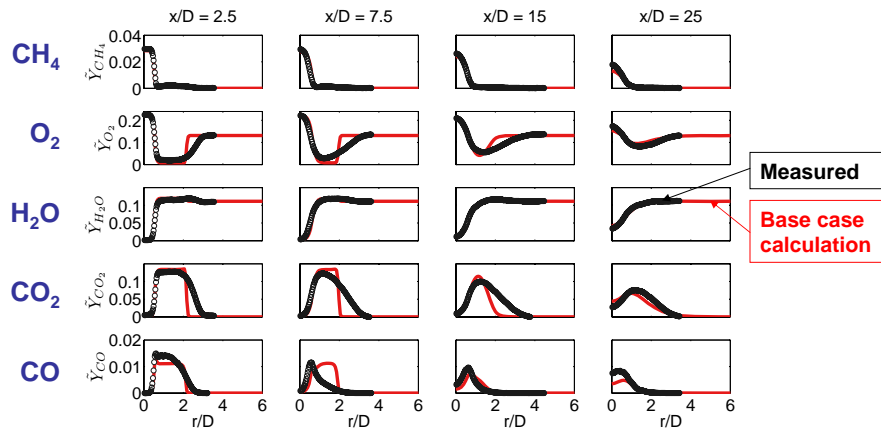
July 30, 2010

10th TNF Workshop

7/28

## Base case PM1-50

### PM1-50, mean mass fraction of selected species



- Discrepancy in pilot/coflow mixing evident
- Otherwise, good agreement in major species

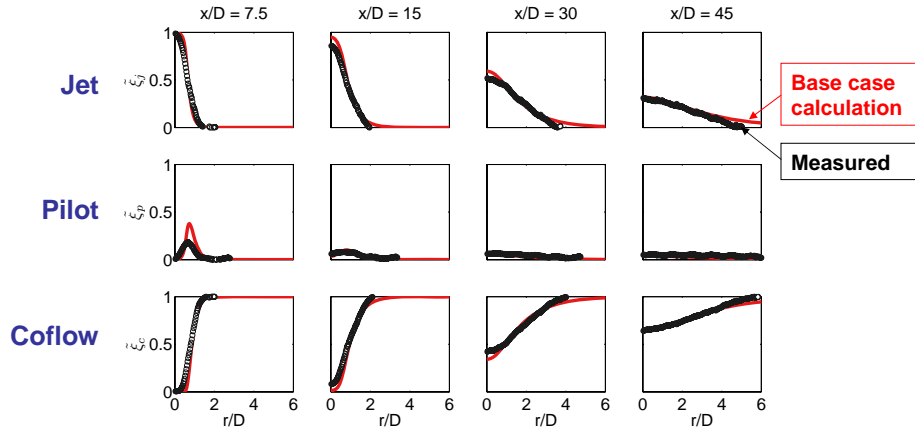
July 30, 2010

10th TNF Workshop

8/28

## Base case PM1-200

### PM1-200, mean mixture fraction fields



- Excellent agreement in mixture fractions downstream
- Rapid decay of  $\tilde{\zeta}_p$  due to strong jet entrainment

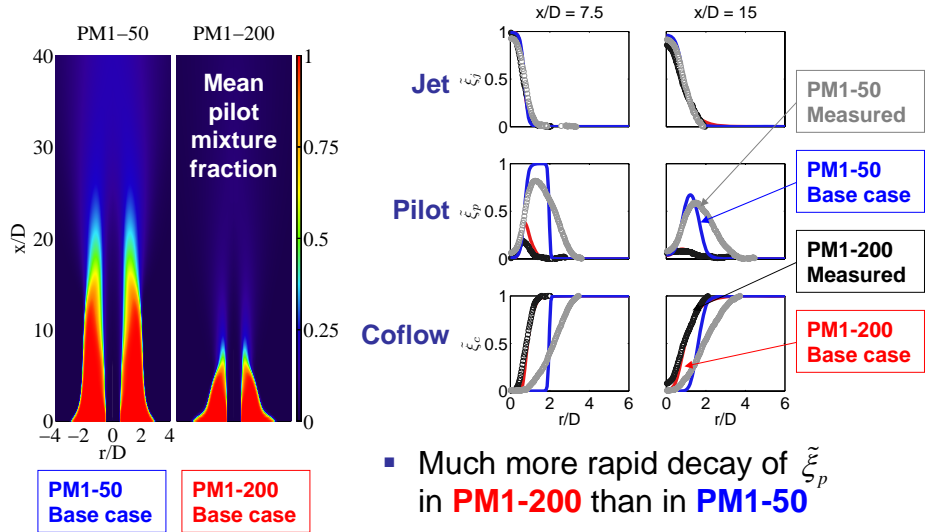
July 30, 2010

10th TNF Workshop

10/28

## Coflow entrainment / pilot shielding

### PM1-200 and PM1-50, mean mixture fraction fields



- Much more rapid decay of  $\tilde{\zeta}_p$  in **PM1-200** than in **PM1-50**

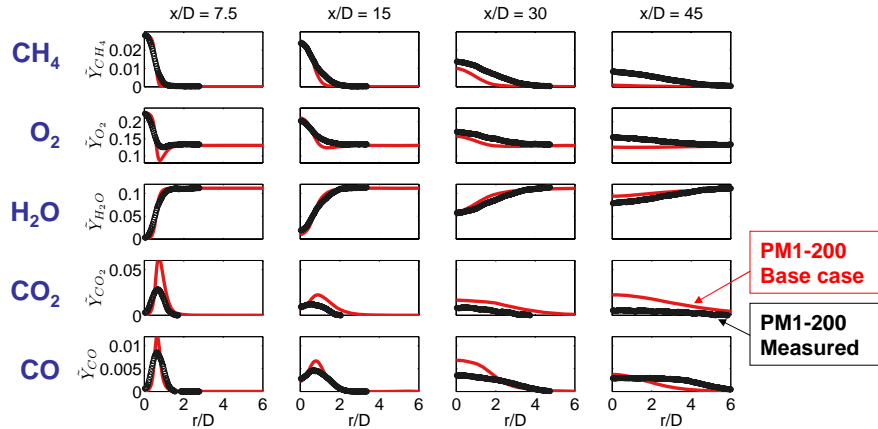
July 30, 2010

10th TNF Workshop

11/28

## Base case PM1-200

- PM1-200, mean mass fraction of selected species



- Despite accurate calculations of mixture fraction, reaction progress is overpredicted in PM1-200, unlike PM1-50

July 30, 2010

10th TNF Workshop

12/28

## Base case

- Summary of base case calculations
  - PM1-50
    - Both mixture fractions and major species in reasonable agreement with measurements in jet/pilot region
  - PM1-200
    - Mixing pattern of streams in good agreement with measurements
    - Reaction progress overpredicted downstream

July 30, 2010

10th TNF Workshop

13/28

## Sensitivity studies of PM1-200

- Inlet boundary specification ( $\tilde{u}, u'', \omega, T$ )
- Turbulence spreading constant,  $C_{\omega 1}$ , from 0.5 to 0.75
- Mixing models and constants
  - EMST, IEM, MC;  $C_{\phi}$  from 1 to 12
- Chemical mechanisms (ARM-1, GRI 3.0, ...)
- Radiation treatment (optically-thin radiation model)
  
- Approximately 60 runs in this set
- Finding: no studied combination of parameters above produces the observed reaction progress in PM1-200

July 30, 2010

10th TNF Workshop

14/28

## Sensitivity studies of PM1-200

- Inlet boundary specification ( $\tilde{u}, u'', \omega, T$ )
- Turbulence spreading constant,  $C_{\omega 1}$ , from 0.5 to 0.75
- Mixing models and constants
  - EMST, IEM, MC;  $C_{\phi}$  from 1 to 12
- Chemical mechanisms (ARM-1, GRI 3.0, ...)
- Radiation treatment (optically-thin radiation model)
  
- Approximately 60 runs in this set
- Finding: no studied combination of parameters above produces the observed reaction progress in PM1-200
  
- Modeling of molecular mixing remains most likely cause of inaccuracy

July 30, 2010

10th TNF Workshop

15/28

## Diagnostic tests

- Extent of reaction progress overprediction investigated by artificially attenuating chemistry
- Factor  $f_R$  introduced, chemical source term  $S$  replaced by  $f_R S$
- Reaction fractional step performed for time  $f_R \Delta t$  (instead of  $\Delta t$ )
- $f_R = 1$  unperturbed
- $f_R = 0$  inert (no change due to reaction)

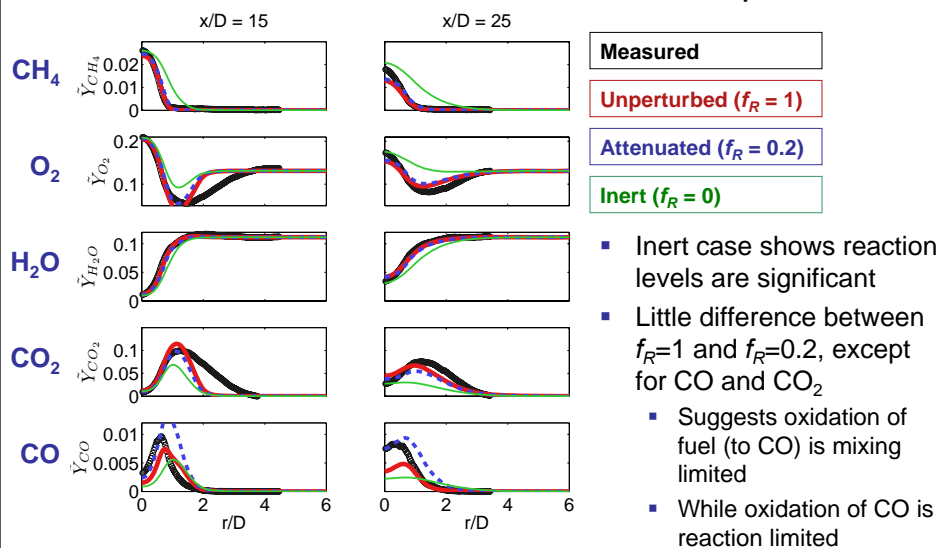
July 30, 2010

10th TNF Workshop

16/28

## Diagnostic tests

- PM1-50, mean mass fraction of selected species



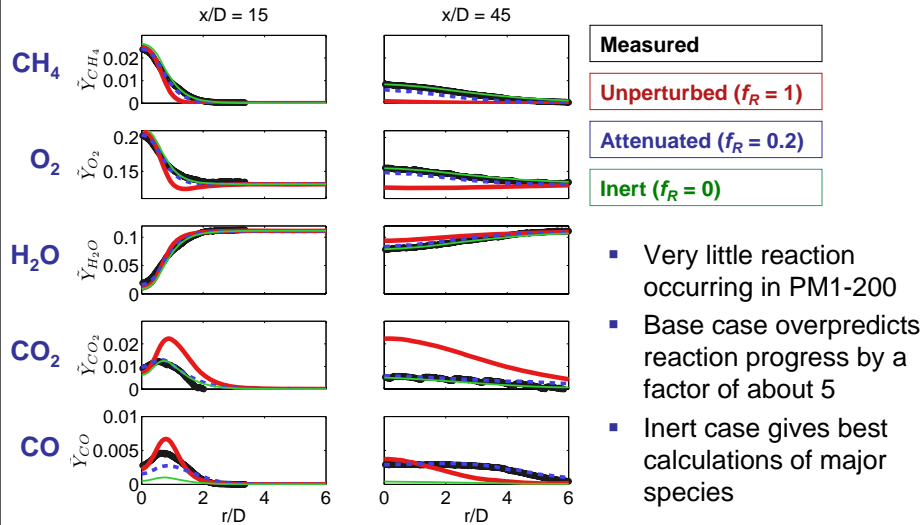
July 30, 2010

10th TNF Workshop

17/28

## Diagnostic tests

### PM1-200, mean mass fraction of selected species



July 30, 2010

10th TNF Workshop

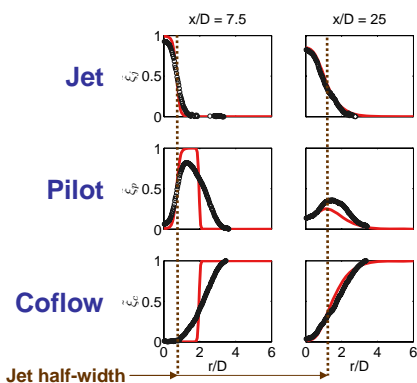
18/28

## Finite-rate chemistry

- As in Dunn et al. (2009), finite-rate chemistry effects investigated by comparison to simpler laminar flames
- PM1-50 is dominated by jet and pilot

### Mean mixture fractions at jet half width:

- $x/D = 7.5$ 
  - Jet: 0.5
  - Pilot: 0.5
  - Coflow: < 0.01
- $x/D = 25$ 
  - Jet: 0.45
  - Pilot: 0.25
  - Coflow: 0.3



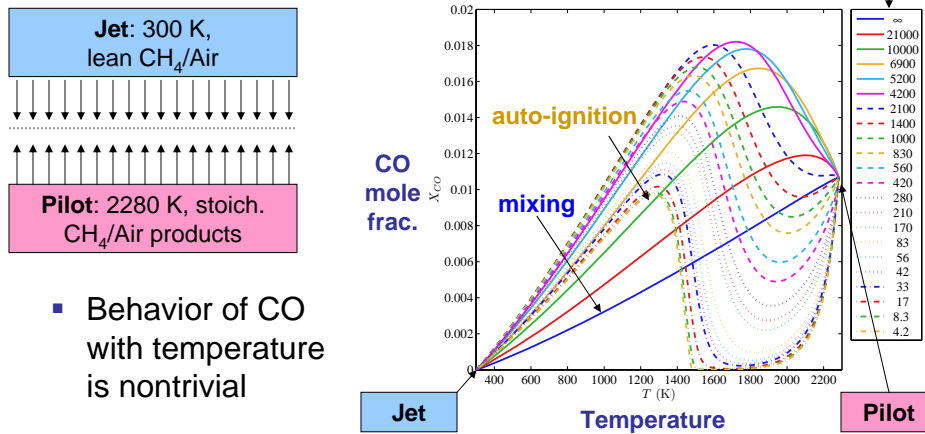
July 30, 2010

10th TNF Workshop

19/28

# Finite-rate chemistry in PM1-50

- PM1-50 compared to laminar opposed flow flame of the **jet** and **pilot** compositions



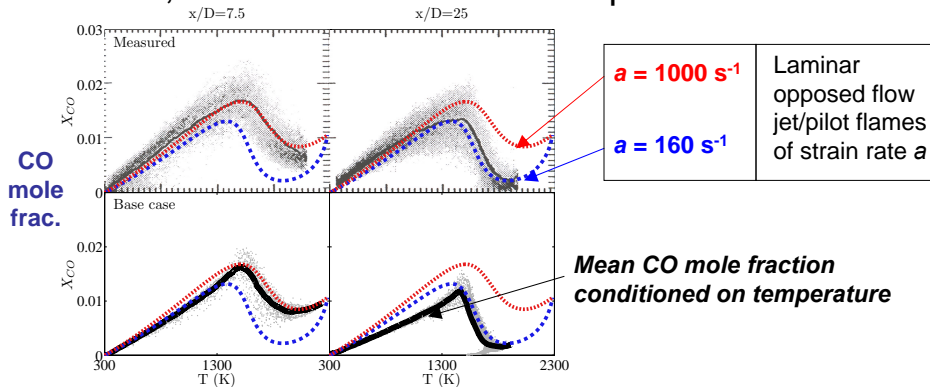
July 30, 2010

10th TNF Workshop

20/28

# Finite-rate chemistry in PM1-50

- PM1-50, CO mole fraction vs. Temperature



- Both calculations and measurements of CO vs.  $T$  in PM1-50 resemble that in laminar jet/pilot flames
- Strain rate of corresponding laminar flames decreases downstream

July 30, 2010

10th TNF Workshop

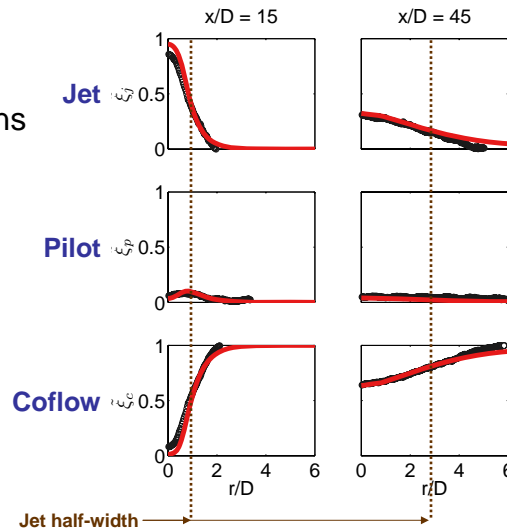
21/28

## Finite-rate chemistry in PM1-200

- PM1-200 is dominated by jet and coflow at regions of interest

- Mean mixture fractions at jet half width:

- $x/D = 15$ 
  - Jet: 0.4
  - Pilot: 0.1
  - Coflow: 0.5
- $x/D = 45$ 
  - Jet: 0.15
  - Pilot:  $< 0.01$
  - Coflow: 0.85



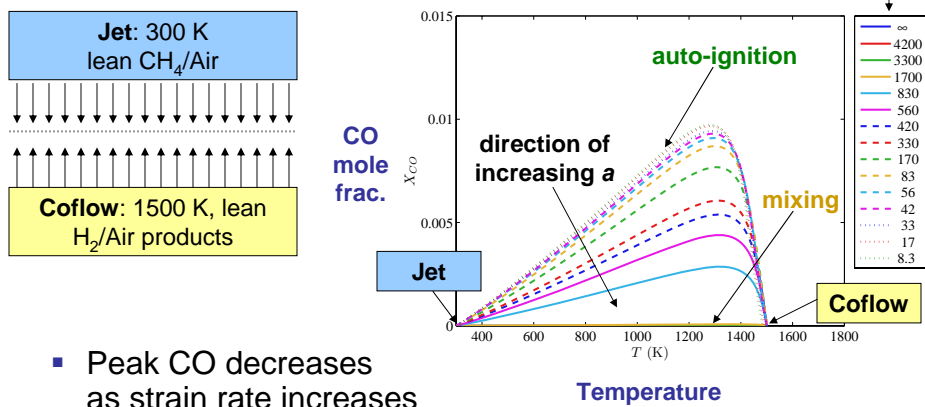
July 30, 2010

10th TNF Workshop

22/28

## Finite-rate chemistry in PM1-200

- PM1-200 compared to **a different flame**: laminar opposed flow flame of the **jet** and **coflow** compositions



- Peak CO decreases as strain rate increases

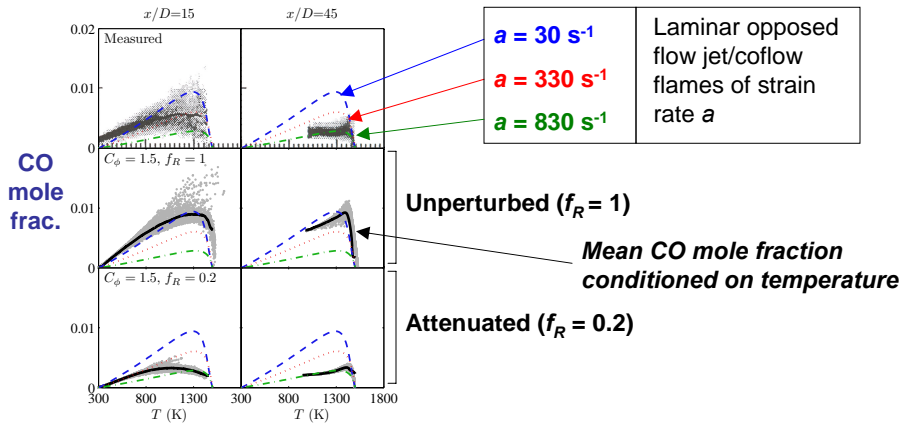
July 30, 2010

10th TNF Workshop

23/28

## Finite-rate chemistry in PM1-200

### PM1-200, CO mole fraction vs. Temperature



- Strain rate of corresponding laminar flame increases downstream
- Unperturbed chemistry corresponds to laminar flames of lower  $a$
- Laminar flames of higher strain rate correspond with  $f_R=0.2$

July 30, 2010

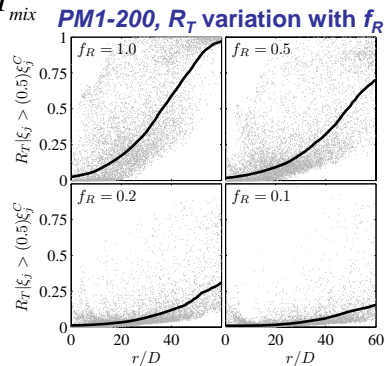
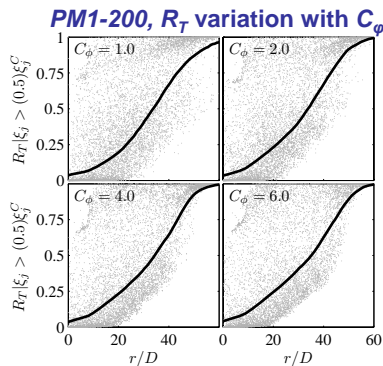
10th TNF Workshop

24/28

## Finite-rate chemistry

- To assess level of reaction progress, reaction index based on temperature is evaluated

$$R_T = \frac{T - T_{mix}}{T_{eq} - T_{mix}}$$



- $C_\phi$  has little effect on  $R_T$
- Most likely  $R_T$  from  $f_R$  of 0.1-0.2 is most accurate, needs to be tested

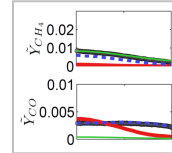
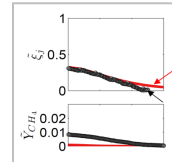
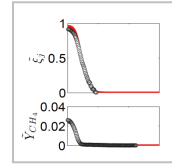
July 30, 2010

10th TNF Workshop

25/28

## Conclusions

- Good performance of RANS-PDF and base case models in PM1-50
  - Mixture fractions, major species, CO vs. T
- Calculations of PM1-200 prove more difficult
  - Mixture fractions calculated accurately
  - Reaction progress overpredicted
- Sensitivity studies of PM1-200 show no set of models/parameters that produce observed reaction progress
  - However, diagnostic calculations with  $f_R=0.2$  agree well, help validate measurements, and confirm base case overprediction of reaction progress



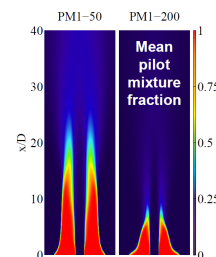
July 30, 2010

10th TNF Workshop

26/28

## Conclusions

- Most likely cause of reaction progress discrepancy identified as modeling of molecular diffusion by the mixing models
  - Transport appears to be calculated adequately
  - Reaction is treated exactly
- The flames are not geometrically similar; the jet/pilot region is much shorter in PM1-200.
  - Flame behavior appears very different in jet/pilot and jet/coflow regions
  - Raises the question as to whether the differences among the flames in this series are due to the change in  $U_j$  or the difference in geometry ( $U_p/U_j$ )



July 30, 2010

10th TNF Workshop

27/28

## Future work

- Importance of pilot shielding
  - Could be tested experimentally by maintaining a constant ratio  $U_p/U_j$  among the flames
- Quantification of reaction levels
  - Could be determined from measurements through  $R_T$  or similar progress variable
- Understanding details of mixing process
  - Could be brought to light through examining instantaneous and conditional diffusion obtained from either (1) measurements or (2) more detailed calculations (e.g., LES-PDF, DNS)

July 30, 2010

10th TNF Workshop

28/28

## Open Discussion Topics for PDF Calculations

- Time scale ratio models? Are time scale ratio models enough?
- Problems with model assumptions?
- How to improve mixing models for PDF calculations?
  - How to incorporate molecular properties
  - How to incorporate Re dependence
  - Future measurements? How helpful would an experimental measurement (high Re) of conditional diffusion be?
  - Could DNS databases be useful?

TNF 10 Workshop, Beijing 2010

## Stanford LES Calculations



### Modeling of a Premixed Flame with Strong Finite-rate Chemistry effects

Varun Mittal<sup>4</sup>

Heinz Pitsch<sup>4</sup>

<sup>4</sup>*Stanford University*

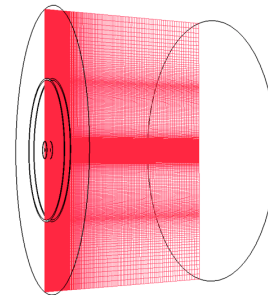
## Simulation Parameters

- High Order Kinetic energy conserving code<sup>1</sup>
- Structured Domain
- Cylindrical coordinate system
- LES with
  - Dynamic Smagorinsky model
  - Lagrangian averaging

<sup>1</sup> O. Desjardins, G. Blanquart, G. Balarac, H. Pitsch, High order conservative finite difference scheme for variable density low Mach number turbulent flows, Journal of Computational Physics 227 (2008) 7125-7159

## Simulation Grid

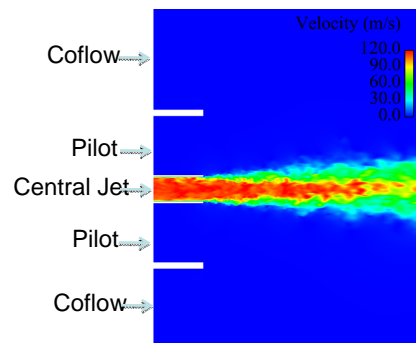
- Entire setup modeled using a structured grid
- Two different grid size used
  - 4.2 million (Coarse)
  - 9.4 million (Refined)
- Stretching used to accurately resolve the shear regions in the domain
- Points across Central Jet
  - 48 (Coarse)
  - 92 (Refined)



Simulation Grid

## Boundary Conditions

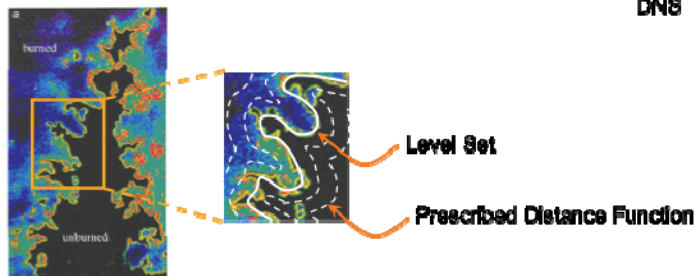
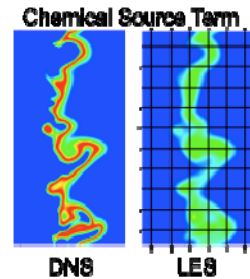
- Inlet
  - Central Jet
    - » Inflow profile generated through simulation of a fully developed pipe
    - » Profile prescribed 2D (8 mm) upstream of the nozzle
  - Pilot, Coflow
    - » Uniform velocity profile
- Outlet
  - Convective outflow used



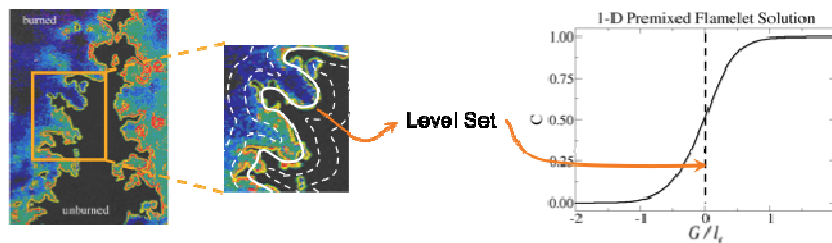
Simulation Domain near Central Jet

## Combustion Model

- Premixed flames unresolved in LES for high turbulence
- Our approach
  - Track front accurately using a level set,  $G$
  - Smooth gradients prescribed for  $G$



## Level Set and Flamelet Coupling



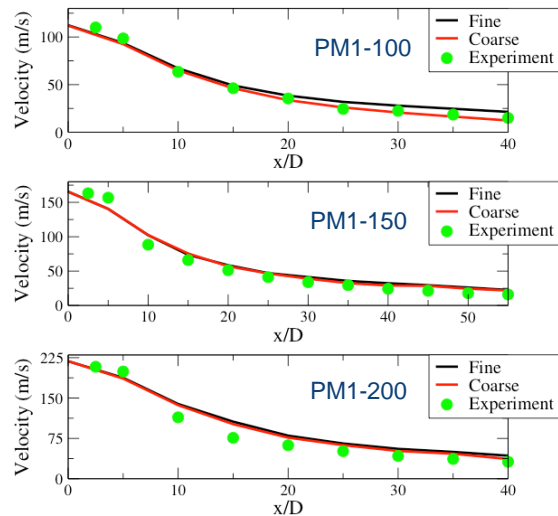
- Coupling Procedure (Moureau et al. 2009)
  - Assume progress variable profile based on level set
  - Calculate progress variable source term based on 1D premixed flamelets
  - Advance transported progress variable
  - Calculate density

## Constant Density Non-Reacting (CDNR) Comparisons

- Experimental studies were carried out with air injection in the central jet, pilot and coflow
- The temperature for all the streams is 300 K
- Simulation carried out for PM1-100, PM1-150 and PM1-200 cases
- Different grids are used to check for convergence
- Mean and fluctuating velocity profiles are compared for different downstream locations

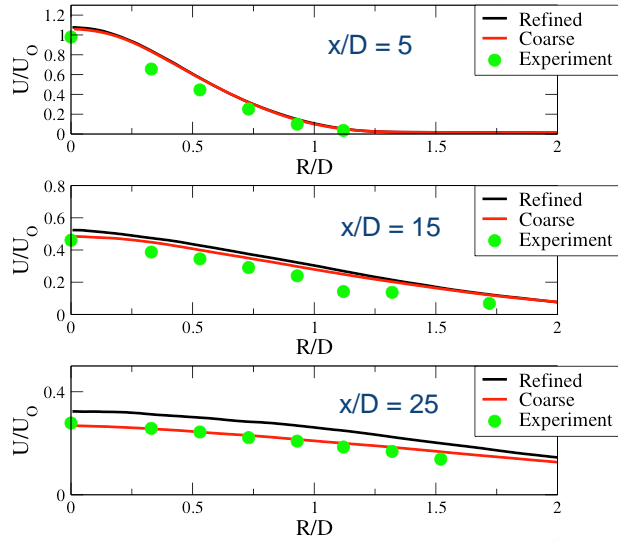
## CDNR Centerline Velocity Comparison

- Reasonable comparison away from centerline
- Simulation results are same for both grids
- Wider shear layer in the simulation



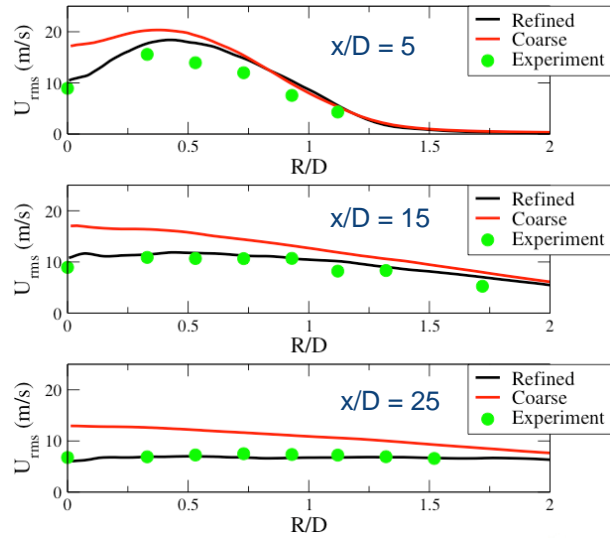
### CDNR Mean velocity : PM1-100

➤ Higher velocity in simulation

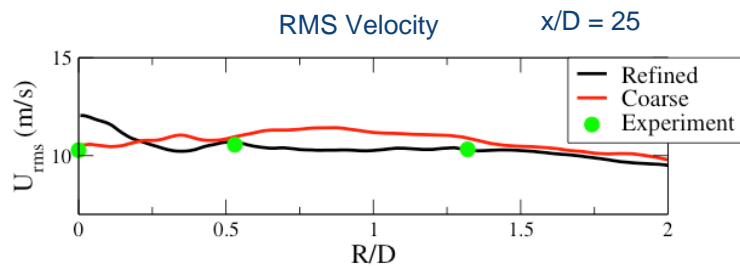
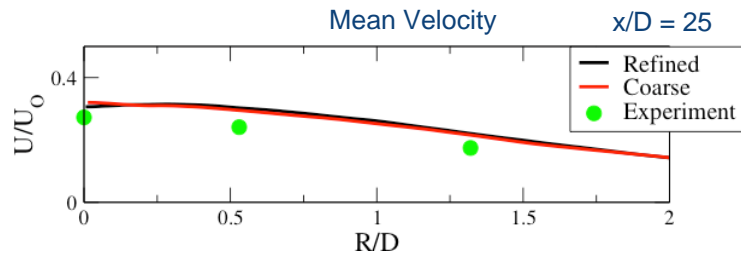


### CDNR Velocity Fluc : PM1-100

➤ Good comparison for the refined simulation

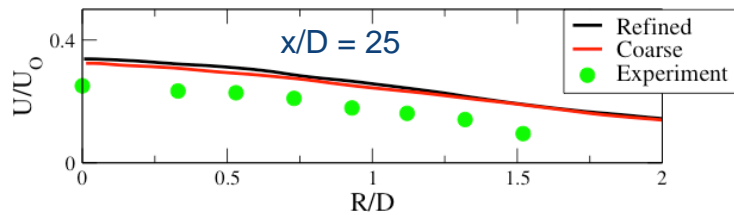
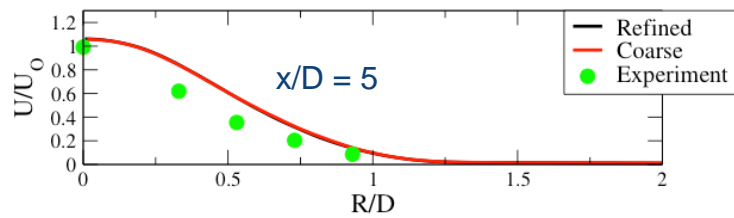


### CDNR velocity : PM1-150

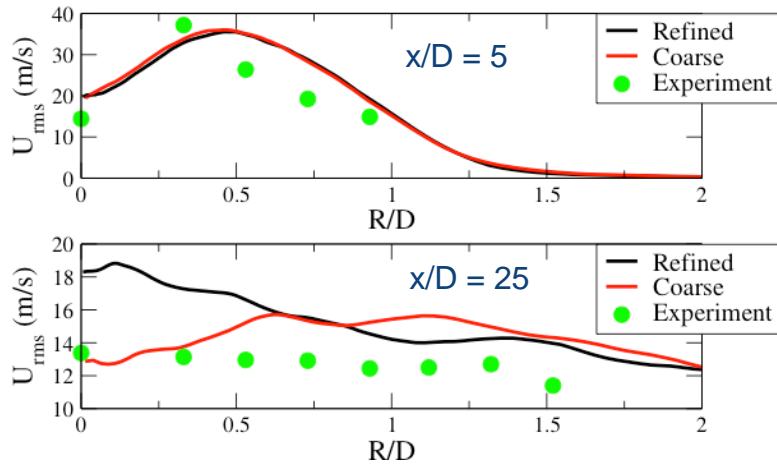


### CDNR Mean velocity : PM1-200

- Higher velocity in simulation
- Similar results for both grids



## CDNR Velocity Fluc : PM1-200

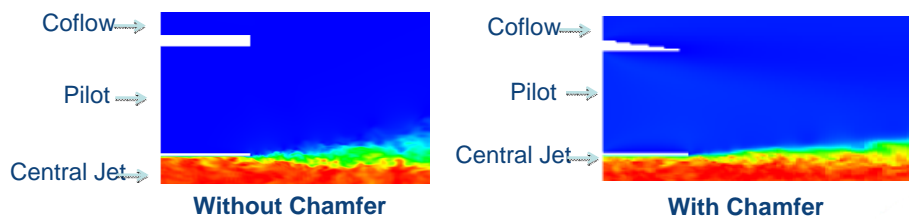


## Reactive Comparisons

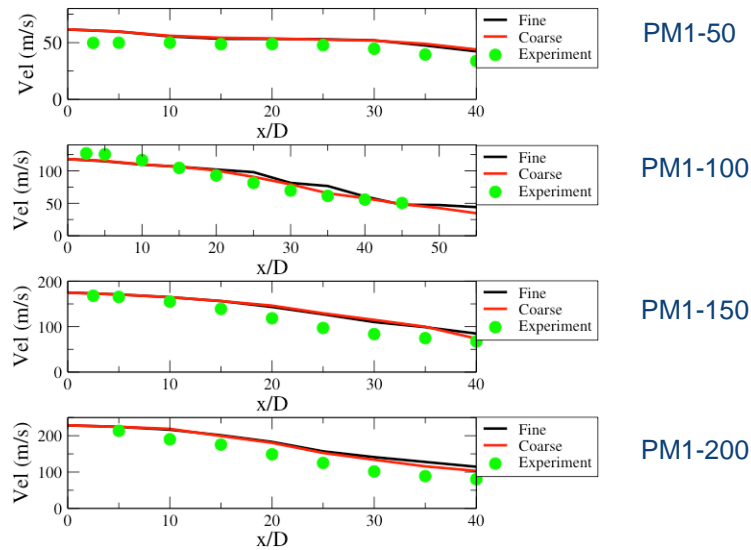
- Jet conditions
  - Central Jet : 0.5 equivalence ratio natural gas
  - Pilot : Stoichiometric natural gas combustion
  - Coflow
    - » 1500 K, 0.43 eq. ratio  $H_2$  combustion
    - » Simulated by matching eq. ratio of natural gas combustion to obtain the correct density
- Simulation carried out for PM1-50, PM1-100, PM1-150 and PM1-200 cases
- Mean and fluctuating velocity and species profiles are compared for different downstream locations

## Effect of Chamfer

- Including the chamfer of the nozzle between the pilot and coflow stream is important
  - Induced Radial velocity affects the mixture entrainment
- All results shown include the chamfer

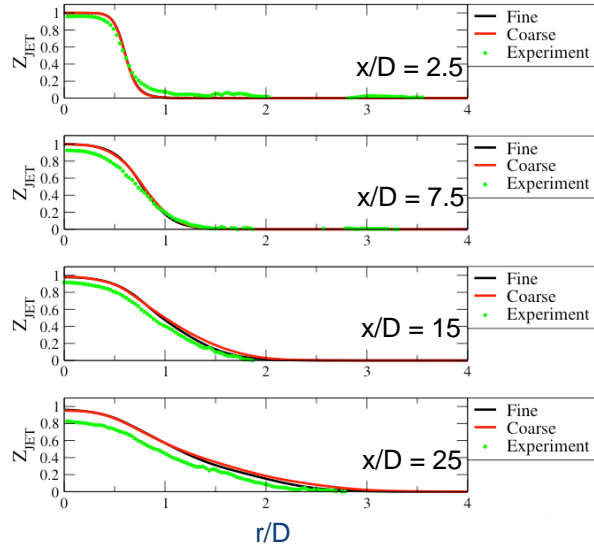


## Centerline Velocity



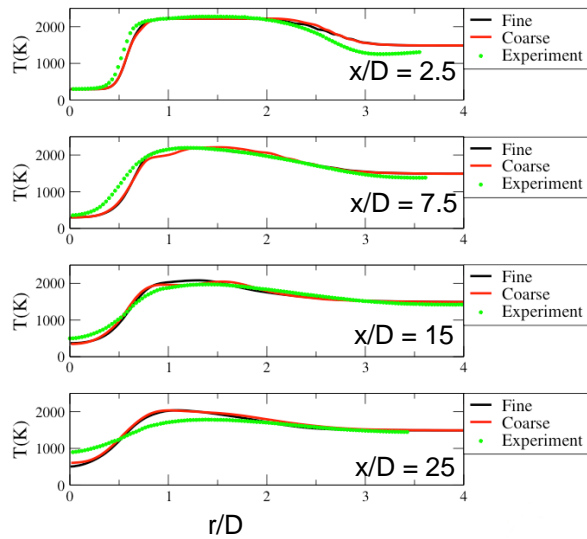
## Jet Mixture fraction : PM1-50

- Jet mixture fraction compares well at different downstream locations
- Results similar between the different grids
- Similar trends seen for the other PM1 cases



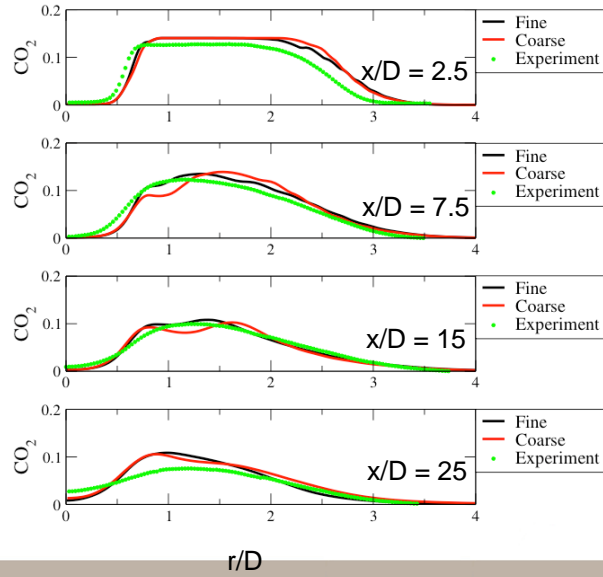
## Temp : PM1-50

- Good comparison away from centerline
- Reasonable prediction close to the centerline
- Lower temp. in simulation at downstream locations
- Higher temperature in shear layer than experiments



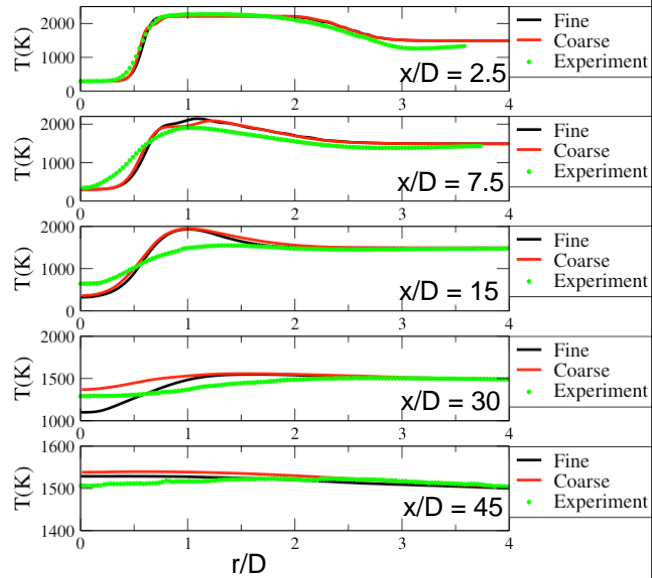
## CO<sub>2</sub> comparison : PM1-50

- Similar trends as the temperature profile
- Higher value corresponding to more combustion in the shear layer downstream

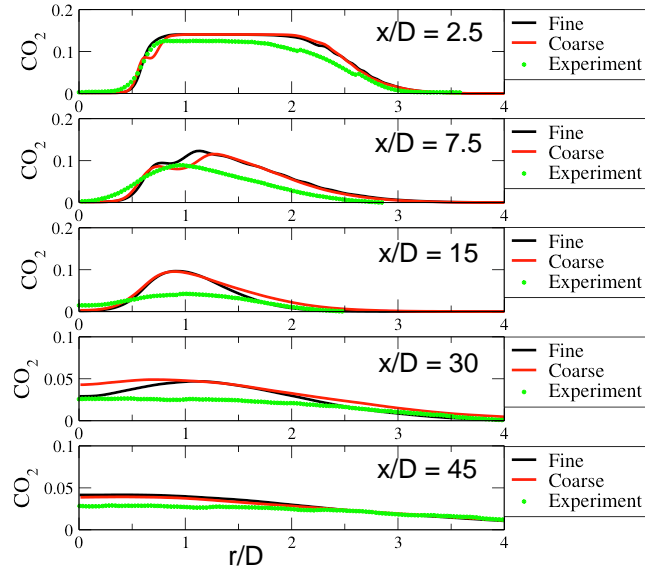


## Temp : PM1-100

- Similar trend as PM1-50 for intermediate downstream locations
- Good agreement at the final location

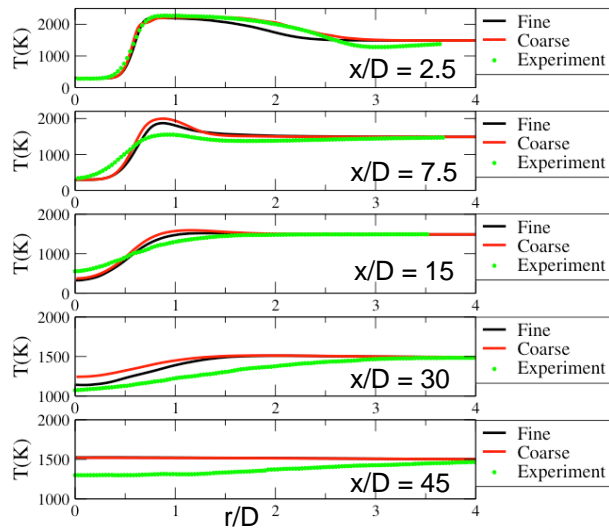


## CO<sub>2</sub>: PM1-100



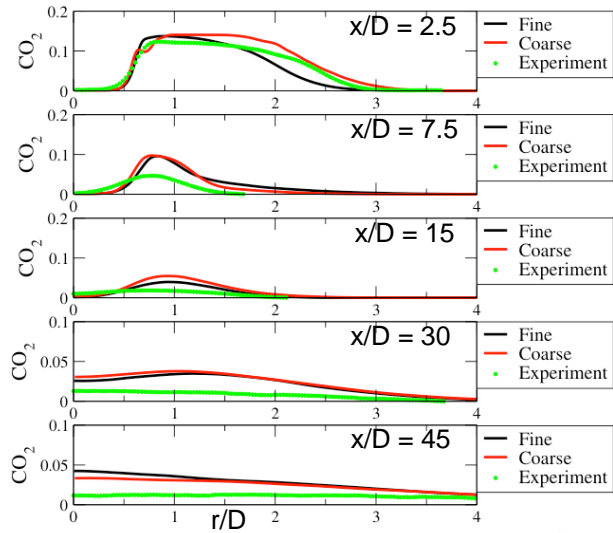
## Temp : PM1-150

- Higher temperature in shear layer
- At final downstream location, higher temperature in simulation



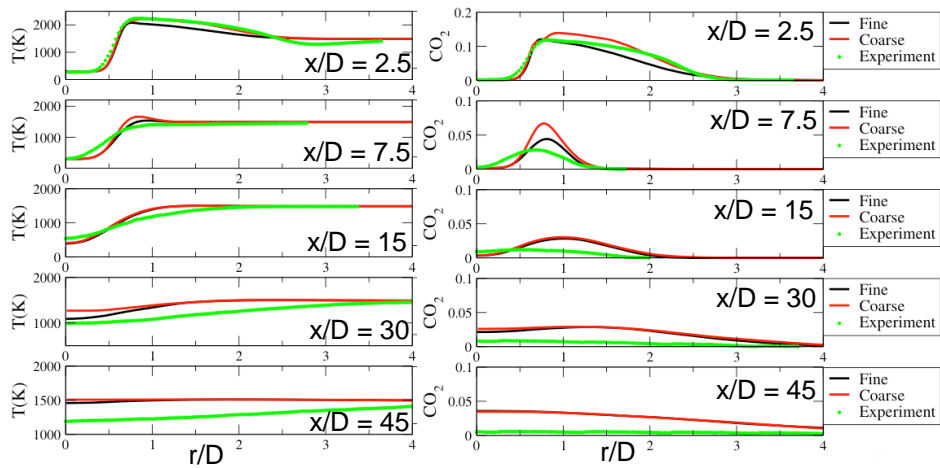
## CO<sub>2</sub>: PM1-150

- Higher value at downstream location
- Model predicts a higher level of combustion than experiment



## Temp : PM1-200

- Same trend as PM1-150 case



## Summary

- Non-reactive and reactive simulations done for the PM1 flame series
- Reasonable comparison for the non-reactive simulations
- Lower T along centerline, higher T in the shear layer region
- Better prediction for lower speed flames
- Over prediction of temperature in the downstream region for the higher speed flames -> predicted reaction rates too high
- Model needs to be improved to simulate those accurately

## Lund LES Calculations



**LUND**  
UNIVERSITY

### Lund LES Calculations

Christophe Duwig<sup>\*,5,6</sup>

Karl-Johan Nogenmyr<sup>7</sup>

Cheong-ki Chan<sup>7</sup>

<sup>5</sup>Dept. of Energy Sciences, Lund University, Sweden

<sup>6</sup>Haldor Topsøe A/S, DK-2800 Lyngby

<sup>7</sup>Dept. Applied Mathematics, The Hong Kong Polytechnic University

\*Primary contact Dr Christophe Duwig (Christophe.Duwig@energy.lth.se)

TNF 10 Workshop, Beijing 2010

## Lund LES Calculations - Motivation

- Develop a scalable LES solver for the simulation of lean premixed gas and lean pre-vaporized gas turbine combustors
- Unstructured code necessary for complex practical geometries
- Want to be able to account for complex chemistry
- PPJB ideal test case: A well documented burner in terms of the velocity and scalar fields (minor species indicative of reaction rates), well defined boundary conditions.

TNF 10 Workshop, Beijing 2010

## Lund LES Calculations

- Detailed chemistry and grid study for PM1-100
  - Submitted CTM 2010, C. Duwig, K. Nogenmyr, C. Chan, M.J. Dunn

CASE	MECHANISM	MESH
I	W&D, 5 species, 1 reaction	860k
II	W&D, 6 species, 2 reactions	860k
III	DRM19, 20 species, 82 reactions	860k
IV	W&D, 5 species, 1 reaction	1.5M

- Preliminary results for PM1-50 and PM1-150
  - Work in progress for a future publication

TNF 10 Workshop, Beijing 2010

## Solver

- Develop custom ILES solver in OpenFOAM, couple to CANTERA to compute reaction rates
- Unstructured solver
  - Still can apply high quality numerics, e.g. central schemes for scalars
- Favre filtered Navier-Stokes with species and enthalpy transport
- Classical Smagorinsky model
- Low Mach number assumption
- Equation of state to determine density

TNF 10 Workshop, Beijing 2010

## Combustion model

- Reaction rates determined directly from filtered species transport equations

$$\overline{\dot{w}_j(Y_i, T)} = \dot{w}_j(\tilde{Y}_i, \tilde{T})$$

- This approach fails in the RANS frame work but is exact in the DNS limit
- In LES this assumes that each cell acts like a PSR
  - Validate this assumption in a couple of slides

TNF 10 Workshop, Beijing 2010

## Complex Chemistry

- CASE I: Westbrook and Dryer: 5 species 1 reaction
  - (CH<sub>4</sub> O<sub>2</sub> N<sub>2</sub> CO<sub>2</sub> H<sub>2</sub>O)
- CASE II: Westbrook and Dryer: 6 species 2 reactions
  - (CH<sub>4</sub> O<sub>2</sub> CO N<sub>2</sub> CO<sub>2</sub> H<sub>2</sub>O)
- CASE III: DRM19, skeletal mechanism derived from GRI1.2, 19 reactive species + N<sub>2</sub>, 82 reactions
  - (H<sub>2</sub> H O O<sub>2</sub> OH H<sub>2</sub>O HO<sub>2</sub> CH<sub>2</sub> CH<sub>2</sub><S> CH<sub>3</sub> CH<sub>4</sub> CO CO<sub>2</sub> HCO CH<sub>2</sub>O CH<sub>3</sub>O C<sub>2</sub>H<sub>4</sub> C<sub>2</sub>H<sub>5</sub> C<sub>2</sub>H<sub>6</sub> N<sub>2</sub>)

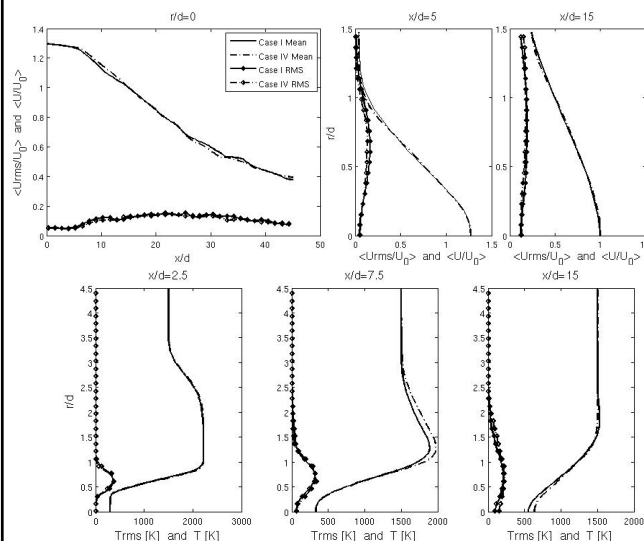
CASE	MECHANISM	CPU cost*
I	W&D, 5 species, 1 reaction	1
II	W&D, 6 species, 2 reactions	1.05
III	DRM19, 20 species, 82 reactions	2.35

- \*CPU cost =1, Δt = τ for CASE I = 2.8hrs 2.8hrs on 4x2.8GHz core, single node
- Base statistics on sampling of 570 τ ~2.3ms

TNF 10 Workshop, Beijing 2010

## PM1-100 Grid sensitivity

- Grid sensitivity, CASE I 860k cells, CASE IV 1.5M cells both W&D 1step

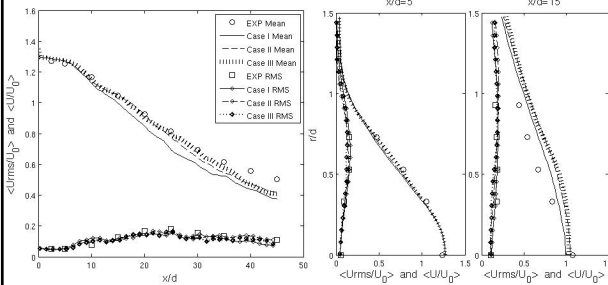


- CASE I grid 40 cells across jet diameter 860k cells
- CASE IV 1.5M cells both W&D 1step, ~twice resolution as case I in the jet proximal region
- Well justified to use 860k grid with confidence

TNF 10 Workshop, Beijing 2010

## PM1-100 Chemical Mechanism Sensitivity (1/5)

- 860k cell grid for chemical mechanism sensitivity analysis



- Centerline mean and rms velocity well predicted

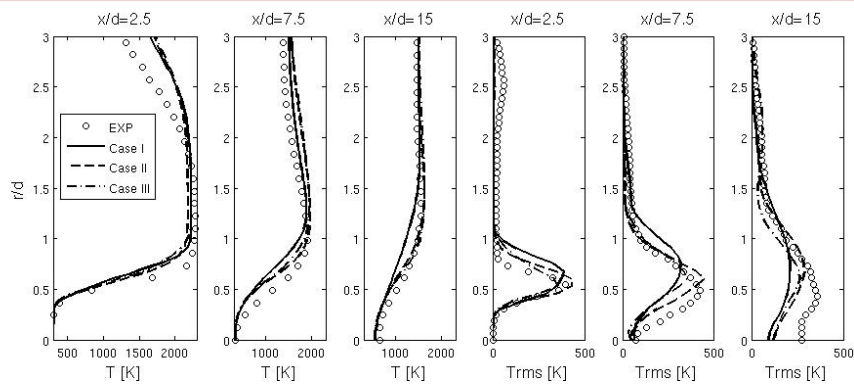
- Good initial results at  $x/D=5$

CASE	MECHANISM
I	W&D, 5 species, 1 reaction
II	W&D, 6 species, 2 reactions
III	DRM19, 20 species, 82 reactions

- Slightly higher mean velocity in the shear layer at  $x/D=15$

TNF 10 Workshop, Beijing 2010

## PM1-100 Chemical Mechanism Sensitivity (2/5)

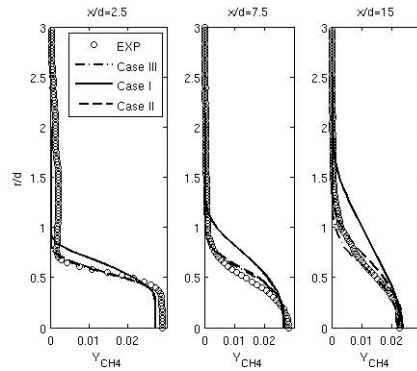


- In general mean and rms Temperature radial profiles well predicted

- Cases II and III perform better than Case I (as expected)

TNF 10 Workshop, Beijing 2010

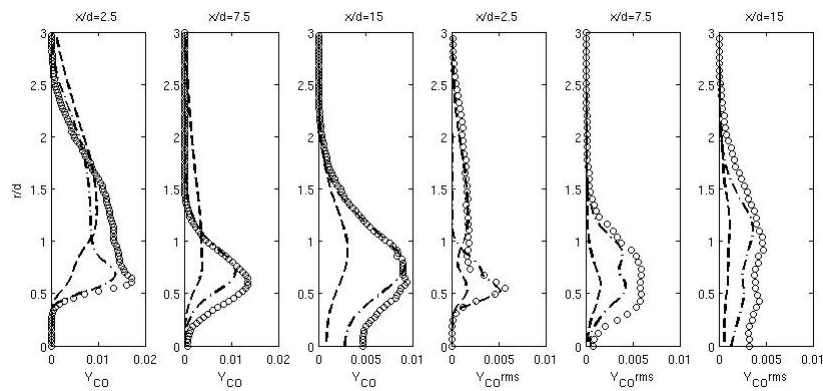
## PM1-100 Chemical Mechanism Sensitivity (3/5)



- CH<sub>4</sub> profiles highlight Case I (single step) issues
- Jet mixing and reaction field well predicted in Cases II and III

TNF 10 Workshop, Beijing 2010

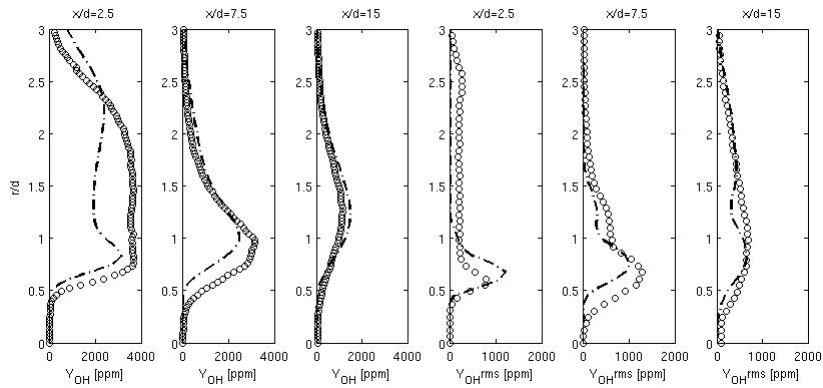
## PM1-100 Chemical Mechanism Sensitivity (4/5)



- Only Cases II and III can compute CO
- Case III good results
- As expected Cases III (DRM19) always much better than Case II (2 step)
- Highlights non-adiabatic minor species mass fractions in pilot gases

TNF 10 Workshop, Beijing 2010

## PM1-100 Chemical Mechanism Sensitivity (5/5)



- Only Case III (DRM19) can compute OH
- Case III good results, considering the challenges with initial conditions

TNF 10 Workshop, Beijing 2010

## PM1-100 *a posteriori* check of modeling assumptions (1/3)

- Consider Case III exclusively
- Compute a local Karlovitz number ( $Ka_{\Delta}$ ):

$$Ka_{\Delta} = \left( \frac{u_{\Delta}}{S_L} \right)^{3/2} \left( \frac{\delta_L}{\Delta} \right)^{1/2} \quad Ka_{\Delta} = \left( \frac{\varepsilon \delta_L}{S_L^3} \right)^{1/2}$$

- $Ka_{\Delta}$  Independent of filter width in the inertial subrange, indicator of turbulence chemistry interaction
- Compute a local Damköhler number ( $Da_{\Delta}$ )

$$Da_{\Delta} = \frac{\tau_{\Delta}}{\tau_c} = \frac{\Delta}{\delta_L} \cdot \frac{S_L}{u_{\Delta}}$$

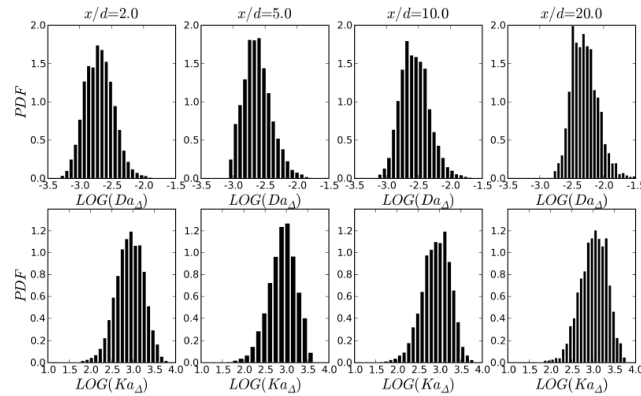
- $Da_{\Delta}$  does depend on filter width, small values (<1) indicate the filter box is well stirred and homogenous check of model assumptions to be valid

TNF 10 Workshop, Beijing 2010

## PM1-100 *a posteriori* check of modeling assumptions (2/3)

➤ Both  $Ka$  and  $Da$  confirm:

- modeling assumptions confirmed  $Da \ll 1$
- Significant turbulent chemistry interaction ( $Ka \gg 1$ )



TNF 10 Workshop, Beijing 2010

## PM1-100 *a posteriori* check of modeling assumptions (3/3)

➤ Desirable to have a local measure of grid resolution/criteria for ILES

- From measurements instantaneous temperature gradient  $\nabla T$  can be as large as  $\sim 4000\text{K/mm}$  in the shear layer
- Consider worst case for  $\Delta T = 1500 - 300 = 1200\text{K}$

$$\nabla T_{\Delta} = \frac{\Delta T_{\text{exp}}}{\nabla T_{\text{exp}}} \frac{1}{\Delta_{\text{LES}}} \quad \Delta T_{\text{LESMAX}} < \nabla T_{\text{exp}} \Delta_{\text{LES}}, \Delta T_{\text{LESMAX}} \approx 50\text{K} ?$$

- For these conditions  $\nabla T_{\Delta} = 0.3 \frac{1}{\Delta_{\text{LES}}}$ ,  $\Delta_{\text{LES}} = \sim d/50$  at nozzle and  $d/25$  downstream,  $0.3\text{mm} = d/12$ , expect no more than  $20\text{K/cell}$  which is an encouraging quality check
- Still more work to be done to finalize definition but promising concept to link LES resolution to high resolution scalar measurements

TNF 10 Workshop, Beijing 2010

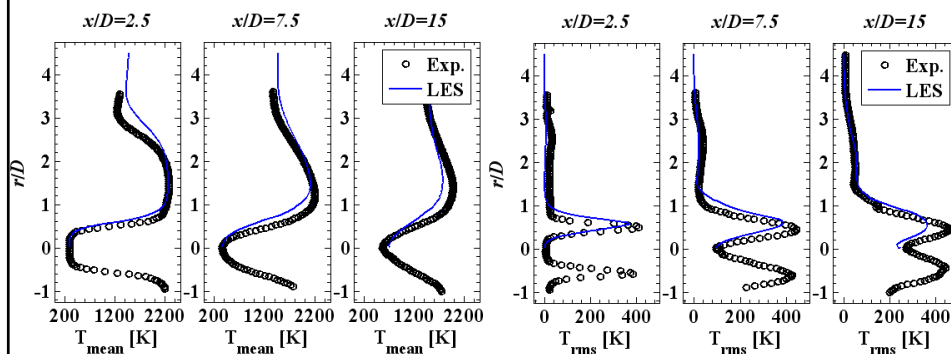
## PM1-50 Case

- Run a single simulation for the PM1-50 case
- Same grid (860k), mechanism (DRM19) and solver as PM1-100 Case III
- Only significant boundary condition change from PM1-100 is the central jet velocity

TNF 10 Workshop, Beijing 2010

## PM1-50 Results: Temperature

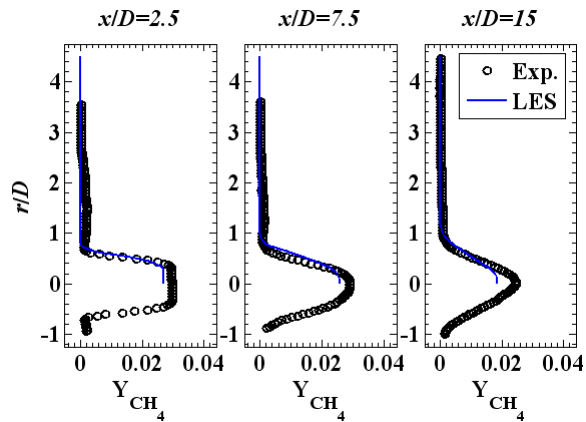
- Mean and rms temperature fields show good agreement with experiments



TNF 10 Workshop, Beijing 2010

## PM1-50 Results: $Y_{CH_4}$

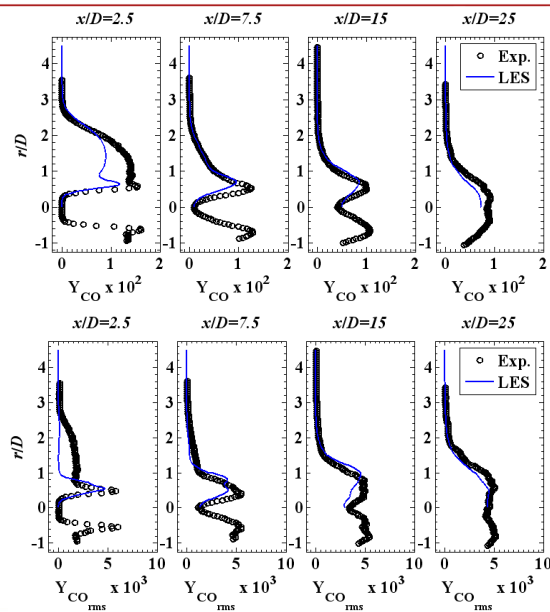
- Mean  $CH_4$  mass fraction fields ok
- Slightly too high  $CH_4$  at  $x/D=15$  – under-prediction of reaction rate



TNF 10 Workshop, Beijing 2010

## PM1-50 Results: $Y_{CO}$

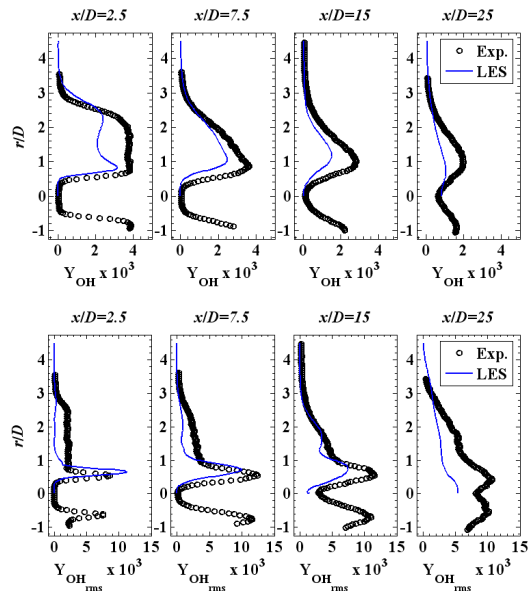
- At  $x/D=2.5$  difference due to non-adiabatic pilot products
- Generally good agreement for Mean and rms CO profiles



TNF 10 Workshop, Beijing 2010

## PM1-50 Results: $Y_{OH}$

- At  $x/D=2.5$  difference due to non-adiabatic pilot products
- Generally agreement with experimental data for OH is not as good as CO



TNF 10 Workshop, Beijing 2010

## PM1-50 Results: Summary

- Results for the PM1-50 flame are generally encouraging
- Generally the  $CH_4$  consumption rate is slightly under predicted as a function of axial distance
- CO and OH are under predicted near the pilot due to the non-adiabatic conditions for these species near the pilot stream
- Higher minor species concentration in pilot inlet stream would likely improve results (increase  $CH_4$  consumption rate)
- Improved prescription of the boundary conditions should increase the accuracy of the simulation results

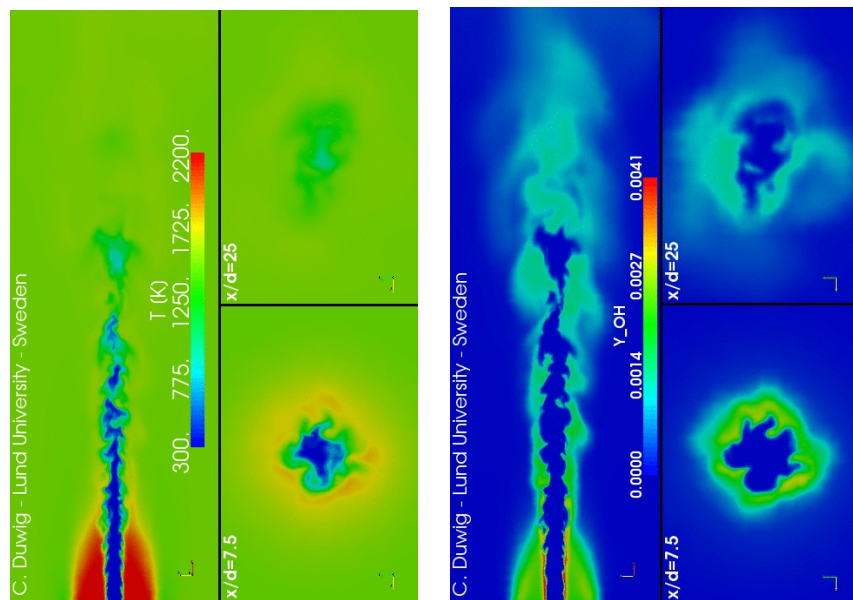
TNF 10 Workshop, Beijing 2010

## PM1-150 Case

- Run special case on small domain up to  $x/D=40D$ , 1.5M cells, DRM19, well resolved only up to  $x/D=30$
- See if can capture some of the very complex turbulence chemistry interaction featured by the PM1-150 flame: initial ignition then a dramatic reduction in the reaction rate in the region  $x/D=0$  to 30

TNF 10 Workshop, Beijing 2010

## PM1-150 Flame Structure

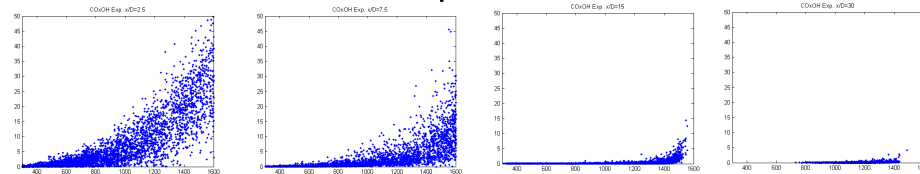


TNF 10 Workshop, Beijing 2010

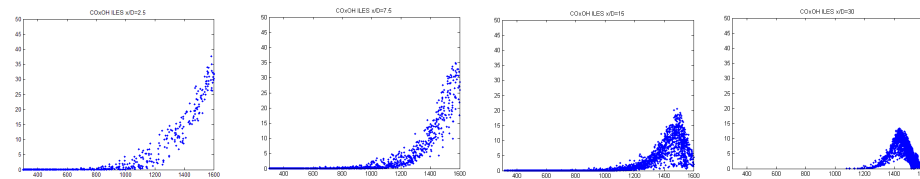
## PM1-150 Turbulence Chemistry Interaction (1/2)

- How do the computations compare with the experiments? Consider a very challenging measure: COxOH|T and a very challenging flame (PM1-150)?

### Experiment



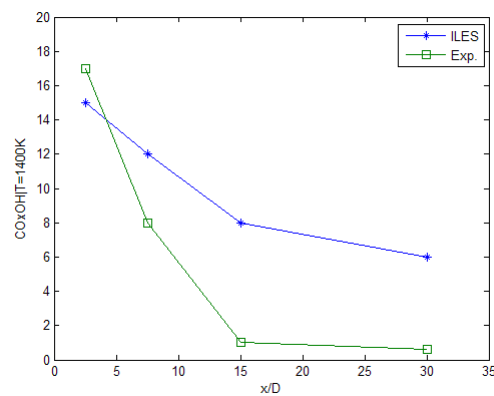
### ILES



TNF 10 Workshop, Beijing 2010

## PM1-150 Turbulence Chemistry Interaction (2/2)

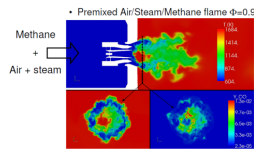
- Encouraging qualitative prediction of reduction of reduction in reaction rate
  - However not to the same extreme degree as experiment



TNF 10 Workshop, Beijing 2010

## Current and Future work

- Basic applicability and validity of the ILES model tested by the PPJB
- Current work on ILES model:
  - Higher velocity flames (PM1-150)
  - Simulation of a realistic gas turbine combustor: Triple Annular Research Swirler combustor (TARS) using this model:
    - » P. Ludiciani, C Duwig, R.Z. Szasz, L. Fuchs, H. Grosshans, M. Åberg\*



- Complex chemistry description mandatory!
- ~5.6M cells

TNF 10 Workshop, Beijing 2010

## General LES Calculation Conclusions/Findings

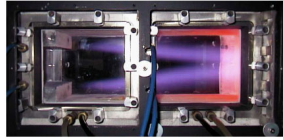
- Confidence in the grid independence can be achieved by utilizing the non-reacting velocity measurements to isolate combustion model from the grid independence
- Boundary condition treatment can be very important
  - Accounting for the curvature of pilot shroud to correctly predict the initial radial velocity and initial entrainment rate
  - Correctly specifying the minor species profiles for pilot inlet
  - Inlet turbulence generation method for jet
- Need to have a model that can account for complex chemistry (explicit or tabulated) to correctly simulate the higher velocity flames

TNF 10 Workshop, Beijing 2010

## LES Calculation Discussion

- Differences in (combustion) modeling approaches
- Are tabulated chemistry capable of describing the chemical manifold that is accessed in the higher velocity flames?
- Need to have a model that can account for complex chemistry (explicit or tabulated) to correctly simulate the higher velocity flames
- Should tabulated chemistry methods utilize (at least) two mixture fraction transport equations?
- How to build a better validation link between LES and experiments?

TNF 10 Workshop, Beijing 2010



## Overview of Stratified Experiments

Simone Hochgreb<sup>1</sup>, Robert Barlow<sup>2</sup>

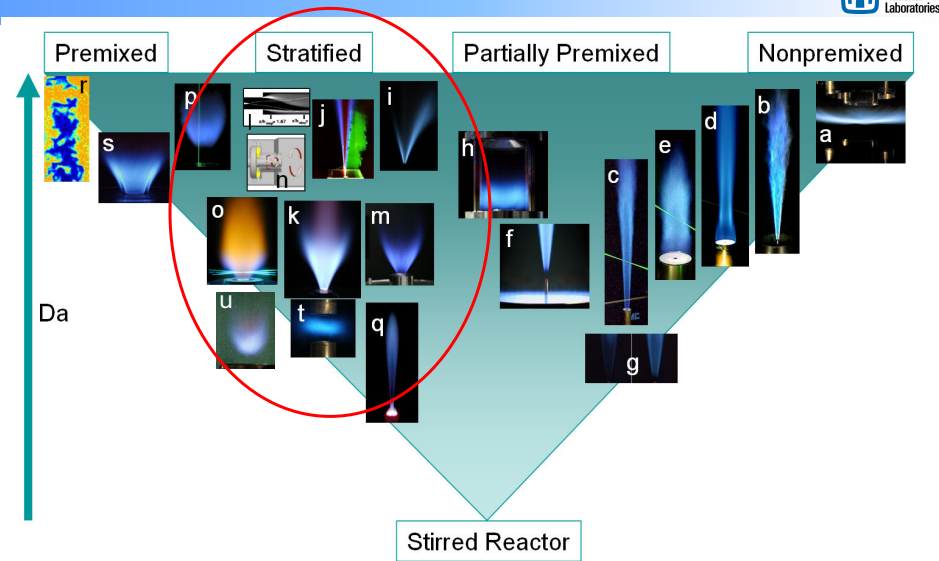


<sup>1</sup>University of Cambridge  
<sup>2</sup>Sandia National Laboratories



TNF10 - Beijing  
 30 Jul 2009

## Stable Flames TNF



# Outline

- Previous work on stratified flames
  - Laminar flames
  - Turbulent flames
  - Practical turbulent flames



- Current experiments
  - Slot burner (Cambridge/Sandia)
  - Co-annular swirl burner (Cambridge/Sandia)
  - Co-annular burner (Darmstadt/Sandia)

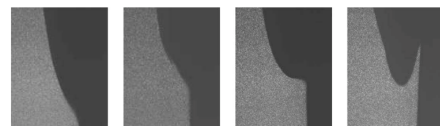
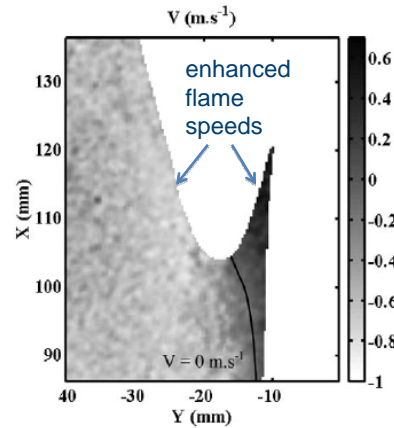
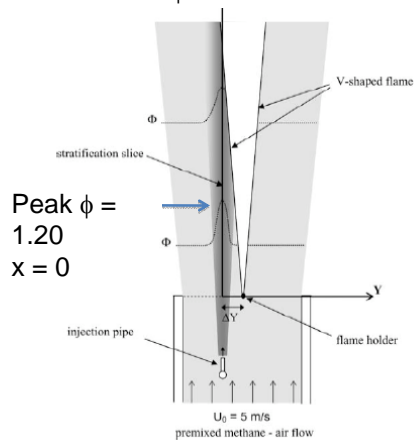


3

# Laminar stratified flames

Galizzi & Escudié (2006)

- V-flame  $\phi = 0.58$



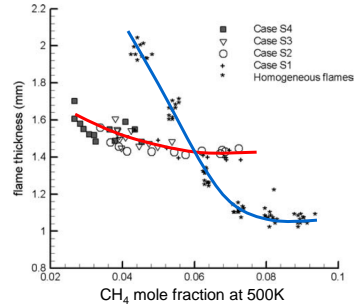
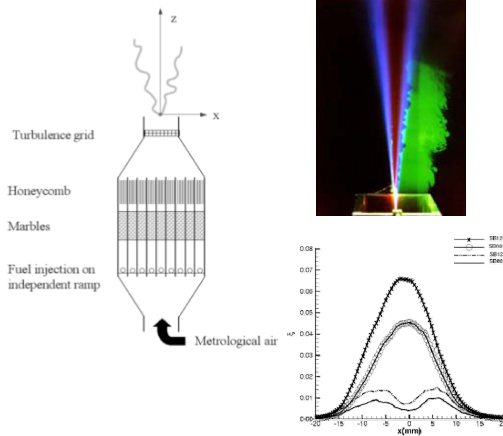
4

# Turbulent stratified flames –

Degardin et al, Exp Fluids (2006); Robin et al, CNF (2008)



- $u'/S_{L_T} \sim 1-8, L_z/L_T \sim 0.5-1$
- Rayleigh/acetone: flame thickness

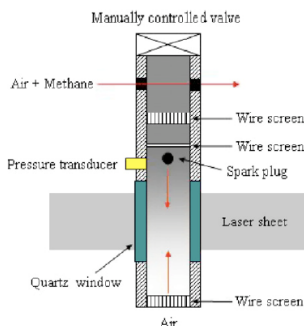


- Flame thickness less sensitive to  $\phi$  in stratified cases
- Extensive modelling comparison in Robin et al. paper

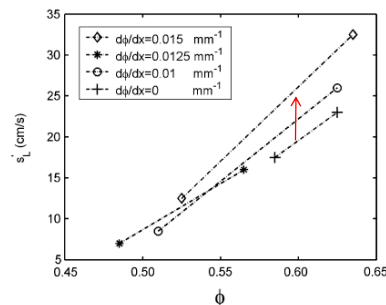
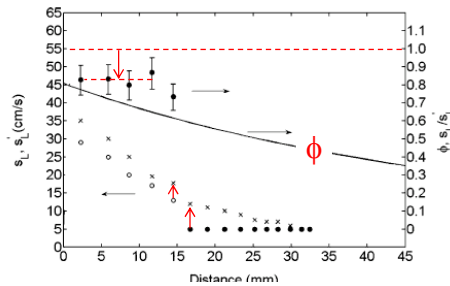
5

# Laminar stratified flames

Kang & Kyritsis, PCI 31 (2007)



- Enhancement of laminar burning rate in the lean range
- Extension of flammable limit
- Effects depend on magnitude of gradient in  $\phi$

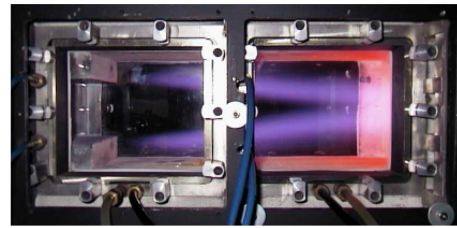
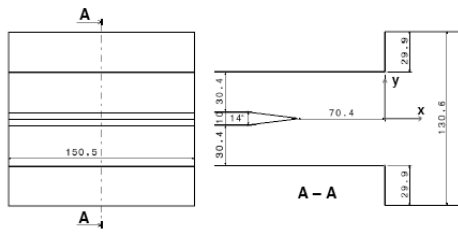
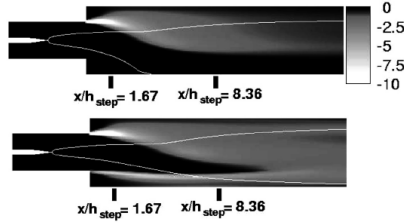


6

# Turbulent stratified flames

Besson et al, IJHT (2000)(2001)

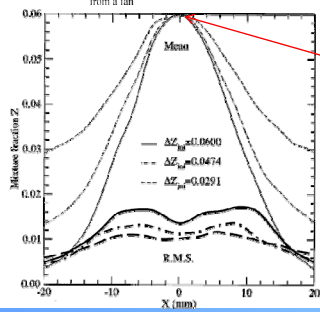
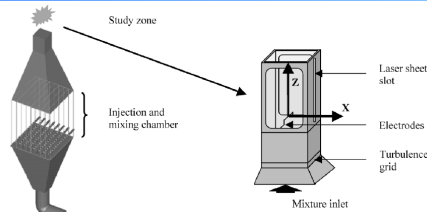
- ORACLES rig (Poitiers)
- $Re = 25,000$
- $\phi_1/\phi_2 = 0.9/0.3, 0.9/0.7$
- New closure models required (Robin et al, CST 2004, 2006)



7

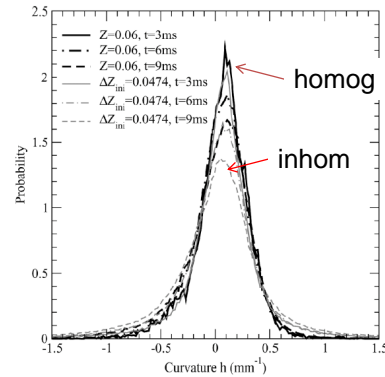
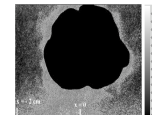
# Turbulent stratified flames

Renou et al, CST (2004)



$\phi \sim 1$   
propane

acetone PLIF



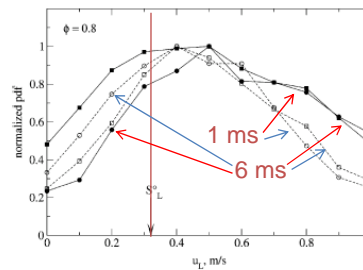
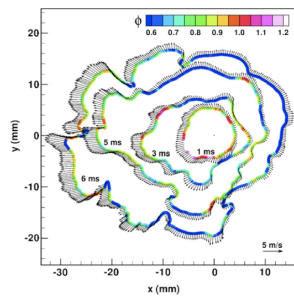
- Broader curvature distribution
- Enhanced wrinkling

8

# Turbulent stratified flames

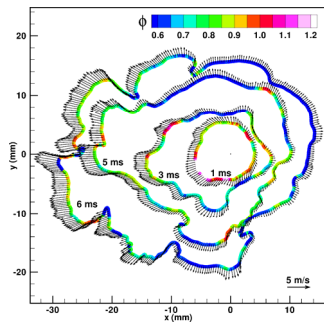
Pasquier et al, PCI 31 (2007)

- ▶ Expanding propane flames (constant volume chamber)
- ▶ PIV/PLIF → local 2D 'displacement speed'



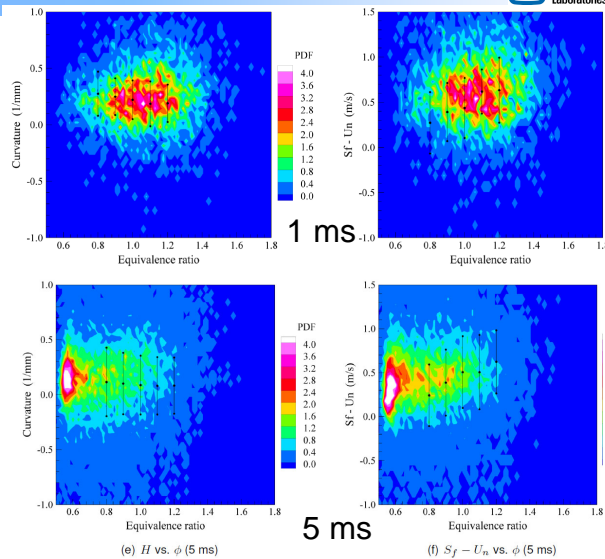
- Extension of burning limit into leaner range
- Higher burning rate when propagating rich into lean

# Conditional measurements and analysis



Pasquier, N., Lecordier, B., Trinité, M., Cessou, A., Proc. Comb. Inst. 31(2007) 1567-1574

Balusamy S., PhD in preparation

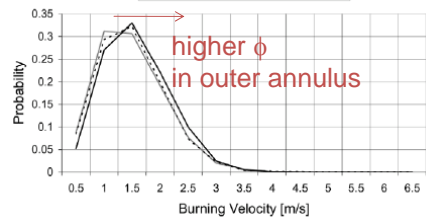
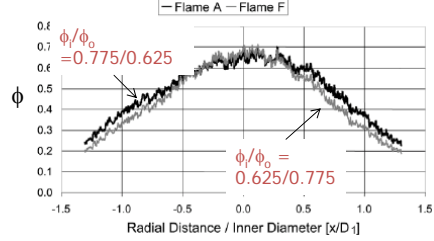
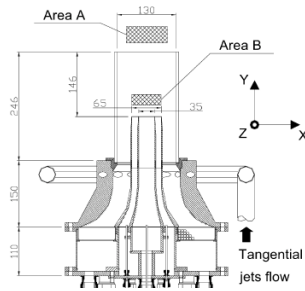
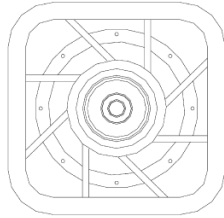


(e)  $H$  vs.  $\phi$  (5 ms)

(f)  $S_f - U_n$  vs.  $\phi$  (5 ms)

# Flat turbulent stratified flame

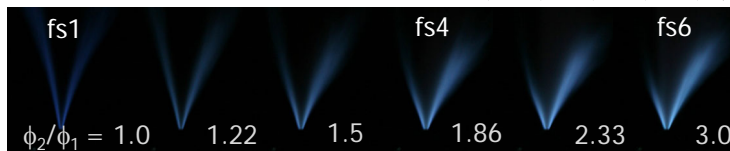
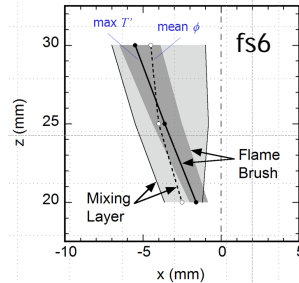
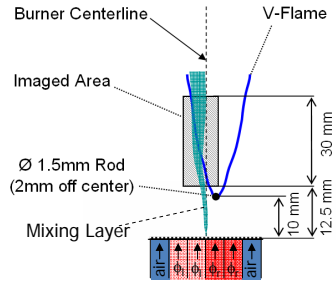
Bonaldo & Kelman, CNF2008



11

# Cambridge Stratified Slot Burner

Anselmo-Filho et al, AIAA 2009, PCI2009



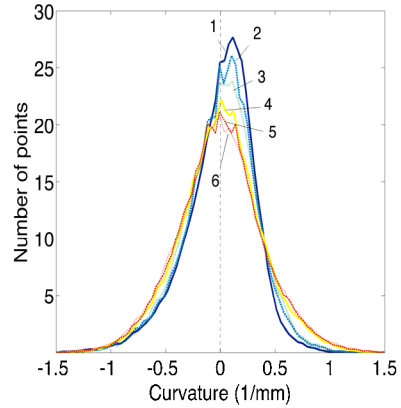
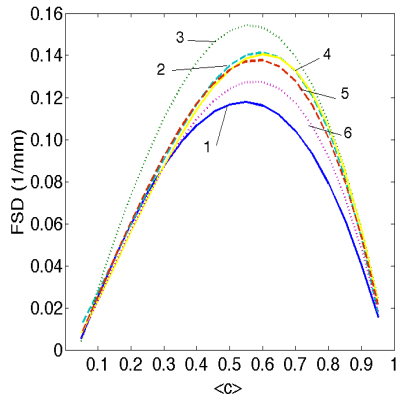
Flame	Combustion Regime	$\phi_{lean}$	$\phi_{rich}$	$\frac{\phi_{rich}}{\phi_{lean}}$	$\bar{u}$	$u'$	$\frac{u'}{S_L}$	$\Lambda$	$\eta$	$Re$	$Re_\Lambda$
		(-)	(-)	(-)	(m/s)	(m/s)	(-)	(mm)	(mm)	(-)	(-)
fs1	Premixed	0.73	0.73	1.00	3.1	0.3	1.3	1.9	0.09	2,316	38
fs6	Stratified	0.37	1.10	3.00							

P. Anselmo-Filho, R.S. Cant, S. Hochgreb, R.S. Barlow, *Proc. Combust. Inst.* 32, 1763-1770 (2009)

12

# Cambridge Stratified Slot Burner

Anselmo-Filho et al, AIAA 2009, PCI2009

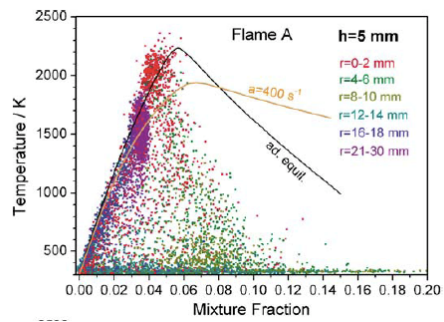
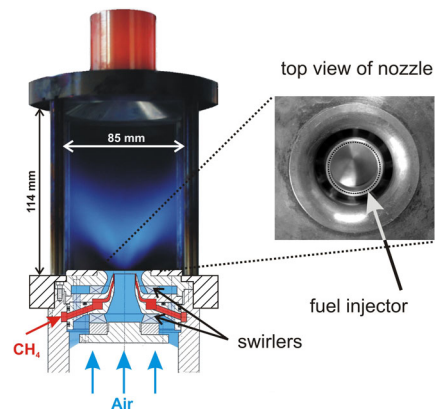


P. Anselmo-Filho, R.S. Cant, S. Hochgreb, R.S. Barlow, *Proc. Combust. Inst.* 32, 1763-1770 (2009)

13

# Practical turbulent stratified flames

Meier et al, CNF (2006), Nogenmyr (2005)

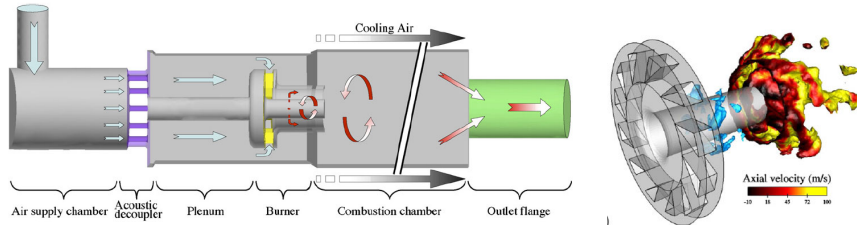


- Detailed species database
- Non-flamelet behaviour
- Product recirculation, quenching, stratification

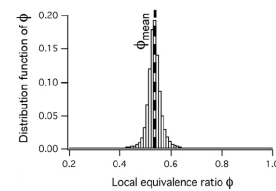
14

## Practical unsteady stratified flames

Sengissen et al, CNF (2007)



- Designed for instability investigation
- Many model parameters, limited database (cold velocity, CH\*)



15

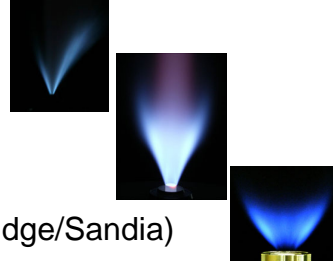
## Previous experimental work – Summary

- Evidence for:
  - Enhancement of lean flammability limit
  - Enhanced burning rate into leaner mixtures
  - Broader and more symmetric curvature pdf
  - Increased flame surface density
- However:
  - Limited data on local structure of turbulent stratified flames
  - More complete data sets needed for model validation

16

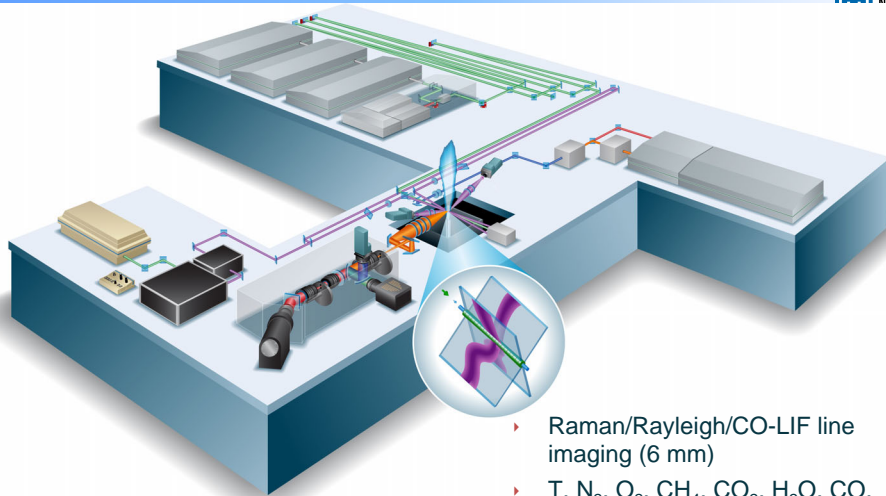
## Outline

- Previous work on stratified flames
  - Laminar flames
  - Turbulent flames
  - Practical turbulent flames
- Current experiments
  - Slot burner (Cambridge/Sandia)
  - Co-annular swirl burner (Cambridge/Sandia)
  - Co-annular burner (Darmstadt/Sandia)



17

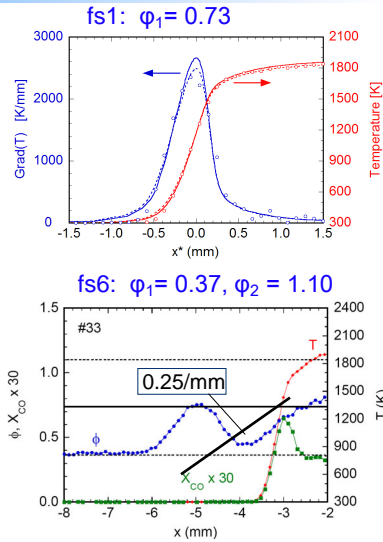
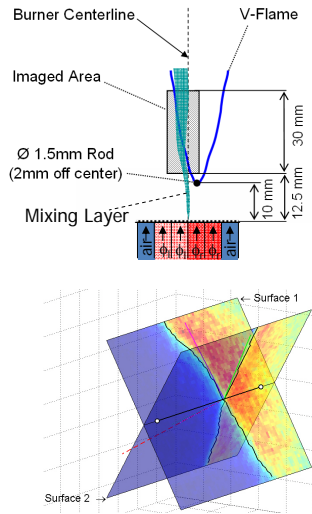
## Sandia Multiscalar Measurements



- ▶ Raman/Rayleigh/CO-LIF line imaging (6 mm)
- ▶ T, N<sub>2</sub>, O<sub>2</sub>, CH<sub>4</sub>, CO<sub>2</sub>, H<sub>2</sub>O, CO, H<sub>2</sub> (104 mm spacing)
- ▶ Crossed OH PLIF

18

# Cambridge-Sandia Slot Burner: near normal flame structure analysis



19

# Dissipation terms for stratified flames

- ▶ Determination of local  $c$  requires measurement of local  $Z$

$$c(x, Z) = \frac{T(x) - T_u}{T_{\text{equil}}(Z) - T_u}$$

- ▶ Scalar dissipation terms

$$\chi_c = D_c \nabla c \cdot \nabla c$$

$$\chi_Z = D_Z \nabla Z \cdot \nabla Z$$

$$\chi_{Zc} = D_{Zc} \nabla Z \cdot \nabla c$$

- ▶ Current focus: Dissipation of reaction progress

$$\chi_c(T, Z) = \alpha(T, Z) \nabla c \cdot \nabla c$$

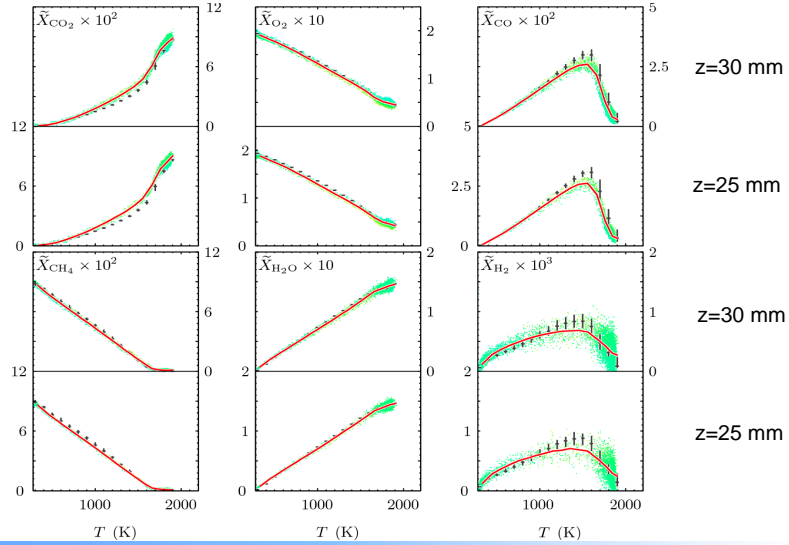
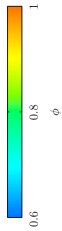
20

# Cambridge/Sandia Stratified Slot Burner

Sweeney, Hochgreb, Barlow, Dunn



$\phi_2/\phi_1 = 1.0$



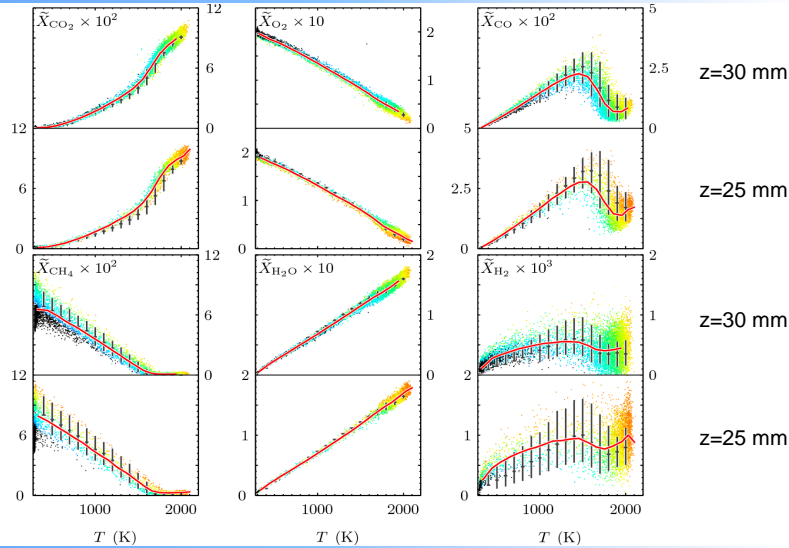
21

# Cambridge/Sandia Stratified Slot Burner

Sweeney, Hochgreb, Barlow, Dunn



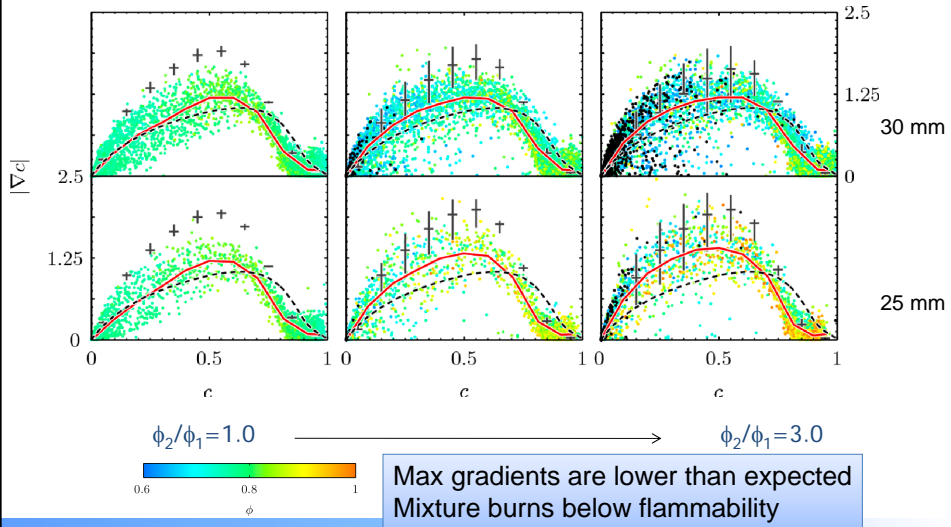
$\phi_2/\phi_1 = 3.0$



22

# Cambridge/Sandia Stratified Slot Burner

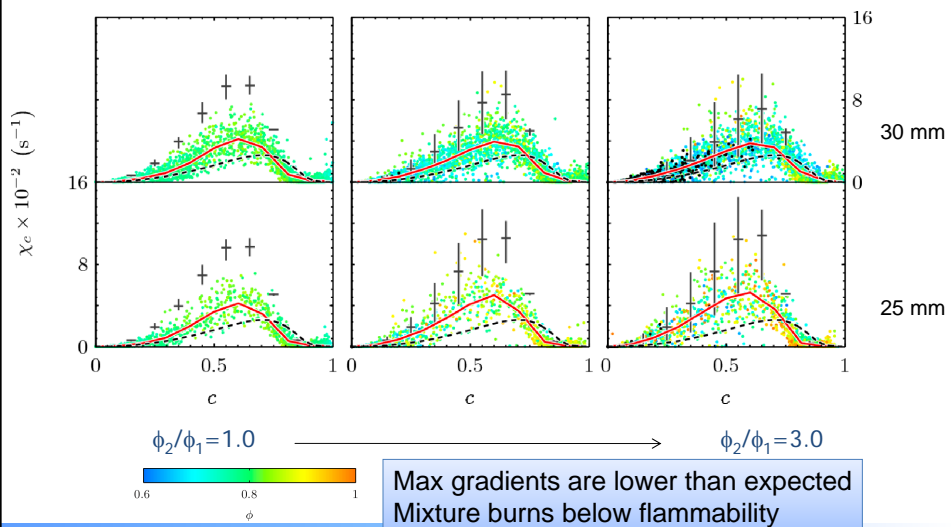
Sweeney, Hochgreb, Barlow, Dunn



23

# Cambridge/Sandia Stratified Slot Burner

Sweeney, Hochgreb, Barlow, Dunn

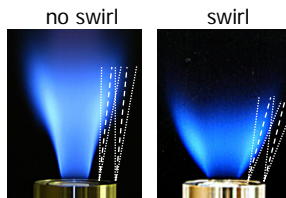
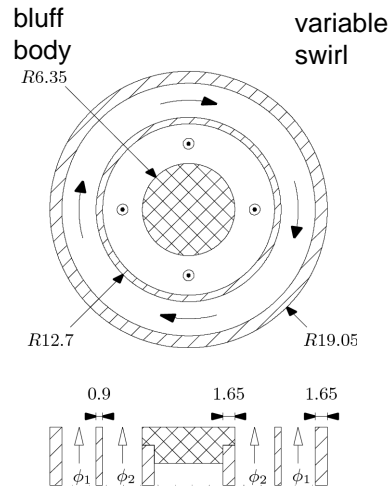


24

# Cambridge/Sandia Stratified Swirl Burner

Sweeney, Hochgreb, Barlow, Dunn

- Higher turbulence levels:  
 $U_1 = 7.5 \text{ m/s}$ ,  $U_2 = 15 \text{ m/s}$
- $Re_{h1}=5800$ ,  $Re_{h2}=10800$
- Long development length
- Optical access
- Increases flow complexity compared to TUD burner



25

# Cambridge/Sandia Stratified Swirl Burner

$U_i = 7.5 \text{ m/s}$     $U_o = 15 \text{ m/s}$     $U_{cf} = 0.4 \text{ m/s}$   
 $Re_i = 5,800$     $Re_o = 11,000$

Vary stratification ratio and swirl

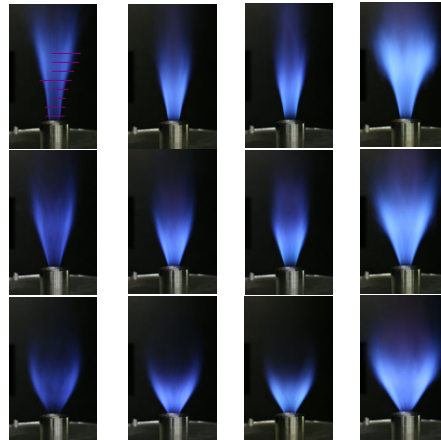
- Radial profiles
  - $z = 10, 20, 30, \dots \text{ mm}$
  - 300 shots at each location, 1500 in flame brush
  - $103 \mu\text{m}$  data spacing
- Long records
  - crossing of flame & mixing layer
  - 30,000 shots
  - $20 \mu\text{m}$  data spacing
  - Wavelet denoising

SR = 1	SR = 2	SR = 3	SR = 1
$\phi_i = 0.75$	$\phi_i = 1.0$	$\phi_i = 1.125$	$\phi_i = 1.0$
$\phi_o = 0.75$	$\phi_o = 0.5$	$\phi_o = 0.375$	$\phi_o = 1.0$

no swirl

25% swirl

33% swirl

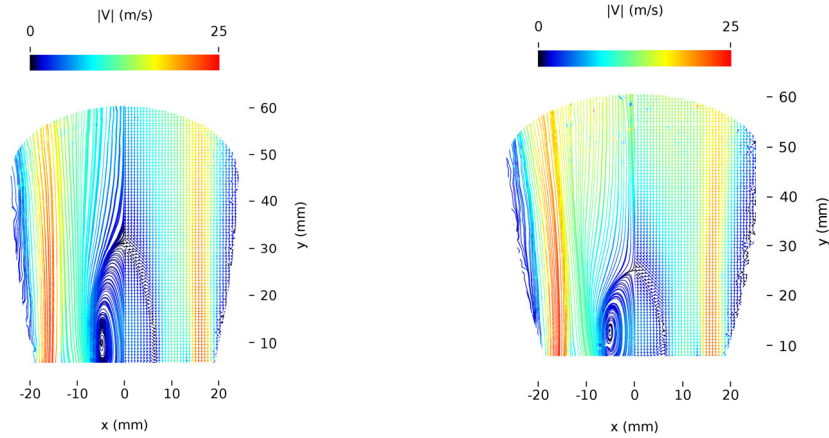


Experiments conducted April – October 2009 / Mark Sweeney, visiting student

26

# Cambridge Stratified Swirl Burner

Sweeney, Hochgreb, Barlow, Dunn



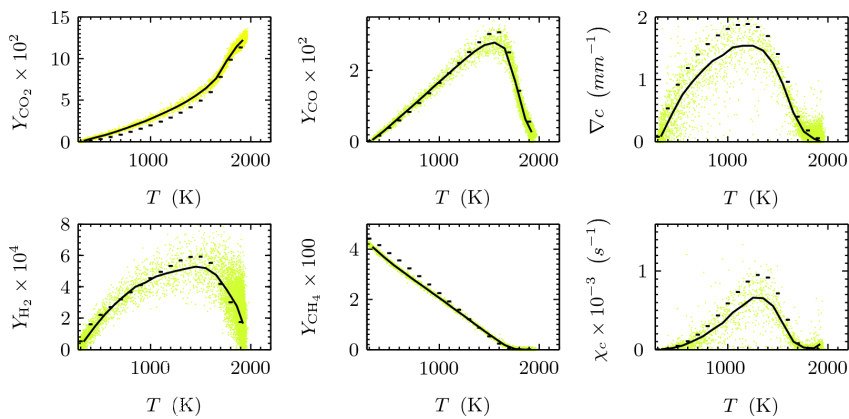
SwB1, premixed, non-swirling

SwB9, stratified, non-swirling

27

# Cambridge Stratified Swirl Burner

Sweeney, Hochgreb, Barlow, Dunn



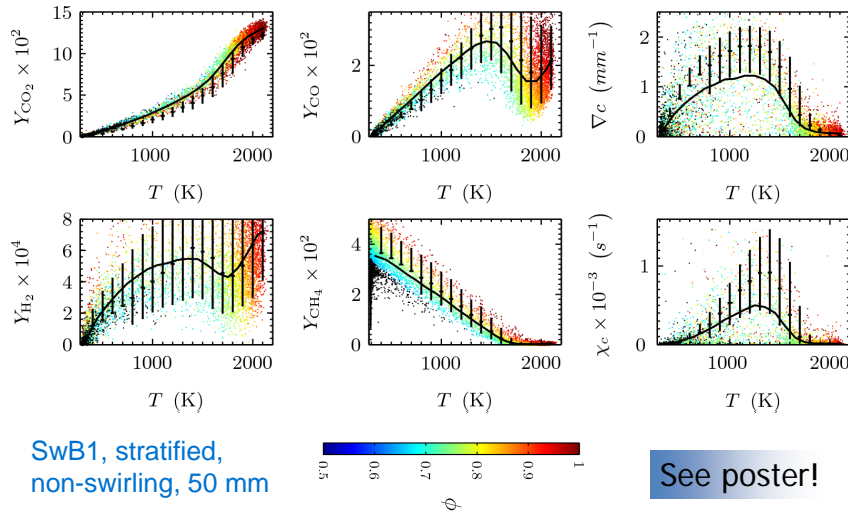
SwB1, premixed, non-swirling, 30 mm

See poster!

28

# Cambridge Stratified Swirl Burner

Sweeney, Hochgreb, Barlow, Dunn



29

## Summary – (Weakly) Stratified Flames



- Overall observations
  - Extension of lean flammability limit by stratification of lean flames
  - Evidence of effect of gradients on laminar flame speeds
  - Higher FSD, broader curvature distribution
- Flame structure
  - Largely consistent with premixed flamelets (some differences due to differential diffusion (?))
  - Measured gradients generally lower than expected from laminar calculations: strain and curvature?

30

## What experiments should be done next?

- Higher stratification ratios crossing into edge flames
- Higher turbulence levels
- Higher Re
  
- Focus on scalar-velocity interactions (curvature, strain)?

31

## Thanks

- R. Barlow, M. Dunn, Sandia National Labs
- M. Sweeney, University of Cambridge
- A. Cessou, B. Renou (Rouen), N. Guilbert (Poitiers)
  
- The Leverhulme Trust

32

# TNF 10 Session Abstract: Partially Premixed Combustion Modeling

Session Chairs: E. Knudsen and E. S. Richardson

## Abstract Of Session Presentation

The goal of this session was to review the current of state of stratified, partially premixed, and mixed regime turbulent combustion models, and to suggest directions for future work that will help to advance the fidelity of model performance in these challenging conditions.

The first half of the presentation reviewed the combustion physics that characterize mixed-regime burning, and that must be accounted for by any relevant modeling approach. So-called ‘front-supported’ and ‘back-supported’ premixed flames were used as example cases that motivate this discussion. In these flames, the equivalence ratio of a co-flow is set as either farther from stoichiometric (front-supported) or closer to stoichiometric (back-supported) than a central jet stream. Newly available DNS data was referenced to demonstrate how these different configurations change the premixed flame’s structure and burning speed. Once the possible effects of stratification are understood, it becomes important to understand the conditions under which these effects are expected to appear. Therefore, in an effort to more rigorously distinguish between stratified combustion and purely premixed combustion, the controlling variables that might appear in a regime diagram for stratification were discussed. These include the ratio of the maximum possible change in burning speed to the mean burning speed, the ratio of the Kolmogorov length scale and the mean flame thickness, and the mixing timescale associated with the local fuel concentration.

In the second half of this presentation, several of the most widely used LES combustion models were discussed with respect to how they handle multi-regime burning. The approaches considered were the flamelet model, the thickened flame model, filtered density function approaches, and the linear eddy model. Each of these approaches was noted to have some particular advantages and particular disadvantages in the context of partially premixed combustion. For example, the flamelet model is expected to predict flame structure very accurately in both the non-premixed and premixed limits, but the extent to which descriptions of these asymptotic regimes can be combined to describe a mixed mode flame structure remains unclear.

Finally, several approaches to locally distinguishing between premixed and non-premixed regimes in an LES were discussed. The simplest of these approaches is the flame index, but more detailed approaches that rely on coordinate transformations that explicitly distinguish regimes were also discussed. These approaches are now being actively applied in LES, and are the subject of ongoing model development efforts.

## Items Of Discussion

- One point that was raised throughout the workshop was the particular challenge that premixed combustion presented, and how this challenge was distinct from the non-premixed modeling challenge. Because stratified and partially premixed combustion inherently have premixed-like behavior, models for premixed flame propagation and flame structure are essential for any predictive multi-regime approach.

## Comments On Future Work

- A continuing need exists for the improvement of regime distinguishing indicators. These indicators will be needed in most combustion models that involve tabulated chemistry, but have only begun to be developed.
- Beyond the need for regime indicators to be used within models, a broad framework (e.g. regime diagrams) for classifying and comparing different partially premixed flows – and the resultant combustion physics – will be helpful. Further study of the stratified and partially-premixed data sets presented at this workshop may help determine the relevant effects of various equivalence ratio and equivalence ratio length-scale distributions.

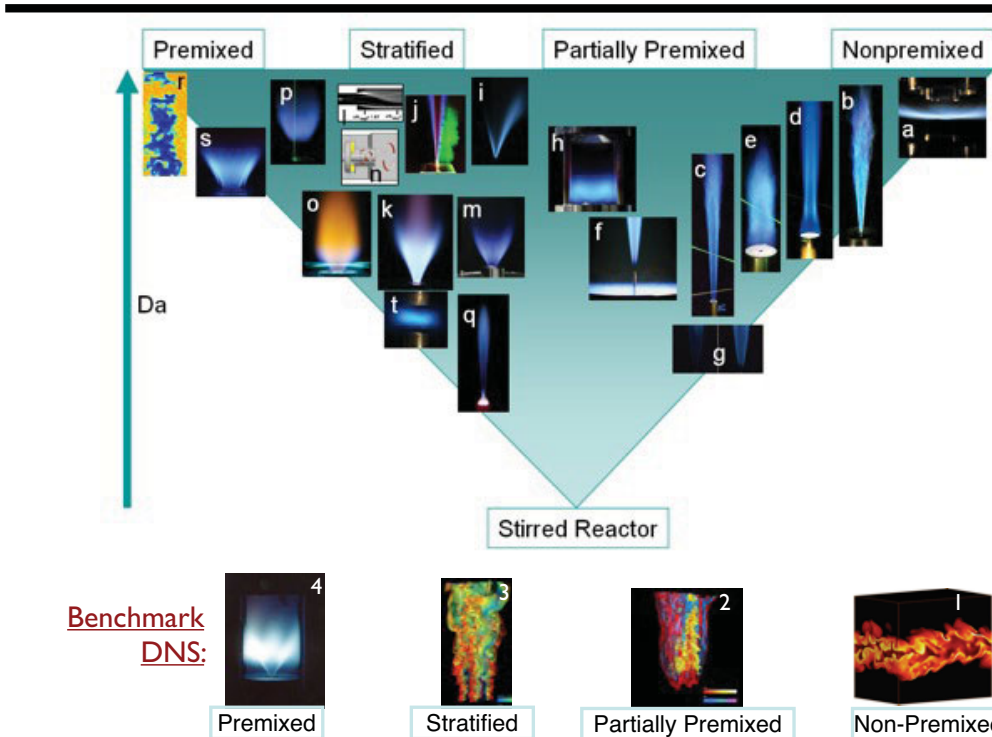
# Modeling Approaches For Stratified And Partially Premixed Combustion

E. S. Richardson  
Sandia National Laboratories

E. Knudsen  
Stanford University

TNF 10 Workshop, July 30<sup>th</sup> 2010

## The Partially-Premixed Spectrum



# Index of flames plotted above

## Experimental data

a	TUD turbulent opposed jet burner.	Geyer2005, Böhm2006
b	DLR simple jet flames of CH <sub>4</sub> /H <sub>2</sub> /N <sub>2</sub> in air.	Bergmann1998, Meier2000, Hult2005, Wang2007, Wang2008, Frank2008
c	Sandia piloted CH <sub>4</sub> /air air jet flames.	Barlow1998, Schneider2005, Barlow2005, Karpetis2005, Wang2007
d	Sydney bluff-body flames of CH <sub>4</sub> /H <sub>2</sub> .	Dally1998, Dally2003
e	Sydney swirl/bluff-body flames.	Kalt2002, Al-Abdeli2003, Masri2004
f	Berkeley/Sydney nonpremixed lifted jet flames in vitiated H <sub>2</sub> /air coflow.	Cabra2002, Cabra2005, Gordon2007
g	Adelaide nonpremixed jet flames in vitiated coflow (low O <sub>2</sub> levels)	Dally2002, Medwell2007
h	DLR model gas turbine combustor (steady and unsteady cases).	Duan2005, Gizendanner2005, Meier2005, Weigand2005, Weigand2006, Meier2006, Meier2007
i	Cambridge stratified slot burner, CH <sub>4</sub> /air V-flame.	Anselmo-Filho2009, Barlow2009
j	CORIA-INSA stratified V-flame.	Renou2004, Degardin 2006, Robin2008
k	TUD piloted annular stratified burner.	Dreizler et al.
l	ORACLES burner.	Nguyen2003, Domingo2005, Robin2006, Duwig2007
m	Cambridge stratified swirl burner Work in progress.	
n	Twente stratified swirl combustor (steady and oscillating cases).	Sengissen2007
o	TECFLAM premixed swirl burner.	Schneider2005, Freitag2005, Freitag2007, Schneider2008
p	TUD premixed low-swirl burner.	Nogenmyr2007
q	Sydney piloted premixed jet in vitiated Coflow.	Dunn2007, Dunn2008
r	Place holder for various premixed flames with low u'/SL	
s	Sandia premixed swirling dump combustor	Oefelein2006
t	Premixed and stratified flames, turbulent counter flow, high u'/SL	Coppola 2009, Coriton 2010

## DNS data

1a	Non-premixed temporal jets with extinction and re-ignition, CO-H <sub>2</sub> , and C <sub>2</sub> H <sub>4</sub> fuels with simple soot model.	Hawkes 2007, Lignell 2009
1b	Non-premixed temporal jet with CH <sub>4</sub> and H <sub>2</sub> fuel.	Knaus 2009
2a	Lifted planar fuel jets, H <sub>2</sub> and C <sub>2</sub> H <sub>4</sub>	Richardson 2009, Yoo 2009, Yoo 2010
2b	Lifted round H <sub>2</sub> jet	Mizobuchi 2002
2c	Autoigniting plume	Kerkemeier
3*	Stratified slot Bunsen jet configurations, realistic CH <sub>4</sub> chemistry.	Richardson 2010
4a	Premixed laboratory swirl burner, tabulated chemistry.	Vervisch 2010
4b	Slot Bunsen jet configurations, realistic CH <sub>4</sub> chemistry.	Sankaran 2007, Richardson 2010
4c	Laboratory scale methane-air slot Bunsen, realistic CH <sub>4</sub> chemistry.	Bell 2007
4d	Isotropic turbulence, high u'/SL, H <sub>2</sub> fuel.	Poludnenko 2010

\*Other stratified turbulent DNS data in decaying turbulence are provided by Malkeson (Malkeson and Chakraborty 2010a, 2010b), Grout (Grout et al. 2009), Hélie (Hélie and Trouvé 1998), and Haworth (Haworth et al. 2000, Jiménez et al. 2002).

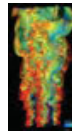
3

# Outline

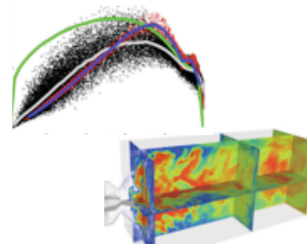
STANFORD UNIVERSITY



## 1. Partially Premixed Physics



## 2. Modeling Approaches



## 3. Modeling Applications



## 4. Modeling Needs

3/ 29

# Stratified Combustion Effects

- Starting from the turbulent premixed combustion paradigm:

$$\frac{S_T}{S_L} = I_0 A' \quad A' = A_{wrinkled} / A_{flat}$$

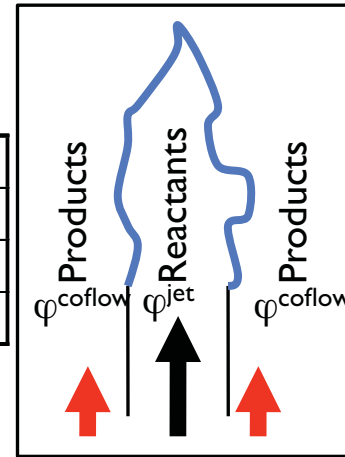
- How does stratification affect flame area  $A'$ ?
- And burning intensity  $I_0$ ?

- Compare slot Bunsen flame DNS in three cases:



	Reactants	Products
Premixed	$\varphi^{jet}=0.7$	$\varphi^{coflow}=0.7$
Back supported	$\varphi^{jet}=0.4$	$\varphi^{coflow}=1.0$
Front supported	$\varphi^{jet}=1.0$	$\varphi^{coflow}=0.4$

$\text{CH}_4$  fuel, jet Reynolds number = 2,100, identical boundary conditions.



# Stratified Combustion Effects

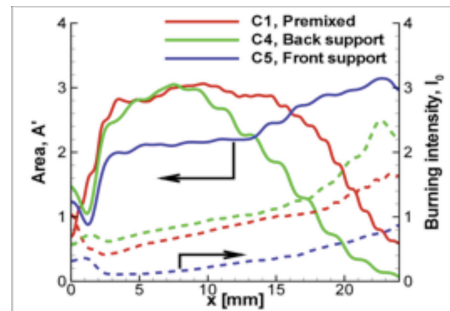
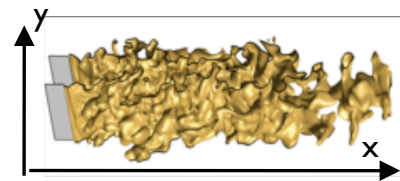
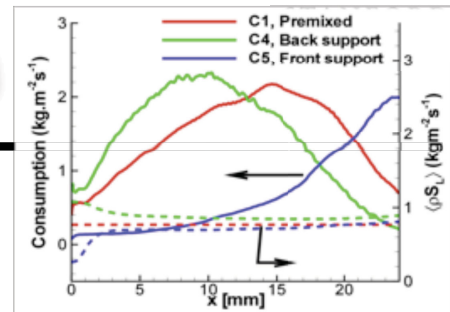
- Integrated consumption rate is greatly reduced for front supported flame, and increased for back support.

$$\int_0^{z+\Delta} \int_0^{Ly} \int_0^{x+\Delta} \dot{\omega}_c dx dy dz$$

- Average equivalence ratio and averaged laminar flame speed similar in each case, with average laminar flame speed indicated by :

$$\overline{\rho_u S_L} = \frac{\int_0^{z+\Delta} \int_0^{Ly} \int_0^{x+\Delta} \rho_u S_L |\nabla c| dx dy dz}{\int_0^{z+\Delta} \int_0^{Ly} \int_0^{x+\Delta} |\nabla c| dx dy dz}$$

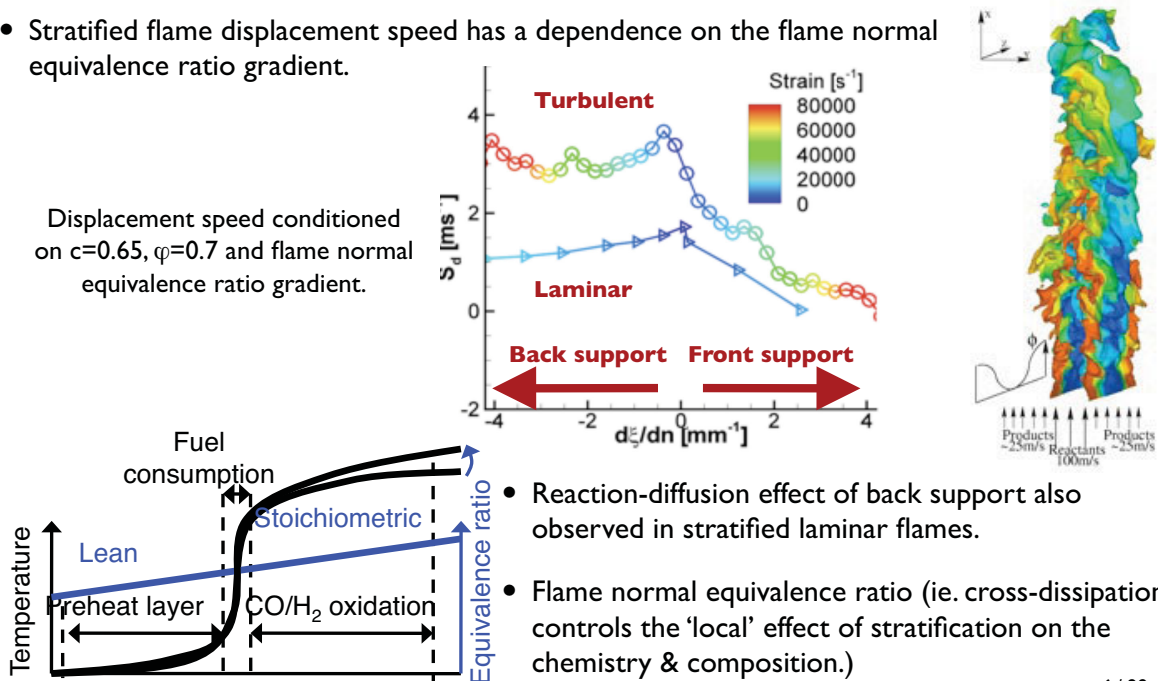
- Need for modeling to account for evolution of flame area – differential propagation?
- Need to understand the effect on burning intensity...



# Stratified Combustion Effects - Flame Speed

- Stratified flame displacement speed has a dependence on the flame normal equivalence ratio gradient.

Displacement speed conditioned on  $c=0.65$ ,  $\varphi=0.7$  and flame normal equivalence ratio gradient.



- Reaction-diffusion effect of back support also observed in stratified laminar flames.
- Flame normal equivalence ratio (ie. cross-dissipation controls the 'local' effect of stratification on the chemistry & composition.)

Richardson et al, 2010 6 / 29

# Characterizing Partially-Premixed Combustion

## Two-regime combustion indicators

- Non-premixed / Premixed: (Yamashita 1996). Improved by (Fiorina 2005)

$$\alpha = \frac{\nabla Y_{Fu} \cdot \nabla Y_{Ox}}{|\nabla Y_{Fu} \cdot \nabla Y_{Ox}|}$$

- Autoignition / Deflagration: Zeldovich criterion (J.H. Chen 2006)

$$I = S_L \nabla \tau_{ign} \cdot \underline{n}$$

## Multi-regime combustion indicators

- Domingo 2008 
$$\frac{\partial Y_i}{\partial Y_c} = \frac{1}{Da^{DF}} \frac{\partial^2 Y_i}{\partial Z^2} + \frac{1}{Da^{PF}} \frac{\partial^2 Y_i}{\partial Y_c^2} + \frac{1}{Da^{PPF}} \frac{\partial^2 Y_i}{\partial Z \partial Y_c} + \dot{\omega}_i$$

$$Da^{DF} = \frac{\dot{\omega}_{Y_c}}{\rho \chi_z} \quad Da^{PF} = \frac{\dot{\omega}_{Y_c}}{\rho \chi_c} \quad Da^{PPF} = \frac{\dot{\omega}_{Y_c}}{\rho \chi_{z,Y_c}}$$

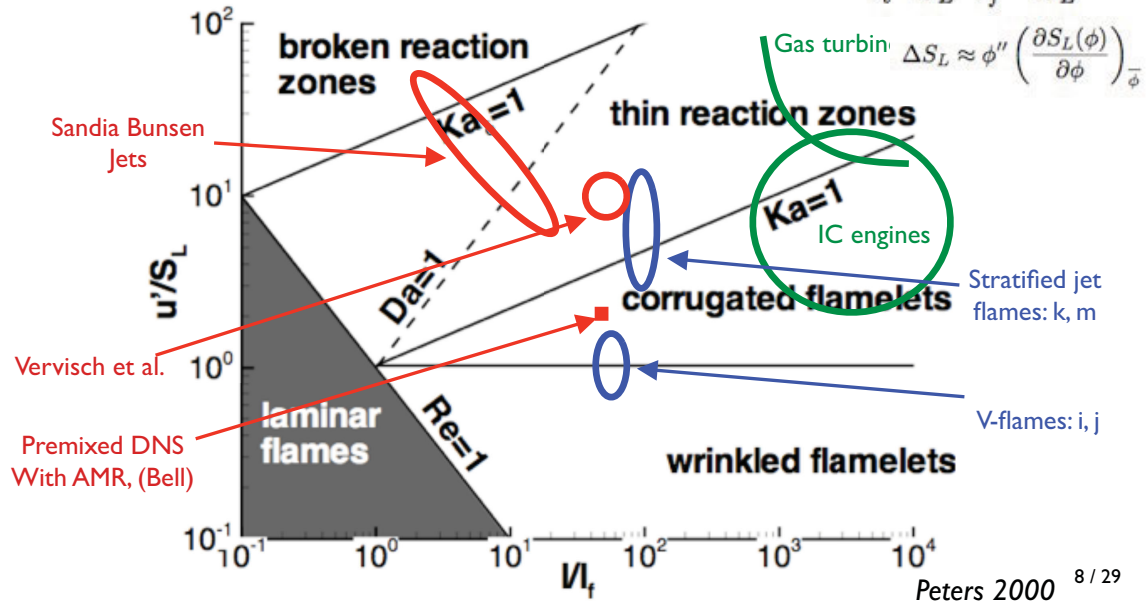
- Knudsen 2009, based on 2-D flamelet transformation – more later

7 / 29

# Characterizing Partially-Premixed Combustion

What additional parameters describe *turbulent* stratified combustion?

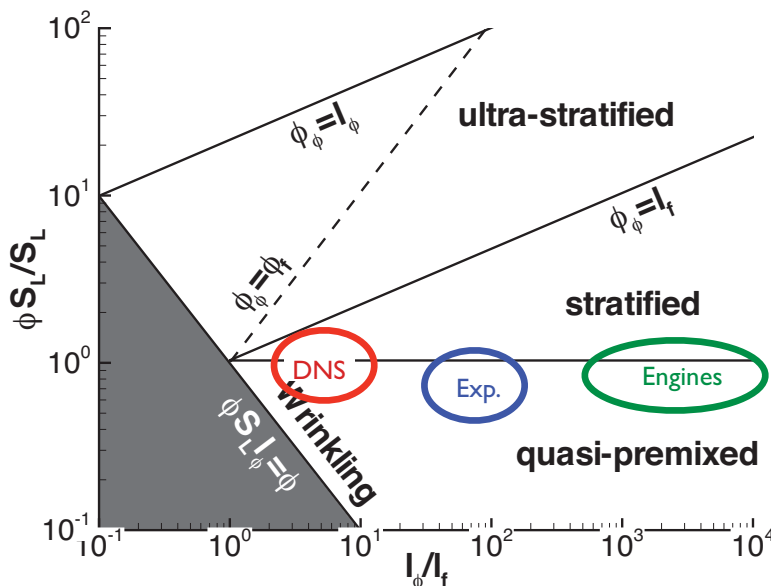
$$l_\phi, \phi'', D_\phi, l_t, u', \nu, l_f, S_L, \alpha \xrightarrow{\nu \approx D_\phi \approx \alpha \approx S_L l_f} \frac{l_\phi}{l_t}, \frac{u'}{S_L}, \frac{l_\phi}{l_f}, \frac{\Delta S_L}{S_L}$$



# Characterizing Partially-Premixed Combustion

Assuming stratification scales are imposed by the turbulence cascade: (rather than by spray evaporation, for example)

$$\begin{aligned} l_\phi &\approx l_t, \lambda_\phi \approx \eta_k \\ \tau_f &= l_f / S_L \\ \tau_\phi &= D_\phi / l_\phi^2 \approx l_f S_L / l_\phi^2 \end{aligned}$$



$\tau_\phi \ll \tau_f$  flame too slow to respond to stratification

$\lambda_\phi < l_f$ : Stratification affects internal flame structure

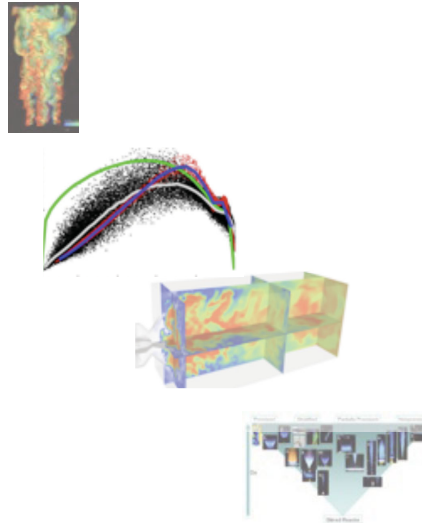
$\tau_\phi \ll \tau_f$  flame too slow to respond to stratification

$\Delta S_L \Lambda_\phi < S_L l_f$  stratification too small - scale to wrinkle flame.

$\Delta S_L \gg S_L$  unlikely to occur.

# Outline

1. Partially Premixed Physics
2. Modeling Approaches
3. Modeling Applications
4. Modeling Needs



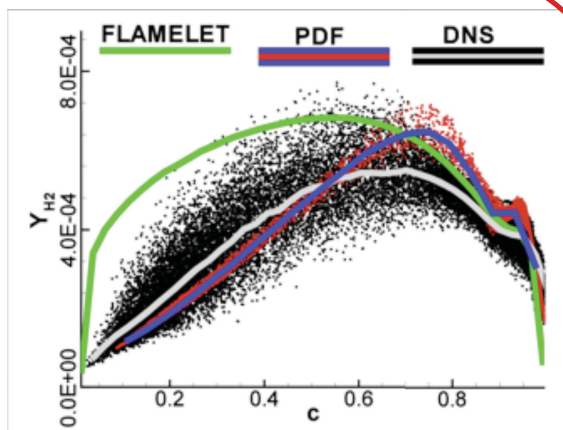
10 / 29

# Modeling Overview

## Structural models

Built on assumed flame structure

Laminar flamelets, Thickened Flame Model



Premixed CH<sub>4</sub> Bunsen DNS (Sandia DNS flame CI) in the thin reaction zones regime: H<sub>2</sub> mass fraction conditioned on progress variable c. Unstrained flamelet (green), EMST PDF model (red scatter and blue conditional mean) DNS (black scatter, grey conditional mean).

## Statistical models

No flame assumptions regarding the flame structure  
→ regime independent, but difficult to capture correct reaction-diffusion physics using 1-point statistics.

e.g. PDF methods (including Stochastic fields), (conditional-)moment methods.

## Models combining statistical and structural components

For example the Linear Eddy Model (Kerstein):

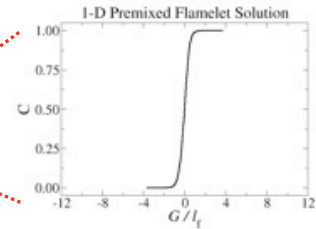
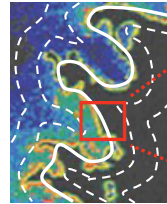
Combines detailed transport for small-scale reaction-diffusion + statistical representation of the turbulent convection.

11 / 29

# Flamelet Models

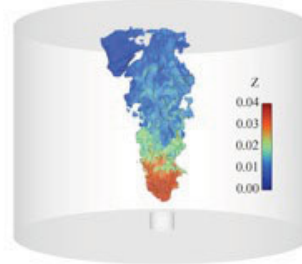
- Modeling approach
  - Solve asymptotic combustion problems
  - Tabulate solutions for mapping in LES
 
$$\phi_i = \phi_i(Z, C, \dots)$$
  - Arbitrarily detailed chemistry

OH In Premixed Flame (Buschmann, 1996)



- Partially premixed application
  - I-D counterflow flames (Fiorina 2005), 2-D spray flame (Domingo 2005), Stratified swirl burner (Knudsen 2009)
  - How should local regime be selected?
  - How should regime interactions be described (I-D or 2-D flamelets?)

LES of Swirl Burner (Knudsen, 2009)



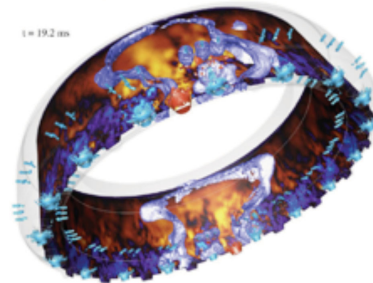
Swirl Burner Exp. (Cheng, LBNL)

12 / 29

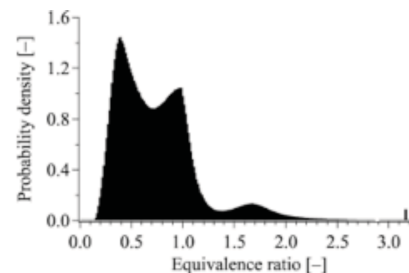
# Thickened Flame Models

- Modeling approach
  - Explicitly broaden flame structure by factor  $F$ 

$$\frac{D\phi_i}{Dt} = E \left( F \cdot \text{Diff} + \frac{\dot{\omega}_i}{F} \right)$$
  - Relatively inexpensive; typically 1-step chemistry
  - Regimes not distinguished
- Partially premixed application
  - Helicopter spray combustor: good agreement w/ exp.
  - Can flame quenching (stability) be predicted?
  - How does the thickening affect minor species? Soot?



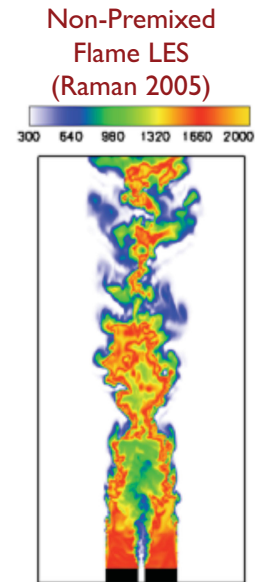
Helicopter Combustor LES (Boileau 2008), (Boudier 2008)



13 / 29

# FDF / PDF Models

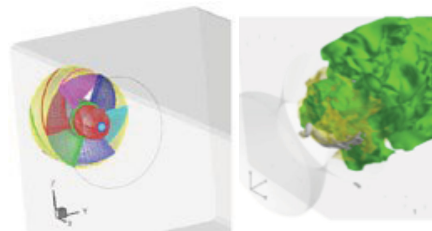
- Modeling approach
  - Solve chemistry realizations using particles
  - Model mixing between realizations
  - Regime distinction not required (Xu 2000) ...
  - ... but often used (Anand 1987, Raman 2005, Lindstedt 2006)
- Partially premixed application
  - Limited, partly due to limited premixed studies, especially for LES
  - Mixing model continues to be critical
  - Is regime selection appropriate?



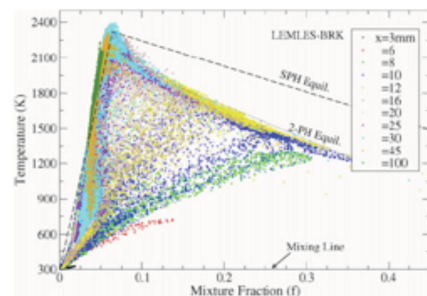
14 / 29

# Linear Eddy Models (LEM)

- Modeling approach
  - Solve 1-D problems in each mesh cell
$$\Delta\phi_i = \Delta t \left( -u' \frac{d\phi_i}{dx} + \text{Diff} + \dot{\omega}_i \right)$$
  - Typically 2- or 3- step mechanisms
  - Regimes not distinguished
  - Stratification effects appear through fuel / O<sub>2</sub> interactions on 1-D meshes
- Partially premixed application
  - Aircraft spray combustor LES: predicts many mixed but unburned realizations
  - 1-D micro-scale sufficient for stratification?
  - Are there constraints on 3-D vs. 1-D resolution?

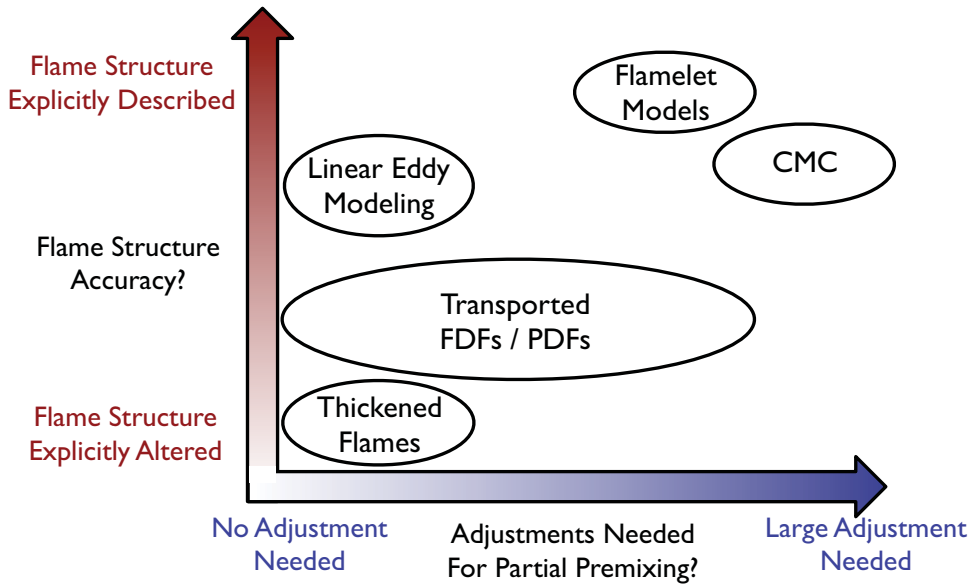


Aircraft Combustor LES (Patel, 2008)



15 / 29

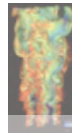
# Assessing Partially Premixed Capabilities



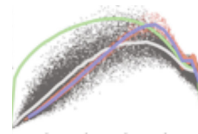
A useful model does not need to accurately predict **all quantities**, but should **consistently** predict **a few quantities** with reasonable accuracy

# Outline

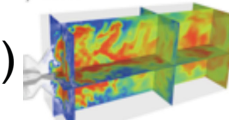
1. Partially Premixed Physics



2. Modeling Approaches



3. Modeling Applications (Flamelet Models)



4. Modeling Needs



# Multi-Regime Flamelet Model

- Transform scalar transport equation ...

$$\rho \frac{\partial \phi_i}{\partial t} + \rho \mathbf{u} \cdot \nabla \phi_i = \nabla \cdot (\rho \mathbf{D}_i \nabla \phi_i) + \rho \dot{\omega}_i$$

- ... Into regime-specific coordinate basis

$$\Theta_{\text{premix}} = \partial_{\Lambda} C [\rho_u s_{L,u} |\nabla \Lambda| - \nabla \cdot (\rho D \nabla \Lambda)]$$

$$\Theta_{\text{nonpre}} = -\rho \frac{\chi Z}{2} \partial_Z^2 C$$

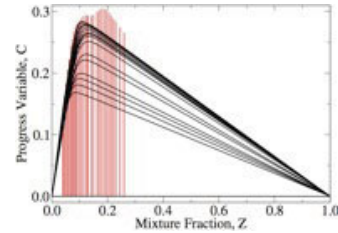
- Locally examine regime strength

$$\xi = \frac{\int_V \Theta_{\text{premix}} dV}{\max(\int_V \Theta_{\text{premix}} dV + \int_V \Theta_{\text{nonpre}} dV, \epsilon)}$$

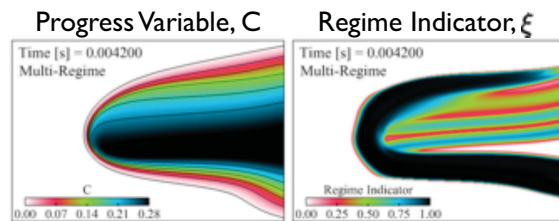
## Flamelet Database

Black: Non-Premixed Flamelets

Red: Premixed Flamelets



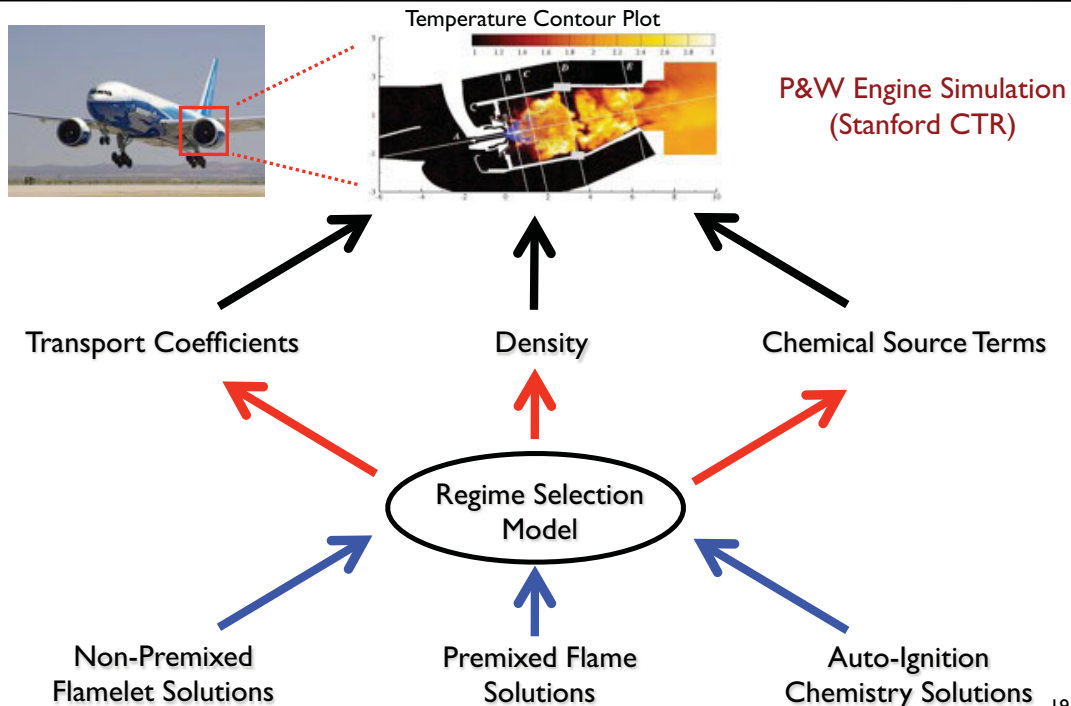
## Laminar Triple Flame



Knudsen & Pitsch, Comb. Flame 2009

18 / 29

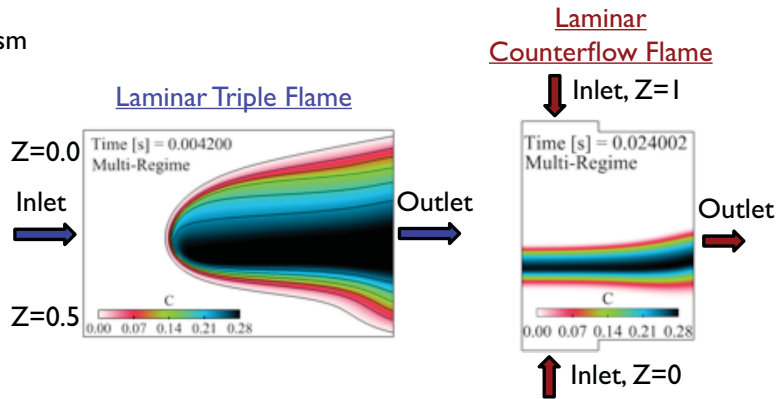
# Multi-Regime Model Schematic



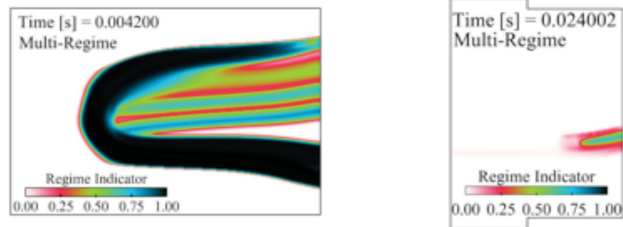
19 / 29

# Regimes In Laminar *n*-Heptane Flames

- 44 species *n*-heptane mechanism (Liu et al., 2004)
- Unity Lewis numbers
- Flamelet variables
  - Mixture fraction:  $Z$
  - Progress variable:  $C$
  - Level set:  $G$
- 4 combustion model cases
  - Finite rate (true solution)
  - Non-premixed ( $Z, C$ )
  - Premixed ( $Z, C, G$ )
  - Multi-regime ( $Z, C, G$ )

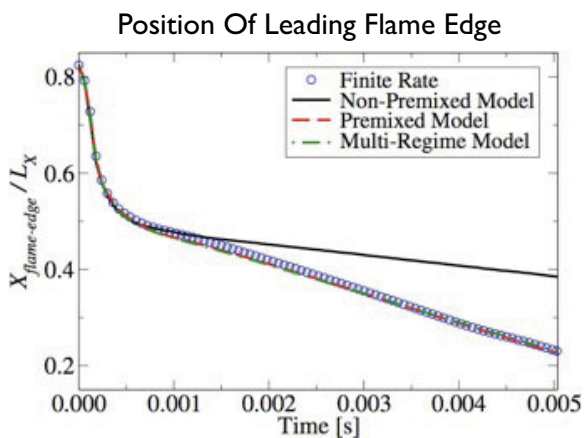


## Regime Indicator Predictions

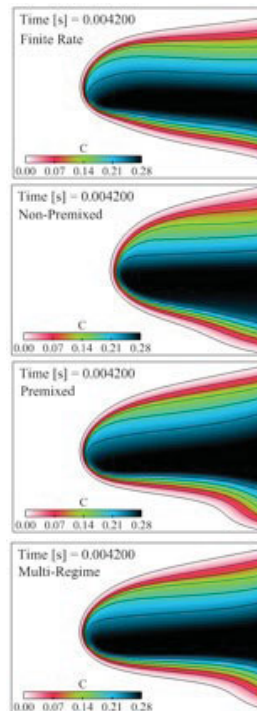


20 / 29

# Triple Flame Propagation Speed



The premixed flamelets' dependence on  $Z$  captures stratified propagation speeds



Finite Rate  
(True Solution)

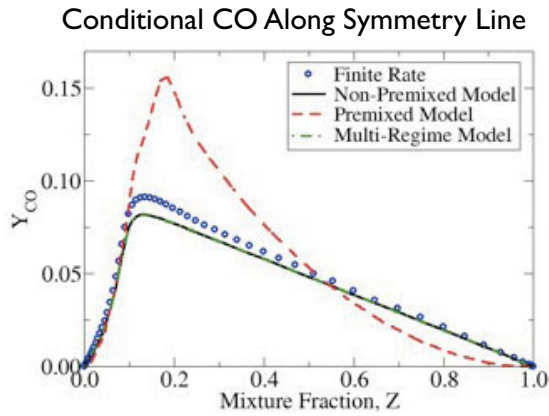
Purely Non-Premixed  
Model

Purely Premixed  
Model

Multi-Regime Model

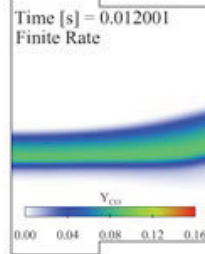
21 / 29

# CO Species In Counterflow Flame

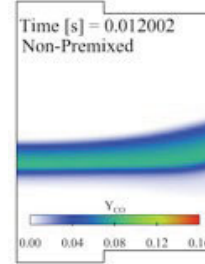


Non-premixed regime captures CO well;  
multi-regime model correctly selects flamelets

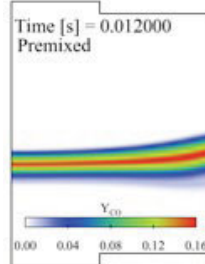
Finite Rate  
(True Solution)



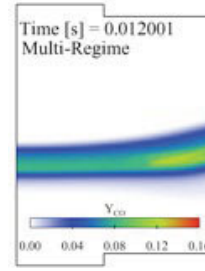
Purely Non-Premixed  
Model



Purely Premixed  
Model

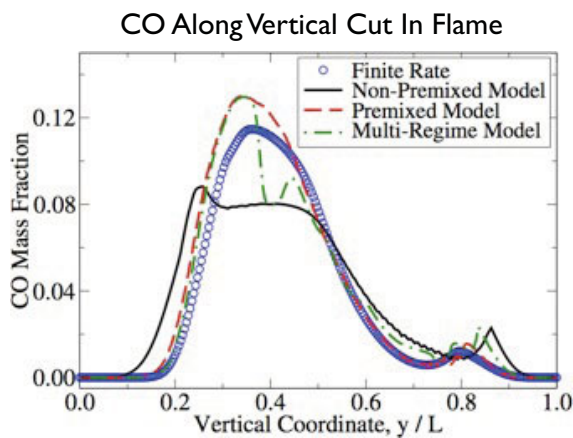


Multi-Regime Model

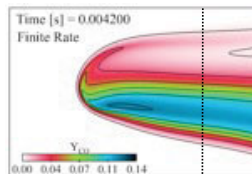


22 / 29

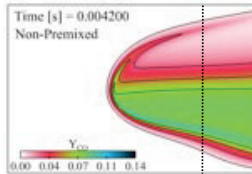
# CO Species In Triple Flame



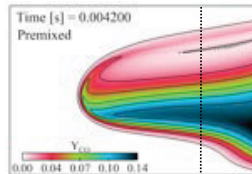
Neither pure regime is adequate ...  
appropriately blending regimes is the challenge



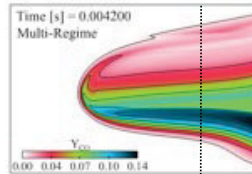
Finite Rate  
(True Solution)



Purely Non-Premixed  
Model



Purely Premixed  
Model



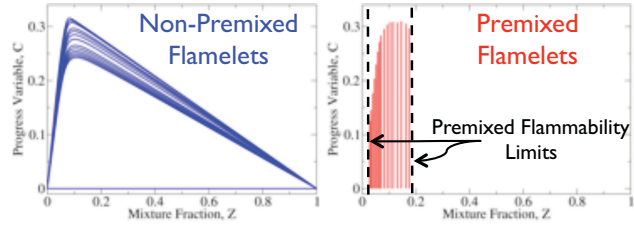
Multi-Regime Model

23 / 29

# Multi-Regime LES Application

- LES of NASA's LDI combustor

- Liquid jet A fuel
- $Re \sim 30,000$
- 122 species mechanism

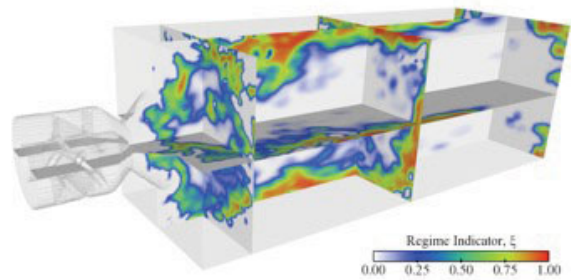


- Is post-evaporation **premixing** important?

$\xi = 0$  (White): Non-premixed mapping  
 $\xi = 1$  (Red): Premixed mapping

- **Multi-regime** model

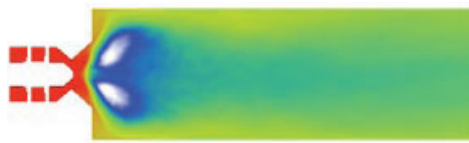
- Tabulate 1-D flamelet sets
- Map chemistry with regime indicator,  $\xi$



\*Knudsen & Pitsch, Comb. Flame 2009

# LES Of LDI Spray Combustor

Time averaged mixture fraction: **multi-regime model** vs. purely **non-premixed model**



Multi-Regime

Mixture Fraction, Z  
0.00 0.04 0.08 0.12 0.16

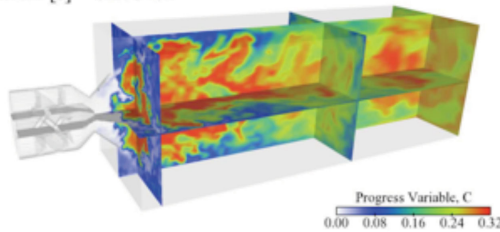


Non-Premixed

Mixture Fraction, Z  
0.00 0.04 0.08 0.12 0.16

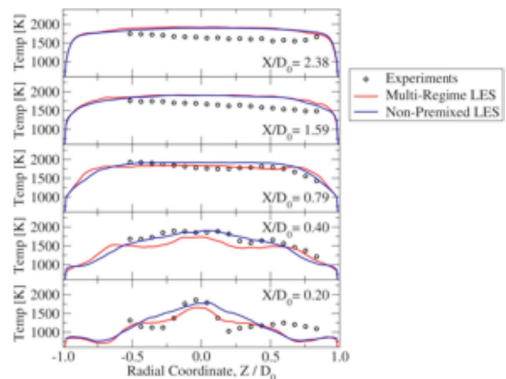
→ Inclusion of premixed regime leads to increased evaporation

Time [s] = 0.176401

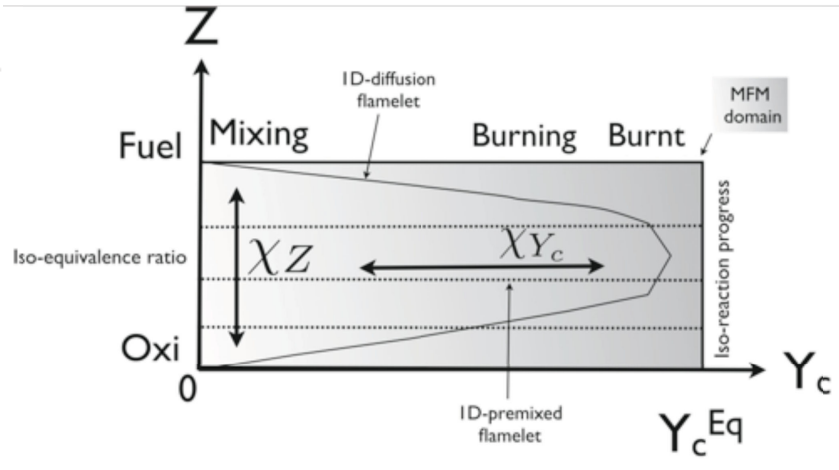
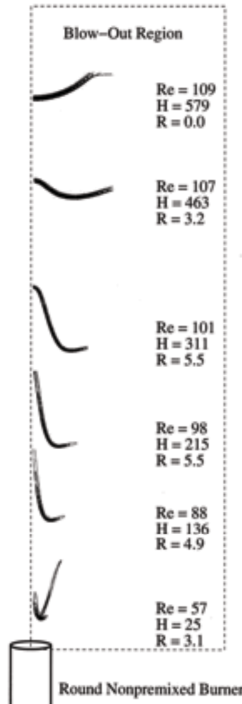


Progress Variable, C  
0.00 0.08 0.16 0.24 0.32

- **Partial premixing** leads to
  - $\sim 100$  K temperature differences **near injector**
  - Large changes in **minor species**



## MFM - Chemistry tabulation Z-Yc coupled

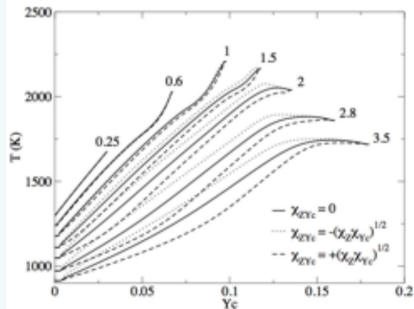


P.-D. Nguyen et al., Combust. Flame 157(1): 43-61 (2010)

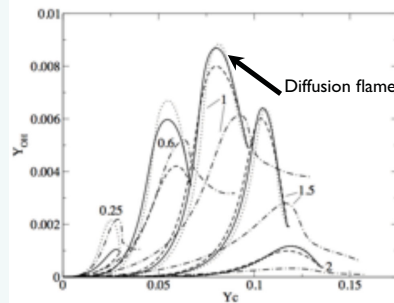
26 / 29

$$\rho \frac{\partial Y_i}{\partial \tau} + \sum_{j=1}^M \frac{\partial Y_i}{\partial \phi_j} (\dot{\omega}_j + \nabla \cdot (\rho D_i^* \nabla \phi_j)) = \sum_{j=1}^M \sum_{k=1}^M \frac{\rho \chi_{jk}}{Le_i} \frac{\partial^2 Y_i}{\partial \phi_j \partial \phi_k} + \dot{\omega}_i$$

Equivalence ratio variation and progress  
of reaction fully coupled



Manifolds depend on flame topology as captured by cross-scalar dissipation rate

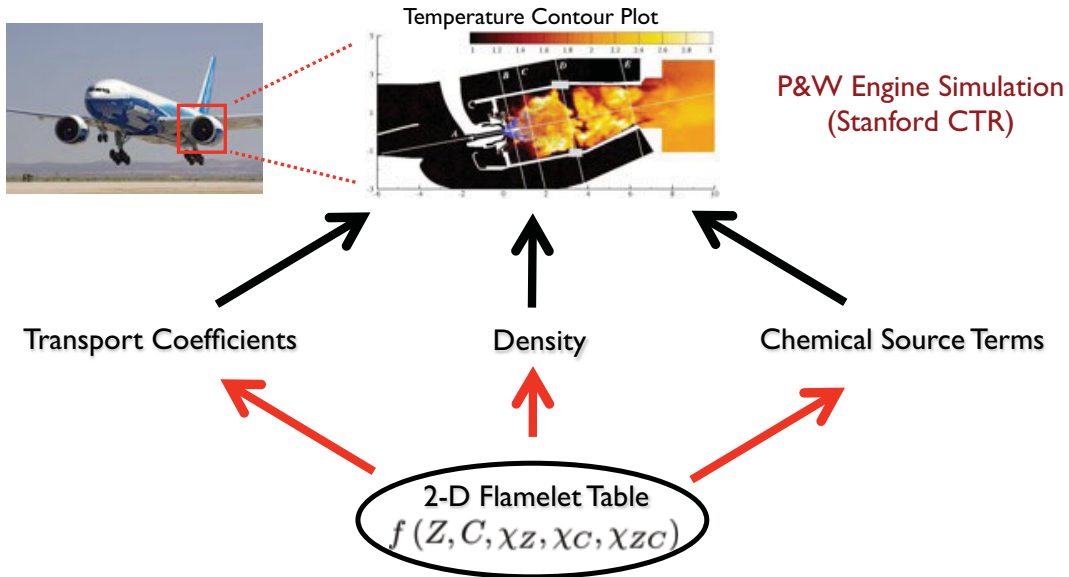


Composition space responses for various strain rates, comparison with diffusion-flamelet: strong differences are observed.

P.-D. Nguyen et al., Combust. Flame 157(1): 43-61 (2010)

27 / 29

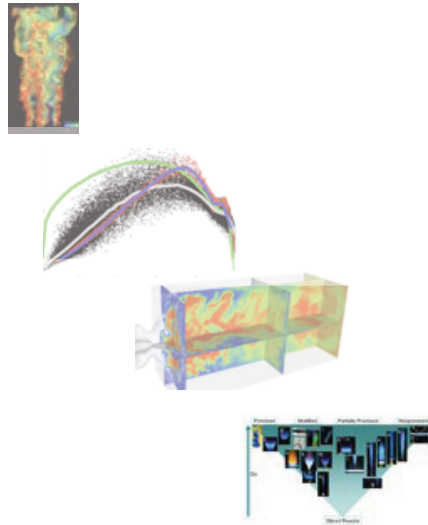
# 2-D Flamelets Model Schematic



- **Advantage:** Regimes implicitly accounted for by table coordinates
- **Challenges:** Memory to store table; modeling the dissipation rates

# Outline

1. Partially Premixed Physics
2. Modeling Approaches
3. Modeling Applications
4. Modeling Needs



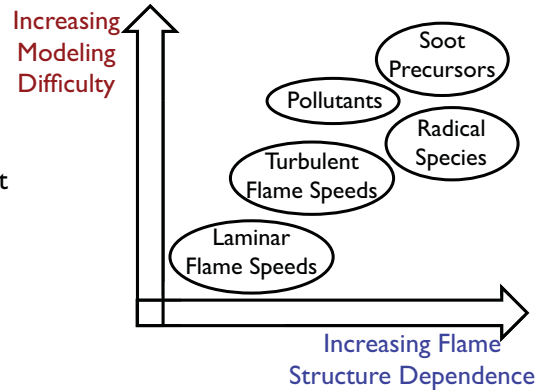
# Partially Premixed Modeling Needs

## General Needs

- Firmer relationships between a given model's errors and combustor conditions
- Flame structure dependence on Z & C alignment
- Turbulent flame speed for partial mixing
- Pollutant / soot formation for partial mixing
- Data on post-evaporation regimes

## Model-Specific Needs

- Mixed 1-D flamelets or 2-D flamelets? When?
- Better (more efficient) chemistry tabulation
- Can global chemistry models predict flame stability/quenching? When do they fail?



## Promising Trends

- Increasing variety, detail of experimental data
- Detailed chemistry DNS data across regimes
- Increasing simulation of industrially relevant (partially premixed) flows

29 / 29

## References (I)

- Al-Abdeli, YM, Masri, AR, *Exp. Thermal Fluid Sci.*, 27 (2003) 655–665.
- Anand MS, Pope SB, *Combust. Flame* 67 (2) (1987) 127–142.
- Anselmo-Filho, P, Hochgreb, S, Cant, RS, Barlow, RS, *Proc. Combust. Inst.* (2009).
- Barlow, RS, Frank, JH, *Proc. Combust. Inst.* 27 (1998) 1087–1095.
- Barlow, RS, Frank, JH, Karpetis, AN, Chen, JY, *Combust. Flame* 143 (2005) 433–449.
- Barlow, RS, *Proc. Combust. Inst.* 31 (2007) 49–75.
- Barlow, RS, Wang, GH, Anselmo-Filho, P, Sweeney, M, Hochgreb, S, *Proc. Combust. Inst.* (2009).
- Bell JB, Day MS, Grcar JF, Lijewski MJ, Driscoll JF, Filatyev SA. *Proc. Combust. Inst.* 31 (2007) 1299–1307.
- Boileau M, Staffelbach G, Cuenot B, Poinso T, Berat C, *Combust. Flame* 154 (2008) 2–22.
- Boudier G, Gicquel LYM, Poinso T, Bissieres D, Berat C, *Proc. Combust. Inst.* 31 (2007) 3075–3082.
- Buschmann A, Dinkelacker F, Schäfer T, Schäfer M, Wolfrum J, *Proc. Combust. Inst.* 26 (1996) 437–445.
- Bergmann, V, Meier, W, Wolff, W, Stricker, W, *Appl. Phys. B* 66 (1998) 489–502.
- Böhm, B, Geyer, D, Dreizler, A, Venkatesan, KK, Laurendeau, NM, Renfro, MW, *Proc. Combust. Inst.* 31 (2007) 709–717.
- Böhm B, Frank JH, Dreizler A, *Proc. Combust. Inst.* (2010).
- Bonaldo A, Kelman JB. *Combustion and Flame* 156 (2009) 750–762.
- Cabra, R, Myhrvold, T, Chen, JY, Dibble, RW, Karpetis, AN, Barlow, RS, *Proc. Combust. Inst.* 29 (2002) 1881–1888.
- Cabra, R, Chen, JY, Dibble, RW, Karpetis, AN, Barlow, RS, *Combust. Flame* 143 (2005) 491–506.
- Cai J, Jeng S-M, Tacina R, *ALAA Paper* 2005-1424, 2005.
- Chen JH, Hawkes ER, Sankaran R, Mason SD, Im HG, *Combust. Flame* 145 (2006) 128–144.
- Coppola G, Coriton B, Gomez A. *Combust. Flame* 156 (2009) 1834–1843.
- Coriton B, Frank JH, Hsu AG, Smooke MD, Gomez A. *Proc. Combust. Inst.* (2010).
- Dally, BB, Masri, AR, Barlow, RS, Fiechtner, GJ, *Combust. Flame* 114 (1998) 119–148.
- Dally, BB, Masri, AR, Barlow, RS, Fiechtner, GJ, *Combust. Flame* 132 (2003) 272–274.
- Dally, BB, Karpetis, AN, Barlow, RS, *Proc. Combust. Inst.* 29 (2002) 1147–1154.
- Domingo, P, Vervisch, L, Payet, S, Hauguel, R, *Combust. Flame* 143 (2005) 566–586.
- Domingo P, Vervisch L, Veynante D. *Combust. Flame* 152 (2008) 415–432.
- Duan, XR, Meier, W, Weigand, P, Lehmann, B, *Appl. Phys. B* 80 (2005) 389–396.
- Dunn, MJ, Masri, AR, Bilger, RW, *Combust. Flame* 151 (2007) 46–60.
- Duwig, C, Fureby, C, *Combust. Flame* 151 (2007) 85–103.
- Fiechtner, *Combust. Flame* 114 (1998) 119–148.
- Fiorina B, Gicquel O, Vervisch L, Carpentier S, Darabiha N, *Combust. Flame* 140 (2005) 47–160.
- Frank, JH, Kaiser, SA, *Exp. Fluids* 44 (2008) 221–233.
- Freitag, M, Klein, K, *Flow Turb. Combust.* 75 (2005) 51–66.
- Freitag, M, Janicka, J, *Proc. Combust. Inst.* 31 (2007) 1477–1485.
- Geyer, D, Kempf, A, Dreizler, A, Janicka, J, *Proc. Combust. Inst.* 30 (2005) 681–689.
- Gizendanner-Thoben, R, Meier, U, Meier, W, Aigner, M, *Flow Turb. Combust.* 75 (2005) 317–333.
- Gordon, RL, Masri, AR, Pope, SB, Goldin, GM, *Combust. Flame* 151 (2007) 495–511.
- Grout, RW, Swaminathan, N, Cant, RS, *Combust. Theor. Model.* 13(5) (2009) 823–852.
- Hawkes ER, Sankaran R, Sutherland JC, Chen JH, *Proc. Combust. Inst.* 31 (1) (2007) 1633–1640.
- Haworth, DC, Blint, RJ, Cuento, B, Poinso T, *Combust. Flame* 121 (2009) 395–417.
- Hélie, J, Trouvé, A, *Proc. Comb. Inst.* 27 (1998) 891–898.
- Hult, J, Meier, U, Meier, W, Harvey, A, Kaminski, CF, *Proc. Combust. Inst.* 30 (2005) 701–709.
- Janicka, J, Sadiki, A, *Proc. Combust. Inst.* 30 (2005) 537–547.
- Janus, B, Dreizler, A, Janicka, J, *Flow Turb. Combust.* 75 (2005) 293–315.
- Jiménez, C, Cuenot, B, Poinso T, Haworth, D, *Combust. Flame* 128 (2002) 1–21.
- Kalt, PAM, Al-Abdeli, YM, Masri, AR, Barlow, RS, *Proc. Combust. Inst.* 29 (2002) 1913–1919.
- Karpetis, AN, Barlow, RS, *Proc. Combust. Inst.* 30 (2005) 665–672.
- Knaus R, Pantano C, *J. Fluid Mech.* 626 (2009) 67–109.
- Knudsen, EW, Pitsch, H, *Open Thermodynamics J.*, submitted, 2009.

## References (2)

- Knudsen, E, Pitsch, H, *Combust. Flame*, 156 (3) (2009) 678-696.
- Lignell DO, Hewson JC, Chen JH, *Proc. Combust. Inst.* 32 (1)(2009) 1491-1498.
- Lindstedt RP, Vaos EM, *Combust. Flame* 145 (3) (2006) 495-511.
- Malkeson, SP, Chakraborty, N., *Numerical Heat Transfer A* (accepted) 2010
- Malkeson, SP, Chakraborty, N., *Combust. Sci. Tech.* (accepted) 2010
- Masri, AR, Kalt, PAM, Barlow, RS, *Combust. Flame* 137 (2004) 1-37.
- Medwell, PR, Kalt, PAM, Dally, BB, *Combust. Flame* 148 (2007) 48-61.
- Meier, W, Barlow, RS, Chen, YL, Chen, JY, *Combust. Flame* 123 (2000) 326-342.
- Meier, W, Duan, XR, Weigand, P, *Proc. Combust. Inst.* 30 (2005) 835-842.
- Meier, W, Duan, XR, Weigand, P, *Combust. Flame* 144 (2006) 225-236.
- Meier, W, Weigand, P, Duan, XR, Giezendanner-Thoben, R, *Combust. Flame* 150 (2007) 2-26.
- Mizobuchi, Y, Tachibana, S, Shinio, J, Ogawa, S, Takeno, T, *Proc. Combust. Inst.* 29 (2) (2002) 2009-2015.
- Mizobuchi, Y, Shinjo, J, Ogawa, S, Takeno, T, *Proc. Combust. Inst.* 30 (1) (2005) 611-619.
- Nguyen, P.-D., Vervisch, L, Subramaniam, V, Domingo, P, *Combust. Flame* 157(1) (2010) 43-61.
- Nguyen, PD, Bruel, P, 41st Aerospace Sciences Meeting and Exhibit, Reno, January 2003, Paper 2003-0958.
- Nogenmyr, KN, Petersson, P, Bai, XS, Nauert, A, Olofsson, J, Brackman, C, Seyfried, H, Zetterberg, J, Li, ZS, Richter, M, Dreizler, A, Linne, M, Alden, M, *Proc. Combust. Inst.* 31 (2007) 1467-1475.
- Oefelein, JC, Schefer, RW, Barlow, RS, *ALAA Journal* 44 (2006) 418-433.
- Pasquier, N, Lecordier, B, Trinité, M, Cessou, A, *Proc. Combust. Inst.* 31 (2007) 1567-1574.
- Patel, N, Menon, S, *Combust. Flame* 153 (2008) 228-257.
- Peters N, *Turbulent Combustion* 2000 Cambridge University Press.
- Poludnenko AY, Oran ES, *Combust. Flame* 157 (2010) 995-1011.
- Raman, V, Pitsch H, *Combust. Flame* 142 (2005) 329-347.
- Raman, V, Pitsch H, Fox, RO, *Combust. Flame* 143 (2005) 56-78.
- Renou, B, Samson, E, Boukhalfa, A, *Combust. Sci. and Tech.* 176 (2004) 1867-1890.
- Richardson, ES, Yoo, CS, Chen, JH, *Proc. Combust. Inst.* 32 (2) (2009) 1695-1703.
- Richardson ES, Granet VE, Eyssartier A, Chen JH. *Combust. Theor. Model.* 2010 accepted.
- Richardson ES, Sankaran R, Grout RW, Chen JH. *Combust. Flame* 157 (2010) 506-515.
- Robin, V, Mura, A, Champion, M, Plion, P, *Combust. Sci. Tech.*, 178 (2006) 1843-1880.
- Robin, V, Mura, A, Champion, M, Degardin, O, Renou, B, Boukhalfa, M, *Combust. Flame* 153 (2008) 288-315.
- Schneider, C, Dreizler, A, Janicka, J, *Flow, Turb. Combust.* 74 (2005) 103-127.
- Schneider, E, Maltsev, EA, Sadiki, A, Janicka, J, *Combust. Flame* 152 (2008) 548-572.
- Sengissen, AX, Van Kampenb, JF, Huls, RA, Stoffels, GGM, Kok, JBW., Poinsot, TJ, *Combust. Flame* 150 (2007) 40-53.
- Sweeney MS, Hochgreb S, Dunn MJ, Barlow RS, *Proc Combust. Inst* (2010).
- Vervisch L et al. DNS of a premixed swirl burner, awaiting publication 2010.
- Wang, GH, Karpetis, AN, Barlow, RS, *Combust. Flame* 148 (2007) 62-75.
- Wang, GH, Clemens, NT, Varghese, PL, Barlow, RS, *Combust. Flame* 152 (2008) 317-335.
- Weigand, P, Meier, W, Duan, XR, Giezendanner-Thoben, R, Meier, U, *Flow Turb. Combust.* 75 (2005) 275-292.
- Wehr, L, Meier, W, Kunte, P, Hassa, C, *Proc. Combust. Inst.* 31 (2007) 3099-3106.
- Weigand, P, Meier, W, Duan, XR, Stricker, W, Aigner, M, *Combust. Flame* 144 (2006) 205-224.
- Yamashita H, Shimada M, Takeno T, *Proc. Combust. Inst.* 26 (1) (1996) 27-34.
- Yoo CS, Sankaran R, Chen JH, *J. Fluid Mech.* 640 (2009) 453-481.
- Yoo CS, Richardson ES, Sankaran R, Chen JH, *Proc. Combust. Inst.* (2010).

# Stratified flames from TUD

Summary by Andreas Dreizler



Institute Reactive Flows and Diagnostics  
Center of Smart Interfaces  
Faculty of Mechanical Engineering  
TU Darmstadt  
Petersenstr. 32, 64287 Darmstadt, Germany



TNF 10 | A. Dreizler | 1



# Stratified flames from TUD

Summary by Andreas Dreizler



## Contributors:

TUD-people (Seffrin, Böhm, Fuest, Karimi, Ketelheun, Künne, Janicka)  
Sandia (Frank, Barlow)

TNF 10 | A. Dreizler | 2



## Contents



- Burner design
- Operational conditions
- Diagnostics: applied, in progress
- Next steps

TNF 10 | A. Dreizler | 3



## Features of the burner design



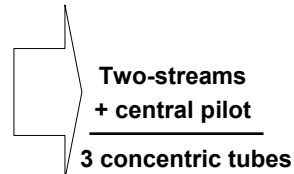
- Provide benchmark for intentionally stratified flames
- Statistically stationary flames (no propagating flames)
- Simple flow field, high Re-Nos., fully developed turbulent pipe flows
  - Should suit geometry-inflexible codes for validation
- Generate regions with (steep) mixture stratification parallel and perpendicular to flame front
  - Significant stratification relative to typical LES resolutions
- Full optical access, open flame, shielded by large coflow

TNF 10 | A. Dreizler | 4



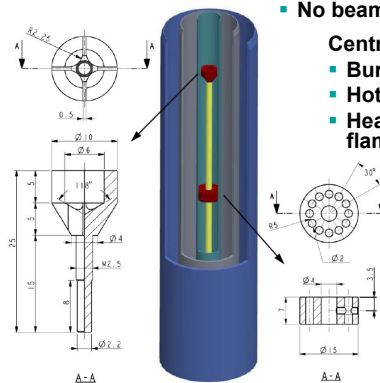
## Features of the burner design

- Flame stabilization without recirculation
  - therefore pilot flame with minimal influence on region of interest and not disturbing laser diagnostics (beam steering, radiation trapping)
- Potential for wide parametric variation of
  - Stratification
    - lean-lean
    - lean-rich, including stoich. conditions
  - Shear
  - Fuel



## Burner design

### ■ Sketch



### General features

- Three streams, individual MFCs
- Staggered exit tubes, full optical access for f# 2.0
- No beam steering because of central pilot

### Central pilot

- Burning inside ceramic tube
- Hot exhaust velocity matched with gases from slot 1
- Heat transfer from pilot tube to slot 1 minimized by flame holder design

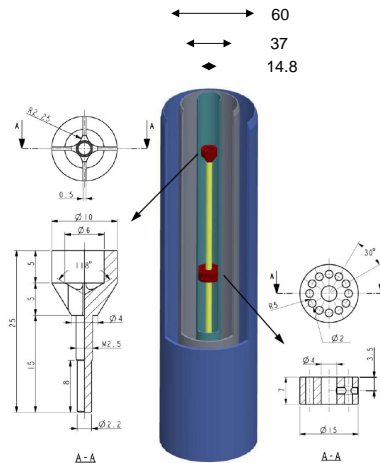
### Slot 1

- Cold gases velocity matched to exhaust from pilot
- Thin rim to slot 2 to avoid recirculation
- Same  $\phi$  as pilot

### Slot 2

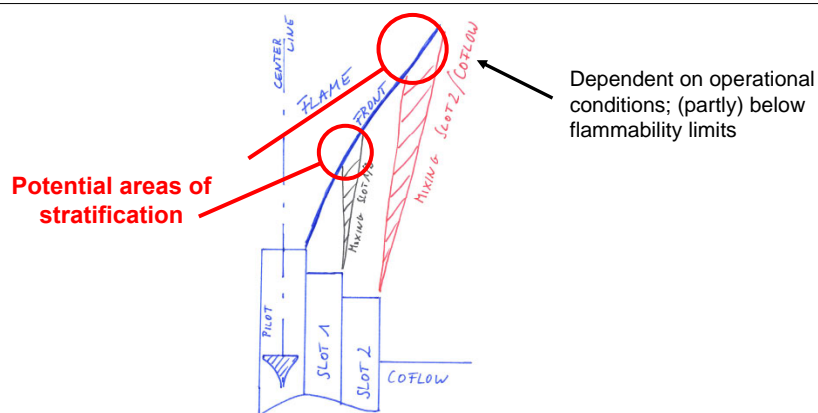
- Variation of  $\phi$  and exit velocities relative to slot 1

## Burner design



- Hydraulic diameter of slot 1  $\approx$  slot 2
- Inflow:  $>25$  hydraulic diameters (version with 40 hydraulic diameter long tubes resulted in almost identical nozzle exit velocity profiles)

## Burner design



### Some issues for future work

- Relevance of stratification (overall topology/ flame brush; flame structures; flame speeds changes because of back/ front support; ...)
- Understanding effects of stratification and come up with suitable model approaches

## Operational conditions (1)

- Mainly operation as lean( $\phi_1$ )-lean( $\phi_2$ ) or premixed (cases A – K)  
(w and w/o stratification between slot 1 and 2)
- One case lean-rich, including stoichiometric conditions (L)
- Base fuel methane, parametric variation
  - stratification but no shear (A, B, F)
  - shear but no stratification (E)
  - shear and stratification (C, D, H ethylene, J)
  - neither shear nor stratification (G, I ethylene, K)

## Operational conditions (2)

configuration	$\Phi_{Pilot}$	$v_{Pilot}$ [m/s]	$\Phi_{Slot1}$	$v_{Slot1}$ [m/s]	$Re_{Slot1}$	$\Phi_{Slot2}$	$v_{Slot2}$ [m/s]	$Re_{Slot2}$	$P_{total}$ [kW]	$l$ [mm]
TSF_A_r	0.9	1	0.9	10	13 600	0.6	10	13 100	72	120
TSF_A_il	0.9	1	0	10		0	10			
TSF_A_i2	0	10	0	10		0	10			
TSF_B_r	0.9	1.5	0.9	15	20 400	0.6	15	19 600	109	150
TSF_B_il	0.9	1.5	0	15		0	15			
TSF_B_i2	0	15	0	15		0	15			
TSF_C_r	0.9	1	0.9	10	13 600	0.6	5	6700	53	110
TSF_C_il	0.9	1	0	10		0	5			
TSF_D_r	0.9	1	0.9	10	13 600	0.6	20	26 200	111	130
TSF_D_il	0.9	1	0	10		0	20			
TSF_E_r	0.9	1	0.9	10	13 600	0.9	5	6600	64	110
TSF_F_r	0.9	1	0.9	10	13 600	0.75	10	13 100	83	120
TSF_G_r	0.9	1	0.9	10	13 600	0.9	10	13 100	94	130
TSF_H_r	0.9	0.6	0.6 (C <sub>2</sub> H <sub>4</sub> )	10	14 000	0.9 (C <sub>2</sub> H <sub>4</sub> )	5	6800	53	110
TSF_I_r	0.9	0.6	0.6 (C <sub>2</sub> H <sub>4</sub> )	10	14 000	0.6 (C <sub>2</sub> H <sub>4</sub> )	10	13 400	63	150
TSF_J_r	0.9	0.6	0.6	10	13 500	0.9	5	6600	52	(320)
TSF_J_il	0.9	0.6	0	10		0	5			
TSF_J_i2	0	6	0	10		0	5			
TSF_K_r	0.9	0.6	0.6	10	13 500	0.6	10	13 100	61	(250)
TSF_L_r	0.9	1	1.4	10	13 700	0.6	10	13 100	90	220

## Visual impressions

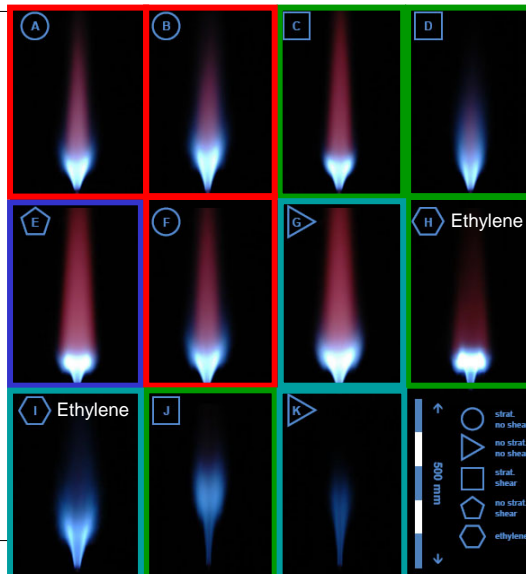
### ■ Flame photographs

Stratification, no shear

No stratification, shear

Stratification, shear

No stratification, no shear

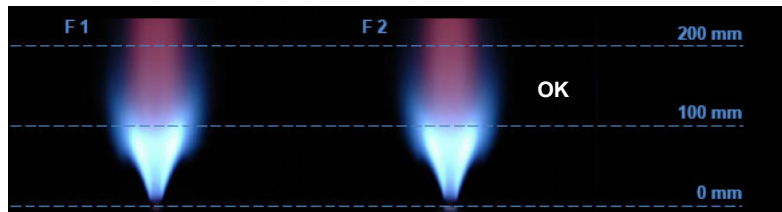


TNF 10 | A. Dreizler | 11

S.M.

## Copy of the burner

### ■ Second burner transferred to Sandia



- Flames are sensitive to proper alignment of three tubes
  - Experience from lab
  - Indicated by numerical simulations (Verena Klapdor)
- If aligned correctly, reproducible flame appearance, HWA-flow field (cold)

TNF 10 | A. Dreizler | 12

RSM

## Diagnosics (1)



- **Flow field (TUD, Seffrin & Ludwig)**
  - **LDV: radial profiles at typically 5 selected axial heights up to 250mm**
    - **2 velocity components, axi-symmetry is checked**
    - **Means, rms, 1 Reynolds-stress, auto-correlations, integral time scales**
  - **High speed PIV: at selected regions (Seffrin)**
    - **2 velocity components, gradients (vorticity, etc.)**
    - **Auto- and cross-correlations, integral length scales**
  
- **Details: F. Seffrin, F. Fuest, D. Geyer, A. Dreizler, Combust. Flame 157 (2010) 384–396.**

TNF 10 | A. Dreizler | 13



## Diagnosics (2)



- **Scalar field (Sandia, TUD: Böhm & Frank)**
  - **2D-Rayleigh (10Hz) & OH PLIF (10Hz, 10kHz): selected regions up to 80mm above exit (CS: 2A13, Tuesday 17:15)**
    - **Temperature fields → length scales to be analysed**
    - **Flame structures**
    - **Flame brush**
  - **Acetone PLIF & OH PLIF (10Hz): selected regions up to 80mm**
    - **Mixing fields prior to flame**
    - **Identification of regions with actually stratified flames**
  - **High speed acetone PLIF (10kHz) (Heeger&Gordon)**
    - **...**

TNF 10 | A. Dreizler | 14



## Diagnostics (3)

- **Scalar field, (TUD, Seffrin, Fuest, Stahler, Karimi, Geyer)**
  - **1D-Raman/Rayleigh**
    - **Temperature field**
    - **Main species concentrations and local equivalence ratios**
    - **Mean, rms, scatter plots**

## Experimental steps coming next

- **Rerun the measurements and final evaluation of 1D Raman/Rayleigh data (Seffrin, Fuest, Stahler, Karimi)**
- **Aim for measurements of scalar gradients**
- **Simultaneous CO LIF and Rayleigh measurements (Frank)**
- **Different operational conditions**
  - **Taking the flame faster to mixing region between slot 1 and 2 by increasing  $s_L$  ( $\rightarrow$  H<sub>2</sub> or C<sub>2</sub>H<sub>4</sub> addition, oxygen enrichment?)**
  - **Slot 2 fed by air?**
  - **Suggestions (faster and narrower coflow, ...) ?**

# Darmstadt Stratified Flames

## Model Comparisons

*W.P. Jones, S. Navarro-Martinez, K. Vogiatzaki, Imperial*  
*G. Kuenne, J. Janicka, Darmstadt*  
*A. Roux, H. Pitsch, Stanford*  
*F. Cavallo Marincola, A. Kempf, Imperial*  
*F. Seffrin, F. Fuest, D. Geyer, A. Dreizler, Darmstadt*

The Darmstadt Stratified Flames were presented as a new test case for the TNF 10 workshop. These flames were developed at Darmstadt university and have been investigated by Seffrin, Fuest, Geyer and Dreizler.

Preliminary experimental data for temperature (Rayleigh, Raman-Rayleigh), mixture fraction and CO<sub>2</sub> mass fraction (Raman) was also made available and presented at the workshop in comparison to the numerical simulations. (This preliminary experimental scalar data was only made available for presentation at TNF10, it has not been included here, as improved data will become available and be published soon.)

A set of flames was chosen as preferred target for the comparisons, and contributors were encouraged to simulate at least the non-reactive case TSFAi2 and the basic stratified case TSFAr. Only the Stanford group submitted further data for case TSFG.

Cases in descending order of priority

- |                                    |                                 |
|------------------------------------|---------------------------------|
| 1. TSFAi2 (isothermic)             | 2. TSFAr (stratified, no shear) |
| 3. TSFG (not stratified, no shear) | 4. TSFCr (stratified, shear)    |
| 5. TSFEr (no strat, shear)         |                                 |

All groups performed Large-Eddy Simulations, using (i) a sub-grid pdf/stochastic fields method in combination with the static Smagorinsky model (Imperial, Jones' Boffin-LES code), (ii) a flamelet model combined with the G-Equation and the Germano model (Stanford, NGA-3DA), (iii) premixed flamelet generated manifolds with local flame thickening and the Germano model (Darmstadt, FASTEST) and (iv) Fureby's flame surface density model with the static Smagorinsky model (Imperial, Kempf's PsiPhi code).

Two approaches were taken to represent the computational domain: Darmstadt and Stanford simulated the flow upstream, using one large domain with local refinement (Darmstadt) and a cascade of precursor simulations (Stanford). Both groups obtained results that were in good agreement with the experimental velocity data. Both groups from Imperial used a more compact computational domain, starting simulations at the outlet of the inner nozzle, prescribing the experimental velocity data.

Overall, all groups achieved good predictions of the data, particularly considering that a new TNF case was simulated. As the scalar data (temperature, mixture fraction and CO<sub>2</sub> mass fraction) only became available very late, the predictions of these quantities can be considered as 'blind'; modellers had no opportunity to tune their simulations to match the data.

The features of the flames that were found to be most challenging were the intricate geometry of the flame holder, the chamfer on the nozzle exits, and the relatively low co-flow velocity of only 0.1 m/s, which makes a long simulation time necessary.

For TNF11, it is recommended that the Darmstadt stratified flame series be considered as a test case. The lessons learned for TNF10 should enable all groups to accurately predict the flow and mixing, so that the focus can be shifted towards the effect of stratification on flame-turbulence interaction. It is hoped that groups will be able to start the TNF11 simulations earlier in the cycle than was the case for TNF10, thus allowing sufficient time for detailed simulations to be completed and potentially interesting comparisons to be made.

Any groups interested to contribute simulations of these flames for TNF11 should contact Andreas Kempf ([a.kempf@imperial.ac.uk](mailto:a.kempf@imperial.ac.uk)) to be included in the mailing list.

These slides were presented at the TNF 11 workshop. The slides contain information that is unfinished or still work in progress, provided in the spirit of discussing fresh, non-final results. The original authors have provided this information under the condition that the data will only be used for the TNF presentation and proceedings.

You may only use these slides in agreement with the rules set out in the TNF proceedings. In particular, you must not refer to or cite the information from these slides in any publication.

Andreas M Kempf, [a.kempf@imperial.ac.uk](mailto:a.kempf@imperial.ac.uk)

# Darmstadt Stratified Flames

## Model Comparisons

Guido Kuenne, Johannes Janicka | Darmstadt  
Anthony Roux, Heinz Pitsch | Stanford  
Konstantina Vogiatzaki, Navarro-Martinez, Bill Jones | Imperial  
Fabrizio Cavallo Marincola, Andreas M Kempf | Imperial

TNF 10

# Overview

- ✦ Cases
- ✦ Contributions
- ✦ Modelling Approaches
- ✦ Results
- ✦ Findings
- ✦ Discussion

# Cases

## TSF-A-i2 isothermal

- Pilot: 10 m/s
- Slot 1: 10 m/s
- Slot 2: 10 m/s
- Coflow: 0.1 m/s

## TSF-A-r reactive

- Pilot: 1 m/s, 0.9
- Slot 1: 10 m/s, 0.9
- Slot 2: 10 m/s, 0.5
- Coflow: 0.1 m/s
- 72 KW

# Contributions

**DA** | Guido Kuenne (PhD student), Johannes Janicka

**SU** | Anthony Roux (PD), Heinz Pitsch

**ICB** | *Boffin*: Salvador Navarro-Martinez (staff)  
Konstantina Vogiatzaki (PD), Bill Jones

**ICP** | *PsiPhi*: Fabrizio Cavallo Marincola (PhD student)  
Andreas M Kempf

# Simulations

	<b>Grid</b> mm	<b>Domain</b> mm	<b>Code</b>	<b>Cost</b> CPUh
<b>DA</b>	block-structured 0.8M, 6.5M cells	-120<x<600 r=300	<b>FASTEST</b> incompressible	5,400 43,000
<b>SU</b>	$0.5 < \Delta < 4$ 7.5M cells	Multiple precursor simulations	<b>NGA/3DA</b> incompressible	~20,000 1,500
<b>ICB</b>	$0.33 < \Delta$ 3M, 1.5M cells	600x600 500x500	<b>Boffin</b> incompressible	700 10,000
<b>ICP</b>	$\Delta = 1$ mm 6.4M, 20M cells	160x200x200 260x280x280	<b>PsiPhi <math>\Psi\Phi</math></b> incompressible	500 6,400

5

TNF 10

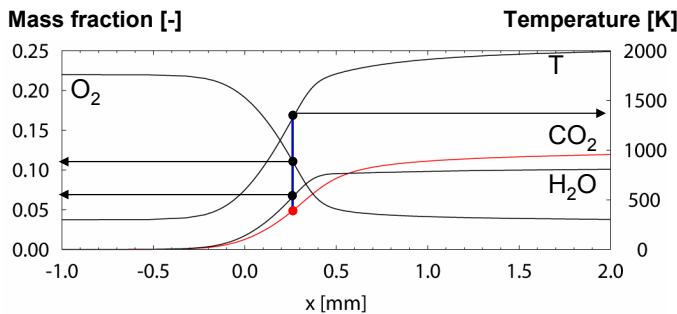
# Modelling Approaches

	<b>Combustion</b>	<b>Turbulence</b>
<b>DA</b>	Premixed Flamelet Generated Manifolds with Artificially Thickened Flame approach	Germano
<b>SU</b>	G-Equation model with tabulated Chemistry	Germano, Lagrangian
<b>ICB</b>	Transported FDF Model Stochastic Fields Method	Smagorinsky
<b>ICP</b>	Flame Surface Density model (Fureby) $S_f$ depends on mixture fraction	Smagorinsky

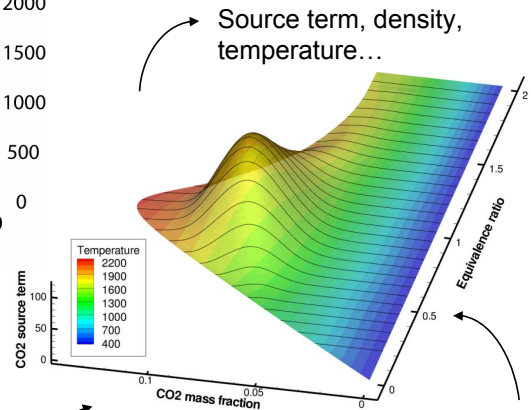
# DA | FGM

## Flamelet Generated Manifolds

- Detailed chemistry calculation of a 1-Dimensional premixed flame at constant equivalence ratio



- Selecting a monotone progress variable ( $\text{CO}_2$ )
  - Repeat the procedure for different equivalence ratios
- 2-Dimensional table, parameterized by the two controlling variables
- $\text{CO}_2$  mass fraction
  - Mixture fraction
- Controlling variables are transported by FASTEST



$$\frac{\partial}{\partial t}(\bar{\rho} \tilde{f}) + \frac{\partial}{\partial x_i}(\bar{\rho} \tilde{u}_i \tilde{f}) = \frac{\partial}{\partial x_i} \left( \bar{\rho} (\tilde{D} + D_t) \frac{\partial \tilde{f}}{\partial x_i} \right)$$

$$\frac{\partial}{\partial t}(\bar{\rho} \tilde{Y}) + \frac{\partial}{\partial x_i}(\bar{\rho} \tilde{u}_i \tilde{Y}) = \frac{\partial}{\partial x_i} \left( \bar{\rho} (\tilde{D} + D_t) \frac{\partial \tilde{Y}}{\partial x_i} \right) + S$$



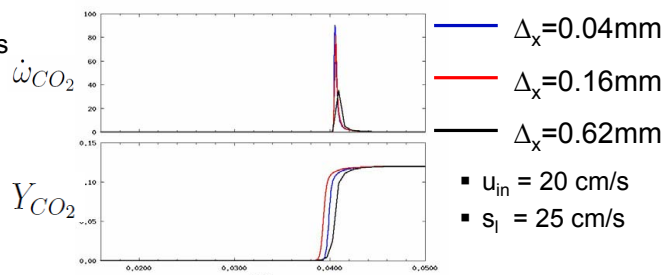
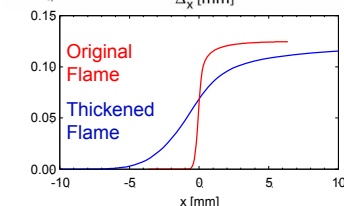
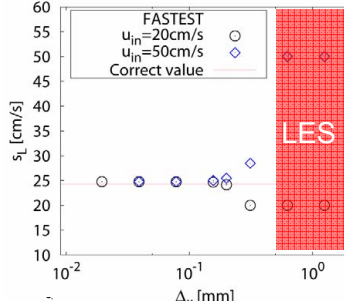
Guido Künne  
Johannes Janicka

TNF 10

# DA | ATF

## Artificially Thickened Flames

- Important flame characteristics can only be reproduced on very fine grids
- A large error occurs on LES-typical meshes



- Artificial thickening is used to extend the region of correct coupling to LES-meshes

(modeling according to: O. Colin *et al.* and F. Charette *et al.*)

$$\frac{\partial \rho Y_k}{\partial t} + \frac{\partial}{\partial x}(\rho u_i Y_k) = \frac{\partial}{\partial x} \left( \rho D_k \frac{\partial Y_k}{\partial x} \right) + \dot{\omega}_k$$

$$\frac{\partial \rho Y_k}{\partial t} + \frac{\partial}{\partial x_i}(\rho u_i Y_k) = \frac{\partial}{\partial x_i} \left( \rho \mathcal{F} \mathcal{E} D_k \frac{\partial Y_k}{\partial x_i} \right) + \frac{\mathcal{E}}{\mathcal{F}} \dot{\omega}_k$$

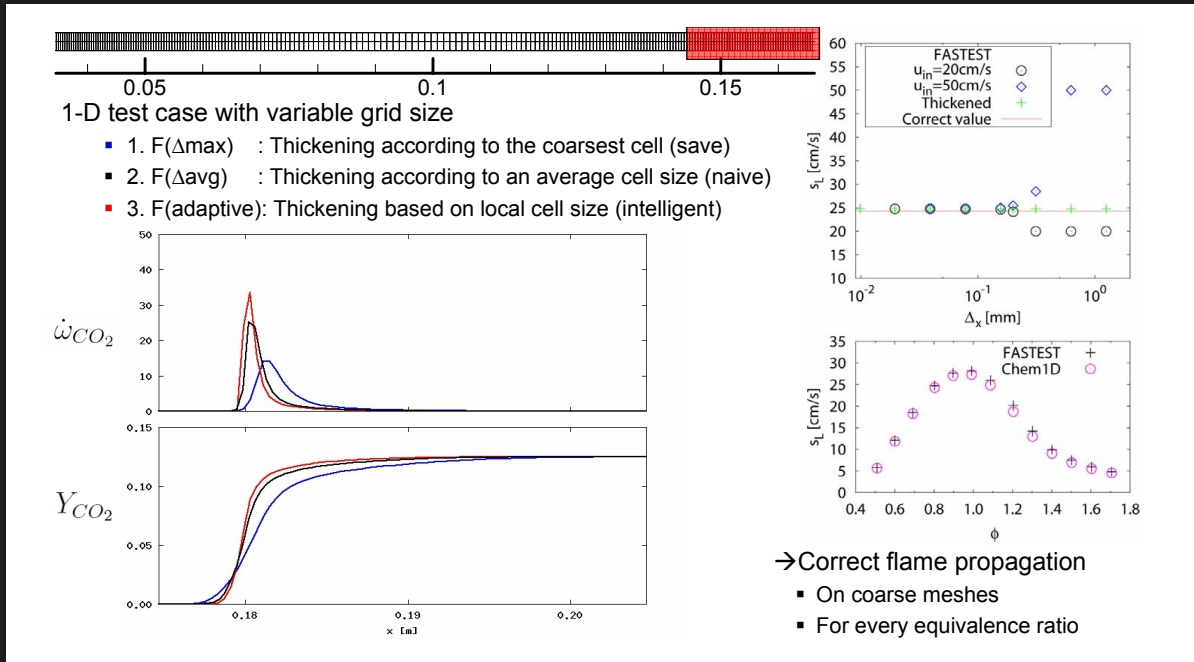
- Thickening is based on
  - Flame sensor to act only in the reactive layer
  - Local grid size



Guido Künne  
Johannes Janicka

202

29-31 July 2010, Beijing, China TNF 10

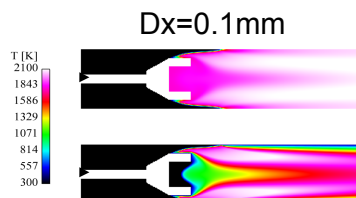


\* **Different series of inflow profiles are used:**

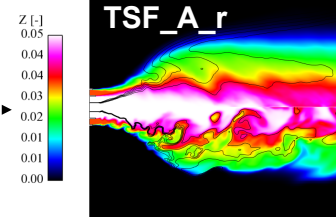
Solutions of 3 LES periodic pipes

Fed → Solution of LES of the flame holder

Fed → TSF Burner



$L = 0.4\text{m}$ ,  $R=0.2\text{m}$   
580x200x64  
 $Dx=0.5\text{mm}$   
(close to injection)



× **Flamelets model (Peters):**

- ◆ Solve both non-premixed and premixed 1D flames and tabulate solutions. Detailed chemistry from Gri-Mech 3.0.

$$\phi_i = \phi_i(\tilde{Z}, \tilde{Z}''^2, \tilde{C})$$

- ◆ Presumed PDF to describe subfilter distributions such as:

$$\tilde{P}(Z, C) = \tilde{P}_1(Z; \tilde{Z}, \tilde{Z}''^2) \times \tilde{P}_2(C|C; \tilde{Z})$$

$\tilde{P}_1$  is modeled using a  $\beta$ -PDF while  $\tilde{P}_2$  is approximated by a  $\delta$ -function.

- ◆ An algebraic equation is used to describe mixing.
- ◆ Multi-regime approach according Knudsen & Pitsch (CF, 2009).
- ◆ Enthalpy transported and used to correct temperature, density and source term directly.

× **Combustion model combines:**

- ◆ G-equation approach: Levelset model coupled with a transported progress variable (Knudsen & Pitsch, PoF, submitted).
- ◆ Flamelet-Progress Variable approach (C.D. Pierce, PhD, 2004)

× **Turbulence:**

- ◆ Dynamic Smagorinsky model with a Lagrangian-type statistical averaging procedure.



× **Semi-implicit finite difference code NGA/3DA (Desjardins et al, JCP, 2008):**

- Low-Mach number limit,
- AMG pressure solver,
- Second order accurate in both space and time, semi-implicit Crank-Nicolson scheme,
- weno3 scheme for scalar advection,
- Cylindrical coordinate mesh

× **Cost:**

- 68s per iteration on 64 pros Intel Xeon 2.33 GHz,
- 4 iterations of the velocity solver and 5 for the pressure solver
- $\Delta t = 2.5 \times 10^{-5}$  s,



# ICB | Imperial 'Boffin'

## Transported FDF Method

Fine grained PDF:  $\mathcal{F}(\underline{\psi}; \mathbf{x}, t) = \prod_{\alpha=1}^{N_s} \delta(\psi_\alpha - \phi_\alpha(\mathbf{x}, t))$

Sub-grid (filtered) PDF  $P_{sgs}(\underline{\psi}; \mathbf{x}, t) = \int_{\Omega} \mathcal{F}(\underline{\psi}; \mathbf{x}', t) G(\mathbf{x} - \mathbf{x}', \Delta) d\mathbf{x}'$

$$\begin{aligned} \bar{\rho} \frac{\partial \tilde{P}_{sgs}(\underline{\psi})}{\partial t} + \bar{\rho} \tilde{u}_j \frac{\partial \tilde{P}_{sgs}(\underline{\psi})}{\partial x_j} &+ \sum_{\alpha=1}^{N_s} \frac{\partial}{\partial \psi_\alpha} \left[ \bar{\rho} \dot{\omega}_\alpha(\underline{\psi}) \tilde{P}_{sgs}(\underline{\psi}) \right] = \\ \text{Gradient closure} &- \frac{\partial}{\partial x_j} \left[ \overline{\rho(\underline{\psi}) \mathcal{F}(\underline{\psi})} u_j - \bar{\rho} \tilde{u}_j \tilde{P}_{sgs} \right] \\ \text{LMSE/IEM Model} &- \sum_{\alpha=1}^{N_s} \frac{\partial}{\partial \psi_\alpha} \left( \frac{\mu}{\sigma} \frac{\partial \phi_\alpha}{\partial x_i \partial x_i} \mathcal{F}(\underline{\psi}) \right) \end{aligned}$$

# ICB | Imperial 'Boffin'

## Stochastic Fields Method

Represent **PDF** by **N** stochastic fields (Valiño 1998)  
(N stochastic fields for each of the  $N_s$  scalars)

$$\begin{aligned} \bar{\rho} d\xi_\alpha^n = &- \bar{\rho} \tilde{u}_i \frac{\partial \xi_\alpha^n}{\partial x_i} dt + \frac{\partial}{\partial x_i} \left[ \Gamma \frac{\partial \xi_\alpha^n}{\partial x_i} \right] dt + \bar{\rho} \sqrt{\frac{2\Gamma}{\bar{\rho}}} \frac{\partial \xi_\alpha^n}{\partial x_j} dW_i^n \\ &- \frac{\bar{\rho}}{2\tau_{sgs}} (\xi_\alpha^n - \tilde{\phi}_\alpha) dt + \bar{\rho} \dot{\omega}_\alpha^n(\xi_\alpha^n) dt \end{aligned}$$

Where

$$\Gamma = \frac{\mu}{\sigma} + \frac{\mu_{sgs}}{\sigma_{sgs}}, \quad dW_i^n \text{ time-step increments } \eta_i^n \sqrt{dt}, \quad \eta_i^n \text{ is a } \{-1, +1\}$$

# ICB | Imperial 'Boffin' Implementation

## CODE

**BOFFIN – LES** (*In-house block structured parallel code*)

## CHEMICAL MECHANISM:

*15 step 19 species (from GRI 3.0) Sung et al (2001)*

# ICB | Imperial 'Boffin' Grid

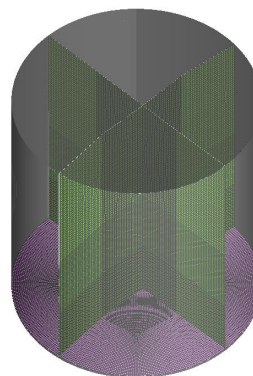
## GRID

### **TSF\_A2** (*Isothermal*)

- ✓ 500x500 mm
- ✓ **2.986.000** cells

### **TSF A\_r**

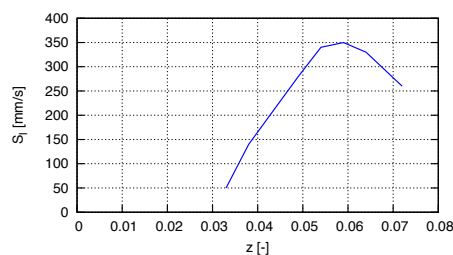
- ✓ 600 x 600 mm
- ✓ **1.572.864** cells
- ✓ smallest mesh size 0.322 mm, stretched towards the shear layer
- ✓ 1 and 8 stochastic fields



ANSYS  
Noncommercial use only



- New case: Start simple, see where it fails
- Solve transport equation for mixture fraction and for progress variable
- Use Fureby's FSD model for premixed combustion
- Use laminar flamespeed according to Aung et al.:



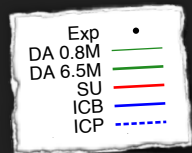
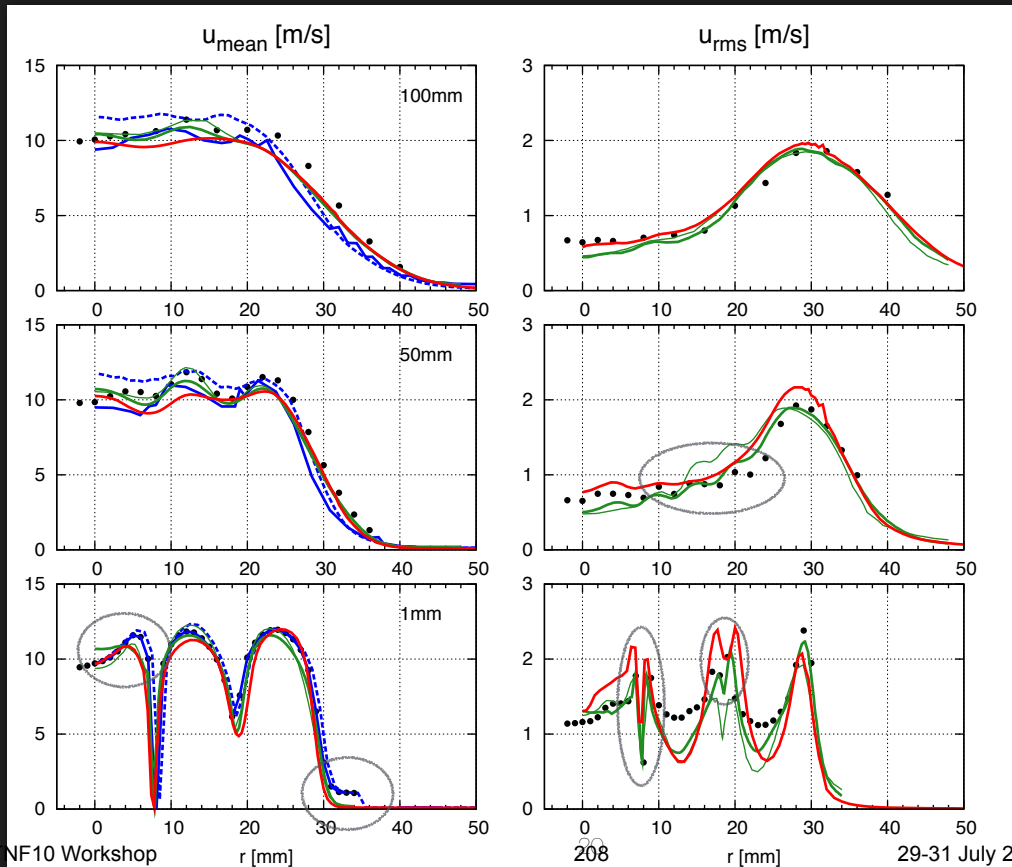
Aung, K. T. Tseng L-K, Ismail M. A. and G. M. Faeth.  
Combustion and Flame, 102:526-530, 1995.

- ▶ Transported quantities:
  - ▶ Momentum, Density, Mixture fraction, Progress variable
- ▶ CDS for momentum, TVD for scalars
- ▶ 3<sup>rd</sup> order explicit low-storage Runge-Kutta for time integration
- ▶ Combustion modeled using Fureby's Flame Surface Density model with varying flame speed
- ▶ Artificial turbulence generated at inflow
- ▶ Cell (filter) width of 1mm
  - ▶ Domain of 260x280x280 ~ 20.3M cells for reactive case
  - ▶ 6400 CPUh for 30000 time steps

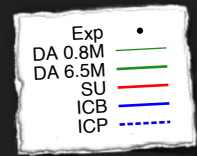
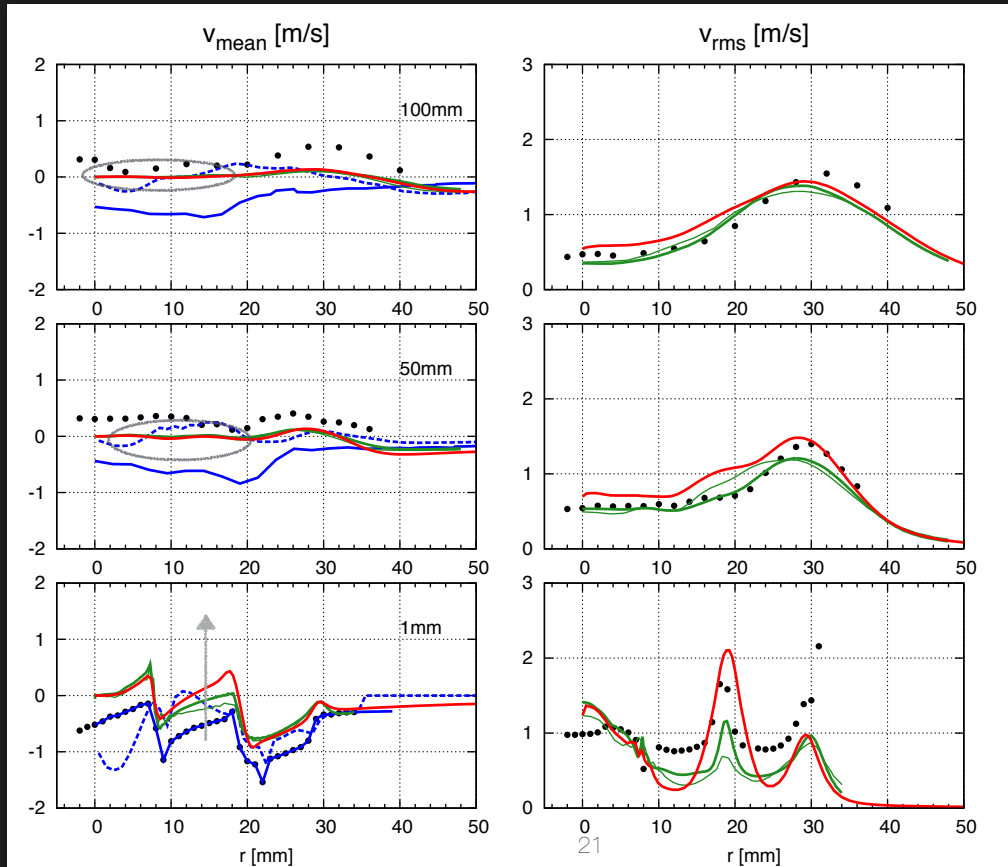
Problems with inflow data: preliminary

# Results: Non-Reactive

## TSF-A-i2 | Axial velocity



# TSF-A-i2 | Radial velocity



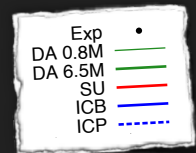
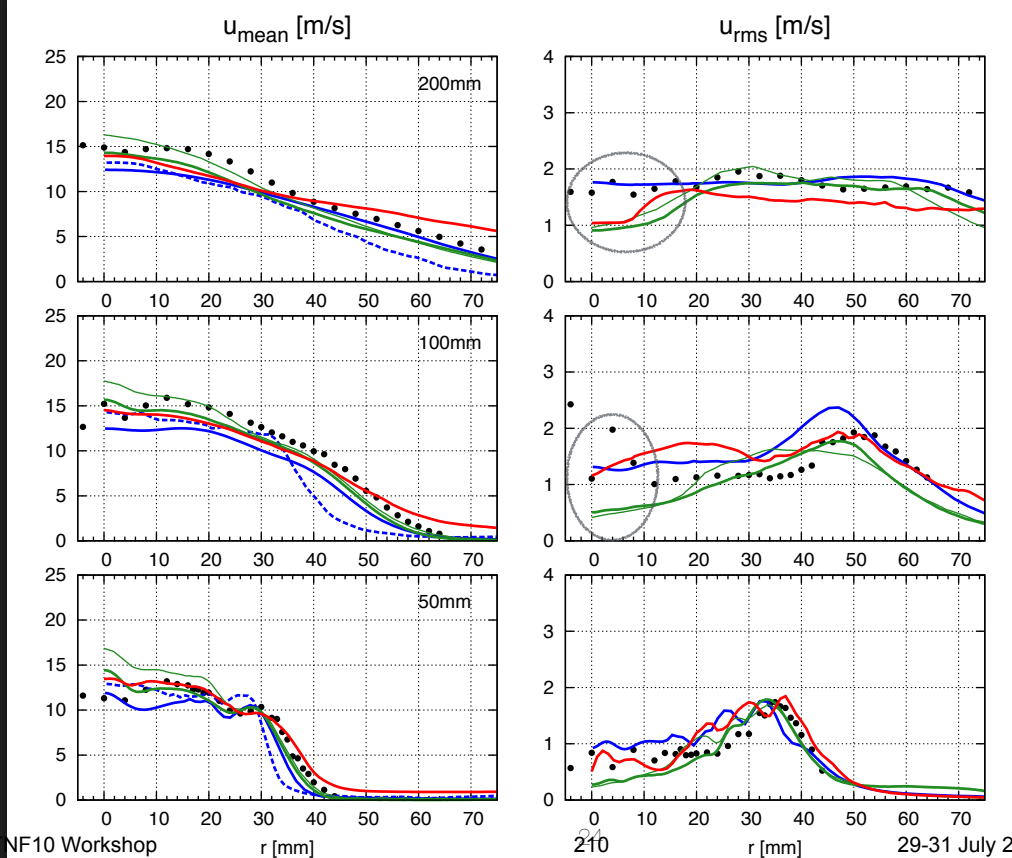
TNF 10

## Non-Reactive Simulations

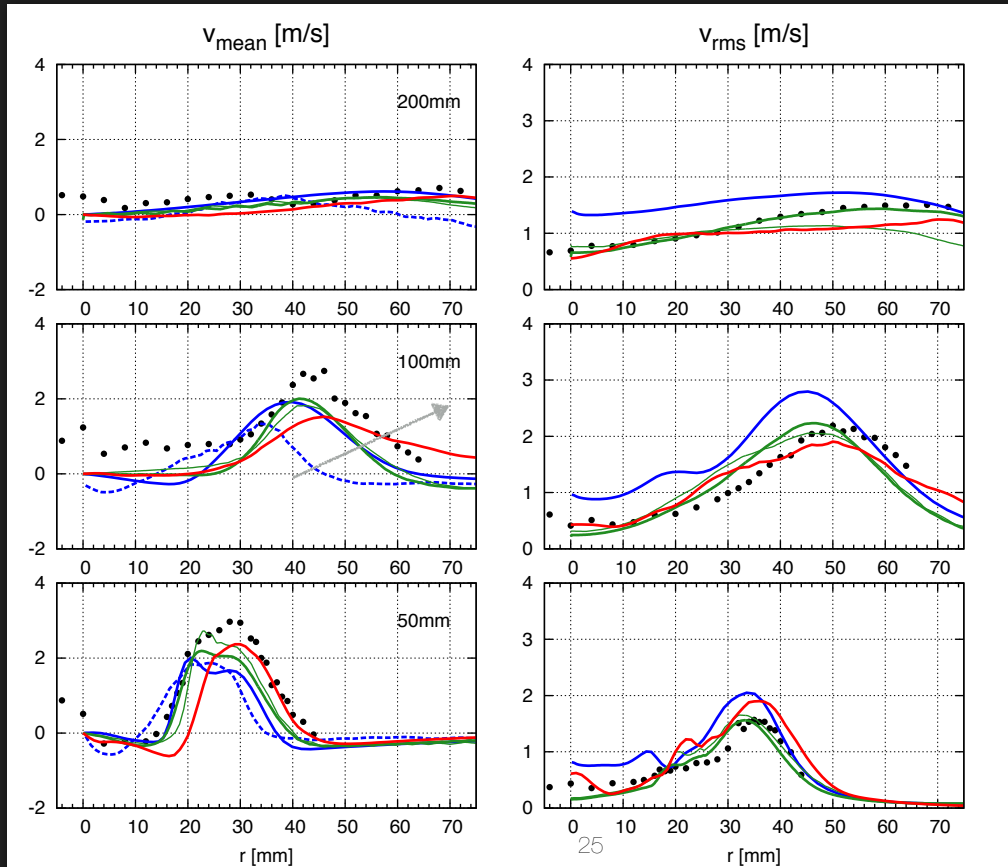
- Excellent agreement for new TNF test case
- Darmstadt, Stanford simulate inflow very successfully
- Real grid study from Darmstadt (0.8M, 6.5M)
- Cost/CPUh: DA 5,400, SU 1,500, ICB 700, ICP 500

# Results: Reactive

## TSF-A-r | Axial velocity



# TSF-A-r | Radial velocity



TNF 10

## Reactive Simulations

- Very encouraging for a new TNF test case
- Darmstadt, Stanford simulate inflow very successfully
- Real grid study from Darmstadt (0.8M, 6.5M)
- Cost/CPUh:

DA 43,000, SU 20,000, ICB 10,000, ICP 6,400

# Difficulties

- Low coflow velocity (0.1 m/s)
  - Need for long initialisation time
  - Need for large domain (radial)
- Fine structures in pilot (flame holder)
- A better understanding of sensitivities is required to enhance results

27

TNF 10

# Comments

- Good experimental data, with improved measurements to follow  
data will be processed again
- Simulations are getting there  
TNF10 work on getting the flow field, mixing, temperature  
TNF11 focus on flame turbulence interaction  
Simple combustion models seem quite useful  
*Probably first publications soon*

**Thank you for your attention...**  
**...and for your questions!**

Special thanks to Fabrizio Cavallo Marincola for his help with plotting.



## **Progress on Kinetics and Diagnostics for “New” Fuels**

**Coordinators: J-Y Chen and Peter Lindstedt**

### **Contributors**

Frederik Fuest and Andreas Dreizler, TU Darmstadt.

Rob Barlow, Matt Dunn and Jonathan Frank, Sandia National Laboratories.

Roger Robinson and Sung-Woo Park, Imperial College.

Imperial College  
London

### **Background/Targets**

- ❑ To introduce new fuels that have different properties to current hydrocarbons (basically methane or methanol) and that are of practical interest.
- ❑ The choices made at the last TNF meeting were DME and ethanol.
- ❑ The fuels have comparatively simple structures and very different chemistries. Ethanol has a RON of 129, while the DME value is very low – the cetane number is 55-60.
- ❑ The current talk will update on progress.

## What do we need to do?

- ❑ To provide a systematic determination of high quality thermodynamic data – some oxygenated species are more problematic.
- ❑ To derive and test detailed reaction mechanisms with validation to include flame structures and ignition related properties.
- ❑ To identify critical reaction pathways and, if need be, determine (or encourage others to obtain) the relevant reaction rate parameters.
- ❑ To reduce the resulting mechanisms to an acceptable size.
- ❑ To procure high quality experimental data in a “friendly” burner configuration (c.f. Sandia A-F series).

## What has been done?

- ❑ Validation of existing reaction mechanisms for DME and ethanol (Berkeley and Imperial).
- ❑ The identification of critical reaction pathways and progress on the determination or selection of appropriate reaction rate constants (Berkeley and Imperial).
- ❑ The derivation and evaluation of a systematically reduced reaction mechanism for DME (Berkeley).
- ❑ The development of experimental techniques for DME and ethanol flames with a focus on the former (Darmstadt and Sandia).
- ❑ The application and evaluation of the developed experimental techniques to laminar and turbulent DME flames (Berkeley, Darmstadt and Sandia).

## Extension of Raman/Rayleigh methods to other fuels

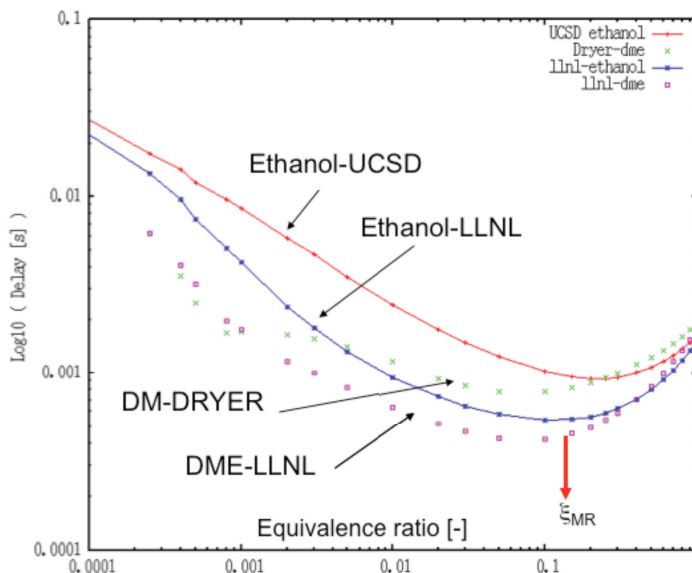
- Exploratory experiments at Sandia to measure Raman spectra and assess feasibility
  - ethane, ethylene, dimethyl ether, propane
  - cold/heated flows, laminar jet flames, turbulent piloted flames
  - focus on DME as most Raman friendly (lowest fluorescence interference)



Imperial College  
London

### Existing Reaction Mechanisms

- ❑ Reaction mechanisms for DME and ethanol have been produced by a number of groups.
- ❑ The suggestions include ethanol from the USCD, LLNL and Dryer groups and DME from the Dryer and LLNL groups.
- ❑ How do they perform in the context of auto-ignition in a coflow from a lean hydrogen flame (c.f. the Cabra burner)?



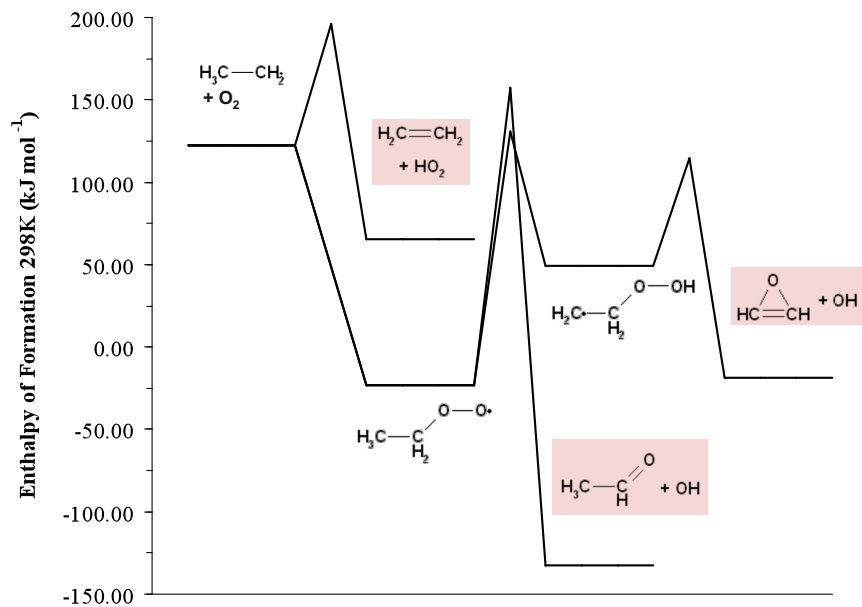
- The result suggests that the LLNL ethanol mechanism predicts faster ignition than the DME Dryer variant.
- The LLNL mechanisms appear self-consistent.
- Predicted delay times also vary by multiples depending on conditions.
- The outcome is perhaps surprising.
- Possible causes?

### Comparisons of Heat of Formation G3B3 Level for Species Involved in Ethanol Ignition

Calculated G3B3 and CBS QB3 Enthalpies of Formation at 298 K.

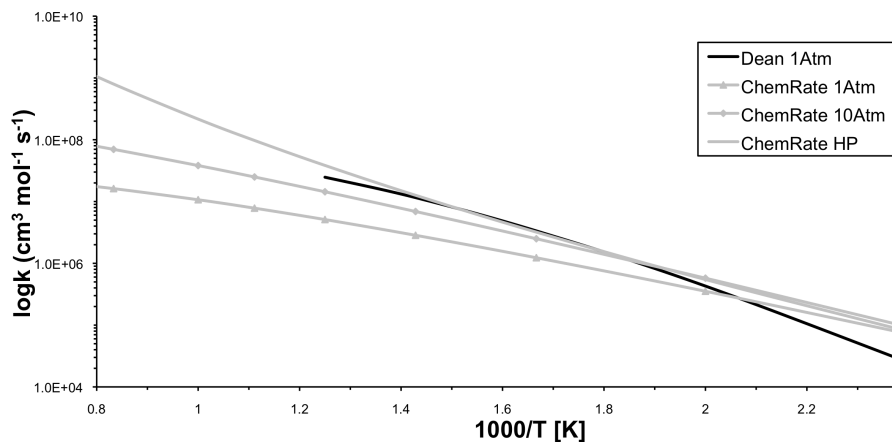
Species	Imperial G3B3	Carstensen <i>et al.</i> (2005) CBS-QB3
	kJ mol <sup>-1</sup>	kJ mol <sup>-1</sup>
OH	35.01	38.53
HO <sub>2</sub>	12.85	13.10
C <sub>2</sub> H <sub>5</sub>	120.51	122.38
C <sub>2</sub> H <sub>4</sub>	51.47	52.13
C <sub>2</sub> H <sub>5</sub> OO	-22.88	-22.01
CH <sub>3</sub> CHO	-167.44	-170.54
C <sub>2</sub> H <sub>4</sub> OOH	49.58	51.25

## PES of Ethyl Oxidation (G3B3 Level)



## $C_2H_5OO \rightarrow CH_3CHO + OH$

- Reaction rates were calculated using Rice-Ramsperger-Kassel-Marcus / Master Equation theory (RRKM/ME) using ChemRate 1.5.8 temperature range extended to 500 - 2500 K.



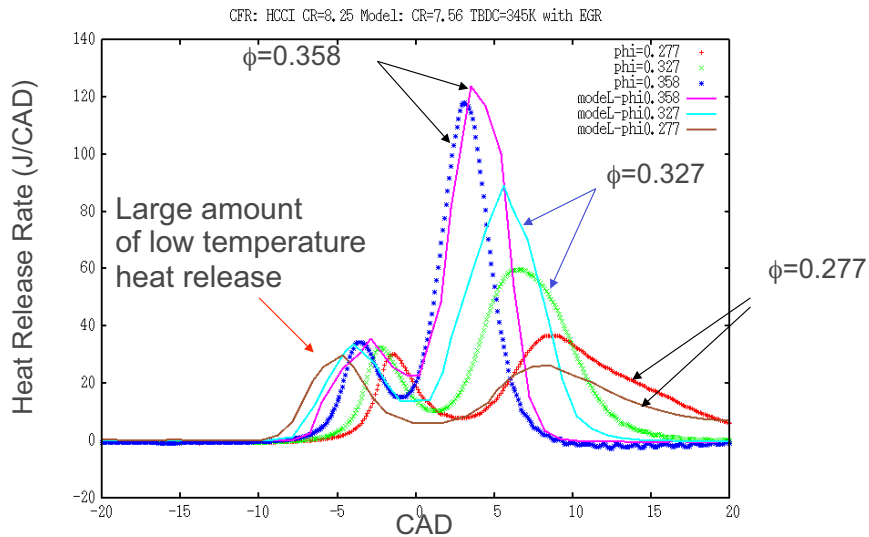
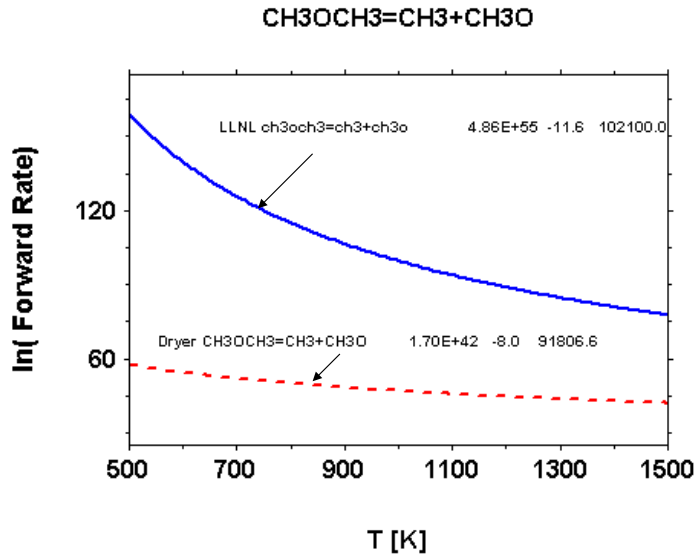
**Channel:  $C_2H_4OOH \rightarrow cy-C_2H_4O + OH$**

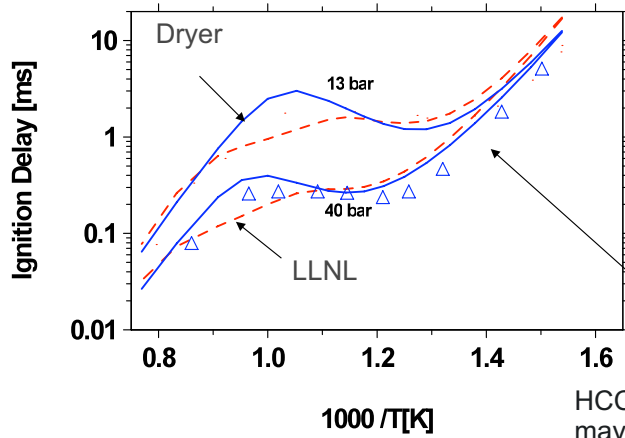
	Carstensen et al. (2005)	Taatjes et al. (2003)	RRKM/ME 1 Atm	RRKM/ME 10 Atm	RRKM/ME HP-Limit
A	2.130E+41		8.03E+40	8.28E+32	3.28E+10
n	-9.810		-8.798	-6.18528	0.909009
Ea kJ	192.125		218.467	209.678	180.746
T	cm <sup>3</sup> mol <sup>-1</sup> s <sup>-1</sup>				
300	3.8E-17	7.7E-16	1.2E-19	1.2E-19	2.0E-19
400	5.2E-10	1.1E-09	3.0E-11	2.8E-11	1.9E-11
500	6.0E-06	3.3E-06	2.2E-06	2.1E-06	1.2E-06
600	2.2E-03	5.1E-04	2.8E-03	3.0E-03	2.0E-03
700	1.2E-01	1.5E-02	3.7E-01	4.7E-01	4.1E-01
800	2.0E+00		1.3E+01	1.9E+01	2.3E+01
900			1.7E+02	3.0E+02	5.1E+02
1000			1.3E+03	2.6E+03	6.3E+03
1200			2.0E+04	5.6E+04	2.8E+05
1400			1.2E+05	4.3E+05	4.3E+06
1600			3.8E+05	1.8E+06	3.4E+07

Sensitivity of delay time for DME  
 $\phi = 0.1$  coflow H<sub>2</sub>/air ( $\phi = 0.4$   
and 1350 K).

LLNL-DME				Dryer-DME			
<u>1</u>	8	-7.8409E-01	h+o2<=>o+oh	<u>1</u>	1	-7.3517E-01	H+O2<=>O+OH
<u>2</u>	12	-5.2730E-01	hco+M<=>h+co+M	<u>2</u>	234	-3.9151E-01	CH3OCH3<=>CH3+CH3O
<u>3</u>	273	-4.7457E-01	ch3och3<=>ch3+ch3o	<u>3</u>	26	-3.7815E-01	HCO+M<=>H+CO+M
<u>4</u>	46	3.0607E-01	hco+o2<=>co+ho2	<u>4</u>	47	-3.6522E-01	CH3+HO2<=>CH3O+OH
<u>5</u>	22	-2.5433E-01	ch3+ho2<=>ch3o+oh	<u>5</u>	27	3.5185E-01	HCO+O2<=>CO+HO2
<u>6</u>	49	1.8095E-01	ho2+oh<=>h2o+o2	<u>6</u>	13	2.6166E-01	HO2+OH<=>H2O+O2
<u>7</u>	275	1.7753E-01	ch3och3+h<=>ch3och2+h2	<u>7</u>	40	-1.5400E-01	CH2O+OH<=>HCO+H2O
<u>8</u>	11	-1.2818E-01	oh+h2<=>h+h2o	<u>8</u>	53	1.3824E-01	CH3+HO2<=>CH4+O2
<u>9</u>	33	9.8764E-02	ch2o+h<=>hco+h2	<u>9</u>	48	1.3463E-01	2CH3(+M)<=>C2H6(+M)
<u>10</u>	32	-8.5356E-02	ch2o+oh<=>hco+h2o	<u>0</u>	38	1.2679E-01	CH2O+H<=>HCO+H2
..	..	..	..	..	..	..	..

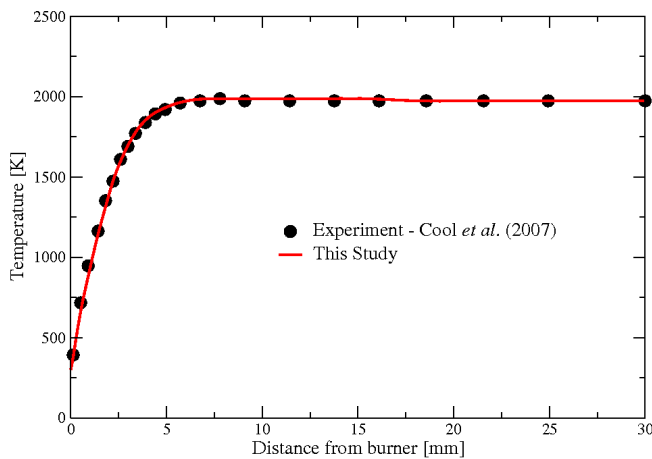
Shows that  $CH_3OCH_3 \rightarrow CH_3 + CH_3O$  is the key step under this condition.





HCCI regime at low temperature  
may require a more accurate  
mechanism

**Low Pressure Flat Flame : DME**



**Cool et al. (2007)**

$P = 4.0 \text{ kPa}$

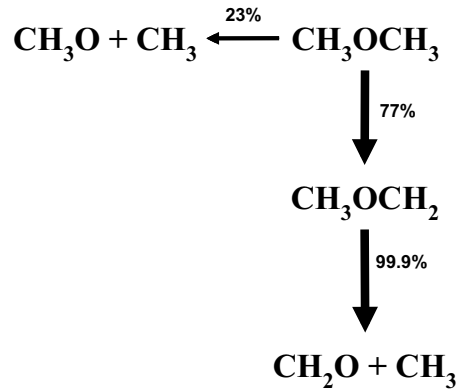
$\Phi = 1.2$

$X_{Ar} = 0.703$

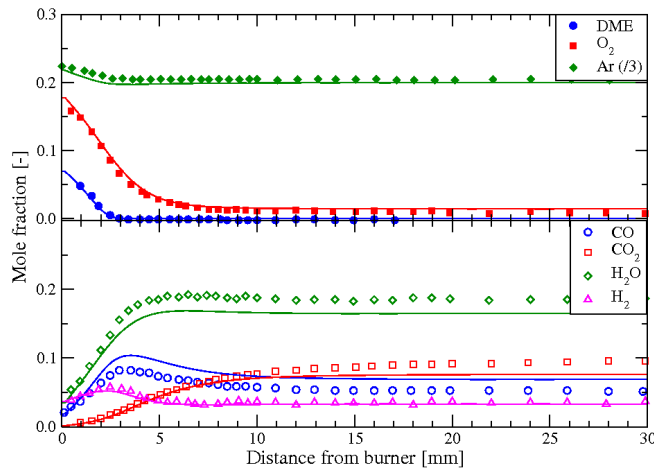
$T_u = 300 \text{ K}$

$v_u = 82.7 \text{ cm/s}$

## Low Pressure Flat Flame : DME Consumption Paths (LLNL Rate)



## Low Pressure Flat Flame : DME Major Species



Cool *et al.* (2007)

$P = 4.0 \text{ kPa}$

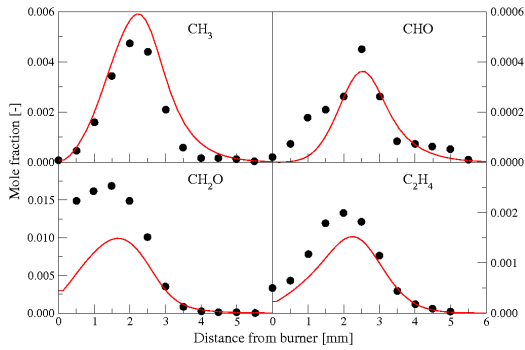
$\Phi = 1.2$

$X_{\text{Ar}} = 0.703$

$T_u = 300 \text{ K}$

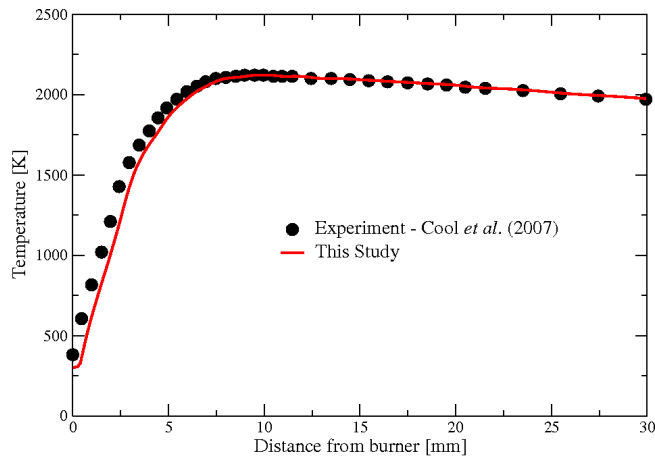
$v_u = 82.7 \text{ cm/s}$

## Low Pressure Flat Flame : DME Intermediate Species



Species	Experiment		This Study	
	X <sub>max</sub>	HAB	X <sub>max</sub>	HAB
CH <sub>3</sub>	4.7E-03	2.0	6.0E-03	2.3
CH <sub>4</sub>	6.4E-03	2.5	8.7E-03	2.0
C <sub>2</sub> H <sub>2</sub>	6.2E-04	3.0	9.2E-04	3.0
C <sub>2</sub> H <sub>4</sub>	2.0E-03	2.0	1.5E-03	2.3
CHO	4.5E-04	2.5	3.5E-04	2.5
CH <sub>2</sub> O	1.7E-02	1.5	9.9E-03	1.6
CH <sub>3</sub> OH	1.0E-03	1.5	2.4E-04	1.4
C <sub>2</sub> H <sub>2</sub> O	6.0E-05	2.0	8.1E-05	2.9
CH <sub>3</sub> CHO	2.8E-04	1.5	1.8E-05	1.5

## Low Pressure Flat Flame : DME



**Cool *et al.* (2007)**

$P = 2.67$  kPa

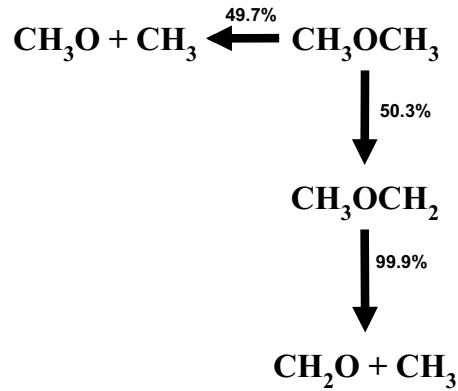
$\Phi = 1.68$

$X_{\text{Ar}} = 0.506$

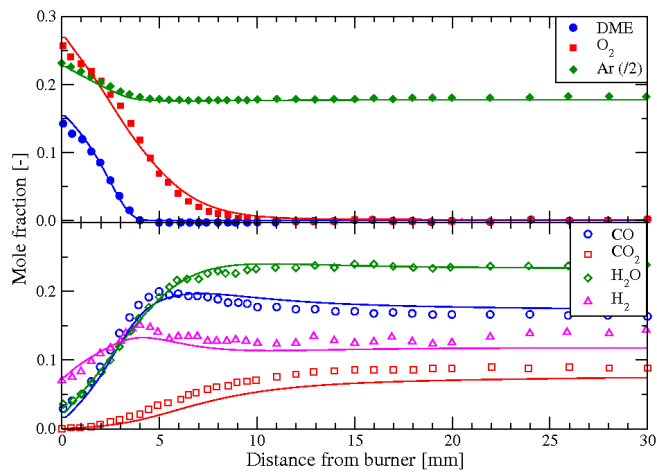
$T_u = 300$  K

$v_u = 97.1$  cm/s

## Low Pressure Flat Flame : DME Consumption Paths



## Low Pressure Flat Flame : DME Major Species



Cool *et al.* (2007)

$P = 2.67 \text{ kPa}$

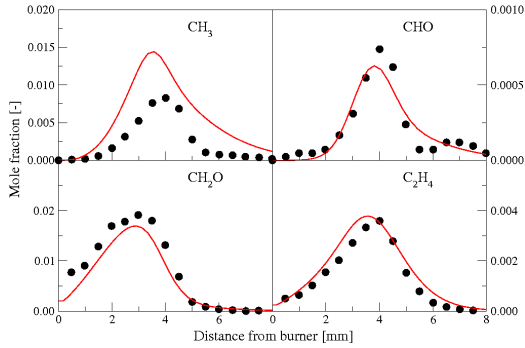
$\Phi = 1.68$

$X_{\text{Ar}} = 0.506$

$T_u = 300 \text{ K}$

$v_u = 97.1 \text{ cm/s}$

## Low Pressure Flat Flame : DME Intermediate Species



Species	Experiment		This Study	
	Xmax	HAB	Xmax	HAB
CH <sub>3</sub>	8.3E-03	4.0	1.5E-02	3.4
CH <sub>4</sub>	1.4E-02	3.5	2.5E-02	3.3
C <sub>2</sub> H <sub>2</sub>	2.7E-03	4.5	3.8E-03	5.0
C <sub>2</sub> H <sub>4</sub>	3.6E-03	4.0	3.8E-03	3.6
CHO	7.4E-04	4.0	6.0E-04	3.8
CH <sub>2</sub> O	1.9E-02	3.0	2.0E-02	2.9
CH <sub>3</sub> OH	7.1E-04	3.0	7.1E-04	3.2
C <sub>2</sub> H <sub>2</sub> O	1.1E-04	4.0	2.2E-04	5.0
CH <sub>3</sub> CHO	2.1E-04	3.0	2.0E-05	2.5

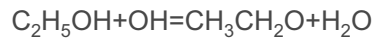
Sensitivity of ignition delay time for ethanol  $\phi = 0.1$  in coflow H<sub>2</sub>/air ( $\phi = 0.4$  and 1350 K)

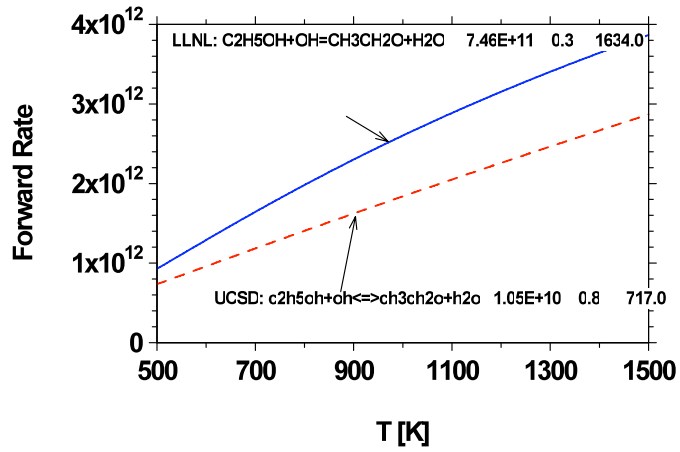
### Ethanol-UCSD

<u>1</u>	1	-9.2023E-01	h+o2<=>oh+o
<u>2</u>	25	-5.2932E-01	hco+M<=>co+h+M
<u>3</u>	15	5.2168E-01	ho2+oh<=>h2o+o2
<u>4</u>	30	4.6551E-01	hco+o2<=>co+ho2
<u>5</u>	134	-4.0263E-01	<u>E2h5oh+oh&lt;=&gt;ch3ch2o+h2o</u>
<u>6</u>	133	2.9935E-01	c2h5oh+oh<=>ch3choh+h2o
<u>7</u>	149	2.9633E-01	ch3ch2o+M<=>ch3+ch2o+M
<u>8</u>	148	-2.4378E-01	ch3ch2o+M<=>ch3cho+h+M
<u>9</u>	76	-2.4249E-01	c2h4+oh<=>c2h3+h2o
<u>10</u>	132	-2.0640E-01	c2h5oh+oh<=>ch2ch2oh+h2o
<u>11</u>	139	1.9476E-01	c2h5oh+o<=>ch3choh+oh
<u>12</u>	48	-1.8958E-01	ch3+ho2<=>ch3o+oh
<u>13</u>	87	-1.4152E-01	c2h3+o2<=>ch2cho+o
<u>14</u>	49	-1.3442E-01	ch3+o2<=>ch2o+oh
<u>15</u>	142	1.3356E-01	c2h5oh+ch3<=>ch3choh+ch4

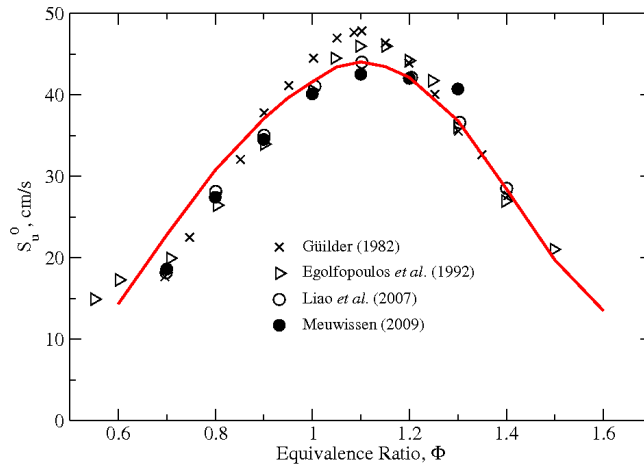
### Ethanol-LLNL

<u>1</u>	2	-6.5416E-01	o+OH<=>o2+H
<u>2</u>	130	-4.5548E-01	HCO+M<=>H+CO+M
<u>3</u>	129	4.4820E-01	HCO+O2<=>CO+HO2
<u>4</u>	159	3.0505E-01	CH3CH2O+M<=>CH3+CH2O+M
<u>5</u>	34	-2.9196E-01	CH3+HO2<=>CH3O+OH
<u>6</u>	158	-2.7652E-01	<u>CH3CH2O+M&lt;=&gt;CH3HCO+H+M</u>
<u>7</u>	145	-2.3109E-01	<u>C2H5OH+OH&lt;=&gt;CH3CH2O+H2O</u>
<u>8</u>	9	1.9203E-01	OH+HO2<=>H2O+O2
<u>9</u>	144	1.8984E-01	C2H5OH+OH<=>CH3CHOH+H2O
<u>10</u>	243	-1.7991E-01	CH2HCO<=>CH2CO+H
<u>11</u>	175	-1.4602E-01	CH3HCO+OH<=>CH2HCO+H2O
<u>12</u>	213	-1.4513E-01	C2H3+O2<=>CH2HCO+O
<u>13</u>	214	1.4202E-01	C2H3+O2<=>C2H2+HO2
<u>14</u>	35	1.4166E-01	CH3+HO2<=>CH4+O2
<u>15</u>	21	-1.4003E-01	H2O2<=>H2O2+O2



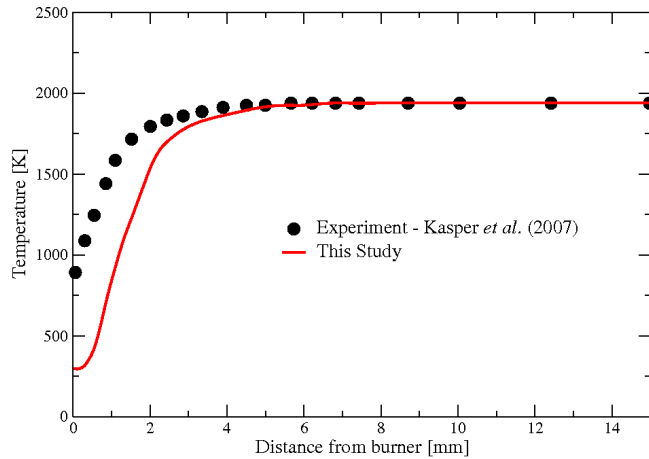


**Laminar Burning Velocity : Ethanol**



$P = 1 \text{ atm}$   
 $T_u = 298 \text{ K}$

## Low Pressure Flat Flame : Ethanol Temperature Profile



**Kasper *et al.* (2007)**

$P = 50 \text{ mbar}$

$\Phi = 1.0$

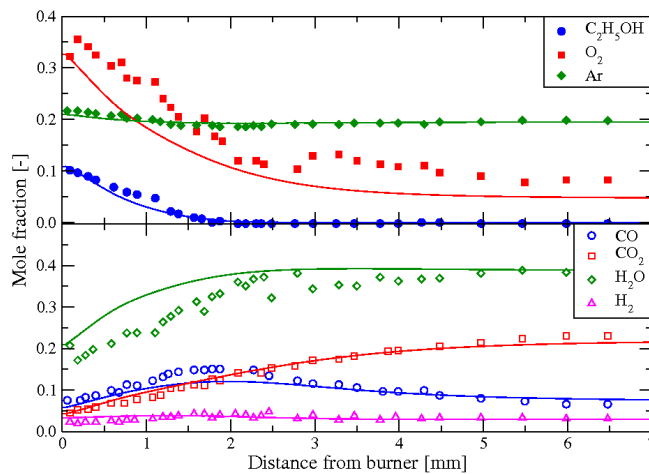
$C/O = 0.286$

$X_{Ar} = 0.25$

$T_u = 298 \text{ K}$

$v_u = 50 \text{ cm/s}$

## Low Pressure Flat Flame : Ethanol Major Species Mole Fractions



**Kasper *et al.* (2007)**

$P = 50 \text{ mbar}$

$\Phi = 1.0$

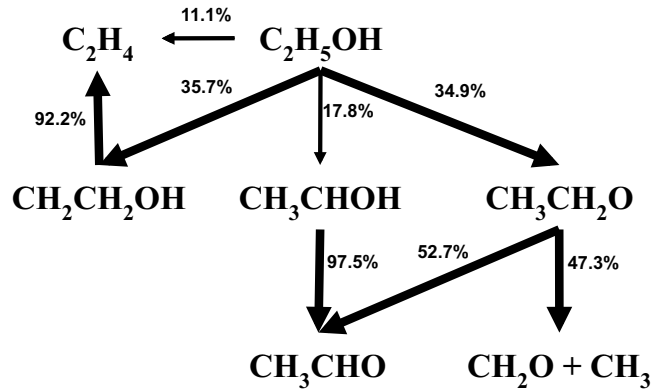
$C/O = 0.286$

$X_{Ar} = 0.25$

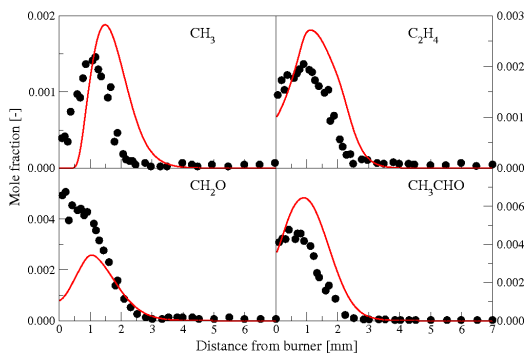
$T_u = 298 \text{ K}$

$v_u = 50 \text{ cm/s}$

## Low Pressure Flat Flame : Ethanol Path Analysis ( $\Phi=1.0$ )

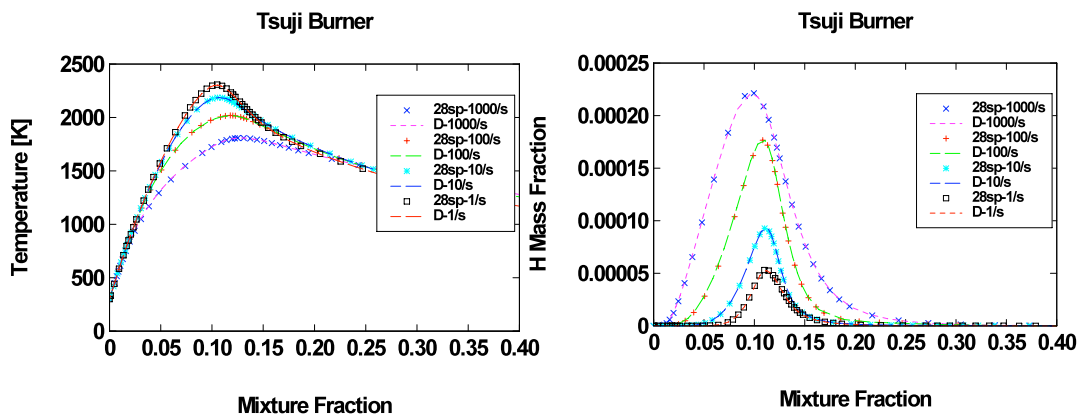


## Intermediate Species Mole Fractions ( $\Phi=1.0$ )

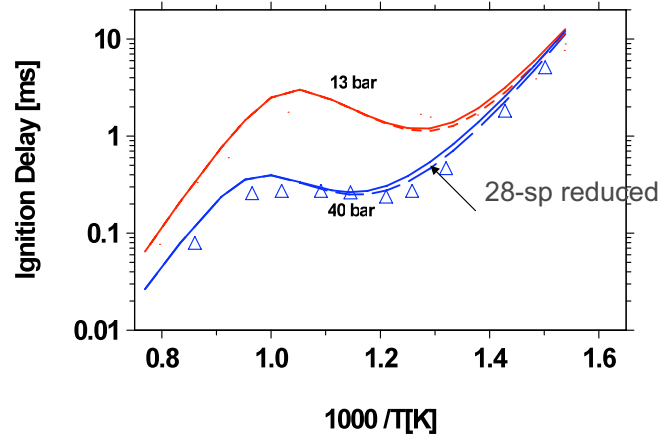


Species	Experiment		This Study	
	Xmax	HAB	Xmax	HAB
CH <sub>3</sub>	1.5E-03	1.2	1.9E-03	1.5
CH <sub>4</sub>	3.3E-03	0.9	3.3E-03	0.9
C <sub>2</sub> H <sub>2</sub>	4.8E-04	1.6	1.1E-03	1.9
C <sub>2</sub> H <sub>4</sub>	2.1E-03	0.9	2.7E-03	1.1
CHO	1.9E-03	0.4	1.1E-04	1.7
CH <sub>2</sub> O	5.1E-03	0.2	2.6E-03	1.1
C <sub>2</sub> H <sub>2</sub> O	6.1E-04	0.4	2.5E-03	0.9
CH <sub>3</sub> CHO	4.8E-03	0.4	6.4E-03	0.9
C <sub>3</sub> H <sub>6</sub>	4.6E-04	0.6	2.4E-03	1.4
C <sub>3</sub> H <sub>8</sub>	2.7E-03	0.6	6.1E-04	0.9

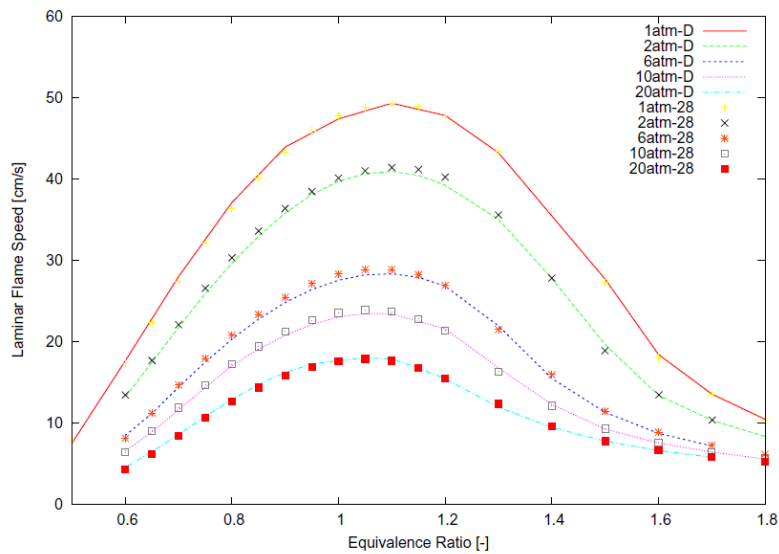
- The derivation and evaluation of a systematically reduced reaction mechanism for DME (Berkeley).



Nearly perfect agreement is seen between 28-species reduced chemistry and the detailed Dryer mechanism.



28-Species reduced DME mechanism compares well with the detailed mechanism for shock-tube data

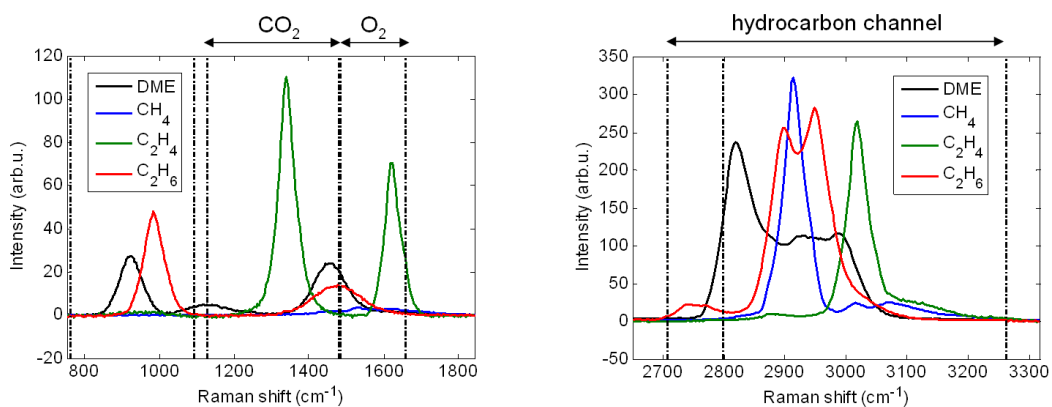


## Experimental Data Sets

- The development of experimental techniques for DME and ethanol flames with a focus on the former (Darmstadt and Sandia).
- The application and evaluation of the developed experimental techniques to laminar and turbulent DME (and ethanol) flames (Berkeley, Darmstadt and Sandia).



## Main findings: Distinct spectral signatures (295 K)

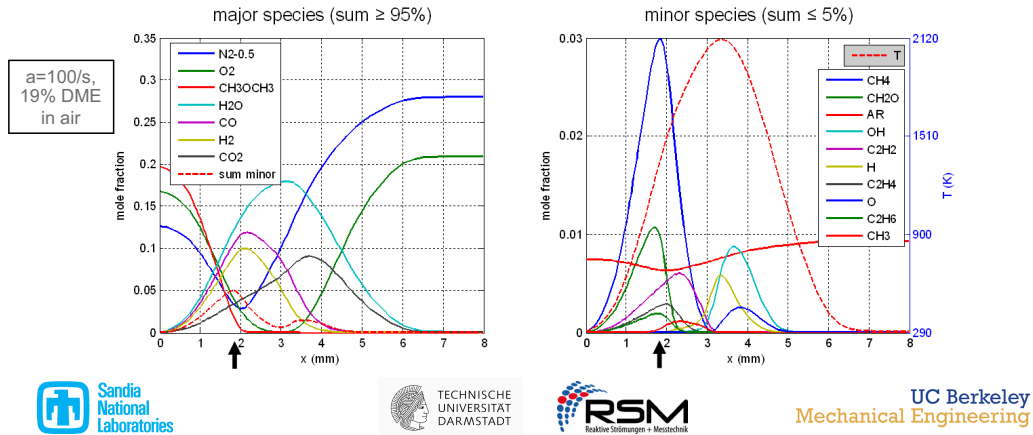


- Different HC fuels have distinct Raman spectra but also significant crosstalk onto CO<sub>2</sub> and O<sub>2</sub> Raman channels



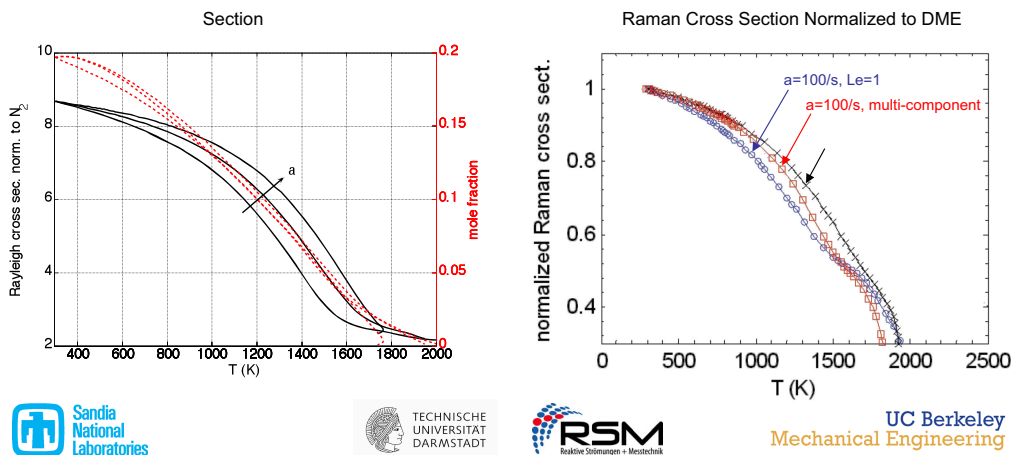
## Main findings: Must account for intermediates

- Raman/Rayleigh data for DME flames cannot be interpreted usefully without accounting for combustion intermediates ( $\text{CH}_4$ ,  $\text{CH}_2\text{O}$ ,  $\text{C}_2\text{H}_2$ ,  $\text{C}_2\text{H}_4$ ,  $\text{C}_2\text{H}_6$ )
- Use strained laminar partially premixed flame calculations (Zhao et al. 2009) to evaluate composition and develop methods for data evaluation



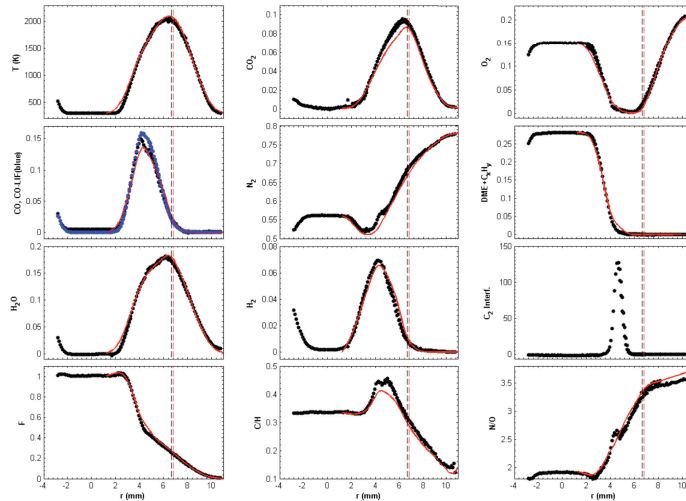
## Main findings: Variation of effective cross sections

- Based on mole fractions of hydrocarbons from laminar calculations, literature values for cross sections, and relative measurements from the lab
- Results sensitive to strain rate and transport assumption



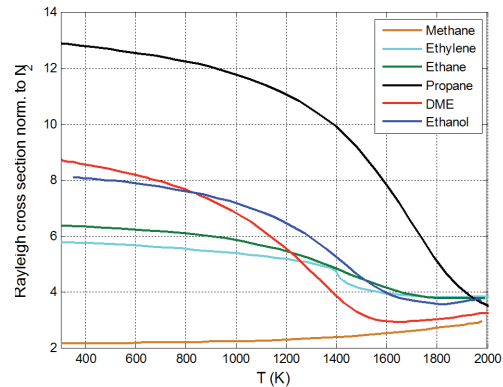
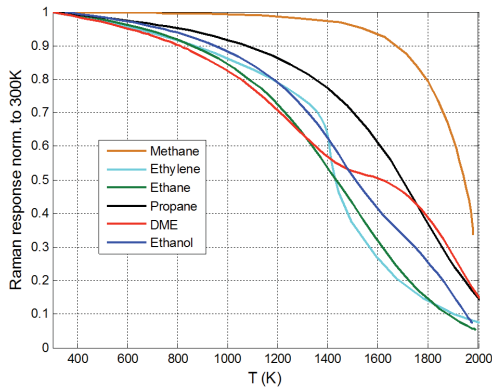
## The Fuest approach to DME data interpretation

- Use one laminar flame calculation to represent effective cross sections of hydrocarbon mixture as a function of temperature.



UC Berkeley  
Mechanical Engineering

## Similar issues for ethane, ethanol, ethylene, ...

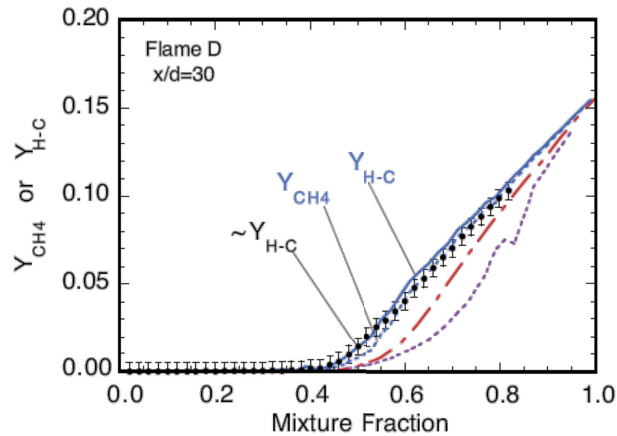


- Average molar mass and C:H:O atom ratios for the hydrocarbon mixture also vary though the calculated laminar flames.



UC Berkeley  
Mechanical Engineering

## Less important in CH<sub>4</sub> flames

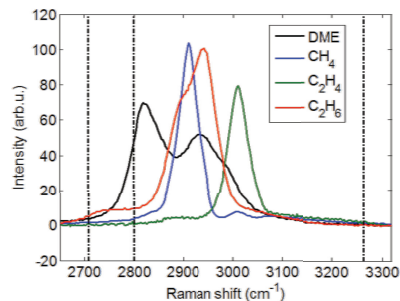
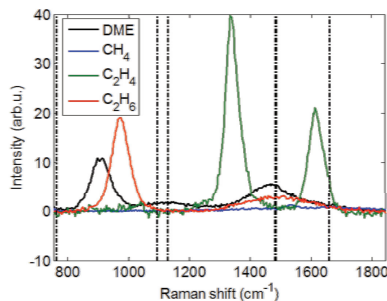


- In previous CH<sub>4</sub> flame measurements the Raman response curve was tuned to approximate the total hydrocarbon mass fraction (Barlow et al. CNF 127:2102-2118, 2001)

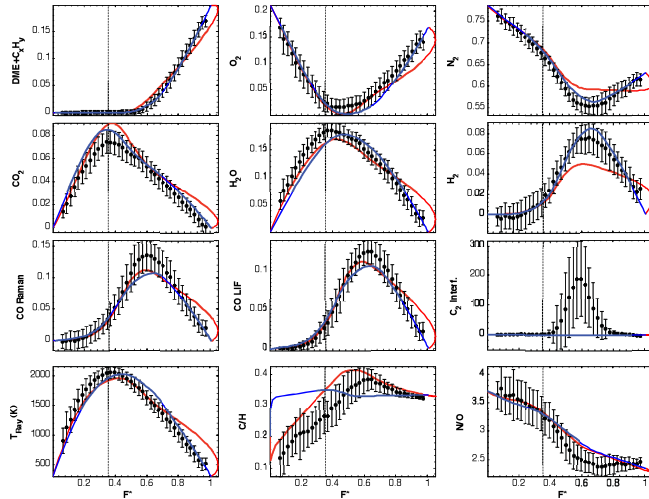


## Speculation regarding all higher hc fuels

- May need more general Raman/Rayleigh approach for turbulent flames across different combustion modes and regimes
- Consider spectrally resolved measurement of hc bands and fitting based on experimentally generated libraries for fuel and intermediates



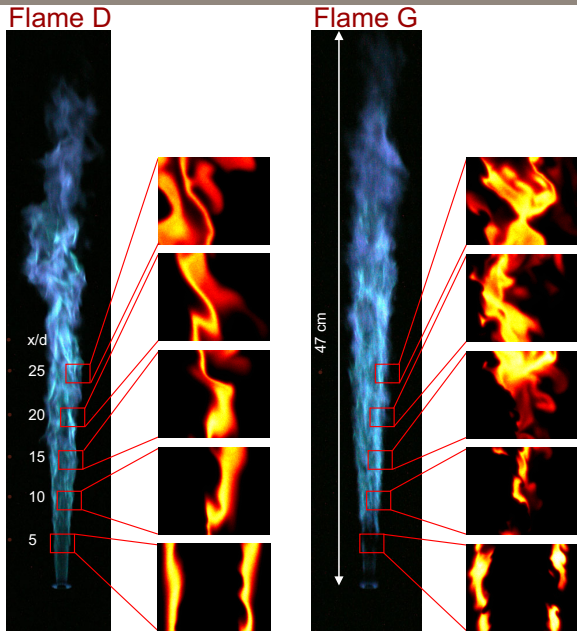
## Turbulent Case: 19.7% DME in air (Flame D, $x/d=15$ )



- Comparison of measured mole fractions as conditional mean and standard deviation from 195 single-shot measurements in mixture fraction space.
- Flamelet calculation (Zhao, Tsuji,  $a=400s^{-1}$ , red line: full molecular transport, blue line: equal diffusivities).
- About 30-40% of the apparent standard deviation is addressed to measurement uncertainties and not to turbulent fluctuations.



## Sandia Piloted DME/air Jet Flame Series



Fuel mixture: 20% DME, 80% air  
 $\xi_{st} = 0.353$

Sydney burner

$d_{nozzle} = 7.2$  mm

$d_{pilot} = 18.2$  mm

$u_{coflow} = 0.9$  m/s

pilot:  $C_2H_2$ ,  $H_2$ , air,  $CO_2$ ,  $N_2$

Flame	$Re_d$
D	~27,000
E	~41,000
F	~54,000
G	~68,000

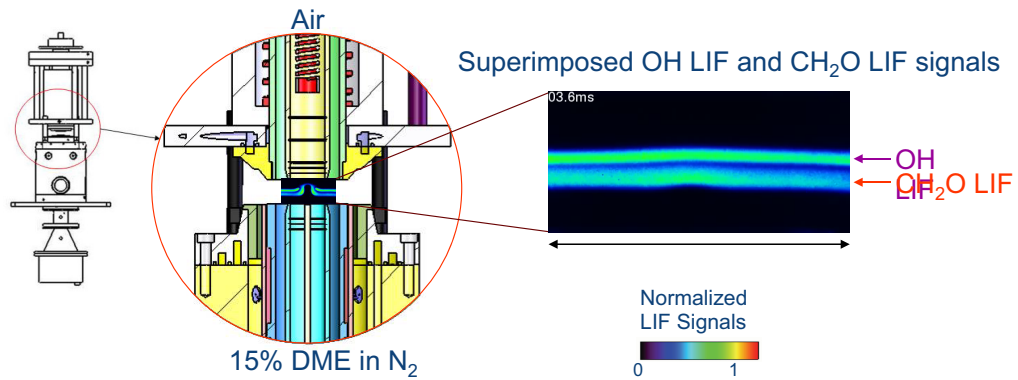
- Analogous to the Sandia  $CH_4$ /air flame series, DME/air flames D-G have varying amounts of localized extinction and re-ignition



Poster: J. H. Frank, A.G. Hsu, J.L. Kuhl



## Extinction and Re-ignition of DME/air Counterflow Flames



- Localized extinction induced via impulsively driven toroidal vortex
- Parametric studies: strain rate, preheat temperature, fuel concentration, additive/diluent



Y. T. Guahk and J. H. Frank



Imperial College  
London

### Summary

- Progress on mechanisms for two oxygenated fuels and their validation has been discussed.
- A first generation reduced reaction mechanism has been developed for DME and will serve as the basis for future revisions.
- Some validation performed – should ideally be extended to cover a wider range of conditions.
- Good progress on experimental techniques and their evaluation.
- Data sets for DME will become available along with a validated chemistry submodel during the coming months.

*It is easy to forget that the current work is often not funded despite the obvious importance to the community.*

## **Session on Highlights from Posters and Other Recent Work**

(Coordinators: Jonathan Frank, Andreas Kronenburg)

This session included presentations on a few selected topics that were not central themes for TNF10 but may be important for future workshops.

- 1) Pros and Cons of the Counterflow Flame as a Potential TNF target
- 2) Development of Suitable TNF Burners for Sooty Fuels
- 3) Unexpected Effects of Preferential Transport in Turbulent Premixed CH<sub>4</sub>/Air Flames
- 4) An Emerging Class of “Real Flow DNS”

## PROS AND CONS OF THE COUNTERFLOW FLAME AS A POTENTIAL TNF TARGET



Bruno Coriton and Alessandro Gomez  
Yale University, New Haven, USA

With Contributions from  
Peter Lindstedt, Henri Goh and Philip Geipel,  
Andreas Kempf and Michael Pettit  
Imperial College, London

10<sup>th</sup> Workshop on Turbulent Non-Premixed Flame – July 29-31, 2010 Beijing, China

## The Counterflow Configuration

### Advantages:

- The configuration is suitable for non-premixed, partially premixed and premixed flames;
- The geometry is compact and has good optical access;
- The flames stabilize away from solid boundaries.

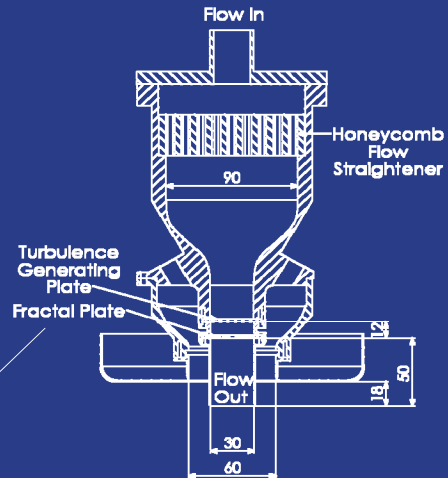
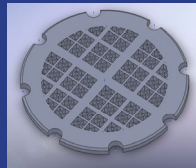
### Challenges:

- Main limitation has been the small turbulent Reynolds numbers  $Re_t \sim O(50-100)$   
(e.g., Mastorakos *et al.*, 1992, Kostiuk *et al.*, 1993, Sardi *et al.*, 1998, Geyer *et al.*, 2005)
- Young turbulence;
- For premixed flames, turbulent Karlovitz numbers  $Ka_t \sim O(1)$  limited by bulk strain rate;
- Intrinsic instabilities cause large scale oscillations of the stagnation surface.

10<sup>th</sup> Workshop on Turbulent Non-Premixed Flame – July 29-31, 2010 Beijing, China

## Increasing $Re_t$ by Fractal Plates

- ❑ The geometry of Geyer et al. (2005) was used with bulk velocities varied from 4.0 to 8.0 m/s giving Reynolds numbers in the range 7,700 to 15,400.
- ❑ Turbulence levels were enhanced using fractal grids located 10 mm downstream of the perforated plates.
- ❑  $Re_t$  doubled from 48-125 to 109-220



IC Burner (top nozzle)  
Geipel *et al.*, 2010

10<sup>th</sup> Workshop on Turbulent Non-Premixed Flame – July 29-31, 2010 Beijing, China

Y

## Yale Counterflow Burner (YCB)

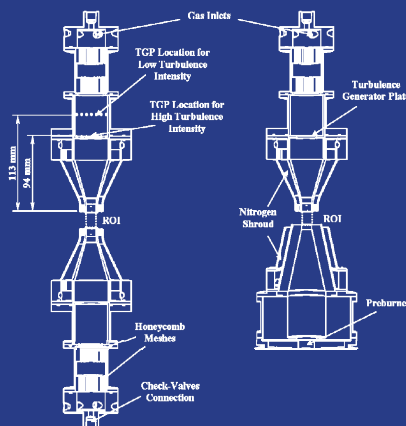
To achieve a tenfold increase in  $Re_t$  to  $O(1000)$  (Coppola, Coriton and Gomez, 2009):

- Operate at high flow rates with oxygen enrichment to prevent flame extinction at large ( $O(1500) s^{-1}$ ) strain rates .
- Force flow through a strategically positioned high-blockage turbulence generator plate.
- Let turbulence develop *inside* contraction nozzle.

Opposed turbulent jets of fresh reactants

Suitable for:

- Non-premixed flames
- Partially-premixed flames
- *Twin*-premixed flames

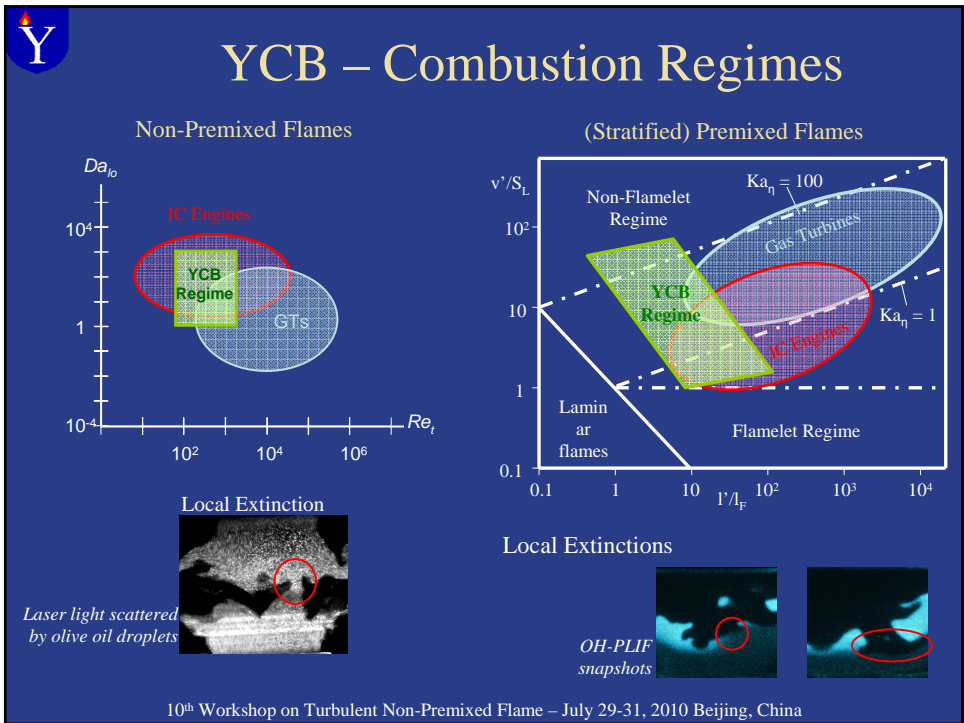
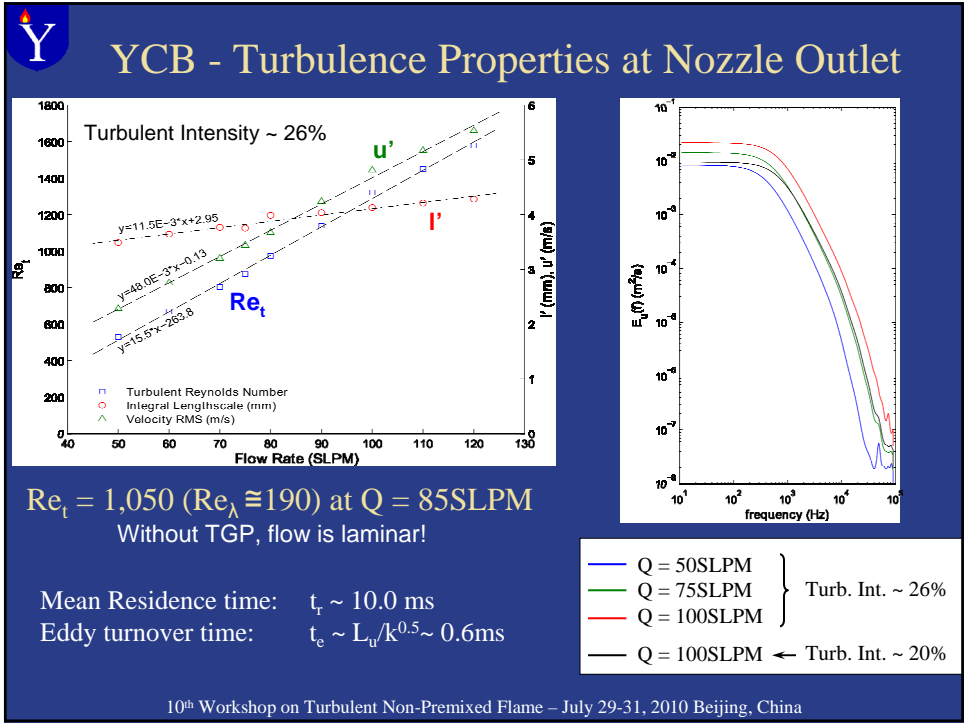


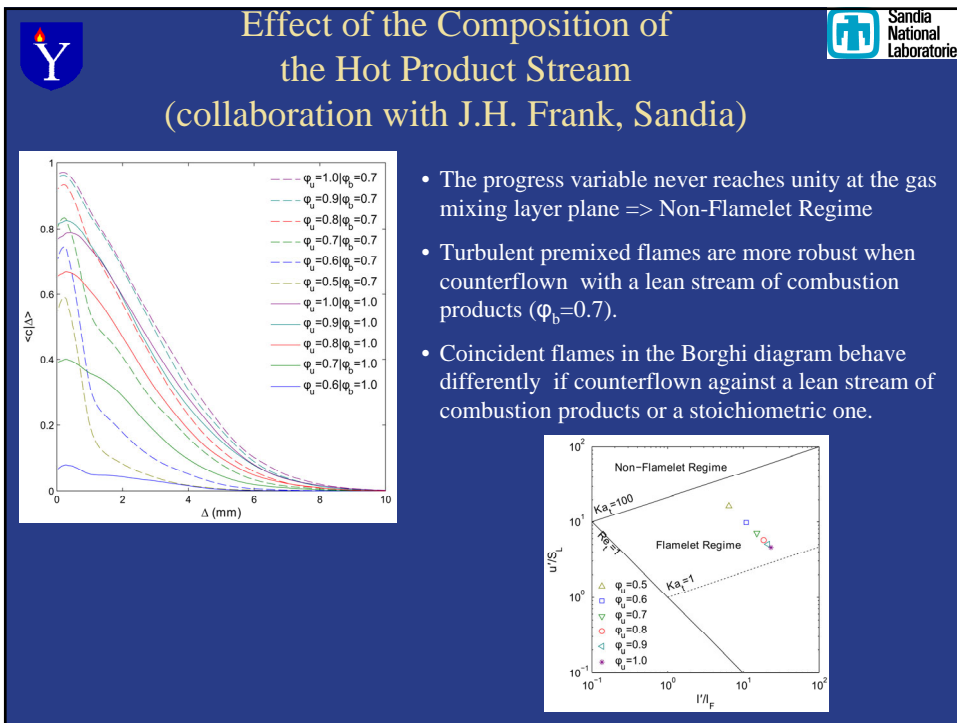
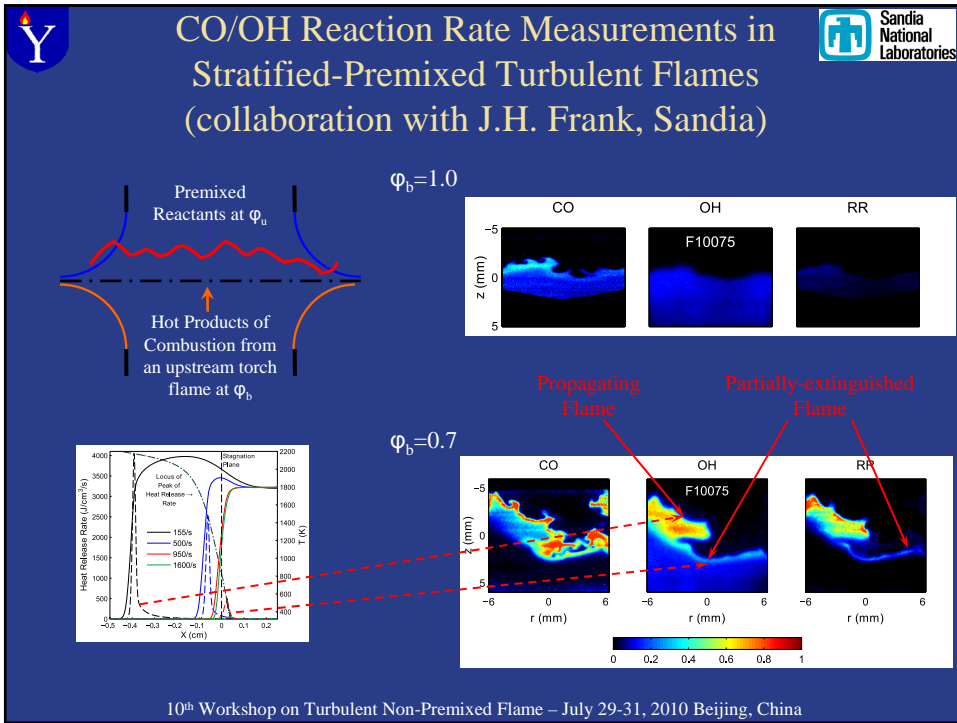
Turbulent jet of fresh reactants opposed to a stream of hot products of combustion (see poster)

Suitable for:

- Premixed flames
- Flamelet and non-flamelet regimes
- Mixture stratification studies

10<sup>th</sup> Workshop on Turbulent Non-Premixed Flame – July 29-31, 2010 Beijing, China

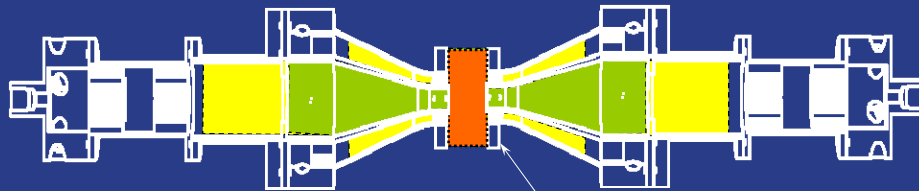




# Modeling Challenges

10<sup>th</sup> Workshop on Turbulent Non-Premixed Flame – July 29-31, 2010 Beijing, China

## Computational Modeling Approaches



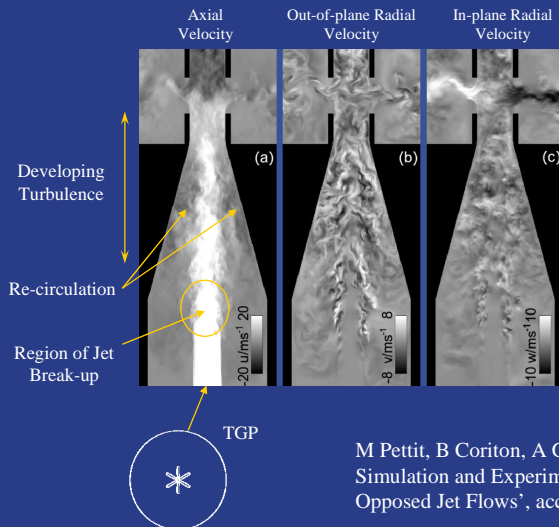
Are flanges necessary?

- Model just the counterflow domain (orange region) directly. Challenge to prescribe sufficiently detailed turbulent BC.
- Model the counterflow domain plus the flow inside the nozzles up to the plate (green region) by LES (e.g., Pettit and Kempf)
- First, model the flow inside the nozzles using a commercial code (e.g., FLUENT) starting upstream of the plate (yellow region) to provide simple, unambiguous boundary conditions for subsequent PDF-based simulations of the counterflow (orange) domain (Pope's suggestion).

10<sup>th</sup> Workshop on Turbulent Non-Premixed Flame – July 29-31, 2010 Beijing, China

# YCB - LES Simulation

Pettit, Kempf, Imperial



Flow is simulated within the nozzles to investigate complex turbulence-generating mechanisms and sensitivity to jet break-up:

- Each image shows 590x240 cells
- Performed at  $\Delta = 0.2\text{mm}$
- 58 million cells
- Two CPU-years

M Pettit, B Coriton, A Gomez, A M Kempf, 'Large-Eddy Simulation and Experiments on Non-Premixed Highly Turbulent Opposed Jet Flows', accepted PCI 2010

10<sup>th</sup> Workshop on Turbulent Non-Premixed Flame – July 29-31, 2010 Beijing, China

# YCB - LES Simulation

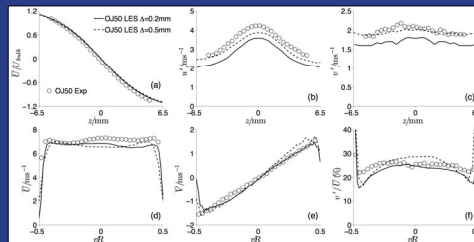
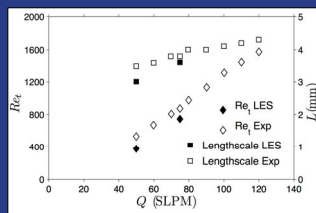
Pettit, Kempf, Imperial



## Non-Reactive Opposed Jets

### Observations:

- Good agreement for all measured quantities
- Sensitivity of jet break-up point leads to under-prediction of velocity fluctuations
- Length-scales determined by auto-correlation of axial velocity –  $Re_t \sim 800$  at 75SLPM
- See the poster for more info!

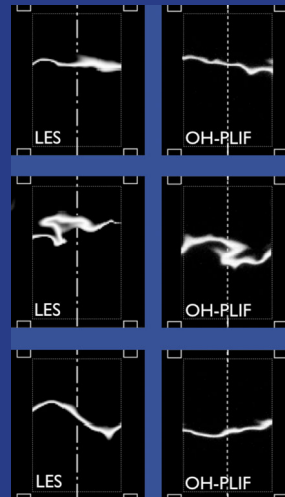
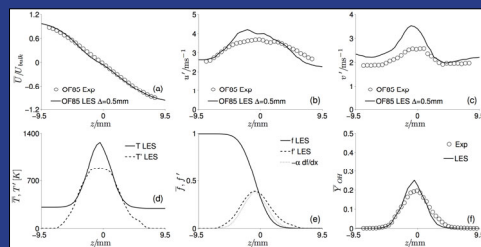


10<sup>th</sup> Workshop on Turbulent Non-Premixed Flame – July 29-31, 2010 Beijing, China

## Non-Premixed Counterflow Flames

### Observations:

- Normalised  $Y_{OH}$  can be interpreted as probability distribution for the flame position
- $Y_{OH}$  from LES and OH-PLIF directly comparable
- Similarity of morphologies supports model validation

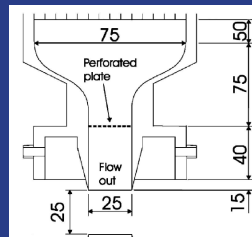


10<sup>th</sup> Workshop on Turbulent Non-Premixed Flame – July 29-31, 2010 Beijing, China

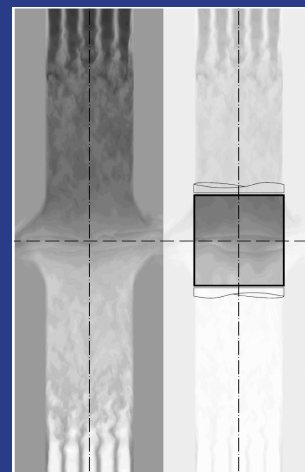
### Snapshots of axial velocity field (LES)

## TOJ: Experimental Set-Up

- Two identical opposed nozzles vertically aligned
- Turbulent conditions ( $Re$  5,000+) established by perforated plates 55 mm upstream of the nozzle exits
- Premixed case: Twin flames stabilised back-to-back
- Excellent optical access and a wealth of experimental validation data available [e.g. Lindstedt et al. (2005, 2007), Geyer et al. (2005), Geipel (2009) and others]
- Previous LES analyses: Kempf et al. (2000), Kempf (2003)



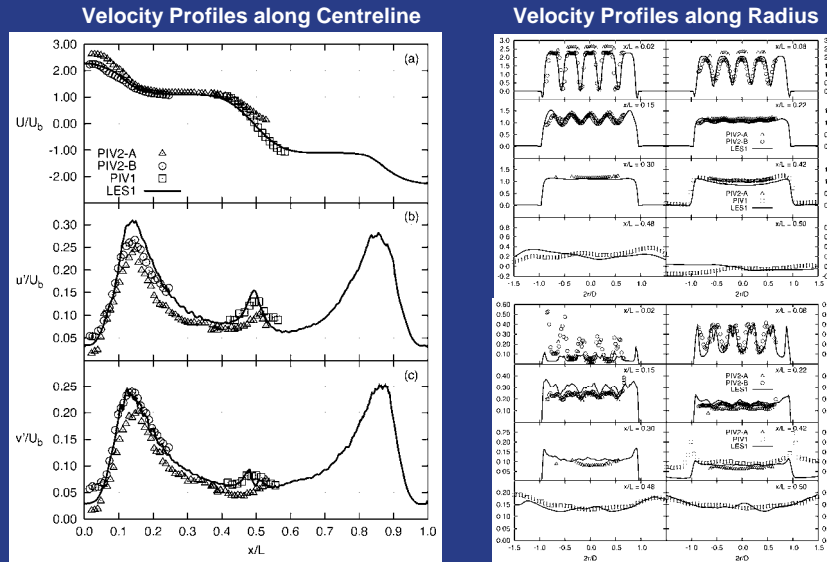
Schematic of a TOJ nozzle adapted from Luff et al. (2003)



Snapshots of axial Velocity field (LES)

10<sup>th</sup> Workshop on Turbulent Non-Premixed Flame – July 29-31, 2010 Beijing, China

## TOJ: Isothermal Results (quasi DNS)



10<sup>th</sup> Workshop on Turbulent Non-Premixed Flame – July 29-31, 2010 Beijing, China



## Counterflow vs. Coflow Flames: Compactness

Configuration	$Q_{CH_4}$ (SLPM)	$X_{CH_4}$	$Re_o$	$Re_t$
Counterflow	8.5	0.1	9,480	1050
Piloted Jet	5.3	0.15	10,000	957

- Counterflow  $\sim 50$  times smaller than coflow
- Advantageous experimentally and numerically
  - Computational cost dramatically reduced
  - Residence time:  $t_r \sim 1/S_b \sim 1.0$  ms, where  $S_b \sim dV/dr \sim 1000s^{-1}$
  - Typical DNS simulation flow time,  $t_s \sim 4$  ms
  - $t_s > t_r$
- Better statistics at the same computational cost

(Coppola *et al.*, 2009)



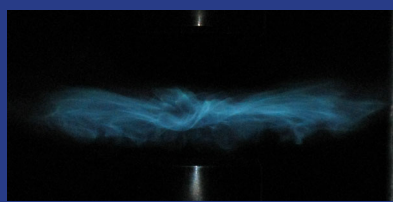
10<sup>th</sup> Workshop on Turbulent Non-Premixed Flame – July 29-31, 2010 Beijing, China

**Y** **Imperial College London**

## Advantage from a Soot Perspective

In counterflow, mean residence time < 1 ms. Soot complications are avoided and one can study turbulence even for fuels with high soot propensity.

$X_f$	0.10	0.15	0.20
$Re$	9,480	10,400	10,000
$Re_t$	1050	995	995

$C_2H_4$  (YCB vs. Coflow)

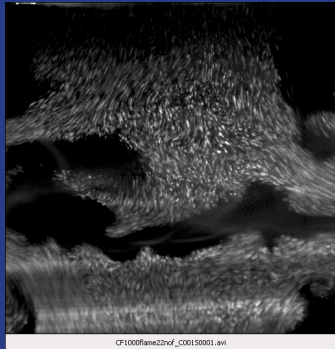
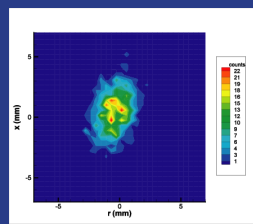
JP-10 (Imperial College)

10<sup>th</sup> Workshop on Turbulent Non-Premixed Flame – July 29-31, 2010 Beijing, China

**Y** **Imperial College London**

## Large Scale Instabilities

Large scale oscillations of the stagnation surface seem inevitable and may require screening. Should we care?

- The examples shown are the PDFs of the instantaneous stagnation point locations for a bulk velocity of 4.0 m/s.
- The movement of the stagnation point is not only a result of turbulent motion but also due to a low frequency bulk movement of the flow.

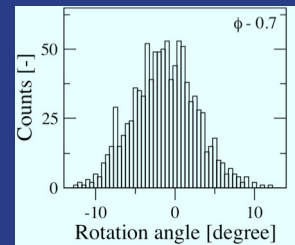
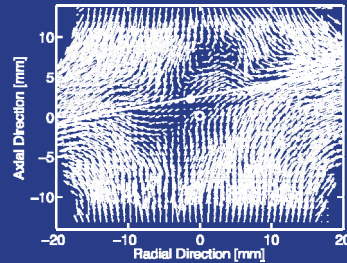
R.P. Lindstedt, P. Geipel and K. H. H. Goh

10<sup>th</sup> Workshop on Turbulent Non-Premixed Flame – July 29-31, 2010 Beijing, China

# Statistical Analysis of the Stagnation Point Location

R.P. Lindstedt, P. Geipel and K. H. H. Goh

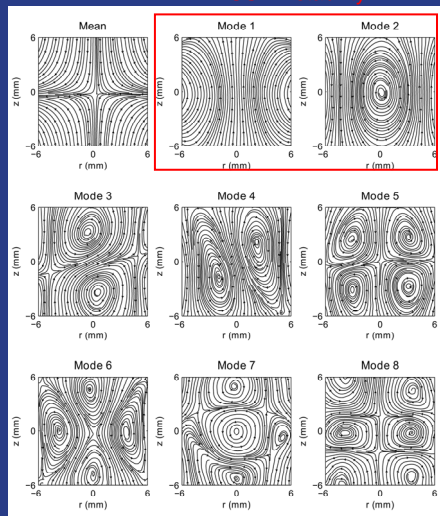
- An algorithm that produces a linear approximation of the stagnation plane location based on streamlines determined from instantaneous vector fields was also developed (see example to the right for a methane/air flame).
- The algorithm enables a quantification of the rotation of the instantaneous stagnation plane.
- A probability density function of the angle of rotation is given for 1000 instantaneous vector fields is shown to the right and reveals a movement of the stagnation plane within 12 degrees.



10<sup>th</sup> Workshop on Turbulent Non-Premixed Flame – July 29-31, 2010 Beijing, China

# Coherent Structures and their Effects

Mean and POD modes 1-to-8  
GSP instability



Coherent structures are large-scale, geometry-dependent, vortical structures.

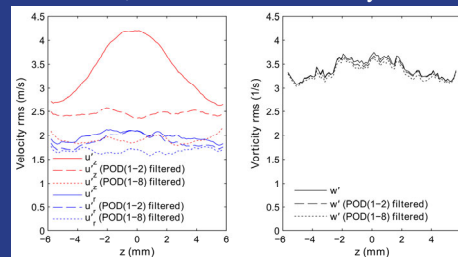
Coherent structures exist in any “experimental” turbulent flow.

Coherent Structures were identified by Proper Orthogonal Decomposition (POD).

$$u(x,t) = \underbrace{a_0(t)u_0(x)}_{\text{Mean Fluctuations}} + \underbrace{\sum_{k=1}^8 a_k(t)u_k(x)}_{\text{Coherent Fluctuations}} + \underbrace{\sum_{k=9}^{\infty} a_k(t)u_k(x)}_{\text{Incoherent Fluctuations}}$$

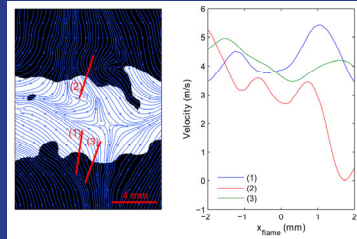
Velocity RMS

Vorticity RMS

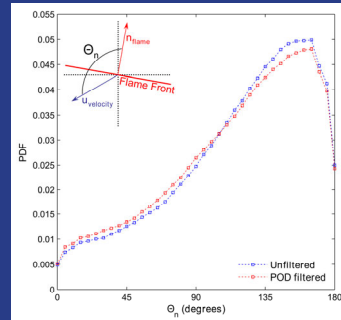


10<sup>th</sup> Workshop on Turbulent Non-Premixed Flame – July 29-31, 2010 Beijing, China

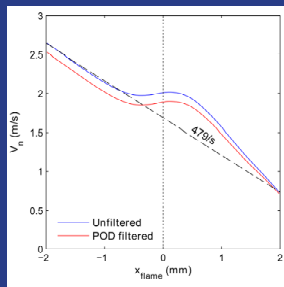
# Y Impact of GSP instability on local flow field as *seen* by premixed flame front



Flame front orientation with respect to local velocity vectors



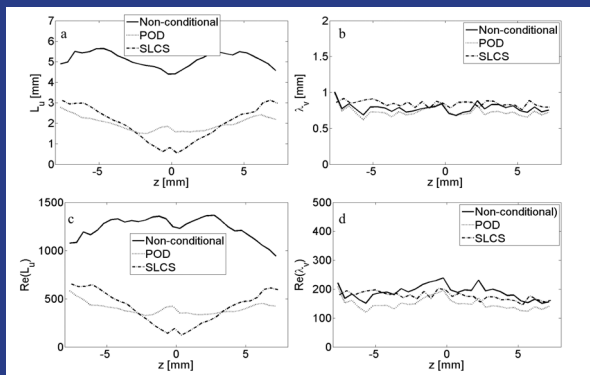
Filtering of POD modes 1&2 has minor impact on conditional statistics



Conditional averaged velocity

10<sup>th</sup> Workshop on Turbulent Non-Premixed Flame – July 29-31, 2010 Beijing, China

# Y Turbulent Scales and Reynolds numbers (Coppola and Gomez, to appear in Phys. Fluids)



Large scale oscillations affect the integral-scale based Re but not the Taylor-scale based Re estimates

10<sup>th</sup> Workshop on Turbulent Non-Premixed Flame – July 29-31, 2010 Beijing, China



## General Conclusions

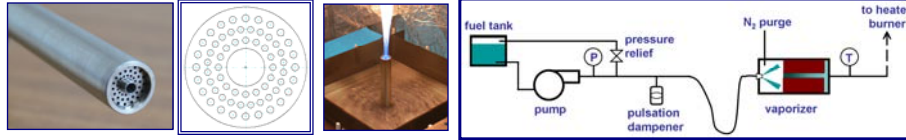


- Turbulent counterflow flames successfully stabilized at large  $Re_t$  and  $Ka_t$ ;
- Versatile and compact system, potentially advantageous for computational modeling;
- Need well-concerted experimental and modeling effort: future target flame?

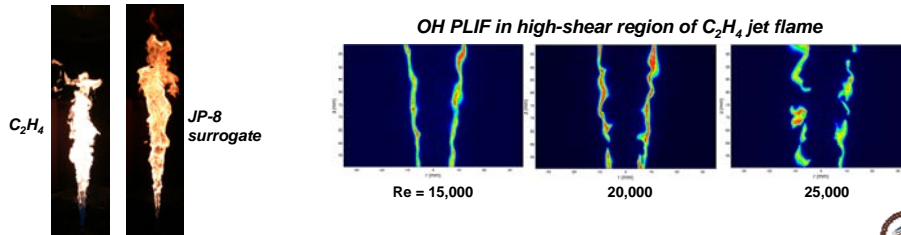
10<sup>th</sup> Workshop on Turbulent Non-Premixed Flame – July 29-31, 2010 Beijing, China

## Development of Suitable TNF Burners for Sooty Fuels

- Piloted jet burners for gaseous or prevaporized liquid fuels, similar as Sydney burner
  - 3-row pilot
  - Smaller fuel tube (ID: 3.2 mm and 2.5 mm vs. 7.2 mm of Sydney burner)

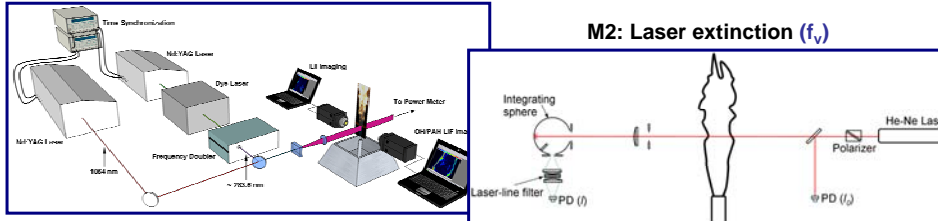


- Canonical flames chosen with  $Re = 20,000$ , to avoid significant local extinction

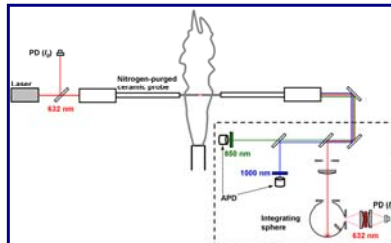


## Measurements in Ethylene and JP-8 Surrogate Flames

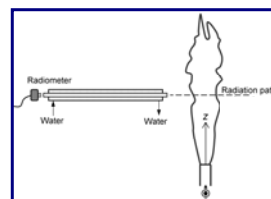
### M1: Simultaneous OH/PAH PLIF and PLII ( $f_v$ )



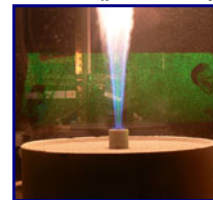
### M3: 3-color extinction emission ( $f_v$ , T)



### M4: Local radiant emission

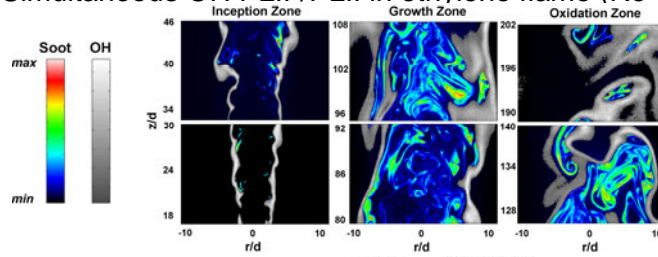


### M5: PIV (preliminary)

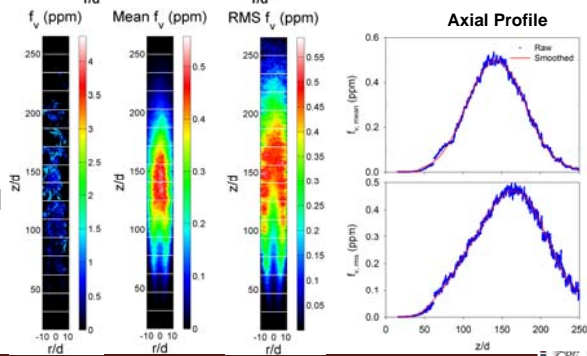


## Representative Data from Experiments

- Simultaneous OH PLIF/PLII in ethylene flame ( $Re = 20000$ )



- Soot volume fraction in ethylene flame ( $Re = 20000$ ) from calibrated LII



## Diagnostic Challenges

- Heavy soot load (esp. in JP-8 flame) strongly attenuates light: shorter  $\lambda$  (e.g. UV), stronger attenuation

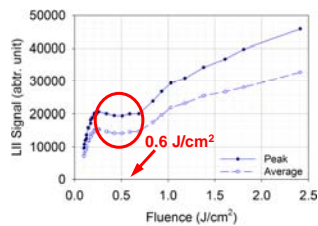
- Laser attenuation
- Signal trapping

$$\frac{I}{I_0} = \exp \left[ - \underbrace{K_e}_{\text{extinction coeff.}} \cdot \underbrace{\left( \int_L f_v(l) dl \right)}_{\text{path-integrated soot volume fraction}} \right] / \underbrace{\lambda}_{\text{wavelength}}$$

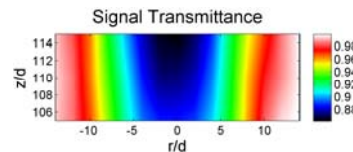
**Beer-Lambert Law**

- Solutions for LII

S1: Laser fluence chosen at high end of "plateau" region

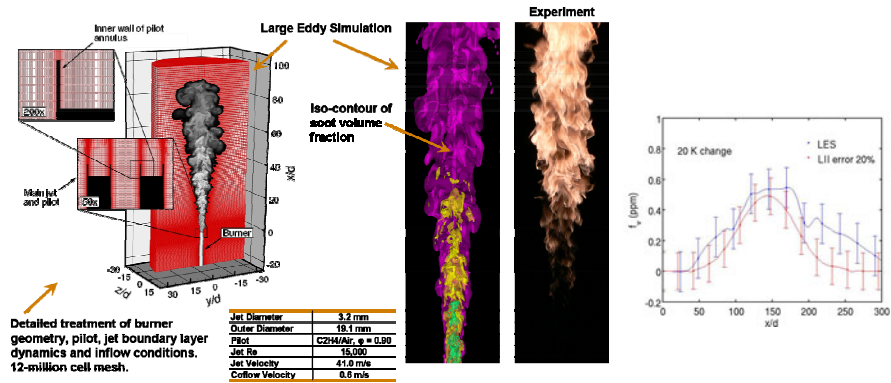


S2: Mean signal transmission estimated from laser extinction



## Modeling Comparisons

- Joe Oefelein



- Heinz Pitsch, Guillaume Blanquart, and David Lignell have plans to model these flames
- Data to be posted on CRF website (soon)



## Unexpected Effects of Preferential Transport in Turbulent Premixed CH<sub>4</sub>/Air Flames

- Rob Barlow, Matt Dunn (Sandia)  
Mark Sweeney, Simone Hochgreb (Cambridge)
- Stratified (and premixed) Swirl Burner experiments
- Initial observation: Mean  $\phi$  not constant across the flame brush in premixed cases
- **MUST BE AN ERROR?!**
- Reassessment of calibrations and data processing did not reveal any significant errors
- Appears to be real and significant effect of differential diffusion in turbulent premixed flames

z=10 mm

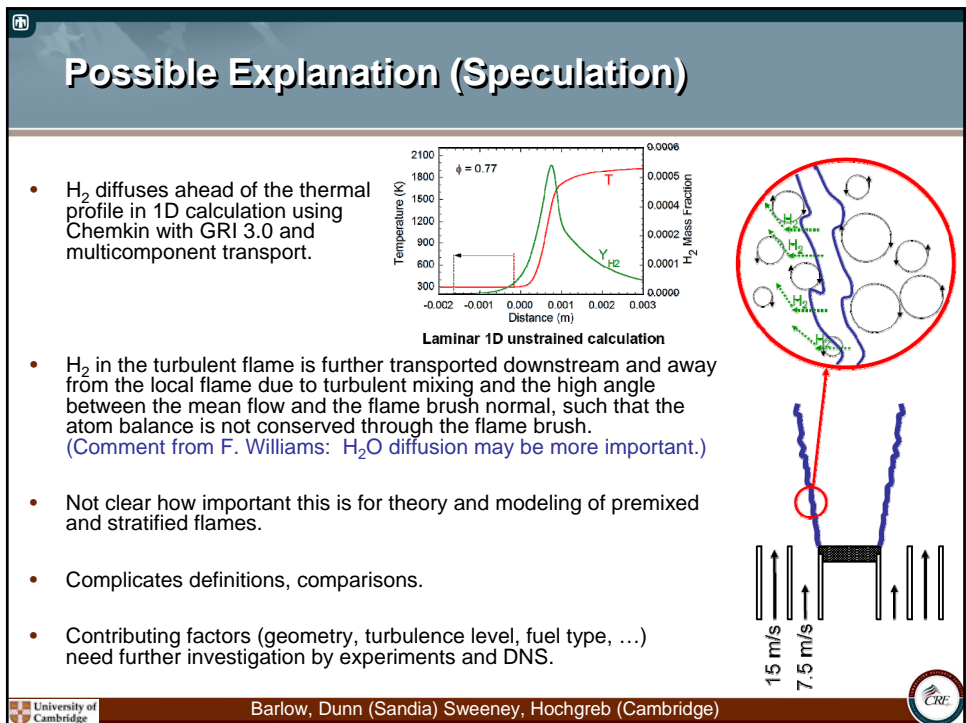
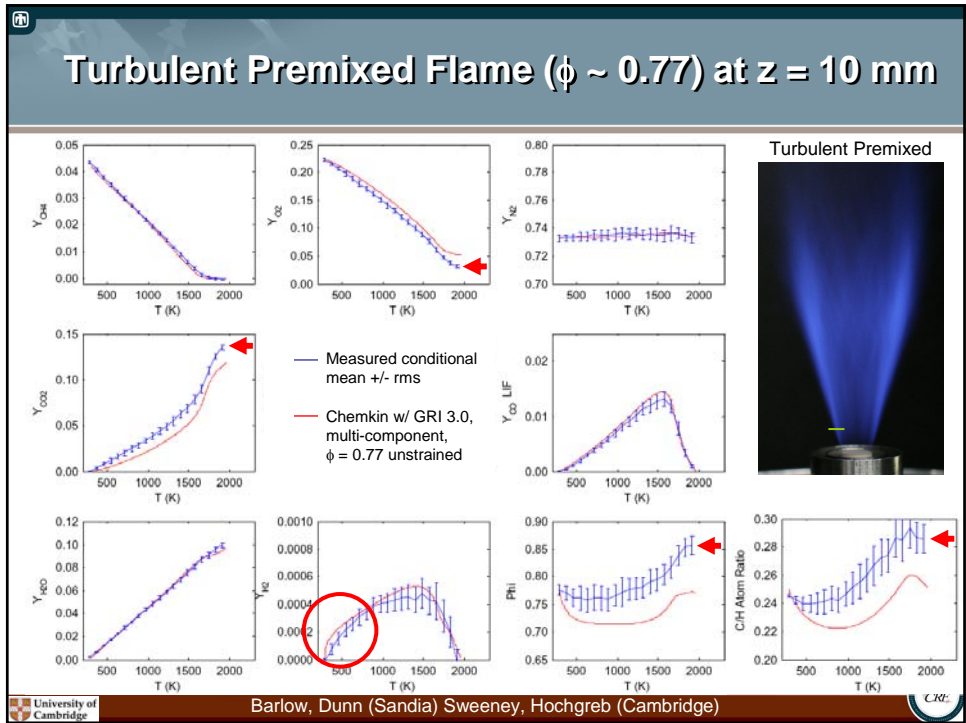
Case 1:  $\phi_i = \phi_o = 0.75$ ; no swirl

## Laminar Unstrained Premixed Flame ( $\phi = 0.73$ )

— Measured conditional mean +/- rms  
— Chemkin w/ GRI 3.0, multi-component,  $\phi = 0.73$  unstrained

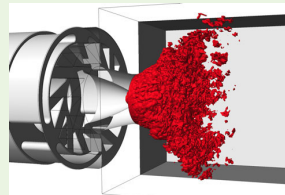
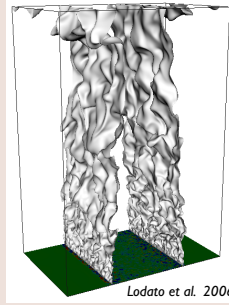
“Vertical Flame”

Barlow, Dunn (Sandia) Sweeney, Hochgreb (Cambridge)



## Canonical flow configurations

- **Synthetic turbulence**
- **Chemistry:**
  - ✓ Single-step
  - ✓ Reduced
  - ✓ Tabulated
  - ✓ Detailed chemistry
- **Transport:**
  - ✓ Simple
  - ✓ Velocity correction
  - ✓ Complex
- **Low Reynolds number**
- **Very limited range of scales, integral length scale of the order of flame thickness.**



## Real turbulent shear flows

- **Real (organically grown) turbulence**
- **Chemistry:**
  - ✓ Single-step
  - ✓ Tabulated detailed
- **Transport:**
  - ✓ Simple
- **Realistic Reynolds number**
- **Real length scales ratios**
- **Real energy distribution over turbulent scales**

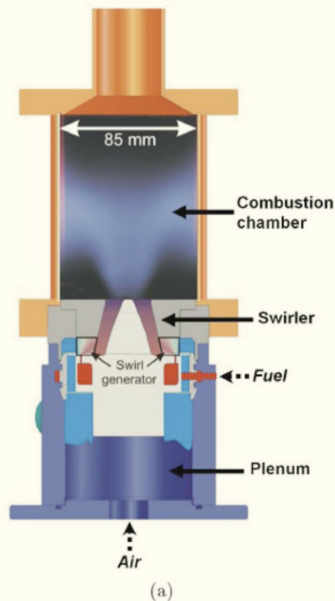
V. Moureau, P. Domingo, L. Vervisch

1

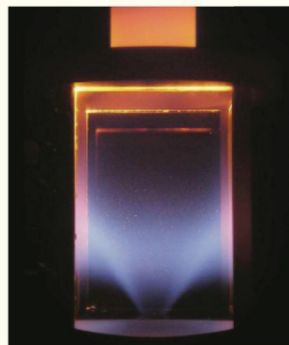
TNF-10

lundi 19 juillet 2010

## Target experiment



W. Meier et al.  
Combust. Flame  
150 (1/2) (2007) 2–26.



## YALES2

Vincent Moureau

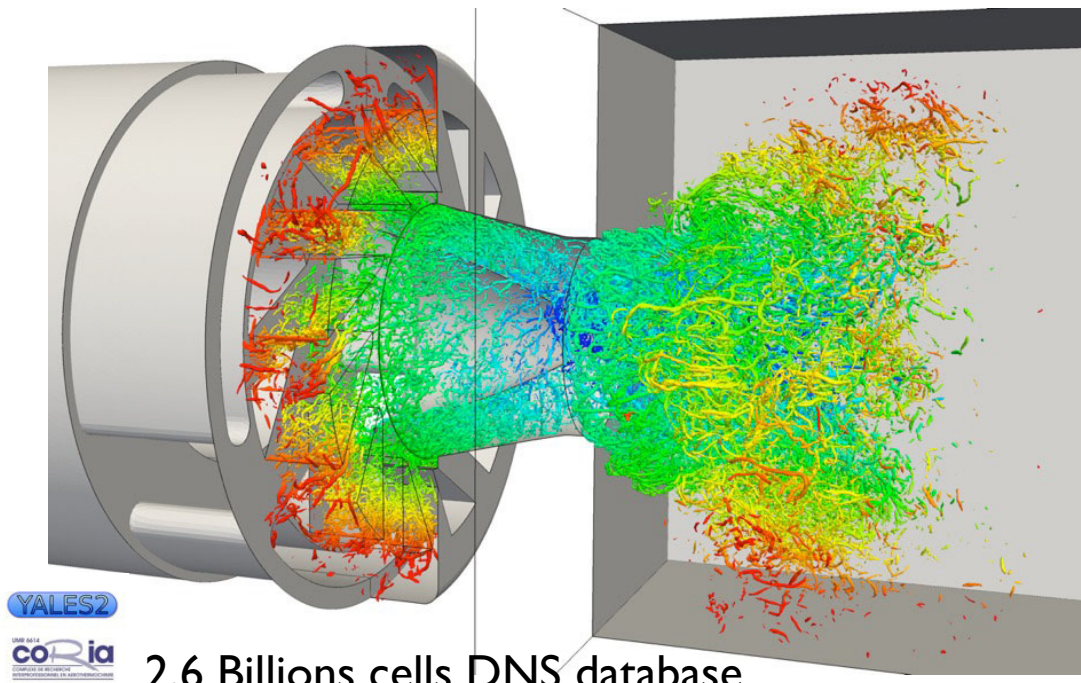
- **YALES2 DNS-LES solver**
  - ✓ Low Mach
  - ✓ Novel numerics for unstructured grids
  - ✓ HPC data architecture (ready for hundred of thousand of cpus)
- **Chemistry:**
  - ✓ Tabulated
- **Transport:**
  - ✓ Simple
- **HPC grid refinement**

V. Moureau, P. Domingo, L. Vervisch

2

TNF-10

lundi 19 juillet 2010

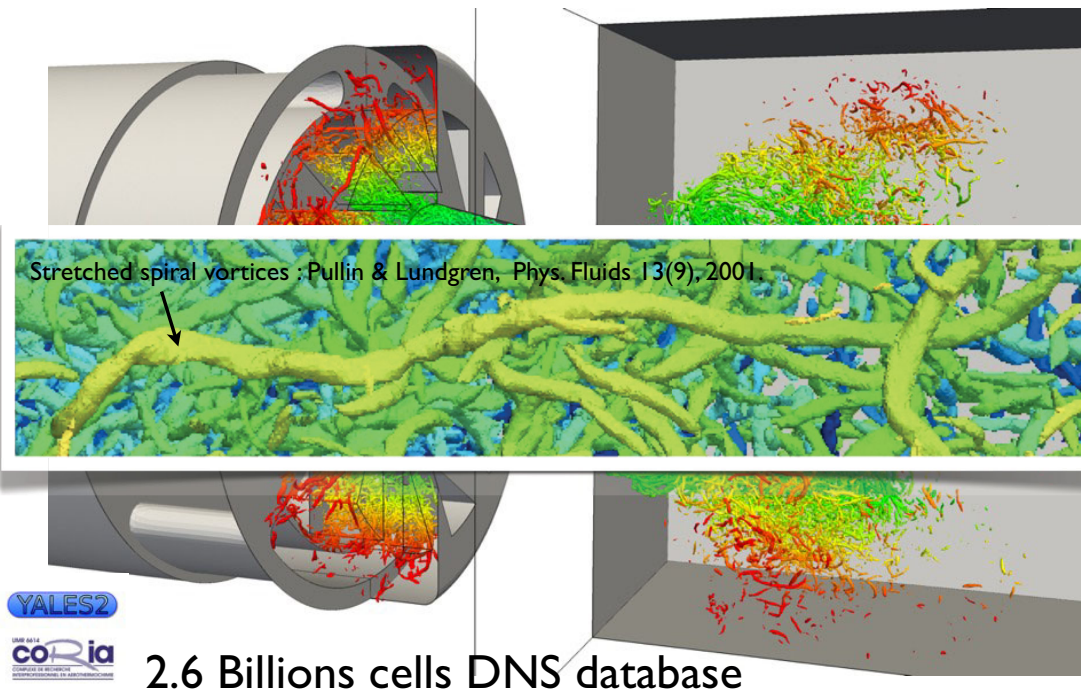


V. Moureau, P. Domingo, L. Vervisch

3

TNF-10

lundi 19 juillet 2010



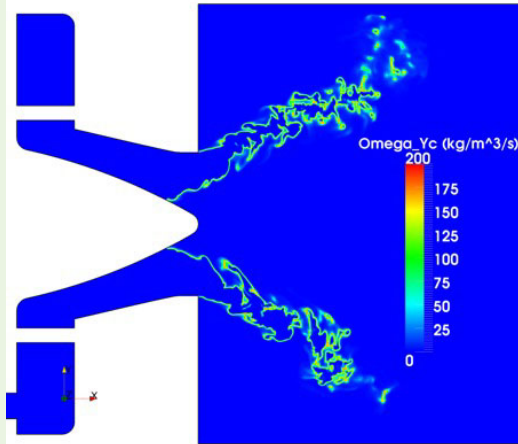
V. Moureau, P. Domingo, L. Vervisch

3

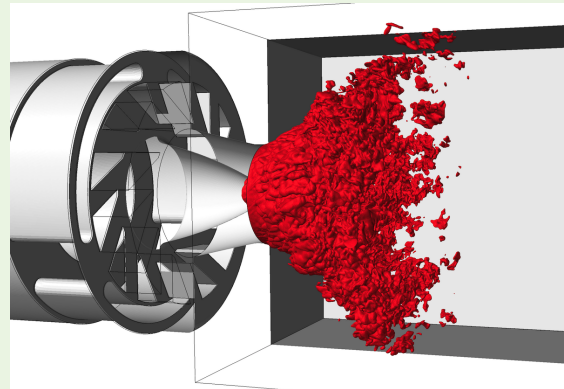
TNF-10

lundi 19 juillet 2010

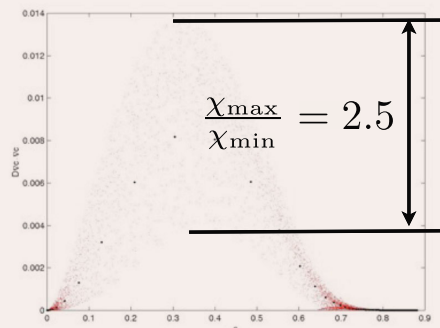
## Burning rate



## Flame Surface

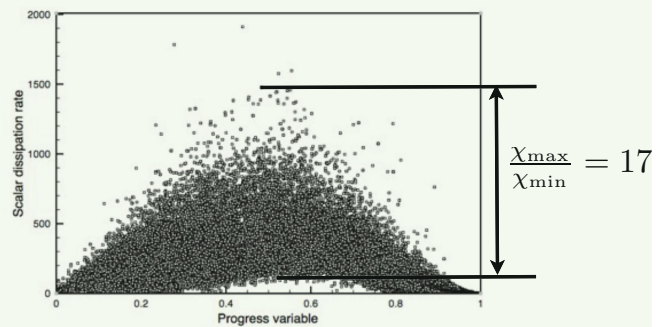


## Canonical flow configurations



From K. Bushe web page  
(<http://kbspc.mech.ubc.ca/scadisscat.jpg>)

## Real turbulent shear flows



Large spreading of scalar dissipation rate response (only 1/4096 of the database shown)

# Open Discussion

**Steve Pope & Assaad Masri**

- Discussion points:
  - Objectives of TNF modeling studies
  - Sensitivities and uncertainties
  - Variation of important parameters
  - PPJB
  
  - Darmstadt stratified burner
  - Lifted flames in vitiated co-flow
  - LES and high-speed OH imaging

1

## Objectives of TNF modeling studies

- NOT to champion particular approaches
- Establish capabilities and limitations of different approaches
- Understand sensitivities of flames to uncertainties in experimental conditions and sub-models
- Question: how to share information more effectively?
  - TNF presentations and web site;
  - publications; supplementary material

2

## Variation of Parameters

- Capability of models to represent effects of most influential experimental conditions

- Stream velocities, fuel, temperatures, ...

- PPJB, Barlow & Frank, ... vary  $U_j$  and  $U_p$

- Important non-dimensional parameters:

$$\frac{U_p}{U_j}, \quad Da \equiv \frac{d}{U_j \tau_c}, \quad Re = \frac{U_j d}{\nu}, \quad (Ma, Fr, \dots)$$

$$\text{Note: } Da Re = \frac{d^2}{\nu \tau_c}$$

- Question: do we know how TNF flames depend on  $Re$  at fixed  $Da$ ?

- Prediction from PDF methods

3

## Calculations of PM1-200

- Stanford LES and Cornell PDF both significantly over-predict extent of reaction

- Chemistry based on GRI

- Question: how to determine if the chemical mechanism is the source of discrepancy?

- Opposed flow laminar flame experiment:

- Jet ( $\phi = 0.5$ ) vs. co-flow (lean burnt  $H_2$ /air)

4

## Stratified Flames (Darmstadt)

- Excellent burner design
- Good evolving data set
- Promising initial calculations

### Suggestion/discussion:

- With respect to each controlling parameter:
  - Select a sequence of 3-4 flames
  - Tabulate data set on the web
  - Start next round of calculations early
- Is the value  $u'/S_L$  sufficiently high?

## LES and High Speed Imaging

- Evolving fields
- Time sequences of reactive scalars
- Massive data sets

### Questions:

- How best to present the images?
- What do we compare?
- How best to make comparisons?

## More complex fuels

- Chemistry is evolving
- Need additional data in piloted flames and lifted, auto-igniting flames

### Suggestions

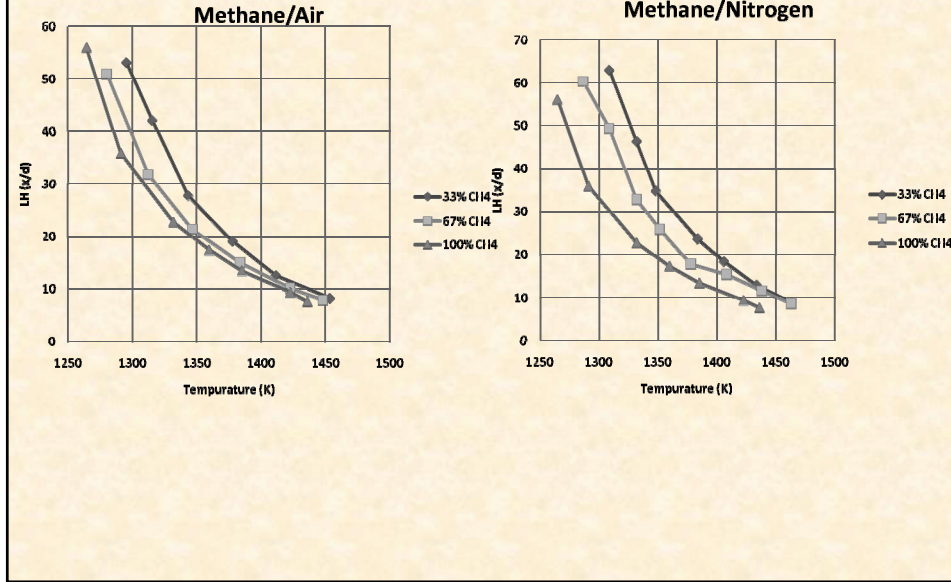
- Computation of pure methane flames
- Data set in methane as well as DME flames

## Additional Measurements in Lifted Auto-igniting Flames

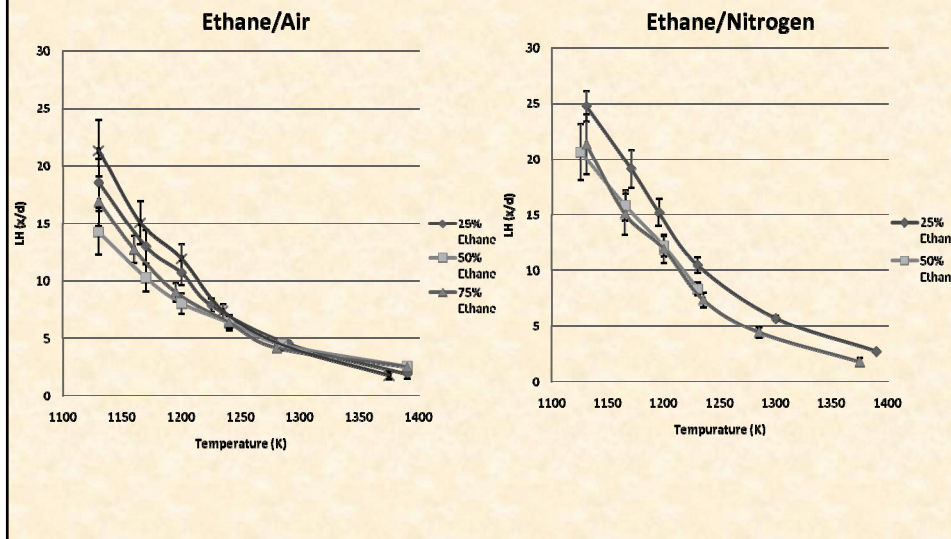
Three fuels, different levels of dilution and partial premixing:

- |  |  |  |
|--|--|--|
| ● CH <sub>4</sub> ,                    | C <sub>2</sub> H <sub>6</sub>                      | C <sub>3</sub> H <sub>8</sub>                      |
| ● CH <sub>4</sub> -Air=33%             | C <sub>2</sub> H <sub>6</sub> -Air=25%             | C <sub>3</sub> H <sub>8</sub> -Air=25%             |
| ● CH <sub>4</sub> -Air=67%             | C <sub>2</sub> H <sub>6</sub> -Air=50%             | C <sub>3</sub> H <sub>8</sub> -Air=50%             |
| ●                                      | C <sub>2</sub> H <sub>6</sub> -Air=75%             | C <sub>3</sub> H <sub>8</sub> -Air=75%             |
| ● CH <sub>4</sub> -N <sub>2</sub> =33% | C <sub>2</sub> H <sub>6</sub> -N <sub>2</sub> =25% | C <sub>3</sub> H <sub>8</sub> -N <sub>2</sub> =25% |
| ● CH <sub>4</sub> -N <sub>2</sub> =67% | C <sub>2</sub> H <sub>6</sub> -N <sub>2</sub> =50% | C <sub>3</sub> H <sub>8</sub> -N <sub>2</sub> =50% |
| ●                                      | C <sub>2</sub> H <sub>6</sub> -N <sub>2</sub> =75% | C <sub>3</sub> H <sub>8</sub> -N <sub>2</sub> =75% |

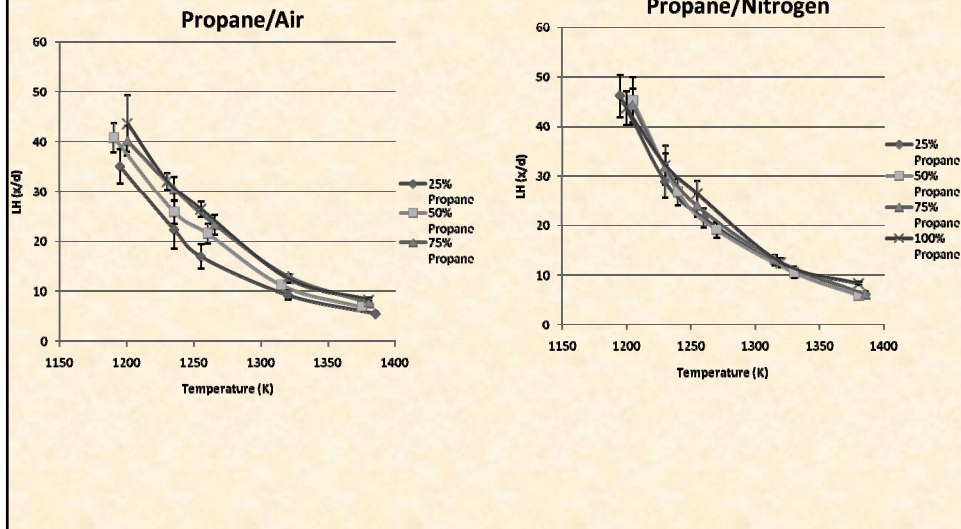
## Lift-off Heights vs T(coflow)



## Lift-off Heights vs T(coflow)



## Lift-off Heights vs T(coflow)



## Discussion Points

- Objectives of TNF modeling studies
- Sensitivities and uncertainties
- Variation of important parameters
- PPJB
  
- Darmstadt stratified burner
- Lifted flames in vitiated co-flow
- LES and high-speed OH imaging

**T<sub>N</sub>F10 Workshop – Poster Abstract Titles and Authors**  
(Beijing, 29-31 July 2010)

1. **Development and Validation of a Manifold Based Method for the Simulation of Non-Premixed and Partially Premixed Combustion Processes**  
J.E. Anker, N. Beishuizen, K. Claramunt, Ch. Hirsch
2. **Analysis of Monte Carlo Approach for the Solution of Filtered Mass Density Function Transport Equation in LES**  
A. Attili, F. Bisetti
3. **Artificial Flame Broadening Effects on the LES Quality**  
P. Auzillon, N. Darabiha, O. Gicquel, D. Veynante, B. Fiorina
4. **Unexpected Effects of Preferential Molecular Transport in Turbulent Premixed CH<sub>4</sub>/Air Flames**  
R.S. Barlow, M.J. Dunn, M. Sweeney, S. Hochgreb
5. **Assessment of Nonlinear Regime Two-Line Atomic Fluorescence (NTLAF) in Sooty Flames**  
Q.N. Chan, P.R. Medwell, P.A.M. Kalt, Z.T. Alwahabi, B.B. Dally, G.J. Nathan
6. **Effects of the Composition of the Hot Product Stream on Turbulent Counterflow Premixed Flames**  
Bruno Coriton, Jonathan H. Frank, Alessandro Gomez
7. **Numerical Investigation of Natural Gas Jet-In-Hot-Coflow Flames**  
A. De, E. Oldenhof, P. Sathiah, D.J.E.M. Roekaerts
8. **Hybrid RANS/PDF Calculations of a Swirling Bluff Body Flame (SM1)**  
R. De Meester, B. Naud, B. Merci
9. **Stratified Lifted Jet Flames in a Hot (1280 K) Cross-Flow**  
James F. Driscoll, Danny Micka
10. **Application of a Wavelet Based Denoising Algorithm Enabling High Resolution Measurements of Scalar Dissipation in Flames**  
Matthew J. Dunn, Robert S. Barlow
11. **Turbulent Partially Premixed Dimethyl Ether/Air Jet Flames: A New Series of Target Flames for Experiments and Modeling**  
Jonathan H. Frank, Andrea G. Hsu, Johannes Kuhl
12. **Raman/Rayleigh-Scattering and CO-LIF Measurements in Laminar and Turbulent Jet Flames of Dimethyl Ether**  
F. Fuest, R.S. Barlow, J.-Y. Chen, M.J. Dunn, A. Dreizler
13. **Conditional Statistics in Turbulent Premixed Opposed Jet Flames**  
K.H.H. Goh, P. Geipel, R.P. Lindstedt

**T<sub>N</sub>F10 Workshop – Poster Abstract Titles and Authors**  
(Beijing, 29-31 July 2010)

14. **Developments in Turbulent Autoignition Experiments – Fuel Droplet Autoignition in a Heated Cross Flow**  
R.L. Gordon, C.N. Markides, E. Mastorakos
15. **Prediction of Autoignition in a Lifted Methane/Air Flame Using an Unsteady Flamelet/Progress Variable Model**  
Matthias Ihme, Yee Chee See
16. **Grid Convergence Analysis for the Large-Eddy Simulation of the Sandia Piloted Methane-Air Flames D, E, and F**  
Jean-Francois Izard, Fabrizio Bisetti
17. **LES of TSF\_A and TSF\_G Flames Using the SGS PDF Equations/Eulerian Stochastic Field Method**  
W.P. Jones, S. Navarro – Martinez, K. Vogiatzaki
18. **DQMOM Approach for Modeling Soot Formation of C<sub>2</sub>H<sub>4</sub>/Air Turbulent Non-Premixed Flame**  
T.H. Kim, J. Lee, Y. Kim
19. **Modeling of Turbulent Nonpremixed Flames in Supercritical Condition**  
T.H. Kim, S. Park, Y. Kim, S.-K. Kim
20. **A Flamelet Based Model for Auto-Ignition in Turbulent Conditions: Validation Using DNS**  
E. Knudsen, E. S. Richardson, H. Pitsch, J. H. Chen
21. **LES of a Lean Premixed Stratified Burner Using a Thickened Flame Approach Coupled with FGM Tabulated Chemistry**  
G. Künne, A. Ketelheun, J. Janicka
22. **Comparison of Flame Surface Density Models for LES**  
T. Ma and A.M. Kempf
23. **LES-CMC Modelling of Turbulent Non-Premixed Flames with Rate-Controlled Constrained Equilibrium (RCCE) and Level of Importance (LOI) Mechanism Reduction**  
Salvador Navarro-Martinez, Terese Løvås, Stelios Rigopoulos
24. **Transported PDF Modeling of a Lifted H<sub>2</sub>/N<sub>2</sub> Jet flame in a Vitiated Coflow Using Detailed Chemistry: Study of Some Numerical Accuracy Issues**  
Bertrand Naud
25. **LES of Lifted Flames in a Gas Turbine Model Combustor Using Top-Hat Filtered PFGM Chemistry**  
C. Olbricht, O.T. Stein, J. Janicka, J.A. van Oijen, S. Wyosocki, A.M. Kempf

## T<sub>N</sub>F10 Workshop – Poster Abstract Titles and Authors

(Beijing, 29-31 July 2010)

26. **Flame Stabilisation of the Delft Jet-In-Hot-Coflow Flames**  
E. Oldenhof, M.J. Tummers, E.H. van Veen, D.J.E.M. Roekaerts
27. **Development of High-Speed Rayleigh and Raman Scattering Imaging to Investigate Dynamics in Turbulent Jets and Flames**  
Randy A. Patton, Kathryn N. Gabet, Naibo Jiang, Walter R. Lempert, Jeffrey A. Sutton
28. **Large-Eddy Simulation and Experiments on Non-Premixed Highly Turbulent Opposed Jet Flows**  
M.W.A. Pettit, B. Coriton, A. Gomez, A.M. Kempf
29. **Characterization of a Turbulent Dilute Hydrogen Diffusion Flame Using Spontaneous Raman Scattering, OH-PLIF and Large Eddy Simulation**  
J. Ranalli, P. Strakey
30. **Analysis of Turbulent Mixing Statistics in Stratified Combustion**  
Edward S. Richardson, Jacqueline. H. Chen
31. **PDF Calculations of Piloted Premixed Jet Flames**  
D.H. Rowinski, S.B. Pope
32. **Reduced State Spaces for Laser-Diagnostics in Combustion: Checks with DNS Data**  
Robert Schießl, Ulrich Maas, Christiane Zistl, Gordon Fru
33. **A Turbulent Stratified Flame Series for Model Validation**  
F. Seffrin, F. Fuest, T. Stahler, N. Karimi, D. Geyer, A. Dreizler
34. **Analysis of Auto-Ignition of Turbulent Hydrogen Jets with Different Detailed Reaction Mechanisms**  
I. Stankovic, A. Triantafyllidis, E. Mastorakos, C. Lacor, B. Merci
35. **Cambridge Stratified Swirl Burner**  
Mark Sweeney, Matt Dunn, Simone Hochgreb, Robert Barlow
36. **Measurements of Blowoff Dynamics in Stratified, Vitiated Bluff-Body Flames**  
S.G. Tuttle, S. Chaudhuri, S. Kostka, K.M. Kopp-Vaughan, B.M. Cetegen, M.W. Renfro
37. **Modeling of Jet in a Hot Coflow with Tabulated Unsteady Non-Premixed Flamelets in RANS and LES**  
R. Vicquelin, B. Fiorina, O. Gicquel
38. **Modeling of Sandia Flame E using Hybrid Binomial Langevin–MMC Model**  
Andrew P. Wandel, R. Peter Lindstedt
39. **Development of an LES/PDF Code and Its Application to Flame D**  
Haifeng Wang, Stephen B. Pope

Blank Page

# Development and validation of a manifold based method for the simulation of non-premixed and partially premixed combustion processes

J. E. Anker, N. Beishuizen, K. Claramunt, Ch. Hirsch\*  
NUMECA Int., Chaussée de la Hulpe/Terhulpesteenweg 189,  
B-1170 Brussels, Belgium  
www.numeca.com  
\*charles.hirsch@numeca.be

## Synopsis

The poster describes the implementation and validation of the Flamelet Generated Manifold (FGM) method for non-premixed and partially-premixed combustion in the unstructured CFD solver package FINE<sup>TM</sup>/Hexa. The flow solver has been assessed on a comprehensible set of test cases ranging from simple verification test cases to geometrically complex, industrially relevant configuration. A key element in the validation procedure is the numerical simulation of TNF target flames. As the various TNF flames feature specific physical phenomena, they are suited to verify that the flow solver is able to reproduce fundamental aspects of non-premixed and partially premixed combustion. Results from the simulation of various target flames together with examples from runs of industrial test cases are used to discuss the capabilities and the limitations of the developed manifold modeling approach.

## Introduction

Since there is a demand for reliable and accurate simulation tools for reactive flows, NUMECA Int. is developing advanced combustion models in cooperation with partners from several renowned research institutions in Europe. Recently NUMECA has incorporated the Flamelet Generated Manifold (FGM) method of TU Eindhoven in its unstructured CFD software system. To assess this approach, various TNF target flames have been used. Since those flames are well defined, ample experimental data are available and they exhibit specific characteristics of non-premixed and partially premixed flames, the test cases of the TNF workshop have proved to be very useful in the validation procedure.

## Numerical method

The FINE<sup>TM</sup>/Hexa integrated CFD solver software package in which combustion models have been implemented consists of HEXPRESS<sup>TM</sup> for the automatic generation of unstructured, hexahedral meshes, the flow solver FINE<sup>TM</sup>/Hexa, and CFView<sup>TM</sup> for post-processing and visualization. FINE<sup>TM</sup>/Hexa solves the Reynolds-Averaged Navier-Stokes equations (RANS) for compressible flows by means of an explicit time-marching finite volume scheme. The solution scheme used ensures monotonous solutions and allows thus a robust and accurate resolution of both reactive and inert flow fields. By using agglomeration multigrid, novel convergence acceleration techniques and parallelization with automatized domain decomposition, the solution scheme is highly efficient.

## The Flamelet Generated Manifold approach

The method applied in the current work is based on the Flamelet Generated Manifold (FGM) approach, which was devised by van Oijen and de Goey [1,2]. In this method a low dimensional manifold is used to represent a complex reaction mechanism. This mixedness-reactedness method is both suitable for the simulation of premixed and non-premixed combustion processes; while the mixture fraction variable describes the stoichiometry of a reacting mixture, the progress variable tracks the advance of the chemical reactions.

As the name suggests, the idea of the method is to construct a manifold based on a set of flamelets. In the current work, an igniting unsteady flamelet, a library of steady premixed, or a library of steady non-premixed flamelets have been used as a basis for the table generation. These libraries were created using TU Eindhoven's 1D-chemistry code Chem1D.

## Verification and validation procedure

The verification and validation procedure of combustion models developed in FINE<sup>TM</sup>/Hexa comprises three distinct components. In the first part the consistency of the implemented transport equations for flow, turbulence and combustion is verified by carrying out elementary test cases like the flat diffusing plate, the mixing of two streams, et cetera. In some instances also the method of manufactured solutions is employed for model verification. This phase of the testing procedure consists also of conducting simulations for non-reacting jets (TNF's propane jet, TNF's inert swirling test cases) and laminar flames. By conducting grid refinement studies and comparing the computational results with analytical data, experiments and detailed simulations, it is verified that the implementation has the expected numerical order of accuracy.

In a second step well-established test cases for turbulent, non-premixed and partially premixed flames are carried out to validate and to calibrate the models for turbulent non-premixed combustion. An important part in this phase is the TNF-10 Workshop

validation of the flow solver on several of the TNFs target flames (e.g., Cabra [3], Flame D, HM1e). As an example for one of the test cases conducted for the validation of FGM method in FINE<sup>TM</sup>/Hexa, the computed and measured carbon dioxide mass fractions are plotted in Fig. 1 for the TNF Bluff-body HM1e test case [4]. The results show that the FGM method leads to better predictions compared to the classical flamelet approach.

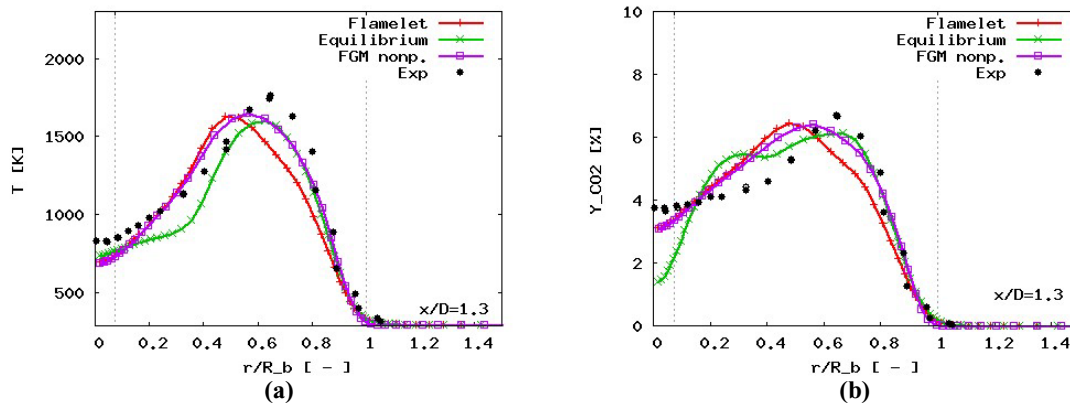


**Fig. 1:** Comparison of computational results and measurement data of the TNF Bluff-body test case (HM1e): (a) Temperature, (b) Mass fraction of CO<sub>2</sub>. The results show that the FGM method leads to better predictions compared to the classical flamelet approach

In the last part of the development and testing procedure, the robustness, the reliability, and the efficiency of the implemented combustion models are examined by conducting computations of geometrically complex, industry like test cases. In this part of the overall quality assessment procedure, the combustion models implemented in FINE<sup>TM</sup>/Hexa were for instance used to simulate the reactive flow field in the generic gas turbine (GGT) combustor of EKT/TU Darmstadt [5]. In Fig. 2 the simulated temperature fields in the GGT combustor are shown; with the standard flamelet approach an attached flame is falsely predicted, whereas when the FGM approach is used, the lifting of the flame is captured.

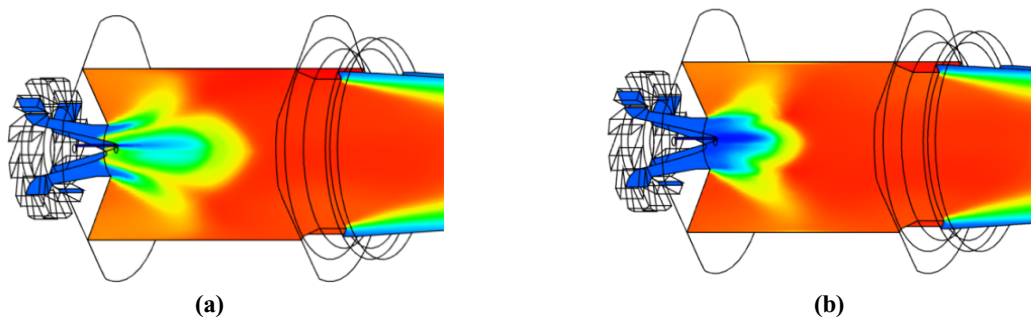


**Fig. 2:** Simulation of the temperature field in the GGT combustor of TU Darmstadt: (a) With the standard flamelet approach an attached flame is predicted; (b) using the FGM approach, the lifting of the flame is captured

### Acknowledgement

A part of this work was accomplished under the EU funded Marie Curie COMBINA project in which NUMECA is collaborating with TU Eindhoven (NL), EKT/TU Darmstadt (DE), INSA Coria (FR), Middle-East Technical University (TR) and Pars Makina Ltd. (TR). The authors would like to thank Mr. Ramaekers, Dr. van Oijen and Prof. de Goey (TU Eindhoven) for providing us knowledge in the generation of FGM. Furthermore, the authors are grateful for various fruitful discussions with Prof. Vervisch (INSA Coria) on the modeling of partially premixed combustion processes.

### References

- [1] van Oijen, J. A. (2002): *Flamelet-Generated Manifolds: Development and Application to Premixed Laminar Flames*, PhD Thesis, TU Eindhoven, 2002
- [2] van Oijen, J. A.; de Goey, L. P. H. (2000): Modelling of Premixed Laminar Flames using Flamelet-Generated Manifolds, *Combustion Science and Technology*, Vol. 161(1), pp. 113-137
- [3] Cabra, R.; Chen, J.Y.; Dibble, R. W.; Karpetis, A. N.; Barlow, R.S. (2005): Lifted methane-air jet flames in a vitiated coflow, *Combustion and Flame*, Vol. 143, pp. 491-506
- [4] Dally, B. B.; Masri, A. R.; Barlow, R. S.; Fiechtner, G. J. (1998): *Combustion and Flame*, Vol. 114, pp. 119-148
- [5] Janus, B.; Dreizler, A.; Janicka, J. (2004): *ASME Paper GT2004-53340*

# ANALYSIS OF MONTE CARLO APPROACH FOR THE SOLUTION OF FILTERED MASS DENSITY FUNCTION TRANSPORT EQUATION IN LES

A. Attili<sup>\*</sup>, F. Bisetti

*King Abdullah University of Science and Technology, Saudi Arabia*

[antonio.attili@kaust.edu.sa](mailto:antonio.attili@kaust.edu.sa)

The ‘filtered mass density function’ (FMDF) methodology is a method for the simulation of reactive turbulent flows (Jaberi et al. 1999). The FMDF is a mass weighted joint density function of subgrid-scale quantities. It can be obtained by solving a transport equation, in which the evolution of the FMDF is related to four phenomena: convection and diffusion (molecular and turbulent) in physical space; convection in composition space, due to subgrid mixing; and reactions among chemical species.

Finite-difference solutions of the equations are impractical because of the large dimensionality of the FMDF, and a particle-based Monte Carlo (MC) method is routinely used; the MC method can be formulated with Lagrangian (Pope 1994) or Eulerian (Chen 2007) approaches. In the Lagrangian approach the stochastic differential equations (SDEs), which yield statistically equivalent results to those of the FMDF transport equation, are used (Jaberi et al. 1999). The spatial transport of the FMDF (due to convection related to the filtered mean velocity and diffusion) is represented by the SDEs of a diffusion process. The drift and diffusion coefficients of the stochastic equations are obtained by comparing its corresponding Fokker-Planck equation with the FMDF transport equation (Gardiner 1985). The subgrid mixing and reaction are obtained evolving the composition of each particle. One of the most important features of this approach is the fact that the reaction source term appears in closed form in the FMDF transport equation.

The aim of this work is to investigate the performance of the Lagrangian approach for non-reactive turbulent flows by comparing LES results to a DNS database. Even if the reaction source term is in closed form, the SGS convection and mixing terms in the FMDF transport equation are unclosed and modeled in a manner consistent with conventional LES of isothermal flows. Those unclosed terms appear as mass-weighted conditional filtered means. Monte Carlo FMDF is capable of modeling extinction and reignition (Xu & Pope 2000) but the quality of the results depends sensitively on the parameters used in the unclosed terms.

In order to focus on the performance of the models for the unclosed convective and mixing terms, the effect of heat release on the flow is neglected. The hydrodynamic Favre-averaged equation of continuity and momentum are solved in a low Mach number formulation following the approach presented by Desjardins et al. (2008). Statistical errors, related to the finite number of particles, affect the numerical behavior of the solver and are always a critical point in Monte Carlo solutions.

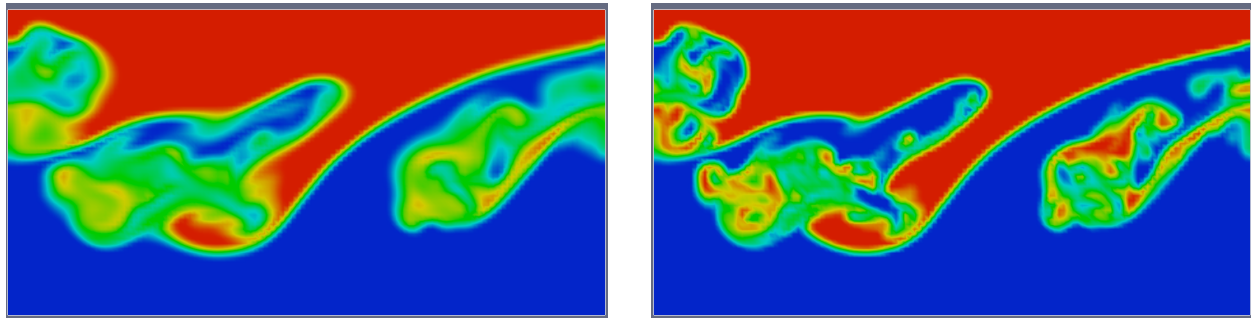
The methodology is applied to a spatially developing mixing layer. The flow exhibits several features, which are relevant in the context of turbulent non-premixed combustion.

A direct numerical simulation of the flow has been performed; the detailed results and the statistics available from DNS are compared to the results obtained with the LES Monte Carlo approach. The unclosed terms in the FMDF transport equation and the models used to achieve closure are analyzed in detail using the mass-weighted conditional statistics available from the DNS.

A detailed parametric analysis is performed varying the parameters of the numerical representation of the equations. The effect of the grid size is investigated, both for Large Eddy Simulation with finite difference solution of the scalar transport equations and FMDF approach. In the FMDF formulation, additional numerical parameters appear, related to the Monte Carlo particles representation; the average number of particles per grid cell and the size of the ensemble domain, used to obtain the statistics at the finite difference nodes, are the two most important. Ideally, it is desirable to obtain the statistics when the size of the sample domain is infinitely small and the number of particles infinitely large. With a finite number of particles, if the sample domain is too small there may not be enough particles for reliable

statistics; a larger sample domain increases the spatial error with artificial diffusion in the statistical results. The effects of the choice of these parameters are also investigated.

The picture contains a comparison of the isocontours of mixture fraction obtained from conventional LES and Monte Carlo FMDF approaches. Both simulations have been performed with zero diffusion (molecular and turbulent) to analyze the artificial diffusion originating from the averaging procedure and field reconstruction from the Monte Carlo particles. For the conventional LES a bquick scheme (Herrmann et al. 2005) has been used for the mixture fraction transport equation; for the MC simulation an average of 100 particles per grid node and a sample volume equal to the grid cell size have been used. It can be observed that the artificial diffusion in the Monte Carlo approach is less than in the case of conventional LES, where numerical diffusion has strong effects on the field.



Isocontours of mixture fraction for conventional LES (left) and FMDF-LES (right).

## References

- DESJARDINS O., BLANQUARD G., BALARAC G. & PITSCH H. (2008) High order conservative finite difference scheme for variable density low Mach number turbulent flows. *J. Comput. Phys.* **227**, 7125-7159
- CHEN J. Y. (2007) A Eulerian PDF scheme for LES of nonpremixed turbulent combustion with second-order accurate mixture fraction. *Combustion Theory and Modelling* **11,5**, 675-695
- GARDINER C. W. (1985) Handbook of stochastic methods. *Springer Berlin*.
- HERRMANN M., BLANQUART G. & RAMAN V. (2005) Flux corrected finite-volume scheme for preserving scalar boundedness in large-eddy simulations. *43rd AIAA Aerospace Sciences Meeting and Exhibit*, 10–13 jan 2005, Reno, NV
- JABERI F. A., COLUCCI P. J., JAMES S., GIVI P. & POPE S. B. (1999) Filtered mass density function for large-eddy simulation of turbulent reacting flows. *J. Fluid Mech.* **401**, 85-121
- POPE S. B. (1994) Lagrangian PDF methods for turbulent flows. *Annual review of fluid mechanics.* **26**, 23-63
- XU J & POPE S. B. (2000) PDF calculations of turbulent nonpremixed flames with local extinction. *Combustion and Flame.* **123,3**, 281-307

# ARTIFICIAL FLAME BROADENING EFFECTS ON THE LES QUALITY

*P. Auzillon, N. Darabiha, O. Gicquel, D. Veynante and B. Fiorina*

*EM2C - CNRS, UPR 288, Ecole Centrale Paris, 92295 Châtenay Malabry, France*

[benoit.fiorina@em2c.ecp.fr](mailto:benoit.fiorina@em2c.ecp.fr)

Large Eddy Simulation is an attractive tool to predict flame dynamics and pollutant emissions in industrial combustion chambers [1]. However, the recurrent problem in LES is that the flame thickness is typically thinner than the grid size. To overcome this issue, different strategies have been developed. The level-set or G-equation approach consists in tracking the inner layer by solving a propagation equation [2, 3]. However as level-set techniques provide information only on the thin reaction zone position and not on the filtered flame structure, the coupling with the flow equations remains challenging. An artificial broadening of the thermal flame thickness is still usually required[4]. Another solution to propagate a flame front on a coarse grid is to artificially thicken both thermal and reactive layers (Thickened Flame model for LES)[5]. Finally, an alternative is the implicit filtering of the flame front at a scale larger than the mesh size (Filtered-Tabulated Chemistry for LES (F-TACLES) model [6]. All these techniques imply an artificial broadening of the thermal layer in order to ensure the coupling with the flow equations.

The objective of the present study is to investigate the effects of the flame front artificial broadening on the flame dynamics. The configuration retained is a 2-D simplification of the Schuller *et al.* [7] experimental set-up. It consists on a 2-D laminar flame submitted to acoustic excitation. The flow is modulated harmonically according to  $\bar{v} = 0.97 \text{ m.s}^{-1}$ ,  $v_{RMS} = 0.19 \text{ m.s}^{-1}$  and  $f = 62.5 \text{ Hz}$  where  $\bar{v}$ ,  $v_{RMS}$  and  $f$  are the mean inflow velocity, the inflow velocity RMS and the excitation frequency. This configuration allows to evaluate the ability of LES combustion model to reproduce unsteady flame behavior when flow motions are fully resolved (no sub-grid scale flame front wrinkling) but not the internal flame structure. A Direct Numerical Simulation (DNS) is first performed on a 1.1 millions grid elements. As the laminar flame structure is fully resolved, it serves as a reference solution. Then TFLES and F-TACLES models are tested on this configuration for various scales of flame front broadening. Results are analyzed after ten excitation cycles to ensure the solution independency from initial conditions.

Two scales are affected by LES combustion models: the reaction rate and the thermal thicknesses. The thermal flame thickness is here defined as:  $\delta_T = (T_b - T_f) / \max(|dT/dx|)$  where  $T_f$  and  $T_b$  are the fresh and burnt gases temperature. The flame front artificial broadening will affect the ratio  $\delta_{\bar{T}}/\delta_T$  where  $\delta_{\bar{T}}$  and  $\delta_T$  are respectively the thermal flame thicknesses computed from the LES and from the DNS temperature fields. The reaction rate thickness  $\delta_r$  is given by the full width at half maximum (FWHM) of the reaction rate. As for the thermal thickness, the ratio  $\delta_{\bar{T}}/\delta_r$  is affected by artificial broadening. Both reaction rate and thermal thicknesses may be affected differently depending on the retained models. For instance  $\delta_{\bar{T}}/\delta_r = \delta_T/\delta_r$  for TFLES by construction while  $\delta_{\bar{T}}/\delta_r \approx 1$  for F-TACLES. Figure 1 shows instantaneous snapshots of the pulsed Bunsen flame front position. Simulations with F-TACLES formalism are conducted for  $\delta_{\bar{T}}/\delta_T$  equal to 1.1 and 2.6. In both simulations, the LES solution (left) is compared to the reference DNS solution (right). A quantitative analysis is conducted by computing the LES flame response relative to the DNS under different broadening conditions. The heat release rate integrated over the computational domain,  $\tilde{h}_r$  and  $h_r$ , are computed at a given time period for LES and DNS simulations, respectively. The ratio  $\tilde{h}_r/h_r$  is plotted as a function of the ratio  $\delta_{\bar{T}}/\delta_T$  and  $\delta_{\bar{T}}/\delta_r$  in Fig. 2. Both F-TACLES and TFLES simulations have been used to construct this diagram. As expected, for moderate values of artificial broadening, the flame response is accurately reproduced as the ratio  $\tilde{h}_r/h_r$  remains close to unity. However for intense artificial broadening, the flame response is affected as the flame wrinkling is damped by the LES. It has been shown in Ref.[7] that a flame behaves as a low-pass filter. The thermal layer thickness broadening tends to decrease the filter cut-off frequency, increasing the flame response time. Fig. 2 shows that when the

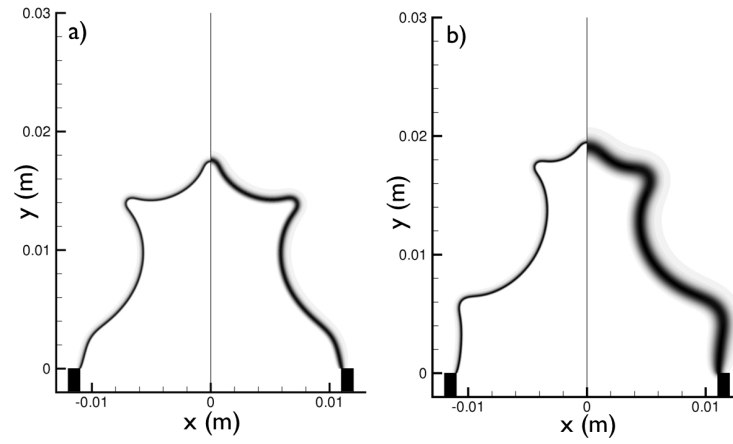


Figure 1: Snapshots of the reaction rate profile for the acoustic 2-D pulsed flame. a) Left: DNS, Right: LES with  $\delta_{\tilde{r}}/\delta_T = 1.1$  b) Left: DNS, Right: LES with  $\delta_{\tilde{r}}/\delta_T = 2.5$

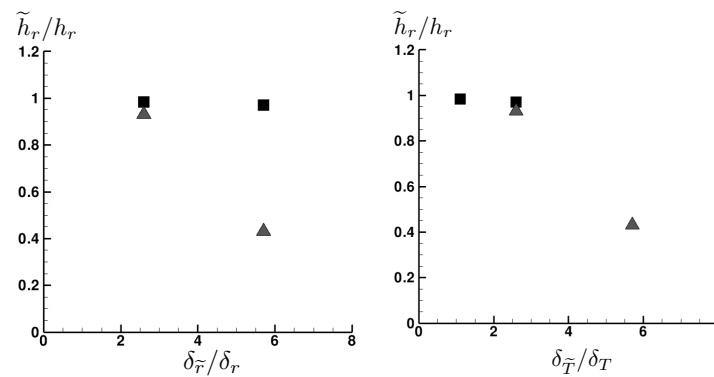


Figure 2: LES flame response relative to the reference DNS flame response as a function of the flame front broadening  $\delta_{\tilde{r}}/\delta_r$  and  $\delta_{\tilde{r}}/\delta_T$ . Square : TACLES, Delta : TFLES

thermal thickness is used as a reference length scale, data collapse on a single curve but scatter when using the reaction rate thickness. This study should be complete with supplementary computations with other LES models.

## References

- [1] T. Poinso, D. Veynante, Theoretical and Numerical Combustion, R. T. Edwards, Inc., 2005.
- [2] N. Peters, Turbulent Combust., Cambridge University Press, 2000.
- [3] S. Menon, W. Jou, Combust. Sci. and Tech. 75 (1991) 53–72.
- [4] V. Moureau, B. Fiorina, H. Pitsch, Combust. Flame 156 (4) (2009) 801–812.
- [5] O. Colin, F. Ducros, D. Veynante, T. Poinso, Physics of Fluids 12 (7) (2000) 1843–1863.
- [6] B. Fiorina, R. Vicquelin, P. Auzillon, N. Darabiha, O. Gicquel, D. Veynante, Combust. Flame 157 (2010) 465–475.
- [7] T. Schuller, S. Ducruix, D. Durox, S. Candel, Proc. Combust. Inst. 29 29 (2002) 107–113.

# Unexpected Effects of Preferential Molecular Transport in Turbulent Premixed CH<sub>4</sub>/Air Flames

RS Barlow<sup>1</sup>, MJ Dunn<sup>1</sup>, M Sweeney<sup>2</sup>, S Hochgreb<sup>2</sup>

<sup>1</sup>Sandia National Laboratories, Livermore, CA USA

<sup>2</sup>Cambridge University, Cambridge UK

Preferential transport of low molecular weight species is a well recognized phenomenon in laminar flames and in turbulent flames with low to moderate Reynolds number. Significant attention has been given to the effects of differential molecular diffusion in turbulent nonpremixed and partially premixed flames, through both experimental and computational research. Generally, differential molecular diffusion can be important in low Reynolds number turbulent jet flames, particularly near the nozzle exit. However, as Re increases, the relative importance of turbulent transport increases, such that measured conditional mean species mass fractions beyond the first several nozzle diameters may be well predicted by models that neglect differential diffusion [1].

In turbulent premixed combustion the influence of Lewis number and preferential molecular diffusion on flame structure, particularly at low to moderate values of  $u'/S_L$ , is also well recognized and documented [2-4]. Preferential molecular diffusion has been described in DNS studies of turbulent premixed flames as causing focusing or defocusing of H<sub>2</sub> and radicals depending on the sense of curvature of the reaction zone. This transport effect changes the scalar structure and local displacement speed of the flame relative to a planar flame. However, the prevalent view for modeling of turbulent premixed flames with Lewis number near unity is that molecular transport effects are only important locally within the thin reaction zone and may be neglected.

In the present work we show experimental evidence that preferential molecular transport can have significant effects on the conditional mean scalar structure of turbulent premixed methane-air flames, such that atom balances within the reactant stream are not necessarily conserved through the turbulent flame brush and into the product stream. These unexpected results come from Raman/Rayleigh/CO-LIF measurements [5] obtained in a co-annular burner, jointly developed by Cambridge University and Sandia, for investigation of turbulent stratified and premixed flames in a flow geometry somewhat more complex than that of the TU Darmstadt Stratified Burner [6]. The double-annular burner (Fig. 1) has a central bluff body for flame stabilization, and the outer annular flow has variable swirl. Here we consider only fully premixed flames (same equivalence ratio in both annular flows).

Figure 2 demonstrates that measurements in a lean premixed unstrained laminar flame are in good agreement with results from Chemkin using GRI 3.0 and multicomponent transport. Here, experimental results are plotted as mean and rms conditioned on temperature. Equivalence ratio,  $\phi$ , is calculated from the measured species (N<sub>2</sub>, O<sub>2</sub>, CH<sub>4</sub>, CO<sub>2</sub>, H<sub>2</sub>O, CO, and H<sub>2</sub>) for both the measured and calculated curves. Variations in  $\phi$  and atom ratios are due primarily to preferential diffusion of H<sub>2</sub> away from the reaction zone. Note that the initial trajectory of the  $Y_{H_2}$  curve vs. temperature is nearly vertical.

Results from a turbulent lean premixed flame are shown in Fig. 3. Here, the profile of  $\phi$  in the burnt gas does not return to the reactant value of 0.75, but increases to nearly 0.85. Similarly, the C/H atom ratio in the burnt gas does not return to 0.25, but increases by roughly 10%. The CO<sub>2</sub> mass fraction finishes higher than expected (with near zero H<sub>2</sub> and CO), while  $Y_{O_2}$  finishes lower. The observed behavior of these conditional mean scalar profiles vs. temperature is outside experimental uncertainty



Fig. 1. Burner photo.

and is believed to be result from preferential transport of  $H_2$  toward the front edge of the preheat zone followed by further molecular and turbulent transport downstream from the locally measured flame brush. In the present burner, the flame brush is far from normal to the mean velocity vectors, and this high flame angle may be a major factor. The magnitude of the effect relaxes somewhat with increasing streamwise distance, but it does not go away. Further work is needed to understand this phenomenon and to determine whether it is of practical importance,

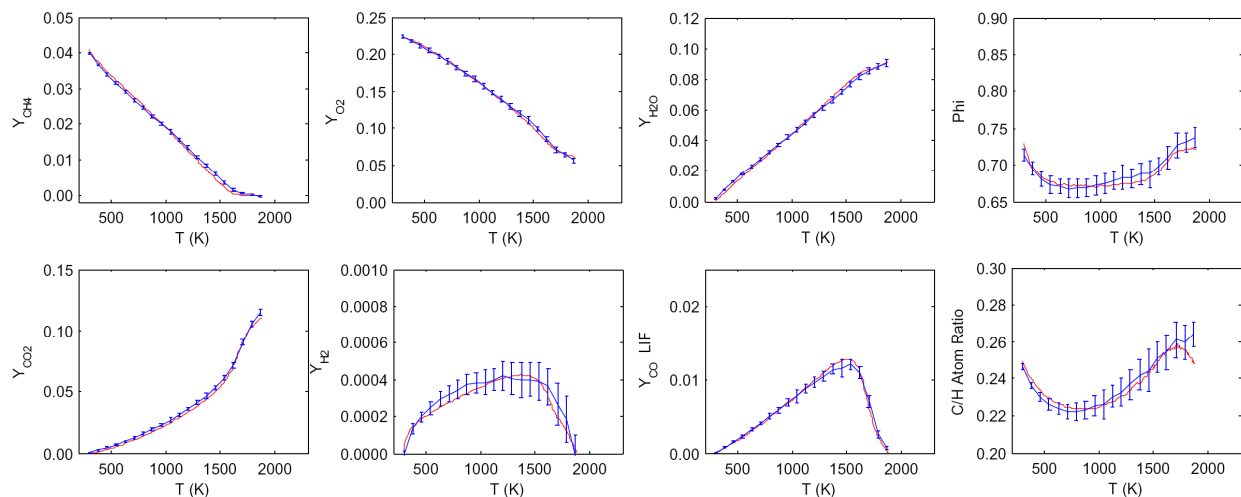


Fig. 2. Measured mean (blue curves) and rms ( $\pm\sigma$ ) species mass fractions,  $\phi$ , and C/H atom ratio compared with a Chemkin calculation (red) for an unstrained laminar premixed  $CH_4$ /air flame at  $\phi = 0.73$ .

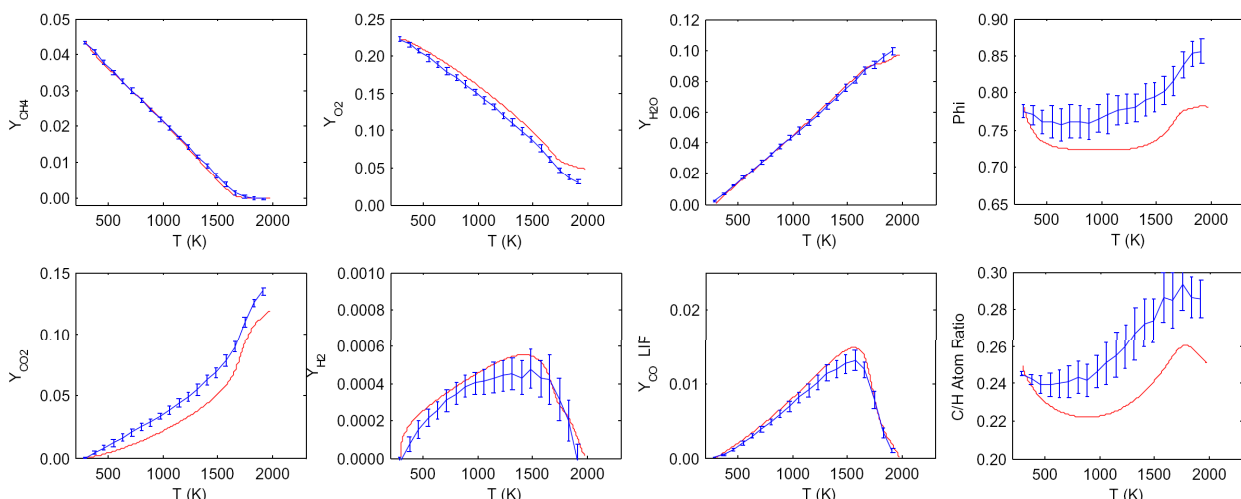


Fig. 3. Measured species mass fractions conditional on temperature (blue curves) in a turbulent premixed flame at a location 10 mm downstream of the exit plane, with standard deviation ( $\pm\sigma$ ) plotted as error bars. The red curves show results of a Chemkin calculation (GRI 3.0 and multicomponent transport) of an unstrained premixed flame at  $\phi = 0.78$ , which gives good agreement with measured reactant composition.

## References

- [1] RS Barlow, JH Frank, AN Karpetis, JY Chen, *Combust. Flame* 143 (4) (2005) 433–449.
- [2] YC Chen, RW Bilger, *Combust. Flame* 138 (2004) 155–174.
- [3] R Hilbert, F Tap, H El-Rabii, D Thevenin, *Prog. Energy Combust. Sci.* 30 (2004) 61–117.
- [4] J Bell, RK Cheng, MS Day, IG Shepherd, *Proc. Combust. Inst.* 31 (2007) 1309–1317.
- [5] RS Barlow, GH Wang, P Anselmo-Filho, MS Sweeney, S Hochgreb, *Proc. Combust. Inst.* 32 (2009) 945–953.
- [6] F Seffrin, F Fuest, D Geyer, A Dreizler, *Combust. Flame* 157 (2010) 384–396.

# ASSESSMENT OF NONLINEAR REGIME TWO-LINE ATOMIC FLUORESCENCE (NTLAF) IN SOOTY FLAMES

Q.N. Chan<sup>1,2</sup>, P.R. Medwell<sup>1,3</sup>, P.A.M. Kalt<sup>1,3</sup>, Z.T. Alwahabi<sup>1,2</sup>, B.B. Dally<sup>1,3</sup> & G.J. Nathan<sup>1,3</sup>

<sup>1</sup>Centre for Energy Technology

Schools of <sup>2</sup>Chemical and <sup>3</sup>Mechanical Engineering, The University of Adelaide, Australia

qing.chan@adelaide.edu.au, paul.medwell@adelaide.edu.au, peter.kalt@adelaide.edu.au, zeyad.alwahabi@adelaide.edu.au, bassam.dally@adelaide.edu.au, graham.nathan@adelaide.edu.au

Two-line Atomic Fluorescence (TLAF), with indium as the seeded thermometric species [1, 2], is one of the laser diagnostic techniques that has been shown to hold promise in sooting environments. The inelastic nature of the technique enables optical filtering to be used to minimise spurious scattering, thus allowing temperature measurements to be performed in particle-laden environments. By extending the technique into the nonlinear excitation regime, the capability of TLAF in providing single-shot imaging has been further improved by the authors [3–6]. Non-linear excitation regime two-line atomic fluorescence (NTLAF) has been shown to provide significant improvement to the signal-to-noise ratio (SNR) and hence better precision when compared to the conventional linear regime TLAF approach [5].

NTLAF has been shown to provide accurate temperature measurements in slightly sooty flames [5]. However, the capacity of NTLAF to perform temperature measurements in flames with higher soot loading is yet to be assessed. The accuracy of the NTLAF technique may be affected by interferences such as increasing spurious scattering or laser-induced incandescence from increasing soot particles, when the soot loading within the flame is high. NTLAF may also be susceptible to interference from fluorescence background, generally ascribed to polycyclic aromatic hydrocarbon compounds (PAHs) [7] present at soot locations, when the soot level of the flame is high.

The present work therefore aims to compare the emission signals when induced at two different laser wavelengths (on- and off-wavelength). The emission signals (1) when induced on-wavelength give an indication of the total signal achievable and (2) when induced off-wavelength, give an estimate on the contribution of background interferences to the total signal observed, for the flame conditions of interest. Laser-induced incandescence (LII) is used **simultaneously** with the NTLAF to measure the soot concentration for the flame under investigation. A Jet in Hot Coflow (JHC) burner is employed to generate the laminar ethylene-air nonpremixed flame used in the present work.

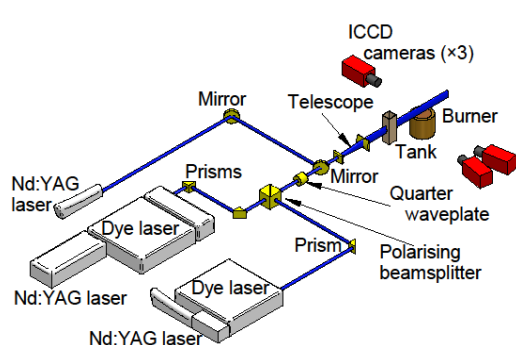
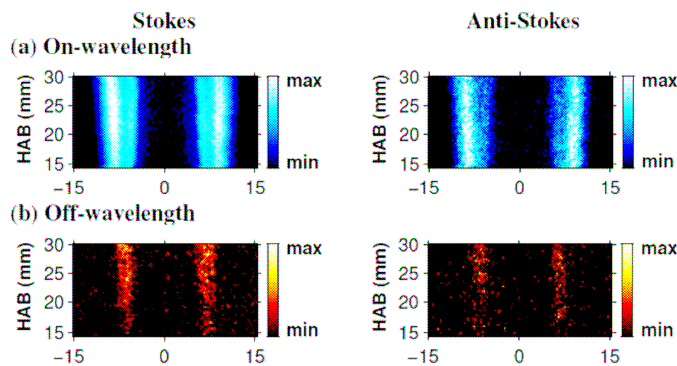


Figure 1: Experimental Setup

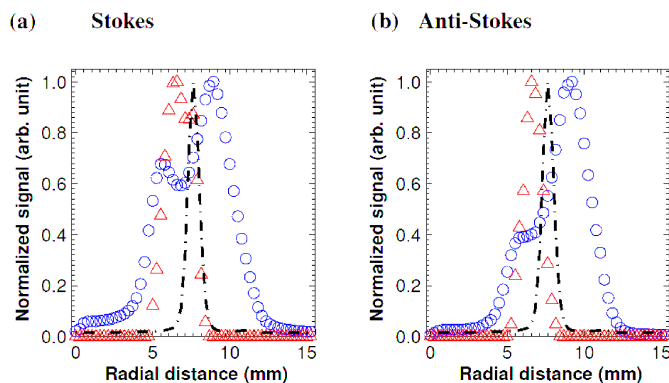
The experimental setup used is shown in Figure 1. For the NTLAF technique, two Nd:YAG pumped dye lasers were fired simultaneously (~100 ns separation) to produce the 410 & 450 nm excitation beams, which were circularly polarised and combined into a coplanar light sheet. The emission signals were detected through narrowband interference filters using two ICCD cameras. A tank containing fluorescing dye is used to facilitate correction of laser energy variation. For LII, an Nd:YAG laser (1064 nm) is operated at a mean fluence of ~0.5 J/cm<sup>2</sup>. The LII process is delayed approximately ~800 ns after the NTLAF measurements, which were found to avoid cross-talk between the two techniques [4]. The LII signals are collected with another ICCD camera, fitted with a 410 nm interference filter. The images from the cameras are spatially matched and morphed to sub-pixel accuracy.

Figure 2(a) and 2(b) show the typical single-shot, on- and off-wavelength emission signals, for Stokes & anti-Stokes measurements. It is worth noting that both the on- and off-wavelength measurements were performed at the same laminar flame conditions, but it was not possible to collect these measurements concurrently. The peak soot volume fraction of the present flame was measured to be ~2.5 ppm (not shown).

Figure 3 presents the average radial profiles (150 images) extracted at a height above burner (HAB) of 25 mm. It can be seen that the off-wavelength emission signals are present on a relatively wide zone and peaks at a radial distance of ~6.5 mm from the burner centreline. By contrast, soot particles are confined to a thinner zone and the soot



**Figure 2: Typical emission signals for (a) on- and (b) off-wavelength measurements.**



**Figure 3: Average radial profiles for Stokes and anti-Stokes measurements. Circle: on-wavelength; triangle: off-wavelength; dashed line: soot volume fraction.**

in sooty flames. The ability to collect single-shot temperature images using TLAF, in conjunction with soot volume fraction, in sooty turbulent nonpremixed flames will form an invaluable data set or future studies on soot. This will, for the first time, enable instantaneous and simultaneous two-dimensional imaging of soot and temperature in turbulent nonpremixed flames.

## References

- [1] J. E. Dec, J. O. Keller, Proceedings of the Combustion Institute 21 (1986) 1737–1745.
- [2] C. F. Kaminski, J. Engström, M. Aldén, Proceedings of the Combustion Institute 27 (1998) 85–93.
- [3] Q. N. Chan, P. R. Medwell, P. A. M. Kalt, Z. T. Alwahabi, B. B. Dally, G. J. Nathan, Applied Optics 49 (2010) 1257–1266.
- [4] Q. N. Chan, P. R. Medwell, P. A. M. Kalt, Z. T. Alwahabi, B. B. Dally, G. J. Nathan, Proceedings of the Combustion Institute 33 (2010) **accepted**.
- [5] P. R. Medwell, Q. N. Chan, P. A. M. Kalt, Z. T. Alwahabi, B. B. Dally, G. J. Nathan, Applied Optics 48 (2009) 1237–1248.
- [6] P. R. Medwell, Q. N. Chan, P. A. M. Kalt, Z. T. Alwahabi, B. B. Dally, G. J. Nathan, Applied Spectroscopy 64(2) (2010) 175–176.
- [7] C. Schoemaeker Moreau, E. Therssen, X. Mercier, J. F. Pauwels, P. Desgroux, Applied Physics B 78 (2004) 485–492.
- [8] A. Ciajolo, R. Ragucci, B. Apicella, R. Barbella, M. de Joannon, A. Tregrossi, Chemosphere 42 (2001), 835–41.

maximum appears on a radial distance of  $\sim 7.5$  mm from the burner centreline. Also, the off-wavelength emissions signals appear closer to the central part of the burner (fuel rich) whereas the soot particles appear closer to the lean side. This difference in trends between these radial profiles suggests that spurious scattering and laser-induced incandescence from soot do not contribute significantly towards the off-wavelength emission signals. Rather, this suggests the filtering capability of the NTLAF is adequate in suppressing spurious scattering from soot. This observation also suggests that the low operating fluence of NTLAF avoids soot incandescence, albeit in the nonlinear fluence regime [5].

A closer inspection on the radial profiles reveals that the off-wavelength emission signals maximum appears at the radial location which corresponds to the onset of the soot. This observation suggests that the compound(s) resulting in the observed off-wavelength emission signals participates with the soot formation process since the consumption of the species coincides with the appearance of the soot particles. Possible candidates include polycyclic aromatic hydrocarbon compounds (PAHs) [7] and condensed species (CS) [8]. The maximum contribution of these off-wavelength measurements to the total emission signals is estimated to be  $\sim 5\%$ , for the present flame.

Whilst this work is still in the development stage, the identification of these potential sources of interference is important to the establishment of NTLAF as a viable laser-based thermometry tool

## Effects of the Composition of the Hot Product Stream on Turbulent Counterflow Premixed Flames

Bruno Coriton<sup>1</sup>, Jonathan H. Frank<sup>2</sup> and Alessandro Gomez<sup>1#</sup>

<sup>1</sup>Yale Center for Combustion Studies, Department of Mechanical Engineering,  
Yale University, New Haven, CT 06520-8286, U.S.A

<sup>2</sup>Combustion Research Facility, Sandia National Laboratories, Livermore, CA 94551, USA

<sup>#</sup>Corresponding Author: *alessandro.gomez@yale.edu*

Laboratory scale benchmarks typically employ either swirl flow, or a bluff-body or a pilot flame (e.g., [1-4]), individually or in combination, to enable turbulent flames to be stabilized in intense turbulence and at large Karlovitz number. All of these methods rely on mixing of the reactants with hot combustion products. We present a counterflow system where a turbulent jet of premixed reactants at a turbulent Reynolds number of  $O(1000)$  is opposed to a stream of hot products of combustion. One of the aims of this configuration is to pinpoint the effects of the hot product stoichiometry on turbulent premixed flames. The importance of controlling the hot product composition was recently evidenced in a numerical study on laminar counterflow flames showing that heat release rate and, therefore, flame extinction are sensitive to hot product stratification [5].

The burner is composed of two nozzles with different characteristics (Fig.1). The top nozzle was designed to deliver a stream of turbulent cold reactants with equivalence ratio  $\phi_u$ , at turbulent Reynolds number of  $O(1,000)$  using a carefully-designed turbulence generator plate [6,7]. The bottom nozzle is made out of ceramic cast to thermally insulate the product stream from a preburner flame positioned upstream. Temperature and composition of the combustion products are controlled by the equivalence ratio,  $\phi_b$ , and dilution of the preburner reactant mixture.

Turbulent premixed flames, with  $\phi_u$  between 0.5 and 1.0, were nominally in the Flamelet Regime in the Borghi diagram shown in Fig.2. The equivalence ratio  $\phi_b$  of the counterflowing hot gases was kept at either 0.7 or 1.0. The degree of nitrogen dilution in the preburner reactant mixture was adjusted such that the temperature of the hot products was maintained at 1850K for both cases. Although variations in the composition of the combustion products are not accounted for in the Borghi diagram, they have significant effects on the turbulent premixed flames, as illustrated in Fig.3 in terms of the mean progress variables plotted in the reference frame of the gas stagnation plane. Turbulent premixed flames are more robust when opposed to a lean stream of combustion products ( $\phi_b=0.7$ ). In addition, the progress variable in Fig.3 never reaches unity at the gas stagnation plane ( $X_{GSP}=0$ ), which indicates the presence of local extinction and therefore departure from the Flamelet Regime, in disagreement with the Borghi diagram.

Additional work will be presented in the poster, including joint statistics on the flame front structure and the CO/OH reaction rate measured by OH-PLIF, CO-PLIF.

## References

- [1] Mansour, M.S., Chen, Y.C., Peters, N., Proc. Combust. Inst. 27 (1998) 767-773.
- [2] Dinkelacker, F., Soika, A., Most, D., Leipertz, A., Polifke, W., Döbbling, K., Combust. Inst. 21 (1998) 857-865.
- [3] Dunn, M.J., Masri, A.R., Bilger, R.W., Barlow, R.S., Wang, G.H., Proc. Combust. Inst 32 (2009) 1779-1786.
- [4] Chaudhuri, S., Kostka, S., Renfro, M.W., Cetegen, B.M., Combust. Flame (2010).
- [5] Coriton, B., Smooke, M.D., Gomez, A., Combust. Flame (2010).
- [6] Coppola, G., Gomez, A., Exp. Therm. Fluid Sci. 33 (2009) 1037-1048.
- [7] Coppola, G., Coriton, B., Gomez, A., Combust. Flame 156 (2009) 1834-1843.

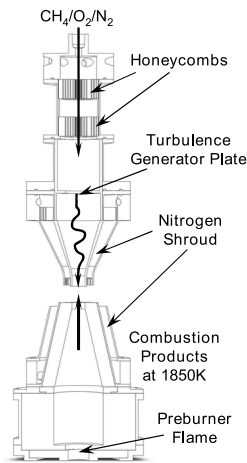


Figure 1. Schematics of Counterflow Burner.

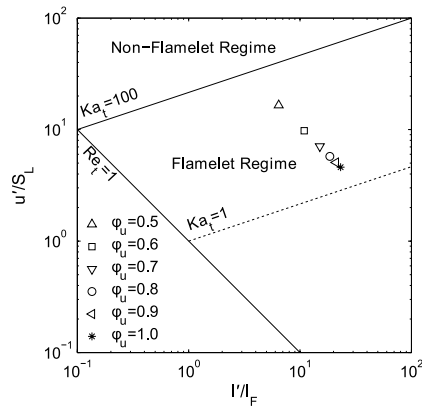


Figure 2. Estimated Flamelet positions in the Borghi diagram

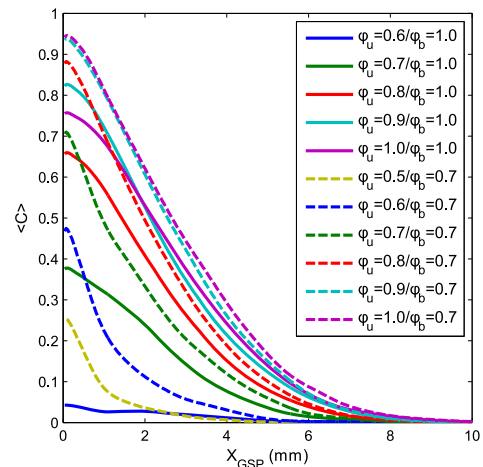


Figure 3. Mean progress variables in the gas stagnation plane reference frame. Solid and dashed curves are cases with stoichiometric ( $\phi_b=1.0$ ) and lean ( $\phi_b=0.7$ ) combustion products, respectively.

# NUMERICAL INVESTIGATION OF NATURAL GAS JET-IN-HOT-COFLOW FLAMES

A. De<sup>\*</sup>, E. Oldenhof, P. Sathiah, D.J.E.M. Roekaerts

*Department of Multi-Scale Physics, Delft University of Technology, The Netherlands*

*A.De@tudelft.nl*

Flames from the Delft-Jet-in-Hot-Coflow (DJHC) burner, emulating MILD (Moderate and Intense Low Oxygen Dilution) combustion, have been investigated numerically using models available in Fluent [1]. The jet fuel is natural gas; the coflow consists of products of a lean natural gas burner, with temperature lower than adiabatic. The main focus of this study is to assess the performance of different turbulence models, combustion models, and chemical mechanisms in predicting JHC flames by comparing predictions with experimental measurements. In particular, two different flame conditions (DJHC-I\_S and DJHC-X\_S) for two different jet Reynolds number ( $Re=4500$  and  $Re=8500$ ) are simulated, corresponding to two different oxygen levels (10.8% and 8.4%) in hot coflow. These flames are known to stabilize by auto-ignition rather than flame propagation [2]. A detailed study using three different turbulence models, i.e. Standard  $k-\varepsilon$  (SKE), Realizable  $k-\varepsilon$  (RKE), Renormalization group  $k-\varepsilon$  (RKG), three different turbulent-chemistry interaction models i.e. Eddy Dissipation Concept (EDC), presumed shape PDF with equilibrium flame table (PDF-EQ), presumed shape PDF with steady flamelet table (PDF-SF), and different chemical kinetics have been carried out.

Because of the symmetry of the burner, a 2D axisymmetric grid can be used. The computational domain starts 3 mm downstream of the jet exit and extends up to 225 mm in the axial direction. In the radial direction, the grid extends up to radial distance 80 mm to take into account the effect of entrainment of ambient cold air. Radially varying inlet velocity, turbulence and temperature boundary conditions are specified from measurements [2]. The radial profile of the composition of the hot coflow is specified as equilibrium composition at the measured mean temperature and oxygen concentration. A steady solution of the mean transport equations is computed. In the solution of the mean transport equations and the turbulence model, a SIMPLE algorithm is used for pressure-velocity coupling. The second order discretization scheme is consistently used for all the terms. In addition to the energy equation in Fluent [1], an additional transport equation for temperature variance is solved via a user defined subroutine, but the variance computed in this way is not used to modify the models for the mean reaction rate. In-Situ Adaptive Tabulation, with an ISAT tolerance of  $10^{-5}$  is used for EDC calculations.

The solutions are found to be grid independent if a stretched mesh of 180x125 cells or finer is used. For DJHC-I\_S ( $Re=4500$ ) case, the mean velocity and turbulent kinetic energy predicted by different turbulence models (SKE, RKE, RNG, modified SKE) are in good agreement with data without exhibiting any significant differences among the model predictions. RKE model shows some improvement in mean velocity profiles but under-predicts the peak values of turbulent kinetic energy. Similarly, using modified SKE improves mean velocity predictions, but significantly under-predicts turbulent kinetic energy profiles. Furthermore, different chemical kinetics show slight differences in mean temperature profiles due to presence of  $C_2H_6$  at the inlet fuel composition. While using the Fluent version of EDC combustion model for reaction, the mean temperature profiles show a peak indicating too early ignition (Fig. 1). Improved results are obtained by tuning the EDC model parameters, as shown in Fig. 1. Two different modifications to EDC model constants are made. Firstly, the time scale constant is increased from default value of  $C_\tau = 0.4082$  to  $C_\tau = 3.0$ . Secondly, the volume fraction constant is decreased from default value of  $C_\xi = 2.1377$  to  $C_\xi = 1.0$ . A theoretical analysis of the EDC model has shown that the mean reaction rate becomes unphysical at values of turbulent Reynolds number lower than 65 (for the default values of model constants). For lower  $Re_t$  the reaction rate is clipped and model predictions can become sensitive to this procedure. This seems to play a role in the too early prediction of ignition in the DJHC burner. Predictions using mixture fraction based models do not show good agreement for the radial mean temperature profile and conceptually the fast-chemistry assumption is not in agreement with the measurements which show ignition delay effects, not present in fast chemistry / PDF models.

In the case of high  $Re$  (DJHC\_I-S,  $Re=8500$ ), SKE model shows poor performance for mean temperature profile predictions as shown in Fig. 2. While, RKE model predictions appear to perform well over SKE model. These results confirm the limitation of SKE model in predicting JHC burner at higher turbulence levels. For the case with higher oxygen concentration in the coflow (DJHC\_X-S,  $Re=4500$ ), general trends of predictions are found to be

similar to the other cases although temperatures in the flow field are lower due to the lower coflow temperature. In both cases, better results are obtained while using modified EDC model parameters. The reported results form a baseline for more detailed studies using transported PDF methods and LES.

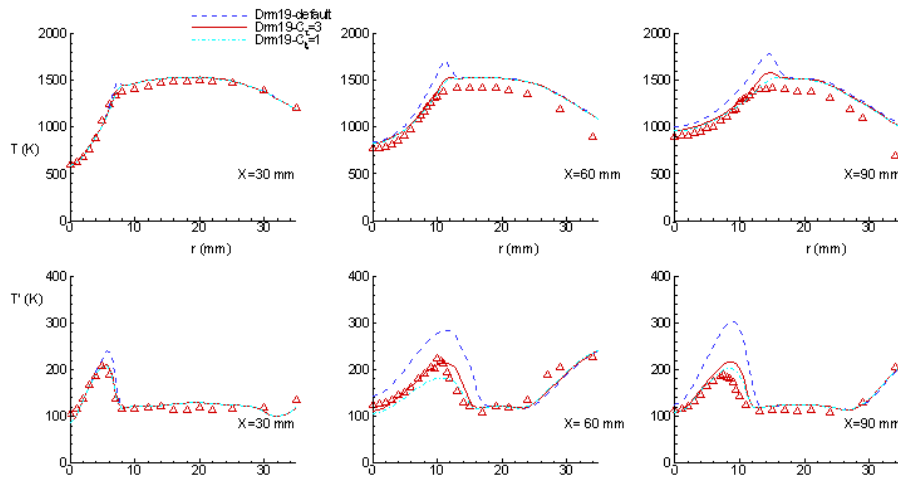


Figure 1. Radial profiles of mean Temperature ( $T$ ) and standard deviation of temperature ( $T'$ ) for case DJHC-I\_S at  $Re=4500$ . Comparison of results using different values of EDC model parameters (with turbulence model SKE and kinetic mechanism DRM19). Symbols are measurements and lines are predictions

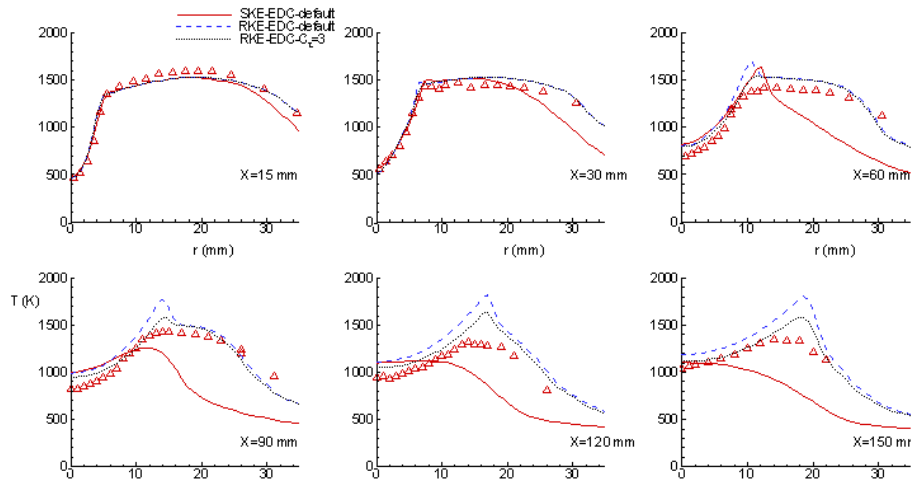


Figure 2. Radial profiles of mean Temperature ( $T$ ) for case DJHC-I\_S at  $Re=8500$ . Comparison of results using different values of EDC model parameters (with kinetic mechanism DRM19) and turbulence models. Symbols are measurements and lines are predictions

**Acknowledgement:** this work is supported financially by the Technology Foundation STW and the Dutch Flame Committee (NVV).

## References

- [1] Ansys Inc. : Ansys Fluent 12.0 User's guide, April (2009).
- [2] Oldenhof, E., Tummers, M., van Veen, E., Roekaerts, D., *Comb. and Flame*, 157 (2010) 1167-1178.
- [3] Christo, F. C., Dally, B. B., *Comb. and Flame*, 141(2005), 117-129.
- [4] Cavaliere, A., de Joannon, M., *Prog. in Energy and Comb. Sci.*, 30(2004), 329-366.

# Hybrid RANS/PDF calculations of a swirling bluff body flame (SM1)

R. De Meester<sup>1</sup>, B. Naud<sup>2</sup>, and B. Merci<sup>1</sup>

<sup>1</sup>Department of Flow, Heat and Combustion Mechanics, Ghent University, Belgium,

<sup>2</sup> Modeling and Numerical Simulation Group, Energy Department, Ciemat, Spain  
[reni.demeester@ugent.be](mailto:reni.demeester@ugent.be)

## 1. Introduction

The objective of this paper is to study the capability of hybrid RANS/PDF calculations in combination with tabulated chemistry techniques to capture local extinction and mixing of unburnt and burnt mixtures. This study is performed for the specific case of the swirling bluff-body flame SM1 [1]. LES results of this flame have been reported in [2], but this was with flamelet chemistry and a presumed scalar PDF, whereas here a transported (scalar) PDF is used in order to study turbulence – chemistry interaction. A comparable quality of results is obtained.

## 2. Experimental Set-up

Experiments have been performed by Sydney University and Sandia National Laboratories [1]. The bluff body (50mm diameter) contains the central fuel jet, consisting of  $CH_4$  (3.6mm diameter). Swirling air is provided through a 5mm wide annulus surrounding the bluff-body. The burner is placed inside a wind tunnel with a square cross section.

## 3. Numerical Description and Modeling

All steady, axisymmetric calculations are performed with the same code PDFD [3]. The 0.3m long computational domain starts at the burner exit and extends 0.15m in the radial direction. A non-uniform rectangular grid of 160x128 cells is used. A non-linear  $k-\varepsilon$  turbulence model [4] is used, as it takes into account the effect of streamline curvature and rotation on turbulence.

Two pre-tabulated combustion models are compared, assuming equal diffusivities and unity Lewis number. First, we use a single steady laminar flamelet with a strain rate of  $100s^{-1}$ , calculated in the opposed-flow diffusion flame configuration using the detailed mechanism GRI2.11. In the flamelet, mixture fraction is the only independent parameter, determining density, temperature, viscosity and all species mass fractions. Second, a REDIM [5] is used which can be seen as an extension of the ILDM concept to incorporate the effect of coupling of reaction and diffusion processes. Here, the REDIM concept was used to reduce the mechanism of [6] for  $CH_4$  to a 2-dimensional manifold with mixture fraction and  $Y(CO_2)$  as independent parameters. The largest difference between the flamelet and the REDIM is the extra independent parameter  $Y(CO_2)$ , describing reaction progress.

The turbulence – chemistry interaction, is modeled with a transported scalar PDF, using a turbulent Schmidt number  $\sigma_T=1.5$ . Two micro-mixing models are compared: the Modified Curl's CD model [7] and the EMST model [8].

## 4. Results

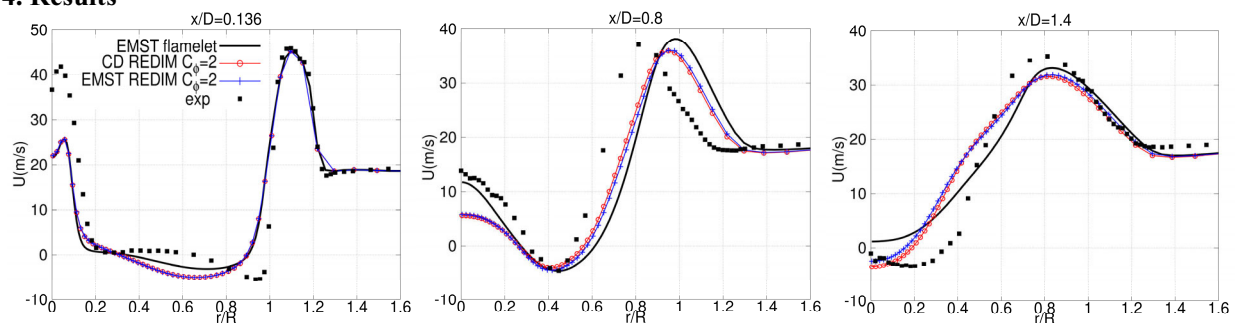
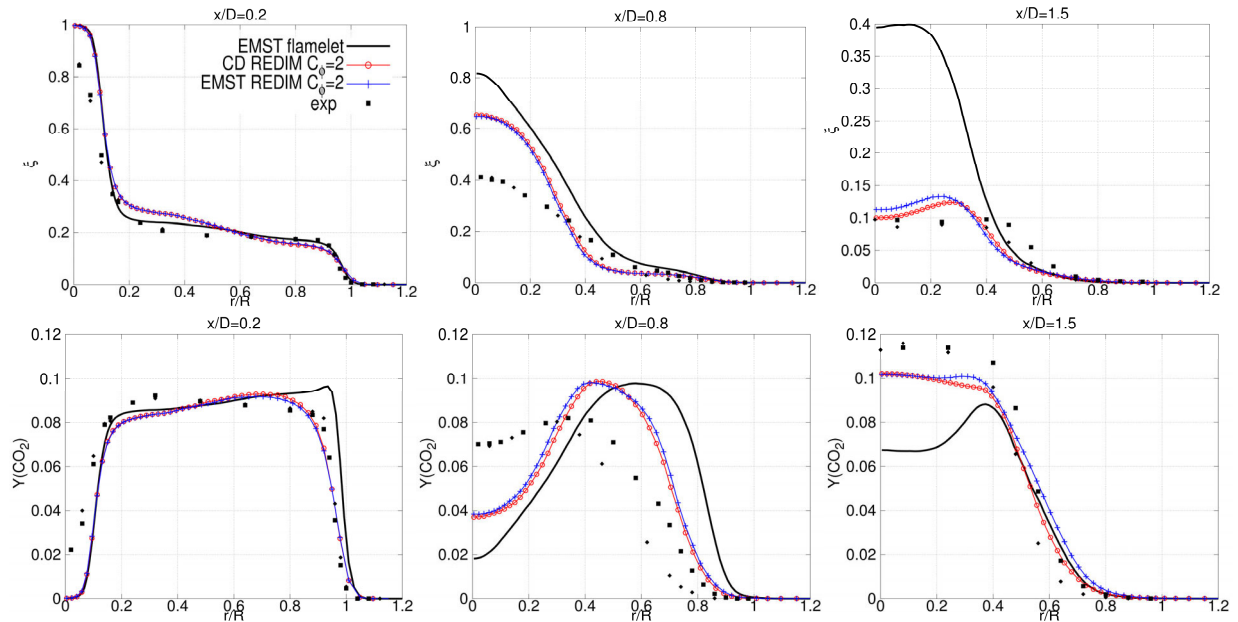


Figure 1: Profiles of mean axial velocity

The flow field of SM1 contains two recirculation zones: one close to the bluff body and one further downstream near the central axis. Both recirculation zones are captured to some extent with both combustion models. A substantial difference in flow fields is seen between the flamelet and the REDIM. This is due to the difference in density field predicted by the two combustion models. The difference between the flamelet and REDIM calculations is even more pronounced for the mean mixture fraction and  $YCO_2$ . The predictions of the REDIM calculations are satisfactory, except for in the region in between the two recirculation zones.



**Figure 2: Profiles of mean mixture fraction and  $Y_{CO_2}$**

The REDIM clearly benefits from the second independent parameter describing reaction progress, as this makes it possible to describe mixing of two mixtures at any point in the reaction progress. Whereas with the single flamelet there is only mixing along the flamelet. (Fig. 3) For the REDIM calculations, there are only minor differences between the two mixing models in physical space (Fig. 2). However, in composition space, there is more scatter with the CD model leading to better predictions of the conditional means and fluctuations. (not shown).

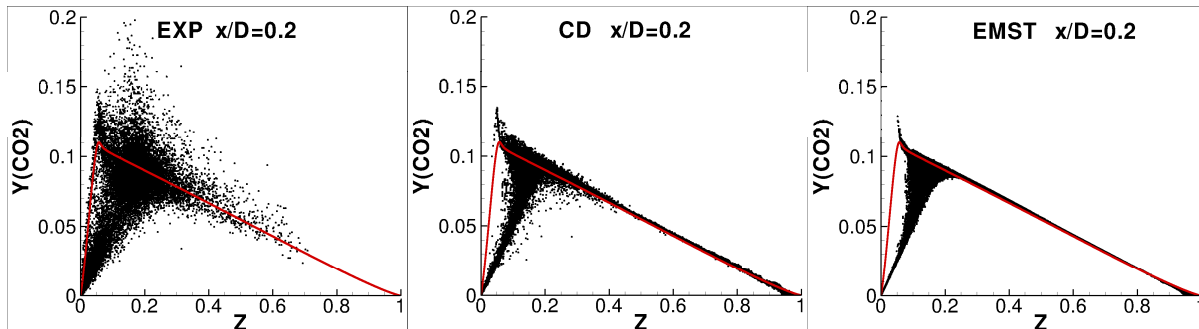


**Figure 3: Scatter plot of  $Y_{CO_2}$  at  $x/D=0.2$  for the experiments and REDIM calculations with CD and EMST. Flamelet for strain rate  $100 \text{ s}^{-1}$  (red line) also shown**

### Acknowledgements

This work is funded by the Special Research Fund of Ghent University under project BOF07/DOC/210 and is also supported by the Comunidad de Madrid through Project HYSYCOMB, P2009/ENE-1597 and by the Spanish Ministry of Science and Innovation under Project ENE2008-06515-C04-02. Many thanks to Prof. U. Maas for providing the REDIM tables and for the many enlightening discussions on REDIM

### References

- [1] Masri, A, Kalt, P., Al-Abdeli, Y.M. and Barlow, R.S. , *Comb. Theory and Mod.* 11 653-673, 2007
- [2] Kempf, A., Malalasekera, W., Ranga-Dinesh, K.K.J. and Stein, O., *Flow Turb. and Comb.* 81 523-561, 2008
- [3] Naud, B., Jimenez, C., Roekaerts, D., *Prog. in Comp. Fluid Dyn.* 6 (1-3) 146-157, 2006
- [4] Merci, B. and Dick, E., *Int. J. of Heat and Mass Transfer* 46 469-480, 2003
- [5] Bykov, V., Maas, U., *Comb. Theory and Mod.* 11 839-862, 2007
- [6] Warnatz J., Maas, U., Dibble R, *Combustion*, 2<sup>nd</sup> edition, Springer, 1999
- [7] Janicka, J., Kolbe W., Kollman, W., *J. Non-Equil. Thermodyn.* 4 47-66, 1979
- [8] Subramaniam, S., S.B. Pope, *Comb. and Flame* 115 487-514, 1998

# Stratified Lifted Jet Flames in a Hot (1280 K) Cross-Flow

James F. Driscoll, Danny Micka  
 University of Michigan  
 jamesfd@umich.edu

Recently J.H. Chen, A. Gruber, and J. Janicka [1,2] demonstrated that it is possible to achieve DNS and LES solutions for a fuel jet that is injected into a hot cross-flow of air. This problem is interesting because it has similarities to the Berkeley burner, except that here the heated air is in a cross-flow rather than a co-flow. In both cases in the liftoff region ahead of the stratified flame base there is premixing and auto-ignition. Cross-flow injection is used in ramjet and gas turbine engines. The present study has:

- (a) Provided measured metrics that can be used for comparison to DNS and LES. These metrics include flame lengths, heat release distributions, and wall pressure distributions;
- (b) Provided images of the primary reaction layers (using CH PLIF) to determine if there are flamelets, or large homogeneous distributed reaction regions, or distributed reactions that are confined to thick coherent layers. (The latter is shown to occur). Images of flame structure are a useful way to assess DNS and to guide the use of the proper LES submodels.
- (c) Provided images of the auto-ignition process; large distributed reaction zones are seen to create formaldehyde upstream of the primary flame, due to the high air temperature of 1280 K.

Figure 1 includes a schematic of a jet in a cross-flow [3] as well as an image of the CH\* chemiluminescence from the Michigan experiment [4]. Mungal et al. [3] have measured scaling relations for many of the jet mixing properties, which depend on the fuel-to-air momentum ratio. To achieve a realistic air temperature of 1280 K in the Michigan experiment, two large air heaters (electrical and vitiated) heated 0.5 kg/s of air that flowed into the 25.4 mm by 38.1 mm test section at 476 m/s. A 50% H<sub>2</sub>, 50% ethylene fuel mixture was injected at sonic velocity through a 2.49 mm diameter wall port.

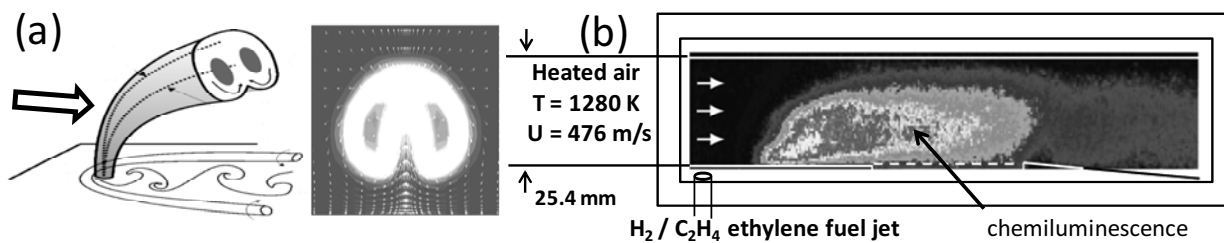


Fig. 1. Jet in Cross-flow: (a) schematic [1] and (b) chemiluminescence imaged in Michigan facility [4].

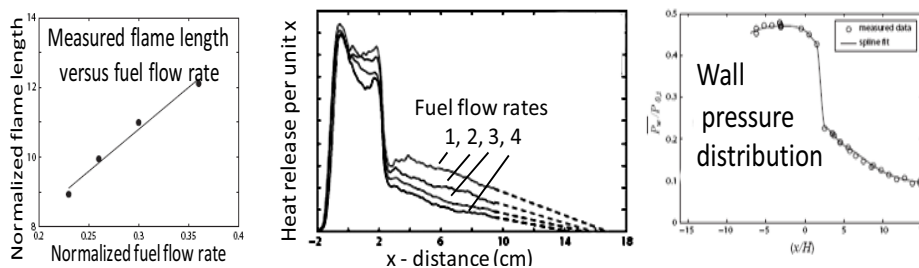


Fig. 2. Three measured metrics useful for assessment of DNS and LES: flame lengths, heat release profiles and wall pressure distributions for various fuel flow rates.

Fig. 2 describes three global metrics that can be used to assess DNS and LES simulations; the flame length was measured to increase linearly with the fuel flow rate, which is expected and is consistent with co-flow and low temperature jets in cross-flow. The heat release distribution was measured from the CH\* chemiluminescence, which was integrated over planes perpendicular to the flow. Wall pressure decreases in the flow direction as the heat addition drives the flow in the duct toward Mach one.

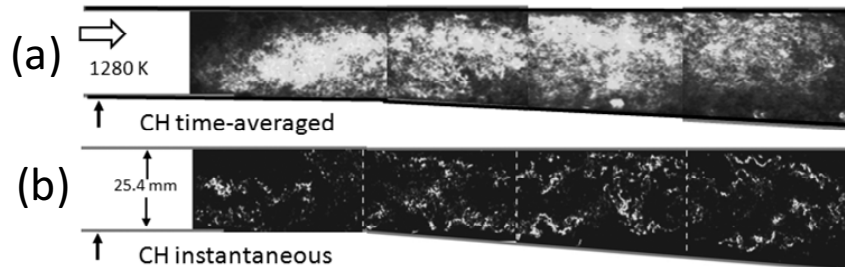


Fig. 3. Structure of CH reaction zones (thickened shredded layers) in highly-preheated jet in cross-flow.

CH PLIF was used to record the primary reaction zones seen in Fig. 3. While time-averaged PLIF provides only flame length and heat release rates (as does CH\* chemiluminescence) the instantaneous CH PLIF indicates that there are no thin flamelets, either near the premixed flame base or in the diffusion flame downstream. There also are no large homogeneous reaction zones. Instead what is observed is a thick layer, which is coherent and follows a wavy pattern on the outside of the fuel jet. This CH layer is shredded and several mm thick, indicating that distributed reactions occur within the layer.

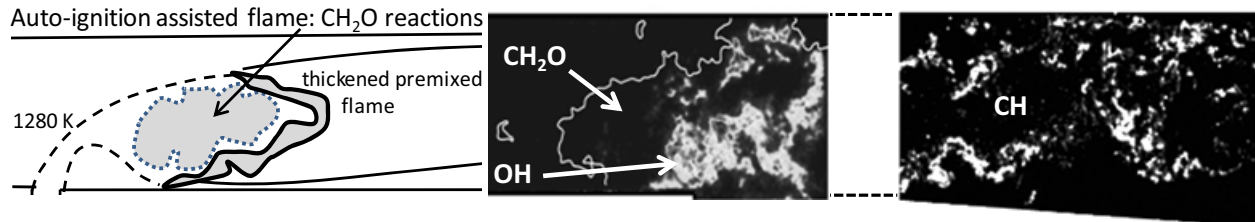


Fig. 4. Formaldehyde observed in distributed reactions (auto-ignition) upstream of OH (flame edge)

While CH PLIF identifies the primary reactions, formaldehyde PLIF indicates that far upstream of the CH reaction layer there are secondary fuel breakdown reactions that occur in a homogeneous distributed reaction region. The white line in Fig. 4 surrounds the CH<sub>2</sub>O region, while the white zones labeled OH indicate the upstream boundary of the primary reactions. This flame is denoted an “auto-ignition-assisted” flame. In the formaldehyde region there are only weak gradients and thus no flame structure. The base of the CH\* region has the properties of a stratified premixed flame, having large thermal gradients, while downstream the structure resembles that of a shredded diffusion flame. The strain rates are larger on the upper surface of the jet, causing the primary reactions there to start farther downstream than on the lower side. The jet in a cross flow offers a realistic geometry in which the mixing now is well understood, but the chemistry of the auto-ignition / flame physics still represent a challenge.

1. A. Gruber, et al., technical presentation, NORDITA conference, Stockholm, May 2010.
2. Olbricht, C, Janicka, J. et al., Int J. Heat and Fluid Flow 28, 6, 1215, 2007.
3. Hasselbrink, E. and Mungal, M.G., J. Fluid Mech 443, 1, 2001.
4. Micka, D, Driscoll, J.F., Proc Comb Inst 32 (2009) 2397. Also AIAA paper 2008-5071.

# Application of a Wavelet Based Denoising Algorithm Enabling High Resolution Measurements of Scalar Dissipation in Flames

Matthew J. Dunn\* and Robert S. Barlow  
Sandia National Laboratories, Livermore, CA, 94551-0969 USA

\*Corresponding author: [m.dunn@usyd.edu.au](mailto:m.dunn@usyd.edu.au)

Measurement of mixture fraction and its dissipation in nonpremixed combustion is a particularly challenging task due to the competing requirements of low noise and high spatial resolution. A wavelet based denoising algorithm has been developed in an attempt to separate the true signal from the measured signal, which is composed of the true signal plus noise. The algorithm is generalized in the sense that there are no user defined parameters to be adjusted on a cases-by-case basis; the only required input parameters are the camera readout noise and the camera gain ( $e^-/ADU$ ). The algorithm is applied in the spatial direction to the raw line-imaged data of the fourteen Raman channels, the Rayleigh signal, and the CO-LIF signal. A spatial oversampling strategy is used, with pixel of  $\sim 20 \mu\text{m}$  in all three images, in order to more easily separate pixel-to-pixel noise from the true spatial scales for turbulent fluctuations. The utility of the developed wavelet based denoising algorithm is highlighted by applying the algorithm to measurements of the DLR-B flame. This flame has been the target of many experimental and numerical investigations both in literature and within the TNF workshop.

The results of the application of the algorithm to a single instantaneous measurement of two scalars (temperature and mixture fraction) are presented in Fig. 1. The predicted noise or residual signals, determined by subtracting the signals with wavelet denoising from the original signals, are shown in Figs. 1b and 1e for temperature and mixture fraction, respectively. These graphs show that the mean of the predicted noise signal is essentially zero on a single shot basis, and that the wavelet filtering introduces no systematic bias in profiles of temperature or mixture fraction. Figures 1c and 1f show the square of the radial gradient of temperature and mixture fraction, which is essentially the dissipation of these scalars but without multiplying by the corresponding diffusivity. The maximum value on the ordinate axis of Figs. 1c and 1f has been truncated so that variation of the wavelet denoised signal can be displayed. The advantage of wavelet denoising becomes most obvious when observing the results in terms of dissipation. The wavelet denoised signal for the temperature dissipation is free of high frequency noise, and the peaks and valleys in the dissipation profile can be easily correlated with the original structures in the scalar profile. Without the wavelet denoising it is difficult to correlate the dissipation profile to the original profile, and it is obvious the dissipation profile is significantly polluted with high frequency noise. The wavelet denoised dissipation profile of mixture fraction displays peaks that can be correlated to the mixture fraction profile. It is also clear that there is no significant contribution of high frequencies in the denoised profile. The degree of noise pollution in the profile of mixture fraction dissipation without wavelet denoising is so large that the mean value of dissipation is approximately two orders of magnitude larger than mean dissipation derived from the wavelet denoising, it is also not possible to reconcile any correlation of the dissipation profile without denoising with the original scalar profile of mixture fraction, these final two observations are not clearly visible in Fig. 1f) because the ordinate axis has been scaled so that the denoised signal may be interpreted.

Sample normalized dissipation spectra of the inverse Rayleigh scattering signal (a proxy for temperature) and mixture fraction are presented in Fig. 2 and are compared with the Pope Model dissipation spectrum [1] and with the corresponding spectra without the wavelet algorithm. Figures 2a and 2b) show that the application of the wavelet algorithm does not interfere with the small wavenumbers (large length scales) in measured spectra. This is important because the contribution of noise to the dissipation at these small wavenumbers is effectively zero. For the inverse Rayleigh scattering signal in Fig. 2a, it can be seen that the signal with the wavelet algorithm closely follows the Pope model dissipation spectra down to about 5 decades from the peak dissipation level, however even without the application of the wavelet algorithm it can be seen this measurement is resolved down to the dissipation cutoff scale at  $\kappa_1 \lambda_B = 1$  ( $2\pi$  times the Bachelor scale), which corresponds to roughly 2% of the peak in the model dissipation spectrum. For the dissipation spectra of mixture fraction in Fig. 2b, it can be seen that there is a much larger difference between the results with and without the wavelet algorithm at wavenumbers near the dissipation cutoff scale. With the application of the wavelet algorithm the dissipation spectra of mixture fraction can be seen to follow the decay of the model dissipation spectrum for two decades beyond the peak level, which was not previously possible in this flame [2]. Furthermore, because the wavelet algorithm is a locally adaptive noise filter, the instantaneous dissipation and conditional mean dissipation may be determined directly, without additional filtering.

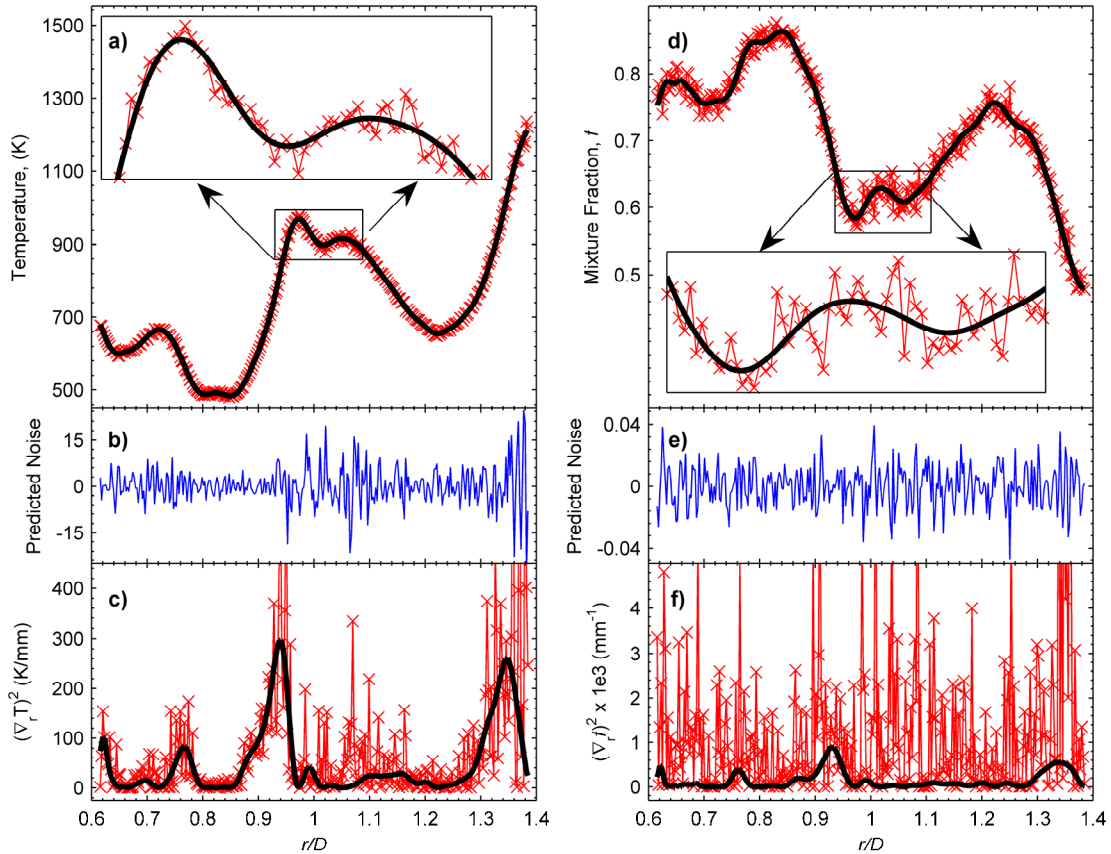


Fig. 1. Results applying the wavelet denoising algorithm to temperature a), b), c), and mixture fraction d), e), f). a) and d): Unfiltered results with no denoising (thin red line with red X markers) and wavelet denoised results (thick black line) for a single shot profile of temperature and mixture fraction. b) and e): The predicted noise contained in the instantaneous profile, derived by subtracting the signal with wavelet denoising from the signal without wavelet denoising. c) and f): The square of the radial gradients of temperature and mixture fraction, respectively.

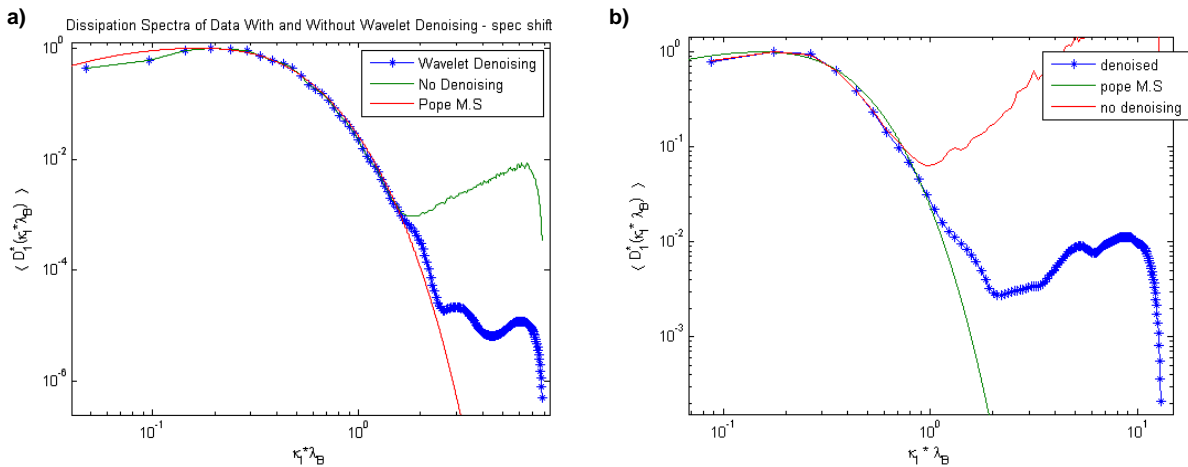


Fig. 2. Normalized dissipation spectra for the inverse Rayleigh scattering signal a), and mixture fraction b) with no denoising and with wavelet denoising compared to the Pope model dissipation spectrum.

### References:

- [1] S. B. Pope, *Turbulent Flows*, Cambridge University Press, Cambridge, 2000.
- [2] G.-H. Wang, A. N. Karpetis, R. S. Barlow, *Combust. Flame* 148 (2007) 62-75

# Turbulent Partially Premixed Dimethyl Ether/Air Jet Flames: A New Series of Target Flames for Experiments and Modeling

Jonathan H. Frank<sup>1,\*</sup>, Andrea G. Hsu<sup>1</sup>, Johannes Kuhl<sup>2</sup>

<sup>1</sup>*Combustion Research Facility, Sandia National Laboratories, Livermore, CA 94551 USA*

<sup>2</sup>*Lehrstuhl für Technische Thermodynamik and Erlangen Graduate School in Advanced Optical Technologies, Friedrich-Alexander-Universität Erlangen Nürnberg, D-91058, Erlangen, Germany*

\*Corresponding Author: [jhfrank@sandia.gov](mailto:jhfrank@sandia.gov)

We introduce a new series of benchmark flames consisting of partially premixed piloted dimethyl ether (DME)/air jet flames. These flames provide an opportunity to understand turbulence-flame interactions for oxygenated fuels and to develop predictive models for these interactions. The development of accurate models for DME/air flames would establish a foundation for studies of more complex oxygenated fuels. This series of four jet flames spans jet exit Reynolds numbers,  $Re_d$ , from approximately 27,000 to 68,000 (see Table 1). The flames are stabilized on the same burner [1] as the piloted methane/air jet flames that have been studied extensively within the context of the TNF Workshop [2-4]. The nozzle diameter is  $d = 7.2$  mm, and the pilot diameter is 18.2 mm. The burner is surrounded by an air coflow with a velocity of 0.9 m/s. The fuel mixture consists of 20% DME and 80% air, by volume, resulting in a stoichiometric mixture fraction of  $\xi_{st} = 0.353$ , which is the same as that of the piloted  $\text{CH}_4$ /air flames with 25%  $\text{CH}_4$  and 75% air. The annular pilot burns a mixture of  $\text{C}_2\text{H}_2$ ,  $\text{H}_2$ , air,  $\text{CO}_2$ , and  $\text{N}_2$  having the same enthalpy and equilibrium composition as a DME/air flame with an equivalence ratio  $\phi = 0.70$ . Compared with the previous series of piloted  $\text{CH}_4$ /air jet flames, the pilot for the DME/air flames is slightly leaner, and the pilot flow rates are a smaller percentage of the total flow rate. Flames D-G have an increasing probability of localized extinction. Flame D has very low probability of localized extinction, and Flame G has a high probability of localized extinction and subsequent re-ignition.

In an initial survey of these flames, we use laser-induced fluorescence (LIF) imaging of OH to measure the reaction zone structure and the degree of localized extinction as a function of downstream location. Figure 1 shows sample OH-LIF measurements at  $x/d = 5-25$  in Flames D and G. Probabilities of localized extinction and the size distributions of the extinguished regions will be evaluated from large sets of OH-LIF images. Plans are underway for further imaging measurements combined with detailed species, temperature, and velocity measurements in collaboration with Rob Barlow (Sandia).

Flame	$Re_d$
D	$\sim 27,000$
E	$\sim 41,000$
F	$\sim 54,000$
G	$\sim 68,000$

Table 1: Jet exit Reynolds numbers of DME/air flames based on the fuel mixture at 294 K.

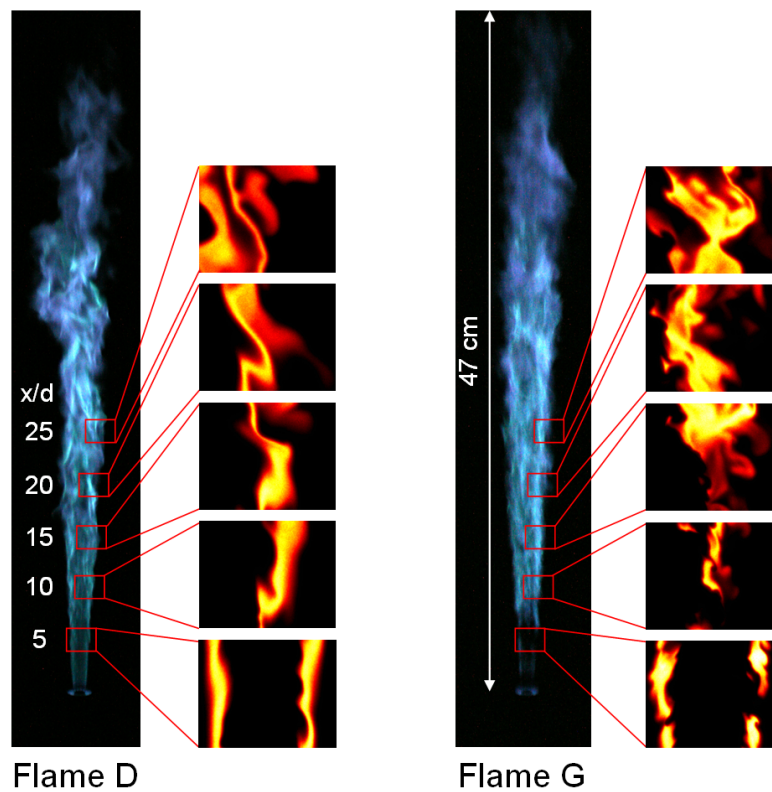


Fig. 1. Chemiluminescence and OH-LIF images of the DME/air partially premixed piloted jet flames D and G with jet exit Reynolds numbers of approximately 27,000 and 68,000, respectively. Exposure times for the chemiluminescence images are 313  $\mu\text{s}$  and 200  $\mu\text{s}$  for flames D and G, respectively.

## References

- [1] A. R. Masri, R. W. Dibble, R. S. Barlow, *Prog. Energy Combust. Sci.* 22 (1996) 307-362.
- [2] R. S. Barlow, J. H. Frank, *Proc. Combust. Inst.* 27 (1998) 1087-1095.
- [3] R. S. Barlow, J. H. Frank, A. N. Karpetis, J. Y. Chen, *Combust. Flame* 143 (2005) 433-449.
- [4] International Workshop on Measurement and Computation of Turbulent Nonpremixed Flames (TNF), <http://www.sandia.gov/TNF>

# Raman/Rayleigh-scattering and CO-LIF measurements in laminar and turbulent jet flames of dimethyl ether

F. Fuest<sup>1</sup>, R.S. Barlow<sup>2</sup>, J.-Y. Chen<sup>3</sup>, M.J.Dunn<sup>2</sup>, A. Dreizler<sup>1</sup>

<sup>1</sup> FG Reactive Flows and Diagnostics, Center of Smart Interfaces,  
TU Darmstadt, Petersenstr. 32, 64287 Darmstadt, Germany

<sup>2</sup>Sandia National Laboratories, 7011 East Avenue, Livermore, CA, USA

<sup>3</sup>Department of Mechanical Engineering, University of California, Berkeley, CA 94720, USA

To reduce the impact of combustion of fossil fuels on air quality and climate change, dimethyl ether (DME) is a promising alternative diesel fuel candidate. Technical combustion processes, including formation of pollutants, are influenced by turbulence-chemistry interaction. Therefore, accurate prediction by computational combustion models of combustion systems burning DME must account for multiple scalars and scalar gradients. The testing of such models requires detailed experiments. Here a study is presented on the feasibility of simultaneous species and temperature measurements in turbulent DME flames, using line-imaged Raman/Rayleigh-scattering of the major species H<sub>2</sub>, O<sub>2</sub>, N<sub>2</sub>, CO, CO<sub>2</sub>, H<sub>2</sub>O, C<sub>2</sub>H<sub>6</sub>O and laser induced fluorescence of CO.

The measurement system and data evaluation methods developed to investigate methane-air flames are extended to address DME flames. The Raman signal intensity and spectral shape of the Raman scattering from DME over a range of temperature are presented, based on measurements in electronically heated flows and laminar jet flames. These data are used to develop an iterative method for data evaluation that allows determination of indispensable crosstalk correction terms for the concentration measurements of O<sub>2</sub> and CO<sub>2</sub>. Issues of fluorescence interferences, mainly from C<sub>2</sub> radicals on the fuel-rich side of the reaction zone, and their corrections are discussed. Opposed-flow laminar flame calculations are used to investigate the role of the intermediate species (CH<sub>4</sub>, CH<sub>2</sub>O, C<sub>2</sub>H<sub>4</sub>, C<sub>2</sub>H<sub>2</sub>, C<sub>2</sub>H<sub>6</sub>, CH<sub>3</sub>) in the reaction zone. The spatial distribution of the intermediate species is shown in the Fig. 1b and their sum as red dashed line in Fig. 1a to illustrate the relative importance compared to the major species. In particular, their effect on the mixture fraction calculation and its relationship to the experimentally determined mixture fraction is examined.

A different method of calculating the mixture fraction is introduced to account for experimental characteristics evoked by the intermediate species. Deviations to the commonly used definition by Bilger are discussed. The impact of the intermediate species on deviations in concentration and temperature profiles due to different resulting Raman- and Rayleigh scattering cross sections is demonstrated. To allow for reasonable comparison between numerical calculations and the applied measurements, all corrections are discussed on measurements of two partially-premixed rich laminar jet flames of DME. Finally, species concentrations and temperature profiles from measurements in a turbulent piloted jet flame of DME are presented as shown for two selected scalars in Fig. 2.

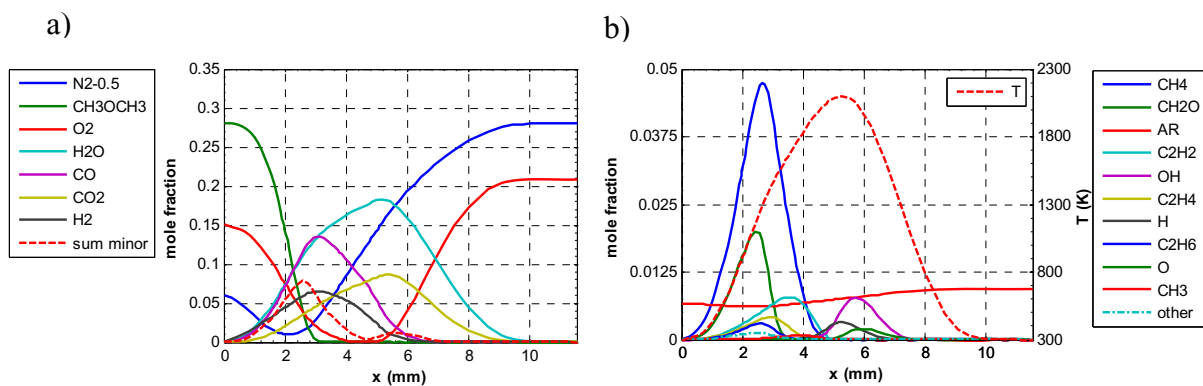


Figure 1: Species and temperature profiles from a laminar flame calculation in the Tsuji geometry, using Chemkin with a detailed chemical reaction mechanism for DME from Zhao et al [1]. The dashed line in a shows the sum of the species from Fig. b except Ar. The names of the species in the legends are sorted in descending order by their maximum occurrence in mole fraction.

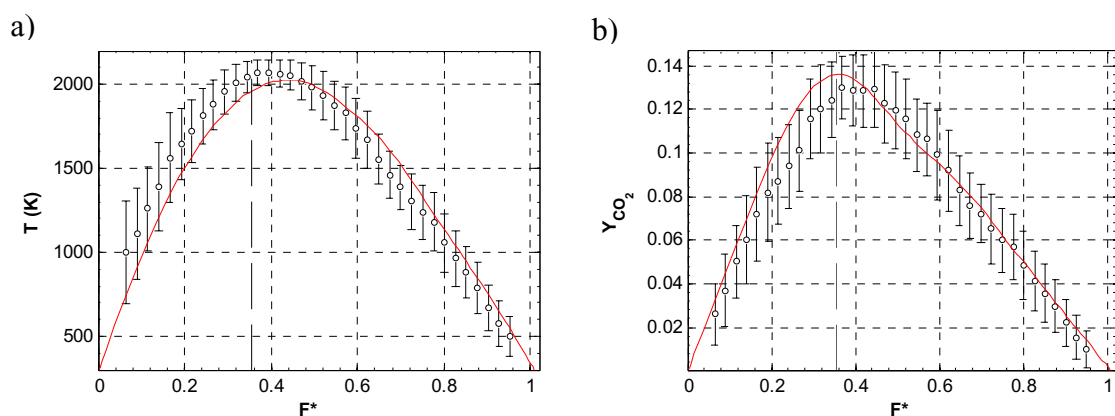


Figure 2: Experimental results from a turbulent partially-premixed jet flame of DME/air, shown with results from a laminar flamelet calculation with  $a=400s^{-1}$  (red solid line). Ninety-five shots are shown as conditional average in mixture fraction space for a) temperature and b) mass fraction of  $CO_2$ . Error bars indicate plus/minus one standard deviation. The mixture fraction calculation has been slightly modified to account for the intermediate species on the fuel-rich side and is here denoted as  $F^*$ .

[1] Zhao Z, Chaos M, Kazakov A, Dryer FL (2008) Thermal Decomposition Reaction and a Comprehensive Kinetic Model of Dimethyl Ether. *Int. J. Chem. Kinet.* 40:1-18.

# Conditional statistics in turbulent premixed opposed jet flames

K. H. H. Goh, P. Geipel, R. P. Lindstedt  
Imperial College London, UK  
p.lindstedt@imperial.ac.uk

The opposed jet configuration presents a particularly attractive geometry for evaluating the impact of strain on burning properties of laminar and turbulent flames. The geometry has the advantage of good optical access and comparatively simple boundary conditions. Disadvantages include potential low frequency flow motion at high nozzle separations (e.g. [1, 2]) and, for turbulent flames, relatively low turbulence levels causing bulk strain to exceed the turbulent contribution at small nozzle separations [3]. In the current work, fractal generated turbulence has been used to ameliorate the latter problem by significantly increasing turbulent strain. The use of additional fractal grids has been shown to increase the turbulent Reynolds number by a factor of two from 48 for conventional perforated plates to 109 for a bulk velocity of 4.0 m/s [4].

The aim of the present work is to explore the contribution of large scale fluid motion on measured turbulence quantities through the use of conditional statistics. Algorithms were developed to determine the instantaneous location of the stagnation point and to estimate the orientation of the stagnation plane using measured 2-D velocity data. The instrumentation comprised particle image velocimetry (PIV) using 3–5 micron  $\text{Al}_2\text{O}_3$  particles. Velocity statistics are shown for methane flames approaching extinction in Fig. 1. At first, the stagnation point was determined using a square window of fixed size that was moved around each PIV image and a vector summation of the velocities was computed. The location of the instantaneous stagnation point was defined as the centre of the window with the lowest magnitude of the vector sum [4].

Probability density functions for the instantaneous location of the stagnation point obtained using the window algorithm are shown in Fig. 2 for methane at stoichiometries of 0.7 and 0.9 and at a bulk velocity of 4.0 m/s. A movement of the instantaneous stagnation point location of the order of the integral length scale (3.1 +/- 0.1 mm) in axial and radial direction was found. Filtered velocity data rejecting stagnation point locations beyond 2.5 mm and 3.5 mm in the axial direction is shown in Fig. 1 for

normalised Reynolds stress components. The unfiltered Reynolds stress components show a certain degree of asymmetry, especially when approaching the lean extinction limit. An axial threshold of 3.5 mm, slightly above the integral length scale, increases the symmetry of the flow. A cause of the observed behaviour can be found in comparatively infrequent large scale events, typically due to a shear layer instability, that exert an influence on the velocity statistics. The symmetry is further improved by a reduction in the threshold to 2.5 mm with some impact on velocity statistics.

Filtering using an axial threshold of 3.5 mm away from the nominal stagnation point leads to a rejection between 2.5% at  $\phi = 0.9$  and 6.6% at  $\phi = 0.7$  vector fields. A threshold of 2.5 mm rejects up to 17.5%. Applying a circular threshold with a diameter of 3.0 mm, close to the integral length scale, rejects up to 15.9% of the instantaneous vector fields. The determined axial Reynolds stress stays almost unchanged, whereas the radial stress is somewhat reduced.

A second algorithm that produces a linear approximation of the stagnation plane location based on streamlines determined from instantaneous vector fields was also developed. An example is shown in Fig. 3, which highlights the linear approximation. The algorithm enables a quantification of the rotation of the instantaneous stagnation plane. A probability density function of the angle of rotation is given for 1000 instantaneous vector fields and two stoichiometries in Fig. 4 and shows a movement of the stagnation plane within 12 degrees. The stagnation point locations obtained using the window algorithm, shown in Fig. 2, and the streamline algorithm, shown in Fig. 3, differ by less than 1 mm.

The work has shown that filtering algorithms may be used to explore the impact of low frequency flow motion on measured turbulence statistics. The results are encouraging and suggest that in the current experimental configuration the impact is moderate. Furthermore, an algorithm has been developed that allows the extraction of data related to PDFs of the orientation of the stagnation plane. The lat-

ter information can be useful as part of comparisons with time-dependent simulation techniques such as LES/FDF.

## Acknowledgements

The current work was carried out with the financial support of the US Office of Naval Research under grant N00014-07-1-0993. The support of Dr Gabriel Roy and Dr Robert Barlow is gratefully acknowledged.

## References

- [1] C. Mounaïm-Rousselle, I. Gökalp, in: *Spring Annual Meeting of the Western States Section of the Combustion Institute*, 1993.
- [2] L. Kostiuk, K. Bray, R. Cheng, *Combust. Flame* 92 (1993) 396–409.
- [3] D. Luff, E. Korusoy, R. P. Lindstedt, J. H. Whitelaw, *Exp. Fluids* 35 (2003) 618–626.
- [4] P. Geipel, K. H. H. Goh, R. P. Lindstedt, *Submitted to Flow, Turbulence and Combustion*.

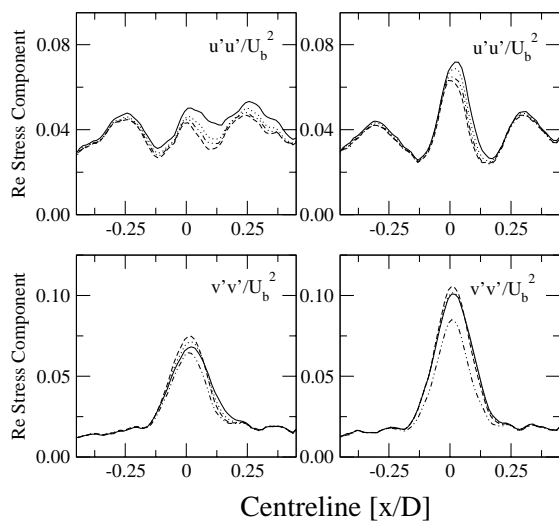


Figure 1: Comparison of the Reynolds stress components along the centreline using axial thresholds of 2.5 mm (dashed line) and 3.5 mm (dotted line), shifting the instantaneous vector fields into the origin (dashed-dotted line) and PIV-data (solid line) at  $\phi = 0.7$  (left) and  $\phi = 0.9$  (right) and a bulk velocity of  $U_b = 4.0$  m/s.

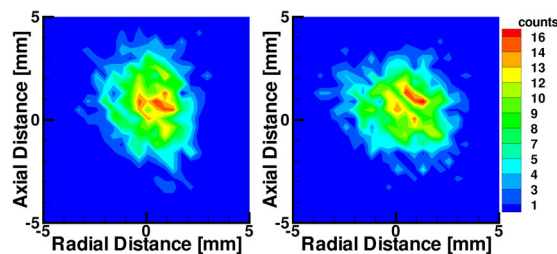


Figure 2: Probability density functions of the instantaneous stagnation point for methane flames at  $\phi = 0.7$  (left) and  $\phi = 0.9$  (right) and a bulk velocity of 4.0 m/s.

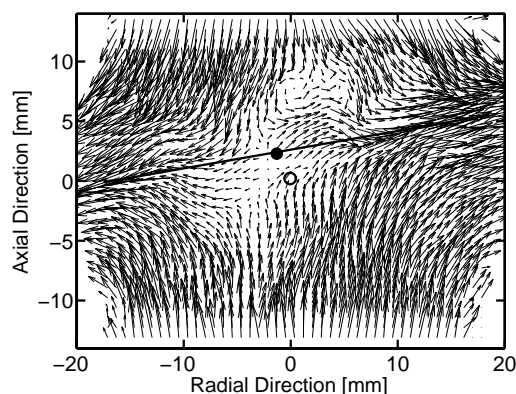


Figure 3: Stagnation plane determination of an instantaneous vector field at a bulk velocity of 4.0 m/s. Approximation of the stagnation plane (solid line), instantaneous (dot) and nominal stagnation point (circle).

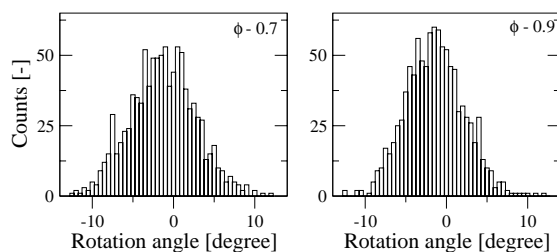


Figure 4: PDFs of the rotation of the stagnation plane for  $\phi = 0.7$  (left) and  $\phi = 0.9$  (right) at a bulk velocity of 4.0 m/s.

## Developments in Turbulent Autoignition Experiments - Fuel Droplet Autoignition in a Heated Cross Flow

R.L. Gordon<sup>1,\*</sup>, C.N. Markides<sup>2</sup>, E. Mastorakos<sup>1</sup>

<sup>1</sup>*Department of Engineering, University of Cambridge, UK;*

<sup>2</sup>*Department of Chemical Engineering, Imperial College London, UK*  
[r.gordon@eng.cam.ac.uk](mailto:r.gordon@eng.cam.ac.uk)

The turbulent autoignition of liquid fuels is of significance to the operation of many combustion systems, particularly diesel engines, HCCI engines, and lean-burn gas turbines. Autoignition in non-premixed turbulent flows is a complex transient phenomenon that involves significant interactions between turbulence and chemical kinetics. Experimental research into these phenomena in gaseous fuels has benefited from the use of generic burners where the source of the hot, turbulent oxidants has been decoupled from the combustion processes, enabling detailed parametric investigations of the processes of turbulent autoignition. A natural development of these investigations is to the autoignition properties of liquid fuels, which is of more practical relevance to the combustion engines listed above. The investigation of liquid fuels will also enable the assessment of the combustion properties of bio-fuel ignition properties.

This poster details a new experiment designed to investigate the autoignition of individual droplets of liquid fuel in a turbulent air flow. Droplets are generated in an almost mono-disperse chain and injected into a cross-flow of heated air inside a vacuum insulated glass tube. The velocity, turbulence and temperature boundary conditions are reported, along with estimated droplet size distributions. The ignition location downstream from the injection point is tested for its sensitivity to the air flow temperature and velocity and droplet generation frequency for ethanol and n-heptane. Additionally, OH\* chemiluminescence is recorded at 5kHz to provide some insight into the mode of ignition and subsequent combustion. For heptane, it was found that stable ignition conditions correspond to an ignition in the vapour phase, into which droplets pass and combust in isolation. For ethanol that vaporizes quickly, the ignition spots resemble previous results with gaseous fuel. The data can assist the validation of two-phase turbulent combustion models. Data will also be presented for biodiesel droplets.

The autoignition lengths were found to vary by 175 mm with changes in air temperature of 30K, and by 150 mm with a 30% change in bulk velocity. The frequency of the droplet generator's piezoelectric diaphragm was also found to have an impact on the flame structure and ignition length. Movies of OH\* chemiluminescence showed a statistically-steady condition with autoignition appearing in isolated spots, probably associated with evaporated fuel from the droplets, into which larger droplets enter and ignite giving rise to isolated burning trails.



Figure 1. Long exposure photograph (1/125s) of n-Heptane autoignition. Droplet generation at 1600Hz. Injected droplet stream is visible on the left hand side of the image. Flow is horizontally from left to right.

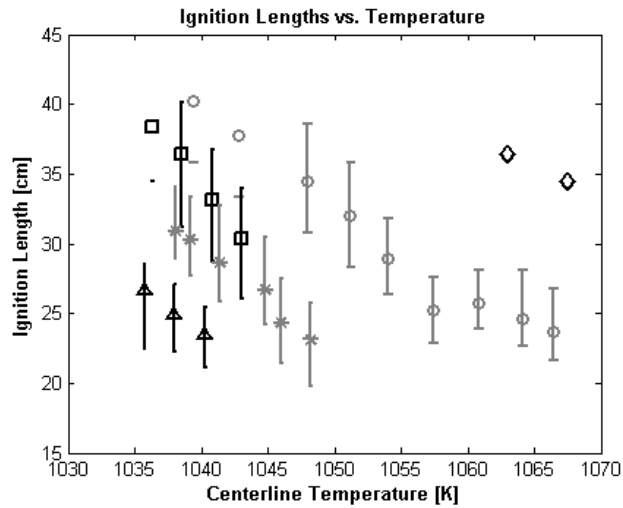


Figure 2. Autoignition lengths for n-Heptane and Ethanol. Lengths measured from RMS images of over 1000 uncorrelated images taken at 1/1000s exposure. Symbols denote location of steepest gradient, lower error bar denotes 10% of peak RMS, upper error bar denotes peak RMS. Key: Diamonds - Ethanol ( $U_b = 12.6 \text{ m.s}^{-1}$ ), remaining plots n-Heptane: circles -  $U_b = 12.6 \text{ m.s}^{-1}$ , squares -  $U_b = 11.1 \text{ m.s}^{-1}$ , stars -  $U_b = 9.9 \text{ m.s}^{-1}$ , triangles -  $U_b = 8.6 \text{ m.s}^{-1}$ .

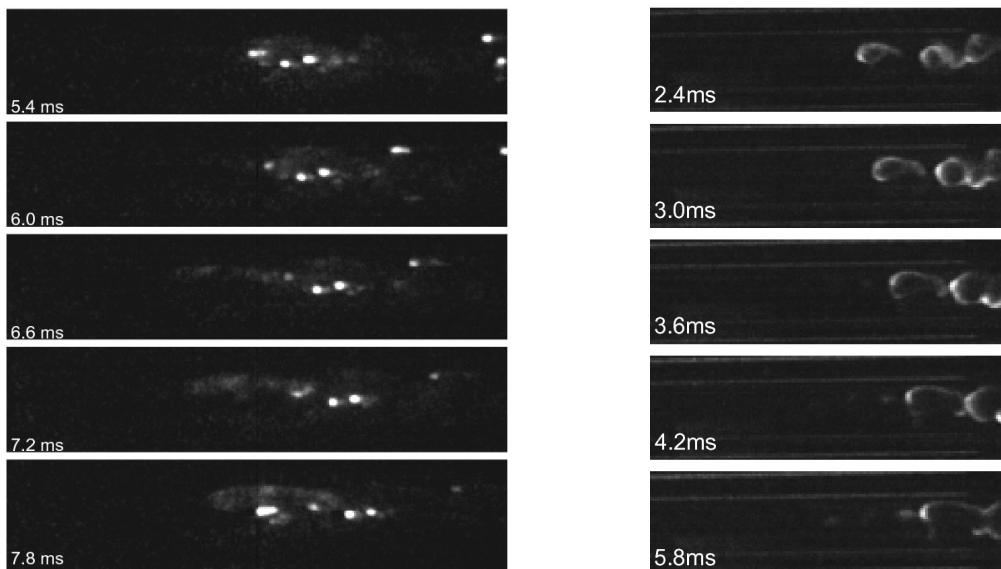


Figure 3. Sequences of  $\text{OH}^*$  Chemiluminescence for n-Heptane (left) at 1054 K, 1750 Hz droplet generator frequency and Ethanol (right) at 1034 K, 1800 Hz droplet generator frequency. Bulk velocity 12.5 m/s (flow from left to right). Images taken at 5 kHz with 1/20000s exposure on an intensified CMOS camera. Every third image shown.

The simultaneous presence of turbulent dispersion of the droplets, vapour release in the turbulent field, autoignition of this vapour, and individual droplet combustion following this autoignition event, make the present experiment a very challenging test case for turbulent spray combustion models, without the usual complication of primary and secondary atomization present in realistic sprays.

# Prediction of Autoignition in a Lifted Methane/Air Flame Using an Unsteady Flamelet/Progress Variable Model

Matthias Ihme\* and Yee Chee See

*Department of Aerospace Engineering, University of Michigan, Ann Arbor, MI 48109*

An unsteady flamelet/progress variable (UFPV) model has been developed for the prediction of autoignition in turbulent lifted flames [1]. The model is an extension to the steady flamelet/progress variable (SFPV) approach [2,3], and employs an unsteady flamelet formulation [4] to describe the transient flame evolution during the ignition process. In this UFPV model, all thermochemical quantities are parameterized in terms of mixture fraction  $Z$ , reaction progress parameter  $C$ , and stoichiometric scalar dissipation rate  $\chi_{Z,st}$ . A potential advantage of this UFPV-formulation is that it eliminates the explicit dependency on the time-scale information which leads to significant simplifications in the computation and parameterization of the thermodynamic state space. For application to LES, a presumed FDF closure model is employed to evaluate

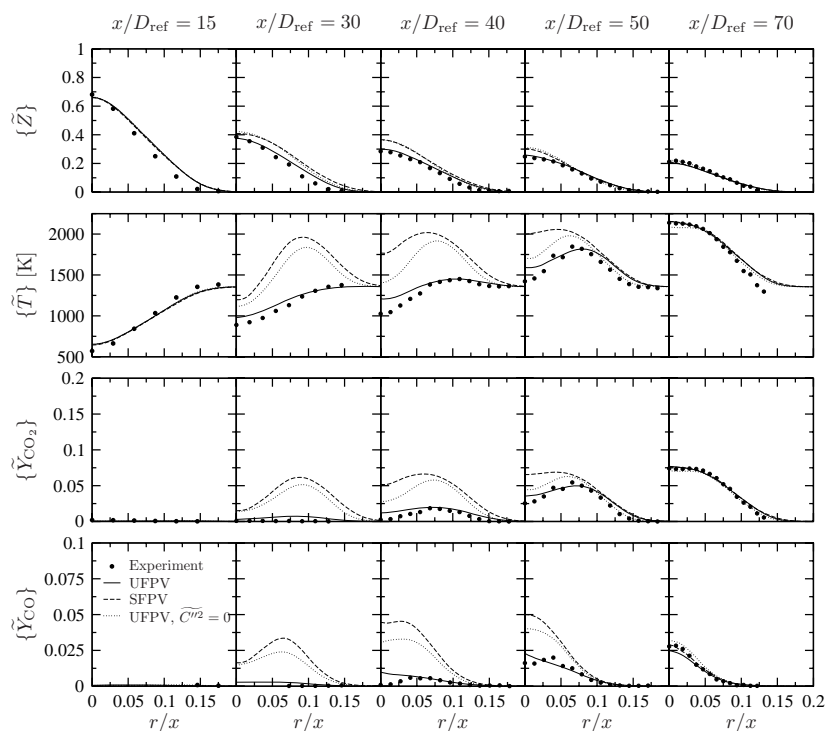


**Figure 1:** Comparison of radial profiles for mixture fraction, temperature, and species mass fractions of  $CO_2$  and  $CO$ . The dashed lines show results obtained from the steady flamelet model (SFPV) and the dotted lines correspond to UFPV results in which effects of the turbulence/chemistry interaction have been neglected by approximating the FDF of the progress variable by a Dirac delta function.

Favre-averaged thermochemical quantities. For this, a beta-distribution is used for the mixture fraction, a so-called statistically most-likely distribution is employed for the reaction progress parameter, and the distribution of the stoichiometric scalar dissipation rate is modeled by a Dirac delta function. To close the UFPV-model, four additional transport equations for mean and variance of mixture fraction and progress variable are solved, and the scalar dissipation rate is obtained from an algebraic relation.

The UFPV model is applied to the lifted methane/air jet flame of Cabra *et al.* [5]. Additional calculations with the SFPV model and a modified UFPV formulation are carried out to investigate transient effects and to

\*Corresponding author: mihme@umich.edu

quantify the significance of turbulence/chemistry interaction *a posteriori*. The governing equations are solved in a cylindrical coordinate system employing a low Mach-number, finite volume code [2]. The computational mesh contains 256 cells in axial direction, 150 in radial direction, and 64 grid points in circumferential direction on a computational domain of  $90 D_{\text{ref}} \times 30 D_{\text{ref}} \times 2\pi$  in axial, radial, and circumferential directions, respectively.

Simulation results for three different LES calculations are presented in Figs. 1 and 2. Figure 1 shows a comparison of radial profiles for temperature and species mass fractions for  $\text{CO}_2$  and  $\text{CO}$  at five axial locations in the flame. Compared to the SFPV model (dashed lines), results from the unsteady flamelet model (solid lines) are in good agreement with experimental data. In addition, results from a UFPV calculation are shown, in which effects of turbulence/chemistry interaction have been omitted by approximating the FDF of  $C$  by a Dirac delta function. This comparison shows that this leads to a significant reduction of the lift-off height which is reflected by the over-prediction of the temperature and species profiles between  $30 \leq x/D_{\text{ref}} \leq 50$ . In this context it is also noted that Raman measurements for the  $\text{CO}$ -comparison have been used. Discussions with Rob Barlow suggested that the  $\text{CO}$ -LIF measurements could be ambiguous, which was also pointed out by Jean-Baptiste Michel and Christian Angelberger.

The PDF of the stabilization location of the flame base is evaluated from the LES results, and is shown in Fig. 2(a). The flame base is characterized as the most upstream point of the  $\tilde{Y}_{\text{OH}} = 10^{-3}$

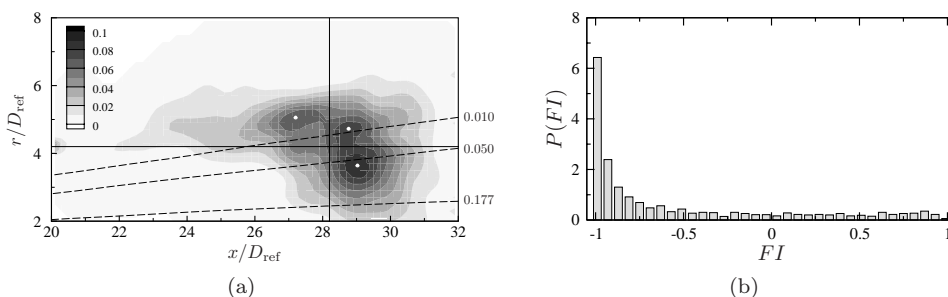


**Figure 2:** (a) PDF of the flame stabilization point; dashed lines correspond to isocontours of the mean mixture fraction with  $\{\tilde{Z}\} = \{0.01, 0.05, 0.177\}$  (from top to bottom), and the solid lines denote the mean axial and radial locations of the stabilization point; (b) PDF of the flame index  $FI$ , evaluated at the flame stabilization point.

and the solid lines denote the mean axial and radial locations of the stabilization point. From this statistical analysis it can be seen that the stabilization point is confined to the fuel lean region, which is in agreement with previous studies [7]. While the flame base fluctuations are confined to a relatively narrow region in radial direction, considerable variations in axial direction are apparent.

To characterize the combustion mode at the stabilization point, the flame index  $FI$  is evaluated (corrected to account for  $\text{O}_2$  in the fuel stream). The PDF of the flame index, evaluated at the stabilization point, is shown in Fig. 2(b). These statistical results show that ignition occurs primarily in the diffusion mode, and a quantitative analysis shows that 50 % of all ignition events occur under conditions in which the alignment angle between fuel and oxidizer gradients exceeds  $3/4\pi$ .

## References

- [1] M. Ihme and Y. C. See., *Combust. Flame*, under review, 2010.
- [2] C. D. Pierce and P. Moin. *J. Fluid Mech.*, 504:73–97, 2004.
- [3] M. Ihme, C. M. Cha, and H. Pitsch. *Proc. Combust. Inst.*, 30:793–800, 2005.
- [4] H. Pitsch and M. Ihme. *AIAA Paper 2005-557*, 2005.
- [5] R. Cabra, J.-Y. Chen, R. W. Dibble, A. N. Karpetsis, and R. S. Barlow. *Combust. Flame*, 143:491–506, 2005.
- [6] C. S. Yoo, R. Sankaran, and J.H. Chen. *J. Fluid Mech.*, 640:453–481, 2009.
- [7] P. Domingo, L. Vervisch, and D. Veynante. *Combust. Flame*, 152:415–432, 2008.

# Grid convergence analysis for the large-eddy simulation of the Sandia piloted methane-air flames D, E, and F.

Jean-Francois Izard and Fabrizio Bisetti,  
*Clean Combustion Research Center,*  
*King Abdullah University of Science and Technology, 23955 Thuwal, KSA.*

Turbulent combustion of non- and partially premixed hydrocarbon fuel mixtures is of practical importance in many technical applications. A series of piloted methane-air jet flames, part of the TNF Workshop [1], defines a common test case. Reactive scalar data from three piloted flames (D, E, and F) is available. These flames are characterized by an increasing velocity in the main diluted methane and pilot jets, increasing the occurrence of localized extinction. Flames D, E, and F have been simulated by several groups [2-7]. Their results show that the representation of local extinction remains a challenging task. The ability of probability or filtered density functions (PDF or FDF for LES applications) methods to capture extinction has been shown in previous studies [2, 6] and current interests are in the extension of PDF approaches to LES. Indeed, by directly solving for the joint FDF of the composition, the reaction source terms appear in closed form and does not require modeling. However, an order-of-magnitude analysis shows that the finite-difference solution of the PDF transport equation is impracticable for more than three scalars, as the computational expense is found to rise exponentially with  $N$ . Monte Carlo method are used, as the computational cost rises only linearly with  $N$ . Nevertheless, stochastic approaches to evolve the FDF in space and time are used together with LES, and attention must be paid to the consistency and accuracy of the simulation.

The computational power of parallel computers is now sufficient to simulate reactive flows with large numerical meshes. However, the use of reaction mechanisms in an FDF calculation with a stochastic solution method is computationally very expensive. The most limiting factor is the mesh size. Consequently, the effect of mesh resolution on LES results become a key question. A grid convergence analysis should be performed for key LES statistics of interest, such as the mean and RMS values of the velocity and mixture fraction fields. Indeed, the mixture fraction is a key parameter for the description of non-premixed flames and it is extensively used within flamelet models [3, 5, 7]. Moreover, resolved momentum is used for the convection step of the Monte Carlo simulation. Since discretization errors are the main source of numerical uncertainties in finite difference/volume methods, grid convergence for the velocity is of great importance for the consistency of the Monte Carlo algorithm.

A grid convergence analysis for flame D greatly important has already been performed by Kemenov et al. [7]. We conduct the same study for all three flames (D, E, and F) utilizing a simple steady flamelet approach and five grids with increasing resolution from 200,000 cells up to 10 millions cells. Though the steady flamelet model might not be a very accurate turbulent combustion model for the Sandia flame series, this work represents a first important step to address the issues of accuracy and grid dependence. Conclusions are given concerning the most appropriate computational grid for each flame.

## References

- [1] TNF Workshop, <http://www.ca.sandia.gov/TNF>, R. Barlow, Eds., Sandia National Laboratories.
- [2] J. Xu, and S. B. Pope, *Combust. Flame*, 123 :281-307, 2000.
- [3] Q. Tang, J. Xu, and S. B. Pope, *Proc. Comb. Inst.*, 28 :133, 2000.
- [4] R. P. Lindstedt, S. A. Louloudi, and E. M. Vaos, *Proc. Comb. Inst.*, 28 :149, 2000.
- [5] H. Pisch, and H. Steiner, *Proc. Comb. Inst.*, 28 :41, 2000.
- [6] V. Raman, and H. Pitsch, *CTR Ann. Res. Briefs*, 2005.
- [7] K. A. Kemenov, H. Wang, and S. B. Pope, *Proc. 6th National Combustion Meeting*, 2009.

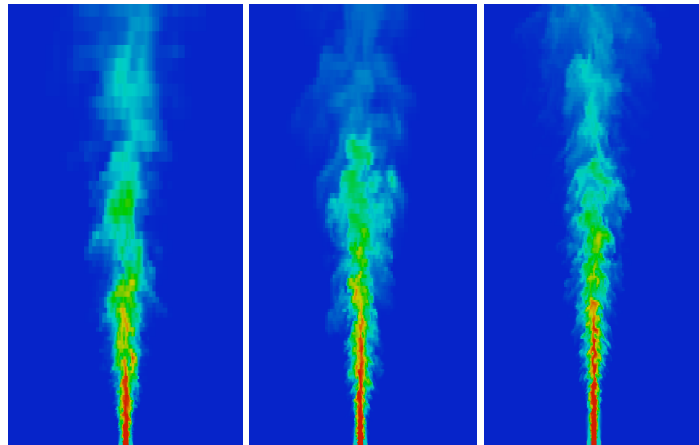


FIGURE 1: Instantaneous fields of mixture fraction for grid1=196,608 cells, grid2=983,040 cells, grid3=2,097,152 cells, and grid 5=10,485,760 cells (from left to right).

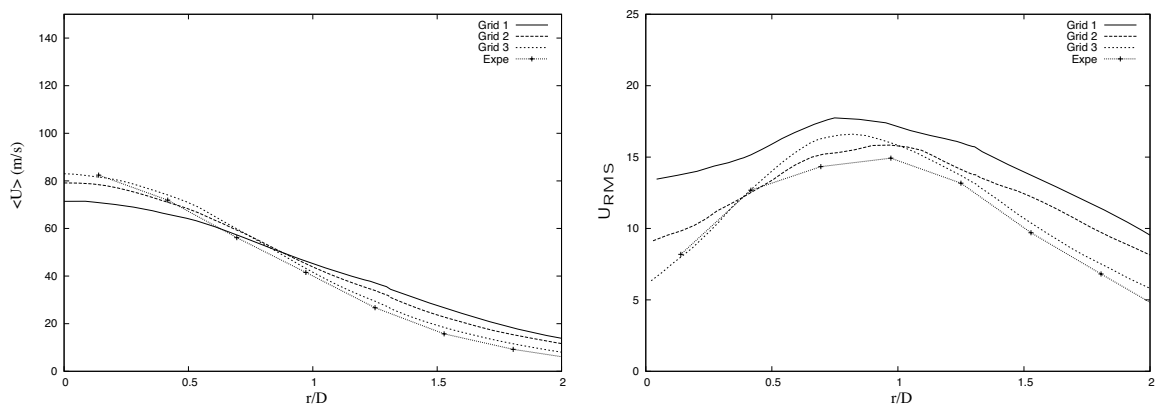


FIGURE 2: Statistics obtained for the mean and RMS values of the velocity at the first location  $x/D=15$  downstream the pipe injector (flame E).

# LES of TSF\_A and TSF\_G flames using the sgs PDF equations/Eulerian stochastic field method

W. P. Jones, S. Navarro - Martinez , K. Vogiatzaki <sup>1</sup>

Department of Mechanical Engineering, Imperial College London, Exhibition Road, London SW7 2AZ, UK

The focus of this poster is Large Eddy Simulation (LES) of a new burner design validated at the University of Darmstadt in 2009 [1]. The burner is shown in Fig1.

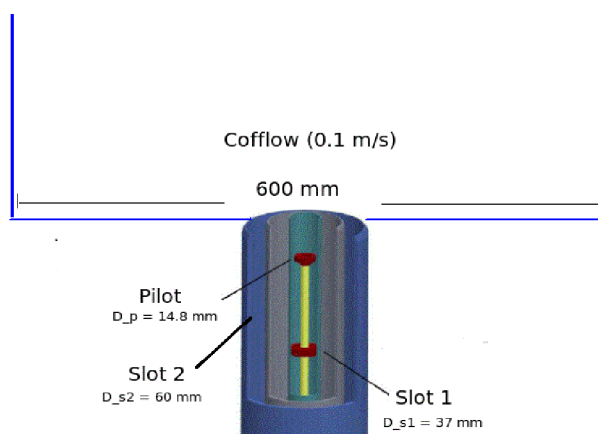


Figure 1: Burner Configuration [1]

Flow field measurements are available at varying operating conditions resulting in 11 flames with different levels of stratification and/or shear at the exit of the annular slots. The focus of the current study is the two reactive cases labelled as TSF\_A\_r and TSF\_G\_r . The operational conditions for the two cases under consideration are given in the table below.

Config	$\Phi_{pilot}$	$U_{pilot}$	$\Phi_{slot1}$	$U_{slot1}$	$\Phi_{slot2}$	$U_{slot2}$	L(mm)
TSF_A_r	0.9	1	0.9	10	0.6	10	120
TSF_G_r	0.9	1	0.9	10	0.9	10	130

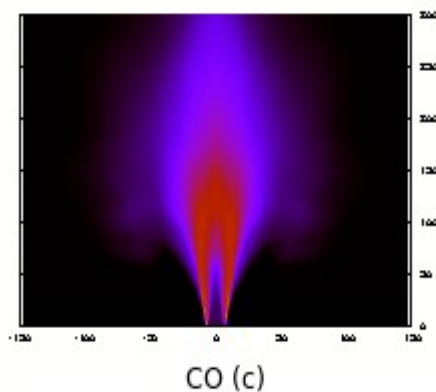
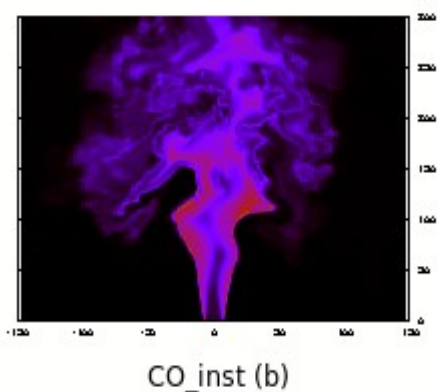
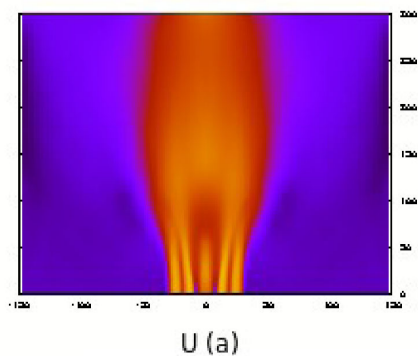
Table 1: Flow parameters for the flames configurations

For the simulations the in-house block-structured, parallel, boundary conforming coordinate LES code, BOFFIN-LES has been used. The LES are performed with filter width equal to the cube root of the local grid cell volume. The dynamic version of the Smagorinski [2] is used for the subgrid stresses and the scalar fluxes are modelled with a simple gradient diffusion approximation. The sub filter scale mixing is modelled with the linear mean-square estimation [3] and the augmented reduced mechanism (AMR) of Sung *et al.* for methane combustion [4] is used to represent chemistry.

The solution domain extends 300mm and 150 mm in the axial and radial direction respectively. The cylindrical mesh used, is comprised of 1,000,000 cells with clustering at the exit of the pipes. . An inflow profile at 1mm downstream, is taken from experimental data and the flow in the pipes is not simulated. Preliminary results have been obtained using a single stochastic field [5,6] i.e. sgs

<sup>1</sup> Corresponding author: k.vogiatzaki@imperial.ac.uk

fluctuations are neglected and a sample of these is shown below. Contour plots of the mean velocity and instantaneous and mean CO for flame TSF\_A\_r are shown in Figs (a) – (c):



#### References:

1. F. Seffrin, F. Fuest, D. Geyer and A. Dreizler, Flow field studies of a new series of turbulent premixed stratified flames, *Combustion and Flame* 157 (2010) 384-396.
2. J. Smagorinsky, General circulation experiments with the primitive equations, *Monthly Weather Review* 91 (1963) 99-164.
3. C. Dopazo and E. O' Brien, Functional formulation of nonisothermal turbulent reactive flows, *Physics of Fluids* 17 (1974) 1968.
4. C. J. Sung, C. K. Law, J. Y. Chen, Augmented reduced mechanisms for no emission in methane oxidation, *Combustion and Flame* 125 (2001) 906- 919.
5. L. Valino, A field Monte Carlo formulation for calculating the probability density function of a single scalar in a turbulent flow, *Flow turbulence and Combustion* 60 (1998) 157-172.
6. W. P. Jones and V. N. Prasad, Large Eddy Simulation of the Sandia Flame Series (D, E and F) using the Eulerian stochastic field method, *Combustion and Flame*, in press.

# DQMOM APPROACH FOR MODELING SOOT FORMATION OF C<sub>2</sub>H<sub>4</sub>/AIR TURBULENT NON-PREMIXED FLAME

T.H. Kim<sup>1</sup>, J. Lee<sup>1</sup>, Y. Kim<sup>1\*</sup>  
<sup>1</sup>Hanyang University, Korea  
[ymkim@hanyang.ac.kr](mailto:ykim@hanyang.ac.kr)

The Method of Moments (MOM) is one of the convenient and accurate methods in the statistical approach. This approach basically provides a means for modeling the particle probability density function using any number of low-order moments. The basic MOM is easy to handle the  $n^{\text{th}}$  moment's distribution but has difficulties to represent the poly-dispersion system. Another MOM called the Quadrature Method of Moments (QMOM) which was demonstrated to be an efficient and accurate method for tracking the moments of the particles distribution. But QMOM is hard to apply to multi-variable distribution. Hence, the most general and accurate MOM is the Direct Quadrature Method of Moments (DQMOM) which is based on the idea of tracking directly the variables appearing in quadrature approximation. DQMOM is easy to extend to the multi-variables case encountered in the poly-dispersion system. In this study, for the solution of the population balance equation, DQMOM has been adopted due to its inherent advantages in terms of accuracy and availability of extension for multiple inner-variables.

The population balance equation is a continuity statement represented in terms of a number density function. The number density function defines how a population of particles is distributed versus particular properties, called internal coordinates (inner-variable), to distinguish them from the particle external coordinates [1]. For simulation of soot formation using population balance equation, we set the number of spherules in each aggregate ( $N$ ) as inner-variable because it seems that soot aggregates are constituted by number of primary particles [3]. The present model is able to account import physical processes involved in soot formation and evolution mechanism such as nucleation, surface growth, oxidation and aggregation. These processes represent the particle dynamics characteristic when the number concentration of particles is high enough, they can collide and stick to each other and it has a decisive effect on soot volume fraction and particle's distribution. Fig. 1 shows these soot evolution mechanism at a glance.

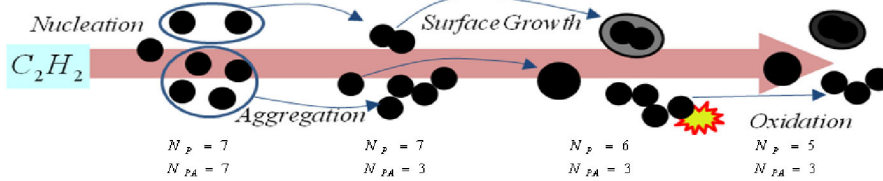


Fig. 1 Schematic of soot formation process

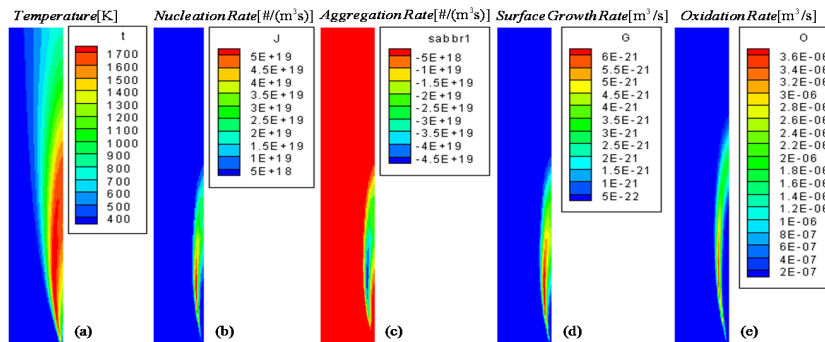


Fig. 2 Contour of Temperature (a), Nucleation (b), Aggregation (c) Surface growth (d), Oxidation rate (e)

In Fig.1,  $N_p$  is number of primary particles and  $N_{PA}$  is number of aggregates. The nucleation, surface growth oxidation rate affects the number of primary particles and aggregation makes soot aggregates. The number of primary particles loses their identity by surface growth rate and disappears by oxidation. This continuous rate of change doesn't affect the number of aggregates but change their size or shape. The related physical sub-models were proposed in the previous studies [4], [5], [6]. Fig. 2 shows the flame pattern of C<sub>2</sub>H<sub>4</sub>/AIR turbulent nonpremixed sooting flame such as temperature and rates of nucleation,

aggregation, surface growth, and oxidation rate. As would be expected, the nucleation and surface growth rate are high at fuel rich and high temperature region. The aggregation rate is high around at the location with the high soot particle concentration. The high level of oxidation rate exists at the outside oxygen-rich flame zone with the high temperature.

In this numerical simulation, turbulence is represented by the  $k-\varepsilon$  model, the mixture fraction based flamelet model is employed to account for the turbulent-chemistry interaction and the P-1 approach is utilized to model the radiation. To validate the present DQMOM approach, numerical results are compared with experimental data in terms of soot volume fraction, total aggregate number density, total primary particle number density and soot properties including mean radius of gyration and mean number of primary particles per an aggregate.

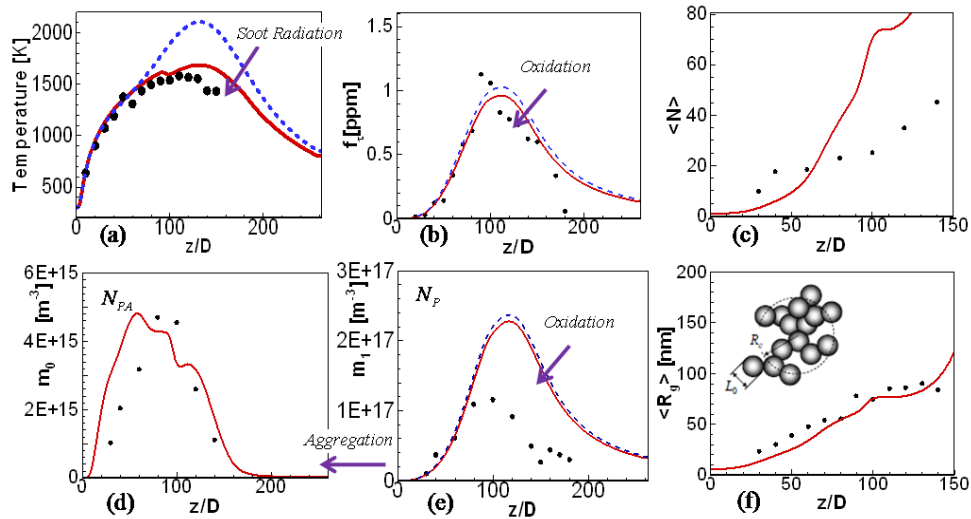


Fig. 3 Axial profiles along the centerline (a) temperature with soot radiation(solid-line), without radiation(dashed-line), (b) soot volume fraction(solid-line), without oxidation(dashed-line), (c) mean number of primary particles per aggregate (d) total aggregates number density, (e) total primary particles number density(solid-line), without oxidation(dashed-line), (f) mean gyration radius of aggregates.

Numerical results displayed in Fig. 3 (a) clearly indicate that the soot radiation considerably influences the flame structure. When the soot radiation is neglected in modeling this sooting flame, the temperature is substantially overestimated especially in the hot flame zone and downstream region. As shown in Fig 3(b) and 3(e), the present approach noticeably overestimates the soot volume fraction and the primary particles number density in the soot oxidation zone. These discrepancies are directly tied with the defects of the soot oxidation used in this study which does not account for the soot oxidation by OH. In terms of the soot aggregation process illustrated in Figures 3(d) and 3(f), the predicted results are reasonably well agreed with experimental data. These numerical results imply that the DQMOM approach has the great potential in dealing with the soot formation processes in the flame field.

- [1] D.L. Marchiso et al, 2008, "Investigation of soot formation in turbulent flames with a pseudo-bivariate population balance model", Chemical Engineering Science
- [2] D.L. Marchiso, R.O. Fox, 2005, "Solution of population balance equations using the direct quadrature method of moments" Journal of Aerosol Science 36, 43-73.
- [3] Koçylu et al., 2003, "Soot measurements at the axis of an ethylene/air non premixed turbulent jet flame", Combustion and Flame
- [4] Fairweather et al, 1992, "Predictions of radiative transfer from a turbulent reacting jet in a cross-wind" Combustion and Flame 89, 45-63.
- [5] Lee et al, 1962, "On the rate of combustion of soot in a laminar soot flame", Combustion and Flame 6.
- [6] N.A. Fuch, 1964, "Mechanics of Aerosols", Pergamon Press, New York.
- [7] T.H. Kim et al, 2010, "Numerical modeling of soot formation in C<sub>2</sub>H<sub>2</sub>/Air turbulent non-premixed flames using Direct Quadrature Method of Moments", The 40<sup>th</sup> KOSCO SYMPOSIUM

## MODELING OF TURBULENT NONPREMIXED FLAMES IN SUPERCRITICAL CONDITION

T.H. Kim<sup>1</sup>, S. Park<sup>1</sup>, Y. Kim<sup>1\*</sup>, S.-K. Kim<sup>2</sup>

<sup>1</sup>Hanyang University, Korea

<sup>2</sup>Korea Aerospace Research Institute, Korea

[ymkim@hanyang.ac.kr](mailto:ymkim@hanyang.ac.kr)

It has been widely recognized that droplet vaporization and spray combustion in supercritical conditions have long been matters of serious practical concern in the high-pressure combustors especially for the cryogenic liquid propellant rocket engines. The modeling of the droplet vaporization process under high-pressure conditions requires taking into account the additionally complex effects such as the real gas behavior, the variation of thermodynamic properties and the non-ideality of the latent heat of evaporation. Numerical modeling of near-critical mixing and combustion processes is a quite challenging task, due to the non-ideal thermodynamic effects and the abrupt variation of the transport properties. In the supercritical conditions, the surface tension and the vaporization heat approach zero, and the isothermal compressibility and the specific heat increase significantly. Compared to the subcritical propellant mixture properties, the propellant mixtures in the supercritical environment have the distinctly different characteristics such as liquid-like density, gas-like diffusivity.

The present study has been mainly motivated to numerically model the supercritical mixing and reacting flow processes encountered in the liquid propellant rocket engines. In the present approach, turbulence is represented by the  $k-\varepsilon$  turbulence model. In order to realistically represent the turbulence–chemistry interaction in the turbulent nonpremixed flames encountered in the supercritical propellant combustion processes, the flamelet approach based on the real-fluid flamelet library has been adopted. To account for the non-ideal thermodynamic effects, the propellant mixture properties are calculated by using SRK (Souve-Redlich-Kwong) equation of state model and this SRK model is validated against NIST data of oxygen thermodynamic properties presented in Fig. 1. The real-gas effects are incorporated in the present flamelet library. To validate the present physical and numerical model for the supercritical mixing and combustion processes, the RCM-1[1] and RCM-3[2] are chosen as the benchmark cases. By utilizing this SRK model, the real-fluid based flamelet library is generated.

Fig. 2 represents the non-reacting cryogenic N<sub>2</sub> jet injection [P=59.8bar, T=128.7K]. It can be clearly seen that the cryogenic N<sub>2</sub> jet has the distinctly different structure from the ideal state near injector. Numerical results predicted by the real-fluid flamelet model are well agreed with experimental data while ideal-gas flamelet model yields the erroneous distribution. Numerical results of GH<sub>2</sub>/LO<sub>x</sub> coaxial shear injector [P=60 bar, GH<sub>2</sub>(287K)/LO<sub>x</sub>(85K), O/F=1.43] are displayed in Fig. 3. The real-fluid based flamelet model predicts the essential features of the turbulent nonpremixed GH<sub>2</sub>/LO<sub>x</sub> flame at supercritical condition, compared to the ideal-gas flamelet model. Numerical results indicate that the present supercritical combustion model is capable of realistically predicting the mixing and reacting flow processes at the supercritical conditions.

[1] J. Telaar, G. Schneider, J. Hussong, W. Mayer, Cryogenic jet injection: Description of test case RCM 1, in: Proceedings 2<sup>nd</sup> International Workshop on Rocket Combustion Modeling, Lampoldshausen, Germany, March 25-27, 2001.

[2] Thomas JL, Zurbach S. Test case RCM-3: supercritical spray combustion at 60bar at Mascotte. In: 2nd International Workshop on Rocket Combustion Modeling. Lampoldshausen, Germany, 2001.

[3] G. Ribert, N. Zong, V. Yang, L. Pons, N. Darabiha, S. Candel, “Counterflow diffusion flames of general fluids: Oxygen/hydrogen mixtures”, *Combustion and Flame*, 319-330, 2008.

[4] L. Cutrone, P. De Palma, G. Pascazio, M. Napolitano, “A RANS flamelet-progress-variable method for computing reacting flows of real-gas mixtures”, *Computers & Fluids*, 485-498, 2010.

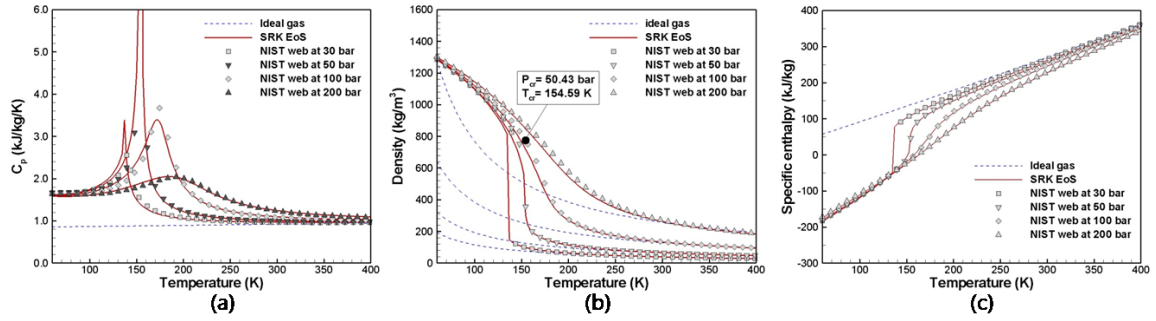


Fig. 1 (a) Specific heat, (b) Density and (c) Specific enthalpy of Oxygen with NIST data

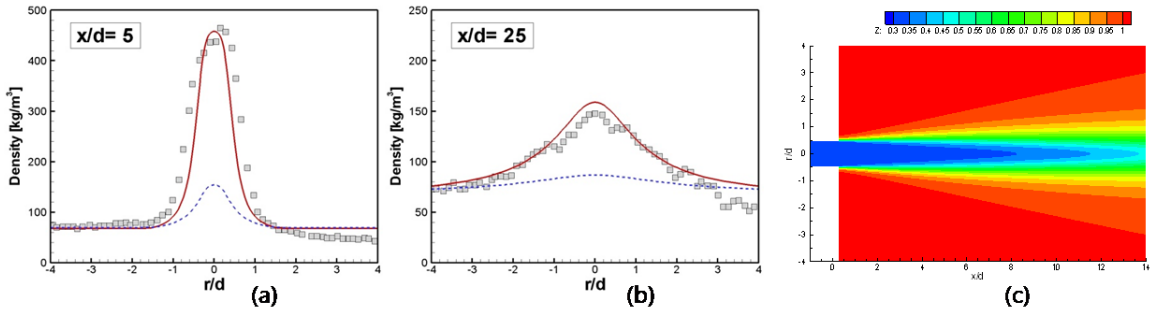


Fig.2 RCM 1 Case Results: (a), (b) Radial profiles of density (line: Real-fluid based flamelet model, dashed: Ideal-gas based flamelet model, points: measurements), (c) Compressibility factor near injector

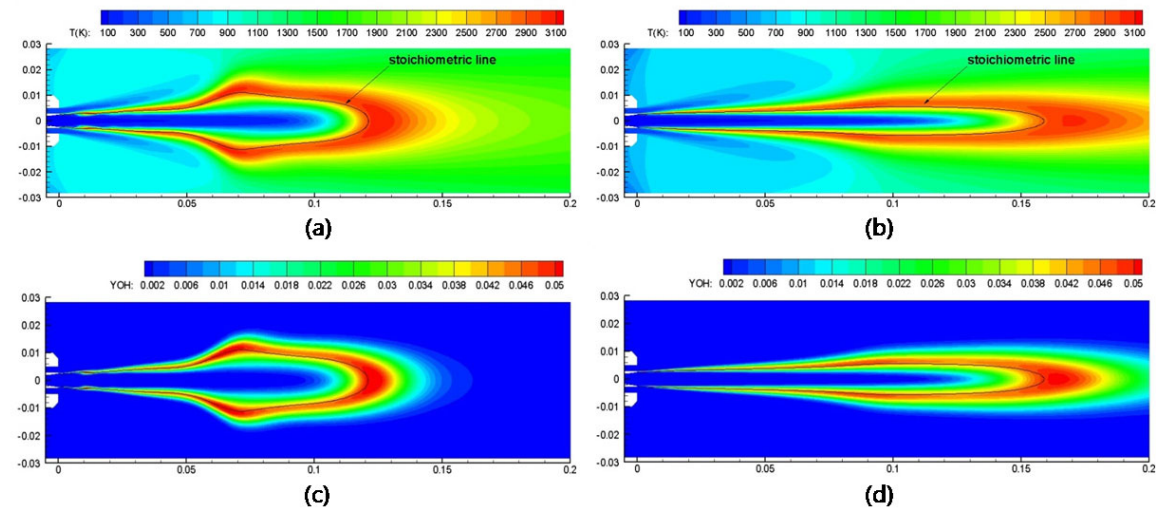


Fig. 3 RCM 3 Case Results: (a)Temperature and (c) OH mass fraction of Real-fluid based flamelet model, (b)Temperature and (d) OH mass fraction of Ideal-gas based flamelet model.

# A FLAMELET BASED MODEL FOR AUTO-IGNITION IN TURBULENT CONDITIONS: VALIDATION USING DNS

TNF 10 Workshop: Poster Submission

E. Knudsen<sup>1</sup>, E. S. Richardson<sup>2</sup>, H. Pitsch<sup>1</sup>, J. H. Chen<sup>2</sup>

<sup>1</sup>Stanford University, USA; <sup>2</sup>Sandia National Laboratories, USA

Corresponding author's email address: ewk@stanford.edu

In this study, a combustion model for large eddy simulation (LES) is analyzed and validated through comparison with a direct numerical simulation (DNS) of a non-premixed  $C_2H_4$  turbulent flame. The turbulent flame that is simulated tends to stabilize due to auto-ignition. In the context of turbulence, however, true asymptotic auto-ignition behavior is rarely observed. Rather, turbulent mixing tends to influence the ignition timescale and the evolution of combustion products.

Flamelet based models for LES that attempt to describe turbulence and auto-ignition interactions often make use of unsteady non-premixed flamelets. In statistically steady problems such as jet flames, this leads to modeling complexity. Either the time scale from a single unsteady flamelet must be correlated with the distance from the jet, or a time-like variable must be used to parameterize a large, computationally expensive set of unsteady non-premixed solutions. Here, these modeling issues are addressed by appropriately combining information from the pure steady non-premixed regime and from the pure auto-ignition regime. Separating these regimes eliminates the need to interpret the unsteady time scale, and dramatically reduces the computational memory needed for chemistry storage.

The case that is considered is a lifted  $C_2H_4$  flame with a jet Reynolds number of  $Re=10,000$ . This flame is not an experimental case, but is rather the subject of a compressible DNS study by Yoo *et al.* (*Proc. Comb. Inst.* 2010). The DNS employs high order numerics, a 1.29 billion cell mesh, and a 22 species mechanism describing  $C_2H_4$  combustion. Schematics of both the DNS and LES are shown in Fig. 1. Results of the DNS demonstrated that, at the high temperature of the air coflow, auto-ignition is the primary flame stabilization mechanism. Additionally, however, results showed that turbulent mixing could locally inhibit the auto-ignition process, and that this inhibition led to an oscillating flame stabilization point.

LES runs of this flame are performed on meshes consisting of between 1.4 million and 7.1 million cells. These runs use a combination of auto-ignition solutions and steady non-premixed flamelet solutions to describe quantities such as the density and the progress variable source term. In general, solutions from these different regimes may be locally combined using a method proposed by Knudsen and Pitsch (*Comb. Flame* 2009). This method determines the combustion regime by explicitly considering which transport processes balance the chemical source term. Once known, information about the combustion regime can be used to map tabulated chemistry solutions into the flow field. This method has the ability to quantitatively relate the importance of auto-ignition and mixing.

Two LES runs have been performed to determine whether the limiting cases of this modeling approach bound the DNS results. In both of these runs the density is mapped into the LES flow field according to

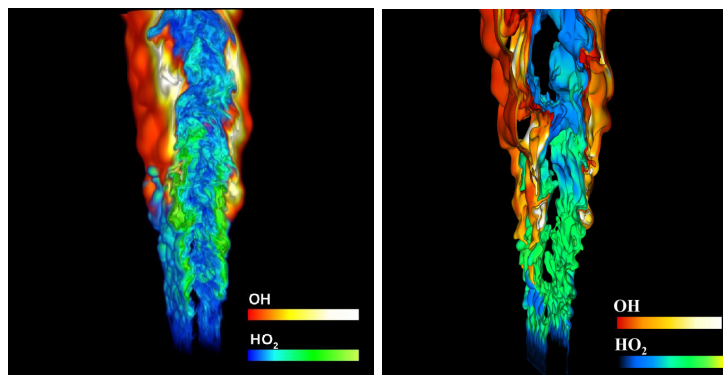


Figure 1: OH and  $HO_2$  radicals in the DNS (Left), and in the LES (Right).

the local combustion regime. In the first run, however, the progress variable source term is taken solely from auto-ignition chemistry solutions. Conversely, in the second run the source term is taken solely from non-premixed flamelets. Time averaged results from the simulations are compared with the DNS in Fig. 2.

Figure 2 shows that the auto-ignition and steady non-premixed limits do envelop the DNS solution, and that both regimes are important. For example, at locations close to the jet nozzle (small  $X/H$ ), the LES based on the auto-ignition source terms over-predicts the temperature in the DNS. This over-prediction occurs because the source term is not directly affected by dissipation and is relatively large. Conversely, the non-premixed source terms are affected by the dissipation rate in flamelet space. LES values based on these non-premixed source terms correctly predict temperature near the nozzle, but under-predict it at downstream (large  $X/H$ ) locations. This is consistent with the DNS observation that auto-ignition processes occur in the flame, and that they must be accounted for if the lift off height is to be predicted.

LES runs that use combustion regime information to appropriately combine progress variable source terms are now being performed, and will be presented. The agreement between these runs and the DNS results will be analyzed, and the implications for the regime selection model will be highlighted. The full resolution flow information available from the DNS solution will be mined to understand any discrepancies.

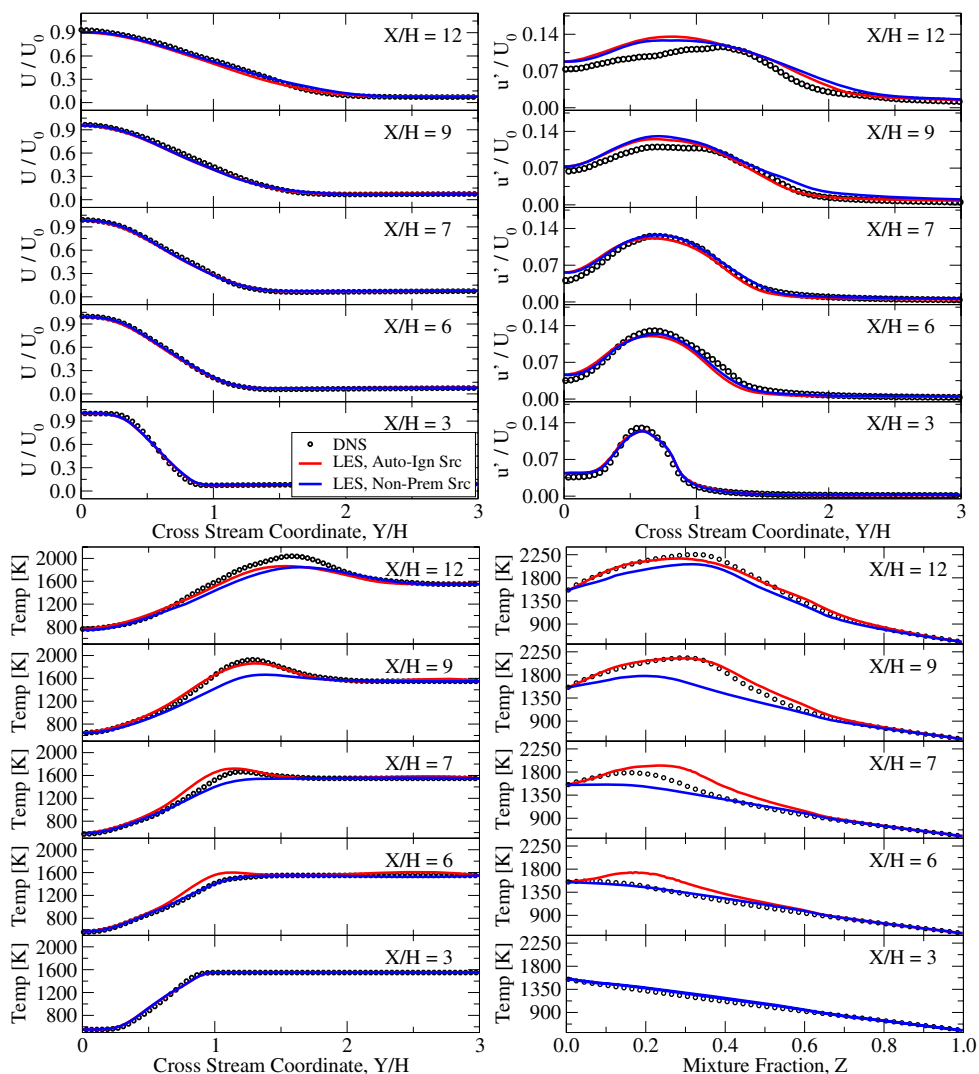


Figure 2: Time averaged axial velocity (upper left), velocity fluctuations (upper right), temperature (lower left), and conditional temperature (lower right) in the  $C_2H_4$  flame. DNS data is compared to LES data where the progress variable source term is taken either from 0-D auto-ignition calculations (red line), or from steady non-premixed flamelets (blue line).

# LES OF A LEAN PREMIXED STRATIFIED BURNER USING A THICKENED FLAME APPROACH COUPLED WITH FGM TABULATED CHEMISTRY

G. Künne, A. Ketelheun, J. Janicka

Institute for Energy and Power Plant Technology, Darmstadt University of Technology, Germany

[kuenne@ekt.tu-darmstadt.de](mailto:kuenne@ekt.tu-darmstadt.de)

Stratification (i.e. non-uniform mixture distribution) can be observed in various technical applications either due to incomplete mixing or intentionally to improve the efficiency such as in direct injection IC engines. Within this work a new burner<sup>1</sup> designed to explore stratification effects is investigated numerically. The configuration including the boundary conditions is depicted in figure 1 where a section of the computational grid has been added to illustrate the blocking strategy. In the inner tube a pilot flame is stabilized by a flame holder to ignite the premixed fresh gases issuing from the concentric annular slots. These slots operate at different equivalence ratios of the methane-air mixture to generate the stratification. The burner is placed inside an air coflow to create defined boundary conditions and prevent penetration by dust particles. To minimize the sensitivity related to boundary conditions the upstream geometry as shown in figure 1 has been included into the computational domain.

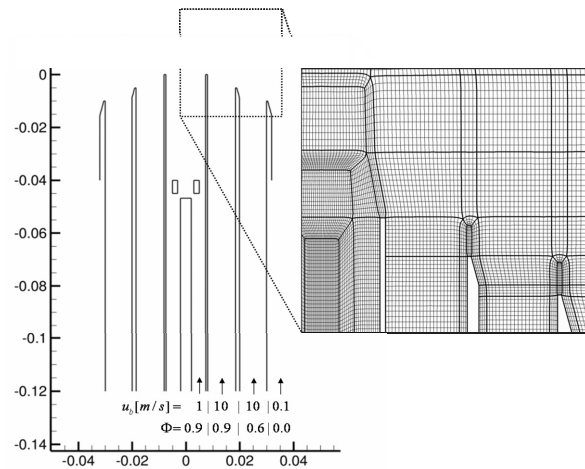


Figure 1

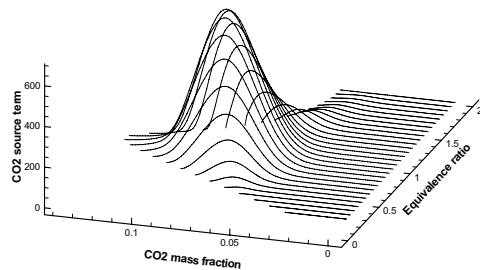


Figure 2

source term is shown as a function of these controlling variables. Simulations of one dimensional flames were used to verify the coupling of the tabulated chemistry and the LES-solver where important features as the grid dependence of flame propagation were carefully addressed.

Two cases will be presented on the poster. The first one is the isothermal case TSF\_A\_i2. Results for this case are given in Figure 3 where the mean and standard deviation of the axial velocity is shown in comparison with experimental data. Overall, there is a good agreement indicating that the upstream geometry can be sufficiently represented by the numerical grid and that the boundary conditions are well defined. These results form a good basis for the reacting flow simulations since an accurate prediction of the unburnt gas velocity is very important to assess the correct flame propagation. The

For the reactive flow simulation the thickened flame approach<sup>2</sup> has been implemented in the academic code FASTEST which uses block-structured, hexahedral, boundary fitted grids to represent complex geometries. For the accurate prediction of the mixing process upstream of the reaction layer the dynamic formulation based on a flame sensor is used for the thickening. To include detailed chemistry effects the model is coupled with FGM (Flamelet Generated Manifolds) tabulated chemistry<sup>3</sup>. The two-dimensional manifold to describe mixing and reaction is parameterized using the mixture fraction and CO<sub>2</sub> mass fraction as progress variable.

The tabulation is illustrated in figure 2 where the CO<sub>2</sub>

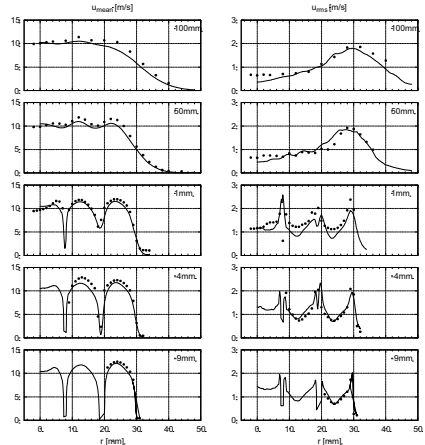


Figure 3

second configuration is the reacting case TSF\_A\_r with the boundary conditions depicted in figure 1. As a first step regarding the reactive flow, the primary goal is to quantify whether or not the simulation is able to predict the correct flame behaviour (e.g. mixing, flame position, turbulent flame brush). In addition, it is of interest how the effect of stratification modifies the flame and to evaluate the consequences for the combustion model.

In figure 4 the instantaneous field of the chemical source term is shown. Here, the pilot flame above the flame holder can be observed. The hot exhaust gases exiting the pilot tube enable the formation of the stratified flame illustrated by isolines of the mixture fraction. In this figure two differing combustion situations can be observed. In region 1 a homogeneous premixed flame can be observed while in region 2 the mixing layer is interacting with the reaction zone. In this region different alignments of mixture fraction and progress variable can be observed (isolines are either orthogonal, parallel or at an angle to each other). To illustrate these different zones figure 5 shows the reaction path extracted along straight lines through the chemical source term\*. Here a two-dimensional plot of figure 2 is shown where the two paths through the flame have been added and one can clearly see the different behavior of both regions while proceeding from the unburnt to the burnt state.

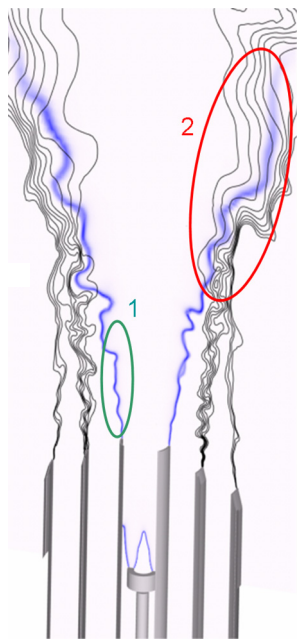


Figure 4

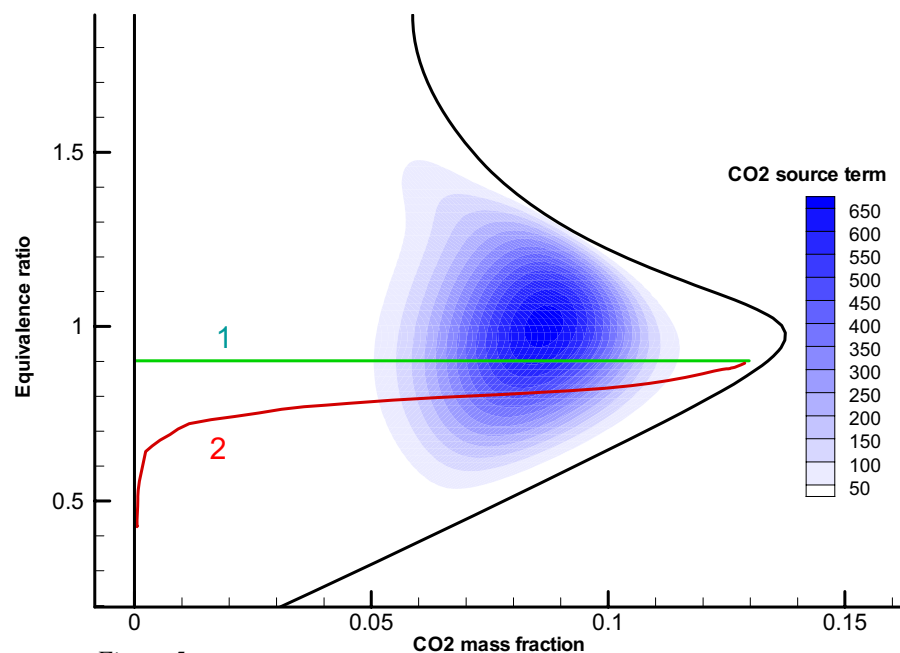


Figure 5

Results of velocity, temperature and species obtained on two different grids containing 0.9 million and 6.5 million grid points, respectively, will be compared with experimental data up to 200mm above the burner exit. Details about the measurements of scalar quantities recently obtained by 1D-Raman/Rayleigh scattering will also be presented at the TNF on the poster from F. Seffrin et al..

1. F. Seffrin et al., *Combust. Flame* 157: 384-396.
2. O. Colin et al., *Phys. Fluids* 12: 1843-1863.
3. J. A. van Oijen et al., *Combust. Flame* 127: 2124-2134.

\* This should be seen as a qualitative illustration since the correct chemistry path to evaluate the effect of stratification is difficult to choose in this situation.

## COMPARISON OF FLAME SURFACE DENSITY MODELS FOR LES

T. Ma and A.M. Kempf

*Imperial College London, UK*  
*[a.kempf@imperial.ac.uk](mailto:a.kempf@imperial.ac.uk)*

Premixed combustion is a common trend in the design of combustion devices for power generation, as it permits to reduce harmful pollutants from burning fossil fuels. Large Eddy Simulation (LES) is a powerful tool in the prediction of turbulent reactive flows in these devices and its concept involves explicitly computing large-scale structures whilst modeling the effect of small-scale structures below a certain filter width. In its application to premixed combustion, the flame front is generally too thin to be resolved on the computational mesh and so a model for the reaction rate closure is required. The combined effect of the molecular diffusion and reaction rate can be modelled as a function of the generalised flame surface density  $\Sigma_{gen}$  [1], which in itself can be expressed as the product of the wrinkling factor  $\Xi$  and the gradient of the progress variable  $|\nabla\bar{c}|$ , or as a constant multiplied by  $\bar{c}(1-\bar{c})$ . The latter expression is similar to the classical Bray-Moss-Libby (BML) formulation that is used widely in the context of RANS [2], but is adjusted for the LES context with variables of filter width and a model constant. An alternative definition for  $\Xi$  is the ratio of turbulent to laminar burning velocity and various models for this parameter exist as listed in [3]. Eleven models as outlined and extended for LES by Chakraborty and Klein [3], were applied to a well known plane symmetric dump combustor known as the ORACLES rig [4], taking into account the combustion instabilities that arose in the experiment. A schematic of the rig is shown in Fig. 1 with the computational domain highlighted by the dashed line.

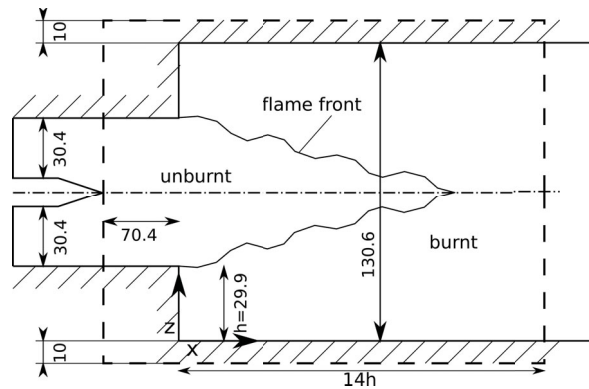


Fig. 1 Schematic of the ORACLES rig (not to scale). Dashed line denote computational domain.

Experimental data consisted of mean and instantaneous velocities for the stream-wise and transverse directions at various points inside the combustor. The LES of this rig was carried out using an in-house code ‘PsiPhi’ and the non-reactive case was examined first to ascertain the level of accuracy that LES can deliver. A grid sensitivity study has also been carried out for both reactive and non-reactive cases with approximately 1.60, 0.48, and 0.20 million cells corresponding to isotropic grid resolutions of 2mm, 3mm and 4mm respectively. It has been found that there is generally good agreement between numerical and experimental results for the non-reactive case. The asymmetric nature of the mean flow, as well as the fluctuating velocity peaks behind the backward facing steps, are well captured with grid refinement. For the reactive case, two complications are introduced: the combustion instability that was found in the experiment, and an unrealistically thick flame brush from LES. These two features can be illustrated by an instantaneous visualisation of the flame in Fig. 2(a). Similar to previous work [5], the instability was emulated by introducing pulsing at the inflow with amplitude of 27% bulk velocity and frequency of 50Hz to match experimental RMS velocity values. The pulsing induces an excitation that creates large pockets of unburnt gases that travel a fairly long distance downstream in the combustor. To resolve the issue of a thick flame brush, a higher turbulent viscosity was used, by applying a 2x and 4x higher

Smagorinsky constant ( $C_s$ ) than the normal value of 0.173. This helps to allow faster dissipation of smaller eddies and therefore avoids the thickening of the flame brush through the smallest eddies. The visualisations of the flame (Fig. 2) do indeed show a reduction in the flame brush thickness as well as in the amount of wrinkling.

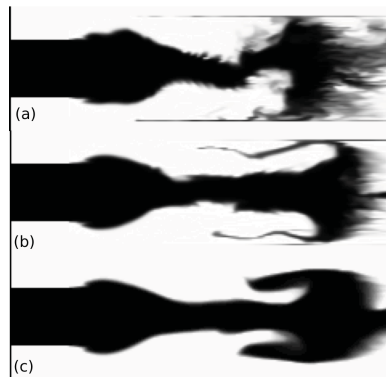


Fig. 2 Instantaneous visualisations of the flame brush for (a)  $C_s = 1 \times 0.173$ , (b)  $C_s = 2 \times 0.173$  and (c)  $C_s = 4 \times 0.173$

The reactive case comparison of FSD models using the fine grid at two locations ( $x = 2h$  and  $x = 7h$ ) is shown in Fig. 3. With the exception of one model, the simulated results show good agreement to experimental data. Using  $\sum_{gen} = |\nabla \bar{c}|$  (denoted by ‘GradC’ in Fig. 3) significantly under-predicts the filtered reaction rates due to the omission of the wrinkling factor, but the proximity of the LES results to the experimental data suggests that most of the wrinkling is actually resolved on the fine grid.

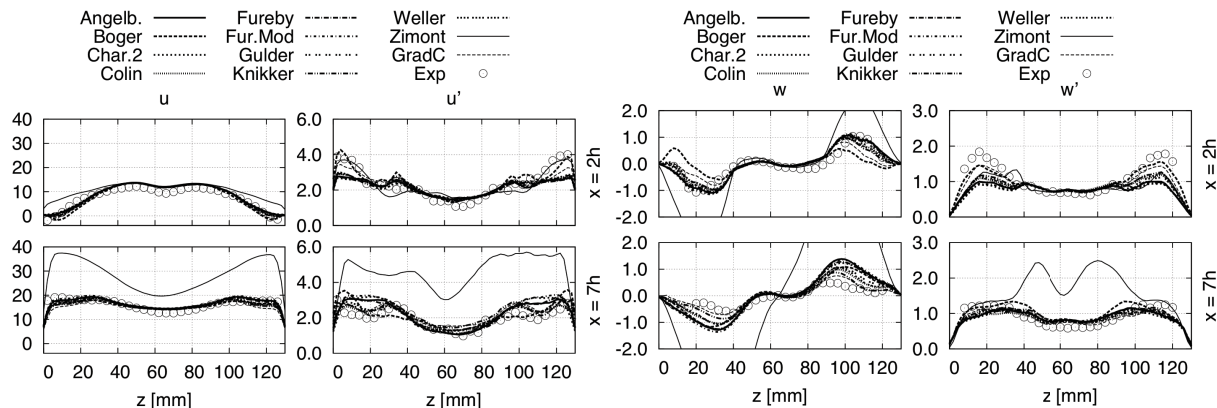


Fig. 3 Mean and fluctuating velocities in axial and transverse directions at locations  $x = 2h$  and  $x = 7h$

A clearer assessment of the models’ performances was gained from a detailed error analysis from which there is little indication of the best performing model, and one can conclude that the majority of the models describe the reaction rate to a reasonable extent.

- [1] M. Boger, D. Veynante, H. Boughanem, and A. Trouvé, *Sym. (Int.) Combust., [Proc.]* **27**, 917 (1998)
- [2] K. Bray, M. Champion, P. Libby, *Springer, New York*, 541-563
- [3] N. Chakraborty and M. Klein, *Phys. Fluids.*, **20**, 085108 (2008)
- [4] P. Nguyen, P. Bruel, and S. Reichstadt, *Flow Turb. Combust.*, **82**, 155-183 (2009)
- [5] C. Duwig and C. Fureby, *Combust. Flame.*, **151**, 85-103 (2007)

## LES-CMC Modelling of Turbulent Non-Premixed Flames with Rate-Controlled Constrained Equilibrium (RCCE) and Level of Importance (LOI) Mechanism Reduction

Salvador Navarro-Martinez<sup>1\*</sup>, Terese Løvås<sup>2,3</sup> and Stelios Rigopoulos<sup>4</sup>

<sup>1</sup>Department of Mechanical Engineering, Imperial College London  
Exhibition Road, South Kensington, London, SW7 2AZ, UK

<sup>2</sup>Department of Energy and Process Technology, Norwegian University of Science and Technology  
Kolbjorn Hejes vei 1b, 7491 Trondheim, Norway

<sup>3</sup>School of Engineering and Material Sciences, Queen Mary University of London  
Mile End Road, London E1 4NS, UK

<sup>4</sup>School of Mechanical, Aerospace and Civil Engineering, The University of Manchester  
PO Box 88, Sackville Street, Manchester M60 1QD, UK

Simulation of turbulent flames presents a major challenge in combustion modelling. The two main stumbling blocks are the treatment of the turbulence-chemistry interaction and the modelling of combustion chemistry. With respect to the first, a number of models (eddy dissipation, steady/unsteady flamelet, conditional moment closure - CMC, transported probability density function - PDF) exist to provide closure at varying levels of detail. Most of these models were originally developed in the context of Reynolds-Averaged Navier Stokes (RANS), but in recent years their coupling with Large Eddy Simulation (LES) has been investigated and found to yield very good predictions of combustion in situations where the large-scale structure of the flow field plays an important role in determining the mixing and reacting processes.

The modeling of combustion chemistry remains a major problem, particularly in advanced combustion models, as a large number of integrations of the chemical kinetics ODEs must be performed during a flame simulation. For comprehensive kinetic modeling, both the major and intermediate species must be resolved dynamically, resulting in a very large number of ODEs (e.g. about 60 for methane, much more for complex fuels) which are also very stiff. Mechanism reduction, i.e. the derivation of models that incorporate the main features of combustion chemistry while involving a small number of variables, is a necessity for practical turbulent combustion simulations. The traditional way to carry out mechanism reduction is by eliminating of species and reactions based on quasi-steady state approximations (QSSA) and partial equilibrium assumptions respectively, a procedure that requires considerable chemical insight and must be carried out for each mechanism individually. Recently, interest has arisen in systematic methods of mechanism reduction, and the literature on mechanism reduction approaches has grown considerably (see e.g. the reviews by Tomlin et al. [1] and by Lu and Law [2] for a review of various approaches).

In this poster we present results of the application of the Rate-Controlled Constrained Equilibrium (RCCE) approach for mechanism reduction to turbulent non-premixed flames, coupled with an LES-CMC approach for modeling of the turbulent flow and turbulence-chemistry interaction. The RCCE concept dates from the 70's [3] and has been recently developed further and applied to laminar non-premixed [4] and premixed [5] flames. Assuming that some species are governed by much shorter timescales than others, the principle of RCCE can be phrased as follows: the 'fast' species are assumed to be temporarily in an equilibrium state which is constrained by the concentrations of the leading species and can therefore be called a "constrained equilibrium state". As the reacting system evolves, so do the constraints for this state - i.e. the concentrations of the leading species - according to the differential

---

\* email: s.navarro@imperial.ac.uk

equations of chemical kinetics, while the 'fast' or 'equilibrated' species are computed by the algebraic equations of constrained equilibrium. Thus the dynamical evolution of the system is governed by a set of differential-algebraic equations, where the algebraic equations force the system to evolve on a manifold which is parametrised by the selection of leading species. RCCE is not a method for investigating the time-scale separation, but rather a method that yields a system of differential-algebraic equations (DAEs) describing the reduced system given a certain selection of fast and slow species, like QSSA and partial equilibrium. A major advantage of RCCE is that it results in a general system of DAEs, readily parametrised by the selection of fast and slow species, which does not need to be derived for each reduced mechanism individually. The selection of fast/slow species, or equilibrated/constrained in the RCCE terminology, can be made either based on traditional heuristics or on systematic methods such as CSP [6] or Level-of-Importance (LOI) [7].

The results presented in this poster include both heuristically-derived RCCE mechanisms and mechanisms where the RCCE constraints have been selected with the aid of the LOI approach. The former approach is applied to an investigation of the Cabra flame, which has been previously simulated by a number of authors (e.g. [8]). Results for this flame highlight its sensitivity to chemistry, as previously reported [8], while when more species are considered, the flame burns sooner, therefore moving the lift-off height upstream. The differences arise from the errors in the chemical models associated with the low temperature transition. The latter approach is applied to a turbulent non-premixed ethylene flame, and the reduced schemes capture very well the instantaneous structure of the flame. Overall, the poster demonstrates the potential of the RCCE and RCCE-LOI approaches to provide a comprehensive framework for the implementation of chemistry in turbulent LES-based combustion models.

## References

- [1] A. Tomlin, T. Turanyi, M. Pilling (1997), Mathematical Tools for the Construction, Investigation and Reduction of Combustion Mechanisms, in: R.G. Compton, G. Hancock and M.J. Pilling, Editors, Comprehensive Chemical Kinetics Vol. 35, Elsevier, New York, NY, 1 p283
- [2] T. Lu, C. K. Law (2009), Toward accommodating realistic fuel chemistry in large-scale computations Progress in Energy and Combustion Science 35 (2), pp. 192-215
- [3] J. C. Keck and D. Gillespie (1971), Rate-controlled partial-equilibrium method for treating reacting gas mixtures. Combust. Flame, 17(2):237–241,
- [4] W. P. Jones and S. Rigopoulos (2005) Rate-controlled constrained equilibrium: Formulation and application to nonpremixed laminar flames. Combust. Flame, 142(3):223–234.
- [5] W. P. Jones and S. Rigopoulos (2007) Reduced chemistry for hydrogen and methanol premixed flames via rcce. Combustion Theory and Modelling, 11(5):755–780, 2007.
- [6] S. H. Lam and D. Goussis (1988), Understanding complex chemical kinetics with computational singular perturbation. Proc. Combust. Inst., 22:931–941.
- [7] T. Løvås, D. Nilsson, F. Mauss (2000), Automatic reduction procedure for chemical mechanisms applied to premixed methane/air flames, Proc. Comb. Inst. 28 1809-1817.
- [8] K. Gkagkas and R. P. Lindstedt (2007), Transported PDF modelling with Detailed Chemistry of Pre and Auto-Ignition in CH<sub>4</sub>/Air mixtures. Proc. Combust. Inst., 31:1559–1586

# Transported PDF modeling of a lifted $H_2/N_2$ jet flame in a vitiated coflow using detailed chemistry: study of some numerical accuracy issues

Bertrand Naud

Modelling and Numerical Simulation Group, Energy Department, Ciemat, Madrid, Spain  
*bertrand.naud@ciemat.es*

Joint velocity-composition probability density function (PDF) modeling of the lifted turbulent  $H_2/N_2$  jet flame in vitiated coflow (Cabra burner) [1] using detailed chemistry is considered. The purpose of this poster is to focus attention on numerical issues that can have special relevance in this flame where autoignition plays an important role. On the one hand, different transported PDF calculations are performed where some numerical settings are varied (tolerance error in chemistry integration, time steps values). On the other hand, the simplified configuration of a Partially Stirred Reactor (PaSR) is considered in order to study the different errors in more detail.

The integration of the evolution of the composition vector due chemical reaction is done using the DDASSL solver [2]. A first numerical issue consists in using a low enough tolerance error in this case where autoignition may suppose particularly stiff points to integrate. Figure 1 shows results from two different transported PDF calculations. The value  $1.e-8$  seems to be low enough (as in PaSR calculations). Nevertheless, in the whole study we use the value  $1.e-9$ .

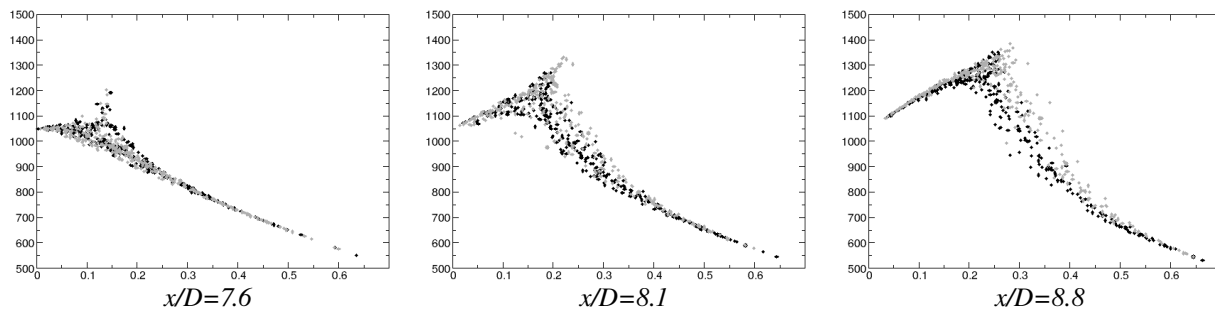


Figure 1: Scatter plots of temperature against mixture fraction at different axial locations around the ignition point (joint velocity-composition PDF calculation with EMST mixing model). Black dots:  $ATOL=1.e-9$  / Grey dots:  $ATOL=1.e-8$ .

One of the main purpose of this study is to consider the “splitting error”, the error related to the use of fractional steps [3] for the integration of the Lagrangian evolution of particle properties, where mixing and reaction are treated successively.

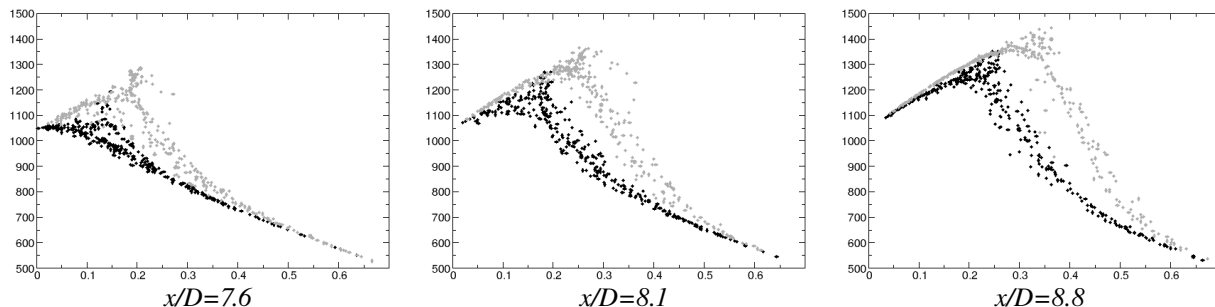


Figure 2: Scatter plots of temperature against mixture fraction as in Fig. 1. Black dots: standard local time step  $\Delta t(CFL)$  / Grey dots:  $\Delta t(CFL)/10$ .

Autoignition implies very short time scales and this error could be more important than for other turbulent flames. This seems to be observed in Figure 2 which shows that by reducing the time step by a factor 10, the flame numerically ignites earlier.

In order to better study this error, a PaSR is considered corresponding to the conditions of the vitiated  $H_2/N_2$  flame where one stream of oxidizer (mixture fraction  $Z = 0$ ) and one stream of fuel/oxidizer mixture at  $Z = 0.4$  enter with mass flow rates such that the mean mixture fraction of the PaSR is 0.05. We specify a turbulent frequency value of  $\omega = 2500s^{-1}$  (typical for the ignition zone of the flame considered) and a residence time of  $6 \cdot 10^{-4}s$ . First, different calculations are performed with the IEM mixing model, since in this case we can make the integration of mixing and reaction together (without the need of fractional steps). We verify that a time step of  $\Delta t = 2 \cdot 10^{-7}s$  is small enough in order to make the splitting error negligible (not shown here). Figure 3 shows the importance of the splitting error when using the EMST mixing model.

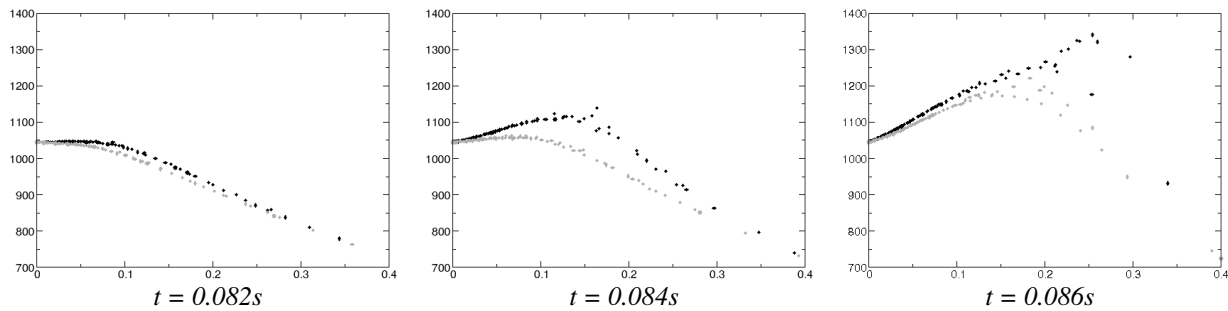


Figure 3: Scatter plots of temperature against mixture fraction at different times in the PaSR. Black dots:  $\Delta t = 2 \cdot 10^{-6}s$  / Grey dots:  $\Delta t = 2 \cdot 10^{-7}s$ .

Finally, we consider the errors due to the use of a finite number of particles (statistical and bias errors). We make two PaSR calculations with EMST mixing model and  $\Delta t = 2 \cdot 10^{-7}s$ , either with 100 particles (as in the previous results), either with 10000 particles. Instead of plotting the results at the same time as in Figure 3, we rather plot the results at different times in Figure 4 in order to better reflect the difference in autoignition time.

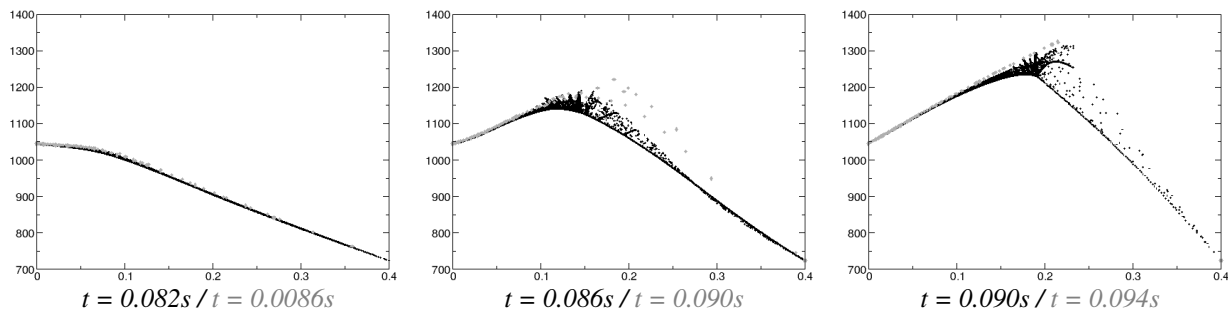


Figure 4: Scatter plots of temperature against mixture fraction in the PaSR with different number of particles. Grey dots: 100 particles / Black dots: 10000 particles.

[1] R. Cabra, T. Myhrvold, J.Y. Chen, R.W. Dibble, A.N. Karpetis, R.S. Barlow, *Proc. Combust. Inst.* 29 (2002) 1881-1888.

[2] L.R. Petzold, *Proc. IMACS World Congress* (1982).

[3] S.B. Pope, *Prog. Energy Combust. Sci.* 11 (1985) 11-119.

# LES of lifted flames in a gas turbine model combustor using top-hat filtered PFGM chemistry

C. Olbricht, O. T. Stein, J. Janicka, J. A. van Oijen, S. Wysocki, A. M. Kempf  
a.kempf@imperial.ac.uk

Progress variable approaches permit the cost effective large eddy simulation (LES) of complex industrial combustion systems, where assumed shape filtered density functions ( $\beta$ -FDFs) are widely used to account for sub-grid scale effects. Floyd et al. [1] have shown that for a well-resolved LES, a top-hat (TH) FDF will result in a more accurate description of the subgrid distribution. In this study a new modelling approach for the LES of partially premixed combustion is used. The approach is based on top-hat filtered premixed flamelet-generated manifolds (TH-PFGM), which are consistent with the LES methodology.

A Premixed Flame-Generated Manifold (PFGM)  $\Psi_j$  is constructed from a set of pre-calculated laminar premixed flamelets at equivalence ratios within the burning limits [2]. The thermo-chemical state  $\Psi_j = f(T, Y_\alpha, \rho, \nu\dots)$  is then described by the mixture fraction and the evolution of one or more progress variables. A progress variable  $\mathcal{Y}$  is typically a linear combination of the product species mass fractions  $Y_\alpha$  weighted by  $w_\alpha$ , according to  $\mathcal{Y} = \sum_\alpha w_\alpha Y_\alpha$ .

In a well-defined look-up table the progress variable must increase monotonically with the reaction progress for each flamelet. The PFGM  $\Psi_j$  is then parameterised by the mixture fraction  $f$  and the progress variable  $\mathcal{Y}$ . The source term and the equilibrium value of the progress variable are evaluated by summing up the weighted contributions of the product species  $\mathcal{Y}_{eq} = \sum_\alpha w_\alpha Y_{\alpha,eq}$  and  $\mathcal{S} = \sum_\alpha w_\alpha S_\alpha$ .

Since flamelet solutions cannot be obtained away from the flammability limits, an extrapolation has to fill the whole range of mixture fractions from 0 to 1. A technique, developed by Ketelheun and Olbricht [3, 4], was chosen that considers the thermo-chemical behaviour of each variable. The species mass fractions  $Y_i$  and hence the progress variable are extrapolated linearly, whereas the density  $\rho$  and the molar mass of the gas mixture  $M_{mix}$  follow a hyperbolic law for mixing. The temperature was calculated from the

density according to the perfect gas law. In this work the species mass fraction of  $\text{CO}_2$  was chosen for the progress variable, which is a fairly sensitive indicator of the reaction progress over a wide range of the flame.

TH-PFGM is applied to a lifted swirl flame in a model gas turbine combustor [5, 6], as shown in fig. 1. A central fuel port provided compressed natural gas ( $\approx 96\%$  methane) with a low inlet velocity. A thin sheet separated the fuel port from a co-axial annulus through which preheated air was fed to the combustion chamber with a high inlet velocity. The species measurements were conducted using traversing gas sampling probe, temperatures were measured using thermocouples and a LDV system was used to measure the velocities.

The PsiPhi LES program is used for the numerical modelling [7, 8]. The effect of subgrid scale turbulence is represented by the classical Smagorinsky model. Two different grid resolutions were used and are summarized in table 1. The time step width was adjusted to meet a relatively stringent CFL number of 0.15 that was required by the reaction model.

Using the top-hat FDF, the pre-integration of the chemistry table can be performed without any numerical difficulty and without adding any further dimensions to the table. Therefore, a top-hat integrated table has only half as many dimensions compared to a table created from any other FDF (except Dirac Delta), so that table access is fast and storage requirements are low. (These advantages only apply to LES, as a top-hat function is not a suitable representation of the PDF in RANS.)

Results show that THFGM captures the flame lift off dynamics governed by a low frequency penetration of the flame into the fuel supply leading to fluid acceleration and - in turn - flame lift off [6]. The statistical data for flow and species concentration fields from LES are in good accordance with the experimental evidence.

Figure 1 shows the upstream part of the computational domain and an instantaneous snapshot of the

temperature field from LES, where white represents hot regions. It can be seen that the flame partially penetrates the fuel supply and attaches to the separation sheet between the fuel port and the annulus in the upper half of the combustor, while the flame is lifted from the rim in the lower half.

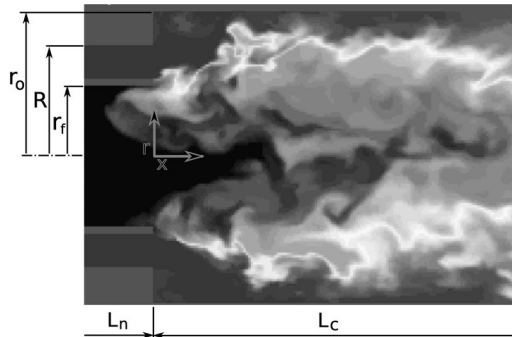


Figure 1: Temperature contour from the LES of the model gas turbine combustor [6] (inlet section). The computational domain includes a part of the nozzle of length  $L_n$  and the length of the combustion chamber is  $L_c$ .

Figure 2 presents radial profiles of the  $\text{CO}_2$  (left) and CO (right) mole fraction. The comparison of simulation and experiments for both combustion products is encouraging, with the experimental profiles captured well throughout the combustor, except for the peak of the CO mole fraction at  $x/R = 0.21$ . It is interesting to note that downstream at  $x/R = 7.47$  the CO mole fraction near the axis is considerably higher than the corresponding value of  $\text{CO}_2$ . This possibly stems from the fact that most of the oxygen is depleted in the annular region, as was demonstrated in fig. 2 (right), leading to a lack of oxygen to convert CO into  $\text{CO}_2$  near the axis.

Overall, the TH-PFGM method was shown to work well, it is computationally highly efficient, easy to implement, and consistent with the LES approach - as opposed to models based on the  $\beta$ -function.

Table 1: LES grid resolutions

grid	$n_x$	$n_y$	$n_z$	$n_{tot}$	$\Delta$
coarse	260	64	64	1,064,960	2 mm
fine	484	128	128	7,929,856	1 mm

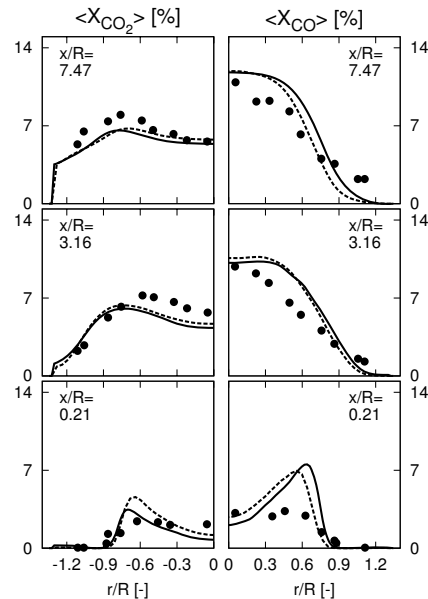


Figure 2: Radial profiles of  $\text{CO}_2$  (left) and CO (right) mole fractions at three downstream locations  $x/R$ . (●) experiments, (--) coarse grid, (—) fine grid.

## References

- [1] J. Floyd, A. M. Kempf, A. Kronenburg, R. H. Ram, *Combust. Theory Modelling* 13 (2009) 559–588.
- [2] J. van Oijen, *Flamelet-Generated Manifold: Development and application to premixed laminar flames*, Ph.D. thesis, Technische Universiteit Eindhoven (2002).
- [3] A. Ketelheun, C. Olbricht, F. Hahn, J. Janicka, in: *ASME Turbo Expo: Power for Land, Sea and Air*, Orlando, USA, 2009.
- [4] C. Olbricht, *Numerische Berechnung technischer Verbrennungssysteme*, Ph.D. thesis, TU Darmstadt, Germany (2009).
- [5] H. Pitsch, M. Ihme, *43rd AIAA Aerospace Science Meeting and Exhibit*, Reno, NV, 2005.
- [6] F. K. Owen, L. J. Spadaccini, C. T. Bowman, *Proc. Combust. Inst.* 16 (1976) 105–117.
- [7] A. M. Kempf, *Large-Eddy Simulation of Non-Premixed Turbulent Flames*, Ph.D. thesis, TU Darmstadt (2003).
- [8] M.W. Pettit, B. Coriton, A. Gomez, A. M. Kempf, *Large-Eddy Simulation and Experiments on Non-Premixed Highly Turbulent Opposed Jet Flows*, accepted for Proc. Combust. Inst. (2010)

# FLAME STABILISATION OF THE DELFT JET-IN-HOT-COFLOW FLAMES

E. Oldenhof, M.J. Tummers, E.H. van Veen, D.J.E.M. Roekaerts  
Multi-Scale Physics, Faculty of Applied Sciences, Delft University of Technology, The Netherlands  
[e.oldenhof@tudelft.nl](mailto:e.oldenhof@tudelft.nl)

## Flameless Combustion

Flameless oxidation is a combustion technique that combines reduction of fuel consumption in industrial furnaces with low  $\text{NO}_x$  emissions. These environmental and economical benefits are realized by the utilization of a heat recovery system (recuperators or regenerators) combined with an injection system that forces mixing of products into the fuel and/or combustion air stream before reaction takes place [1,2]. The reaction rates in this type of combustion are lower due to the low combustion temperatures, posing a modelling challenge for turbulence-chemistry interaction in these flames.

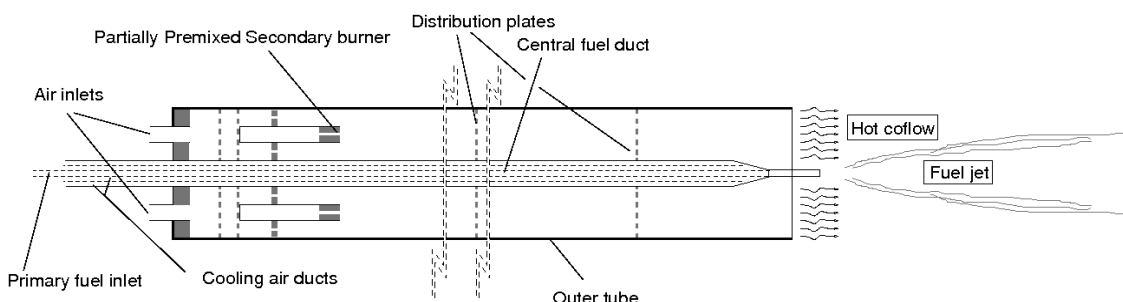


**Figure 1:** Schematic design drawing of the Delft JHC burner

## The Delft Jet-in-Hot Coflow burner

The goal of the experimental work is to investigate the detailed flame structure of the produced flames of the Delft Jet-in-Hot-Coflow burner and to generate a detailed dataset of statistics of velocities, temperatures and species of flames relevant to flameless combustion, to be used for validation of turbulence-chemistry interaction models.

Three different coflows have been used, varying in temperature and oxygen mass fraction. The hottest coflow, DJHC-I, has a peak temperature of 1540 K. DJHC-V and DJHC-X have a coflow peak temperature of 1460 K and 1395 K, respectively. The temperature profile at  $z=3$  mm is shown in Figure 2.

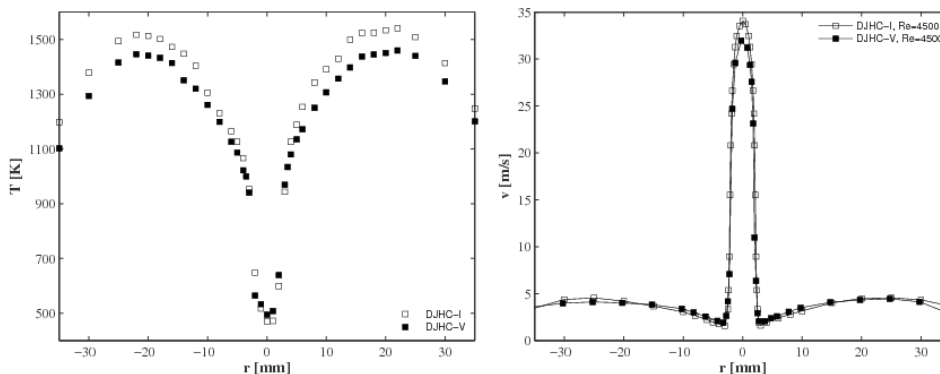


**Figure 2:** Coflow temperature (left) and velocity (right) at  $z=3$  mm, DJHC-I and DJHC-V,  $Re=4500$ .

## Flame stabilisation: autoignition kernel formation and growth

By means of flame luminescence measurements with an intensified high-speed camera, the flame stabilisation process in the lower part of the flame (the “lift-off region”) has been identified as being a combination of the random formation of ignition kernels followed by their growth due to flame propagation [4]. A snapshot of this process is provided in Figure 3, along with ensemble averaged flame evolutions for four different jet Reynolds numbers (3,000 top left to 9,500 bottom right) in the DJHC-V flame.

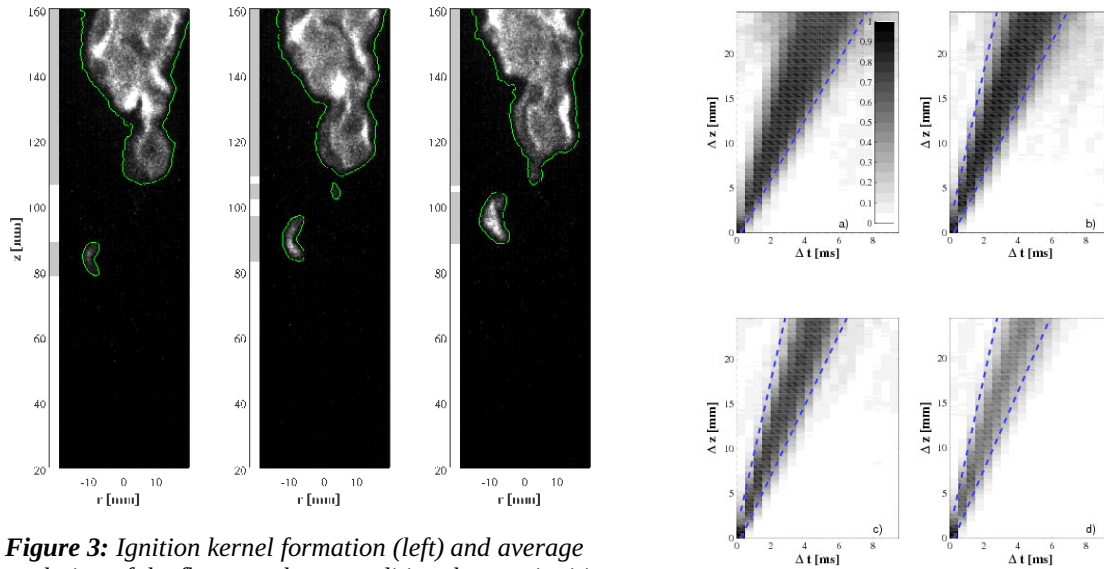


**Figure 3:** Ignition kernel formation (left) and average evolution of the flame pockets, conditional on an ignition event at (0,0) for four different Reynolds numbers (right).

The influence of entrainment on the lift-off height

For all flames, a decrease in the height where ignition kernels are first observed as a function of jet Reynolds number was found. This decrease can be related to the gradient in coflow temperature combined with the faster entrainment at higher jet velocities.

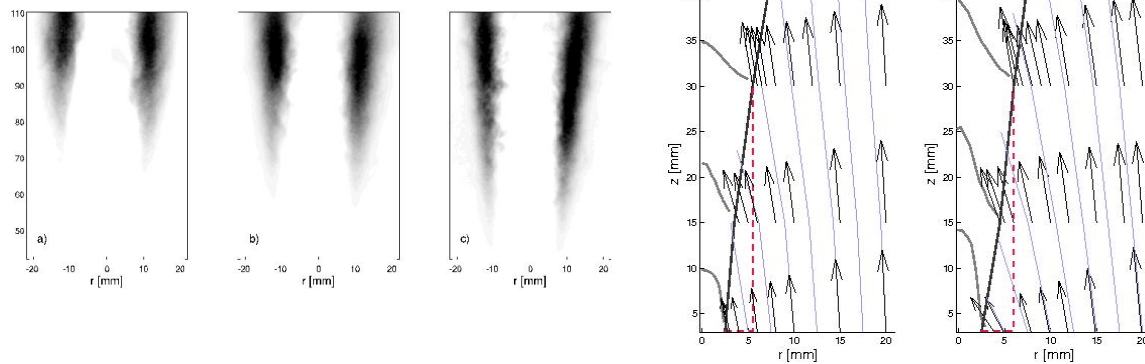


**Figure 4:** Decreasing lift-off height, as identified by the RMS of OH-PLIF measurements, DJHC-I,  $Re = 3,000, 4,500$  and  $8,500$  (left) and streamlines showing the stronger entrainment at the higher jet Reynolds number, as determined with LDA measurements for  $Re=4,500$  and  $Re=8,500$  (right).

[1] Wüning J.A. & Wüning J.G. *Flameless oxidation to reduce thermal NO-formation*, Progress in Energy and Combustion Science, 1997, 23, 81-94

[2] Tsuji, H. Gupta, A. Hasegawa, T. Katsuki, M. Kishimoto, K. & Morita, M. *High temperature air combustion*, CRC Press, 2003

[3] Dally B.B., Karpetis A.N. & Barlow R.S. *Structure of turbulent non-premixed jet flames in a diluted hot coflow*, Proceedings of the Combustion Institute, 2002, 29, 1147-1154

[4] Oldenhof E., Tummers M.J., van Veen E.H. & Roekaerts, D.J.E.M. *Ignition kernel formation and lift-off behaviour of jet-in-hot-coflow flames*, Combustion and Flame, 2010, 157, 1167--1178

# Development of High-Speed Rayleigh and Raman Scattering Imaging to Investigate Dynamics in Turbulent Jets and Flames

Randy A. Patton, Kathryn N. Gabet, Naibo Jiang, Walter R. Lempert, Jeffrey A. Sutton<sup>1</sup>  
Department of Mechanical Engineering, The Ohio State University, Columbus, OH 43210  
<sup>1</sup>sutton.235@osu.edu

## Objectives:

This poster will describe a new class of high-repetition-rate laser-based diagnostics that are being developed to measure the time-varying mixture fraction, temperature, and scalar gradient fields in turbulent jets and non-premixed flames. High-speed Rayleigh and Raman scattering imaging ( $\geq 10$  kHz acquisition rate) will yield unique temporal and spatial statistics that augment direct visualization of the scalar mixing process. This approach allows the time-dependent interaction between the large-scale turbulence and the small-scale mixing properties to be explicitly characterized. In addition this work will support the emergence of LES as a method of modeling *time-varying* turbulent combustion by providing more suitable temporally-based visualization and statistical metrics for assessing model performance under highly unsteady conditions.

## Approach:

We have been developing a new class of high-repetition rate laser diagnostics that take advantage of pulse-burst laser technology [1] to generate a series of high-energy laser pulses ( $\sim 200$  mJ/pulse at 532-nm) that can be used for Raman and Rayleigh scattering diagnostics. From the high-speed imaging, we are able to measure mixture fraction ( $\xi$ ) and temperature in both space and time in turbulent jets and flames.

### High-Speed Mixture Fraction Imaging in Turbulent Non-reacting Jets:

It has been widely regarded that the initial steps in understanding turbulent mixing in combustion environments will stem from an increase in the understanding of the physics of non-reacting turbulent flows. In this regard, a major focus of the current research is to measure  $\xi(x,t)$  in turbulent non-reacting jets. Measurements of  $\xi(x,t)$  were performed in non-reacting jets of propane issuing into a low-speed co-flow of air. Figure 1 shows an example series of mixture fraction measurements at  $Re = 10,000$  at an axial location corresponding to  $x/d = 10$ . What is evident is the high SNR of the images and the amount of small-scale features that are easily identified and resolved. In fact, preliminary tests comparing images acquired with the CMOS camera are very similar in quality to those obtained with a high-resolution, scientific CCD camera.

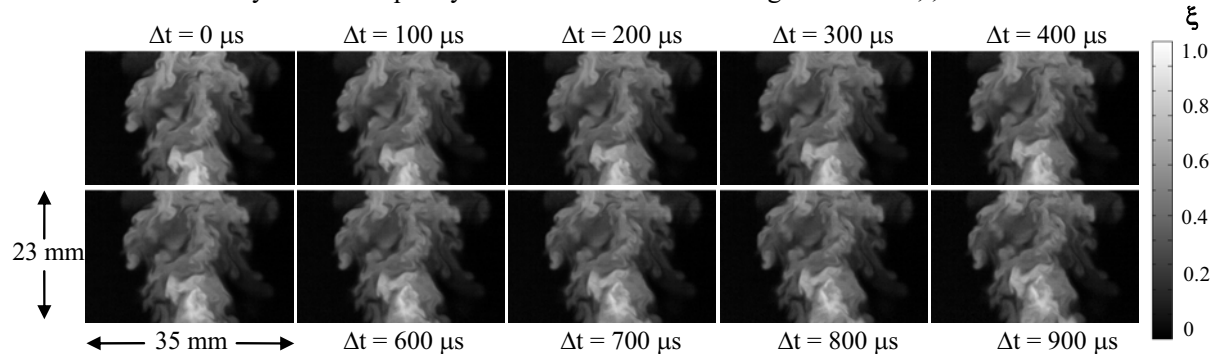


**Fig. 1: 10-kHz sequence of the mixture fraction field in a turbulent ( $Re = 10000$ ) non-reacting propane jet issuing into air. Images are centered at  $x/d = 10$ .**

### High-Speed Temperature Imaging in Turbulent Jet-Flames:

High-speed temperature measurements in turbulent flames using Rayleigh scattering represent an increasing level of complexity as compared to the turbulent non-reacting flows. The turbulent non-premixed flames considered are the DLR flames, which are simple jet-flames that serve as benchmark flames in the TNF workshop [2]. The fuel, which consists of 22.1%  $CH_4$  / 33.2%  $H_2$  / 44.7%  $N_2$ , issues from a 0.775-cm-diameter tube into a 30 cm x 30 cm co-flow. The conditions correspond to jet Reynolds numbers of 15,200 and 22800 on nozzle diameter for DLR flame A and B, respectively. A set of high-repetition rate temperature images are

shown in Fig. 2 from the higher Reynolds number DLR flame B to demonstrate the unique experimental capability developed in highly turbulent reacting flows. Ten images are shown with inter-pulse spacing of 100  $\mu\text{s}$  (10-kHz repetition rate). From the images, features such as the formation of hot pockets and their upstream propagation are clearly seen, showing the time-varying nature of thermal mixing and the introduction of steep thermal gradients due to gas mixing and chemical reaction. To the authors' knowledge, these results represent the first high-speed temperature images acquired in turbulent flames.

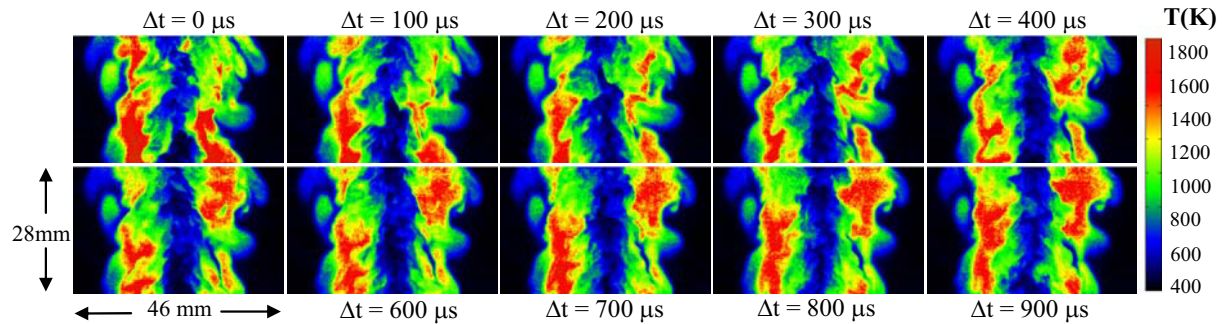


**Fig. 2: 10-kHz sequence of the temperature field in a turbulent non-premixed flame (DLR B,  $\text{Re} = 22800$ ). Images are centered at  $x/d = 10$ .**

#### Development of High-Speed 1D Raman Scattering Line Imaging:

A major motivation of the current and future work is the development high-energy, high-repetition-rate diagnostics that can be used for Raman scattering, thus permitting a measurement of the major species in both space and time and a measurement of  $\xi(x,t)$  in turbulent flames [3]. Towards this goal, we demonstrate high-speed 1D Raman line imaging in a turbulent  $\text{CH}_4/\text{H}_2$  jet issuing into air as shown in Fig. 3. The 7-mm line profiles of  $\text{CH}_4$ ,  $\text{H}_2$ ,  $\text{O}_2$ , and  $\text{N}_2$  are easily identified, although the SNR is modest at this point. However, it should be pointed out that these images were acquired with only 150 mJ/pulse. An increase of a factor of 6 in pulse energy is expected with a new laser system currently being developed, which when combined with a new high-speed intensifier which is optimized in the red wavelength region should yield a total increase in signal levels by more than a factor of 15-20.

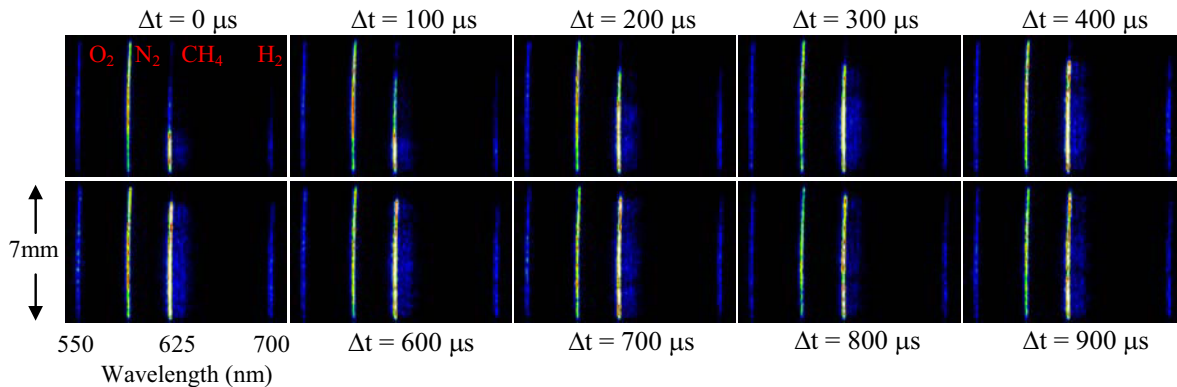


**Fig. 3: 10-kHz sequence of 1D Raman scattering images in a turbulent  $\text{CH}_4/\text{H}_2$  jet issuing into a co-flowing stream of air. Images are centered at  $x/d = 10$ .**

#### References:

- [1] Thurow, B.S., Jiang, N.B., Samimy, M., Lempert, W.R., "Narrow-Linewidth Megahertz-Rate Pulse-Burst Laser for High-Speed Flow Diagnostics", *Applied Optics*, Vol. 43, No. 26, 2005, p. 5064.
- [2] Barlow, R.S., International Workshop on Measurement and Computation of Turbulent Nonpremixed Flames, <http://www.ca.sandia.gov/TNF/abstract.html>
- [3] Bilger, R.W., "Turbulent Diffusion Flames", *Progress in Energy and Combustion Science*, Vol. 1, 1976, p. 87.

# LARGE-EDDY SIMULATION AND EXPERIMENTS ON NON-PREMIXED HIGHLY TURBULENT OPPOSED JET FLOWS

M W A Pettit<sup>1</sup>, B Coriton<sup>2</sup>, A Gomez<sup>2</sup>, A M Kempf<sup>1\*</sup>

<sup>1</sup>*Department of Mechanical Engineering, Imperial College, UK*

<sup>2</sup>*Yale Center for Combustion Studies, Yale University, USA*

[a.kempf@imperial.ac.uk](mailto:a.kempf@imperial.ac.uk)

An experimental and computational study of highly turbulent non-premixed opposed jet flows has been performed, under both isothermal and reactive conditions. Experimentally, Hot Wire Anemometry (HWA), two-dimensional Particle Image Velocimetry (PIV) and Hydroxyl Planar Laser-Induced Fluorescence (OH-PLIF) were used to determine axial and radial velocities and fluctuations, and axial velocity auto-correlation. Computationally, Large-Eddy Simulations (LES) were applied with a steady flamelet model to simulate the flow inside the nozzles and in the opposed flow region, using grid resolutions of 1.0mm, 0.5mm and 0.2mm. These resolutions correspond to domain sizes of 0.5 million, 4.6 million and 70 million cells for the reactive case respectively, with the largest simulation performed requiring approximately 2 CPU-years of computational resource.

The combined approach enabled the cross-validation of the simulation and experiment and provided additional insight into the flow field, particularly within those regions inaccessible by experiment only. Turbulent Reynolds numbers reaching a value of 900 were achieved, demonstrating the capability of the burner to reach conditions of relevance to practical systems. Importantly, the simplicity of a compact, bench-top experiment is retained. The extension of the computational domain to the region within the nozzles reveals the mechanism by which a specially designed turbulence generating plate (TGP) and burner housing (Fig. 1) yield turbulence intensities of over 20%.

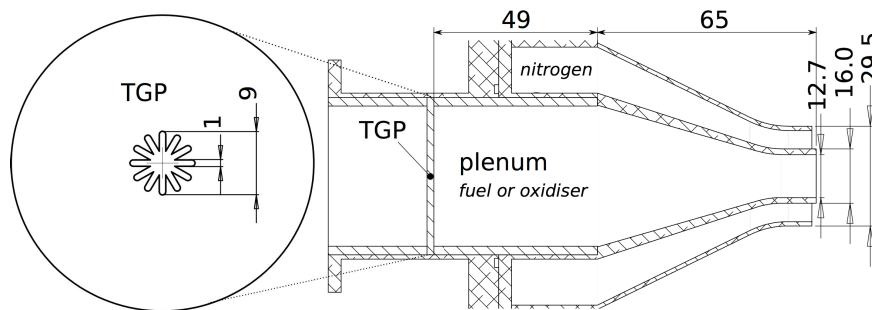


**Figure 1: One of the two opposed nozzles (shown rotated by 90°)**

The study compared results for three different set-ups: a single nozzle case was analysed to obtain detailed velocity statistics in the nozzle exit plane, a second test case involved the non-reactive investigation of the complete opposed jet configuration, and finally, a non-premixed flame was stabilised near the stagnation plane. The flow field within a single nozzle was visualised by adding a marker fluid (Fig. 2), which revealed the formation of a recirculation zone within the nozzle (confirmed by mean axial velocity statistics) as indicated by the counter-flowing marker fluid surrounding the main jet.

Accuracy of the LES was considered by performing a grid sensitivity study and by applying a quality indicator, although it is stressed that the chosen indicator would not be mathematically sufficient to ensure an accurate simulation (of which the same may be said of other existing indicators). However, the study did reveal that simulations on the coarse (1.0mm) grid did not sufficiently resolve the flow near to the walls at the nozzle exits, and as such only results from the medium (0.5mm) and fine (0.2mm) grids were considered.

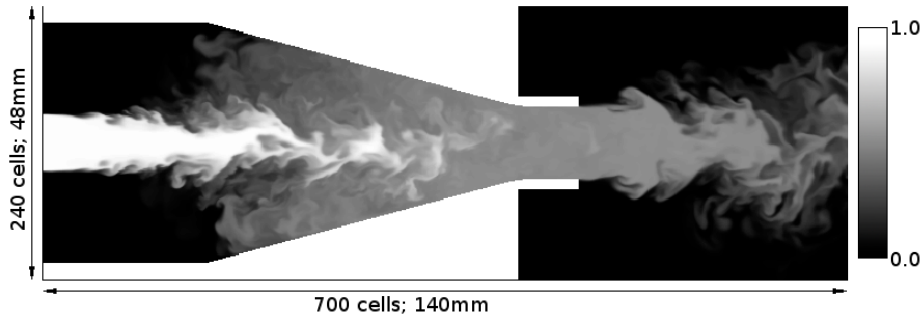


**Figure 2: Instantaneous snapshot of mixing inside a single nozzle (0.2mm grid resolution)**

The simulated and measured data were found to be in good agreement for first and second velocity moments, for the axial velocity auto-correlation function and for the normalised mean OH fluorescence. The prescribed level of simulated turbulence applied at the inflow boundaries was critical to the correctness of the computation, as this level is a key contributor to the position of jet break-up, which itself determines the amount of axial and radial velocity fluctuation at the nozzle exit and on the stagnation plane. Beyond the achieved agreement of statistical flow data, similarity of instantaneous OH-based flame morphology between experiments and computations also confirmed that the LES successfully captured key features of the flow, as shown in Fig. 3.

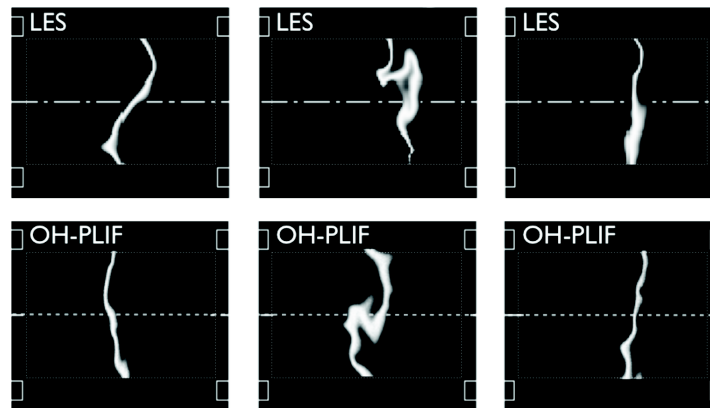


**Figure 3: Instantaneous OH snapshots of the flame from LES (0.2mm grid resolution) and OH-PLIF**

Due to the computational expense, simulated times were typically around one second and were therefore not of sufficient duration to capture low frequency, large-scale oscillatory motions of the flow (as observed in experiments). In addition, the relatively simple approach to solving the flame chemistry did not permit phenomena such as localised flame extinction to be investigated numerically. Reducing the computational domain to the region between the nozzle exits only would reduce the computational effort by around two orders of magnitude, allowing for much longer simulated times, with inflow conditions in the reduced domain determined from the larger simulations already performed.

# Characterization of a Turbulent Dilute Hydrogen Diffusion Flame Using Spontaneous Raman Scattering, OH-PLIF and Large Eddy Simulation

J. Ranalli and P. Strakey (peter.strakey@netl.doe.gov)

National Energy Technology Laboratory  
Morgantown, WV 26508

## Introduction

In an increasingly carbon-constrained world, safe and clean combustion of high-hydrogen fuels is becoming a pertinent research area in the gas turbine community. Due to the potentially troublesome prospect of premixing hydrogen and air for combustion in the gas turbine, the current work is exploring the feasibility of utilizing diffusion flames in the combustor, where the hydrogen can be diluted with about 50% nitrogen by volume, available from the coal gasifier's air separation unit, to help control the combustion temperature. Even with a 50/50 H<sub>2</sub>/N<sub>2</sub> fuel mixture, adiabatic flame temperatures are too high (~2025 K) to fully suppress NO<sub>x</sub> formation, thus additional strategies must be employed to meet the DOE Turbine Program's goal of 2 ppm NO<sub>x</sub> @ 15% O<sub>2</sub>. The primary NO<sub>x</sub> reduction strategy investigated in this work is the reduction of the flame residence time and temperature, which is accomplished by using small, highly strained nitrogen-diluted diffusion flames.

The importance of accurate computational modeling is to provide deeper insight into the complex physical and chemical phenomena that govern flame stability and NO<sub>x</sub> formation. However, in order to ensure the fidelity of such computational models, substantial experimental validation is required. Validation data in the form of concentrations of the major combustion species and temperature in a dilute-diffusion hydrogen flame provides an excellent basis for modeling efforts. Spontaneous Raman Scattering (SRS) diagnostics allow this type of measurement to be made.

## Experimental System

The burner used in this study is similar to that described in Ref. [1]. The burner consists of a stainless steel tube which delivers a fuel jet. Surrounding the fuel jet is a region of high velocity coaxial air delivered at an equivalence ratio of  $\phi = 0.50$ . A surrounding co-flow air is supplied to over-ventilate the flame with an overall equivalence ratio of 0.2. An image of the combustor operating is shown in Figure 1. For the case tested in this study, the fuel jet diameter was 2.118 mm in diameter and the coaxial air jet was 6.35 mm in diameter. A fuel composition of 50% H<sub>2</sub> with 50% nitrogen by volume was delivered at a total flow rate of 15.45 slpm, corresponding to a fuel jet velocity of approximately 75 m/s. The coaxial air velocity was 27 m/s. The laser used for the measurements was a frequency-doubled Nd: YAG emitting 1000mJ/10ns pulse at the 532 nm line. OH-PLIF measurements were conducted using a frequency doubled dye-laser operating at 284 nm. For the Raman measurements the high energy level necessitated use of an optical pulse stretcher to reduce the peak power focused into the probe volume. The design for the pulse stretcher was similar to one described by Kojima and Nguyen [2]. The pulse stretcher reduced the peak power of the laser beam by a factor of ten and eliminated multi-photon ionization breakdown of the gasses at the probe volume. The beam from the pulse stretcher was focused into the probe volume at the burner with a 750 mm focal length lens. The resulting probe volume resolution was approximately 150  $\mu\text{m}$  x 150  $\mu\text{m}$  as defined by the diameter of the probe volume and the on-chip binning employed in the camera. In order to increase the Raman signal, the beam was reflected for a second pass through the same volume. Part of the incident beam was split onto a photodiode for sensing of the shot-to-shot laser power variation.

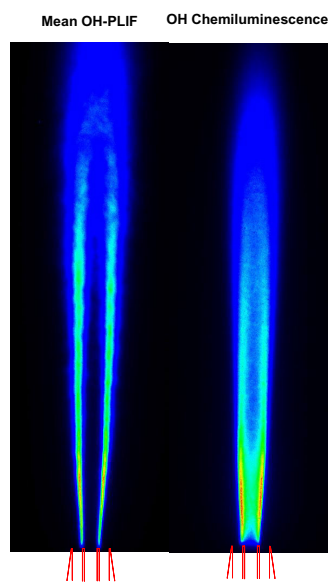


**Figure 1: Images of the H<sub>2</sub> dilute diffusion flame.**

The light from the probe volume was collected by a pair of  $f/2.0$  achromat lenses and focused into a spectrometer. The holographic transmission imaging spectrometer contained a holographic notch filter to remove the Rayleigh line. The output of the spectrometer was imaged by a cooled CCD camera. The holographic transmission grating used in the spectrometer allowed for full capture of the entire visible spectrum from 400 nm to 700 nm, allowing both Stokes and anti-Stokes spectra to be captured. The system imaged a 16 mm segment of the laser beam, resulting in images in which the vertical dimension represents distance along the imaging line and the horizontal dimension is wavelength. The line imaging approach employed here allowed for single shot radial profiles of major species and

temperature. Binning of the images by 8 pixels in the spatial dimension and 4 pixels in the spectral dimension was used to improve the signal-to-noise ratio while allowing reasonable spectral and spatial resolution. A mechanical shutter consisting of a high-speed rotating wheel combined with a mechanical shutter constructed with a hard-drive actuator arm to reduce the exposure to 40  $\mu$ sec. The background light was reduced to a negligible level. An example of the Raman data is shown in Figure 2 which shows the entire Raman spectrum in the horizontal direction and the radial distribution in the vertical direction. The burner nozzle is annotated on the right of the figure.

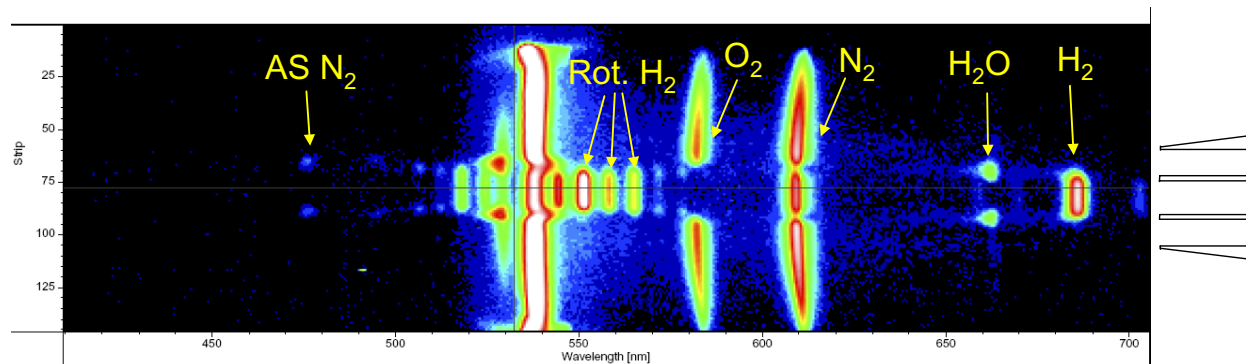


**Figure 2: Single-shot spectrum at an axial distance of 1.5 mm from the fuel tube showing all major species over a line image of 16 mm in length.**

In order to make quantitative measurements of the major species in the flame, it was necessary to calibrate the Raman system in a known flame environment. For this purpose, the hydrogen burner was replaced with a laminar McKenna flat-flame burner and a set of calibration spectra were acquired. To account for the crosstalk between species, a Raman crosstalk calibration matrix was measured, as described by Dibble et. al [3]. To compute the crosstalk terms, judicious selection of operating conditions was used to reduce the number of species present at any one time. The calibration of the system allowed for absolute concentration measurements of all major species including  $N_2$ ,  $O_2$ ,  $H_2O$  and  $H_2$  as well as temperature through either Stokes/anti-Stokes ratio of the nitrogen molecule or through the ideal gas law assumption at temperatures below about 1000 K. The Raman results are currently being analyzed with the calibration matrix data.

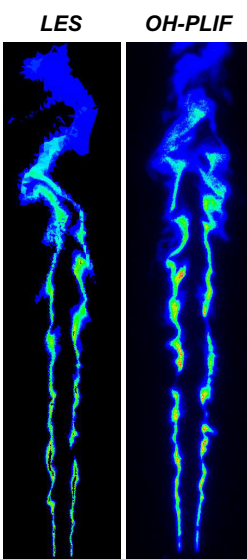


**Figure 3: OH concentration from the LES simulation (left) compared to the OH-PLIF measurements.**

### Computational Studies

LES simulations on the target flame were carried out with the commercial CFD code FLUENT. For the LES studies, a 3D unstructured grid of approximately 3 million cells was used with a detailed hydrogen-air kinetic mechanism. No turbulence-chemistry interaction model was used for the LES studies which is the equivalent of assuming that the sub-grid scalars were perfectly mixed. This is somewhat justified considering the high resolution of the grid which was approximately 100  $\mu$ m in the reaction zone and the fast molecular mixing time-scale of hydrogen. A dynamic Smagorinsky model was used to calculate the sub-grid viscosity. The LES simulations were run until the initial RANS solution was flushed out and a statistically steady-state solution was achieved. A comparison of the instantaneous OH concentration from the LES simulation to the OH-PLIF intensity is shown in Figure 3. The LES simulation appears to predict the flame length and overall heat release distribution fairly well.

### References

- [1] N. Weiland and P. Strakey, "Stability Characteristics of Turbulent Hydrogen Dilute Diffusion Flames," *Combustion Science and Technology*, vol. 181, May, 2009, pp. 756-781.
- [2] J. Kojima and Q. Nguyen, "Laser Pulse-Stretching with Multiple Optical Ring Cavities," *Applied Optics*, vol. 41, Oct. 2002, pp. 6360-6370.
- [3] R. DIBBLE, S. STARNER, A. MASRI, and R. BARLOW, "AN IMPROVED METHOD OF DATA ACQUISITION AND REDUCTION FOR LASER RAMAN-RAYLEIGH AND FLUORESCENCE SCATTERING FROM MULTISPECIES," *APPLIED PHYSICS B-PHOTOPHYSICS AND LASER CHEMISTRY*, vol. 51, Jul. 1990, pp. 39-43.

# Analysis of Turbulent Mixing Statistics in Stratified Combustion

Edward S. Richardson\*, Jacqueline. H. Chen

\*[esrich@sandia.gov](mailto:esrich@sandia.gov)

Combustion Research Facility, Sandia National Laboratories, Livermore, CA 94551-0969, USA

Effects of equivalence ratio stratification on turbulent mixing processes are investigated in this study. Equivalence ratio stratification occurs in a range of applications: in gas turbines, a fuel rich pilot region may be employed in order to enhance the stability of an overall lean, low-emission combustor design. This study uses analysis of new stratified flame Direct Numerical Simulation (DNS) data to improve understanding and modelling of equivalence ratio stratification effects.

Fully resolved three-dimensional DNS data for turbulent stratified methane Bunsen flames with a jet Reynolds number of 2100 have been performed. The flame series displays three stratification levels of equivalence ratio ( $\phi$ ): (C1) premixed,  $\phi=0.70$ ; (C2, C4, C5) low stratification,  $0.41 < \phi < 1.0$ ; and (C3) high stratification,  $0.0 < \phi < 1.46$ . The simulations employ reduced kinetic mechanisms with 13 chemical species, except in case C3 which includes 28 species in order to account for combustion and nitrogen chemistry in the richer mixture. Stratified cases C2 and C3, shown schematically on the left hand side in Fig. 1, have a variation of mixture fraction in the periodic span-wise  $z$ -direction between the equivalence ratio limits given above. The equivalence ratio stratification in cases C4 (shown on the right hand side in Fig. 1) and C5 is introduced parallel to the flame - this provides data more comparable to several recent stratified combustion experiments (Cambridge stratified swirl burner, TUD piloted annular stratified burner, and the ORACLES burner) - with  $\phi$  varying in the cross-stream  $y$ -direction. The inflow composition in C4 is stoichiometric in the products and  $\phi=0.41$  in the reactants, while C5 has these equivalence ratios reversed (the reactants are stoichiometric). The reactant stream issues at  $100\text{ms}^{-1}$  into a  $25\text{ms}^{-1}$  coflowing product stream. The resulting flames span from premixed to partially-premixed combustion modes, and show a high degree of flame-turbulence interaction, with combustion occurring in the thickened flame regime, and extending into the broken reaction zone regime as the mixture approaches its lean flammability limit.

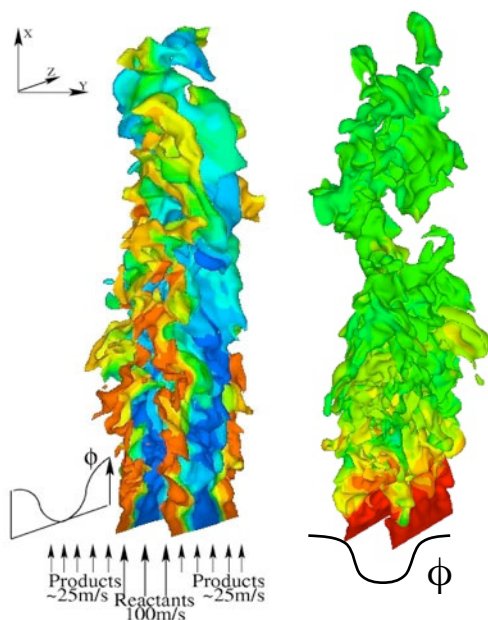


**Figure 1:** Stratified flame configuration C2 (left) and C4 (right), the 1200K temperature isosurface is colored by equivalence ratio from blue at  $\phi=0.41$  to red at  $\phi=1.0$ .

Stratified combustion is characterized by simultaneous mixing between combustion products and reactants, and between mixtures of different equivalence ratio. These local mixing processes are described in both flamelet and statistical moment based modelling approaches by the (cross-)dissipation rates of progress variable and mixture fraction. Comparing scalar dissipation statistics recorded for the different stratification levels provided by the three flames, and between the various combustion regimes which occur at regions of differing mean equivalence ratio and turbulence intensity, indicates that the scalar dissipation is influenced by the modification of the turbulence, chemistry and molecular mixing due to stratification. Mixing statistics are compared in terms of species variances, scalar dissipation rate probability density functions (pdfs), see Fig. 2, and scalar alignments. Figure 2 shows the pdf of the natural logarithm of the progress variable dissipation rate (Fig. 2a), the natural logarithm of the mixture fraction dissipation rate (Fig. 2b) and the mixture fraction - progress variable cross-dissipation rate (Fig. 2c), all conditioned on  $\phi=0.7$  and progress variable of 0.5. The progress variable and mixture fraction dissipation rates exhibit approximately log-normal pdfs (dashed lines in Fig. 2) across the range of scales present in the DNS: little extra likelihood is attributed to the conditional progress variable dissipation rate, indicated by  $\delta_1$  in Fig. 2a, which corresponds to a freely propagating premixed flame. The cross-dissipation pdf is approximately symmetrical for  $\phi=0.7$ , but Fig. 3 shows a distinct variation of the conditionally averaged cross-dissipation with mixture fraction, with the root mean square of the cross-dissipation much greater than the conditional mean. The physical processes governing the scalar dissipation rates are investigated further with reference to the transport equations for the (co-)variance and the mean (cross-)dissipation rates of progress variable and mixture fraction.

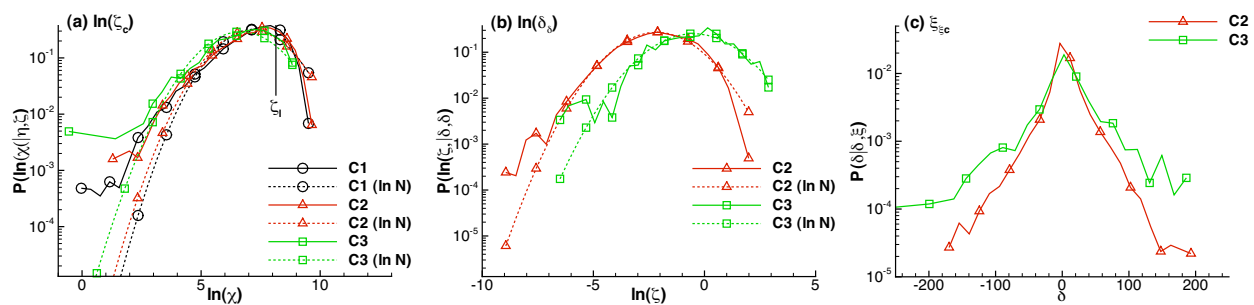


**Figure 2:** Probability density functions of the natural logarithm of the progress variable dissipation rate (a), the natural logarithm of the mixture fraction dissipation rate (b) mixture fraction - progress variable scalar dissipation rate, conditioned on  $\phi=0.7$  and progress variable=0.5 at half of the domain height for C1-C3. Log-normal pdfs are also shown by dashed lines.

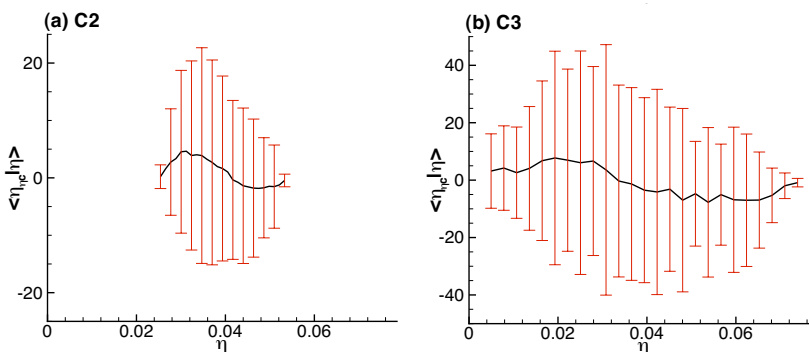


**Figure 3:** Mixture fraction-progress variable cross-dissipation rate conditionally averaged (solid black line) on mixture fraction in flames C2 (left) and C3 (right) at half of the domain height. The bars correspond to  $\pm$  the conditional root mean square cross-dissipation.

# PDF CALCULATIONS OF PILOTED PREMIXED JET FLAMES

D.H. Rowinski\*, S.B. Pope  
 Cornell University, USA  
[dhr46@cornell.edu](mailto:dhr46@cornell.edu)

A series of piloted premixed jet flames with strong finite-rate chemistry effects is studied using the joint velocity-turbulence frequency-composition PDF method. The flames studied here are based on the Sydney piloted premixed jet burner [1, 2] (PPJB). The PPJB consists of a jet of lean premixed methane-air surrounded by a pilot of hot stoichiometric methane-air products and a hot coflow of lean hydrogen-air products. The only parameter variation among these flames is the jet velocity. As the jet velocity increases, extinction and reignition events are observed downstream. The flame with the lowest jet velocity, PM1-50, and the flame with the highest jet velocity, PM1-200, are presented here.

These flames are modeled using the joint velocity-turbulence frequency-composition PDF method [3]. The joint PDF is solved by a Monte Carlo method, where particle velocities are modeled by the simplified Langevin model [4], and the timescale of turbulence is provided by a stochastic frequency model [5]. In the base case, the EMST mixing model [6] is used along with a reduced 16-species methane mechanism [7]. The chemistry is evaluated via the ISAT algorithm [8]. The particle solver is coupled to a finite volume solver which solves the mean equations of mass, momentum, energy, and state [9]. The finite volume solver provides the particle solver with the mean velocity and pressure, while the particle solver provides the turbulence quantities and reaction source term to the finite volume solver.

The numerical accuracy of the calculations is assessed through convergence studies including grid refinement and chemistry tabulation error tolerance refinement; the statistical errors are analyzed by increasing the number of particles per cell and duration of time averaging. Overall, the maximum errors are generally of order 5% for mean quantities and 10% for rms quantities.

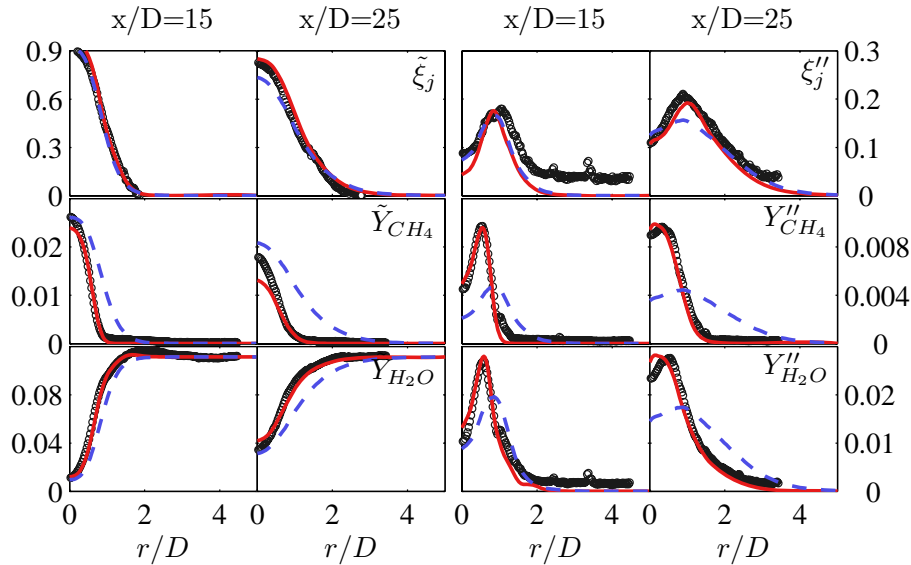


Figure 1: Radial profiles of Favre mean and rms jet mixture fraction ( $\xi_j$ ) and species mass fractions ( $Y$ ) in PM1-50 at  $x/D = 15$  and  $x/D = 25$ . Open circles are measurements, solid lines are base case PDF calculations, dashed lines are inert PDF calculations.

For all base case calculations, good agreement is observed with the measurements of mean and rms mixture fraction fields, while the reaction progress is overpredicted to varying degrees depending on the jet velocity. In

the calculations of PM1-50, species and temperature generally show good agreement with the measurements. Both mean and rms quantities for major species show good agreement with measurements as shown in Fig. 1 for the two measurement stations farthest downstream.

In the calculations of PM1-200, however, the products and temperature are overpredicted while fuel and oxidizer are underpredicted. An extensive set of sensitivity studies on inlet boundary conditions, turbulence model constants, mixing models and constants, radiation treatment, and chemical mechanisms is conducted on this flame. These studies show no combination of models and parameters that yields the observed reaction progress. Diagnostic calculations with artificially slowed chemistry confirm that the reaction progress is overpredicted in the base case calculations; in fact, the major species measured downstream correspond best with those of inert calculations, as shown in Fig. 2 for the two measurement stations farthest downstream.

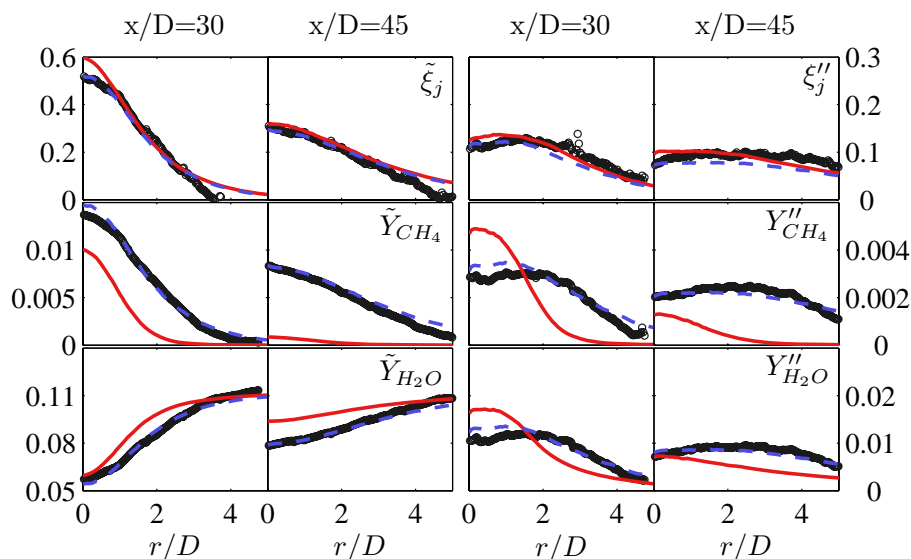


Figure 2: Radial profiles of Favre mean and rms jet mixture fraction ( $\xi_j$ ) and species mass fractions ( $Y$ ) in PM1-200 at  $x/D = 30$  and  $x/D = 45$ . Open circles are measurements, solid lines are base case PDF calculations, dashed lines are inert PDF calculations.

Work is ongoing to investigate the mixing model performance in these flames. More advanced modeling approaches, such as the LES/PDF methodology, are to be employed so that the details of the mixing processes can be abstracted and the performance of the mixing models can be better understood. In summary, a series of calculations of a challenging flame series has been performed, and the mixing models have been identified as possible area for improvement in this combustion regime.

- [1] M.J. Dunn, A.R. Masri, R.W. Bilger, *Combust. Flame* 151 (2007) 46–60.
- [2] M.J. Dunn, A.R. Masri, R.W. Bilger, R.S. Barlow, G.H. Wang, *Proc. Combust. Inst.* 32 (2009) 1779–1786.
- [3] S.B. Pope, *Prog. Energy Combust. Sci.* 11 (1985) 119–192.
- [4] D.C. Haworth, S.B. Pope, *Phys. Fluids* 29 (1986) 387–405.
- [5] P.R. Van Slooten, Jayesh, S.B. Pope, *Phys. Fluids*, 10 (1998) 246–265.
- [6] S. Subramaniam, S.B. Pope, *Combust. Flame* 115 (1998) 487–514.
- [7] C.J. Sung, C.K. Law, J.Y. Chen, *Proc. Combust. Inst.* 27 (1998) 295–304.
- [8] S.B. Pope, *Combust. Theory Modelling* 1 (1997) 41–63.
- [9] M. Muradoglu, S.B. Pope, D.A. Caughey, *J. Comp. Phys.* 172 (2001) 841–878.

## Reduced state spaces for laser-diagnostics in combustion: checks with DNS data

Robert Schießl, Ulrich Maas  
Institut fuer Technische Thermodynamik  
Karlsruhe Institute of Technology (KIT)  
[robert.schiessl@kit.edu](mailto:robert.schiessl@kit.edu)  
Christiane Zistl, Gordon Fru  
Lab. of Fluid Dynamics and Technical Flows  
Univ. of Magdeburg "Otto von Guericke"

This poster contribution aims at motivating and exemplifying the use of reduced state spaces for laser diagnostics in combustion processes (as described at the 2008 combustion symposium, [1]). Examples are studied using data from direct numerical simulations (DNS).

A motivation for the method is given based on synthetic numerical examples, which demonstrate that laser-based signal strengths are typically *per se* not sharply correlated to the quantity they are supposed to measure, if arbitrary combinations of species concentrations and temperature are present. These examples also illustrate how the signals do become correlated quite well to quantities they are supposed to measure if chemical reactions (as they are present in combustion) become active. In Figure 1, this is shown for Rayleigh signals and temperature in a premixed CH<sub>4</sub>/air system. A similar behavior is found for reaction systems where in addition also diffusive processes (mixing of reactors) are allowed. This highlights that the evaluation of laser-based measurements in combustion is intrinsically linked to the dynamics of the combustion process: in most cases, it would be difficult to obtain results from measurements if no additional information about the combustion process was available. Many currently employed measurement techniques implicitly (and mostly, informally) use such additional information, but do so mainly based on empiricism.

The formalized use of additional information about combustion processes (via the concept of reduced state spaces) in laser-based measurements is checked by computing synthetical signals from Direct Numerical Simulation (DNS) data, and then "reconstructing" the data by reading them out from signal-parameterized low-dimensional manifolds of various dimension.

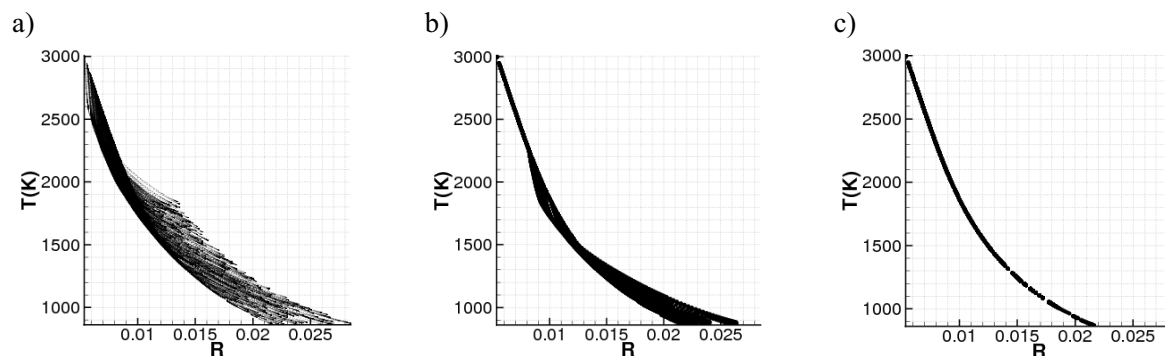


Figure 1 Synthetic example of a correlation between Rayleigh-signal  $R$  (arbitrary units) and temperature  $T$  in a reacting methane/air system (scatter plots). a) Quasi-random initial states. b) Same points, after 20 microseconds of chemical reaction c) after 5 milliseconds of chemical reaction. Combustion reactions create correlations, which allow measurements to be made.

Several low-dimensional manifolds are constructed, including simple manifolds based on conservation laws, and also Reaction Diffusion Manifolds (REDIMs,[2]). It is then checked how well state vectors in the DNS data can be reproduced from (synthetic) signals computed from these data, in particular Rayleigh signals, depolarized Rayleigh signals and LIF-signals from molecular oxygen (O<sub>2</sub>). For DNS data from a non-premixed turbulent hydrogen/air flame [3,4], a one-dimensional state space with the

Rayleigh signal is insufficient to obtain accurate information about temperature. If a two-dimensional state space is used, the reconstruction becomes only marginally better. With three dimensions, however, the reconstruction becomes significantly better, allowing temperature to be determined from the signals with good accuracy (Figure 2 and Figure 3). The fact that, even with the two-dimensional reduced state space spanned by two measurement signals, no accurate determination of temperature is possible, is found to be an effect caused mainly by preferential diffusion, which can be captured by three dimensions. If the DNS data are filtered to exclude points without significant preferential diffusion, two dimensions are sufficient for an accurate temperature determination.

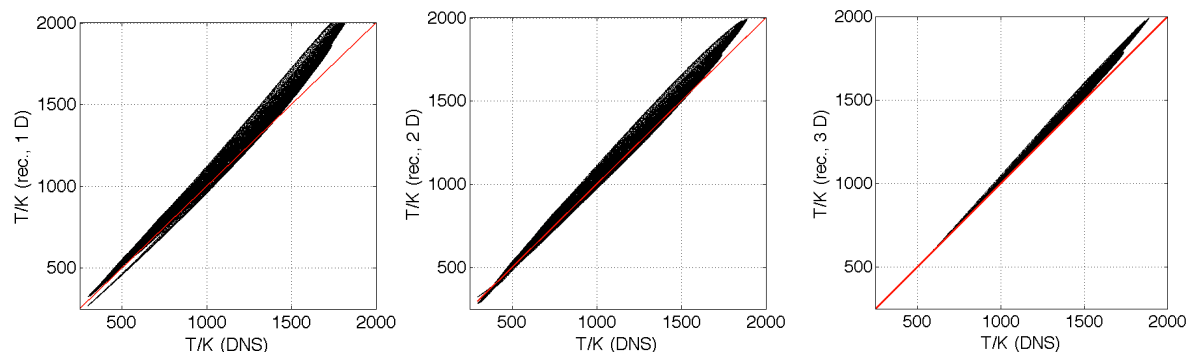


Figure 2 Temperature (DNS data) plotted versus reconstructed temperature for manifolds of various dimension. a) one-dimensional manifold, reconstruction from Rayleigh signal. b) two-dimensional manifold, reconstruction from Rayleigh signal and  $O_2$ -LIF, c) three-dimensional manifold, reconstruction from polarized and depolarized Rayleigh signal and  $O_2$ -LIF. For the example shown, simple manifolds based on conservation laws were used.

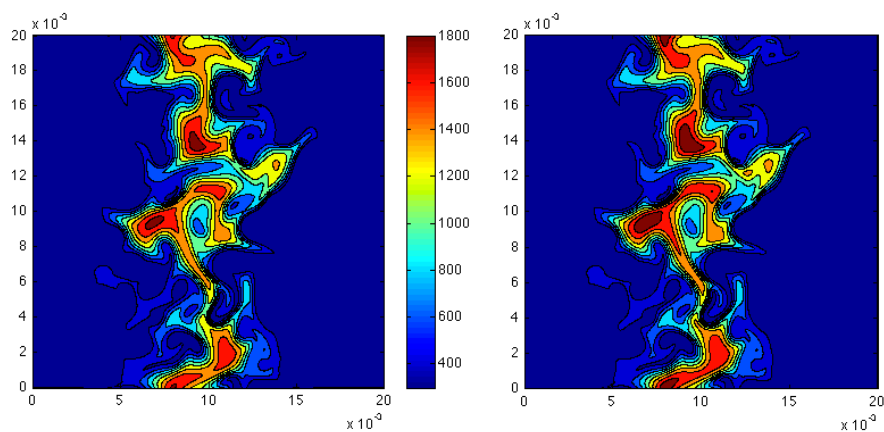


Figure 3 Left: Temperature field from DNS of a non-premixed  $H_2$ /air flame. Right: Reconstructed temperature field, based on three measurement signals and a three-dimensional manifold.

## References

1. Schießl, R., et al., *Application of Reduced State Spaces to Laser-Based Measurements in Combustion*, in *Proceedings of the Combustion Institute*. 2009, The Combustion Institute, Pittsburgh, PA.
2. Bykov, V. and U. Maas, *The extension of the ILDM concept to reaction-diffusion manifolds*. *Combustion Theory and Modelling*, 2007. **11**(6): p. 839-862.
3. Zistl, C., Hilbert, R., Janiga, G. and Thévenin, D.: Increasing the efficiency of postprocessing for turbulent reacting flows, *Comput. Visual. Sci.*, **12**, 2009, 383-395.
4. Fru, G., Thévenin, D., Zistl, C., Janiga, G., Gouarin, L. and Laverdant, A.: 3D Direct Simulation of a nonpremixed hydrogen flame with detailed models, in: *Direct and Large-Eddy Simulation VII*. 2010, (Armenio, V., Geurts, B. and Fröhlich, J., Eds.), Springer, 421-425.

# A TURBULENT STRATIFIED FLAME SERIES FOR MODEL VALIDATION

F. Seffrin<sup>1</sup>, F. Fuest<sup>1</sup>, T. Stahler<sup>1</sup>, N. Karimi<sup>1</sup>, D. Geyer<sup>2</sup>, A. Dreizler<sup>1\*</sup>  
<sup>1</sup> Technische Universität Darmstadt, Germany; <sup>2</sup> Hochschule Darmstadt, Germany  
 dreizler@csi.tu-darmstadt.de

## Introduction

Stratification of the (partially) premixed fuel is rather the norm than the exception in technical combustion processes. The stratification can be caused unintentionally by imperfect mixing of fuel and oxidizer or by transient inlet conditions provoked by combustion instabilities. It may also be created intentionally to reduce fuel consumption and pollutant formation as in direct injection IC engines or gas turbine combustors.

Within the scope of numerical simulations such as Large Eddy Simulation (LES) comprehensive data sets for model validation are required. Only sparse suitable test cases for turbulent premixed and especially stratified flames are presently available (e.g. [1,2,3,4]), thus the aim of this study is to provide flow and scalar field data of a broad series of flames. A burner for turbulent stratified combustion was therefore developed and multiple parametric varied flames were investigated with laser based techniques.

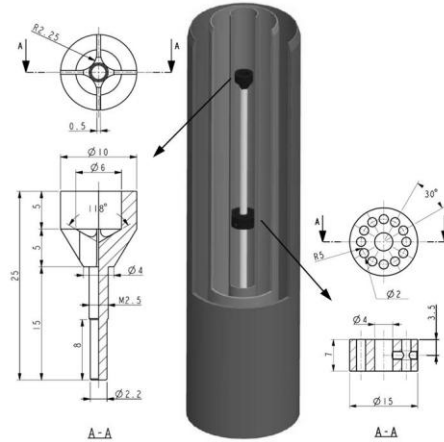


Fig. 1 – Schematic of the burner.

## Burner Design & Operational Conditions

The axisymmetric burner (*Fig. 1*) consists of two concentric annular slots with hydraulic diameters of about 20 mm which can be operated independently to vary shear and stratification between the streams. A small premixed flame (stabilized by a flame holder) burning inside a tube in the center of the burner pilots the main flames. The inlets provide fully developed pipe turbulence.

The flame series comprises 12 different flames along with their isothermal analogs including variations in stratification (with and without, lean-lean, lean-rich), shear, Re number (about 6000 to 27 000, corresponding the thermal powers of about 50 to 110 kW), and fuel type (methane and ethylene) (*Tab. 1*).

## Diagnostics & Experimental Results

Flow fields were characterized with Laser Doppler Velocimetry (LDV) and Particle Image Velocimetry (PIV) (TSF\_A – J). Profiles of the radial and axial

Tab. 1 – Flow configurations for reacting cases with given exit bulk velocities  $v$  and equivalence ratios  $\Phi$  for the two annular slots.

config	$V_{\text{slot 1}}$ [m/s]	$\Phi_{\text{slot 1}}$	$V_{\text{slot 2}}$ [m/s]	$\Phi_{\text{slot 2}}$
TSF_A	10	0.9	10	0.6
TSF_B	15	0.9	15	0.6
TSF_C	10	0.9	5	0.6
TSF_D	10	0.9	20	0.6
TSF_E	10	0.9	5	0.9
TSF_F	10	0.9	10	0.75
TSF_G	10	0.9	10	0.9
TSF_H (C <sub>2</sub> H <sub>4</sub> )	10	0.6	5	0.9
TSF_I (C <sub>2</sub> H <sub>4</sub> )	10	0.6	10	0.6
TSF_J	10	0.6	5	0.9
TSF_K	10	0.6	10	0.6
TSF_L	10	1.4	10	0.6

velocity components, integral time and length scales, and vorticity maps are provided [5].

Scalars were recently quantified using 1D-Raman/Rayleigh scattering (TSF\_A, C, L). Instantaneous temperature and the main species concentrations (fuel, N<sub>2</sub>, O<sub>2</sub>, CO<sub>2</sub>, H<sub>2</sub>O) are inferred using this technique. Thus, the full thermo-kinetic state is probed. Derived quantities such as equivalence ratio and scalar correlations can be calculated and (multi-) conditioning be accomplished. In addition, first numerical simulations are performed (see contribution of G. Künne et al.).

Beside burner schematics and flow configurations the poster comprises selected experimental results emphasizing the not yet published scalar data from Raman/Rayleigh scattering. *Fig. 2* exemplarily shows radial mean profiles of species mole fraction, equivalence ratio, and temperature in TSF\_A configuration.

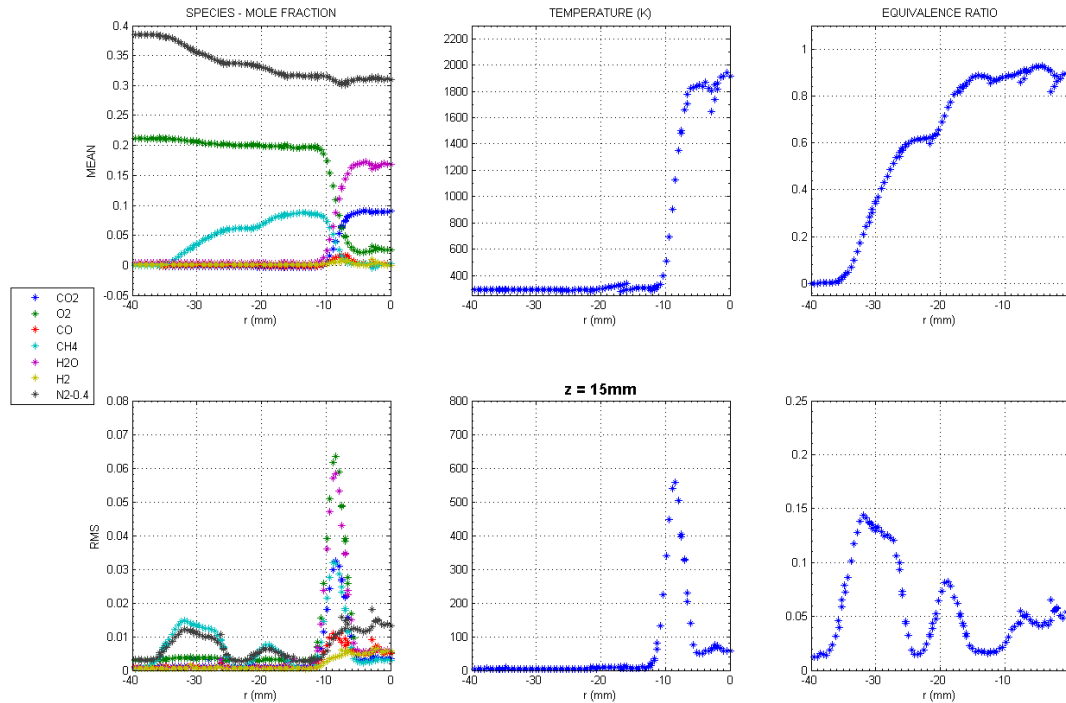


*Fig. 2* – Mean and RMS radial profiles of main species mole fraction, temperature, and equivalence ratio in TSF\_A at an axial height of 15 mm (preliminary results).

## References

- 1 M. Besson, P. Bruel, J.L. Champion, B. Deshaies, J. Thermophys. Heat Transfer 14 (2000) 59-67.
- 2 R.S. Barlow, G.H. Wang, P. Anselmo-Filho, M.S. Sweeney, S. Hochgreb, Proc. Combust. Inst. 32 (2009) 945-953.
- 3 P.D. Nguyen, P. Bruel, S. Reichstadt, Flow Turbul. Combust. 82 (2009) 155-183.
- 4 P. Anselmo-Filho, S. Hochgreb, R.S. Barlow, R.S. Cant, Proc. Combust. Inst. 32 (2009) 1763-1770.
- 5 F. Seffrin, F. Fuest, D. Geyer, A. Dreizler, Combust. Flame 157 (2010) 384–396.

# ANALYSIS OF AUTO-IGNITION OF TURBULENT HYDROGEN JETS WITH DIFFERENT DETAILED REACTION MECHANISMS

I. Stanković<sup>1\*</sup>, A. Triantafyllidis<sup>2</sup>, E. Mastorakos<sup>2</sup>, C. Lacor<sup>3</sup>, B. Merci<sup>1</sup>

<sup>1</sup> Ghent University, Belgium; <sup>2</sup> Cambridge University, UK; <sup>3</sup> Vrij Universiteit Brussel, Belgium  
[Ivana.Stankovic@UGent.be](mailto:Ivana.Stankovic@UGent.be)

Auto-ignition in turbulent non-premixed flows has significant practical applications and quite subtle fundamental aspects [1]. In numerical studies of auto-ignition phenomena, turbulence and unsteady chemistry must be modelled accurately. In order to obtain accurate simulation results for the turbulence, the Large-Eddy Simulation (LES) approach has recently received attention, while for the turbulence-chemistry interaction, the Conditional Moment Closure (CMC) can be used.

Large-Eddy Simulation (LES) results with first-order Conditional Moment Closure (CMC) are presented for a hydrogen jet, diluted with nitrogen, issuing into a turbulent co-flowing hot air stream [2]. We focus here on the case where  $T_{\text{fuel}} = 691\text{K}$  and  $T_{\text{cf}} = 935, 945, 960, 980\text{K}$ . The fuel velocity is 120m/s while the co-flow velocity ranges from 20 to 35m/s. The LES are performed using the VUB in-house CFD code [3], while an in-house code developed in Cambridge [4] is used to solve CMC equations. The full three-dimensional CMC equations are solved on a coarser grid than the LES. The solution domain (67.5mm  $\times$  25mm  $\times$  25mm) contains  $192 \times 48 \times 48$  CFD cells and we compare to the results obtained on a CFD mesh with  $192 \times 48 \times 48$  cells. The basic CMC mesh, covering the same physical space domain as the CFD mesh, consists of  $80 \times 8 \times 8$  cells. The mixture fraction space is discretized into 50 bins, clustered at the lean side in mixture fraction space. The inflow turbulence generator is based on a digital filter [5]. The chosen length and time scales are 4.5mm and 1ms, with turbulence intensity 12.5% [2].

Focus is on assessing the impact of different detailed chemical mechanisms on the auto-ignition predictions. At relatively low temperatures, where there is more uncertainty in the reaction rate constants, the choice of the detailed chemical mechanism can be of great importance. Crucial are intermediate and slow reactions, which increase the pool of reactants. Therefore, we investigate the low temperature non-premixed auto-ignition behavior with different chemical mechanisms: Li et al. [6], Mueller et al. [7] and Yetter et al. [8]. The Li mechanism results in earlier auto-ignition and hence gives shorter lift-off heights than the Mueller and Yetter mechanisms over the entire test range.

The fuel mixes with the air co-flow, ignites, and forms a lifted-like flame. The evolution of HO<sub>2</sub> and OH from inert to burning conditions in mixture fraction space is discussed (Figure 1). Radially averaged and time averaged conditional species mass fractions are shown in Fig. 1. Each line in Fig. 1 corresponds to one CMC cell. Time averaging for the LES and CMC results was performed with data being collected over 10ms. During the auto-ignition process, H<sub>2</sub> and O<sub>2</sub> are also slowly consumed while the concentrations of H, OH, H<sub>2</sub>O increase at the ignition location. The highest values of the H radical are found in the rich region, after ignition, while H<sub>2</sub>O corresponds to the high temperature region. The hot regions, corresponding to high OH mass fraction, are convected downstream out of the domain. Auto-ignition of hydrogen is characterized by destruction of the pre-ignition species (HO<sub>2</sub>) and rapid generation of OH [1]. Consistently, just upstream of the auto-ignition point (i.e. at the flame base), there is a build-up of HO<sub>2</sub> radical. Build-up of HO<sub>2</sub> ahead of the flame edge, prior to creation of H and OH, shows that base of the flame is stabilized by auto-ignition. Therefore HO<sub>2</sub> is a key intermediate species. The other species have low concentration at the ignition point.

The trends in the experimental observations are in general well reproduced: the auto-ignition length decreases with an increase in co-flow temperature and increases with increase in co-flow velocity. With increasing co-flow temperature, the differences between the mechanisms considered diminish. In the statistically steady-state condition of the flow, reaction is balanced by convection at the flame base, showing that auto-ignition is the stabilization mechanism, with scalar dissipation rate and diffusion in physical space being relatively unimportant there.

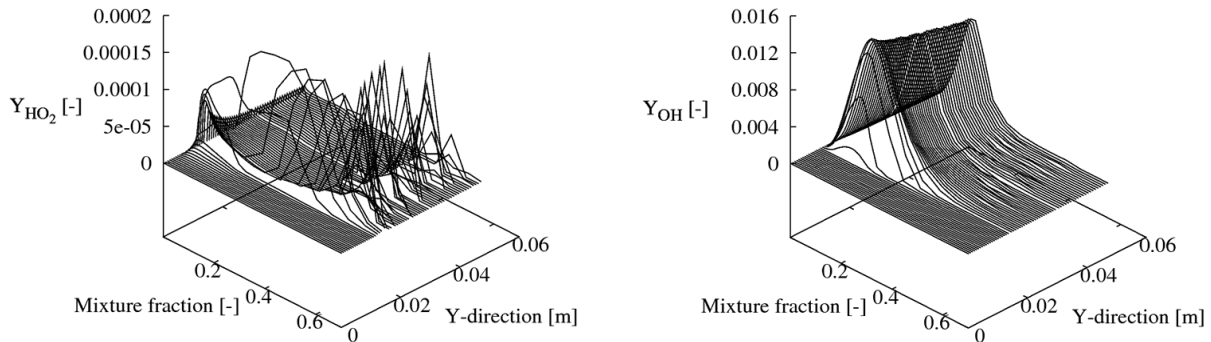


Figure 1: Evolution in the axial direction of time averaged conditional HO<sub>2</sub> and OH mass fractions as a function of mixture fraction (co-flow temperature: 960K, fuel temperature: 691K, mechanism of [6]).

- [1] E. Mastorakos, Prog. Energy Combust. Sci. 35 (2009) 57-97.
- [2] C.N. Markides, E. Mastorakos, Proc. Combust. Inst. 30 (2005) 883-891.
- [3] T. Broeckhoven, PhD Thesis, VUB, Beussels, Belgium, 2007.
- [4] A. Triantafyllidis, E. Mastorakos, R.L.G.M. Eggels, Combust. Flame 156 (2009) 2328-2345.
- [5] M. Klein, A. Sadiki, J. Janicka, J. Computat. Phys. 186 (2003) 652-665.
- [6] J. Li, Z. Zhao, A. Kazakov, and F.L. Dryer, Inter. J. Chem. Kinet. 36 (2004) 566-575.
- [7] M.A. Mueller, T.J. Kim, R.A. Yetter, F.L. Dryer, Inter. J. Chem. Kinet. 31 (1999) 113-125.
- [8] R.A. Yetter, F.L. Dryer, H. Rabitz, Combust. Sci. Technol. 79 (1991) 97-128.

## Cambridge Stratified Swirl Burner

Mark Sweeney<sup>\*+</sup>, Matt Dunn<sup>§</sup>, Simone Hochgreb<sup>+</sup>, Robert Barlow<sup>§</sup>

<sup>+</sup>Department of Engineering, University of Cambridge, UK

<sup>§</sup>Sandia National Laboratories, California, USA

<sup>\*</sup>[marksweeney@cantab.net](mailto:marksweeney@cantab.net)

Many practical combustion applications make use of stratification and swirl to achieve improved performance. The fundamental properties and behaviour of such flames remains an area of active research. A novel co-annular turbulent methane-air burner is presented, as well as preliminary data from a selection of interesting operating conditions. The burner was designed to provide simple exit geometry (see Fig. 1) and well defined boundary conditions to assist modelling.

The inner annulus was run as a non-swirling flow, at a richer equivalence ratio than the outer annulus flow. The outer annulus was run with two CH<sub>4</sub>/air flows split between an axial flow plenum and a swirl plenum depending on the degree of swirl required. The annuli are approximately 25 hydraulic diameters in length to ensure fully developed flow at exit. In all cases the flame is stabilised by a central ceramic bluff body. The exit geometry is summarised in Fig. 1. A low velocity co-flow is used to prevent entrainment of ambient air. This flow system allowed for a range of premixed, stratified, and swirling operating conditions, a selection of which are presented here and are summarised in Table 1.

Operating Condition	Flow Type	$\Phi_{\text{global}}$	$\Phi_{\text{inner}}$	$\Phi_{\text{outer}}$	Stratification Ratio	$U_{\text{inner}}$	$U_{\text{outer}}$
SwB1	Axial						
SwB3	Swirling		0.75	0	1		
SwB9	Axial	0.75				7.5	15
SwB11	Swirling		1.125	0.375	3		

Table 1: Selected operating conditions from Cambridge Swirling Stratified Burner

Velocity data were obtained from 2D particle image velocimetry (PIV). A double-pulsed 532 nm laser (Litron Nano PIV) was used to illuminate calcined aluminium oxide seed particles with mean diameter of 1  $\mu\text{m}$ . The pulse energy was 50 mJ. The resulting scattered light was captured using a CCD camera in double-frame mode (LaVision Imager ProX 4M). The field of view was approximately 85 x 85 mm and the frame resolution was 2048 x 2048 (41.5  $\mu\text{m}$  pixel<sup>-1</sup>). The seed density, camera aperture, and pulse separation  $\Delta t$  were optimised for each operating condition. The inner annulus and outer annulus were seeded separately using a pair of seeding chambers to ensure similar seed densities at different stream velocities. The mean velocity field for the non-swirling SwB1 case is shown in Fig. 2 using vectors and streamlines.

Temperature and species data were obtained from simultaneous line imaging of Rayleigh scattering, Raman scattering, and two-photon CO-LIF. These measurements were recorded at 103  $\mu\text{m}$  resolution. Crossed plane imaging of OH-PLIF was used to determine the instantaneous 3D flame normal at the line measurement axis, allowing the angle correction of gradients of scalars.

Sample profiles of instantaneous mole fractions (CO, CO<sub>2</sub>, O<sub>2</sub>, H<sub>2</sub>O, CH<sub>4</sub>) against temperature are shown in Fig. 3 for the non-swirling SwB1 case. The data is taken at 30 mm downstream from the burner exit. The experimental data generally shows good agreement on the mean with equivalent values obtained from numerical simulations. The most significant deviations are seen for CO<sub>2</sub>, H<sub>2</sub>O and H<sub>2</sub>.

Gradients of progress variable  $c$  and mixture fraction  $Z$  are used to determine the scalar dissipation  $X_c$  and the cross dissipation term  $X_{zc}$ . The progress variable gradient is evaluated using central differencing, while the gradient of the noisier mixture fraction data is evaluated using a wavelet differentiation scheme. Flame surface density derived from angle corrected progress variable measurements using the Pope formulation are also presented.

## References

M. S. Sweeney, S. Hochgreb, M. J. Dunn, R. S. Barlow, *RA comparative analysis of flame surface density metrics in premixed and stratified flames*, 33<sup>rd</sup> International Symposium on Combustion, Beijing, China, 2010

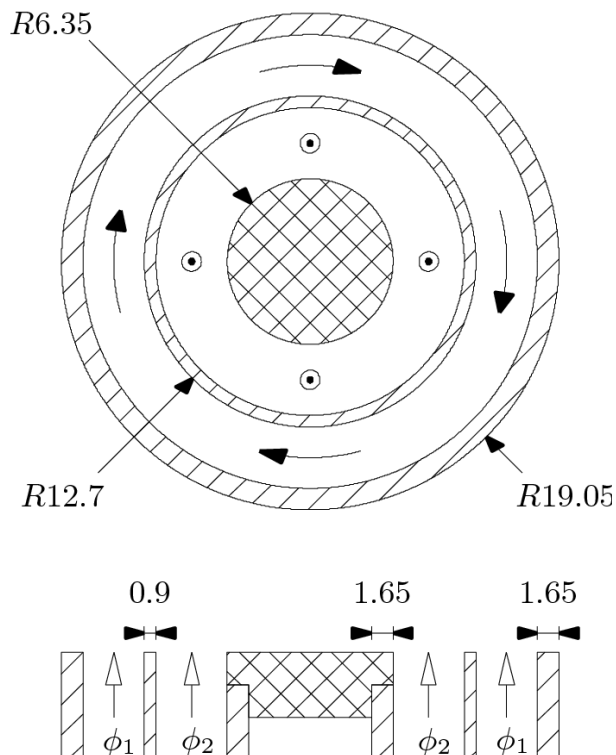


Fig 1: Schematic of swirl burner. All dimensions in mm and shown to scale. Direction of swirl flows in outer annulus shown by curved arrows.

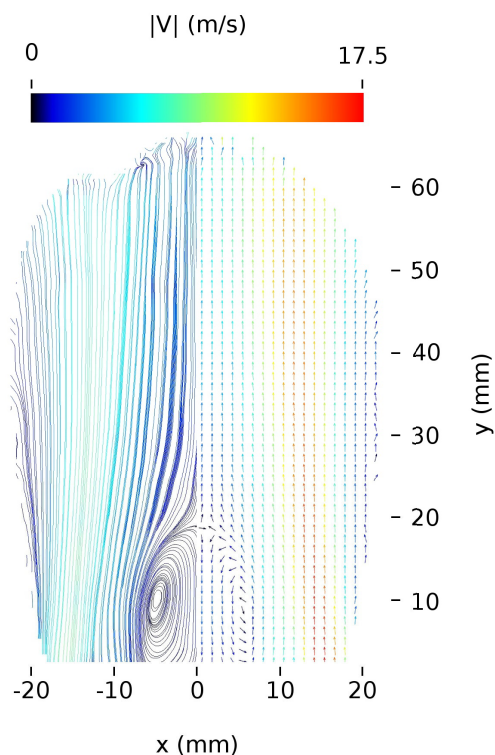


Fig 2: Mean velocities in premixed non-swirling case SwB1, showing streamlines (left) and velocity vectors (right)

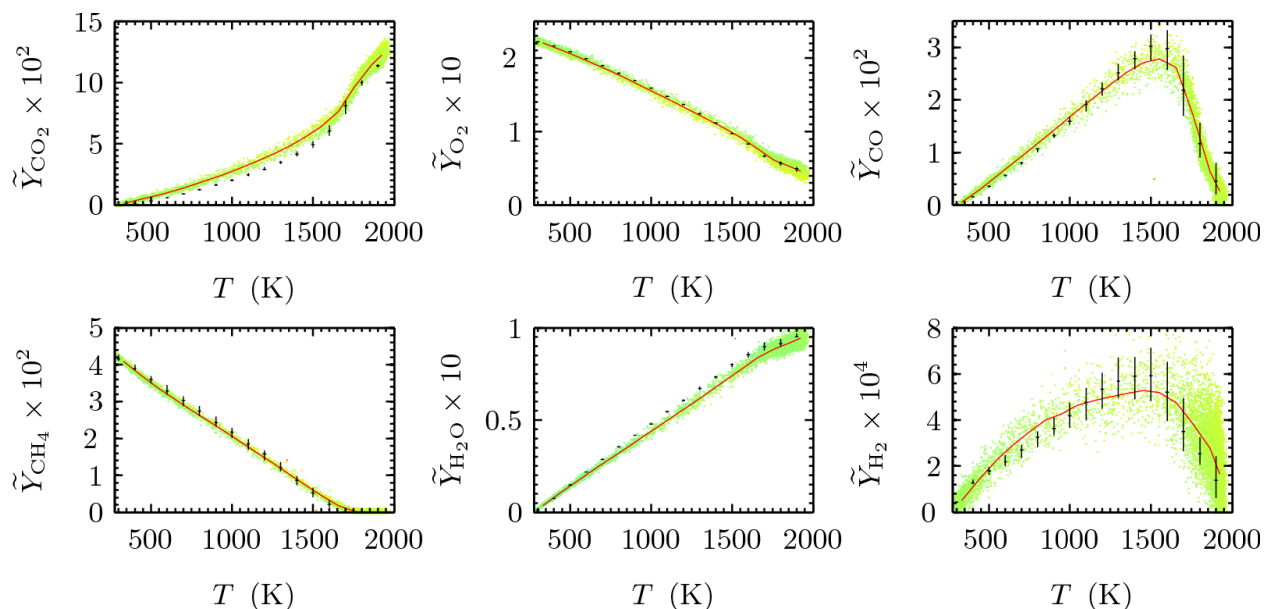


Fig 3: Scatterplots of key species against temperature in SwB1 case, with conditional mean shown by a red line. Laminar calculations at the mean local equivalence ratio are shown by black crosses

# Measurements of Blowoff Dynamics in Stratified, Vitiated Bluff-Body Flames

S. G. Tuttle, S. Chaudhuri, S. Kostka, K. M. Kopp-Vaughan, B. M. Cetegen, M. W. Renfro\*  
 Mechanical Engineering Department, University of Connecticut, Storrs, CT 06269-3139

Experiments were performed in an enclosed duct designed to simulate conditions in an afterburning gas turbine engine with both unvitiated and vitiated air. As shown in Fig. 1, room temperature air entered the duct at (1), passed through a Maxon NP-LE duct burner (2), and then through a settling section to allow the combustion products to mix (3). Downstream, a heat exchanger could be installed or removed, allowing the vitiated flow to be cooled (4). The gases were then accelerated through a contoured convergent nozzle (5) and past three airfoil fuel injectors (6), where gaseous propane was injected. The fuel injectors were designed to produce a flat or tailored fuel profile to investigate the influence of equivalence ratio gradients and fuel placement on the wake combustion.

The vitiated air and fuel mixture then proceeded into the optically-accessible experimental section (7), where a 9.55 mm equilateral triangular bluff body was placed across a duct 76.2 mm wide and 38.1 mm high. The full height of the test section was optically accessible, while a narrow 19 mm window on the top was included for laser access. All four faces of the test sections had 0.8 mm slits at 30° to inject a film of nitrogen to decrease the convective heat transfer to the windows. The duct opened up into a round 15.2 cm section (8), 20.3 cm downstream from the flame holder, with five water spray nozzles that extinguished any flames and cooled the exhaust flow.

Measurements of the velocity and fuel/air distribution upstream of the bluff-body and the bluff-body temperature were made sufficient to characterize the boundary-conditions for numerical simulations. Large-eddy simulations of this experiment are being conducted by groups at Georgia Tech and United Technologies. Investigations were carried out with air flow rates of 0.06-0.09 kg/s and Reynolds numbers based on the bluff body dimension of  $Re_H=1.8 \times 10^4 - 2.0 \times 10^4$ . Rig capabilities are shown in Table 1 for the three upstream combustion regimes.

Optical diagnostics were used to characterize the flames including: (1) a monochromatic high speed camera, Motion Scope from Redlake Imaging, coupled to a Dep-Gen II image intensifier was focused on the bluff-body wake and gathered images of chemiluminescence at 500 frames per second. For some experiments a Phantom v.12 unintensified camera was used for imaging at 5000 to 6500 Hz. (2) a photomultiplier tube (PMT), 432 nm bandpass filter, and objective lens were directed on the bluff-body wake, providing a signal of the CH\* chemiluminescence used to trigger the high-speed imaging and providing a record of the temporal location relative to blowoff for other diagnostics. (3) a particle-imaging velocimetry (PIV) system including a New Wave dual cavity Nd:YAG laser (50 mJ/pulse) and a frame-straddling 1024×1280 CCD camera, model Flow Maser 3S, together with DaVis 7.0 post-processing software. Particle seeding of the flow was performed using a fluidized bed aerosol generator filled with 1 μm alumina seed particles. A separate air line, with a flow rate of 0.0072-0.0098 kg/s was passed through the seeder and the seeded air was injected into the contoured nozzle. Seed density was controlled by adjusting the air flow rate, powder dispenser rate, and through adjustment of the vibration frequency. (4) a Nd:YAG pumped dye laser, Continuum, was used to generate a 283-nm UV sheet for hydroxyl planar laser-induced fluorescence (PLIF). (5) the 4<sup>th</sup> harmonic of an Nd:YAG laser was used to excite acetone fluorescence upstream of the bluff-body to characterize the fuel air distribution. In these experiments, the propane injection was replaced with nitrogen at the same flow rate bubbled through temperature-controlled acetone baths. The PLIF, PIV and chemiluminescence systems could be operated simultaneously, but the acetone measurements of fuel air distribution were performed separately.

Additional experimental details are provided in Refs. 1-3.

Lean blowoff was first investigated at unvitiated and uniformly mixed flow conditions in order to characterize the baseline flame behavior. The lean

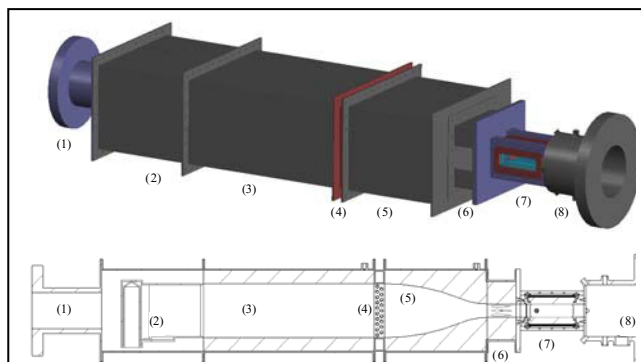


Fig. 1: Layout of experimental rig.

Regime	Ambient	Vitiated	Vitiated & Cooled
Temp (K)	300	700	700
$\phi_p$	0.00	0.15	0.33
U (m/s)	18-27	44-66	44-66
O <sub>2</sub> (%V)	21	18	13
Mach	0.06-0.08	0.08-0.13	0.08-0.13
Re <sub>H</sub>	1.2-1.7×10 <sup>4</sup>	1.7-2.0×10 <sup>4</sup>	1.7-2.0×10 <sup>4</sup>

Table 1: Rig capabilities for three flow regimes.

\* renfro@engr.uconn.edu

blowoff margin was then characterized with upstream air vitiated at overall equivalence ratios of 0.15 and 0.33.

Further studies were performed with non-uniform fuel profiles (rich or lean in the center or asymmetric), thus imposing single and double fuel gradients near the flame holder. Fuel profiles were characterized using laser induced acetone fluorescence. Transitional blowoff behavior was documented with measurements of CH chemiluminescence emission from the wake as well as high-speed imaging of flame dynamics. Simultaneous PIV and OH PLIF measurements were taken at fuel-air ratios near blowoff to capture flame edge and aerodynamic behavior to determine the mechanisms of final blowoff. Post processing of the images and flow field revealed the interaction between the velocity field and flame sheet.

A blowoff stability map was established by decreasing the global equivalence ratio within the test section in steps of  $\Delta\phi=0.01$ , under constant air flow. The flame was first ignited at an equivalence ratio of 0.8. Two minutes was allowed between each step change to allow for the complete stabilization of fuel flow between equivalence ratio changes. As the equivalence ratio decreased, the PMT CH\* signal was monitored for blowoff. Upon blowoff the equivalence ratio,  $\phi$ , from the fuel control system was recorded. Tests were repeated multiple times to quantify repeatability. A blowoff curve for the unvitiating and vitiated air in Fig. 2 shows that the increases in upstream mean velocity resulted in higher blowoff equivalence ratios. This behavior is expected and is generally reflected in a decreasing Damköhler number with increasing velocity. With increases in velocity and decrease aerodynamic time scales, the chemical timescales must also be decreased for the flame to remain attached to the bluff body. This can be accomplished by an increase in flame temperature and a fuel richer mixture, to maintain the same Da at blowoff. The local equivalence ratios were calculated based on the available oxygen remaining in the vitiated flow. In general, the unvitiating blowoff equivalence ratios were within 5% of those predicted from literature values.

The chemiluminescence images of the last 36 ms until blowoff are shown in Fig. 3 for conditions at 23 m/s and an equivalence ratio of 0.69. Extinction of the flame in the near-field shear layer led to burning in the recirculation zone just prior to blowoff for all the cases examined. This recirculation zone combustion intermittently led to reignition of the shear layers as observed in Fig. 3. A sample simultaneous PIV/OH PLIF measurement is shown in Fig. 4. The overlaying vector field is colored by vorticity with vector length scaled to velocity magnitude. Analysis of these results to date have evaluated conditional strain rates to examine conditions leading to local extinction.

1. Chaudhuri, S., Kostka, S., Renfro, M. W., and Cetegen, B. M. (2010). *Combust. Flame*, v. 157, 790-802.
2. Chaudhuri, S., Kostka Jr., S., Tuttle, S. G., Renfro, M. W., and Cetegen, B. M. (2010). Blowoff dynamics of V-shaped bluff body stabilized, partially premixed turbulent flames in a practical scale rig. 48<sup>th</sup> AIAA Aerospace Sciences Meeting, Orlando, FL.
3. Tuttle, S. G., Chaudhuri, S., Kostka Jr., S., Cetegen, B. M., and Renfro, M. W. (2010). Transitional blowoff behavior of wake-stabilized, stratified flames in vitiated flow. 48<sup>th</sup> AIAA Aerospace Sciences Meeting, Orlando, FL.

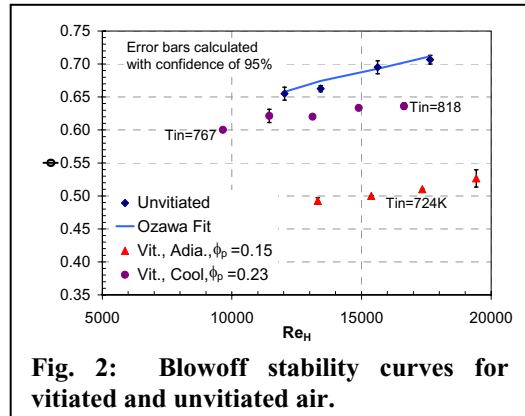


**Fig. 2: Blowoff stability curves for vitiated and unvitiating air.**

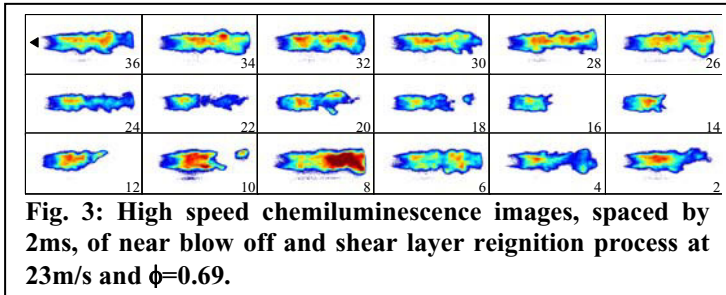


**Fig. 3: High speed chemiluminescence images, spaced by 2ms, of near blow off and shear layer reignition process at 23m/s and  $\phi=0.69$ .**

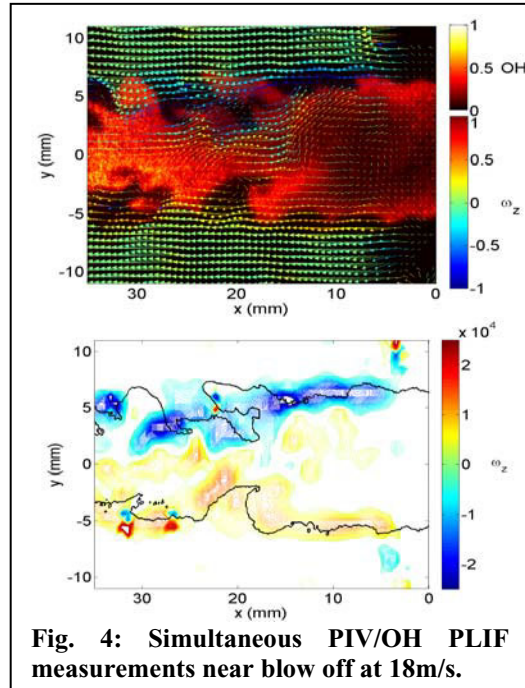


**Fig. 4: Simultaneous PIV/OH PLIF measurements near blow off at 18m/s.**

# Modeling of jet in a hot coflow with tabulated unsteady non-premixed flamelets in RANS and LES

R. Vicquelin\*, B. Fiorina, O. Gicquel

Laboratoire EM2C-CNRS, Ecole Centrale Paris, 92295 Châtenay Malabry, France

\* Corresponding author: ronan.vicquelin@centraliens.net

Tabulated chemistry models have been widely used in RANS to include detailed chemistry effects. Applications of these methods in LES have benefit of both good descriptions of chemistry and turbulence. Most of the time, when RANS models are extended to LES, presumed PDF (Probability Density Function) are replaced with equivalent presumed FDF (Filtered Density Function) and the additional balance equations for averaged parameters of the chemical database are replaced with filtered balance equations in LES. As LES model assumptions apply at subgrid scales only, one expects LES to describe turbulent combustion better than RANS even when the same tabulated chemistry model is used. This is here investigated with the numerical simulation of a jet in a hot coflow performed both in RANS and LES approaches.

A turbulent combustion model called UTaC (Unsteady flamelets Tabulated Chemistry) was developed for diluted combustion where auto-ignition participates to the stabilization mechanism. This model is based on the tabulation of non-premixed igniting flamelet solutions and was applied to a jet in a vitiated coflow [1, 2]. The jet was experimentally studied with two mixtures: hydrogen/nitrogen and methane/air. Both mixtures were computed in RANS simulations. Radial profiles of temperature (Fig. 1) and the flame lift-off height sensitivity to the coflow temperature (Fig. 2) are well retrieved by RANS simulations in the  $H_2/N_2$  case. In the  $CH_4$ /air case, the UTaC model is used in both RANS and LES frameworks (Fig. 3). The RANS simulation underestimates the flame lift-off height ( $H/d = 20$  instead of 30) while the LES predicts a flame lift-off height ( $H/d = 29$ ) closer to the experimental one. Figure 4 shows the axial temperature profile. As the RANS simulated flame is closer to the jet, rich mixtures are burnt too early. The large eddy simulation was post-processed in order to identify reasons of the difference between RANS and LES results in the  $CH_4$ /air case.

A known shortcoming of RANS models such as  $k-\varepsilon$  is the overestimation of the round jet spreading. Standard coefficients of the  $k-\varepsilon$  model were then modified to correct this behavior. LES and RANS computations predict the similar velocity and mixing fields in non-reactive simulations. However, in opposition to LES, the RANS approach with modified coefficients is not universal. Nonetheless, with the same mixing field, LES and RANS do not find the same flame lift-off height. This must therefore be attributed to the turbulent combustion model.

LES post-treatment shows that instantaneous filtered mixture fraction and progress variable (two key coordinates of the database) cannot be assumed independent. Conditional average and mixture fraction/progress variable joint PDF (Fig. 5) demonstrate that progress in reaction depends on the local mixture. Hence, a main difference between RANS and LES is that the RANS combustion model assumed independency at all times and scales whereas LES makes this assumption only at the subgrid level and allows to capture correlation between progress variable and mixture fraction in large scales. This clearly shows the advantage of LES for the same turbulent combustion model.

## References

- [1] R. Cabra, T. Myhrvold, J. Y. Chen, R. W. Dibble, A. N. Karpetis, and R. S. Barlow. *Proceedings of the Combustion Institute*, 29(2):1881–1888, 2002.
- [2] R. Cabra, J. Y. Chen, R. W. Dibble, A. N. Karpetis, and R. S. Barlow. *Combustion and Flame*, 143(4):491–506, 2005.
- [3] Z. Wu, S. H. Starner, and R. W. Bilger. In *Proceedings of the 2003 Australian Symposium on Combustion and the 8th Australian Flame Days*, Monash University, Australia, 2003.
- [4] R. L. Gordon, S. H. Starner, A. R. Masri, and R. W. Bilger. In *Proceedings of the 5th Asia-Pacific Conference on Combustion*, pages 333–336, University of Adelaide, Jul 2005.

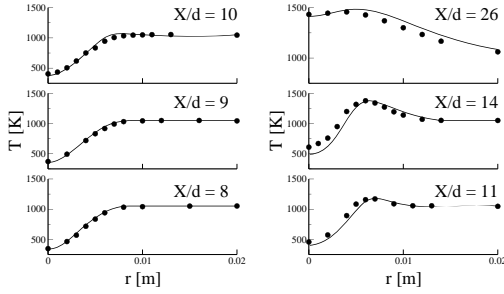


Figure 1: Radial mean temperature profiles comparison between RANS (line) and experimental [1] (symbols) results in the  $H_2/N_2$  case.

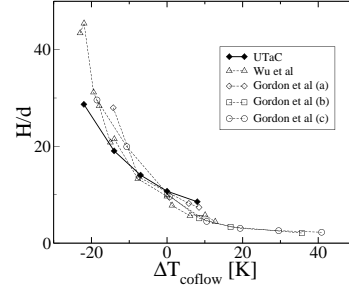


Figure 2: Coflow temperature sensitivity of the flame lift-off height  $H$  (scaled by the jet diameter  $d$ ) in the  $H_2/N_2$  case. RANS simulations performed with the UTaC model are compared with experimental measurements [3, 4].

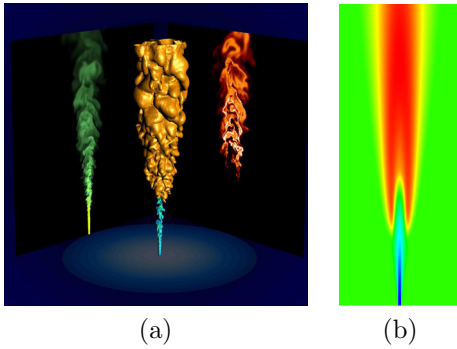


Figure 3:  $CH_4/air$  case: (a) Three-dimensional view of an instantaneous LES solution: isosurfaces of temperature (1600 K) and mixture fraction ( $\tilde{z} = 0.5$ ); planar slices colored by mixture fraction (left) and OH mass fraction (right). (b) Mean temperature contour plot of the RANS solution.

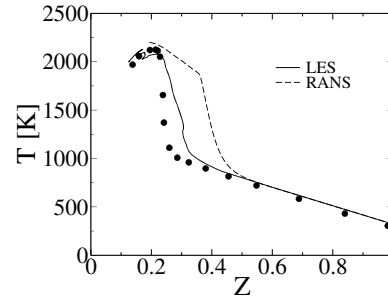


Figure 4: Axial mean temperature profiles plotted as a function of mean mixture fraction in the  $CH_4/air$  case. Lines: RANS (dashed line) and LES (plain line) results. Symbols: experimental data [2].

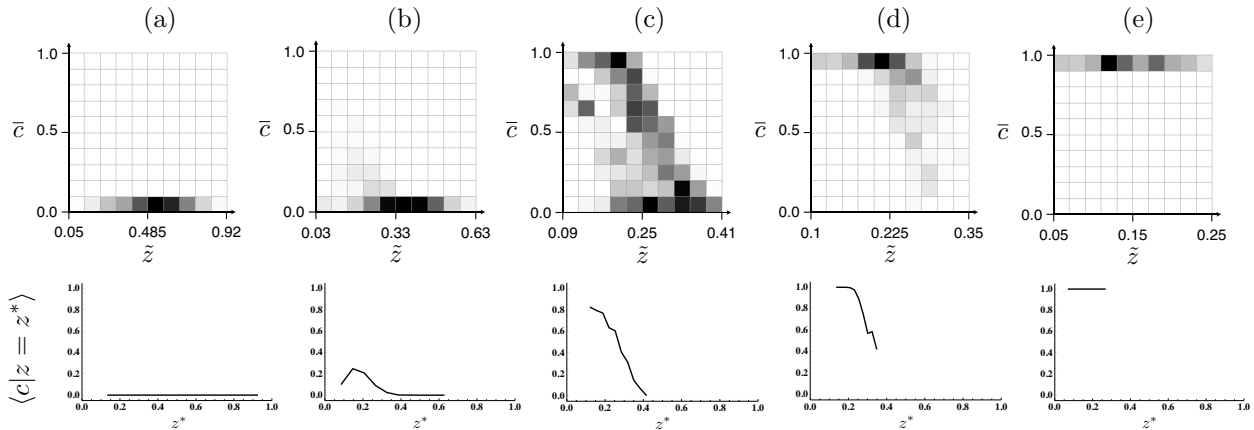


Figure 5: Statistical analysis of time signal of  $\bar{c}$  and  $\tilde{z}$  at several locations on the jet axis in the  $CH_4/air$  case: (a)  $X/d = 20$ ; (b)  $X/d = 30$ ; (c)  $X/d = 40$ ; (d)  $X/d = 50$ ; (e)  $X/d = 75$ . First row: color maps of the joint PDF  $P(\tilde{z}, \bar{c})$  in the discretized  $\tilde{z}$ - $\bar{c}$  plane. Second row: profiles of the progress variable conditional mean  $\langle \bar{c} | \tilde{z} = z^* \rangle$ .

# Modeling of Sandia Flame E using Hybrid Binomial Langevin–MMC Model

Andrew P. Wandel<sup>1</sup> and R. Peter Lindstedt<sup>2</sup>

Authors: [andrew.wandel@usq.edu.au](mailto:andrew.wandel@usq.edu.au), [p.lindstedt@imperial.ac.uk](mailto:p.lindstedt@imperial.ac.uk)

<sup>1</sup>Computational Engineering and Science Research Centre,

Department of Mechanical Engineering, University of Southern Queensland, Toowoomba, 4350, Australia

<sup>2</sup>Department of Mechanical Engineering, Imperial College London, South Kensington, SW7 2BX, UK

In the hybrid binomial Langevin–MMC model [1], the binomial Langevin model [2] is used to simulate the velocity–scalar joint probability density function (pdf) (with the scalar a pseudo mixture fraction), while the Multiple Mapping Conditioning (MMC) method [3] is used to simulate the mixing of all scalars. The compatibility of the hybrid model is ensured by setting the MMC velocity to equal the binomial Langevin velocity, which results in a model for the MMC reference variable—obviating the need to specify the transport coefficients for the reference variable. The mixing is controlled by attempting to minimize the difference between the (MMC) mixture fraction and the (binomial Langevin) pseudo mixture fraction.

The method has previously been used [1,4] to satisfactorily simulate a mixing layer with dilute chemistry [5–7] and Sandia Flame D [8]. Results are presented here for Sandia Flame E, to test the model’s ability to characterize moderately strong local extinction/reignition phenomena. The Euclidean Minimal Spanning Tree (EMST) model [9] has also been used for this case [10], while the EMST subroutines [11] were implemented into the same code as the hybrid model (Piper). This last effort is designed to eliminate any bias that may occur due to the different numerical schemes that are used.

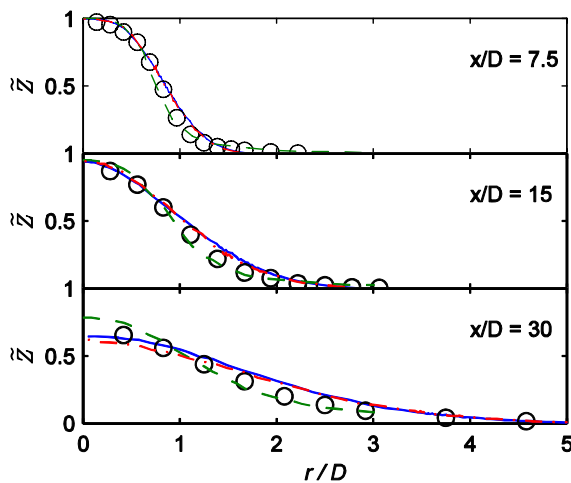


Figure 1: Favre-averaged mixture fraction profiles. Hybrid binomial Langevin–MMC, —; EMST (same code), - -; EMST [10], ···; Experiment [8], ○.

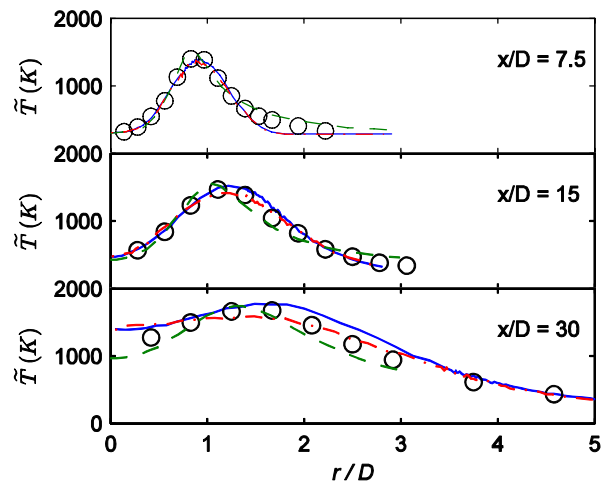


Figure 2: Favre-averaged temperature profiles. As per Fig. 1.

Figures 1 and 2 contain the Favre-averaged mixture fraction and temperature profiles respectively. The hybrid model predictions are slightly higher than the corresponding EMST results, while the previous EMST results [10] are noticeably different, although all predict the experiment [8] reasonably well. Figure 3 shows the rms mixture fraction results where it is clear that the EMST model implemented into the Piper code greatly under-mixes, while the previous EMST results [10] perform well. This under-mixing caused the temperature to remain close to equilibrium (Fig. 4). The hybrid model consistently predicted OH well (Fig. 5), with EMST over-predicting the levels closer to the axis. The Burning Index (BI) is a measure of the extent of combustion near the stoichiometric mixture fraction [12] and is shown in Fig. 6. The hybrid model performed well for temperature and OH, but over-predicted CO; the EMST model [10] performed well for all scalars; while EMST implemented into Piper consistently over-predicted the results, consistent with this model remaining too close to equilibrium. Overall, the hybrid model produced promising results, encouraging further testing for other cases.

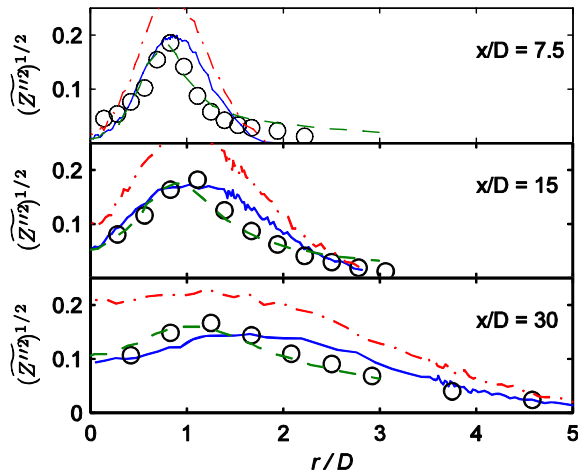


Figure 3: Favre-rms mixture fraction profiles. As per Fig. 1.

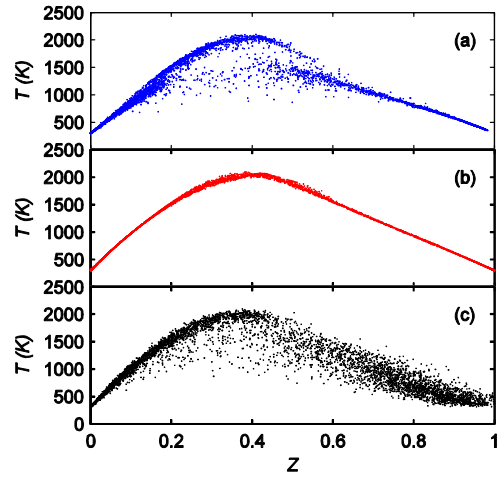


Figure 4: Scatter plots of temperature at  $x/D = 15$  for 5000 randomly-selected samples. (a) Hybrid model; (b) EMST (same code); (c) Experiment [8].

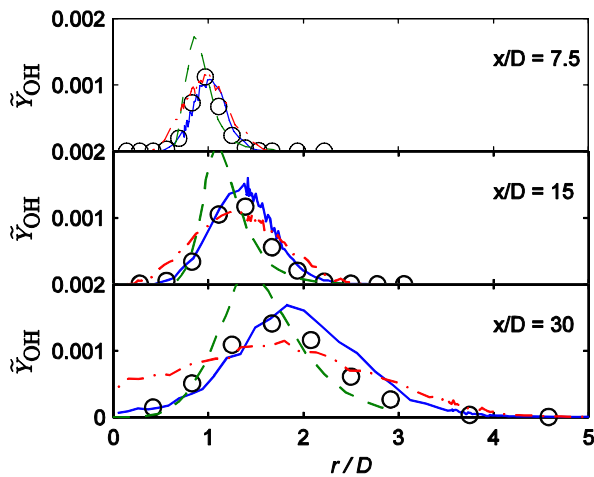


Figure 5: Favre-averaged OH profiles. As per Fig. 1.

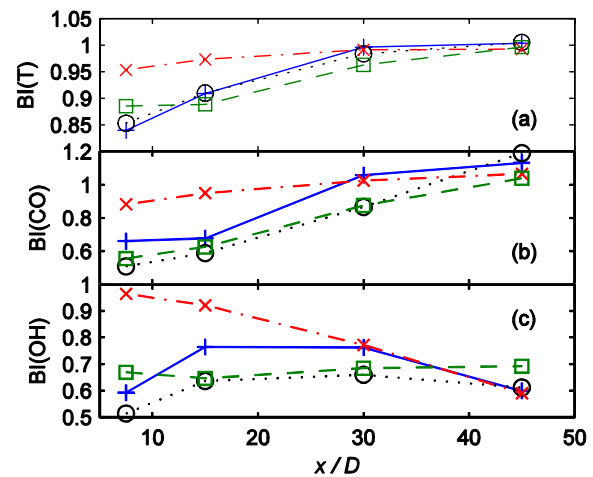


Figure 6: Burning Indices for: (a) temperature; (b) CO; (c) OH. Hybrid model, +; EMST (same code), x; EMST [10], □; Experiment, o.

## References:

- [1] A.P. Wandel and R.P. Lindstedt, *Physics of Fluids*, 21:015103 (2009).
- [2] L. Valiño and C. Dopazo, *Physics of Fluids A*, 3:3034 (1991).
- [3] A.Y. Klimenko and S.B. Pope, *Physics of Fluids*, 15:1907 (2003).
- [4] A.P. Wandel and R.P. Lindstedt, in *Proceedings of the Australian Combustion Symposium 2009*, p. 47 (2009).
- [5] L.R. Saetran, D.R. Honnery, S.H. Stårner and R.W. Bilger, *Turbulent Shear Flows 6*, Springer-Verlag, p. 109 (1989).
- [6] R.W. Bilger, L.R. Saetran and L.V. Krishnamoorthy, *Journal of Fluid Mechanics*, 233:211 (1991).
- [7] J.D. Li and R.W. Bilger, *Physics of Fluids A*, 5:3255 (1993).
- [8] R.S. Barlow and J.H. Frank, *Proceedings of the Combustion Institute*, 27:1087 (1998).
- [9] S. Subramaniam and S.B. Pope, *Combustion and Flame*, 115:487 (1998).
- [10] R.R. Cao, H. Wang and S.B. Pope, *Proceedings of the Combustion Institute*, 31:1543 (2007).
- [11] Z. Ren, S. Subramaniam and S.B. Pope, <http://eccentric.mae.cornel.edu/~tcg/emst> (2002).
- [12] J. Xu and S.B. Pope, *Combustion and Flame*, 123:281 (2000).

# Development of an LES/PDF code and its application to Flame D

Haifeng Wang\*, Stephen B. Pope

*Sibley School of Mechanical and Aerospace Engineering,  
Cornell University, Ithaca, NY 14853, USA*

\*Corresponding author. Email: [hw98@cornell.edu](mailto:hw98@cornell.edu)

Although LES/PDF has been implemented in several previous works (e.g. [1-3]), numerically solving the PDF equation adequately remains to be investigated and validated. A new Monte Carlo particle code (called HPDF) suitable for RANS/PDF and LES/PDF studies is developed as a platform for studying numerical algorithms and for practical turbulent combustion modeling. Accurate numerical schemes are developed and implemented in the code to advance the particles in the physical and compositional space to ensure overall second-order numerical accuracy in both space and time. In contrast, all previous LES/PDF studies achieve only first-order accurate in the time advancement [4]. In addition, the code has the following attributes: scalable up to at least 4096 cores with MPI parallelization; supporting Cartesian and cylindrical coordinate systems; parallelizable by domain decomposition in two dimensions; and having a general interface to facilitate coupling to different existing LES (or RANS) codes.

The HPDF code has been verified comprehensively with a wide range of manufactured test cases, and has been initially combined with an LES code developed by Pierce [5]. The first set of LES/HPDF simulations has been performed for the DLR flame A [6]. For simplicity and computational economy, the flamelet model is used to compute the thermochemical properties based on the mixture fraction. A single scalar (the mixture fraction) is solved for the particles. In this initial study, the following issues are discussed: the verification of the HPDF code, the effect of the LES grid resolution, the consistency between LES and PDF, and the performance of different time-integration schemes (first-order and second-order) in HPDF. Second-order accuracy of the code in space and time is verified by a manufactured 1D test case. Strong grid-dependency is found for the DLR flame A. In order to study consistency, the numerical solutions of the mixture fraction are duplicated in LES and HPDF. At the level of the governing equations, the first two moments of the mixture fraction are consistent in the LES and PDF approaches, so that any discrepancy between their simulation results is due to numerical errors. The results of the mixture fraction fields from LES and HPDF agree well with each other, indicating good numerical consistency. The effect of first and second order time integration schemes are also compared in the flame simulations, and negligible difference is observed due to the very small local CFL number in the flow downstream. The numerical results are compared to the experimental data, and overall good agreement is observed for the velocity, turbulence and scalar fields, which demonstrates the capability of the new code.

In the initial application of HPDF [6], a simple flamelet model is used. One of the goals of this development of new LES/PDF capability is to perform massively parallel LES/PDF computations of the TNF target flames for parametric studies of chemistry mechanisms and turbulence-chemistry interactions. To perform detailed chemistry calculations, direct integration of the reaction ODE is far too expensive for LES/PDF and a chemistry acceleration algorithm is needed, such as ISAT [7,8]. In this work, we combine LES/PDF with ISAT, and perform initial LES/PDF/ISAT simulations for Sandia flame D.

ISAT is combined with LES/PDF for simple local processing in the parallel computations, i.e., a single and independent ISAT table is created on each process. The ISAT parallelization for balancing workloads has been developed in a package called *x2f\_mpi* [8] and will be used in the future.

In the current simulations of flame D, the domain size is  $[80D, 20D]$  in the axial and radial directions, where  $D$  is the jet diameter. The number of  $256 \times 128 \times 32$  nonuniform grid cells are used in the axial, radial and azimuthal directions. A number of 40 particles per cell are used. The ARM1 mechanism is used for chemical reaction and the modified Curl model is used for mixing. One-way coupling is used in the current study, with which the density is obtained from LES with a flamelet model and is provided to HPDF. The contour plots of velocity, density and temperature from LES and HPDF are shown in Figure 1.

- [1] P.J. Colucci, F.A. Jaber, P. Givi, S.B. Pope, *Phys. Fluids* 10 (2) (1998) 499-515.
- [2] V. Raman, H. Pitsch, *Proc. Combust. Inst.* 31 (2007) 1711-1719.
- [3] S. James, J. Zhu, M.S. Anand, *Proc. Combust. Inst.* 31 (2007) 1737-1745.
- [4] H. Wang, P. P. Popov, S. B. Pope, *J. Comput. Phys.* 229 (2010) 1852-1878.
- [5] C.D. Pierce, *Progress-Variable Approach for Large-Eddy Simulation of Turbulent Combustion*, PhD thesis, Stanford University, 2001.
- [6] H. Wang, S.B. Pope, *Large Eddy Simulation/Probability Density Function Modeling of a Turbulent CH<sub>4</sub>/H<sub>2</sub>/N<sub>2</sub> Jet Flame*, *Proc. Combust. Inst.* (2010) (submitted).
- [7] S.B. Pope, *Combust. Theory Modelling* 1 (1997) 41-63.
- [8] L. Lu, S. R. Lantz, Z. Ren, S. B. Pope, *J. Comput. Phys.* 228(15) (2009) 5490-5525.

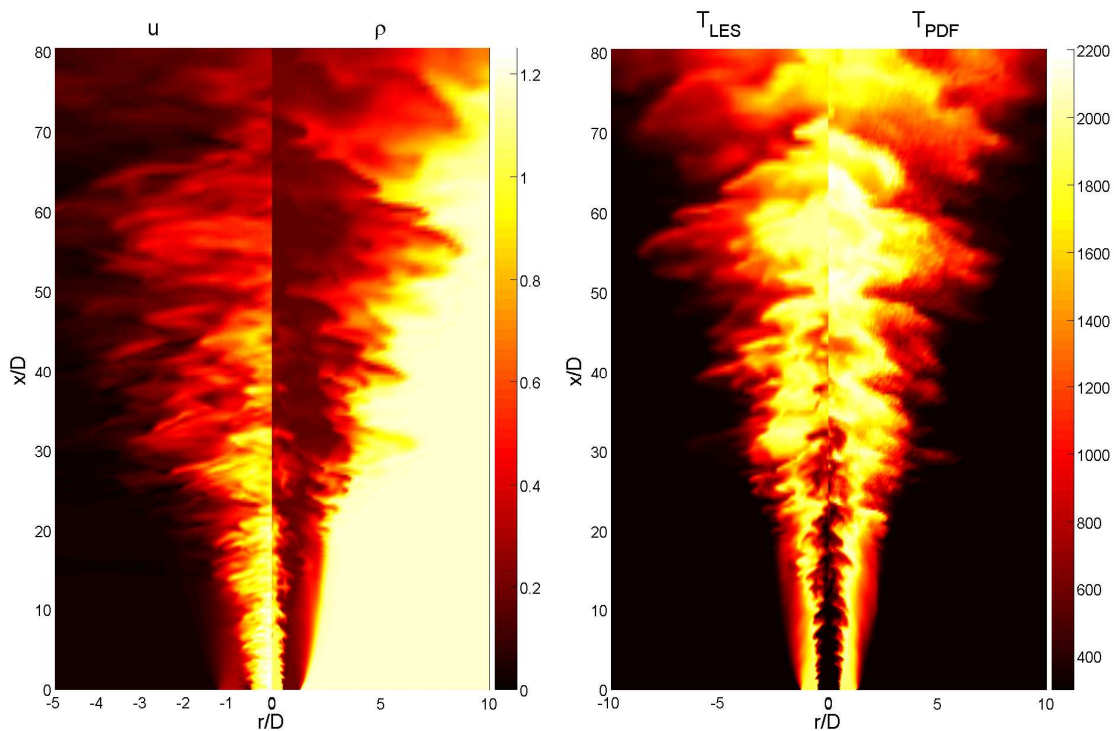


Figure 1: Contour plots of velocity  $u$ , density  $\rho$ , temperature from LES and temperature from HPDF.